JOURNAL OF THE MYANMAR ACADEMY OF ARTS AND SCIENCE

Chemistry and Industrial Chemistry

Vol. XVI, No.1B, October 2018

Myanmar Academy of Arts and Science

Journal of the Myanmar Academy of Arts and Science

Vol. XVI, No. 1B

Contents

Section (i) Chemistry

Journal of the Myanmar Academy of Arts and Science

Vol. XVI, No. 1B

Contents

Section (ii) Industrial Chemistry

SYNTHESIS OF CHITOSAN BASED POLYVINYLALCOHOL HYDROGEL FOR LOADING WITH CONTROLLED-RELEASED FERTILIZER

Aung Than Htwe[1] , Hninn Wutt Yee Htun[2], Daw Hla Ngwe [3]

Abstract

The use of controlled-released fertilizer hydrogel has become a new trend to save fertilizer consumption, and to reduce environmental pollution and safety application in agriculture. In agriculture, loss of nutrient elements is one of the large problems. So controlled-release is a method used to slove this problem. This paper describes the phosphorus release behavior of controlled-released fertilizer (CRF) hydrogels. The CRF hydrogel was prepared by mixing chitosan solution, polyvinyl alcohol hydrogel and fertilizer solution. The swelling ratio, water retention and fertilizer release behavior of prepared CRF hydrogel in water and soil were investigated. Therefore, the chemical nature was important that affected the degree of swelling of the hydrogel. Cultivation of chilli and maize seed tested using the various amount of prepared CRF hydrogel samples. The investigation of agronomical characters of the generation seeds were described.

Keywords: controlled-release fertilizer, hydrogel, chitosan, polyvinyl alcohol

Introduction

Nowadays, fertilizer specially NPK is the vital material for the grough of crops and plays an important role in food security. These NPK fertilizers are added into soil to save the necessary nutrients for plant growth. However, various environmental and economic drawbacks associated with the use of conventional fertilizers have become a focus of worldwide concern. The main problem facing the agrochemical industry is the huge loss of fertilizers added to the soil. One method for overcoming these shortcomings involves the use of slow-release fertilizers, which has demonstrated many advantages over the conventional types, such as decreasing fertilizer loss rate, supplying nutrient sustainably, lowering application frequency, and minimizing potential negative effects associated with over dosage (Diwani *et al.*, 2013).

[1.] Dr, Demonstrators, Department of Chemistry, University of Yangon
[2.] Dr, Demonstrators, Department of Chemistry, University of Yangon
[3.] Dr, Professor and Head, Department of Chemistry, University of Yangon

The growth of plants and its quality are mainly a function of the fertilizer quantity and water used. Depending on application methods and soil condition, some amount of the nutrients from the conventional fertilizers cannot be absorbed by plants and is lost to the environment. This phenomenon not only causes large economic and resource losses, but also causes serious environmental pollution (Salmiaton and Firoozeh, 2015).

Controlled release is a method that release or deliver a compound in a response of time. This method firstly practiced in medical field to optimize the dosage, to minimize the cost and toxic effect, and to increase the drugs overall efficiency. In agriculture field, this method is used to make a controlled release fertilizer. The advantages in this method are (1) to minimize the effect of excess fertilizer, (2) to decrease the operational cost, (3) to release the fertilizer directly to the root of the plants, (4) to decrease the fertilizer loss, and (5) to reduce water and soil pollution (Han *et al.,* 2008).

Chitosan, the second great amount of natural polysaccharide on earth crust, as a compound of chitin deacetylation is a biodegradable and non-toxic material for environment. Chitosan is widely used to produce controlled release materials in various fields, particularly in controlled-released fertilizer (CRF) manufacturing. Chitosan can be successfully processed by a variety of chemical reactions owing to its. Few works have applied chitosan particles in the agricultural field such as incorporation of NPK fertilizer into the chitosan nanoparticles to make fertilizer consumption more efficient. Furthermore, chitosan coated NPK compound fertilizers have demonstrated controlled release properties (Roshanravan *et al.*, 2015).

In this study, the controlled- released fertilizer (CRF) hydrogels were prepared from chitosan, polyvinyl alcohol and polyvinyl alcohol - chitosan, using glutaraldehyde as a crosslinker. Water absorbency, water retention and phosphorus release behavior of such the CRF hydrogels in water and in soil were investigated. The water and soil samples were analyzed for total amount of phosphorus by UV-visible spectrophotometry. In addition, the phosphorus release mechanism of each CRF hydrogel was investigated.

The objective of this research was to obtain materials possessing controlled release properties. This was done by covering granules of mineral fertilizer with a layer of chitosan as an example of biodegradable, natural polymer.

Materials and Methods

Materials

Commercial chitosan sample from shrimp shell was purchased from Asian Technology Groups Co., Ltd., Local Industry, Yangon, Myanmar. Polyvinyl alcohol (Molecular weight 20, 000, degree of hydrolysis 98%) was purchased from the British Drug House (BDH) Chemical Ltd, England. All other chemicals used were of analytical reagent grade. In all investigations, the recommended standard methods and techniques involving both conventional and modern methods were provided.

Preparation of Controlled-Release Fertilizer (CRF) Hydrogel Film

Chitosan solution 1% w/v was prepared by dissolving 1 g of CS in 100 mL of 1% v/v acetic acid to get a clear solution. Clear solution of PVA 20 % w/v in water was put in an autoclave for 20 min at 121 ºC and 0.1 MPa. The fertilizer solution was prepared by dissolving 2.0010 g of ammonium nitrate, 3.3015 g of diammonium phosphate and 2.5275 g of potassium nitrate to make 100 mL aqueous solution. Crosslinking solution was prepared by mixing 50 % methanol, 10 % acetic acid, 1.25 % glutaraldehyde and 10 % sulphuric acid together, making up a 3:2:1:1 weight ratio solution.

The prepared CS solution , PVA solution, glutaraldehyde, fertilizer solution and crosslink solution were mixed with appropriate proportions under constant stirring to obtain a series of CRF hydrogel films. After homogeneous mixing, the gel was formed within 30 min. The CRF hydrogel solutions were kept for sufficient time to remove any bubble formation and were dried on melamine plates at 40 °C in vacuum for overnight.

Determination of Degree of Swelling

The prepared CRF hydrogel film (1 × 1 cm^2) were dipped in 25 mL of water at room temperature. The swelling time was kept as various time intervals. The films were removed from water, blotted gently with tissue paper and weighed. Based on these values, swelling (%) were determined. Each experiment was replicated for three times. The degree of swelling was calculated by the following equation and the results are shown in Table 1 and

Figure 1. DS (%) = $\frac{W_s - W_d}{W_d} \times 100\%$, where W_s and W_d referred to the weight of swollen and dry CRF hydrogels, respectively.

Determination of Water Retention of Soil

A dry sample of CRF hydrogel was buried in dry soil, which was placed in a cup (A). The other dry soil without CRF hydrogel was placed in an identical cup (B) and then each cup was weighed (W). After that, deionized water was added into both cups and reweighed (W_o). The cups were kept under identical conditions at room temperature (Figure 1) and were weighed every day (W_t) over a period of 30 days. Water retention (% WR) of soil was then calculated by the following equation (Cheng and Sun, 2005).

$$WR\ (\%) = \frac{W_t - W}{W_o - W} \times 100\%$$

Figure 1: Experiment for determination of water retention of soil

Determination of Phosphorus Release Behaviors

The release behaviors of phosphorus from the CRF hydrogels, both in deionized water and in soil, were investigated by UV-visible spectrophotometry. A 5.00 mL fertilizer sample solution was pipetted into a 25.00 mL volumetric flask, and then 5.00 mL of molybdovanadate reagent was added. Deionized water was also added to make a 25.00 mL solution. After 30 min, at the room temperature the absorbance of the sample solution was measured at a wavelength of 420 nm by UV spectrophotometer. The amount of phosphorus in the sample solution was calculated using the calibration curve (AOAC,1990).

Cultivation of Chilli and Maize Plants

Cultivation of Chilli and Maize seed samples were conducted in plots of beside fields Chemistry Department, University of Yangon. Five experimental plots (1.5' x 2') were prepared for sowing in 10th November 2016. After 14 days, the germination of plant started. Plant height, number of branches per plant and number of pod per branches were measure and counted in the investigation of agronomical characterization of chilli and maize plant. The selected plant was taken to record height, number of branches and number pod in all investigation.

Results and Discussion

Aspect of Degree of Swelling of CRF Hydrogel Films

The degree of swelling of a series of CRF hydrogel, in form of the water absorbency, films are shown in Table 1 and Figure 2 as a function of immersion time .

As seen in figure the highest degree of swelling of CS-PVA(1:4), CS-PVA(2:3), CS-PVA(3:2) and CS-PVA(4:1) are 877.97, 812.91, 728.64 and 674.23 % respectively. The water absorbency of the hydrogels increases with increasing PVA content. Hydrophilic groups are responsible for such results. This is because PVA is more hydrophilic than CS. Thus, the higher PVA content within the CRF hydrogels caused the higher water absorbency.

It can be seen that all the CRF hydrogels reached maximum amount of swelling in 90 min with in 5 h. The swelling ratio of CS-PVA(1:4) system was found to be higher than other systems.

Table 1: Degree of Swelling of CRF Hydrogels

Time (min)	Degree of Swelling (%) of CRF Hydrogels			
	CS-PVA (1:4)	CS-PVA (2:3)	CS-PVA (3:2)	CS-PVA (4:1)
30	251.47	234.12	197.45	176.29
60	763.80	720.65	630.98	569.29
90	877.97	812.91	728.64	674.23
120	847.94	803.45	709.91	654.47
150	730.75	727.12	692.11	562.19
180	726.43	727.01	672.12	539.98
210	687.11	675.44	614.54	400.19
240	689.25	687.76	524.20	386.13
270	630.32	543.13	510.22	378.98
300	539.99	537.23	493.12	298.87

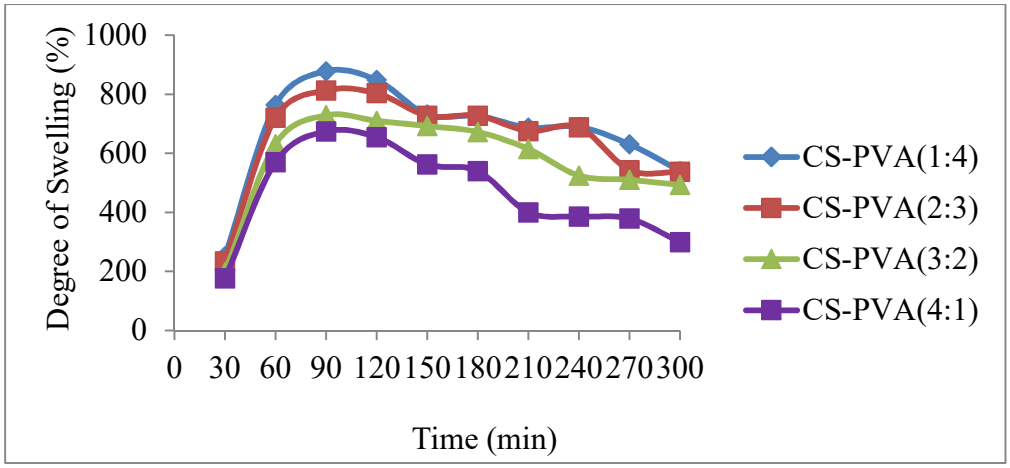

Figure 2: Degree of swelling of CRF hydrogels consisting of different ratios pH1

Aspect of Water Retention Behavior of CRF Hydrogel Films

Table 2 and Figure 3 represent water retention behavior of the soil containing CRF hydrogels. The CS-PVA ratios (1:4, 2:3, 3:2, 4:1) were investigated for water retention of the soil. Table 2 and Figure 2 show that on the 14 days, the soil containing CS-PVA(1:4), CS-PVA (2:3), CS-PVA (3:2) and CS-PVA (4:1) hydrogels have remained water around 15, 12, 10 and 3 % respectively. Therefore the CS-PVA(1:4) ratio of CRF hydrogels affected the highest water retention and CS-PVA(4:1) ratio of CRF hydrogel affected the lowest water retention. That is the water retention of the soil increased with increasing PVA content.

Table 2: Water Retention of Soil Containing CRF Hydrogel Films

Time (Day)	Samples			
	CS-PVA (1:4)	**CS-PVA (2:3)**	**CS-PVA (3:2)**	**CS-PVA (4:1)**
1	89	87	78	68
2	77	74	73	66
3	72	68	61	57
4	60	59	55	52
5	58	52	47	42
6	40	34	31	28
7	36	31	29	23
8	34	27	25	21
9	31	25	23	17
10	29	21	19	16
11	26	17	14	11
12	22	15	13	9
13	19	14	11	5
14	15	12	10	3

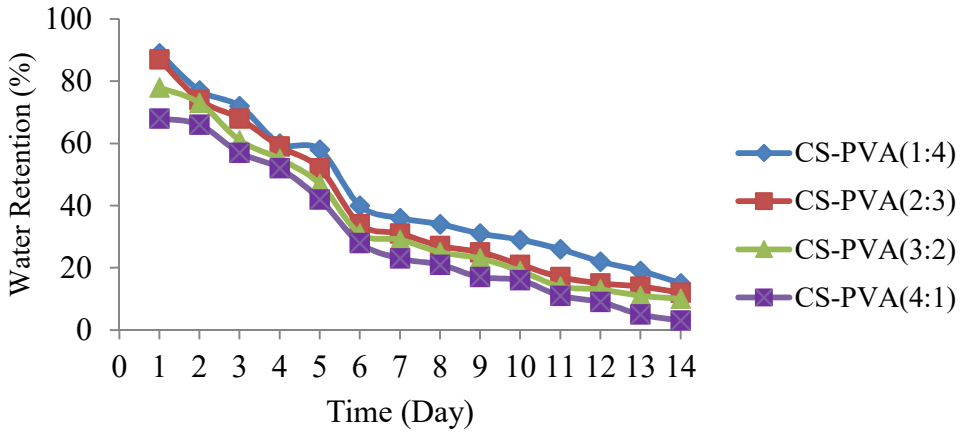

Figure 3: Water retention of soil containing CRF hydrogel films

The Behavior of of CRF Hydrogel Films for Release Phosphorus

The release behaviors of phosphorus of the CRF hydrogels in deionized water at room temperature are shown in Table 3 and Figure 4. It was found that all the CRF hydrogels exhibited initial increased release. The percent cumulative release of phosphorus CS-PVA(1:4), CS-PVA (2:3), CS-PVA (3:2) and CS-PVA (4:1) hydrogels showed of 76, 69, 67 and 63 %, on14th day, respectively. The PVA hydrogels both initial and at equilibrium appeared to show the highest release amount of phosphorus due to its high hydrophilicity. Phosphorus (in the form of diammonium phosphate) in the CRF hydrogels released after the hydrogels absorbed water, leading hydrolysis process taking place.

Table 4 and Figure 5 show the percent phosphorus cumulative release in soil of CRF hydrogels. It was found that the percent cumulative release of phosphorus of CS-PVA(1:4), CS-PVA (2:3), CS-PVA (3:2) and CS-PVA (4:1) hydrogels were 20, 20.8, 22.7 and 25.7 % on the 14th day, respectively. In contrast with phosphorus release behavior in water, the CS-PVA(1:4) hydrogel exhibited the highest percent cumulative release. This is because chitosan is an excellent biodegradable material and is easily degraded by microorganisms and ions existing in soil . Therefore, the existing of different kinds of ions and microorganisms in soil solution, probably increases the degradation rate of the CRF hydrogels.

Table 3: Release Behavior of Phosphorus of CRF Hydrogel Films in Water

Time (Day)	Phosphorus release (%)			
	CS-PVA (1:4)	CS-PVA (2:3)	CS-PVA (3:2)	CS-PVA (4:1)
1	24	21	21	20
2	32	27	26	24
3	34	31	31	26
4	41	39	35	32
5	52	50	47	44
6	62	57	54	51
7	68	63	61	53
8	72	65	64	60
9	75	68	64	61
10	77	72	65	64
11	83	73	71	69
12	81	71	70	69
13	79	69	70	65
14	76	69	67	63

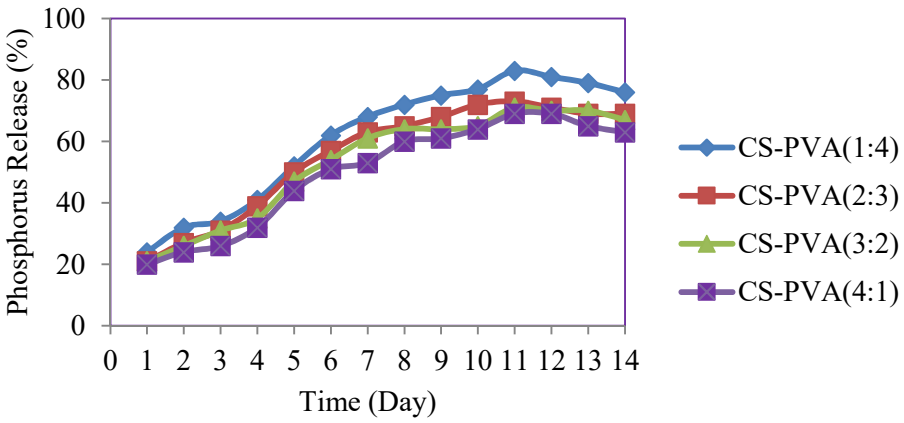

Figure 4: Release behavior of phosphorus of CRF hydrogel films in water

Table 4: Release Behavior of Phosphorus of CRF Hydrogel Films in Soil

Time (Day)	Phosphorus release (%)			
	CS-PVA (1:4)	CS-PVA (2:3)	CS-PVA (3:2)	CS-PVA (4:1)
1	6.0	7.2	7.4	8.5
2	6.5	7.8	8.1	9.4
3	7.2	8.1	8.6	9.7
4	9.5	9.7	10.5	10.6
5	10.2	11.0	11.9	12.6
6	12.4	12.9	13.2	14.2
7	12.9	13.6	14.5	15.3
8	14.0	14.8	15.7	16.7
9	14.9	15.3	16.5	17.2
10	16	16.4	16.9	18.9
11	16.9	16.7	17.3	19.8
12	17.4	17.9	18.4	20.1
13	18.5	19.2	19.9	22.3
14	20.0	20.8	22.7	25.7

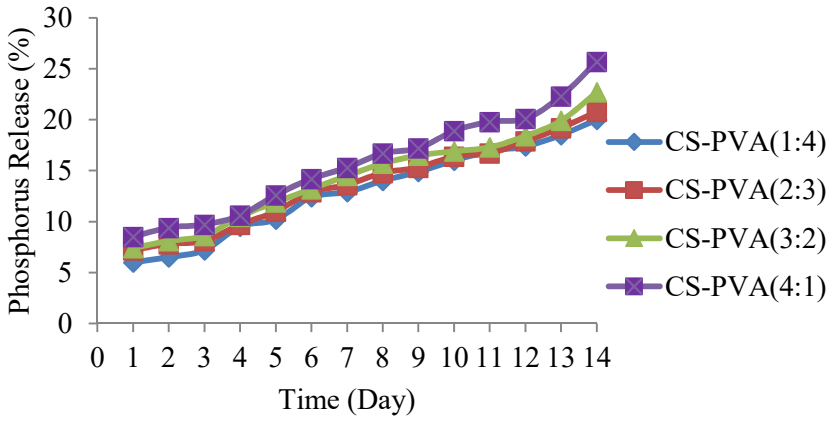

Figure 5: Release behavior of phosphorus of CRF hydrogel films in soil

Application

The growth of plants Chilli using CRF hydrogel were recorded by photos in Figure 6. As seen in Table 5, in all cultivation of the agronomical characteristics of chilli plant, CRF hydrogel showed longer plant height, increasing number of branches and pads when compared with control. According to the data, CS-PVA (3:2) and CS-PVA (4;1)are the more effective than the other hydrogel films. So all CRF hydrogels films have the greater cumulative effect than the control. The growth of plant Maize using CS-PVA (3:2) CRF hydrogel were further investigated by photos in Figure 7. As seen in Figure 7, CS-PVA (3:2) CRF hydrogel showed longer plant height. It can be concluded that all CRF hydrogel films have the greater cumulative effect and these by reducing the environmental pollution.

Control CS-PVA (1:4) CS-PVA (2:3) CS-PVA (3:2) CS-PVA (4:1)

(A) Growing chilli after 1 months

Control CS-PVA (1:4) CS-PVA (2:3) CS-PVA (3:2) CS-PVA (4:1)

(B) Growing chilli after 1.5 months

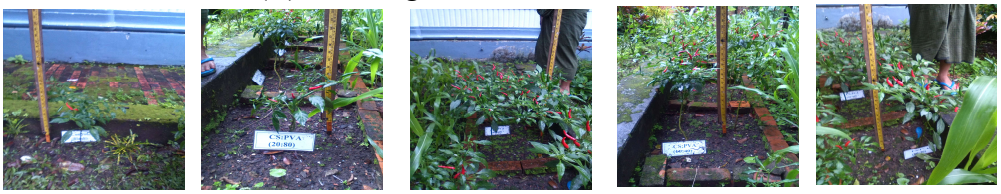

Control CS-PVA (1:4) CS-PVA (2:3) CS-PVA (3:2) CS-PVA (4:1)

(C) Growing chilli after 2 months

Figure 6: Growing plants of Chilli (A) after 1 month (B) after1.5 months (C) after 2

Table 5: Agronomical Characteristic of Chilli Plant

Sample	Plant height (cm)			Number of branches per plant			Number of pad per branch		
	Month			Month			Month		
	1	1.5	2	1	1.5	2	1	1.5	2
control	15.74	19.30	20.32	3	3	3	2	3	4
CS:PVA(1:4)	29.97	33.52	35.81	4	4	4	4	6	7
CS:PVA(2:3)	30.73	34.54	36.83	4	4	4	6	8	11
CS:PVA(3:2)	33.27	34.79	37.08	4	6	6	6	8	13
CS:PVA(4:1)	33.27	35.05	37.59	4	6	6	7	8	13

CS-PVA (2:3)
(A) Growing maize after after 20 days , (15.24 cm) height

CS-PVA (2:3)
(B) Growing maize after 1.5 months , (91.44 cm) height

CS-PVA (2:3)

(C) Growing maize after 2 months, 152.4 cm and above height

Figure 7: Growing plant (A) Maize after 1 month (B) Maize after1.5 months (C)Maize after 2 months

Conclusion

All the synthesized CRF hydrogels exhibited high swelling ratio. With increasing PVA content within the CRF hydrogels, the water absorbency of the hydrogels increases. The soil containing the CRF hydrogels had retained some water, while the soil without CRF hydrogels had already given off most of the water. The amount of the remained water depends on the PVA content in the CRF hydrogel. In deionized water, the release behavior of phosphorus related to PVA content of the CRF hydrogels. The higher the PVA content, the higher the swelling ratio and the more the release amount is. CS hydrogel exhibited the highest the percent cumulative release of phosphorus in soil among the CRF prepared hydrogels. Various agronomical characteristics so measured revealed that CRF hydrogel showed significant changes in terms of retaining water and release of phosphorus when compared with control. So all CRF hydrogels films have the greater cumulative effect than the control. It can be recommended that the synthesis of chitosan based polyvinyl alcohol CRF hydrogel film and its application become a new trend to save fertilizer consumption and to reduce environmental pollution from agriculture.

Acknowledgements

The authors would like to thank the Myanmar Academy of Arts and Science for allowing to present this paper and Professor and Head Dr Daw Hla Ngwe, Department of Chemistry, University of Yangon, for her kind encouragement.

References

AOAC. (1990). Official Methods of Analysis. Washington DC: 15th ed.: Association of Analytical Chemistry

Cheng, M.L. and Sun, Y. M. (2005). "Observation of the Solute Transport in the Permeation through Hydrogel Membranes by using FTIR Microscopy". *Journal of Membrane Science*, vol.253, pp. 191-198

Diwani, G. E., Motawie, N., Shaarawy, H. H. and Shalaby, M. S. (2013). "Nitrogen Slow Release Biodegradable Polymer Based on Oxidized Starch Prepared via Electrogenerated Mixed Oxidants". *J. Appl. Sci. Res.*, vol.9 (3), pp. 1931-1939

Han, X., Chen, S. and Hu, X. (2008) ."Controlled-Release Fertilizer Encapsulated by Starch/Polyvinyl Alcohol Coating". *J. Desalination*, vol. 240, pp.21-26

Jamnongkan, T. and Kaewpirom, S. (2010), "Controlled-Release Fertilizer Based on Chitosan Hydrogel: Phosphrous Release Kinetics", *Sci. J. UBU,* vol. 1, No. 1 , pp. 43-50

Roshanravan, B., Soltani, S. M., Rashid, S. A, Mahdavi ,F. and Yusop, M. K. (2015) . "Enhancement of Nitrogen Release Properties of Urea-Kaolinite Fertilizer with Chitosan Binder". *Chemical Speciation & Bioavailability*, vol.27, 1, pp. 44-51

Salmiaton, A. and Firoozeh. D. (2015) . "Controlled-Release Fertilizers: Advances and Challenges". *Life Science Journal,* vol.12(11), pp. 33-45

SOME METAL CONTENTS IN SEA WATER AND SEDIMENT SAMPLE AROUND CHAUNG THA AREA IN AYEYARWADY REGION, MYANMAR

Jue Jue Khin[1], Aye Aye Lwin[2], Myat Kyaw Thu[3], Kyaw Naing[4]

Abstract

Pollution of heavy metals in aquatic environment is a growing problem worldwide and currently it has reached an alarming rate. There are various sources of heavy metals; most of them originate from anthropogenic activities like draining of sewerage and recreational activities. As heavy metals cannot be degraded, they are continuously being deposited and incorporated in water and sediment, thus causing heavy metal pollution in water bodies. In this research sea water and sediment samples were collected seasonally and annually in (2012-2014). Heavy metal (Cr, Mn, Fe, Cu, Zn, As, Pb, Cd and Hg) contents were determined to identify pollution hot spots in the studied area. Sampling sites were recorded by using GPS detector. The concentrations of metals were determined by atomic absorption spectrometry (AAS) technique and compared with acceptable levels of ASEAN, EPA and CBSQGs standards.

Keywords: sea water, sediment, Chaung Tha, Ayeyarwady Region, ASEAN, EPA standards

Introduction

Marine pollution is a global environmental problem; human activities in the coastal area and marine water contribute to the discharge of various kinds of pollutants such as heavy metals into the marine ecosystems. Heavy metals can be added to an aquatic system either by natural or anthropogenic sources (Kyaw Naing, 2011). Other possible sources of pollution include; domestic effluents, urban storm water runoff, landfill leachate, atmospheric sources and boating activities.

Heavy metals released to aquatic systems are generally bound to particulate matter, which are eventually incorporated into sediments. Thus sediments are an efficient mean of accumulation and downstream transport of

[1]. Dr, Demonstrator, Department of Chemistry, Maubin University
[2]. Dr, Associate Professor, Department of Chemistry, Yenanchaung Degree College
[3]. Dr, Professor, Department of Chemistry, Mandalay University
[4]. Dr, Deputy Director General, Department of Higher Education (Yangon Office)

inorganic contaminants, like heavy metals. It is a proven fact that heavy metals induce toxic effects on living organisms, therefore they can pose a high risk when found in high concentrations in sediments (Censi *et al.,* 2006).

Materials and Methods

The sea water and sediment samples were collected from Chaung Tha area in Ayeyarwady region. The concentrations of metals have been determined by Atomic Absorption Spectrometry (AAS) techniques. The analytical data were tabulated and compared with ASEAN, EPA and CBSQGs Standards.

Study Area

The studied area ChaungTha is the most beautiful beach in Myanmar. It is located on the western coast of Rakhine state near Pathein where the waves of the Bay of Bengal (BOB) and the Indian ocean lap the shores. It is situated between North latitude 160º 179' North and South latitude940º 072' East (Wikipedia, 2013).

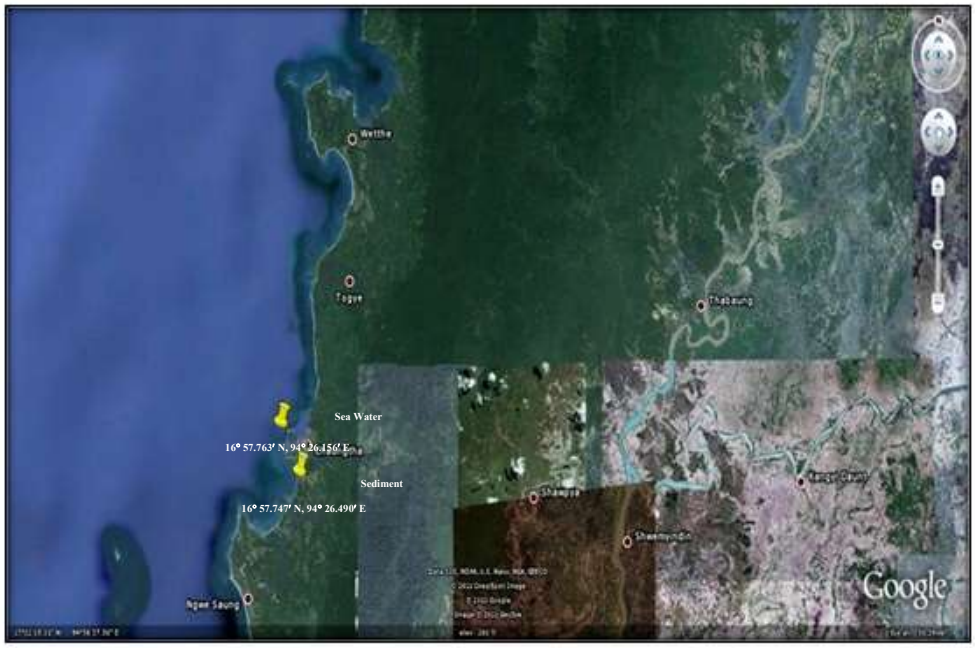

Figure 1: Satellite image of ChaungTha in Ayeyarwady Region Sampling Site for Sea Water - 16° 57.463' N, 94° 26.150' E Sampling Site for Sediment - 16° 57.747' N, 94° 26.490' E

Sample Collection

Sea water samples were taken 1 mile away from the Sea Shore and 2m depth from the surface water level. The water samples were collected by means of a water sampler. Sediment samples were collected about 5 to 10 cm thickness of the surface sediment with a stainless steel grab sampler during low tide.

Results and Discussion

Seasonal Variation of some Metals (Cr, Cu, Mn, Fe, Zn, Pb, Cd, Hg and As) Contents in Sea Water and Sediment Samples Chromium (Cr) content in sea water and sediment samples

In the present study, the chromium (Cr) content in sea water samples were found to be in the annual range of 0.010 - 0.020 ppm in 2012, 0.003 - 0.050 ppm in 2013 and 0.006 - 0.050 ppm in 2014, respectively. Of these three seasons, the highest Chromium (Cr) content(0.050 ppm)was found in cold season due to the decreasing rate of organic matter decomposition and low water temperature. The lowest value 0.003 ppm was found in rainy season. According to the data, all measured values were within the range of ASEAN standard0.05 ppm (Table 1 and Figure 2).

The concentration of chromium (Cr) in sediment samples were found to be in the annual range of 0.00-0.12 mg/kg in 2012, 0.22 - 0.23 mg/kg in 2013 and 0.24 - 0.26 mg/kg in 2014, respectively. The highest value 0.26 mg/kg was found in cold season and the lowest value 0.12 mg/kg was found in rainy season. Observed values were within the CBSQGs (TEC) (2010) value 43 mg/kg for aquatic life protection (Table 1 and Figure 3).

Copper (Cu) content in sea water and sediment samples

The concentration of copper (Cu) in sea water samples were found to be in the annual range of 0.003 - 0.036 ppm in 2012, 0.004 - 0.060 ppm in 2013 and 0.003 - 0.013 ppm in 2014. Of these three seasons, the highest value of 0.036 ppm was found in hot season and the lowest value of 0.003 ppm was found in rainy season. The resultants values exceeded the permissible level of ASEAN standard 0.008 ppm because of the sewage and industrial waste are

the major sources of copper contamination in aquatic environment (Table 2 and Figure 4).

The concentration of copper (Cu) in sediment samples were found in the annual range of 3.18- 3.85 mg/kg in 2012, 4.25- 4.85 mg/kg in 2013 and 6.20- 6.40 mg/kg in 2014, respectively. The highest copper (Cu) value of 6.40 mg/kg was found in hot season and the lowest value of 3.18 mg/kg was found in rainy season. Observed values were within the CBSQGs (TEC) (2010) value of 32 mg/kg for aquatic life protection (Table 2 and Figure 5).

Manganese (Mn) content in sea water and sediment samples

Manganese (Mn) is the naturally occurring metal usually present in many types of rocks. In sea water Mn tends to form particles in the water or settle into the sediment. The manganese (Mn) content in sea water samples were observed in the annual range of 0.003-0.012 ppm in 2012, 0.008-0.026 ppm in 2013 and 0.010- 0.026 ppm in 2014, respectively. The highest value of0.026 ppm was observed in cold season. These values exceeded the EPA standard 0.05 ppm because of the environmental pollution by the waste products of visiting people and villagers (such as, batteries, materials made by iron). The lowest value of 0.003ppm was observed in hot season (Table 3 and Figure 6).

The concentration of manganese (Mn) in sediment samples were in the annual range of 150.5- 152.2 mg/kg in 2012, 156.3-160.2 mg/kg in 2013 and 160.4 - 164.3 mg/kg in 2014, respectively. The highest content of 164.3 mg/kg was observed in cold season and the lowest value of150.5 mg/kg was found in hot season. The resultant data were within the CBSQGs (TEC) (2010) value 460 mg/kg for aquatic life protection (Table 3 and Figure 7).

Iron (Fe) content in sea water and sediment samples

The iron (Fe) concentration in water may be present in varying quantities depending upon the geological area and other chemical component of the water way (Chapman.,1996). The iron (Fe) contents was found to be in the annual range of 0.140-0.143 ppm in 2012, 0.160-0.190 ppm in 2013 and 0.169- 0.210 ppm in 2014, respectively. Fe content is not of concern (NC) in the ASEAN Standard. The highest iron (Fe) content of 0.210 ppm was found

in hot season due to the geological nature of the sewage and some industrial waste and the lowest value0.140 ppm was found in rainy season (Table 4 and Figure 8).

The iron (Fe) content in sediment samples were found to be in the annual range of 1200- 1260 mg/kg in 2012, 1300-1500 mg/kg in 2013 and 1400-1700 mg/kg in 2014, respectively. The maximum value1700 mg/kg was found in hot season and the minimum value 1200 mg/kg was found in rainy season. These values were lower than the CBSQGs (TEC) (2010) value of 20000 mg/kg for aquatic life protection (Table 4 and Figure 9).

Zinc (Zn) content in sea water and sediment samples

The zinc (Zn) concentration in sea water samples were observed in the annual range of 0.060 - 0.130 ppm in 2012, 0.079 - 0.139 ppm in 2013 and 0.088 - 0.130 ppm in 2014, respectively. The maximum Zn value 0.139 ppm was observed in hot season due to the evaporation of water and temperature effect. The minimum Zn value 0.060 ppm was observed in rainy season(Table 5 and Figure 10). Zn value is not of concern (NC) in the ASEAN standard.

The concentration of Zinc (Zn) in sediment samples may be present in the annual range of 50.70- 57.55 mg/kg in 2012, 56.50–58.70 mg/kg in 2013 and 60.20 - 60.80 mg/kg in 2014, respectively. The maximum content of (Zn)60.80 mg/kgwas observed in hot season and the minimum value of (Zn)50.70mg/kg was found in rainy season. The resultant data were within the CBSQGs (TEC) (2010) value of 120 mg/kg for aquatic life protection (Table 5 and Figure 11).

Lead (Pb) content in sea water and sediment samples

The Lead (Pb) concentration in sea water samples were observed in the annual range of 0.001 - 0.003 ppm in 2012, 0.002 - 0.007 ppm in 2013 and 0.003 - 0.008 ppm in 2014, respectively. The highest Pb value 0.008 ppm was observed in hot season. The lowest Pb value 0.001 ppm was observed in cold season (Table 6 and Figure 12). These values were lower than the ASEAN standard 0.009 ppm.

The concentration of Lead (Pb) in sediment samples were in the annual range of 0.016 – 0.019 mg/kg in 2012, 0.024 – 0.028 mg/kg in 2013 and 0.024 – 0.045 mg/kg in 2014, respectively. The highest content 0.045 mg/ kg was observed in hot season and the lowest value of 0.016 mg/kg was found in cold season. Both of sea water and sediment samples the highest values were found in hot season. It would be attributed to the industrial and agricultural discharge as well as from spill of lead petrol from fishing boats and dust (Table 6 and Figure 13).

Cadmium (Cd) content in sea water and sediment samples

Cadmium (Cd) is certainly a dangerous water pollutant, causing a major water quality problem. Source of cadmium is industrial discharge, mining waste, metal plating and water pipes (Strickland and Parsons, 1972). The concentration of cadmium (Cd) in sea water samples were found to be in the annual range of 0.003-0.004 ppm in 2012, 0.004- 0.007 ppm in 2013 and 0.006 - 0.008 ppm in 2014, respectively. Of these three season, the highest value 0.008 ppm was found in cold season due to the decreasing rate of organic matter decomposition and low water temperature. The lowest value of0.003 ppm was found in rainy season (Table 7 and Figure 14). These values were lower than the ASEAN standard of 0.010 ppm.

The concentration of cadmium (Cd) in sediment samples were found to be in the annual range of 0.011-0.021 mg/kg in 2012, 0.020-0.024 mg/kg in 2013 and 0.012-0.031 mg/kg in 2014, respectively. The highest cadmium (Cd) value 0.031 mg/kg was found in cold season and the lowest value 0.011mg/kg was found in rainy season. The high level of cadmium contamination may be due to the soil composition and environmental pollution in the study area (Table 7 and Figure 15).

Mercury (Hg) and Arsenic (As) contents in sea water and sediment samples

The mercury and arsenic contents were not detected in sea water and sediment sample (Tables 8 and 9).

Table 1. Seasonal Variation of Chromium (Cr) Content in Sea Water and Sediment Samples

Year	Season	Sea Water	Sediment
		Cr (ppm)	Cr (mg/kg)
2012	Hot	ND	ND
	Rainy	0.010	0.12
	Cold	0.020	ND
2013	Hot	0.020	ND
	Rainy	0.003	0.22
	Cold	0.050	0.23
2014	Hot	0.040	ND
	Rainy	0.006	0.24
	Cold	0.050	0.26
ASEAN (2010)		0.05	-
EPA (2010)		-	-
CBSQGs (TEC) (2010)		-	43

- ASEAN Standard for human health protection (2010) (for recreational activities)
- EPA standard for aquatic life protection (2010)
- CBSQGs, Consensus Based Sediment Quality Guide lines (2010)
- TEC- Threshold Effect Concentration
- ND- Not Detected

Table 2. Seasonal Variation of Copper (Cu) Content in Sea Water and Sediment Samples

Year	Season	Sea Water	Sediment
		Cu (ppm)	Cu (mg/kg)
2012	Hot	0.036	3.85
	Rainy	ND	3.18
	Cold	0.003	3.45
2013	Hot	0.060	4.85
	Rainy	0.004	4.60
	Cold	0.009	4.25
2014	Hot	0.013	6.40
	Rainy	0.003	6.30
	Cold	0.008	6.20
ASEAN (2010)		0.008	-
EPA (2010)		-	-
CBSQGs (TEC) (2010)		-	32

ND = Not Detected

Table 3. Seasonal Variation of Manganese (Mn) content in Sea Water and Sediment Samples

Year	Season	Sea Water	Sediment
		Mn (ppm)	Mn mg/kg)
2012	Hot	ND	152.2
	Rainy	0.003	150.5
	Cold	0.012	151.5
2013	Hot	ND	156.3
	Rainy	0.008	158.4
	Cold	0.026	160.2
2014	Hot	ND	160.4
	Rainy	0.010	162.5
	Cold	0.026	164.3
ASEAN (2010)		NC	-
EPA (2010)		0.05	-
CBSQGs (TEC) (2010)		-	460

NC = Not of Concern

ND = Not Detected

Table 4: Seasonal Variation of Iron (Fe) content in Sea Water and Sediment Samples

Year	Season	Sea Water	Sediment
		Fe (ppm)	Fe (mg/kg)
2012	Hot	0.140	1260
	Rainy	0.142	1200
	Cold	0.143	1250
2013	Hot	0.190	1500
	Rainy	0.160	1400
	Cold	0.160	1300
2014	Hot	0.210	1700
	Rainy	0.169	1600
	Cold	0.172	1400
ASEAN (2010)		NC	-
EPA (2010)		-	-
CBSQGs (TEC) (2010)		-	20000

NC = Not of Concern

Table 5: Seasonal Variation of Zinc (Zn) Content in Sea Water and Sediment Samples

Year	Season	Sea Water	Sediment
		Zn (ppm)	Zn (mg/kg)
2012	Hot	0.130	57.55
	Rainy	0.060	50.70
	Cold	0.101	55.60
2013	Hot	0.139	58.70
	Rainy	0.079	57.60
	Cold	0.110	56.50
2014	Hot	0.120	60.80
	Rainy	0.088	60.40
	Cold	0.130	60.20
ASEAN (2010)		NC	-
EPA (2010)		-	-
CBSQGs (TEC) (2010)		-	120

NC = Not of Concern

Table 6: Seasonal Variation of Lead (Pb) Content in Sea Water and Sediment Samples

Year	Season	Sea Water	Sediment
		Pb (ppm)	Pb (mg/kg)
2012	Hot	0.003	0.018
	Rainy	0.001	0.019
	Cold	0.001	0.016
2013	Hot	0.007	0.028
	Rainy	0.002	0.024
	Cold	0.004	0.027
2014	Hot	0.008	0.045
	Rainy	0.003	0.024
	Cold	0.006	0.025
ASEAN (2010)		0.009	-
EPA (2010)		-	-
CBSQGs (TEC) (2010)		-	-

Table7: Seasonal Variation of Cadmium (Cd) content in Sea Water and Sediment Samples

Year	Season	Sea Water	Sediment
		Cd (ppm)	Cd (mg/kg)
2012	Hot	ND	ND
	Rainy	0.003	0.011
	Cold	0.004	0.021
2013	Hot	ND	0.020
	Rainy	0.007	0.024
	Cold	0.004	0.021
2014	Hot	ND	0.012
	Rainy	0.006	0.025
	Cold	0.008	0.031
ASEAN (2010)		0.010	-
EPA (2010)		-	-
CBSQGs (TEC) (2010)		-	-

ND = Not Detected

Table 8: Seasonal Variation of Arsenic (As) Content in Sea Water and Sediment Samples

Year	Season	Sea Water	Sediment
		As (ppm)	As (mg/kg)
2012	Hot	ND	ND
	Rainy	ND	ND
	Cold	ND	ND
2013	Hot	ND	ND
	Rainy	ND	ND
	Cold	ND	ND
2014	Hot	ND	ND
	Rainy	ND	ND
	Cold	ND	ND
ASEAN (2010)		0.036	-
EPA (2010)		-	-
CBSQGs (TEC) (2010)		-	-

ND = Not Detected

Table 9: Seasonal Variation of Mercury (Hg) Content in Sea Water and Sediment Samples

Year	Season	Sea Water	Sediment
		Hg (ppm)	Hg (mg/kg)
2012	Hot	ND	ND
	Rainy	ND	ND
	Cold	ND	ND
2013	Hot	ND	ND
	Rainy	ND	ND
	Cold	ND	ND
2014	Hot	ND	ND
	Rainy	ND	ND
	Cold	ND	ND
ASEAN (2010)		0.16	-
EPA (2010)		-	-
CBSQGs (TEC) (2010)		-	-

ND = Not Detected

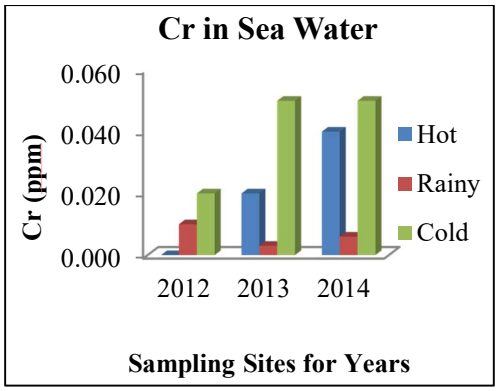

Figure 2: Histogram of Cr in sea water samples Vs study period

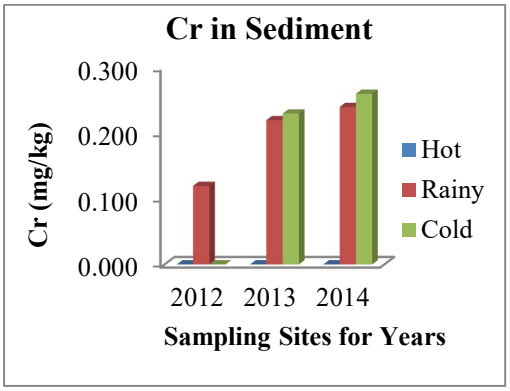

Figure 3: Histogram of Cr in sediment samples Vs study period

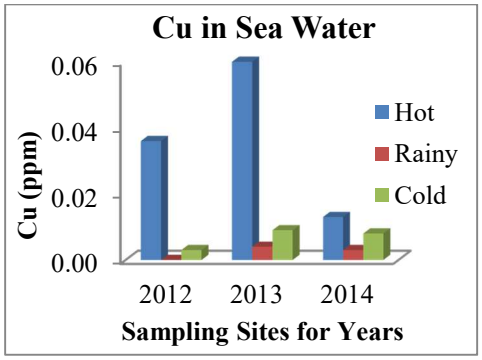

Figure 4: Histogram of Cu in sea water samples Vs study period

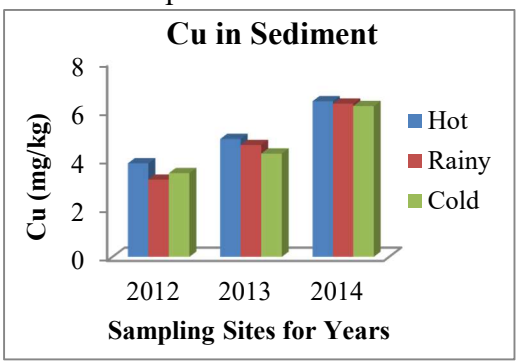

Figure 5: Histogram of Cu in sediment samples Vs study period

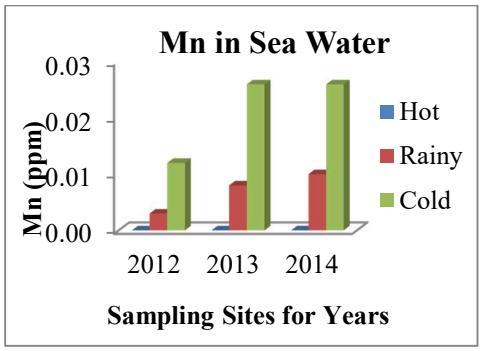

Figure 6: Histogram of Mn in sea water samples Vs study period

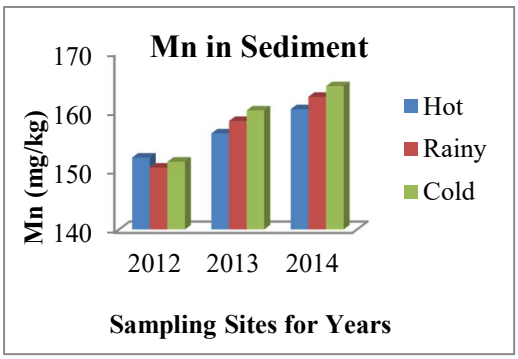

Figure 7: Histogram of Mn in sediment samples Vs study period

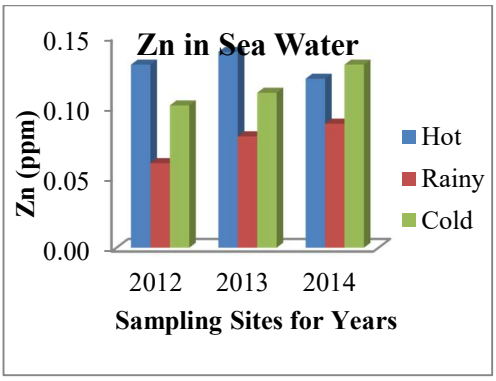

Figure 8: Histogram of Zn in sea water samples Vs study period

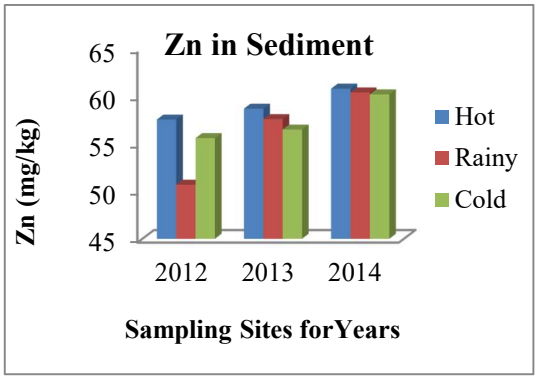

Figure 9: Histogram of Zn in sediment samples Vs study period

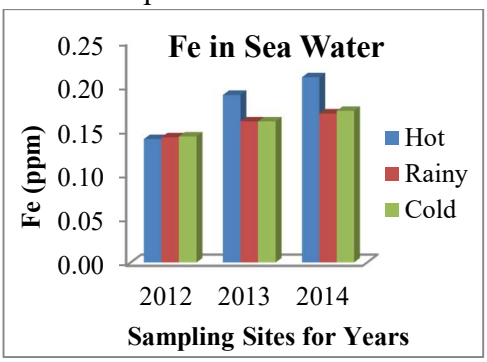

Figure 10: Histogram of Cu in sea water samples Vs study period

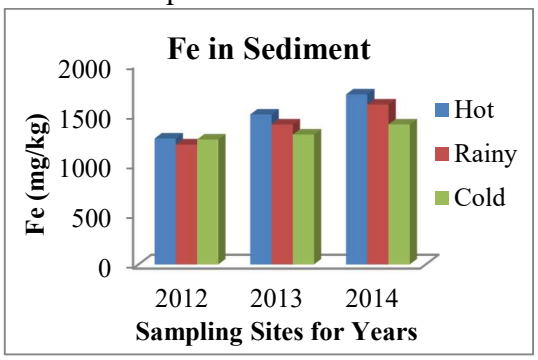

Figure 11: Histogram of Cu in sediment samples Vs study period

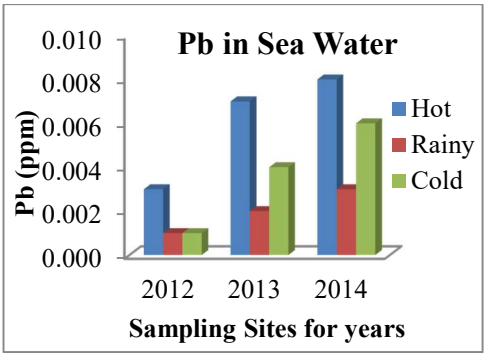

Figure 12: Histogram of Pb in sea water samples Vs study period

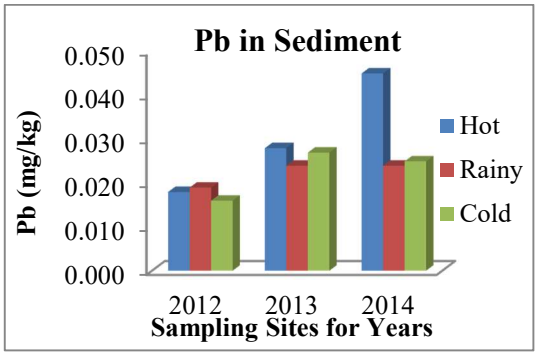

Figure 13: Histogram of Pb in sediment samples Vs study period

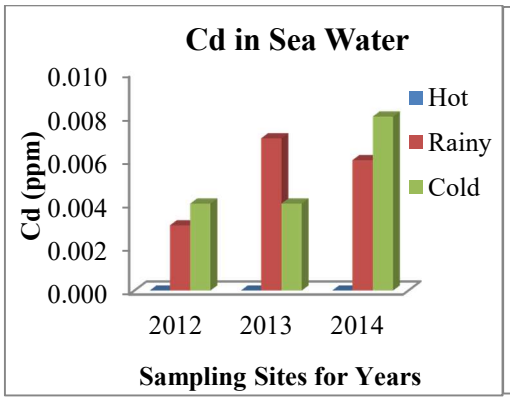

Figure 14: Histogram of Cd in sea water samples Vs study period

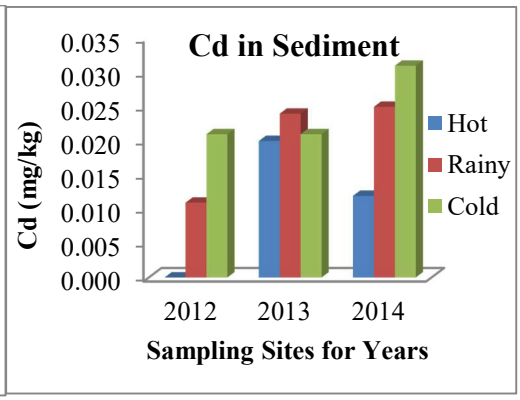

Figure 15: Histogram of Cd in sediment samples Vs study period

Conclusion

By evaluating the heavy metals accumulation content in sea water and sediments, it can be concluded that heavy metals are highly accumulated in sediments than sea water. Some metal (Cr, Mn, Fe, Zn, Pb and Cd) contents in sea water samples (except Cu) were found within the permissible level of ASEAN and EPA standards. In sediment samples (Cr, Cu, Mn, Zn, Fe, Pb and Cd) values were lower than the Consensus Based Sediment Quality Guide lines (TEC) standards for aquatic life protection showing not toxic on aquatic life especially benthic-dwelling organisms. The mercury and arsenic values were not detected during the study period in sea water and sediment sample. Thus the studied region in the period from 2012-2014, is free of heavy metals pollution and the marine ecosy ohm is still Sofe to for aquatic life and fisheries.

Acknowledgements

The authors would like to express their profound gratitude to the Department of Higher Education (Yangon Office), Ministry of Education, Yangon, Myanmar, for provision of opportunity to do this research and Myanmar Academy of Arts and Science for allowing to present this paper.

References

ASEAN Marine Environmental Management.(2010). *Water Quality Criteria and Standards for Freshwater and Marine Aquaculture*. North Vancouver: EVS Environmental Consultants Ltd., 171-189

Censi, P., Spoto, S.E., Saiano, F., Sprovieri, M. and Mazzola, S. (2006). "Heavy Metals in Coastal Water System, A Case Study from the North Western Gulf of Thailand". *Chemosphere,*vol.64, pp.1167-1176

Chapman, D. (1996). *A Guide to the Use of Biota Sediments and Water in Environmental Monitoring in Water Quality Assessment*. London : 2nd Edn. , E & FNSPON, pp.8-91

Consensus-Based Sediment Quality Guidelines (CBSQGs). (2010). *Contaminated Sediment Standing team Recommendations for Use & Application.* Washington DC: Equal Opportunity Office, Department of Interior, pp.1-17

EPA.(2010). *Nutrient Water Quality Standards.* Washington, DC: Office of Water Research

Kyaw Naing. (2011). *National Report of Myanmar on the Coastal Pollution Loading and Water Quality Criteria (Land-based Sources of Marine Pollution).*Rome: Bay of Bengal Large Marine Ecosystem Project to the Food and Agriculture Organization of the United Nations, FAO, 1-53

Strickland, J. D. H. and Parsons, T. R. (1972). *A Practical Handbook of Sea Water Analysis*. Fisheries Research Board of Canada, 21-29

Wikipedia, the Free Encyclopedia. (2013). *Chaung Tha Beach.* http://en.wikipedia.org/wiki/ Chaung Tha. html (Accessed 30 May 2011)

ASSESSMENT ON THE WATER QUALITY AT THE MOUTH OF PATHEIN RIVER, AYEYARWADY REGION, MYANMAR

Poh Poh Win[1], Khin Mar Cho[2], Myat Myat Thaw[3], Kyaw Naing[4]

Abstract

The aim of this paper is to assess the water quality of Patheinriver around the river mouth and to evaluate the pollution loading and water quality criteria of Pathein river. In this paper, a total of 9 river water samples were collected near Payala Village in hot, rainy and cold seasons of the year 2014. Sampling sites were recorded with GPS detector. Some physicochemical properties (pH, DO, TSS, turbidity, chlorinity, salinity, total alkalinity, total hardness, BOD and COD)and nutrient levels (orthophosphate, organic phosphate, total phosphate, total nitrogen and chlorophyll *a*) were determined. Trace metals (As, Cd, Pb, Hg, Fe, Zn, Cr, Mn and Cu) concentrations of the river water samples were determined. (Based on DO (7.16-7.39 ppm),orthophosphate (0.15-0.24ppm) and total nitrogen(1.12-1.56 ppm) values, the river water near Payala village could be identified as low and medium nutrient enrichment, i.e., oligotrophic in hot season and mesotrophic in rainy and cold seasons.)

Keywords: Pathein river, water quality, orthophosphate, DO, total alkalinity, chlorophyll *a*

Introduction

Water is the most vital resource for all kinds of life on this planet. Water is one of the nature's most important gifts to mankind. It is essential and most precious commodity for life. Rivers are vital and vulnerable freshwater systems, and are essential for the sustenance of all life. Rivers supply valuable drinking water to humans, irrigation water to farmlands and provide habitat to many aquatic plants and living organisms. The study of rivers is important sources of natural water apart from serving as a source of drinking water, irrigation and fishing; they are generally of immense importance in geology, biology, history and culture (Anhwange *et al.,* 2012). Rivers can be classified according to the type of flow regime and magnitude of discharge (Chapman, 1996). Myanmar's main rivers run from north to

1. Dr, Demonstrator, Department of Chemistry, Maubin University
2. Dr, Associate Professor, Department of Chemistry, Pyay University
3. Dr, Professor, Department of Chemistry, University of Yangon
4. Dr, Deputy Director General, Department of Higher Education (Yangon Office)

south. About three-fifths of Myanmar's surface is drained by the Ayeyarwady and its tributaries. Flowing entirely through Myanmar, it is navigable for nearly 1, 000 miles (1, 600 km). At the apex of its delta, the Ayeyarwady breaks up into a vast network of streams and empties into the Andaman Sea through multiple mouths. The Ayeyarwady river is one vital artery waterway of Myanmar (Kyaw Naing, 2011).The Ayeyarwady Delta comprises the main arms of Pathein River. The purpose of the study was to investigate the water quality of Pathein river around the river mouth and to evaluate the pollution loading and water quality criteria of Pathein river and to find out seasonal and spatial variation and development of the region the important river flowing water chemistry.

Materials and Methods

In this research, totally 9 river water samples were collected in the year 2014 from Pathein river mouth, vicinity of Payala Village. Figure 1 shows the sampling sites of river water samplesby the GPS detector. All samples are surface river water (2 m depth). Some physicochemical properties (pH, DO, TSS, turbidity, chlorinity, salinity, total alkalinity, total hardness, BOD and COD) and nutrient levels (orthophosphate, organic phosphate, total phosphate, total nitrogen and chlorophyll *a*) were determined. The pH of river water samples were measured in the field by using digital pH meter. The temperature and dissolved oxygen of river water samples was measured in the field by using a DO meter-Temperature sensor probe HANNA Instrument. Chlorinity of the river water samples were determined by titrimetric method. Total alkalinity concentrations of river water samples were determined by titrimetric analysis. Biological oxygen demand of river water samples were determined by incubation method. Chemical oxygen demand of river water samples were determined by permanganate titrimetric analysis. Orthophosphate, organic phosphate and total phosphate were determined by UV-visible spectrophotometric method. Total nitrogenof river water samples were determined by Azo Dye method. Chlorophyll *a* contents of river water samples were measured by UV-Visible spectrophotometer. Trace metals (As, Cd, Pb, Hg, Fe, Zn, Cr, Mn and Cu) concentrations of the river water samples were measured by atomic absorption spectrophotometer (AAS).

Figure 1: Collection areas of river water samples (Site A 94° 27.239′ E, 16° 6.927′ N,Site B 94° 27.187′ E, 16° 6.842′ N , Site C 94° 27.205′ E, 16° 6.702′ N)

Results and Discussion

In this study, some physicochemical properties, nutrient levels and sometrace metals concentrations of the river water samples from Pathein River Mouth, vicinity of Payala village area were determined.

Physicochemical Properties of River Water Samples

pH in river samples

The pH of a water body is very important in determination of water quality since it affects other chemical reactions such as solubility and metal toxicity. In this present work, the pH values of the river water samples were recorded 7.78-7.87 in hot season, 7.71-7.73 in rainy season and 7.75-7.80 in cold season (Table 1).

The maximum value of pH 7.87 was observed in hot season for sampling site (A). The maximum value of pH observed in hot season might be due to biological activity and photosynthetic activities. The pH values are within the permissible level of 6.5-8.5 EPA standard (2009). Most fish can be

observed pH values of about 5-9. So, the observed pH value is suitable for fish and other aquatic life.

Temperature in river water samples

Temperature is a thermodynamic property of a fluid, and is due to the activity of molecules and atoms in the fluid. From the viewpoint of seasonal sample collection, the temperature values of river water were observed in the range of 32.2-32.8°C in hot season, 31.5-32.1°C in rainy season and 31.8-32.5°C in cold season (Table 1).The highest value of temperature 32.8 °C was observed in hot season for sampling site (B). The variation in the water temperature may be due to different timings of collection, influence of season and solar radiation.

Total suspended solids in river water samples

Total suspended solids are particles of sand, silt, clay and organic material moving with the water. In this study, the values of total suspended solids (TSS) in river water samples ranged from 45.42-60.72 ppm in hot season, 58.12-65.41 ppm in rainy season and 47.14-62.48 ppm in cold season (Table 1). The highest value of total suspended solids was observed as 65.41 ppm in rainy season for sampling site (B). The highest value of total suspended solids was recorded during rainy season, which indicates the river run off, industrial effluents and municipal sewage.

Turbidity in river water sample

Turbidity is a measure of the amount of particulate matter and dissolved color that is suspended in water. In this present work, the values of turbidity in river water were observed in the range of 42.53-58.25 FTU (hot), 55.43-69.12 FTU (rainy) 35.35-54.53 FTU (cold) for seasonal sample collection (Table 1). From the studied area results, the highest amount of turbidity was found in rainy season. In this case, a higher turbidity may be because of the soil erosion, river flow, presence of sources of organic pollution and run off factors. According to the results obtained, the values of turbidity were under the permissible level of EPA standard (< 700 FTU).

Chlorinity in river water samples

Chlorinity is one of the important indicators of pollution. Chlorinity are present in sewage, effluents and farm drainage. It is responsible for the brackish taste in water and is an indicator of sewage pollution because of the chlorinity content in urine. Seasonally, the values of chlorinity in river water samples ranged from 2.51-2.56 ppt in hot season, 2.37-2.41ppt in rainy season and 2.42-2.47 ppt in cold season (Table 1).The highest value of chlorinity was found 2.56 ppt in hot season for sampling site A. All chlorinity values were within the permissible level of 250 ppm EPA standard (2009).

Salinity in river water samples

Salinity is a measure of the amount of dissolved salts in the water. In this present work, the salinity values of the river water samples were found 4.53-4.62 ppt in hot season, 4.28-4.35ppt in rainy season and 4.37-4.46 ppt in cold (Table 1). The maximum content of salinity 4.62 ppt was recorded in hot season for sampling site (A). The seasonal variation salinity lowers in rainy season, due to the river run off in this period and high dilution in the estuary.

Total alkalinity in river water samples

Alkalinity is a total measure of the substances in water that have acid neutralizing ability. In this present work, the alkalinity of river water samples in the studied area were in the range of 100-150 ppm in hot season, 70-130 ppm in rainy season and 90-130 ppm in cold season (Table 1). The highest content of total alkalinity 150 ppm was found in the hot season for sampling site (B).The total alkalinity of all river water samples in the studied area were found to be within the permissible level of 30-150 ppm EPA standard (2009).

Total hardness in river water samples

Total hardness is the sum of calcium and magnesium concentration. It is used to measure the capacity of water to precipitate soap. In this research work, the values of total hardness in river water samples were found to

be4965-5213 ppm in hot season, 4981-5192 ppm in rainy season and 4772-4943 ppm in cold season (Table 1). The highest value of total hardness was 5213 ppm in hot season for sampling site (B). Higher value was observed in hot season may be due to increase of salt in water.

Dissolved oxygen (DO) in river water samples

Dissolved oxygen is an important limnological parameter indicating level of water quality and organic pollution in the water body. The dissolved oxygen (DO) values of river water samples were observed in the range of 7.16-7.28 ppm in hot season, 7.26-7.39 ppm in rainy season and 7.17-7.35 ppm in cold season (Table 1). Seasonally, the highest values of DO were found in rainy season and lowest values in hot season and intermediate values were recorded in cold season. The highest value of dissolved oxygen 7.39 ppm was observed in rainy season for sampling site (C). The maximum values of DO in rainy season might be due to the fact that the solubility of DO increases with the decrease in water temperature.

Biochemical oxygen demand in river water samples

Biochemical oxygen demand is a measure of the use dissolved oxygen by life forms, particularly during decomposition. BOD is the amount of oxygen required by bacteria to stabilize organic matter under aerobic conditions. The values of BOD were observed in the range of 2.43-2.76 ppm in hot season, 2.01-2.38 ppm in rainy season and 2.08-2.41 ppm in cold season (Table 1). The highest value of BOD was found to be 2.76 ppm in hot season for sampling site (A). The maximum value of BOD in hot season might be due to biological as well as natural oxidation process with increase in temperature. All BOD values of river water samples were below the permissible level of 5 ppm EPA standard (2009).

Chemical oxygen demand in river water samples

Chemical oxygen demand is defined as the amount of oxygen needed to oxidize the dissolved and particulate matter in water, is a practical indicator of the concentration of organic matter and of water quality (Kawabe and Kawabe, 1997). Seasonally, the concentrations of COD were observed in the

range of 9.18-11.21 ppm in hot season, 6.48-9.29 ppm in rainy season and 7.28-10.23 ppm in cold season, respectively (Table 1). The highest value of COD was observed 11.21 ppm in hot season for sampling site (A). COD high level indicates presence of all forms of organic matter, both biodegradable and non biodegradable and hence the degree of pollution in water. All COD values of river water samples were above the maximum permissible level of 10ppm EPA standard (2009).

Table 1: Some Physicochemical Properties of River Water Samples from Three Sampling Sites (2014)

Parameters	Sampling Sites	Season			Standard	
		Hot	Rainy	Cold	EPA (2009)	ASEAN (2010)
pH	A	7.87	7.73	7.79	6.5-8.5	6.0-8.0
	B	7.78	7.71	7.75		
	C	7.85	7.72	7.80		
Temperature	A	32.2	31.5	31.9	NC	-
	B	32.8	32.1	32.5		
	C	32.5	31.7	31.8		
Total suspended Solids (ppm)(Mean±SD)	A	45.42±0.38	62.23±0.61	61.51±0.61	NC	NC
	B	57.34±0.46	65.41±0.54	62.48±0.55		
	C	60.72±0.38	58.12±0.44	47.14±0.47		
Turbidity (FTU) (Mean±SD)	A	42.53	63.13	41.56	<700	15
	B	49.78	69.12	54.53		
	C	58.25	55.43	35.35		
Chlorinity (ppt) (Mean±SD)	A	2.56±0.06	2.38±0.03	2.42±0.03	250	<19
	B	2.51±0.04	2.37±0.02	2.47±0.08		
	C	2.55±0.05	2.41±0.04	2.44±0.09		
Salinity (ppt) (Mean±SD)	A	4.62±0.09	4.29±0.12	4.37±0.08	NC	NC
	B	4.53±0.13	4.28±0.11	4.46±0.11		
	C	4.60±0.17	4.35±0.09	4.40±0.12		
Total alkalinity (ppm) (Mean±SD)	A	100±4	70±1	90±2	30-150	120
	B	150±3	130±3	130±3		
	C	110±2	100±2	120±2		
Total hardness (ppm) (Mean±SD)	A	4965±72	4981±61	4772±64	NC	NC
	B	5213±65	5192±63	4931±73		
	C	5189±70	5123±59	4943±63		
Dissolved oxygen (ppm)	A	7.16	7.26	7.17	>4	>5
	B	7.28	7.38	7.35		
	C	7.22	7.39	7.31		
Biochemical oxygen demand(ppm)	A	2.76	2.38	2.41	5	>15
	B	2.61	2.28	2.08		
	C	2.43	2.01	2.35		
Chemical oxygen demand (ppm)(Mean±SD)	A	11.21±0.23	9.29±0.22	7.28±0.19	10	40
	B	11.13±0.21	6.48±0.25	10.23±0.21		
	C	9.18±0.19	8.31±0.27	9.24±0.18		

*EPA standards(2009) NC=Not of Concern

*ASEAN standards for aquatic life protection (2010)

Nutrient Levels of River Water Samples

Orthophosphate, organic phosphate, total phosphate, and chlorophyll *a* in river water samples

Phosphate is one of the most important nutrients responsible for eutrophication of rivers which increases algae growth and ultimately reduces dissolved oxygen level in the water (Anhwange, 2012). In seasonal sampling, the orthophosphate values were found to be 0.18-0.24 ppm in rainy season and 0.15-0.19 ppm in cold season (Table 2).The values of orthophosphate were not detected in hot season. The maximum contents of orthophosphate 0.24 ppm were recorded in rainy season for sampling site (C). The amount of organic phosphate ranged from 5.21-5.85 ppm in hot season, 6.02-6.50 ppm in rainy season and 5.66-6.17 ppm in cold season. The contents of total phosphate were in the range of 5.21-5.85 ppm in hot season, 6.24-6.74 ppm in rainy season and 5.85-6.32 ppm in cold season (Table 2). In the present observation, the maximum value of total phosphate was recorded 6.74 ppm in rainy season for sampling site (C). The high phosphate level during the rainy season could be related to the high rate of decomposition of organic matter and from run-off, surface catchment and interaction between the water and sediments from dead plants and animals remains at the bottom of the river. Total nitrogen is an essential nutrient or plants and animals. An excess amount of nitrogen in a waterway may lead to low levels of dissolved oxygen and negatively alter various plant life and organisms. In this research work, total nitrogen values were observed to be 1.12-1.35ppm in hot season, 1.52-1.56 ppm in rainy season and 1.37-1.48 ppm in cold season (Table 2). The contents of chlorophyll *a* were observed in the range of 1.2833-1.4128 μg/ 10 mL in hot season, 2.3741-2.5312 μg/10 mL in rainy season and 1.7289-2.2374 μg/10mL in cold season (Table 2). The maximum value of chlorophyll *a* was found 2.5312 μg/10mL in rainy season for sampling site C. It was found that increasing concentration of chlorophyll *a* in river water is directly proportional to the value of increase DO levels and phytoplankton biomass.

Table 2: Nutrient Levels of River Water Samples from Three Sampling Sites (2014)

Parameters	Sampling sites	Season			Standard	
		Hot	Rainy	Cold	EPA (2009)	ASEAN (2010)
Orthophosphate (ppm) (Mean±SD)	A	ND	0.22±0.02	0.19±0.01	-	0.015
	B	ND	0.18±0.01	0.15±0.02		
	C	ND	0.24±0.03	0.17±0.01		
Organic phosphate (ppm) (Mean±SD)	A	5.48±0.06	6.02±0.09	5.66±0.11	-	NC
	B	5.85±0.04	6.44±0.12	6.17±0.08		
	C	5.21±0.06	6.50±0.09	6.11±0.12		
Total phosphate (ppm) (Mean±SD)	A	5.48±0.06	6.24±0.05	5.85±0.04	-	<0.05
	B	5.85±0.04	6.62±0.06	6.32±0.08		
	C	5.21±0.06	6.74±0.08	6.28±0.05		
Total Nitrogen (ppm) (Mean ± SD)	A	1.29±0.03	1.54±0.03	1.37±0.01	-	NC
	B	1.12±0.01	1.52±0.04	1.39±0.02		
	C	1.35±0.02	1.56±0.03	1.48±0.03		
Chlorophyll *a* (μg/10 mL) (Mean±SD)	A	1.2833±0.0018	2.4435±0.0023	2.2374±0.0031	NC	2
	B	1.4128±0.0017	2.3741±0.0018	1.8921±0.0032		
	C	1.3532±0.0019	2.5312±0.0016	1.7289±0.0028		

*EPA standards (2009) NC=Not of Concern

*ASEAN standards for aquatic life protection (2010)

Trace Elements in River Water Samples

Arsenic in river water sample

Arsenic is ubiquitous element that is comparatively rare, but widely distributed in the atmosphere, soils and rocks, natural water and organisms. From the study area, the concentrations of arsenic in river water samples ranged from 0.0163-0.0195 ppm in hot season and 0.0138-0.0185 ppm in cold season (Table 3). The arsenic content was not detected in rainy season. The highest values of arsenic was observed to be 0.0195 ppm in hot season for sampling site (B). Among these samples, the values of arsenic were found

under the permissible levels of 0.036 ppm of ASEAN standard (2010) and no toxicity of arsenic in the river waters is observed during the studied period.

Cadmium in river water samples

Cadmium is an element that occurs naturally earth's crust. Cadmium is toxic to humans, animals, microorganisms and plants, however only a small amount of cadmium intake is absorbed by the body and will be stored mainly in bones, liver and, in case of chronic exposure, in kidneys. In the present study, the contents of cadmium were observed 0.045-0.048 ppm in hot season, 0.031-0.039 ppm in rainy season and 0.037-0.043 ppm in cold season for seasonally collected samples (Table 3). The highest value of cadmium was observed 0.048 ppm in hot season for sampling site C. According to these data, all measured values were higher than the permissible level of 0.010ppm ASEAN standard (2010).The possible sources of contamination of cadmium might be due to the runoff from the agricultural soil. The entire studied area is covered by agricultural land where rock phosphate is used as phosphorous fertilizer.

Lead in river water samples

Lead is the one of the most common of the some metals. In the present study, the contents of lead in river water samples collected seasonally were found to be 1.095-1.192 ppm in hot season, 0.019-0.045 ppm in rainy season and 0.017-0.038 ppm in cold season (Table 3). The maximum value of lead was found to be 1.192 ppm in hot season for sampling site (B). The excess of lead content may be due to the runoff from agricultural fields where phosphorous fertilizers are applied, in which lead is one of the impurities.

Mercury in the river water samples

Mercury is one of the most toxic metals, interfering seriously with the human central nervous system. In the environment, it can be found in its volatile elemental form, as slightly soluble inorganic salts, and as mono and di-methylated mercury (Lomniczi, 2004). In the present work, the mercury concentrations in river water samples ranged from0.0012 to 0.0025 ppb in cold season. Mercury was not detected in hot and rainy seasons. From the

data results, the values of mercury were below the permissible levels of 0.016 ppb (ASEAN standard, 2010). So, the river water in the studied area was not polluted from viewpoint of toxic element, Hg.

Iron in river water samples

The iron concentrations in river water, samples collected seasonally were observed as 0.034-0.081 ppm in rainy season (Table 3).Iron was not detected in hot and cold seasons. The highest value of iron was found as 0.081 ppm in rainy season for sampling site (A). The increase in iron content might be due to discharge into the river through industrial, agricultural, and other human activities in the area.

Zinc in river water samples

Zinc is an essential element for all living things; including man. Zinc is unusual in that it has low toxicity to man, but relatively high toxic to fish (Badr *et al.,* 2006). In this research work, the zinc concentrations were observed to be0.029-0.035 ppm in hot season, 0.018-0.035 ppm in rainy season and 0.024-0.032 ppm in cold season (Table 3). The maximum content (0.035 ppm) was observed in hot sample for site C.

Among the some metals measured, the rest of elements (Cr, Mn and Cu) were not detected in all river water sample for seasonally collected samples (Table 3).

Table 3: Trace Element Contents in River Water for Seasonally Sampling

Elements	Sampling sites	Seasons			Standard	
		Hot	Rainy	Cold	EPA (2009)	ASEAN (2010)
As (ppm)	A	0.0163	ND	0.0152	0.69	0.036
	B	0.0195	ND	0.0138		
	C	0.0192	ND	0.0185		
Cd (ppm)	A	0.045	0.039	0.043	0.4	0.01
	B	0.047	0.031	0.037		
	C	0.048	0.036	0.041		
Pb (ppm)	A	1.189	0.019	0.017	2.1	0.009
	B	1.192	0.045	0.038		
	C	1.095	0.033	0.032		
Hg (ppb)	A	ND	ND	0.0017	1.8	0.16
	B	ND	ND	0.0025		
	C	ND	ND	0.0012		
Fe (ppm)	A	ND	0.081	ND	-	NC
	B	ND	0.034	ND		
	C	ND	0.047	ND		
Zn (ppm)	A	0.031	0.018	0.028	-	NC
	B	0.029	0.022	0.024		
	C	0.035	0.035	0.032		
Cr (ppm)	A	ND	ND	ND	-	0.05
	B	ND	ND	ND		
	C	ND	ND	ND		
Mn(ppm)	A	ND	ND	ND	-	NC
	B	ND	ND	ND		
	C	ND	ND	ND		
Cu (ppm)	A	ND	ND	ND	4.8	8
	B	ND	ND	ND		
	C	ND	ND	ND		

*EPA standards (2009) NC=Not of Concern

*ASEAN standards for aquatic life protection (2010)

Conclusion

In this study, totally 9 river water samples from different sites were collected from the Pathein river mouth, vicinity of Payala village seasonally during 2014. The river water quality assessment helps to identify the significant parameters of getting better information about source of pollution. From the results that are recorded in the different sites are compared with acceptable levels of EPA and ASEAN standards. From study area data, all measured values (pH, TSS, turbidity, chlorinity, salinity, total alkalinity, total hardness, As, Hg, Fe, Zn, Cr, Mn, Cu, total nitrogen, DO and BOD) were within the permissible levels of EPA (2009) and ASEAN (2010) standards but except (Pb, Cd, orthophosphate, organic phosphate, total phosphate, COD and chlorophyll *a*). Therefore, the observed water quality suggests that the river water could not be used for drinking purpose. It could only be used for irrigation after suitable treatment.

Acknowledgements

The authors would like to express their profound gratitude to the Department of Higher Education (Yangon Office), Ministry of Education, Yangon, Myanmar, for provision of opportunity to do this research and Myanmar Academy of Arts and Science for allowing to present this paper.

References

Anhwange, B. A., Agbaji, E.B. and Gimba, E.C. (2012). "Impact Assessment of Human Activities and Seasonal Variation on River Benue, within Makurdi Metropolis". *International Journal of Science and Technology,* vol. 2 (5), pp. 248-254.

ASEAN Marine Environmental Management.(2010). *Water Quality Criteria and Standards for Freshwater and Marine Aquaculture*. North Vancouver: EVS Environmental Consultants Ltd., pp. 171-189

Badr, M. H., Elewa, A., Shehata, M.B., Mohamed, L.F. and Abdelaziz. G.S. (2006). "Studies on the Effect of EL Rahaway Drain on the River Nile Water Pollution by Some Metals and Major Cations at EL-Kanater-EL Kayria Area Under the Effet of Seasonal Variation". *Ass. Univ. Bull. Environ. Res.*vol. 9 (2), pp. 37-47

Chapman, D. (1996). *Water Quality Assessment, A Guide to the Use of Biota Sediments and Water in Environmental Monitoring*. London : 2nd Edition, E & FN Spon, pp. 9-91

EPA.(2009). *Nutrient Water Quality Standard.*Washington, DC: Office of Water Research.

Hla Phone Aung. (1986). *Analytical Studies of the Water Environment of Hmyin* (*Acetes and Mysides*). MSc (Thesis), Department of Chemistry, University of Yangon, Myanmar

Kawabe, Mi. and Kawabe, M.(1997)."Temporal and Spatial Characteristics of Chemical Oxygen Demand in Tokyo Bay".*Journal of Oceanography,* vol. 53, pp. 19-26.

Kyaw Naing. (2012). "*Some Physicochemical Properties of River Water in Tanintharyi Coastal Zone"*. Bangkok: in the Proceeding of the 4th AUN-SEED-Net: Regional Conference on Global Environment of Seminar of NRCT-JSPS Asian Core Program, pp. 69-72.

Kyaw Naing. (2011). "National Report of Myanmar on the Coastal Pollution Loading and Water Quality Criteria (Land-based Sources of Marine Pollution)" *Bay of Bengal Large Marine Ecosystem Project of the Food and Agriculture Organization of the United Nations, FAO, Rome.* pp. 1-53.

Lomniczi, I., Boemo, A. and Musso, H. (2004). "Mercury Pollution of the Juramento River Water System (Salta Province, Argentina).*The Journal of the Argentine Chemical Society,*vol. 92(4/6), pp. 65-75.

Myint Aung. (1999). *Analytical Study of Water Quality of Ngamoeyeik Dam.* MSc (Thesis), Department of Chemistry, University of Yangon, Myanmar

Win Aung. (1995). *Environmental Studies on Bago River Water, Bago.* MSc (Thesis), Department of Chemistry, University of Yangon, Myanmar

Ye Myint Aung.(1993). *Water Analysis of Bago River near Prawn Hatchery (Tharkayta*). MSc (Thesis), Department of Chemistry, University of Yangon, Myanmar

PREPARATION AND CHARACTERIZATION OF THE CHITOSAN FILM FOR PACKAGING MATERIAL

Sandar Win[1], Khin Than Yee[2], Sandar Tun[3], Kyaw Myo Naing[4]

ABSTRACT

This research work was concerned with the preparation, characterization and application of biodegradable chitosan (C) film to be used as a packaging materials. A series of chtisoan (C) film was prepared using different amounts of chitosan by solvent evaporating method. In this preparation 1%, 2%, 3% and 4% of chitosan solutions kept in an autoclave under 0.1 MPa pressure at 121°C for 20 min were used. The homogeneous chitosan solutions after autoclaving were casted on melamine plate and left for a few days. The chitosan films obtained were characterized according to physicomechanical and physicochemical properties. The prepared C films were characterized by mechanical properties such as tensile strength, elongation at break and tear strength. According to the mechanical properties, 2 % w/v C was the most suitable for preparing C-2 film. Prepared C-2 film was characterized by modern techniques such as SEM, FT IR and TG-DTA. Antimicrobial activities of C-2 film was investigated by agar-disc diffusion method. Biodegradability of prepared C-2 film was studied by soil burial method. The quality controlling factors of mango fruits (water content, titratable acidity, reducing sugar content, crude fiber, total soluble solid, effect of pH, refractive index and weight loss) were investigated by using prepared film (C-2) as packaging materials. It was found that, for all unpackaged (control) mango fruits and packaged fruits, water contents, sugar contents, and crude fiber contents were slightly increased, but the weight loss percents were sharply increased (inverse of pH). One determining quality controlling factor was the total solubility that decreases for unpackaged (control) mango fruit, i.e, control where as it increases for packaged mango fruit, i.e, mangoes packaged by C-2 film. Moreover, unpackaged (control) mango fruits started to undergo spoilage after 10 days. However, it was found that package of mango fruits showed longer shelf life, that is, with a longer ripening time compared unpackaged (control) fruits.

Keywords*:* chitosan, biodegradable film, mango, packaging material

1. Demonstrator, Department of Chemistry, Maubin University
2. Lecturer, Department of Chemistry, University of Yangon
3. Lecturer (Retd.), Department of Chemistry, University of Yangon
4. Professor (Retd.), Department of Chemistry, Kyaingtong University

Introduction

Chitosan

Chitosan is white to ability light yellow color, insoluble in water but it is readily soluble in dilute aqueous organic acid such as acetic acid, propionic acid, formic acid and lactic acid (Dutta *et al*., 2004). These properties include: biodegradability, lack of toxicity, antifungal effects, wound healing acceleration, and immune system stimulation. (Fangkanwanwong *et al*., 2006). Most important feature of chitosan of biodegradable ability flexibility and high resistance to heat due to intra-molecular hydrogen bonds formed hydroxyl and amino group. Chitosan offers a wide range of unique applications in the food industry including preservation of foods from microbial deterioration, formation of biodegradable films, and recovery of material from food processing discards (Aranaz et al., 2009)

Biodegradation

Biodergadability depends not only on the origin of the polymer but also on its chemical structure and the environmental degrading conditions (Vroman and Tighzert, 2009). The three main sectors where biodegradable polymers have been introduced include medicine, packaging and agriculture. The development of biodegradable packaging materials has received in increasing attention. Natural biopolymer usually have good biocompatibility as well as biodegradability (Jamaluddin, 2009).

Food Packaging

The requirements for food packaging, the keeping find food fresh, enhancing organoleptic characteristics of food such an appearance , order, and flavor, and providing food safety. In everyday life, packaging is another important area where biodegradable polymers are used. In order to reduce the volume of waste, biodegradable polymers are often used. Biodegradable polymers used in packaging require different physical characteristics, depending on the product to be packaged and the store conditions. Several polysaccharide-based biopolymers chitosan have been investigated as packaging films (Shahidi *et al*., 1999).

Materials and Methods

Commercial chitosan was purchased from Shwe Poe Company, Hlaing Tharyar Township, Yangon Region, Myanmar. The chemicals (acetic acid) used in the experimental work were from the British Drug House (BDH) Chemicals Ltd., Poole, England. The chemicals were used as received unless stated otherwise. All specific chemicals used are described in detail in each experimental section.

In all the investigations, the recommended standard methods and techniques involving both conventional and modern methods were provided on the statistical basis. The apparatus used in this work were conventional labware and glassware, and modern equipments. These are cited in each experiment. The following were some of the instruments and equipments used in the experiments in this study.

Identification of Commercial Chitosan

Determination of moisture content

Material

Chitosan flakes

Apparatus

Porcelain crucible with cover

Mattler balance AE 160 (160 ± 0.1 mg), Gallenkamp, England

Electric furnance, 100-1100°C, Gallenkamp, England

Procedure

Chitosan 1g was added into a known weight of pure and dry porcelain basin. It was heated up to 105 ºC in an oven for two hours. Then the porcelain basin was placed into a desiccators for an hour to cool down the temperature. It was weighed again. Heating, cooling and weighing were repeated until the constant weight was achieved.

Determination of degree of deacetylation by titrimetric method

Materials

Chitosan flakes, Hydrochloric acid, Sodium hydroxide, Phenolphthalein indicator, Acetone, Methanol

Apparatus

Mettler balance (160 g ± 0.001 mg), Centrifuge, Burette, Pipette, Conical flask

Procedure

Chitosan (2g) was completely dissolved in 200 mL of freshly prepared 0.2 M HCl solution and 100 mL of concentrated hydrochloric acid was then added to the homogeneous chitosan solution with vigorous stirring to precipitate the hydrochloride salt. The resultant solution was centrifuged for 15 min and the supernatant was discarded. The chitosan hydrochloride salt was then filtered off and washed several times with methanol until filtrate was neutral to litmus. Residual moisture in the chitosan hydrochloride salt was removed by stirring for 6 h in acetone. After final filtration, the precipitate was dried in a vacuum desiccators for 12 h to yield white chitosan hydrochloride salt.

The resulted chitosan hydrochloride salt was divided into two portions, one portion was placed in oven at 105°C to determine moisture content. In the other portion, an accurately weighed (approximately 0.2 g) chitosan hydrochloride salt was dissolved in distilled water and the volume made up to 100 mL in the volumetric flask. The resulting solution (25 mL) was titrated against a standard 0.05 M sodium hydroxide solution using phenolphthalein as an indicator.

Antimicrobial Test of Composite Films by Agar Disc Diffusion Method

Materials

Chitosan Film

Chemicals

1% meat extract, 0.5 % sodium chloride, 1% peptone, 2% agar

Bacterials

Bacillus *subitilis* (IFO-3080), *Staphylococcus aureus* (IFO-12732), *Pseudomonas aeruginosa* (IFO-3080), *Bacillus pumilus* (IFO-1210), *Candida ablicans* (IFO-1060), E.coli

Apparatus and Equipments

1) Automatic high speed autoclave, Model S-90N, Tomy Seiko Co.Ltd., Tokyo, Japan.
2) Hot oven Model, GM-10E (DEWG, No.9 B-81051)
3) Clean bench, Hitachi Ltd, Japan
4) Water bath, Yamoto Model BT-18 No. 157
5) Incubator box, Sanyo Co., Ltd.
6) Refrigerated centrifuge, Tomy Seiko, Co., Ltd., Tokyo, Japan.
7) Petridishes, Flat bottle, conical flask, pipette, test tube
8) Balance

Procedure

The Chitosan fim, tested with Bacillus subtilis, Staphylococcus aureus, Pseudomonas aeruginosa, Bacillus Pumilus, Candida albicans and E.coli species to investigate the nature of antibacterial activity.

After preparing the bacteriological medias, the dried films were placed on the agar with flamed forceps and gently pressed down to ensure proper contact. The plates were inclubated immediately or within 30 min after

incubation. After overnight incubation at 37 °C, the result were shown in Table 4 and Figure 5.

Analysis of Soil

Biodegradations was determined by soil burial test examining and morphology changes. The soil sample was obtained from waste disposal area. Three types of soil sample were taken and dried in the shade. After all the soils had been dried the sample was ground and sifted.

Determination of Biodegradability of C Film

The nature of biodegradability of films was determined by soil burial test examining morphology changes.

Materials

Chitosan Film

Apparatus

Balance (Mettler)

Procedure

The chitosan film was cut into 1" × 1" dimension. The films were then accurately weighed and buried in soil at a depth of 5 cm. They were taken out from the soil at an interval of three days. Sample geometry on degradation was also recorded with photos which are presented in Figure 6.

Preparation of chitosan (C) films

A series of chitosan solutions 1 % w/v to 4 % w/v were prepared by using various weight percent of chitosan in 100 mL of 1 %v/v acetic acid and then autoclaved for 20 min at 121 ºC and 0.1MPa to get a clear solution. The prepared films were designated as C-1 for 1 % w/v chitosan, C-2 for 2 % w/v chitosan, C-3 for 3 % w/v chitosan and C-4 for 4 % w/v chitosan. The solutions were then made into films by pouring onto a melamine plate and allowed to take place at room temperature for 15 days.

Determination of Physicomechanical Properties of Chitosan Films

Determination of thickness

Materials

C-1, C-2, C-3, C-4

Apparatus

(NKS) micrometer, slide clipper

Procedure

Thickness of the prepared chitosan film was measured by using (NSK) micrometer. The thickness of the film was measured at 5 locations (centre and four corners) using digital micrometer.

Determination of tensile strength and percent elongation at break

Materials

C-1, C-2, C-3, C-4

Apparatus

Tensile testing machine, (Hounsfield. 5000 E), Cutter (Wallace)

Procedure

The prepared chitosan film was cut off according to JISK 7127 (1987). The shape and dimension of the test pieces were described in Appendix-IV. Both ends of the test piece were firmed clamped in the jaws of a testing machine. One jaw was fixed and the other was movable. The movable jaw moved at a rate of 100 mm/min. The recorder of the machine showed the tensile strength in MPa. The procedure was repeated three times for each result.

The resulting data was presented in Table 1 and Figure 1.

Determination of tear strength

Materials

C-1, C-2, C-3, C-4

Apparatus

Wallace cutter, tensile testing machine (AJ 100 mettler)

Procedure

Test specimen was cut out by a die from prepared chitosan film. Specimen was cut with a single nick (0.05 mm) at the centre of the inner concave edge by a special cutting device using a razor blade. The clamping of the specimen in the jaws of a testing machine was aligned with travel direction of the grip. The speed of the moving grip is 100 mm/min. The recorder of the machine showed the highest force to tear from a specimen nicked. The procedure was repeated three times for each result.

The resulting data was presented in Table 1 and Figure 1.

Results and Discussion

Aspect of Characterization of Pure Chitosan Films

The mechanical properties such as tensile strength, elongation at break (%), tear strength are important parameters which revealed the nature of films. The mechanical property of pure chitosan film as a function of chitosan content are presented in Table 1 and Figure 1. The thickness of pure chitosan film is about 0.10 mm.

It was found that the tensile strength was drastically increased to 23.4 MPa with chitosan content 2% w/v (i.e C-2). Similarly, the percent elongation at break also increased for C-2 film, however it was significantly decreased with increasing chitosan concentration. The maximum tensile strength and the percent elongation at break of C-2 film were found to be 23.4 MPa and 7.8 % respectively.

The tear strength is another mechanical property of the nature of films. It indicated that the tear strength of chitosan film was significantly increased

at C-2, however, it was significantly decreased beyond 2 % w/v of chitosan concentration. It can be concluded that according to the physicomechanical properties such as tensile strength, percent elongation and tear strength, the composition of chitosan for flexible film C-2 (2 % w/v) is the best.

Table 1: Physicomechanical Properties of A Series of Chitosan (C) Films

(%w/v) of Chitosan	Tensile strength(MPa)	Elongation at break (%)	Tear Strength (kN/m)
C - 1	19.1	3.5	26.7
C - 2	23.4	7.8	16.0
C - 3	20.1	2.5	11.4
C - 4	11.0	8.8	11.7

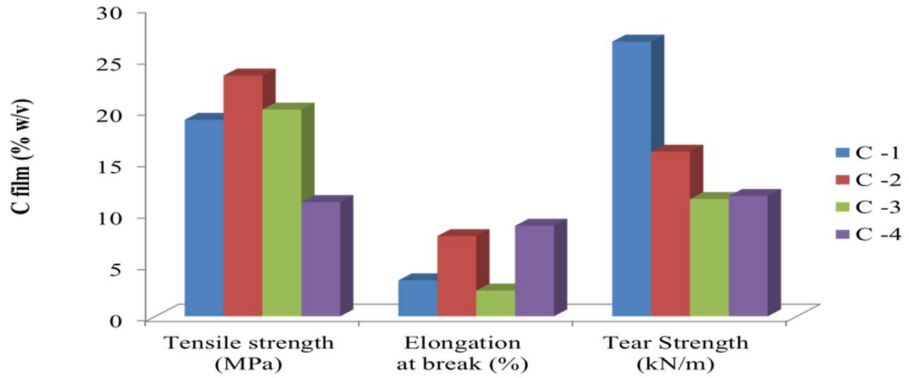

Figure 1: Tensile strength, elongation at break (%) and tear strength of C-2 film

SEM Analysis

Figure 2 shows the SEM photographs of C film (C-2), The surface morphology of pure chitosan film was relatively smooth, homogenous and continuous matrix without cracks with good structural integrity.

Figure 2: Scanning electron micrographs of C-2 Film

FT IR Spectrum of Chitosan C-2 Composite Film

FT IR spectroscopic studies allowed to analyze the characteristics bands corresponding to vibrations of the hydroxyl-, methyl-, methylene-, carbonyl- and amide groups. The FT-IR spectrum of C-2 film, is presented in Figure 3 and Table 2. The broad absorption band of N-H and OH stretching was between 3200 and 3600 cm^{-1}. The IR spectrum of chitosan at 3294 cm^{-1} was the OH stretching, which overlaped the NH stretching in the same region. The band at 1635 cm^{-1} represent C = O stretching ($\nu_{C=O}$) due to amide I band and the band at 1558 cm^{-1} represent (-NH-) amide II band due to N-H bending (δ_{NH}) vibration of secondary amide group chitosan . The band at 1411 cm^{-1} corresponds to the CH symmetrical deformation mode. The peak at 1149 cm^{-1} indicate the saccharide structure and a broad band at 1072 cm^{-1} was due to the C-O stretching vibration in chitosan (Salleh *et al*., 2009).

Table 2: FT IR Band Assignment for C-2 Film

Experimental	**Literature***	
C-2 film	**Frequency (cm^{-1})**	**Band Assignments**
3294	3200-3600	N-H, OH symmetric stretching vibration
2926-2891	2900-2950	Symmetric and asymmetric CH stretching of CH_2
1635	1649-1655	Amide I: C=O stretching vibration
1558	1515-1570	Amide II: NH deformation and C-N stretching vibration
1411	1400-1430	CH symmetrical deformation mode
1327	1322-1325	Deformation vibrations of CH group
1149	1153-1158	Bending vibration of hydroxyl group
1080	1080-1230	C-O stretching vibration

∗Silverstein 1991, Salleh 2009

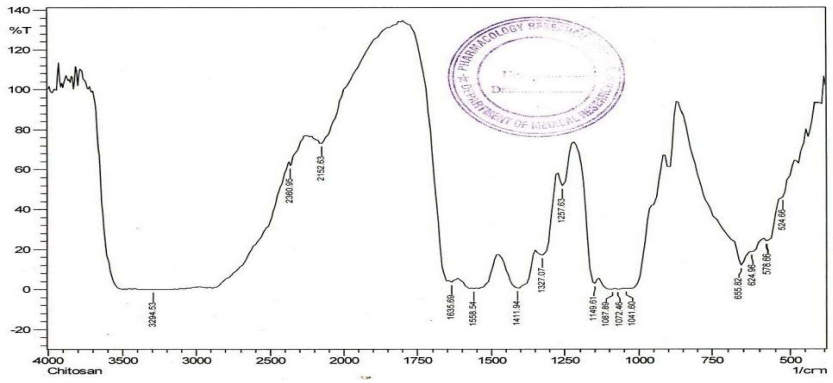

Figure 3: FT IR spectrum of C-2 film

TG-DTA Analysis

The nature and remarks regarding the thermogram profiles are presented in Table 3. The thermogram of uncross-linked chitosan film (C-2) is presented in Figure 4.

According to the TG-DTA thermogram profiles of chitosan film (C-2), three stages of weight loss were observed. In the first stage, the temperature range between 37 °C to 120 °C accompanied with 5.49 % weight loss due to

the dehydration of moisture and surface water. The slight weight loss approximately 17.09 % was observed in the temperature range between 120 °C and 280 °C in the second stage. This weight loss can be attributed to the decomposition of volatile materials. In the third stage, the obvious weight loss 51.08 % was found in the temperature range between 280 °C and 600 °C. In this stage, the weight loss was due to the degradation of polymer backbone and decomposed to monomer fragments up to the formation of residue.

Table 3: Thermal Analysis Data for C-2 Film

TG Thermogram			DTA Thermogram	TG and DTA Remarks
Temperature Range (°C)	**Break in Temperature (°C)**	**Weight loss (%)**		
37-120	-	5.49	-	Dehydration due to moisture and surface water
120-280	-	17.09	-	Loss of volatile materials
280-600	299.43	51.08	exothermic	Degradation of polymer backbone
-	525.94	-	endothermic	Decompose to monomer fragments up to the formation of residue

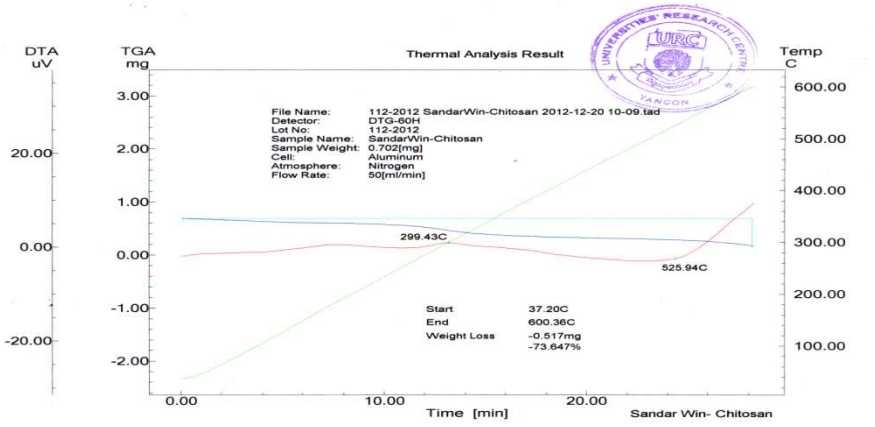

Figure 4: TG-DTA thermogram for C-2 film

Antimicrobial Activity C-2 Film

Antimicrobial activity of C-2 film is shown in Table 4 and Figure 5. The tested organisms were *Bacillus subtilis, Staphylococcus aureus, Pseudomonas aeruginosa, Bacillus pumilus, Candida ablicans and E.coli.* As seen in Figure 5 antimicrobial test of C-2 film was used in the agar medium cultivation. C-2 Film showed the antimicrobial activity such as *Bacillus subtilis, Staphylococcus aureus* and *E.coli* but the other three organisms did not show the activity.

Table 4. Antimicrobial Activity of C-2 Films by Agar Well Diffusion Method

No.	Microorganisms	Antimicrobial Activity of C-2 Film
1.	*Bacillus subtilis*	+
2.	*Staphylococcus aureus*	+
3.	*Pseudomonas aeruginosa*	-
4.	*Bacillus pumilus*	-
5.	*Candida albicans*	-
6.	*E.coli*	+

Agar Well- 10 mm (-), 10 mm ~ 14 mm (+)

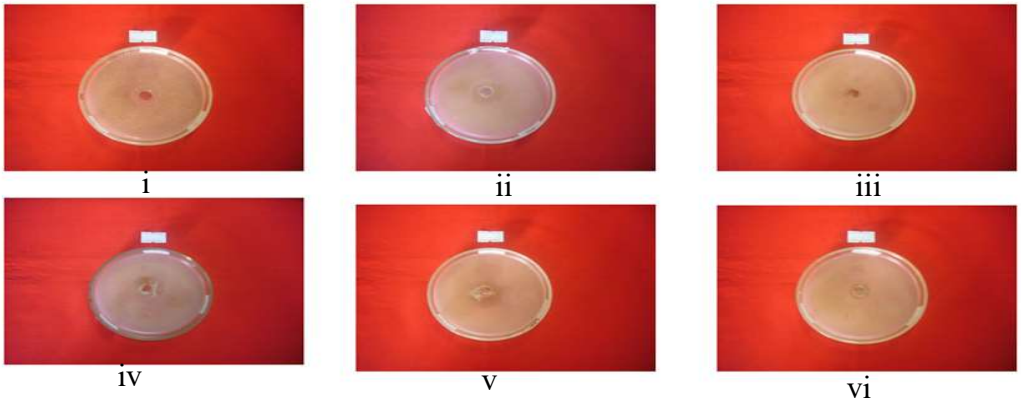

Figure 5: Antimicrobial activity of prepared C-2 film with *(i) Bacillus subtilis (ii) Staphylococcus aureus (iii) Pseudomonas aeruginosa (iv) Bacillus pumilus (v) Candida albicans (vi)E.coli*

On the Aspect Biodegradation

The environmental friendly degradable plastic has been developed by compositing the natural polymer chitosan .One of the objectives of development natural polymer chitosan is to make easy throw away materials from degradable plastic to alleviate waste disposal problems by means of environmental degradation. In this work, biodegradation of chitosan films such as C-2 film was tested by soil burial method. Soil burial is a traditional way to test samples for degradation because of its similarity to actual condition of waste disposal. Uniformly sized samples were buried in the soil from waste disposal. The physical appearance of film by soil burial method were shown in Figure 6. In the dry sand, there were not significantly difference in biodegradability. The biodegradability of C-2 film was found to be more biodegradable in sandy soil, soil and humus soil than the dry sand.

Soil Burial Test

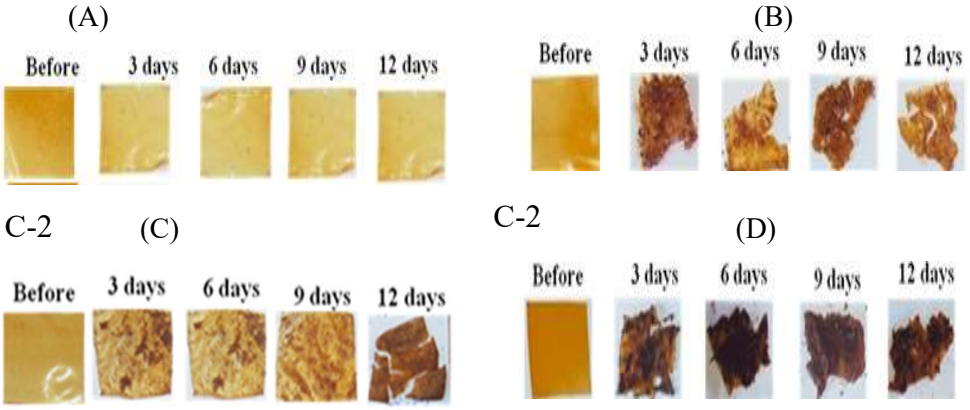

Figure 6: The physical appearances of films by soil burial method (A) Dry sand (B) Sandy soil(C) Soil (D) Humus soil

Packaging of Prepared C-2 Film on Mango

Packaging of prepared C-2 film on mango are shown in Figures 7 and 8. The film packaging is known to have the potential to prolong the storage life and control the decay of fruits. The processed mangoes were packaged in chitosan C-2 film boxes with these film. Packaging fruits with chitosan film

helps the long term storage of fruit because chitosan C-2 film provides a type of active package, which are released from the film deposited on the surface of the fruit. Citrus and other fruits can be stored for long period once they have been packaged with C-2 film which decreases respiration rates and inhibits fungal development and delays ripening by suppressing the evolution of ethylene and carbon dioxide (Dutta *et al*., 1997).

The effectiveness of C-2 film and control (unpackaged mangoes), the weight loss and maintaining the quality of mangoes were also investigated. Weighed mangoes were packaged with C-2 film. The control (unpackaged mangoes) and packaged mangoes were stored for 20 days at room temperature (≈ 28 ± 2 °C). The fruit quality such as water content, titratable acidity (TA), reducing sugar content, crude fibre, total soluble solid , pH , weight loss and refractive index of the unpackaged mangoes and packaged mangoes were also determined within 20 days of storage time.

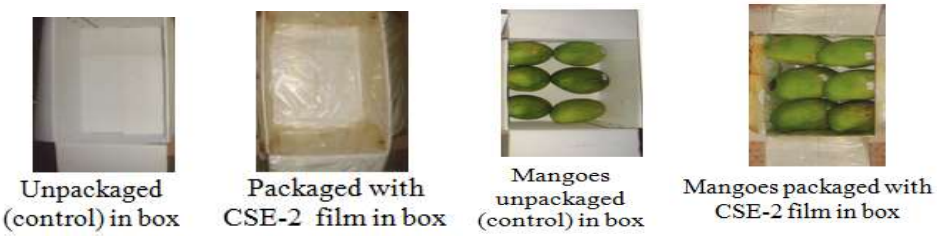

Figure 7: Photographs of film packaging treatments on mangoes

(A) **(B)**

(A) = Unpackaged (control) Mangoes
(B) = Mangoes, packaged with C-2 film
Figure 8: Physical appearance of unpackaged(control) and packaged mangoes

Effect on Water Content and Titratable Acidity

Tables 5 and Figure 9 show that the increase in water content of mangoes packaged with chitosan films as a function of time at room temperature. In this study C-2 beneficially affected postharvest mango and retarded ripening, water loss and decay. Therefore reducing water loss from fruit during storage or ripening helps to maintain the quality of fruit. According to experimental results C-2, promoted the retention of firmness and increased water content. The titratable acidity was significantly decreased during the storage time. The titratable acidity value of C-2 packed fruit were lower than control. The decreasing acidity at the end of storage might be due to the metabolic changes in fruits.

Table 5: Water Content and Titratable Acidity of Unpackaged (control) and C-2 Packaged Mangoes as a Function of Times at Room Temperature

Sample	Water Content (%)			Titratable Acidity (g/100 g)		
	5 days	10 days	15 days	5 days	10 days	15 days
Unpackaged (control)	81.43	83.17	85.32	99.75	10.88	9.32
C-2 Film	80.61	83.17	84.87	108.54	14.04	10.85

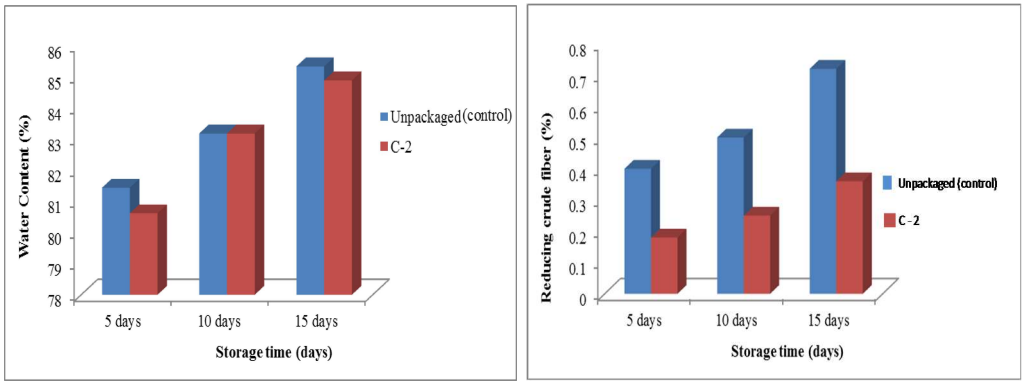

(a) (b)

Figure 9: Variation of (a)water content and(b) titratable acidity of unpackaged (control) and packaged mangoes with storage time at room temperature

Effect on Sugar Content and Crude Fibre

The changes in the sugar content and crude fiber content of packaged and unpackaged fruits are shown in Table 6 and Figure 10.The reducing sugar content and crude fiber content of C-2 packaged fruits were lower than and control. The increasing sugar content was due to breakdown of cell structure in order to senescence phenomena during storage. The crude fibre content of C-2 slightly increases from 0.18 to 0.36 within 15 days at room temperature. But crude fibre content of unpackaged (control) fruits obviously increased from 0.40 to 0.72 during 15 days. So C-2 can control the increasing of crude fibre content in a mango.

Table6: Sugar Content and Crude Fibre Content of Unpackaged (control) and C-2Packaged Mangoes as a Function of Times at Room Temperature

	Sugar content (%)			**Crude fiber (%)**		
Sample	**5 days**	**10 days**	**15 days**	**5 days**	**10 days**	**15 days**
Unpackaged (control)	2.66	2.73	3.43	0.40	0.50	0.72
C-2 Film	2.41	2.69	3.09	0.18	0.25	0.36

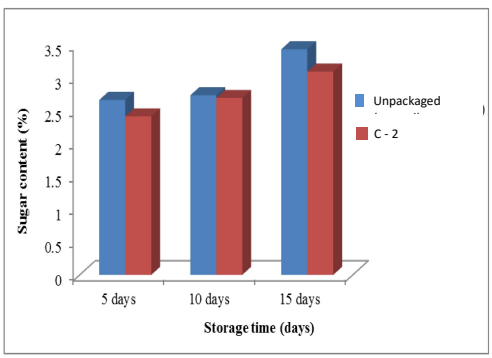

(a)

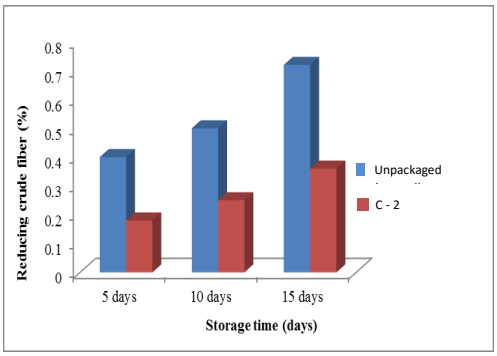

(b)

Figure 10: Variation of (a) sugar content and (b) Crude Fibre Content of unpackaged (control) and packaged mangoes with storage time at room temperature

Effect on Total Soluble Solid and Weight Loss

The changes in the total soluble solid content and weight loss in mangoes are shown in Table 7 and Figure 11. Total soluble solid (TSS) of packaged fruits was gradually increased during the storage except the unpackaged (control) fruit. No significant differences were found packaged with prepared C-2 sample and control fruits (unpackaged mango). There were significant differences about 15 days of storage in C-2 film. The increase packaged mango in TSS contents during storage might be due to the respiration rate and conversion of sugars to carbon dioxide and water. The weight loss associated with C-2 packaged with mangoes were slower than that unpackaged mangoes. Weight loss was lower in coated fruit with C-2 (0.19% to 0.75 %) as compared to control having higher percent weight loss (0.29 % to 0.91%).

Table 7: Total Soluble Solid and Weight Loss of Unpackaged (control) and C-2 Packaged Mangoes as a Function of Times at Room Temperature

Sample	Total Soluble solid (°Brix)			Weight Loss(%)		
	5 days	10 days	15 days	5 days	10 days	15 days
Unpackaged(control)	1.75	1.68	1.50	0.29	0.51	0.91
C-2 Film	1.62	1.76	1.75	0.19	0.40	0.75

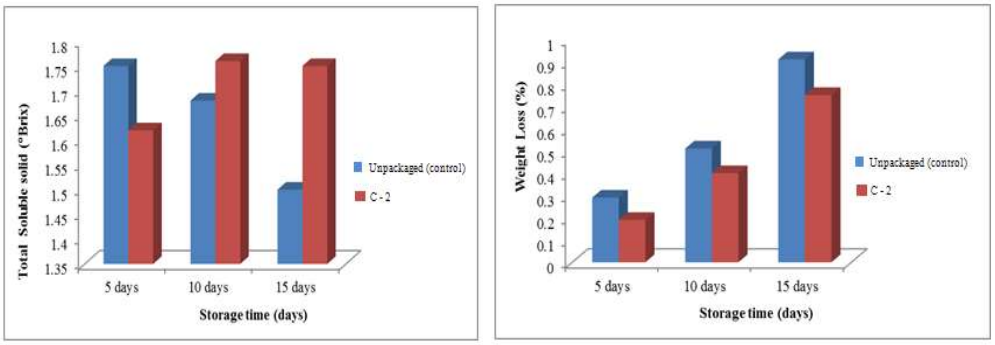

(a) (b)

Figure 11: (a)Total soluble solid and (b) weight loss of unpackaged (control) and packaged mangoes with storage time at room temperature

Effect on pH and Refractive Index

The pH of mangoes were gradually increased during storage time. There were no significant differences between treated and control fruits. These data were shown in Table 8. According to the experimental results, the pH values were gradually increased during storage intervals. It might be due to decrease in acidity through the biochemical changes within the fruits during storage. The refractive index values of unpackaged mangoes and packaged mangoes are presented in Table 8. It was observed that there was no significant changes in the refractive index of the unpackaged mangoes and packaged mangoes were also determined within 15 days of storage time.

Table 8: pH and Refractive Index of Unpackaged (control) and C-2 Packaged Mangoes as a Function of Times at Room Temperature

Sample	pH			Refractive Index		
	5 days	10 days	15 days	5 days	10 days	15 days
Unpackaged(control)	4.04	5.85	6.09	1.3365	1.3365	1.3365
C-2 Film	3.85	5.78	5.93	1.3345	1.3345	1.3345

Conclusion

In this study, chitosan (C) films (C-1, C-2, C-3, C-4) were prepared by solvent evaporating method under autoclaving conditions of 0.1 MPa in a time frame of 20 min at 121°C. The mechanical properties of prepared C-2 film was found to possess the tensile strength (23.4 MPa), elongation at break (7.8 %) and tear strength (16.0 kN/m). According to the FT IR spectrum, the broad absorption band of N-H and OH stretching was between 3200 and 3600 cm^{-1}. The IR spectra of chitosan at 3294 cm^{-1} was the OH stretching, which overlaps the NH stretching in the same region. The band at 1635 cm^{-1} represent C=O stretching ($\nu_{C=O}$) due to amide I band and the band at 1558cm^{-1} represent (-NH-) amide II band due to N-H bending (δ_{NH}) vibration of secondary amide group chitosan . The band at 1411 cm^{-1} corresponds to the CH symmetrical deformation mode. The peak at 1149 cm^{-1} indicate the saccharide structure and a broad band at 1072 cm^{-1} was due to the C-O stretching vibration in chitosan. From the SEM analysis, the pattern of C-2 film was found to be relatively smooth, homogeneous and a continuous matrix

without cracks with good structural integrity. The TG-DTA, in the temperature range between 37°C and 120°C, the weight loss is 5.49% which is due to the dehydration of moisture and absorbed water. The slight weight loss of about 17.09 % was observed in the temperature range between 120 °C and 280 °C in the second stage. This weight loss can be attributed to the decomposition of volatile materials. In the third stage, the significant weight loss 51.08 % was found in the temperature range between 280 °C and 600 °C. In this stage, the weight loss was due to the degradation of polymer backbone and decomposed to monomer fragments up to the formation of residue.

The biodegradability of C-2 film was found to be more biodegradable in sandy soil, soil and humus soil than the dry sand. From the microbial activities, C-2 film showed significant antimicrobial activity such as *Bacillus subtilis, Staphylococcus aureus* and *E-coli* but not on the other three organisms. Application of C-2 as packaging film for mango fruits delayed physicochemical changes such as water content, titratable acidity, sugar content, crude fibre, total soluble solid, effect of pH, refractive index and weight loss. By comparing the unpackaged and packaging films, the mango fruit packaged by C-2 film show 15 days ripening film and can sustain better quality.

Acknowledgments

The authors would like to express their profound gratitude to the Department of Higher Education (Yangon Office), Ministry of Education, Yangon, Myanmar, for provision of opportunity to do this research.

References

Aranaz, I., Mengibar, M., Harris, R., Panos, I., Miralles, B., Acosta, N., Galed, G. and Heras, A. (2009). "*Functional Characterization of Chitin and Chitosan". Current Chemical Biology,* vol. 3, pp. 203-230

Bhuvaneshwari, S Sruthi, D., Sivasubramanian, V., Kalyani, N. and Sugunabai, J. (2008). "Development and Characterization of Chitosan Film". *International Journal of Engineering Research and Application* (IJERA), vol.1(2), pp. 292-299

Dutta, P.K., Dutta, J. and Tripathi, V.S. (2004). "Chitin and Chitosan: Chemistry, Properties and Applications". *Journal of Scientific and Industrial Research*, vol. 63, pp. 20-31

Fangkanwanwong, J., Yoksan, R. and Chirachanchai, S. (2006). "*Chitosan Gel Formation via the Chitosan - Epichloroghydrin Adduct and its Subsequent Mineralization with Hydroxyapatite*". vol. 47, pp. 6438-6445

Hudson, S.M. and Smith, C. (1998). "Polysaccharides: Chitin and Chitosan Chemistry and Technology of their used Structural Material". In: Kaplan DL, Berlin: Springer; pp. 96-118

Jamaluddin, M. F. (2009). "*Fabrication and Characterization of Composite Biodegradable Films from Chitosan and Corn Silk* ". Degree of Bachelor of Chemical Engineering Faculty of Chemical and Natural Resources Engineering, University of Malaysia, Penang, pp. 10-14

Salleh, E., Muhamad, I. I. and Khairuddin N. (2009). "Structural Characterization and Physical Properties of Antimicrobial (AM) Starch-Based Films". *Journal of Engineering and Technology*, vol. 31**,** pp. 430-432

Shahidi, F., Arachchi J.K.V. and Jeon, Y.L. (1999). "Applications of Food Chitin and Chitosan". *Journal of Food Sci. Technol.,* vol. 10*,* pp. 37-51

Silverstein, R. M., Bassler, G. C. and Terence, C.M. (1991). "*Spectrometric Identification of Organic Compounds*". New York: John Wiley and Son, Inc., pp. 99-164

Ting Liu, T. L. (2008). "Edible Films from Starch and Chitosan: Formulation and Gas Permeabilities". *Applied Science in Chemical Engineering Waterloo,* vol. 64, pp. 60-65

Vroman, I . and Tighzert. L. (2009). "Biodegradable Polymers". France, vol. 2, pp. 307-344 http:// www. mdpi. corn/ journal/ materials (Accessed 28 June 2012)

INVESTIGATION OF ANTIOXIDANT, CYTOTOXIC AND ANTITUMOR ACTIVITIES OF *Morinda citrifolia* L. FRUIT (YÈ-YO) AND *Catharanthus roseus* L. WHOLE PLANT (THIN-BAW-MA-NYOE)

Aung Phyo Naing[1], Kyaw Khaing[2], Khin Chaw Win[3],
Khine Zar Win Lae[4], Daw Hla Ngwe[5]

Abstract

The present work focused on the investigation of some biological activities such as antioxidant, cytotoxic and antitumor activities on some crude extracts from locally cultivated *Morinda citrifolia* L. fruits (Yè-yo) and *Catharanthus roseus* L. whole plant (Thin-baw-ma-nyoe). The antioxidant activity of ethanol and watery extracts evaluated by DPPH free radical scavenging assay showed that IC_{50} values of EtOH extract (4.395 μg/mL) and watery extract (8.878 μg/mL) from *C. roseus* were repsectively higher than those of EtOH extract (9.347 μg/mL) and watery extract (8.484 μg/mL) from *M. citrifolia*. The ethanol and watery extracts of both plant samples did not exhibit the cytotoxic effect determined by using brine shrimp cytotoxicity bioassay method. Antitumor activity screening determined by potato crown gall test revealed that ethanol and watery extracts of *M. citrifolia* and *C. roseus* can inhibit tumor growth. Tumor inhibition was significantly observed in the concentration of 0.2 g /mL for each extract.

Keywords: *M. citrifolia*, *C. roseus*, antioxidant activity, cytotoxic effect, antitumor activity

Introduction

Natural plant products have served as the basis of man's medicinal arsenal since time immemorial. The history of herbal medicine in the treatment of many diseases and 3,000 plant species that have been used or recommended in various parts of the world for the treatment of cancer. It has been only within the last 20 years that any product from a higher order plant has been successfully used in cancer chemotherapy. *Morinda citrifolia* L. and

1. 4 PhD, Candidates, Department of Chemistry, University of Yangon
2. 4 PhD, Candidates, Department of Chemistry, University of Yangon
3. Dr, Lecturers, Department of Chemistry, University of Yangon
4. Dr, Lecturers, Department of Chemistry, University of Yangon
5. Dr, Professor and Head, Department of Chemistry, University of Yangon

the *Catharanthus roseus* L. have been used as medicinal plants since long ago. *M. citrifolia*, a shrub originating in tropical Asia, has been extensively used in folk medicine and as a dye in Asian countries (Dittmar, 1993). In Myanmar, the fruits are cooked in curries or eaten raw with salt. The fruit juice of *M. citrifolia* is in high demand in alternative medicine for various illnesses, such as arthritis, diabetes, high blood pressure, muscle aches and pains, menstrual difficulties, headaches, heart disease, Acquired Immune Deficiency Syndrome (AIDS) and cancer (Kamiya *et al*., 2004). *C. roseus* is a medicinal herb found in many tropical and subtropical regions around the world (Farah *et al*., 2011). This plant produces a diverse array of secondary metabolites that are pharmaceutically important like vinblastine and vincristine used as chemotherapeutic agents in the treatment of several types of cancers. The plants are also used in treatment of diabetes, fever, malaria and throat infection. The leaf-juices are used in blood dysentery and leaf decoctions are also to babies in gripping pain. The roots of *C. roseus* are used for the treatment in cancerous wounds and septic wounds. The plant bears active phytoconstituents and exhibits various pharmacological activities like anti-diabetic, anti-oxidant, anti-hypertensive, anti-microbial and cytotoxic etc (Mohd *et al*., 2010).

There were some reports on the investigation of some organic constituents and cholestrol lowering effect of locally cultivated *M. citrifolia* (Ye-yo) (Khin Thida Nyo, 2006) and antidiabetic potency of locally grown *C. roseus* (Thin-baw-ma-nyoe) (Myint Myint Khin, 2007). In the present work, some biological activities: antioxidant, cytotoxic and antitumor activities of the fruits of *M. citrifolia* (Ye-yo) and the whole plant of *C. roseus* (Thin-baw-ma-nyoe) could be evaluated.

Materials and Methods

Collection of Plant Materials

The sample of *M. citrifolia* fruits were collected from Kyaung-su Village, Ke-gyi Township, Ayeyarwady Region and whole plants of *C. roseus* were collected from Mingalar-taung-nyot Township, Yangon. The plant samples were identified in Department of Botany, University of Yangon, Myanmar.

The collected samples were cleaned by washing thoroughly with water were then and air-dried at room temperature. The dried samples were cut into small pieces and ground into powder by a grinding machine. These powder samples obtained were separately stored in air-tight container.

Determination of Antioxidant, Cytotoxicity and Antitumor Activities

Preparation of crude extracts from the samples

For antibacterial activity screening, some crude extracts such as EtOAc, 95 % EtOH and H_2O extracts were firstly prepared from *M. citrifolia* and *C. roseus* samples. Dried powdered samples was refluxed with 95 % EtOH and then filtered. This solution was recovered by distillation and evaporation to dryness to give 95 % EtOH crude extracts. The dried powdered samples were extracted with distilled water within 15 min, by using hot extraction. Water solution was concentrated by evaporation to dryness to give water extract. All extracts are stored in desiccators.

Determination of antioxidant activity

DPPH radical scavenging activity was determined by UV-spectrophotometric method (Ashokkumar and Ramaswamy, 2013). The control solution was prepared by mixing 1.5 mL of 60 μM DPPH solution and 1.5 mL of 95 % ethanol with vortex mixer. The sample solution was also prepared by mixing thoroughly 1.5 mL of 60 μM DPPH solutions and 1.5 mL of test sample solution. The solutions were allowed to stand at room temperature for 30 min. After 30 min, measurement of absorbance at 517 nm were made by using spectrophotometer UV 1601 PC (P\N 206 – 6750), Shimadzu corporation. Absorbance measurements were done in triplicate for each solution and the mean value was obtained, and then used to calculate % inhibition of oxidation by the following equation,

$$\% \text{ oxidative inhibition} = \frac{A_c - (A - A_b)}{A_c} \times 100\ \%$$

% oxidative inhibition = % oxidative inhibition of test sample

A_c = absorbance of the control (DPPH alone)

A_b = absorbance of the blank (EtOH + Test sample solution)

A = absorbance of test sample solution

Then IC_{50} (50 % inhibitory concentration) values were also calculated by linear regressive excel program.

Determination of cytotoxicity

Cytotoxicity of 95 % EtOH and H_2O extracts were determined by using brine shrimp bioassay. Firstly, artificial sea water was prepared by dissolving, sodium chloride (38 g) in 1000 mL of distilled water. Brine shrimp cysts (0.5 g) were added to 1 L of artificial sea water. The bottle was placed near a lamp and supplied O_2 for 24 h. After 24 h incubation, hatching of brine shrimp cysts occurred and the alive brine shrimp (napulii) were ready for cytotoxicity test. Test solution (1 mL) was mixed with 9 mL of artificial sea water and placed in the chamber of ice cup. Alive brine shrimp (10 napulli) were taken with pasteur pipette and placed into each chamber which was kept at room temperature for about 24 h. After 24 h incubation, the number of survival brine shrimp was counted and 50 % lethality dose (LD_{50}) was calculated (Ali *et. al*, 2013; Dockery and Tomkins, 2000).

Screening of antitumor activity by potato discs assay method (potato crown gall test)

Antitumor Activity of 95 % EtOH and H_2O extracts of *M. citrifolia* fruits and the whole plant of *C. roseus* were studied by Potato Discs Assay Method. Tumor producing bacteria, *Agrobacterium tumefacien*, isolated from *Sandoricum koetjape* Merr. (Thitto) leaves was used in this study. The bacterial strain had been maintained as solid slants under refrigeration. For inoculation of the potato discs, 48 h broth cultures containing 5×10^7-5×10^9 cell/mL were used. Fresh, disease free potato tubers were obtained from local markets and were used within 48 h of transfer to the laboratory.

Tubers of moderate sizes were surface-sterilized by immersion in 50 % sodium hypochlorite (Clorox) for 20 min. The ends were removed and soaked

for 10 minutes more in Clorox. A core of the tissue was extracted from each tuber by using surface-sterilized (ethanol and flame) 2.5 cm wide cork borer and 2 cm pieces were removed from each end and discarded and the remainder of the cylinder is cut into 1.0 cm thick discs with a surface-sterilized cutter. The discs were then transferred to 1.5 % agar plates (1.5 g of Difco agar was dissolved in 100 mL of distilled water, autoclaved and 20 mL poured into each petri dish). Each plate contained three discs. This procedure was done in the clean bench in the sterile room.

0.1 g and 0.2 g each of the sample was dissolved in EtOH solvent filtered through Millipore filters (0.22 μm) into a sterile tube. 0.5 mL of this solution was added to 1.5 mL of sterile distilled water and 2 mL of broth culture of *A. tumefaciens* strain (48 h culture containing 5×10^7-5×10^9cells/ mL) were added aseptically. Controls were made in this way; 0.5 mL of DMSO and 1.5 mL of sterile distilled water were added to the tube containing 2 mL of broth culture of *A. tumefaciens* (from the same 48 h culture). Using a sterile disposable pipette, 1 drop (0.05 mL) from these tubes was used to inoculate each potato disc, spreading it over the disc, surface. The process of cutting the potatoes and incubation must be conducted within 30 min. The plates were sealed with tape to minimize moisture loss and incubated at room temperature counted with microscope and compared with control. The antitumor activity was examined by observation of tumor produced or not (Collins, 2001).

Results and Discussion

Antioxidant Activity of *M. citrifolia* and *C. roseus*

Antioxidant compounds in plant play an important role as a health-protecting factor. Scientific evidence suggests that antioxidants reduce the risk for chronic diseases including cancer and heart disease. Primary sources of naturally occurring antioxidants are whole grains, fruits and vegetables. Plant source antioxidants like vitamin C, vitamin E, carotenes, phenolic acids and phytoestrogens have been recognized as having the potential to reduce disease risk. The antioxidant activity of *M. citrifolia* and *C. roseus* were evaluated by DPPH (2, 2- diphenyl-1-picrylhydrazyl) radical scavenging assay. The radical scavenging effects were determined for EtOH and watery extracts of two selected plants. The extracts or their constituents when mixed

with DPPH decolorized due to hydrogen donating ability. The antioxdiant activities of crude extracts were expressed in terms of percent radical scavenging activities (%RSA) and IC_{50} (50 % inhibitory concentration). The resultant data from Table 1 and Figure 1, showed that when the concentrations of samples increased the % RSA also increased. It can be suggested that one requires to scavenge effectively radicals the more concentrated crude extracts will be used. These results are shown in Figure 2. Since the lower the IC_{50} values, the higher the antioxidant activity of the samples have, the *C. roseus* EtOH extract (IC_{50} = 4.395 μg/mL) possessed the highest radical scavenging property among the extracts. The IC_{50} values were found to be *C. roseus* (EtOH) (4.395 μg/mL) < *M. citrifolia* (Watery) (8.484 μg/mL) < *C. roseus* (Watery) (8.878 μg/mL) < *M. citrifolia* (EtOH) (9.347 μg/mL), indicating the order of antioxidant activity of the extracts would be in the order of *C. roseus* (EtOH) > *M. citrifolia* (Watery) > *C. roseus* (Watery) > *M. citrifolia* (EtOH) (9.347 μg/mL). However, their antioxidant potency was found to be sligthly weaker than the that of standard ascorbic acid (IC_{50} = 2.2 μg/mL).

Table 1. % Radical Scavenging Activity of Crude Extracts of *M. citrifolia* and *C. roseus* Compared with Standard Ascorbic acid

Test sample	**% RSA ± SD at Different Concentration (μg/mL)**					**IC_{50} (μg/mL)**
	1.25	**2.5**	**5**	**10**	**20**	
M. citrifolia (watery)	7.225 ± 1.388	8.359 ± 2.008	32.650 ± 5.130	57.558 ± 0.4112	72.356 ± 0.823	8.484
M. citrifolia (EtOH)	10.268 ± 1.848	13.095 ± 2.472	24.107 ± 2.839	53.895 ± 0.454	70.498 ± 0.823	9.347
C. roseus (watery)	3.734 ± 1.607	7.467 ± 1.370	30.032 ± 1.035	55.784 ± 0.654	65.786 ± 0.823	8.878
C. roseus (EtOH)	12.748 ± 2.575	25.994 ± 2.576	57.679 ± 0.753	69.536 ± 0.468	70.349 ± 0.823	4.395
Ascorbic acid	41.192 ± 2.443	52.554 ± 0.701	55.382 ± 0.704	56.595 ± 1.001	64.358 ± 1.365	2.200

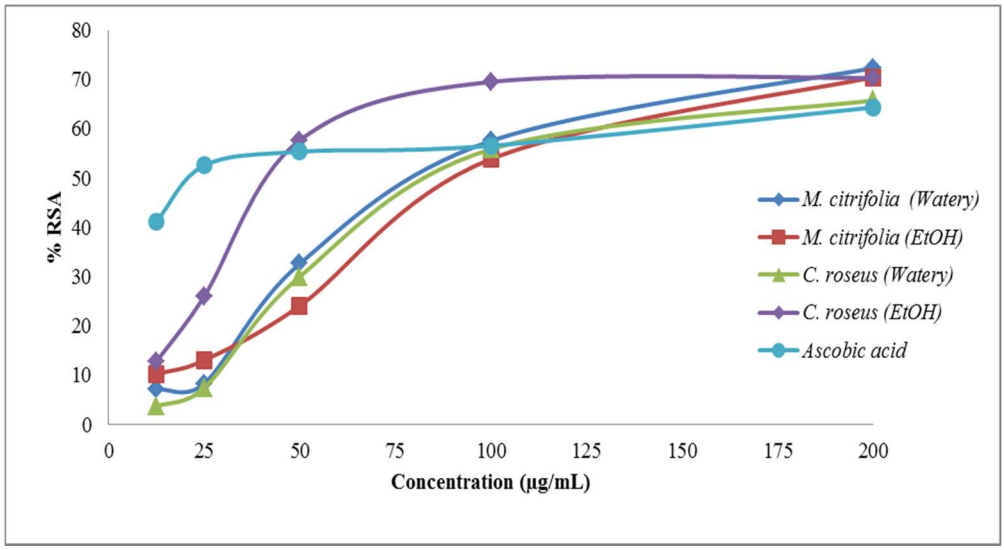

Figure 1: % Radical scavenging activity of crude extract of *M. citrifolia*, *C. roseus* and standard ascorbic acid

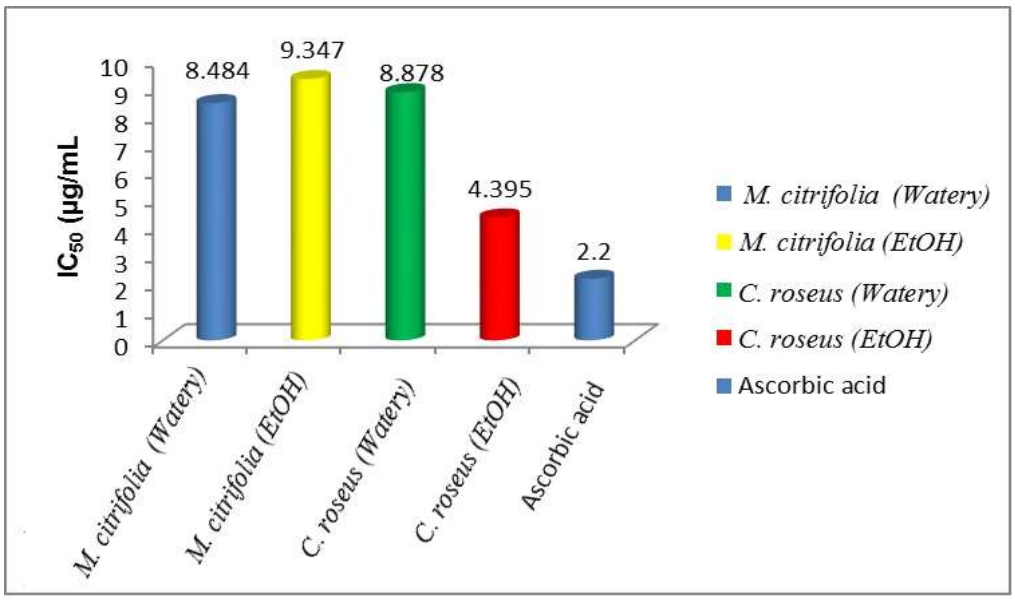

Figure 2: IC_{50} values of crude extracts of *M. citrifolia* and *C. roseus* compared with standard ascorbic acid

Cytotoxicity of *M. citrifolia* and *C. roseus*

The cytotoxicity of watery and ethanol extracts of *M. citrifolia* and *C. roseus* was evaluated by brine shrimp cytotoxicity bioassay. The organisms used were brine shrimp (*Artemia salina*). The cytotoxic effect was expressed as LD_{50} values (50 % Lethality Dose). The resulting cytotoxicity of watery and ethanol extracts of two selected plants are reported in Table 2. According to these results, LD_{50} values could not be detected for both samples until 3200 µg/mL doses. Hence, both samples have no cytotoxic effect compared with $K_2Cr_2O_7$ (LD_{50} = 275 µg/mL) up to the maximum dose of LD_{50} 3200 µg/mL.

Table 2: Cytotoxic Effect of Different Doses of EtOH and Watery Crude Extracts of *M. citrifolia* and *C. roseus*

Samples	No. of Dead Brine shrimp (Mean ± SEM) in various concentration (µg/mL)						LD_{50} (µg/mL)
	100	**200**	**400**	**800**	**1600**	**3200**	
M. citrifolia (Watery)	0.000 ± 0.000	0.000 ± 0.000	0.000 ± 0.000	0.000 ± 0.000	1.000 ± 0.000	2.000 ± 0.000	> 3200
M. citrifolia (EtOH)	0.000 ± 0.000	0.000 ± 0.000	0.000 ± 0.000	0.000 ± 0.000	2.000 ± 0.000	2.333 ± 0.577	> 3200
C. roseus (Watery)	0.000 ± 0.000	0.000 ± 0.000	0.000 ± 0.000	1.000 ± 0.000	2.000 ± 0.000	3.000 ± 0.000	> 3200
C. roseus (EtOH)	0.000 ± 0.000	0.000 ± 0.000	0.000 ± 0.000	1.333 ± 0.577	2.333 ± 0.577	3.000 ± 0.000	> 3200
*$K_2Cr_2O_7$	1.000 ± 0.000	2.000 ± 0.000	10.000 ± 0.000	10.000 ± 0.000	10.000 ± 0.000	10.000 ± 0.000	275

* Used as Cytotoxic Standard ;

** No. of brine shrimp used were 10 for each experiment.

Antitumor Activity of *M. citrifolia* and *C. roseus*

The antitumor activity of EtOH and H_2O extracts of *M. citrifolia* and *C. roseus* was investigated by using PCG test with the isolated tumor producing bacterium *A. tumefaciens.* For inoculation of the potato disc, 48 h broth cultures containing $5x10^9$ cells/mL were used. The tested samples were dissolved in DMSO to dilute and the diluted samples were mixed with the bacterial culture for inoculation. After preparing the inoculums, the bacterial suspension was inoculated on the cleaned and sterilized potato discs, and incubated for 3 days, at room temperature. After that, the tumors were appeared on potato discs and checked by staining the knob with Lugol's (I_2-KI) solution. In the control, the formation of white knob on the blue background indicated the presence of tumor cells because there is no protein in tumor cells. The active test samples did not form any tumors on the potato discs and its surface remained blue as shown in Figures 3 to 5.

Antitumor activity screening revealed that two crude extracts of both samples could inhibit tumor growth. In general, tumor inhibition was significantly observed at the concentration of 0.2 g/mL for each extract.

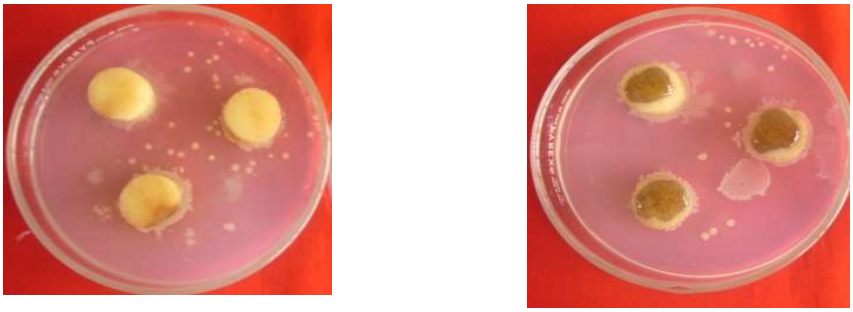

(a) **(b)**

Figure 3. Photographs showing the control potato disc
(a) Before spraying with iodine
(b) After spraying with iodine

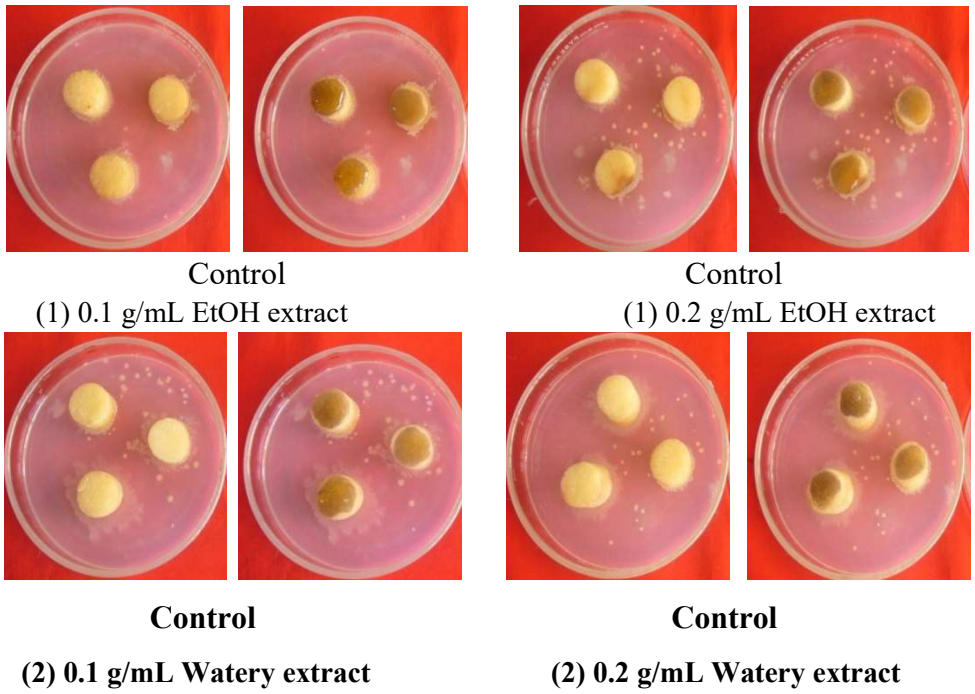

Figure 4. Antitumor assay by potato crown gall test for *M. citrifolia* in different amounts of extracts

Table 3: Antitumor Activity of Different Crude Extracts from *M. citrifolia*

No.	Test Sample	Concentration of samples g/mL	Tumor
1.	Control	0	+
2.	Ethanol extract	0.1	+
3.	Ethanol extract	0.2	-
4.	Watery extract	0.1	-
5.	Watery extract	0.2	-

(+) Tumor appeared ; (-) No tumor appeared

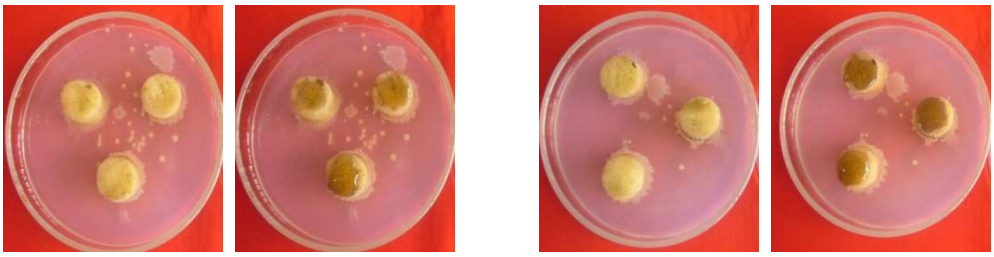

(1) 0.1 g/mL EtOH extract (1) 0.2 g/mL EtOH extract

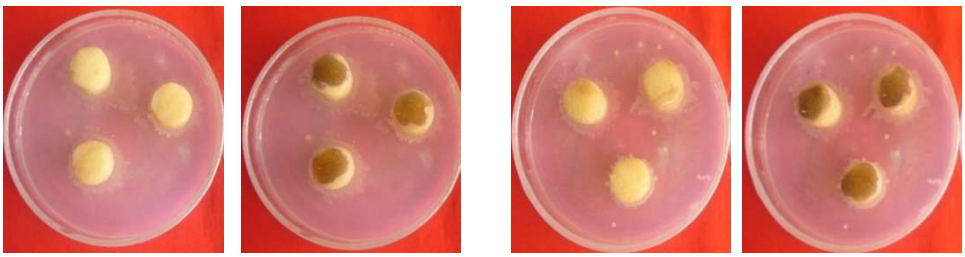

(2) 0.1 g/mL Watery extract (2) 0.2 g/mL Watery extract

Figure 5. Antitumor assay by potato crown gall test for *C. roseus* in different amounts of extracts

Table 3: Antitumor Activity of Different Crude Extracts from *C. roseus*

No.	Test Sample	Concentration of samples g/mL	Tumor
1.	Control	0	+
2.	EtOH extract	0.1	-
3.	EtOH extract	0.2	-
4.	Watery extract	0.1	-
5.	Watery extract	0.2	-

(+) Tumor appeared (-) no tumor appeared

Conclusion

From the present study, it can be concluded that *M. citrifolia* fruits and *C. roseus* whole plant possessed the antioxidant activity in the order of *C. roseus* (EtOH extract) > *M. citrifolia* (Watery extract) > *C. roseus* (Watery extract) > *M. citrifolia* (EtOH extract). The EtOH extract of *C. roseus* exhibited the highest antioxidant potency among the extracts. In general, both of the two samples may be useful for the cure of oxidative stress related diseases. The cytotoxicity was not observed in ethanol and watery extracts of *M. citrifolia* and *C. roseus* determined by using brine shrimp cytotoxicity bioassay. Both of the ethanol and watery extracts of *M. citrifolia* and *C. roseus* were found to exhibit the inhibition of tumor growth up to minimum dose of 0.1 g/mL.

These scientific findings from the present work may contribute to the development of Myanmar traditional medicinal in formulation, especially for the disease related to oxidative stress and is expected to inhibit tumor growth in some forms of cancer.

Acknowledgements

The authors would like to express their profound gratitude to the Department of Higher Education (Yangon Office), Ministry of Education, Yangon, Myanmar, for provision of opportunity to do this research.

References

Ali, N., Allen, U. , Shah, S.W.A. , Shah, I. , Junaid, M. , Ahmed, G., Ali , W. and Ghias, M. (2013). "Acute Toxicity, Brine Shrimp Cytotoxicity, Anthelmintic and Relaxant of Fruits of *Rubus fruiticosis* Agg". *BMC Complement. Altern. Med*, vol. 13, pp. 138 – 143

Ashokkumar, R. and Ramaswamy, M. (2013). "Determination of DPPH Free Radical Scavenging Oxidation Effects of Methanolic Leaf Extracts of Some Indian Medicinal Plant Species". *Journal of Chemical, Bological and Physical Sciences*, vol. 3, no.2, pp. 1273 – 1278

Collins, A. (2001). "*Agrobacterium tumefaciens*". A Class Project for Soilborne Plant Pathogens, North Carolina State University, Department of Plant Pathology, pp. 728

Dittmar, A. (1993). "*Morinda citrifolia* L.-Use in Indigenous Samoan Medicine". *Journal of Herbs Spices and Medicine Plants,* vol. 1, pp. 77 – 92

Dockery, M. and Tomkins, S. (2000). *Brine Shrimp Ecology*. London: 1st Ed., The British Ecology Society,vol. 5, pp. 92 – 93

Farah, F., Mohsen, Z. and Tahereh, N. (2011). "Anti-bacterial Activity of *in Vitro* Produced Alkaloids in *Catharanthus roseus* L.". *African Journal of Microbiology Research*, vol. 3(27), pp. 4769 – 4770

Kamiya, K., Tanaka, Y., Endang, H., Umar, M. and Satake, T.(2004). "Chemical Constituents of *Morinda citrifolia* Fruits Inhibit Copper-Induced Low-Density Lipoprotein Oxidation". *Journal of Agriculture and Food Chemistry,* vol. 52, pp. 5843 – 5848

Khin Thida Nyo, U Kyaw, Ma Hla Ngwe and Maung Maung Htay. (2006). "Hypocholesterolemic effect of locally cultivated Morinda citrifolia Linn. (Rubiaceae) (Ye-yo)". *Jour. Myan. Acad. Arts & Sc*., vol. 4 (1), pp. 269 - 286

Mohd, I., Naeem, M. , Masroor, M. and Khan, A . (2010). "The Superiority of cv 'rosea' over cv 'alba' of Periwinkle (*Catharanthus roseus* L.) in Alkaloid Production and other Physiological Attributes". *Journal of Biol*, vol. 34, pp. 81 – 88

Myint Myint Khin. (2007). *Isolation and Identification of Some Bioactive Compounds from Catharanthus roseus Linn. (Thinbaw-Ma-Nyoe) Leaf and Rauvolfia serpwntina Linn. (Bon-Ma-Ya-Za) Root and Investigation of Hypoglycemia, Antioxidant and Antibacterial Activity*. PhD Dissertation, Department of Chemistry, University of Yangon

EFFECT OF ALKALI CONCENTRATION ON THE PREPARATION OF VOLCANIC MUD AND QUARRY DUST BASED GEOPOLYMER

Aye Aye Than[1], Naw Aye Aye Thein[2], Thi Thi Aye[3]

Abstract

The volcanic mud sample was collected from Yauk Chaung Village, Kyaukphyu Township, Rakhine State and quarry dust from Loikaw Township, Kayah State. The physical properties (moisture content, loss - on -ignition, specific gravity ,fineness, pH and pozzolanic reactivity) of volcanic mud and quarry dust samples were determined and characterized by conventional and modern spectroscopic methods (EDXRF, XRD and SEM).From the EDXRF and XRD analysis, it was observed that the major oxide compositions were present as SiO_2, CaO, Fe_2O_3 and Al_2O_3 in both samples. It was found that the samples were silica-alumina rich compound. From the SEM micrographs, the microstructure of quarry dust appeared to be glassy, hollow and porous structure . In the microstructure of volcanic mud sample, the micrograph indicates crystalline nature. It can be considered that the pores are micro-porosity sized particles. The optimum conditions of sodium hydroxide concentration and the ratio of sodium hydroxide and sodium silicate which are used in the preparation of geopolymer have been determined. The physical properties (apparent porosity, water absorption, apparent density) and the mechanical properties (compressive strength) of prepared volcanicmud based geopolymer were also determined. Compressive strength of geopolymer ranged from 6.70 to 21.41N/mm^2.The mechanical properties compressive strength of prepared volcanic mud-quarry dust based geopolymer (GP) and blended cement (GP: Cement) (1:1, 1:2, 2:1) at different time intervals (7, 14 and 28 days) have been determined.

Keywords: Geopolymer, compressive strength, blended cement, pozzolanic reactivity

Introduction

The global warming problem caused by CO_2 became one of the serious international environmental issues to be solved. In particular, the CO_2 produced in the manufacturing process of Portland cement used in most building and civil constructions are increasing every year. 0.4 ~ 1.0 tons of CO_2 were produced to make 1 ton of cement and it is as much serious as 7% of total CO_2 amount of global production were used for making cement.

[1.] 2PhD, Candidate, Department of Chemistry, University of Yangon
[2.] Lecturer, Department of Chemistry, University of Yangon
[3.] Associate Professor, Department of Chemistry , University of Yangon

Therefore, many researchers have focused on reducing CO_2 production and substitute materials for cement with the consideration of ecological industry in the future. The prospecting materials for non-sintering inorganic binders are fly ash, slag and brick powder from the industrial wastes as well as natural raw materials such as clay and incinerated kaolin (Mc Lellan *et al*., 2011).

The development of geopolymer concrete is an important step towards the production of environmentally friendly concrete. The name geopolymer was formed by a French Professor Davidovits in 1978 to represent a broad range of materials characterized by networks of inorganic molecules. The fundamental chemical and structural characteristics of geopolymer derived from metakaoline, fly ash and slag are explored in terms of the effects of raw material selection on the properties of geopolymer composite (Mc Lellan et al., 2011).

Geopolymers are novel class of materials that are formed by the polymerization of silicon, oxygen and aluminium species to form an amorphous three-dimensional framework structure (Kyi Kyi San,2013). Geopolymerization can transform a wide of waste alumino-silicate materials into building and mining materials with excellent chemical and physical properties, such as fire and acid resistance (Palomo *et al*,1999).

Reuse of various industrial by-products such as flyash, silicafume, rice husk ash foundry waste, quarrydust, et cetera as substitutes to the conventional construction materials in construction has been atgued to be a possible way forward towards achieving an environmentally friendly construction (Neville,2002; Gambhir,1995). Most common alkali activator used in geopolymerization is a combination of NaOH or KOH and Na_2SiO_3 .(Khin Moe Aye,2013).

Geopolymer can be synthesized by the condensation of Si^{4+} and Al^{3+} ions came from the industrial wastes or natural ores by alkaline activators. The general chemical formular is $M.n(-SiO_2)_2-Al_2O_3)_n.\ wH_2O)$ where, M is alkali or alkaline earth elements such as K, Na, and Ca, n is 1, 2, and 3 and it represents the degree of condensation. Geopolymer is one type of alumina-silica cements and they produce less $CO_2$and show better mechanical as well as chemical properties including heavy metal stabilization compared to Portland cement. Therefore, they are the most prospecting materials for

substituting conventional cement. Geopolymers have a three dimensional network structure such as zeolite and an amorphous phase. The prospecting raw materials for geopolymers are industrial wastes containing large amount of amorphous silica such as fly ash, metakaolin, blast furnace slag etc. and natural silicate materials (Chaung and Chiu 2003).

Geopolymer cement is an innovative material and a real alternative to conventional Portland cement for use in transportation infrastructure, construction and offshore applications. It relies on minimally processed natural materials or industrial byproducts to significantly reduce its carbon footprint, while also being very resistant to many of the durability issues that can plague conventional concretes (Davidovits, J., 1991).

Materials and Methods

Sample Collection

The volcanic mud sample was collected from Yauk Chaung Village, Kyaukphyu Township, Rakhine State and quarry dust samples was collected from Loikaw Township, Kayah State.

Sample Preparation

Volcanic mud was piled up into a cone and dividing it into quarters. Opposite quarters were rejected and the remaining half-portion again treated as before, rolling the sample back and forth on a paper. After quartering, the sample was ground in an agitate motor and pestle and then sieving with 200 mesh sieves.

Quarry dust sample is obtained by crushing the stone boulders of size 100 to 150 mm in the stone crushers. The aggregate is sieved and the sieved aggregates which is less than 4.75 mm in size.

Methods

All chemicals used in this work were the products from British Drug House Chemical Ltd., Poole, England and from Kanto Chemical Co. Inc., Japan, unless otherwise stated. All specific chemicals used are described in detail in each experimental section.

All analytical procedure of the experiment were carried out according to recommended standard text such as Vogel (1964).Various conventional and modern instrumental techniques were used throughout the experimental procedure. These include Scanning Electron Microscope (SEM) and X-ray Diffraction (XRD) techniques. Qualitative elemental composition of samples were determined by EDXRF technique. During the experiment, all analytical determinations, instrumental analyses, monitoring of the process systems and the equipment together with the supporting facilities were carried out at Universities ' Research Centre, University of Yangon.

Preparation of Volcanic Mud and Quarry Dust(1:1wt. ratio) Geopolymer and Blended Cement

Volcanic mud and quarry dust in 1:1,1:2 and 2:1 wt. ratios was mixed with 3ml of alkali solution (1:1,1:2,2:1,1:3,3:1) v/v of Na_2SiO_3 :NaOH and 28 % of water were mixed on a non-absorbent base. Immediately the mixture was placed in the plastic mould. After 28 days, the specimens were removed from the plastic mould. The blended cements were prepared by various mixing ratios of prepared GP: commercial cement 1:1,1:2,2:1 w/w.

Table 1: Preparation of Volcanic Mud and Quarry Dust (1:1) based Geopolymer Samples Using Various ratio of NaOH and Na_2SiO_3

GP Sample No	Ratio of Alkali Solutions NaOH : Na_2SiO_3	Concentration of NaOH (M)
A-1	1:1	4
A-2	1:2	
A-3	2:1	
A-4	1:3	
A-5	3:1	
B-1	1:1	8
B-2	1:2	
B-3	2:1	
B-4	1:3	
B-5	3:1	
C-1	1:1	12
C-2	1:2	
C-3	2:1	
C-4	1:3	
C-5	3:1	

Results and Discussions

The result is divided into two parts. The first part is concerned with the physicochemical properties and the characterization of local raw materials volcanic mud and duarry dust**.** The second part is the optimum conditions of sodium hydroxide concentration and sodium silicate for the preparation of volcanic mud and quarry dust based geopolymer.

Physicochemical Properties of Volcanic Mud and Quarry Dust Sample

Moisture content

Moisture content of volcanic mud and quarry dust samples contain 3.7 % and 2.6 % respectively. It is possibly due to basic oxides and those of silicon, iron and aluminium. These oxides are able to absorb moisture. The results are shown in Table 1.

pH

pH values of volcanic mud and quarry dust samples were 11.92 and 9.46 respectively. According to the pH values, the samples were highly alkaline not surprising of the nature of basic oxides. The results are shown in Table 1.

Loss on ignition (LOI)

LOI was essentially a measure of the unburnt carbon in volcanic mud and quarry dust samples. LOI value of volcanic mud was found as 5.3 % and quarry dust as 0.48 %. According to ASTM C 618 guide lines studies, LOI is acceptable for use as a substitute of cement. The results are shown in Table 1.

Specific gravity

The average specific gravity of the volcanic mud and quarry dust were 2.59 and 2.57.They are slightly less than that of Portland Cement (Alpha Cement Brand),thus using volcanic mud and quarry dust samples as a replacement material can reduce the weight of cement. The low specific gravity causes porous, weak and absorptive material and high specific gravity causes good quality of concrete. The results are shown in Table 1.

Fineness

The fineness of volcanic mud and quarry dust depends on the methods of combustion and grinding. The results of fineness of volcanic mud was 27.8 % and quarry dust was 12.9%. The results are shown in Table 1.

Table 1: Physical Properties of Volcanic Mud and Quarry Dust Samples

No.	Sample	Moisture (%)	Loss-on-ignition(%)	pH	Specific gravity	Fineness (%)
1.	Volcanic mud	3.7	5.3	11.92	2.59	27.8
2.	Quarry dust	2.6	0.48	9.46	2.57	12.9

Solubility

The solubility of volcanic mud and quarry dust samples are shown Table 2. According to the experimental results, the samples were slightly soluble in inorganic acids but insoluble in organic solvents. The results are shown in Table 2.

Table 2: Solubility of Volcanic Mud and Quarry Dust Samples

No.	Solvent	Volcanic mud	Quarry dust
1.	Nitric acid	±	±
2.	Sulphuric acid	±	±
3.	Hydrochloric acid	±	±
4.	Acetic acid	-	-
5.	Ethanol	-	-
6.	Methanol	-	-
7.	Sodium hydroxide	-	-
8.	Water	-	-

(+) = soluble (-) = insoluble (±) = slightly soluble

Relative Abundance of the Elements in Volcanic Mud and Quarry Dust Samples by EDXRF method

The relative compositions of the elements in the volcanoic mud and quarry dust samples are shown in Figures 1 and2 and Table 3. According to the experimental results, Si, Ca and Al were found as major constituents and Fe, S and K were found as minor constituents in the volcanic mud sample. In the quarry dust sample, Si and Al were observed as major constituents and Fe, K and Ca as minor constituents.

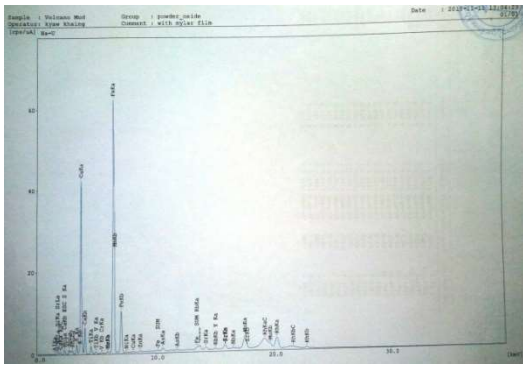

Figure 1. ED XRF spectrum of volcanic mud sample

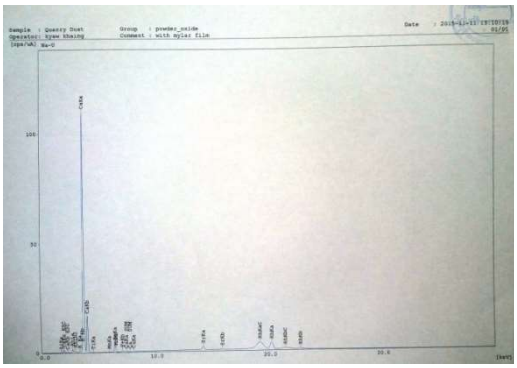

Figure 2. EDXRF spectrum of quarry dust sample

Table 3: Relative Composition of Elements in Volcanic Mud and Quarry Dust Samples

Samples	Relative composition (%)							
	Si	**Ca**	**Al**	**Fe**	**S**	**K**	**Ti**	**Sr**
Volcanic mud	52.06	20.17	16.27	5.10	3.81	1.64	0.64	0.01
Quarry dust	7.74	89.83	-	1.40	-	0.66	0.17	0.12

X Ray Diffractograms of Volcanic Mud and Quarry Dust samples

The X-ray diffractogram of the samples are shown in Figures 3 and 4. It was found to be amorphous form of SiO_2. According to the XRD results, the two samples of the2Θ value from 28 to 32 which is in indication of crystalline form (Figure 3 and 4). The crystalline form of samples can be used as a Portland cement replacement in concrete.

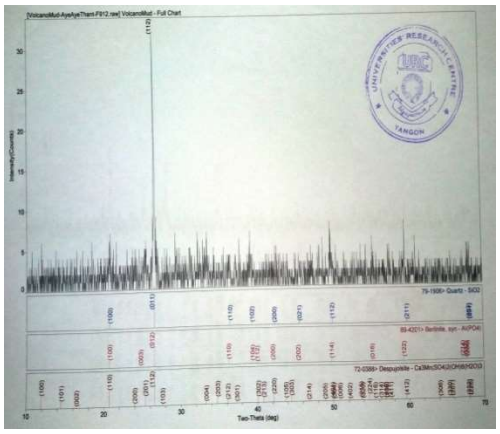

Figure 3. XRD spectrum of volcanic mud sample

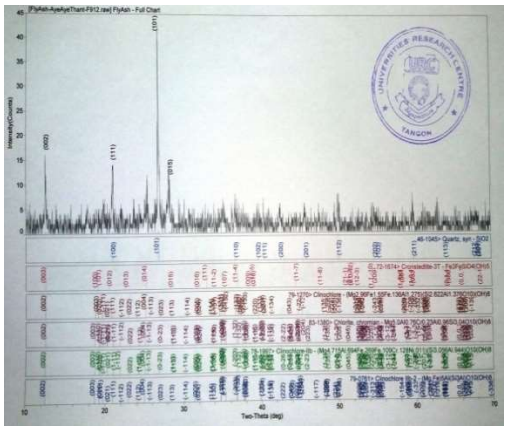

Figure 4. XRD spectrum of quarry dust sample

SEM Micrographs of Volcanic Mud and Quarry Dust Samples

SEM micrographs of volcanic mud and quarry dust samples are shown in Figures 5 and 6**.**Thesefigures showed the diameter of pores that may be approximately 1-10µm range. From the SEM micrographs, the microstructure of quarry dust appeared to be glassy, hollow and porous structure. In the microstructure of volcanic mud sample, the micrograph indicates crystalline nature. It can be considered that the pores are micro-porosity sized particles. It must be note that the cement powder lies in the mixed partial morphological nature of the ingredients.

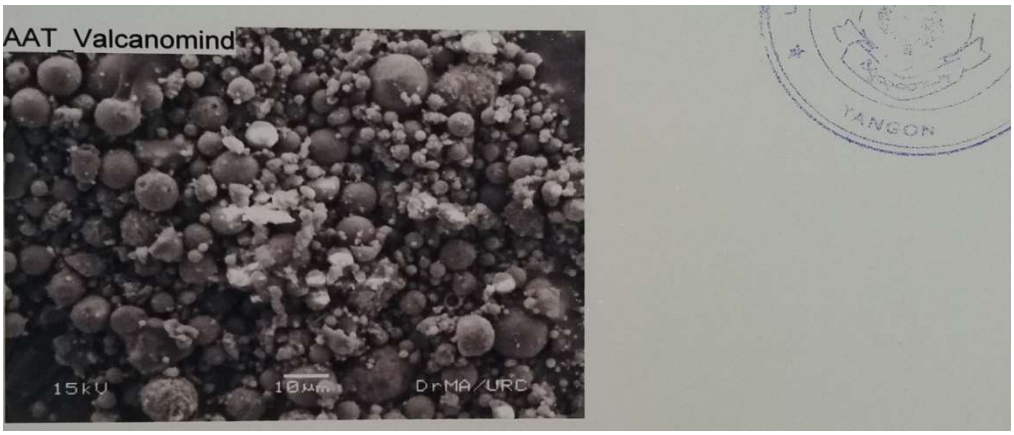

Figure 5: SEM micrograph of volcanic mud sampleat 1000 × magnification

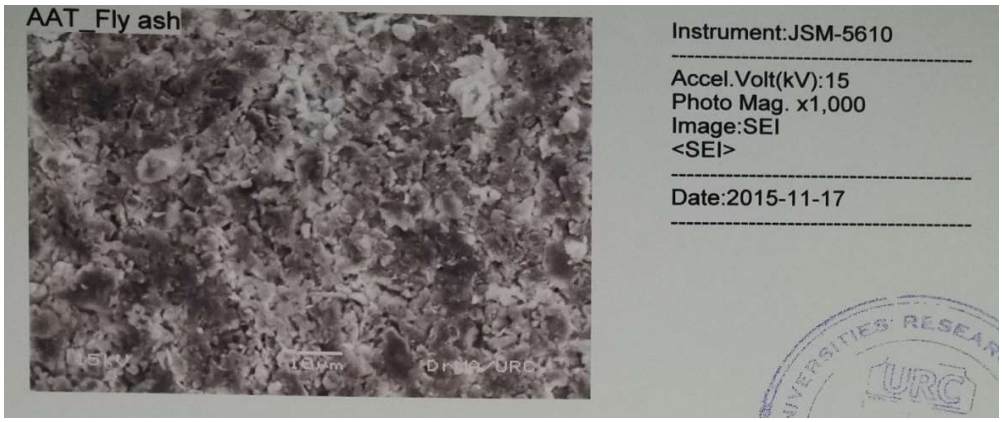

Figure 6: SEM micrograph of quarry dust sample at 1000 × magnification

Pozzolanic Reactivity of Volcanic Mud and Quarry Dust samples

The pozzolanic material of volcanic mud and quarry dust were allowed to react with calcium hydroxide in solution as were as in paste. In case of reaction in solution, volcanic mud and quarry were mixed with saturated solution of calcium hydroxide and definite volume of the solution(filtered) were titrated against standard HCl at different intervals of time. The amount of calcium hydroxide reacted with volcanic mud and quarry dust were determined.

Table 4 and 5 showed that the pozzolanic reactivity of volcanic mud and quarry dust samples. The amount of reacted calcium hydroxide is plotted against time. Figure 7 and 8 showed that the time progressed, the amount of calcium hydroxide reacted were increased. The reactivity was much higher than that at room temperature. The results suggest that volcanic mud and quarry dust are pozzolanic material and its pozzolanic activity increased with the temperature. The pozzolanic reaction can be expressed as:

$$Ca(OH)_2 + SiO2 \longrightarrow C\text{-}S\text{-}H \text{ (calcium silicate hydrate)}$$

The increase of rate above reaction with temperature may be due to increase of dissociation of $Ca(OH)_2$ in solution giving more Ca^{2+} and OH^- ions. The larger number of ions react with amorphous silica at faster rate.

Table 4: Pozzolanic Reactivity of Volcanic Mud Sample

No. of Experiments	Time(min)	Reacted value of $Ca(OH)_2$ (%)
1	30	48.86
2	60	54.55
3	90	60.23
4	120	64.02
5	150	75.58

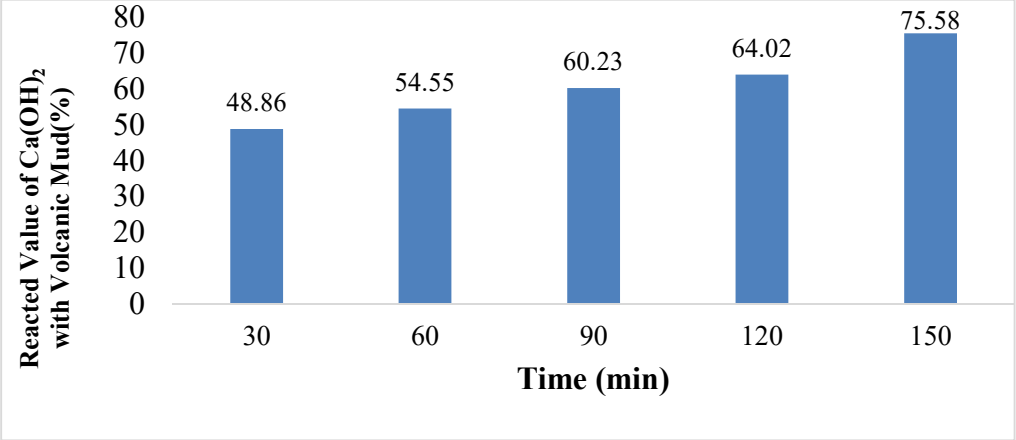

Figure 7: Pozzolanic reactivity of volcanic mud sample

Table 5: Pozzolanic Reactivity of Quarry Dust Sample

No. of Experiments	Time(min)	Reacted value of $Ca(OH)_2$ (%)
1	30	71.59
2	60	75.38
3	90	79.17
4	120	84.85
5	150	88.64

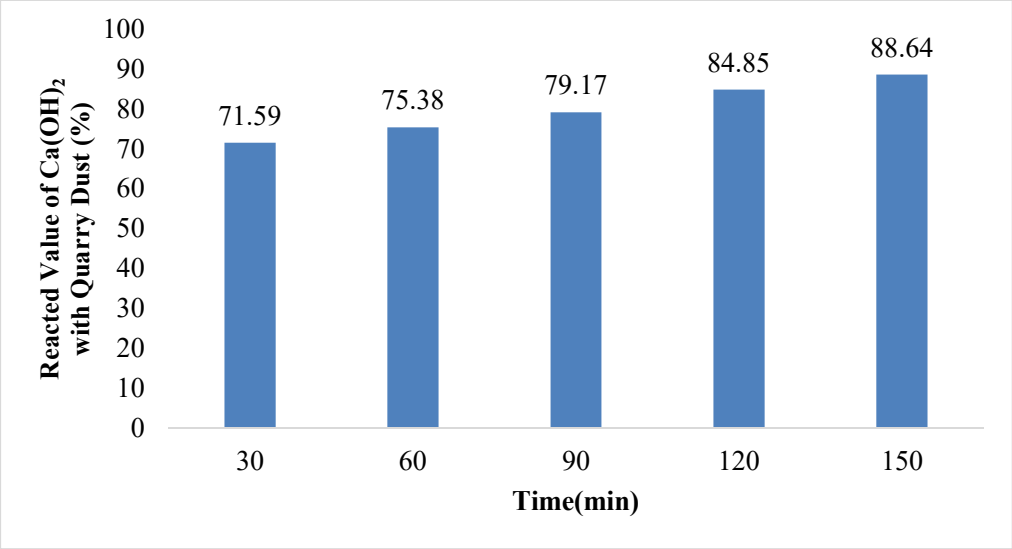

Figure 8: Pozzolanic reactivity of quarry dust sample

The Optimum Condition of Effect of Alkali Concentration on the Prepared Volcanic Mud and Quarry Dust Based Geopolymer

The optimum condition of sodium hydroxide concentration and the ratio of sodium hydroxide and sodium silicate for the preparation ofvolcanic mud and quarry dust based geopolymers were prepared by physical mixing method. Table 6 show that the apparent porosity, water absorption and apparent density of prepared geopolymer samples. In the prepared method, same amount of volcanic mud and quarry dust (1:1) and different volume ratio of (1:1,1:2,2:1,1:3,3:1)of NaOH (4,8,12) M and Na_2SiO_3 were mixed. Table 7 show that the compressive strength of volcanic mud and quarry dust 1:1 based prepared geopolymer at 7,14 and 28 days. The apparent density and compressive strength, (28 days) were found to be maximum when it was prepared with same amount of volcanic mud and quarry dust and (1:3) volume ratio of 12 M NaOH and Na_2SiO_3. Table 8 show that the apparent porosity, water absorption and apparent density of prepared samples (110^0C) and the mechanical properties such as compressive strength (28 days)each of sample were measured to assess the quality of volcanic mud and quarry dust based geopolymer.

Table 6: Apparent Porosity, Water Absorption and Apparent Density of Prepared Geopolymer Samples

Concentration of NaOH (M)	GP Sample No.	Apparent Porosity (%)	Water Absorption (%)	Apparent Density (g/ml))
	A-1	15.5	7.58	0.47
	A-2	11.71	8.54	0.56
4	A-3	13.46	6.47	0.79
	A-4	**16.87**	**9.86**	**0.82**
	A-5	11.74	5.48	0.98
	B-1	17.45	9.58	0.91
	B-2	13.79	8.26	0.63
8	B-3	14.54	6.87	0.79
	B-4	**18.91**	**10.54**	**0.91**
	B-5	16.74	7.24	0.63
	C-1	22.68	12.48	0.76
	C-2	17.63	9.53	1.25
12	C-3	22.45	10.54	1.49
	C-4	**23.96**	**13.58**	**1.01**
	C-5	21.57	10.69	1.00

1= 1:1, 2= 1:2, 3=2:1, 4=1:3, 5=3:1($NaOH:Na_2SiO_3$)

Table 7: Compressive Strength of Volcanic Mud and Quarry Dust (1:1) Based Prepared Geopolymer at 7, 14 and 28 days

Concentration of NaOH (M)	Sample No	7 day (N/mm^2)	14 day (N/mm^2)	28days (N/mm^2)
4	A-1	7.45	9.71	13.26
	A-2	8.11	11.28	14.78
	A-3	5.55	7.56	11.47
	A-4	8.25	12.45	16.49
	A-5	7.23	10.23	14.56
8	B-1	9.54	11.74	15.59
	B-2	6.37	10.53	13.42
	B-3	5.44	8.68	12.37
	B-4	12.74	14.56	17.47
	B-5	5.34	7.44	10.54
12	C-1	10.54	12.77	16.12
	C-2	11.71	14.52	17.47
	C-3	12.46	16.12	18.47
	C-4	14.54	16.65	19.85
	C-5	9.68	12.62	17.95

Table 8. Water Absorption, Apparent Porosity, and Apparent Density Prepared Geopolymer Samples (110˚C)

Group	Mix No(V:Q)	Apparent Porosity (%)	Water Absorption (%)	Apparent Density (%)
4	1:1	25.30	18.53	1.89
	1:2	22.01	10.40	1.51
	2:1	25.02	11.60	1.76
8	1:1	23.43	16.47	1.73
	1:2	22.41	10.34	1.41
	2:1	23.35	12.41	1.31
12	1:1	30.50	19.30	2.41
	1:2	24.40	12.80	1.98
	2:1	28.49	14.56	2.20

Mechanical Strength of Volcanic Mud and Quarry Dust Based Geopolymer

Table 9 show that the compressive strength values was found to be high in (1:1weight ratio) at 28 days. Compressive strength values increased as the densities increased. In this research work, the compressive strength was found to be increased as the curing time increased. Table 10 show that the maximum compressive strength of blended cement: commercial cement (1:2)is 35.76 N/mm^{2}at 28 days.

Table 9. Relationship between Time and Compressive Strength of Prepared Geopolymer (GP) in Various Ratio of Volcanic Mud and Quarry Dust

	Compressive Strength (N/mm^2) in different time intervals								
Prepared GP	4M			8M			12M		
Volcanic mud : Quarry dust (weight ratio)	7 days	14 days	28 days	7 days	14 days	28 days	7 days	14 days	28 days
1:1	8.52	11.96	15.41	14.05	17.63	19.36	16.44	18.58	21.41
1:2	6.70	10.74	13.74	11.88	15.91	15.91	13.40	15.27	18.27
2:1	7.9	11.57	14.57	12.18	17.43	17.43	14.05	17.67	20.67

Table 10. Relationship between Time and Compressive Strength of Prepared Blended Cement in Various Ratio and Cement (Alpha Cement Brand)

Blended Cement (BC)	GP: Commercial Cement (weight ratio)	Compressive Strength (N/mm^2) in different time interval		
		7 days	14 days	28 days
BC 1	1:1	21.83	25.45	28.41
BC 2	1:2	28.34	31.71	35.76
BC 3	2:1	23.39	27.89	30.14
Cement (Alpha Cement Brand)	Cement (Alpha Cement Brand)	35.09	40.89	42.61

Conclusion

In this research, volcanic mud and quarry dust were used for the preparation of geopolymer. The determination of physicochemical properties of volcanic mud sample from Kyaukphyu Township and quarry dust sample from Loikaw Township was carried out. From the experimental work, moisture 3.7%, LOI 5.3and pH 11.92,specific gravity 2.59 and fineness 27.8 were found in the volcanic mud sample. In the quarry dust sample, moisture 2.6 %, LOI 0.48 % and pH 9.46,specific gravity 2.57 and fineness12.9 were observed. From the EDXRF and XRD analysis, it was observed that the major oxide composition were present as SiO_2, CaO, Fe_2O_3 and Al_2O_3 in both samples. From the SEM photographs, the microstructure of quarry dust appeared to be glassy, hollow and porous structure. In the microstructure of volcanic mud sample, the micrograph indicates crystalline nature. It can be considered that the pores are micro-porosity sized particles. Same amount of mud volcanic and quarry dust and different ratio (1:1,1:2,2:1) of NaOH (4,8,12) M and Na_2SiO_3 were used as experimental design. The physiochemical test such as apparent porosity, water absorption, apparent density(110˚**C**) and compressive strength (7, 14 and 28 days) of each sample were measured to assess the quality of mud volcanic-quarry dust based geopolymer. Blended cement (GP: cement) and cement(Alpha Cement Brand) of different mixing ratio were carried out at different times. The mechanical strength of the prepared geopolymer (volcanic mud : quarry dust) increases with the higher amount of volcanic mud added but the best ratio was found to be1:1. For the blended cement, pure cement and geopolymer ratio 2:1 was the best.

Acknowledgements

The authors would like to express their profound gratitude to the Department of Higher Education (Yangon Office), Ministry of Education, Yangon, Myanmar, for provision of opportunity to do this research and Myanmar Academy of Arts and Science for allowing to present this paper.

References

Chaung, T. W. and Chiu, J. P. (2003).“Fire Resistance Geopolymer Produced by Granulated Blast Furnace Slags”. *Minerals Engineering*, vol.16, pp.205-210

Gambhir, M. L. (1995). *Concrete Technology*. New Delhi.
Second Edition, Ta ta Mc Graw-Hill Publishing Company Limited,vol53,pp.1742-1790

Khin Moe Aye.(2013). *A Study on Fly ash-Bentonitc Based Geopolymer in Concrete Production*. PhD Dissertation, Department of Chemistry, University of Yangon, Myanmar

Kyi Kyi San.(2013). *A Study on the use of Kalonitc and Fly Ash-Based Geopolymer for Immobilization of Toxic Material Ions*. PhD Dissertation, Department of Chemistry, University of Yangon, Myanmar

Mc Lellan, B. C .,Williams., R. P., Lay, J., Riessen, A. A. V and Corder, G. D. (2011). “Costs and Carbon Emissions for Geopolymer Pastes in Comparison to Ordinary Portland Cement”. *Journal of Cleaner Production*, vol .19, pp. 1080-1090

Neville, A. M. (2002). *Properties of Concrete* Essex. Fourth Edition, Pearson Education Limited

Palomo A.,M.W Grutzeck and M.T Blanco.(1999) “Alkali-activated Fly Ashes-A Cement for the Furture” Cement and Concrete Reserch, vol. 29 ,1323-1329.

Vogel, A.L. (1964).*A Text Book of Quantitative Inorganic Analysis*. Third Edition., Longmans, Green and Co., Ltd, London

PREPARATION AND CHARACTERIZATION OF HYDROXYAPATITE-MGO NANOCOMPOSITES AND THEIR ANTIMICROBIAL ACTIVITY AND ACUTE TOXICITY

Cho Lwin Lwin Khine[1], San Nwe Zin[2], Ni Ni Sein[3]

Abstract

The application of pure hydroxyapatite (HAp) are restricted to non load-bearing implants due to the poor mechanical properties of hydroxyapatite. To improve the mechanical properties of hydroxyapatite derived from cow bone, incorporation of magnesium oxide was conducted in this research. Hydroxyapatite was prepared by calcination of deproteinised cow bone waste using HCl and NaOH solutions. Magnesium oxide was prepared by wet chemical method treating magnesium nitrate solution with sodium hydroxide solution followed by thermal decomposition of magnesium hydroxide at 600 °C. After addition of magnesium oxide to HAp, the XRD pattern showed the two new peaks corresponding to magnesium oxide peaks at (200) and (220). Crystallite sizes of hydroxyapatite - MgO nanocomposites were 32.17 nm and 37.87 nm for HAp-5 % MgO nanocomposites calcined at 1000 °C and 1100 °C respectively. For HAp-10 % MgO nanocomposites the crystallite sizes were 31.46 nm and 36.70 nm, respectively for calcination temperature of 1000 °C and 1100 °C. Crystal structures of all HAp-MgO nanocomposites and HAp were indexed as hexagonal. FT IR spectral data revealed the characteristics peaks of both hydroxyapatite and MgO in the prepared nanocomposites. HAp-MgO nanocomposites showed mild antimicrobial activities on all tested organisms such as *Bacillus subtilis, Pseudomonas aeruginosa, Candida albicans, Escherichia coli, Staphylococcus aureus and Bacillus pumilus. In vivo* acute toxicity test on albino mice showed no mortality and no toxicity throughout the dosing schedule of 14 days at all dose levels in all groups.

Keywords: hydroxyapatite, magnesium oxide, wet chemical method, hydroxyapatite-MgO nanocomposites, antimicrobial activity, acute toxicity

[1]. 4 PhD, Candidate, Department of Chemistry, University of Yangon
[2]. Dr, Associate Professor, Department of Chemistry, Bago University
[3]. Dr, Professor (Retired), Department of Chemistry, University of Yangon

Introduction

Hydroxyapatite (HAp) is the main biomineral component found in human hard tissues, *i.e*., tooth and bone. Its stoichiometry is represented by the formula ($Ca_{10}(PO_4)_6(OH)_2$). It is comprised of calcium and phosphorus present in the ratio (Ca/P) of 1.67 (Oliveira and Mansur, 2007). It is the main mineral component of the enamel, comprising of more than 60 % of tooth dentin by weight (Goenka *et al*., 2012).

Hydroxyapatite has attracted much interest as a biomaterial for use in prosthetic applications due to its similarity in crystallography and chemical composition to that of human hard tissue. It has outstanding properties like biocompatibility, bioactivity, osteoconductivity, non-toxicity and non-inflammatory nature (Liu *et al*., 1997).

Hydroxyapatite is manufactured in many forms and can be prepared as a dense ceramic, powder, granules, ceramic coating or porous ceramic and various composites as required for the particular applications. However, in recent years, nano-sized hydroxyapatite with appropriate stoichiometry, morphology and purity have a high surface activity and ultrafine structure similar to the mineral found in hard tissues (Sadat-Shojai *et al*., 2013). Hydroxyapatite has got the ability to form a direct chemical bond with living tissues (Sobczak *et al*., 2009).

Synthetic hydroxyapatite can be prepared from an aqueous solution by solid state reaction or by hydrothermal methods (Damien and Revell, 2004). To prepare HAp from those sources needs analytical pure grade chemicals. HAp from natural origins differs from synthetic HAp in composition, crystal morphology, size, shape and physicochemical properties depending on the technology used to obtain the synthetic HAp. Calcination is one of the most used method. Nowadays, natural HAp is prepared (calcination method) from bovine, sheep, pig and goat bones (Sudipo *et al.,* 2012). It is already known that the mechanical properties of HAp are poor, especially in wet environment. For this reason, ceramics of pure HAp cannot be suggested for use in heavy-loaded implants, such as artificial bone or teeth. For improving the mechanical reliability of HAp ceramics, *i.e*., to increase their fracture toughness, incorporation of metallic material, ceramic oxide, whiskers or fibers have been suggested (Demirkol *et al*., 2012).

Magnesium oxide is one of the most successful candidates of reinforcement oxide. Magnesium is also a very important element in human body related to mineralization of calcined tissues, apatite crystallization, destabilization of HAp and thermal conversion of HAp to β-tricalcium phosphate (β-TCP, $Ca_3(PO_4)_2$). Magnesium seemingly reduces risks of cardiovascular diseases, promotes catalytic reactions and controls biological functions of human body (Oktar *et al*., 2007).

Many investigations on the preparation and characterization of hydroxyapatite (HAp) from various aspects have been reported by Myanmar researchers (Thin Thin Nwe, 2005; Than Than Khaing, 2006; Khin Thu Thu Min, 2006; Min Min Than, 2013; Aung Win Thant, 2014 and Zaw Moe Oo, 2014). The present paper is concerned with the preparation and characterization of cow bone HAp-MgO nanocomposites, and investigation of its antimicrobial activity and acute toxicity.

Materials and Methods

The experimental works were conducted at the Department of Chemistry, University of Yangon (UY). Hydroxyapatite (HAp) was prepared from readily affordable biowaste cow bone employing simple unit operations and acid-alkali processes.

Sample Collection

Cow bone samples were collected from Mingalar Taung Nyunt retail market in Yangon Region.

Sample Preparation

Raw cow bone sample worked with distilled water (1 kg) was crushed into splintered bone pieces. It was boiled in a steel pot immersed in 2 L of hot distilled water contained in a steel pot for 4-5 h. Boiling was repeated 3 more times. The boiled sample (800 g) was then pressure cooked in 2 L of distilled water, under pressure of 5-7.5 psi. Pressure cooking was repeated 3 more times with fresh distilled water. Washing, boiling and pressure cooking removed any adhering oil, fat, meaty things plus some contaminated dirt and

microorganisms. Dried bone pieces were then treated with 1M HCl (2 L) in a glass tank for about 24 h accompanied by occasional stirring. After the acidification, bone pieces were washed with distilled water to a nearly neutral state (pH 6.5-7.3) the bone pieces were then immersed in 2 L of 1 M NaOH for about 24 h. The alkali treated bone pieces were repeatedly washed with distilled water to a neutral state. It was air dried and pulverized to a powder form (44 μm). The acid-alkali treatment removed any remaining tissue, fatty matter and making the splintered bones more porous and brittle. It aided the splintered bones to be ground to the powder form. The hydroxyapatite powder was calcined at 900 °C in a muffle furnace.

Synthesis of Magnesium Oxide Nanoparticles

Magnesium oxide nanoparticles were prepared by wet chemical method using magnesium nitrate hexahydrate and sodium hydroxide as precursors and soluble starch as stabilizing agent. Starch act as a stabilizing agent and also prevents the agglomeration of nanoparticles (Agrawal *et al*., 2015). Starch (0.1 % concentration) solution was prepared in 100 mL of distilled water and magnesium nitrate 0.4 mol was added to the above solution. Then the solution was kept under constant stirring using magnetic stirrer for complete dissolution of contents. After complete dissolution, 0.8 mol of sodium hydroxide solution was added in drops along the sides of the container under constant stirring for 2 h and allowed to settle for 24 h. The supernatant liquid was then discarded carefully and the remaining solution was centrifuged (3000 rpm at 25 °C) for 30 min. Centrifugate was washed three times using distilled water and ethanol to remove the by-products and the excessive starch that bound with the nanoparticles. The nanoparticles of magnesium hydroxide were dried in an oven at 100 °C for 4 h and annealed in a muffle furnace at 600 °C for 4 h to obtain magnesium oxide. During this process, conversion of magnesium hydroxide into magnesium oxide took place.

Synthesis of Hydroxyapatite-MgO Nanocomposites

MgO (5 g) was dispersed in 20 mL of distilled water with the help of a magnetic stirrer for 1 h. The hydroxyapatite suspension was also prepared using the ratio of 1:1 for powder (100 g) and water (100 mL) by means of magnetic stirring for 1 h to get homogeneity of the dispersion. In order to prepare HAp-MgO nanocomposites, the weight percentages (wt %) of 5 and 10 were chosen. The prepared MgO suspension was poured into the HAp solution and then was thoroughly mixed using stirrer at 80-90 °C for 1 h. The obtained suspension was cooled to room temperature for 12 h. In addition, it was filtered using a funnel through filter paper. The residues were washed 2 to 3 times with distilled water. Then, it was transferred into porcelain basin and placed in an oven at 120 °C for 4 h to obtain dried sample. Moreover, the resulting products were annealed at 1000 °C and 1100 °C for 4 h.

Characterization Techniques

TG-DTA (DTG-60 H) Thermal Analyzer, Shimadzu, Japan was employed for investigation of the thermal property of prepared magnesium oxide and cow bone hydroxyapatite. The sample was scanned from 40 °C to 600 °C under nitrogen atmosphere with a flow rate of 50 mL min^{-1}. The techniques employed were in accordance with the company's catalogue.

Phase analysis and purity of prepared magnesium oxide, hydroxyapatite and hydroxyapatite-MgO nanocomposites obtained were investigated by X-ray analysis. X-ray diffraction patterns of the samples were recorded on X-ray diffractometer (Rigaku, Tokyo, Japan), using CuK_α radiation (λ= 1.54 Å) at 40 kV and 40 mA. The diffraction angle ranged from 10^o to 70^o of 2θ. The crystallite size was calculated by Scherrer method. The crystallinity percent was obtained by dividing total area of crystalline peaks by total area of all peaks.

Fourier transform infrared (FT IR) spectra of the samples was recorded on a FT IR spectrometer (FT IR-8400 SHIMADZU, Japan). FT IR analysis was in a range of wavenumber from 4000 to 440 cm^{-1}.

The morphology of the samples were observed by scanning electron microscopy (JEOL-JSM 5610 LV, Japan).

In vitro Investigation of Antimicrobial Activity of HAp-MgO Nanocomposites

Antimicrobial activities of HAp-MgO nanocomposites were tested by agar well diffusion method at Pharmaceutical Research Department (PRD), Yangon. The microorganism selected were *B. subtilis*, *S. aureus*, *P. aeruginosa*, *B. pumilus*, *C. albicans* and *E. coli*. Nutrient agar was prepared according to method described by Cruickshank (1975). Briefly, nutrient agar was boiled and 20-25 mL of the medium was poured into a test tube and plugged with cotton wool and autoclaved at 121 °C for 15 min. Then the tubes were cooled down to 60 °C and poured into sterile petri dish and 0.1 mL of spore suspension was also added into the dishes. The agar was allowed to set for 30 min after which 10 mm plate agar well was made with the help of sterilized cork borer. After that, about 0.1 mL of sample was introduced into the agar well and incubated at 37 °C for 24 h. The inhibition zone (clear zone) appeared around the agar well indicated the presence of antimicrobial activity. The extent of antimicrobial activity was measured from the zone of inhibition diameter.

In vivo Acute Toxicity Test of HAp-MgO Nanocomposites

Acute toxicity of HAp-MgO nanocomposites was tested according to the methods of OECD Guidelines for the Testing of Chemicals 423 at Laboratory Animal Services Division, Department of Medical Research (DMR), Yangon.

According to the test description, total number of 54 adult albino mice, weighing (25-30 g) were selected and divided into 9 groups. Each group contained six animals. They were fasted for 18 h before giving the HAp-MgO nanocomposites. Group (A 1 to D 2) mice were orally administered with HAp-MgO nanocomposites 2000 mg/kg dose and 5000 mg/kg dose (Figure 1). Group (E) mice performed as a control group and they were treated with clean water and normal animal food. All groups of mice were kept in the standard aluminium mouse cages and allowed to access food and water in the separate room at the room temperature of 26 ±1ºC. After administration, mortality and behaviour changes were continuously observed. Then the

animals were checked each 24 h for fourteen days. The mortality during this period was noted (Nil or percent death).

(a) Weighing albino mice

(b) Oral administration of HAp-MgO nanocomposite

Figure 1: Acute toxicity test on albino mice

Results and Discussion

TG-DTA Analysis

TG-DTA thermograms of magnesium hydroxide and magnesium oxide are shown in Figures 2 and 3. One decomposition step was observed in TG-DTA thermogram of magnesium hydroxide with a sharp endothermic peak appeared at 335.28 °C because of phase transition from magnesium hydroxide to magnesium oxide. The weight loss is 30.86 % which is in agreement with the theoretical weight loss of water (31.03 %). TG-DTA thermogram of magnesium oxide at 600 °C for 4 h showed a very small endothermic peak around at 280 °C due to loss of water. Furthermore, TG-DTA thermograms of HAp-MgO nanocomposites at 1000 °C and 1100 °C are shown in Figures 4, 5, 6 and 7 and thermal data are presented in Table 1. No inflection of TG curve with small weight loss was observed in each TG curved of HAp-MgO nanocomposites indicating the stability of the sample.

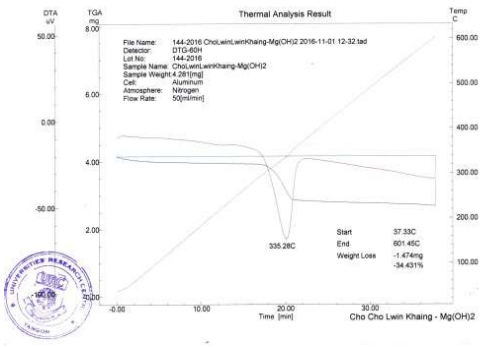

Figure 2: TG-DTA thermogram of magnesium hydroxide

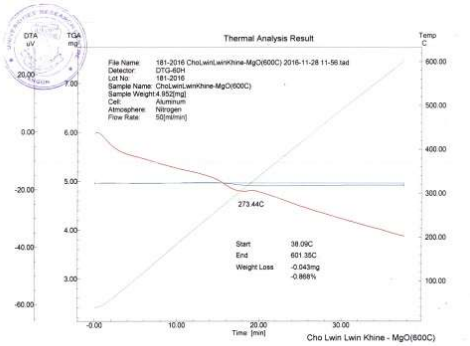

Figure 3: TG-DTA thermogram of magnesium oxide at 600 °C

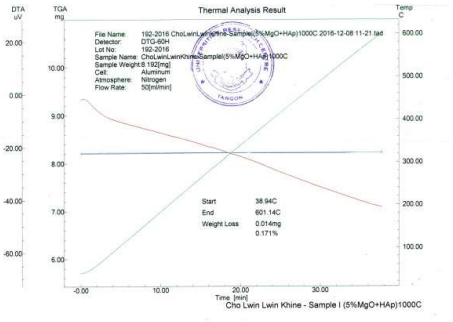

Figure 4:TG-DTA thermogram of HAp-5 % MgO at 1000 °C

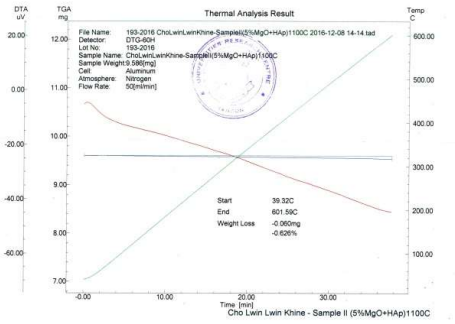

Figure : TG-DTA thermogram of HAp-5 % MgO at 1100 °C

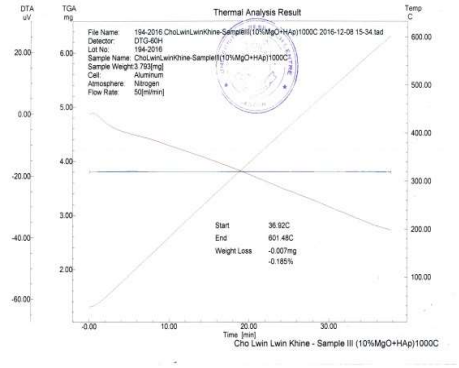

Figure 6: TG-DTA thermogram of HAp-10 % MgO at 1000 °C

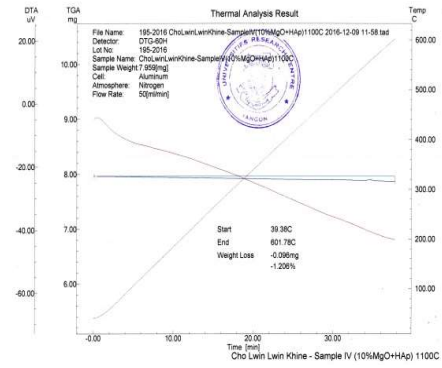

Figure 7: TG-DTA thermogram of HAp-10 % MgO at 1100 °C

Table 1: Thermal Analysis Data of Hydroxyapatite-MgO Nanocomposites

Sample	Temperature range (°C)	Initial weight (mg)	Final weight (mg)	Weight loss (%)	Remark
HAp-5 % MgO 1000 °C	38.94-601.14	8.192	8.178	0.171	Thermally stable
HAp-5 % MgO 1100 °C	39.32-601.59	9.586	9.526	0.626	Thermally stable
HAp-10 % MgO 1000 °C	36.92-601.48	3.793	3.786	0.185	Thermally stable
HAp-10 % MgO 1100 °C	39.38-601.78	7.959	7.863	1.206	Thermally stable

XRD Analysis

The well-resolved XRD pattern of hydroxyapatite (Figure 8) could be easily indexed on the basis of hexagonal crystal system with equal length of a and b axes (a=b= 9.4009 Å) and shorter length of c axis (c= 6.8757Å). The mean crystallite size of hydroxyapatite sample has been estimated from full width at half maximum (FWHM) and Scherrer equation according to the following formula:

$$\tau = \frac{0.9\,\lambda}{\beta \operatorname{Cos} \theta}$$

where τ is the crystallite size (nm), λ is the diffraction wavelength (0.154056 nm for Cu K_α radiation), θ is the diffraction angle (degree) and β is the full width at half maximum (FWHM) for the diffraction peak (radian). The prepared magnesium oxide samples were subjected to XRD analysis and three well-defined diffraction peaks were observed in each diffractogram at Miller indices of (111), (220) and (200) (Figure 9). A single phase of magnesium

oxide with face-centered cubic structure and space group of Fm3m was observed from XRD analysis. After addition of magnesium oxide to hydroxyapatite, the XRD patterns of HAp-MgO nanocomposites showed two new peaks corresponding to magnesium oxide peaks at (200) and (220) (Figure 10). Crystallite sizes of prepared magnesium oxide was found to be 21.71 nm and crystallinity of magnesium oxide is 54.39 % (Table 2). For hydroxyapatite, the crystallite size and crystallinity percent are 78.24 nm and 63.51 %. Crystallite sizes of HAp-MgO nanocomposites were 32.17 nm and 37.87 nm for HAp-5 % MgO nanocomposites calcined at 1000 °C and 1100 °C respectively. For HAp-10 % MgO nanocomposites the crystallite sizes were 31.46 nm and 36.70 nm, respectively, for calcination temperature of 1000 °C and 1100 °C. Crystallinity values of HAp-5 % MgO nanocomposites were 70.65 and 76.49 % and those of HAp-10 % MgO nanocomposites were 68.12 % and 75.39 %, respectively, at 1000 °C and 1100 °C. With increase in temperature the crystallite size and percent crystallinity of HAp-MgO nanocomposites were found to increase. However, the results were reversed as the amount of magnesium oxide was increased. Moreover, peak positions were slightly shifted to lower positions as the temperature increased from 1000°C to 1100°C (Table 3). Crystal structures of all HAp-MgO nanocomposites and HAp were hexagonal and that of MgO was cubic. Comparison of lattice constants of hydroxyapatite, magnesium oxide and HAp-MgO nanocomposites is shown in Table 4. The lattice constants of HAp-MgO nanocomposites noticeably changed from those of HAp and MgO indicating the formation of composite. Among the HAp-MgO nanocomposites, the lattice constants changed slightly with change in temperature and amount of magnesium oxide.

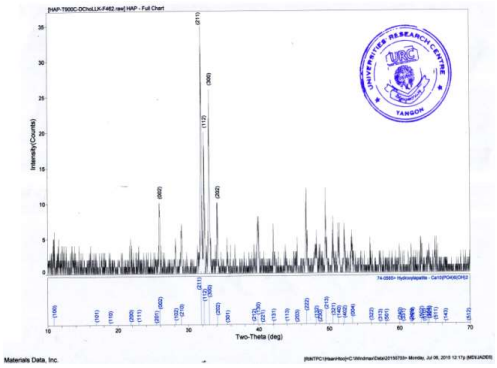

Figure 8: X-ray diffractogram of hydroxyapatite

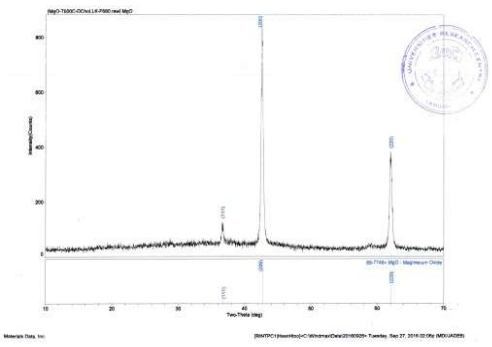

Figure 9: X-ray diffractogram of magnesium oxide at 600 °C

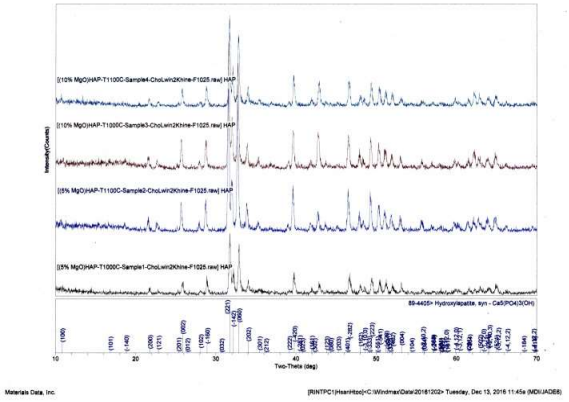

Figure 8: X-ray diffractogram of hydroxyapatite

Table 2: Average Crystallite Sizes and Crystallinity Percents of HAp, MgO and HAp-MgO Nanocomposites

No	Samples	Average crystallite size (nm)	Crystallinity (%)
1	HAp	78.24	63.51
2	MgO	21.71	54.39
3	HAp-5 % MgO Nanocomposite at 1000 °C	32.17	70.65
4	HAp-5 % MgO Nanocomposite at 1100 °C	37.87	76.49
5	HAp-10 % MgO Nanocomposite at 1000 °C	31.46	68.12
6	HAp-10 % MgO Nanocomposite at 1100 °C	36.70	75.39

Table 3: Changes of Peak Positions of HAp-MgO Nancomposites at Different Concentrations of MgO and Different Temperatures

Peak position 2 θ (degree)				Miller Indices hkl	Remark
HAp-5 % MgO 1000 °C	HAp-5 % MgO 1100 °C	HAp-10 % MgO 1000 °C	HAp-10 % MgO 1100 °C		
25.853	25.632	25.772	25.663	002	HAp
31.743	31.548	31.660	31.576	221	HAp
32.169	31.967	32.078	31.987	142	HAp
32.865	32.680	32.788	32.712	060	HAp
39.760	39.588	39.667	39.607	420	HAp
42.852	42.749	42.841	42.745	220	MgO
62.372	62.119	62.165	62.140	200	MgO

Table 4: Comparison of Lattice Costants of HAp, MgO and HAp-MgO Nanocomposites

Sample	Lattice Constants (Å)			Crystal structure
	a	b	c	
HAp	9.4009		6.8757	Hexagonal
HAp-5 % MgO at 1000 °C	9.5469		6.8434	Hexagonal
HAp-5 % MgO at 1100 °C	9.5998		6.9544	Hexagonal
HAp-10 % MgO at 1000 °C	9.5650		6.7985	Hexagonal
HAp- 10 % MgO at 1100 °C	9.5295		6.8878	Hexagonal
MgO	4.2357	4.2357	4.2357	Cubic

FT IR Analysis

FT IR spectra of hydroxyapatite, magnesium oxide and HAp-MgO nanocomposites with different MgO percents at 1000 °C and 1100 °C are shown in Figures 11 to 16. FT IR spectral data revealed the characteristics peaks of both hydroxyapatite and MgO in the prepared nanocomposites (Table 5). The characteristics peaks of hydroxyapatite in nanocomposites were observed between 700-400 cm^{-1} due to P-O bending vibration and between 1200-900 cm^{-1} due to P-O stretching vibration. Similarly, the characteristics peaks of MgO in nanocomposites were observed at 441 cm^{-1} and between 650-440 cm^{-1}due to MgO bending vibration.

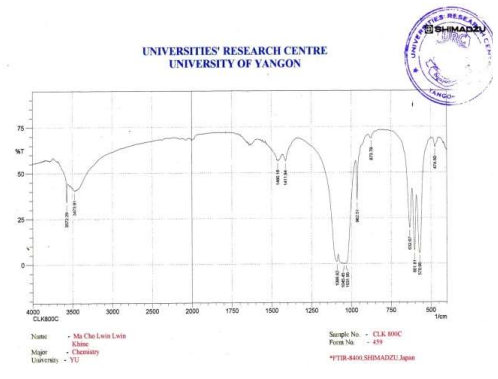

Figure 11: FT IR spectrum of hydroxyapatite

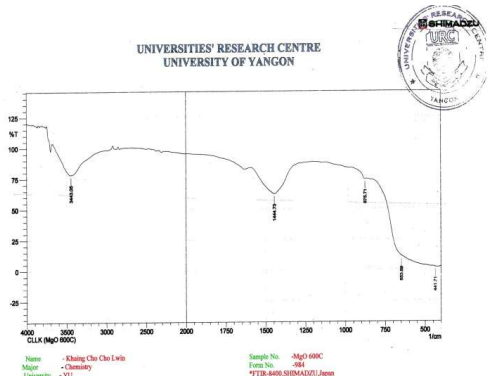

Figure 12: FT IR spectrum of magnesium oxide at 600 °C

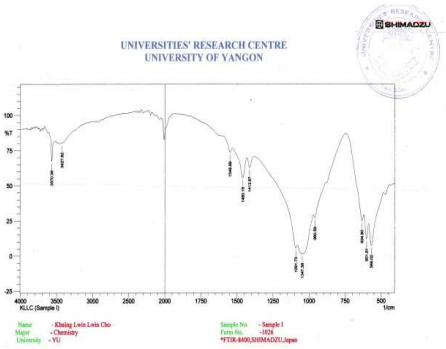

Figure 13: FT IR spectrum of HAp-5 % MgO at 1000 °C

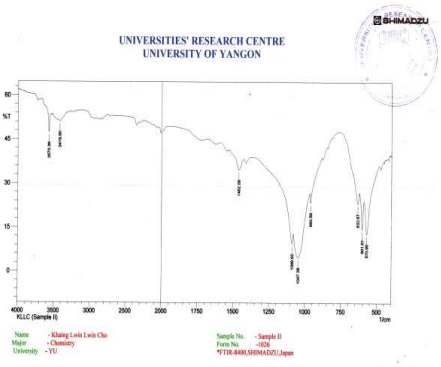

Figure 14: FT IR spectrum of HAp-5 % MgO at 1100 °C

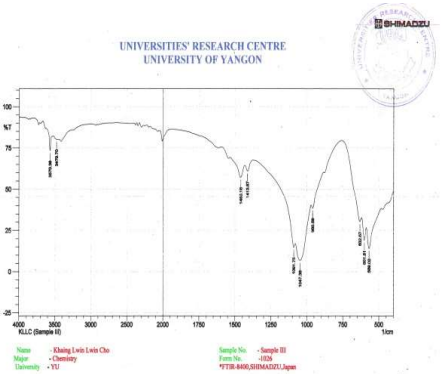

Figure 15: FT IR spectrum of HAp-10 % MgO at 1000 °C

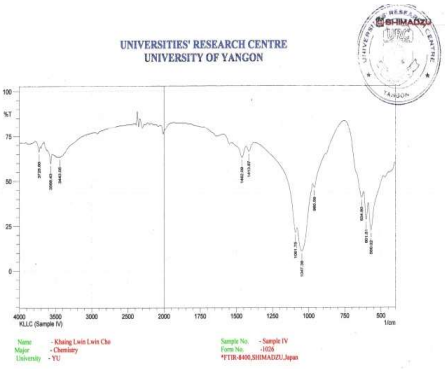

Figure 16: FT IR spectrum of HAp-10 % MgO at 1100 °C

Table 5: FT IR Spectral Data of HAp, MgO and HAp-MgO Nanocomposites

No	HAp	MgO	Wavenumber (cm^{-1})				Reported Values (cm^{-1})	Remark
			5 % MgO at 1000 °C	5 % MgO at 1100 °C	10 % MgO at 1000 °C	10 % MgO at 1100 °C		
1	3697		3570	3570	3510	3568	3500-3100*	Vibration of O-H
2	3443		3427	3419	3479	3443		
3		3440					3444**	O-H stretching vibration of physically adsorbed water molecules
4	1456		1460	1462	1460	1462	1629-1400*	Carbonate group
5	1413		1413		1413	1413		
6		1444					1600-1400**	O-H bending vibration of physically absorbed water molecules
7	1089		1091	1089	1091	1091	1200-900*	P-O stretching of phosphate
8	1047		1047	1047	1047	1047		
9	962		960	960	960	960		
10	877						871*	Carbonate group
11		653					650-450**	Mg-O deformation vibration
12	632		632	632	632	634	700-500*	P-O bending of phosphate
13	601		601	601	601	601		
14	570		569	570	569	569		
15	474	474	472	474	474	474	650-450**	Mg-O deformation vibration

* Nakamoto, 1970 ** Karthikeyan *et al.,* 2016

SEM Analysis

SEM images depict that magnesium oxide nanoparticles are appearing as spherical granule with slight agglomeration (Figure 17). Microscopic observations illustrated that the HAp-5 % MgO nanocomposite calcined at 1000 °C showed elongated shape. As the concentration of MgO increased, irregular shape are observed. Increasing temperature to 1100 °C, the poorly connected particles tend to agglomerate.

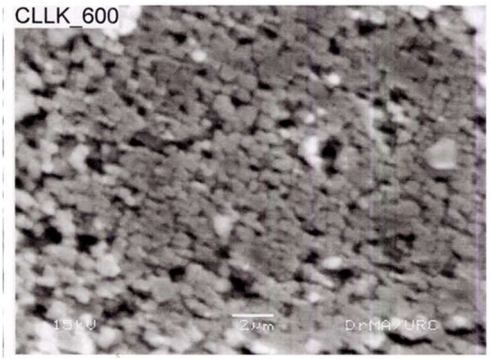

Figure 17: SEM image of magnesium oxide at 600 °C

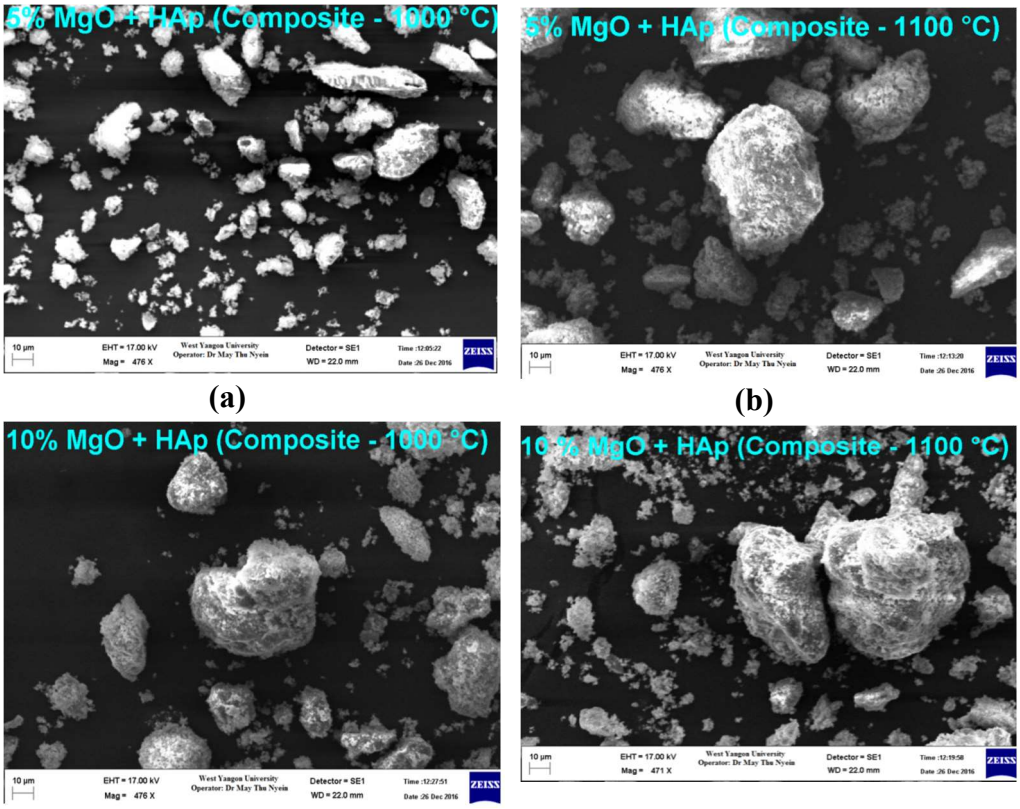

Figure 18: SEM images of HAp-5 % MgO nanocomposite at (a) 1000 °C (b) 1100 °C and HAp-10 % MgO nanocomposite at (c) 1000 °C (d) 1100 °C

Antimicrobial Activity of HAp-MgO Nanocomposites

Antimicrobial activities of HAp-MgO nanocomposites (5 % and 10 %) were investigated against six microorganisms. HAp-MgO nanocomposites (5 % and 10 %) only showed mild antimicrobial activities on all tested organisms such as *Bacillus subtilis, Pseudomonas aeruginosa, Candida albicans, Escherichia coli, Staphylococcus aureus and Bacillus pumilus* (Table 6).

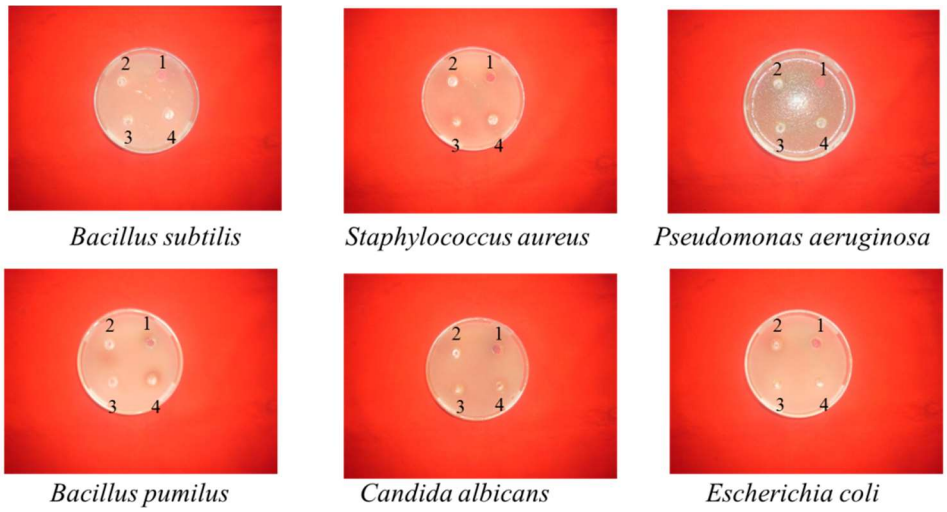

1 = control
2 = HAp
3 = HAp-5 % MgO at 1000 °C
4 = HAp-5 % MgO at 1100 °C

Figure 19: Antimicrobial activity of HAp and HAp-5 % MgO nanocomposites with six tested microorganisms

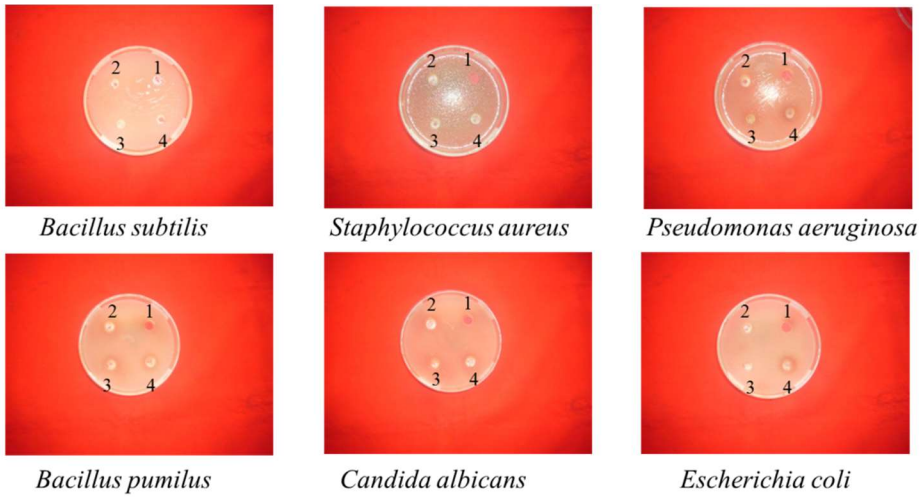

Figure 20: Antimicrobial activity of HAp and HAp-10% MgO nanocomposites with six tested microorganisms

Table 6: Antimicrobial Activities of HAp-MgO Nanocomposites

Samples	Inhibition Zone Diameters (mm)					
	B. subtilis	***S. aureus***	***P. aeruginosa***	***B. pumilus***	***C. albicans***	***E. coli***
Control	DW	DW	DW	DW	DW	DW
HAp	12	12	12	12	12	12
HAp-5 % MgO at 1000 °C	13 mm (+)	13 mm (+)	12 mm (+)	12 mm (+)	13 mm (+)	13 mm (+)
HAp-5 % MgO at 1100 °C	13 mm (+)	13 mm (+)	12 mm (+)	13 mm (+)	13 mm (+)	13 mm (+)
HAp-10 % MgO at 1000°C	13 mm (+)	12 mm (+)	13 mm (+)	12 mm (+)	13 mm (+)	12 mm (+)
HAp-10 % MgO at 1100°C	13 mm (+)	12 mm (+)	13 mm (+)	13 mm (+)	13 mm (+)	13 mm (+)

Agar well – 10 mm
10 mm ~ 14 mm (+)
15 mm ~ 19 mm (++)
20 mm above (+++)

Acute Toxicity Tests of HAp-MgO Nanocomposites on Albino Mice Model

Acute toxicity screening of HAp-MgO nanocomposite was done with the dosage of 2000 mg/kg and 5000 mg/kg body weight in each group of albino mice. The condition of mice groups were recorded after fourteen days administration. No lethality of the mice was observed until 2 weeks with the maximum dose of administration (Table 7). Each group of animals was also observed still alive and did not show any visible symptoms of toxicity like restlessness, respiratory disorders, convulsion, aggressive activities, coma and death. Even with the dose up to 2000 mg/kg and 5000 mg/kg body weight administration, there was no lethality at the day of fourteen.

Table 7: Results of Acute Toxicity Study of HAp-MgO Nanocomposites on Albino Mice Model

Group	Dose (mg/kg)	No. of mice tested	Observed periods (d)	Death per test
A 1	2000	6	14	0/6
A 2	5000	6	14	0/6
B 1	2000	6	14	0/6
B 2	5000	6	14	0/6
C 1	2000	6	14	0/6
C 2	5000	6	14	0/6
D 1	2000	6	14	0/6
D 2	5000	6	14	0/6
E (Control)	-	6	14	0/6

A 1, A 2 = HAp-5 % MgO at 1000 °C C 1, C 2 = HAp-10 % MgO at 1000 °C

B 1, B 2 = HAp-5 % MgO at 1100 °C D 1 D 2 = HAp-10 % MgO at 1100 °C

Conclusion

HAp-MgO nanocomposites were successfully prepared in this research. TG-DTA analysis showed the stability of the HAp-MgO nanocomposites. Higher temperatures lead to higher percent crystallinity resulting in with increasing crystallite sizes. Decrease in MgO content caused the lower percent crystallinity and crystallite size. FT IR spectral data revealed the presence of characteristic peaks of both MgO and HAp in HAp-MgO nanocomposites. On addition of magnesium oxide content and increase in temperature, peak position slightly shifted to lower positions. The shift indicated the change in morphology and crystal orientation. Hydroxyapatite-MgO nanocomposites have mild activity on six tested microorganisms. *In vivo* acute toxicity test revealed that no lethality of the albino mice was observed oven up to fourteen days of administering.

Acknowledgements

The authors would like to express their profound gratitude to the Department of Higher Education (Yangon Office), Ministry of Education, Myanmar for provision of opportunity to do this research.

References

Agrawal, R. M., Charpe, S. D., Raghuwanshi, F. C. and Lamdhade, G. T. (2015). "Synthesis and Characterization of Magnesium Oxide Nanoparticles with 1:1 Molar Ratio via Liquid-Phase Method". *International Journal of Application or Innovation in Engineering and Management,* vol. 4(2), pp.141-144

Aung Win Thant. (2014). *Preparation and Characterization of Hydroxyapatite from Fish Bone*. MSc Thesis, Department of Chemistry, University of Yangon

Cruickshank, R. (1975). *Test for Sensitivity to Antimicrobial Agents in Medical Microbiology*. Edinburgh: 12th Edition, Churchill Livingston Publication, pp.120-122

Damien, E. and Revell, P. A. (2004). "Coralline Hydroxyapatite Bone Graft Substitute; A Review of Experimental Studies and Biomedical Application". *Journal of Applied Biomaterials and Biomechanics*, vol. 2, pp. 65-73

Demirkol, N., Meydanoglu, O., Gokce, H., Oktar, F. N. and Kayali, E. S. (2012). "Comparison of Mechanical Properties of Sheep Hydroxyapataite (SHA) and Commercial Synthetic Hydroxyapatite (CSHA)-MgO Composites". *Key Engineering Material.,* vol. 493-494, pp. 588-593

Goenka, S., Balu, R. and Sampath, K. T. S. (2012). "Effects of Nanocrystalline Calcium Deficient Hydroxyapatite Incorporation in Glass Ionomer Cements". *J Mech Behav Biomed Mater*., vol. 7, pp. 69-76

Karthikeyan, V., Dhanapandian, S. and Manoharan, C. (2016). "Characterization and Antibacterial Behavior of MgO Nanoparticles Synthesized via Co-precipitation Method". *International Journal for Scientific Research and Development,* vol. 10(1), pp. 2321-2323

Khin Thu Thu Min. (2006). *Studies of Bioceramics Iron and Zinc Substituted Hydroxyapatites*. PhD Dissertation, Department of Chemistry, University of Yangon

Liu, C., Wang, W., Shen, W., Chen, T., Hu, L. and Chen, Z. (1997). "Evaluation of the Biocompatibility of A Nonceramic Hydroxyapatite". *J Endod*., vol. 23, pp. 490-493

Min Min Than. (2013). *Removal of Some Heavy Metal Ions by using Synthetic Carbonate Hydroxyapatit*e. PhD Dissertation, Department of Chemistry, University of Yangon

Nakamoto, K. (1970). *Infrared Spectra of Inorganic and Coordination Compounds*. New York: 2nd Edition, Wiley Interscience Publication, pp. 252-254

Oktar, F. N., Agathopoulos, S., Ozyegin, L. S., Gunduz, O., Demirkol, M., Bozkurt, Y. and Salman, S. (2007). "Mechanical Properties of Bovine Hydroxyapatite (BHA) Composite Doped with SiO_2, MgO, Al_2O_3 and ZrO_2". *J. Mater Sci: Mater Med.*, vol. 18, pp. 2127-2143

Oliveira, M. and Mansur, H. S. (2007). "Synthetic Tooth Enamel: SEM Characterization of a Fluoride Hydroxyapatite Coating for Dentistry Applications". *Mater Res.,* vol. 10, pp. 115-118

Sadat-Shojai, M., Khorasani, M. T., Dinpanah-Khoshdargi, E. and Jamshidi, A. (2013). "Synthesis Methods for Nanosized Hydroxyapatite with Diverse Structures". *Acta Biomater*., vol. 9, pp.7591-7621

Sobczak, A., Kowalski, Z. and Wzorek, Z. (2009). "Preparation of Hydroxyapatite from Animal Bones". *Acta of Bioengineering and Biomechanics,* vol. 11(4), pp. 23-28

Sudipo, B. M., Apurba, P. and Sudit, M. (2012). "Studies on Processing and Characterizations of Hydroxyapatite Biomaterials from Different Bio Wastes". *Journal of Minerals and Materials Characterization and Engineering,* vol. 11(1), pp. 55-56

Than Than Khaing. (2006). *Process Development of Biocompatible Calcium Phosphate Powders from Waste Material (Egg shell)*. PhD Dissertation, Department of Chemistry, University of Yangon

Thin Thin Nwe, Kyaw Naing, Khin Mar Tun and Nyunt Wynn. (2005). "Preparation and Characterization of Apatitic Biphasic Calcium Phosphate". *Jour. Myan. Acad. Arts & Sc*., vol. 3(1), pp. 1-7

Zaw Moe Oo. (2014). *Preparation and Characterization of Hydroxyapatite from Fish Scale*. MSc Thesis, Department of Chemistry, University of Yangon

COMPARATIVE STUDIES ON THE PREPARATION AND CHARACTERIZATION OF $LAFeO_3$ NANOCRYSTALLITE POWDER BY CITRATE SOL- GEL METHOD AND CO-PRECIPITATION METHOD

Kay Thi Tun[1], Mya Theingi[2], Nwe Nwe Aung[3]

Abstract

Lanthanum ferrite ($LaFeO_3$) nanocrystalline material is a promising material for its interesting electrical, magnetic, catalytic and thermoelectric properties. In this study, the nanocrystalline $LaFeO_3$ powder was prepared by citrate sol-gel method and co-precipitation method.In the citrate sol gel method, a modified Pechini method based on the polyesterification of citric acid and ethylene glycol for the synthesis of the $LaFeO_3$. The precursor for $LaFeO_3$ will be synthesized by co-precipitation from metal nitrate and carbonate salts. The properties of the $LaFeO_3$ powders were studied by TG-DTA, XRD, SEM, FT IR and EDXRF. The results showed that $LaFeO_3$was formed at the lower temperature in the citrate sol-gel method compared to co-precipitation method. The size of spherical $LaFeO_3$ synthesized by sol-gel was 20-25nm, whereas the sample prepared by co-precipitation yielded nearly tetragonal and flake like powder with particle size of 20-35nm. The difference in preparation methods results in the difference in the structure and morphology of prepared materials.

Keywords*:* Perovskite, $LaFeO_3$, citrate sol-gel method, co-precipitation method

Introduction

Perovskite materials exhibit many interesting and intriguing properties from both theoretical and application point of view. Colossal magneto resistance, ferroelectricity, superconductivity, charge ordering, spin dependent transport, high thermo power the interplay of structural, magnetic and transport properties are commonly observed features in this family. These perovskite compounds are used as sensors and catalyst electrodes in certain type of fuel cells, memory devices and spintronic applications (Kanta and Kumar, 2014). The general formula of perovskite is ABO_3 (where A is rare earth, alkaline earth or an alkali metal cation and B is 3d transition metal).A large ionic radius have12 fold coordination with oxygen atoms, occupying A-

[1.] Ph.D. candidate, Department of Chemistry, University of Yangon
[2.] Dr, Lecturer, Department of Chemistry, University of Yangon
[3.] Dr, Lecturer, Department of Chemistry, University of Yangon

sites and cations with a smaller ionic radius have 6 fold coordination occupying B-sites. The $LaFeO_3$ materials have been prepared by several techniques such as hydrothermal synthesis, micro emulsion, co-precipitation method, sol-gel method, solid state reaction, flame hydrolysis and electrochemical oxidation method (Unikoth *et al*., 2014). For achieving optimum performances and functional properties well defined microstructures are desirable, which in fact strongly depend on the method of synthesis. In this paper, we examined the preparation of $LaFeO_3$nanocrystals via the citrate sol-gel and co-precipitation method and investigated the comparative study of their calcination temperatures, crystal structure, surface morphology and elemental composition by modern techniques. In addition, the structural and morphological difference of $LaFeO_3$ prepared by different methods was investigated.

Materials and Methods

Synthesis of Perovskite $LaFeO_3$ Powder

Perovskite $LaFeO_3$nanocrystallite powder were prepared by two methods i.e. citrate sol-gel method and co-precipitation method. All AR-grade chemicals were used in the preparation of nanocrystallite powder. In the first method,$LaFeO_3$ was prepared by citrate sol-gel method in which the aqueous solution of $La(NO_3)_3$.$6H_2O$ and $Fe(NO_3)_3$.$9H_2O$ were mixed with citric acid that was equivalent in gram mole with that of the total cations (La^{3+}, Fe^{3+})(Anupama and Prasad, 2015). Subsequently 5 mL of ethylene glycol was added to the mixture solution. Resulting yellow coloured solution was heated at 80 °C under continuous stirring. After being heated for about 6 h, the resulting solution became highly viscous and the reddish brown transparent gel was formed. Finally, the xerogel was obtained after the gel was dried completely in an oven at 120 °C for 6 h. The xerogel was ground in the mortar and pestle. The dried powder was calcined at 400°C, 450 °C and 500 °C for 4 h. The citrate sol-gel synthesis occurs according to the following overall reaction (1) which gives rise to a perovskite powder and gaseous species.

$$La(NO_3)_3.6H_2O+Fe(NO_3)_3.9H_2O+nC_6H_8O_7+nC_2H_6O_2 \xrightarrow{\Delta} LaFeO_3+nCO_2\uparrow+nN_2+nH_2O \quad (1)$$

In the second method, $LaFeO_3$ was prepared by co-precipitation method in which nitrate precursors La $(NO_3)_3$ $.6H_2O$ and Fe $(NO_3)_3.9H_2O$ were mixed in the required stoichiometric ratio (i.e. La/ Fe= 1/1) to make aqueous solution. Then $(NH_4)_2CO_3$ solutions was added rapidly with continuous stirring. The precipitate was formed immediately by adding ammonium carbonate solution in nitrate solution, which was continuously stirred for 30 minutes at room temperature. After centrifuging, the precipitate was filtered and washed with deionized water, until pH 7. The prepared precipitate was dried at 110 °C for 6 hours and further calcined separately at 500 °C, 550 °C and 600 °Cfor 4 hours. The precipitation and calcination reactions may be represented by equations (2), (3) and (4) respectively.

$$La\ (NO_{3)3}\ .6H_2O + (NH_4)_2\ CO_3 + nH_2O \longrightarrow La^{3+} + nCO_3^{2-} + nNH_4^{+} + nNO_3^{-} \quad (2)$$

$$Fe\ (NO_3)_3.9H_2O + (NH_4)_2\ CO_3 + nH_2O \longrightarrow Fe^{3+} + nCO_3^{2-} + nNH_4^{+} + nNO_3^{-} \quad (3)$$

$$La^{3+} + Fe^{3+} + nCO_3^{2-} + nNH_4^{+} + nNO_3^{-} \longrightarrow LaFeO_3 + n\ CO_2\uparrow + nN_2\uparrow + nH_2O \quad (4)$$

Characterizations of the sample

The thermal decomposition behaviors of the powder prepared by two different methods were characterized by thermogravimetric and differential thermal analysis (TG-DTA) at a heating rate of 10˚C/min in nitrogen. The phase identification of the as-prepared powder was performed using X-ray diffractometer with CuK_α radiation (λ=1.5405Å).The lattice parameters and the average crystallite size were calculated using PDXL-software. The morphology of the as-prepared powder was characterized by scanning electron microscopy (SEM).The FTIR measurements have been performed in the KBr mode the region from 400- 4000 $cm^{-1}$was measured using 8400 SHIMADZU, Japan FTIR spectrometer. The elemental compositions of $LaFeO_3$ perovskite oxides prepared by two different methods were detected by using energy dispersive X-ray spectrometer (EDXRF).

Results and Discussion

Thermal Analyses

Thermogravimetric and differential thermal analysis (TG-DTA) was performed to study the thermal analysis behavior of the nanocrystallite powder obtained by two different methods. The respective thermograms are shown in Figure 1 and 2. During the citrate sol-gel synthesis, the process of oxides formation involves liberation of gaseous products, which is accompanied by a decrease of mass. The three sharp exothermic peaks (261, 365 and 408°C) were observed.The three broad exothermic lines might relate to the elimination of adsorbed water, the decomposition of nitrates and the combustion of organic residues due to the formation of expected perovskite $LaFeO_3$. Thermal decomposition of lanthanum ferrite prepared by co-precipitation method was investigated TG-DTA. The rate of weight loss takes place above 100 °C with slow rate up to 400 °C;there is no prominent weight loss above 400˚C. The DTA curve indicate small exothermic peak at 329°C which confirms the presence of phase transition behavior. There is no detectable change in both DTA and TGA curves up to 100 °C.

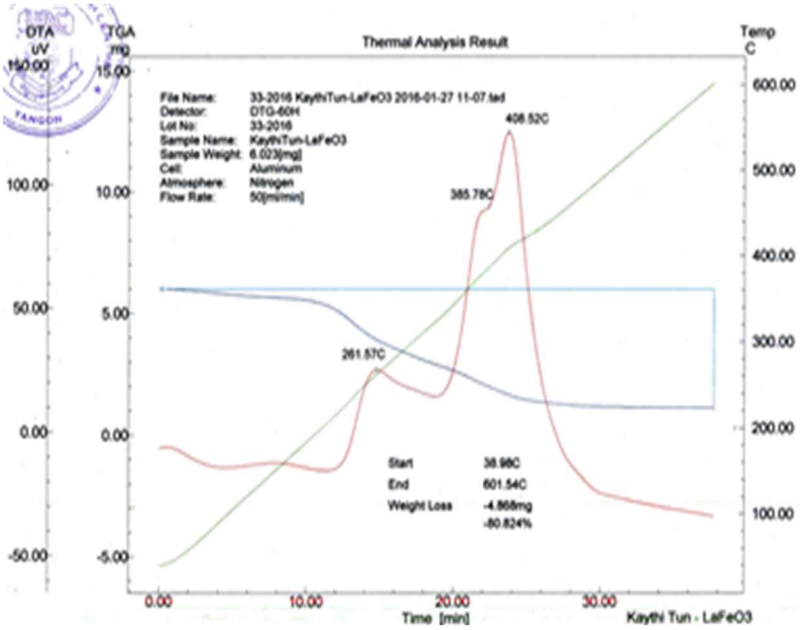

Figure 1: TG-DTA curve for the xerogel $LaFeO_3$ powder prepared by citrate sol-gel method

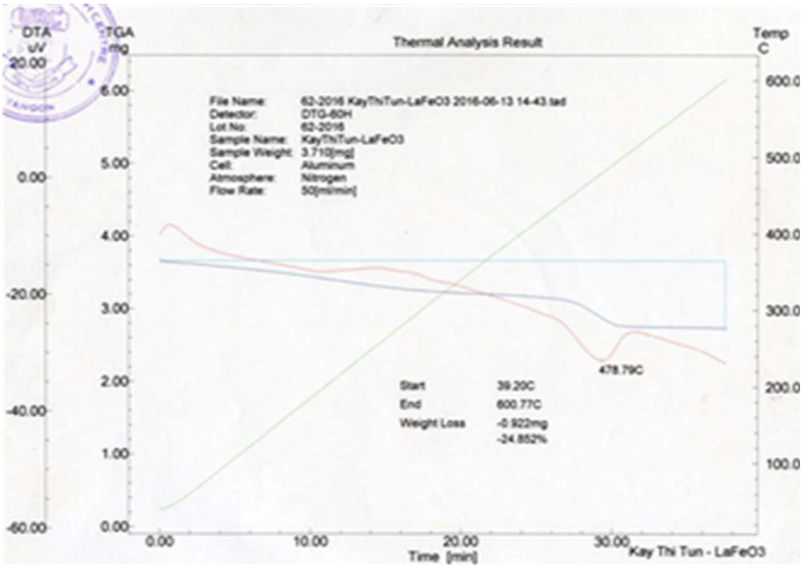

Figure 2: TG-DTA curve for the precursor $LaFeO_3$ powder prepared by co-precipitation method

XRD analysis

Phase confirmation and crystal structure of the compounds were investigated by X-ray diffractometer (XRD) at room temperature in the diffraction angle range of 2θ value 10-70ºC. XRD pattern of $LaFeO_3$ xerogel powder prepared by citrate sol–gel method are shown in Figure 3. Any diffraction peak is not observed in XRD pattern which indicates the prepared gel is mainly amorphous.Figure 4 shows diffraction patterns of $LaFeO_3$ powder calcined at 400˚C, 450˚C and 500˚C for 4 hours. At 400 ˚C for the citrate sol-gel sample, which is difficult to index according to the JCPDS data indicating that the powder is possiblyin amorphous form.The strongest peak and characteristic planes (110) of cubic crystalline structure observed at temperature 450˚C and 500˚C.

Furthermore,the XRD pattern of $LaFeO_3$ powder prepared by co-precipitation method before calcination is shown in Figure 5.Figure6shows the X-ray diffraction patterns of $LaFeO_3$ powder calcined at 500˚C, 550˚C and 600 ˚C for 4 hours in co-precipitation method.The XRD patterns at all calcination temperature that the intensities of three basic peaks of (103) plane

are more than the other peaks. The crystallite size of the sample prepared by different method was in the range of 20-35nm respectively.The difference in crystallite size was due to different preparation conditions for ferrite synthesis. $LaFeO_3$ prepared by the citrate sol-gel method displayed the most intense XRD peak, indicating their highest crystallinity. The XRD diagram of $LaFeO_3$ obtained by co-precipitation method show some diffraction peaks and this may be due to the phase purity is not completely achieved. The crystallite size of synthesized compounds obtained by different methods was calculated by the X-ray line broadening method using the Scherrer formula,

$$D = \frac{0.9\lambda}{\beta \cos\theta}$$

where D is the average crystallite size (nm), λ is the X-ray radiation wavelength (nm) and β is the X-ray diffraction full width peak at half maximum (rad) and θ is the Bragg's angle(degree). It shows a trend that the average crystallite size is larger at higher calcination temperature, which is related to the grain growth(Theingi, 2013). The resultant data are presented in Table 1.

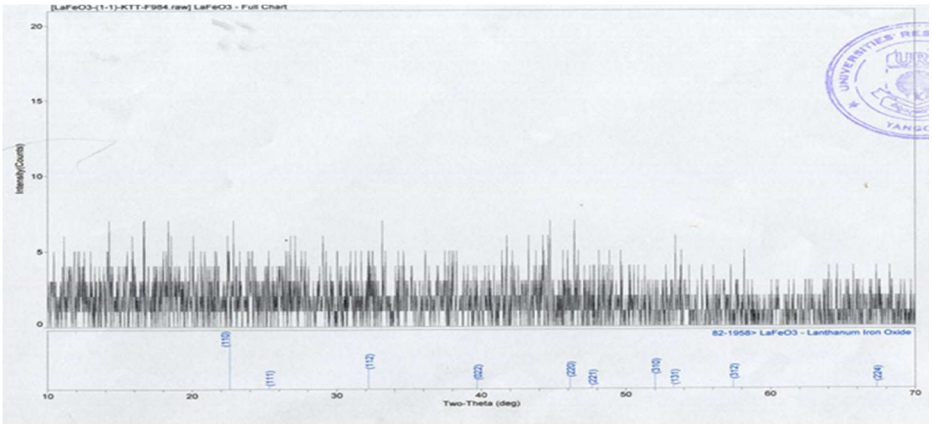

Figure 3: XRD diffraction pattern of xerogel $LaFeO_3$ powder obtained by citrate sol-gel method

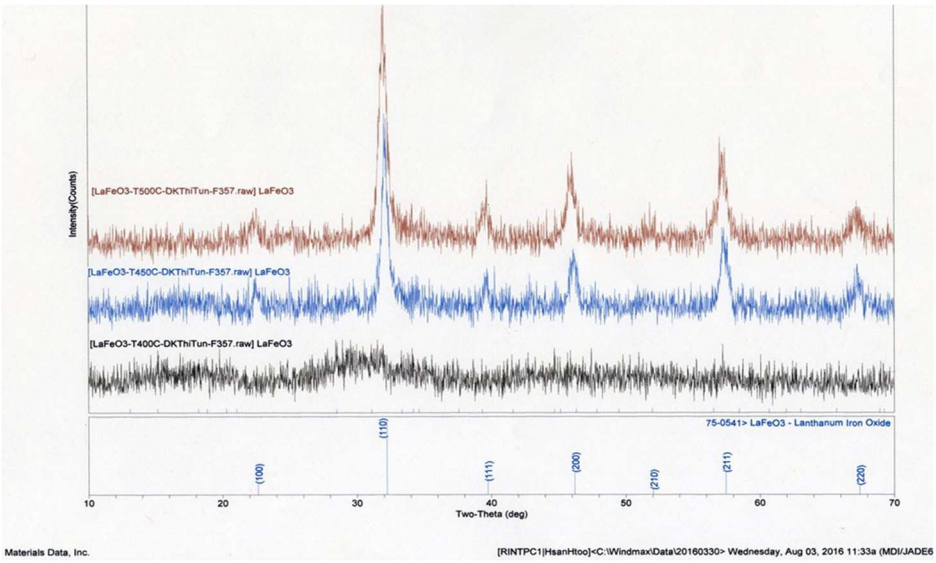

Figure 4: XRD diffraction patterns method of $LaFeO_3$ nanopowder at different calcined temperatures (a) 400˚C (b) 450˚C (c) 500 ˚C

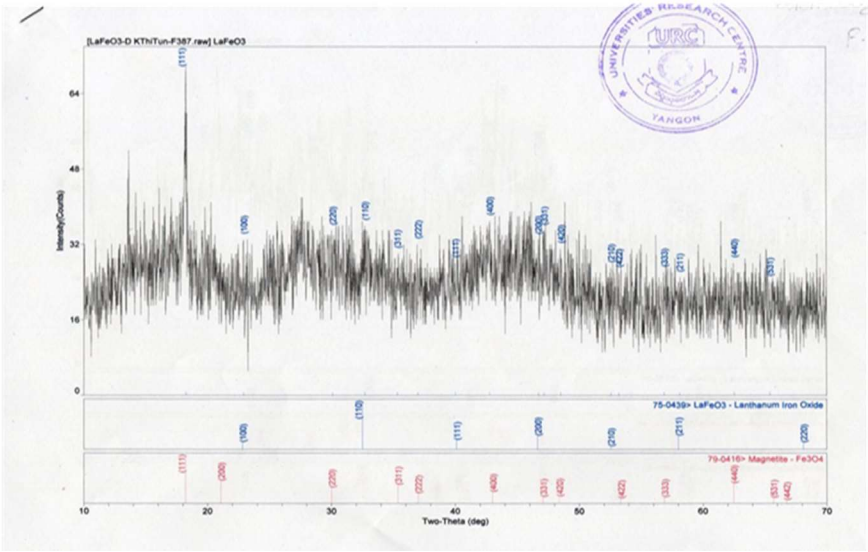

Figure 5: XRD diffraction pattern of $LaFeO_3$ precursor powder obtained by co- precipitation method

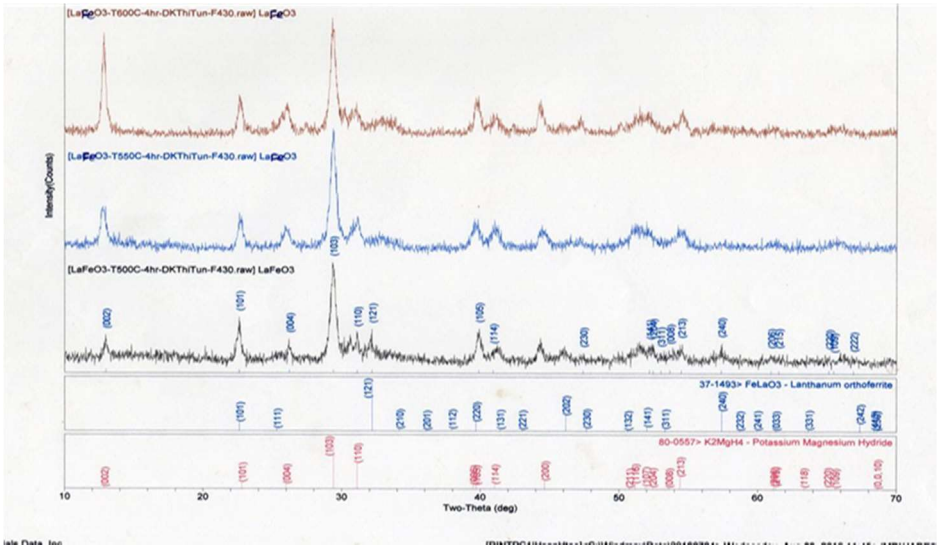

Figure 6: XRD diffraction patterns of $LaFeO_3$ nanopowder at different calcined temperature (a) 500˚C (b) 550˚C (c) 600 ˚C

Table 1: Crystallite size of $LaFeO_3$ Nanoparticle Prepared by Different Methods

Method	Calcination temperature (°C)	Crystallite size/D (nm)
Citrate sol-gel	450	23.26
	500	24.01
Co-precipitation	500	23.01
	550	29.80
	600	34.06

FTIR Analysis

FTIR spectra with wave number ranges from 400 – 4000 cm^{-1} are shown in Figures 7 and 8 for $LaFeO_3$prepared by citrate sol-gel method and co-preipitation method respectively. Both methods showed an intense band around 1629 cm^{-1} are assigned to asymmetric carbonyl group and 545cm^{-1} around the peak corresponds to Fe- O stretching vibration mode. The $LaFeO_3$ prepared byco-precipitation method, showed the absorption band appearing at 3404 cm^{-1} is due to the stretching vibration of hydroxyl group, whereas for

that prepared by citrate sol-gel method has not strong intense peak of the hydroxyl group band. The low intense peak observed in citrate sol-gel at 1483 cm^{-1} and 1383 cm^{-1} are due to the asymmetric stretching of metal carbonates. The absorption bands at around 1361,1448 and 1516 cm^{-1} as strong intense peak shown in $LaFeO_3$ prepared by co-precipitation are indicated the symmetric and asymmetric stretching vibraation mode of NO_2(Ghosh *et al*.,2010).

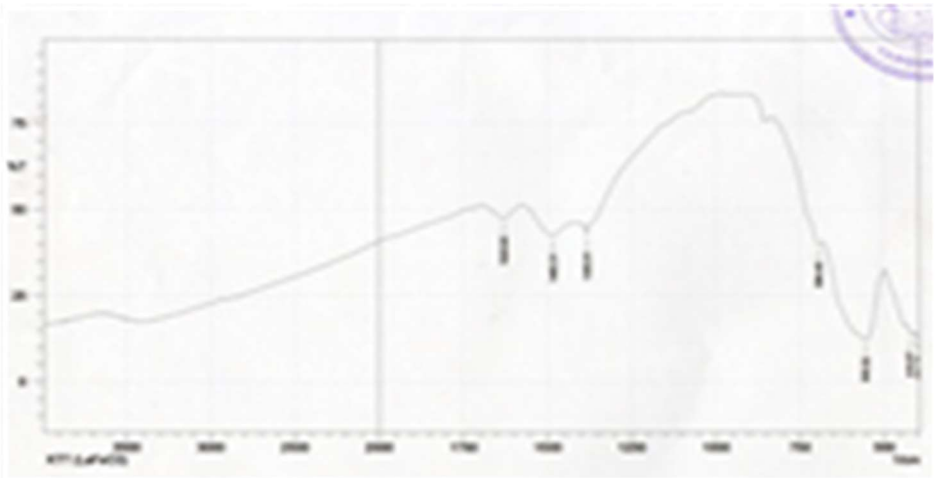

Figure 7: FT IR spectrum of $LaFeO_3$ nanopowder prepared by citrate sol-gel method calcined at 450˚C for 4 hours

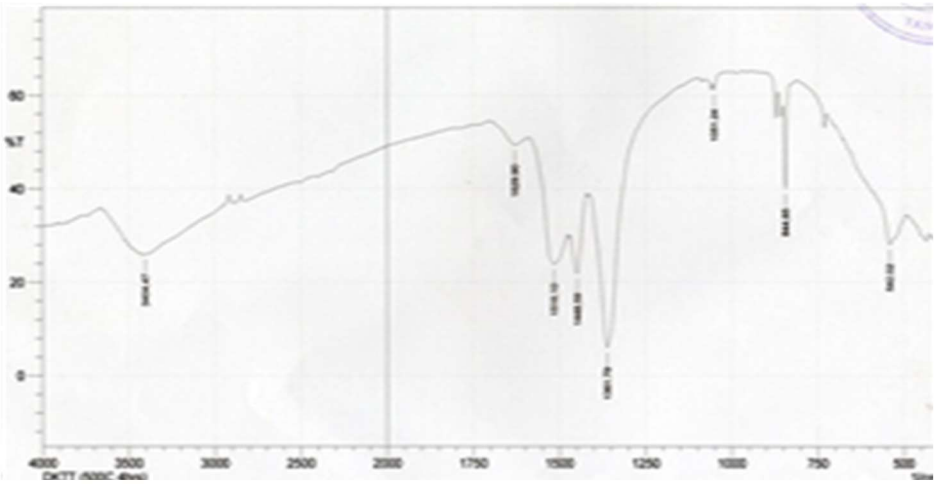

Figure 8: FT IR spectrum of $LaFeO_3$ nanopowder prepared co-precipitation method calcined at 500˚C for 4 hours

EDXRF analysis

For more details, the EDXRF which has higher sensitivity was used to confirm the elemental composition of perovskite $LaFeO_3$ samples synthesised by the two methods. From EDXRF analysis, La and Fe are main constituents elements prepared by two different methods as shown in Figures 9 and 10. The elements present are La, Fe and O with a mole ratio of 1:1:3 corresponding to the stoichiometric composition of $LaFeO_3$ obtained by citrate sol-gel method. It was found that the relative abundance of the $LaFeO_3$ prepared by citrate sol-gel method are match with the molecular formula of $LaFeO_3$.

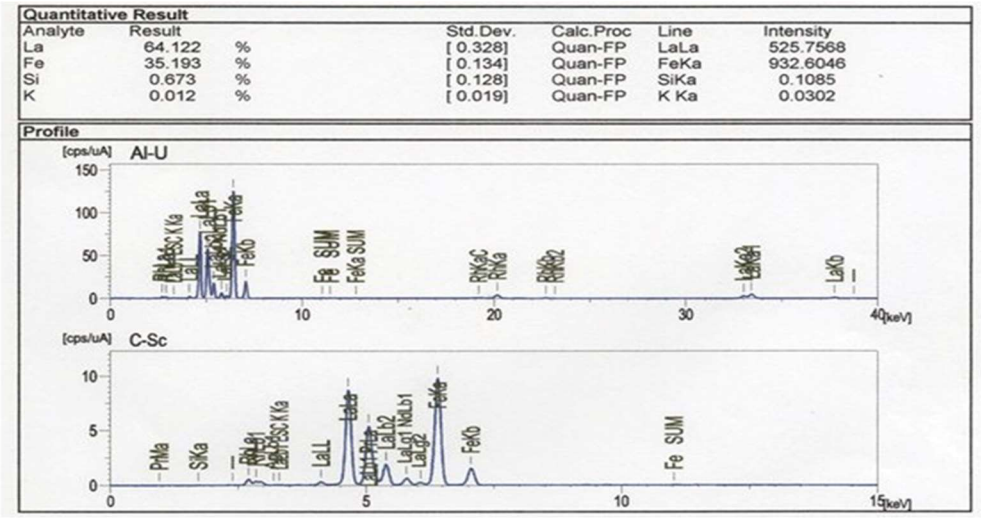

Figure 9: EDXRF spectrum of $LaFeO_3$ nanopowder synthesized by citrate sol-gel method calcined at 450°C for 4 h

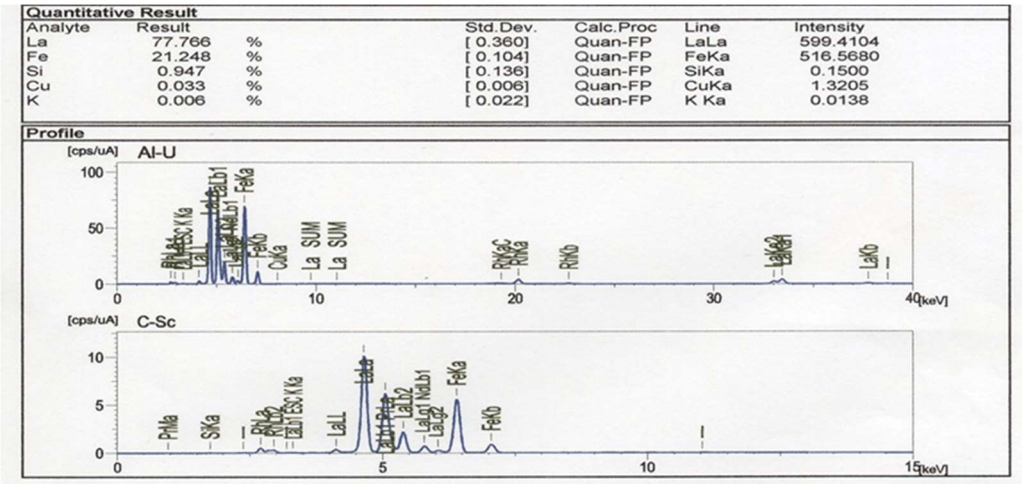

Figure 10: EDXRF spectrum of $LaFeO_3$ nanopowder prepared by co-precipitation method calcined at 500 °C for 4 hours

SEM analysis

Figures11 and12 show the SEM images of the particles synthesized by citrate sol-gel and co-precipitation methods. The citrate sol-gel particles have porous surface with uniform distribution unlike the strong agglomeration with varied size of the sample. The $LaFeO_3$ nanoparticles synthesized by co-precipitation method have different shapes with the size of 30-40 nm such as tetragonal or flake like structure, whereas citrate sol-gel $LaFeO_3$ nanoparticles are more spherical with uniform structure having the size distribution of 20-30 nm.

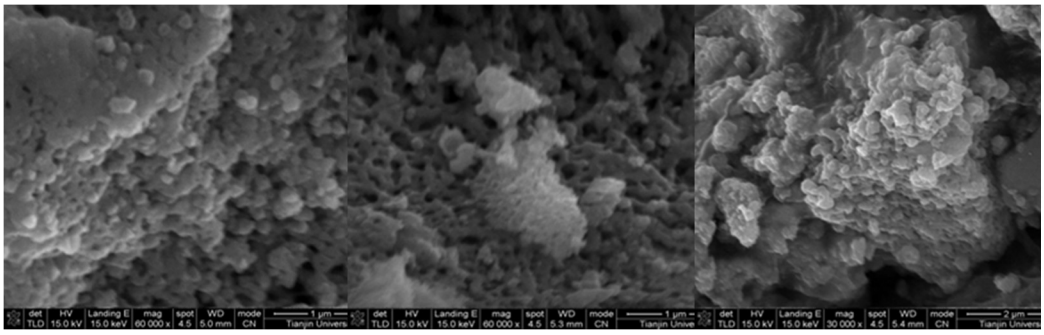

(a) **(b)** **(c)**

Figure 11: SEM micrographs of $LaFeO_3$ nanopowder prepared by citrate sol-gel method calcined at (a) 400˚C (b) 450˚C (c) 500˚C for 4 h

(a) (b) (c)

Figure 12. SEM micrographs of $LaFeO_3$ nanopowder prepared by co-precipitat method at (a)500 °C (b) 550 °C and (c) 600 °C for 4 hours

Conclusion

On the basis of the above systematical investigations, the following conclusions can be drawn. $LaFeO_3$ perovskite nanocrystallites were prepared by citrate sol-gel and co-precipitation methods. From XRD showed that not only existence of $LaFeO_3$phase but also the present of impurity secondary phases for co-precipitation method. On the other hand only single perovskite phase $LaFeO_3$was successfully prepared by citrate sol-gel method at low temperature(~450˚C). Thecrystallite structure of $LaFeO_3$ with cubic crystal structure was obtained in citrate sol-gel method at 450 °C and the tetragonal crystallite structure was obtained via the co-precipitation method at 500 °C. The SEM micrographs of $LaFeO_3$ prepared by two methods shown that the morphologies of $LaFeO_3$ were quite different. It was found that the particle size of the $LaFeO_3$ powder varies from 20 to 40 nm depending on the preparation method. According to FT IR data, the absorption band of metal-oxygen band of $LaFeO_3$ observed at citrate sol-gel method and many absorption bands appear in co-precipitation method. The EDXRF result has a little different these two methods. The major advantage of the citrate sol-gel method is that even at relatively low calcined temperature (450 °C) xerogel precursors are directly transformed into a single perovskite phase without intermediate step. These results are comparable to those for $LaFeO_3$ powder and bulk samples synthesized by co-precipitation methods.

Acknowledgements

The authors wish to thank to Professor Dr Daw Hla Ngwe, Head of the Department of Chemistry, University of Yangon, for her encouragement, providing necessary research facilities and good advice.

References

Anupama, M. and Prasad, R. (2015). "Effect of Preparation Method and Calcination Temperature on $LaCoO_3$ Perovskite Catalyst for Diesel Soot Oxidation.''*J. Chem*, vol. 3(1), pp. 95-107

Ghosh, S. andDasgupta, S. (2010). "Synthesis, Characterization and Properties of Nano Crystalline Peroskite Cathode Materials''. *J. Mater. Sci*- vol. 28 (2), pp. 427 -438

Kenta and Kumar, D. (2014). "Study the Perovskite-Type Mixed Oxides with the General Formula ABO_3." *J. Mater. Sci*., vol. 3 (5), pp. 1-7

Khetre, S. M., H. V. Jadhav and S. R. Bamane. (2010). "Synthesis and Characterization of Nano Crystalline $LaFeO_3$ by Combustion Route''. *J. Chem, vol.*3(1), pp. 82-86

Theingi, M. (2013). *Study of Electrical Properties and Laser Induced Voltage Effect in* $La_{1-x}Ca_xMnO_3$ *Epitaxial Thin Films*. PhD Dissertation, Material Science, Kunming University of Science and Technology, China

Unikoth, M., Shijina, K. and Varghese, G. (2014). "Nano Sized $LaCo_{0.4}Fe_{0.6}O_3$ Perovskite Synthesized by Citrate Sol-Gel Auto Combustion Method''. *Processing and Application of Ceramic*s, vol. 8(2), pp. 87-92

STUDY ON SOME BIOACTIVITIES OF SULAR-NA-PHAR (*OLDENLANDIA CORYMBOSA* L.) PLANT

Khaing Zar Lin[1], Myint Myint Htwe[2], Hnin Hnin Aye[3], Daw HlaNgwe[4]

Abstract

In the present work, some bioactivities such as antitumor, antimicrobial, radical scavenging and cytotoxic activities of Sular-na-phar (*Oldenlandiacorymbosa* L.) plant and its bioactive compound were investigated. The antitumor activity of the H_2O and EtOH extracts of Sular-na-phar was examined by using PCG (Potato Crown Gall) test with the isolated bacterium *A. tumefaciens* and only H_2O extract prevented the formation of tumor. The antimicrobial activity of the crude extracts from this plant sample was determined against six strains of microorganisms by agar well diffusion methods at PRD (Pharmaceutical Research Department). The pet ether extract of Sular-na-phar did not show the antimicrobial activity. However, the EtOH and H_2O extracts possessed medium and EtOAc extract possessed high antimicrobial activities. Radical scavenging activity of EtOH and H_2O extract samples was determined by 1, 1-diphenyl-2-picrylhydrazyl (DPPH) Assay. EtOH extract showed stronger radical scavenging activity than H_2O extract of plant sample. Cytotoxic effect of EtOH and H_2O extracts of whole plant of Sular-na-pharwas investigated against *Artemiasalina*(Brine Shrimp). The cytotoxic effect of plant extracts was not found on Brine Shrimp up to maximum dose of 1000 µg/mL. The bioactive compound(white colour crystal, 0.0285%) was isolated from defatted MeOH extract of *O. corymbosa* (Sular-na-phar) on the silica gel column chromatographic separation. The isolated compound was identified asursolic acid by physico-chemical properties and modern spectroscopic techinques such as UV, FT IR, ^{1}HNMR, ^{13}C NMR spectrometry as well as by comparing with the reported data. Finally, *invitro* cytotoxicity was also screened by using MTS Cell Proliferation Colourimetric Assay, against H1299, Clone no. 9, A549 and MCF-7 cell lines. According to the results, cell viability cannot be inhibited by ursolic acid for H1299 and Clone no. 9 cell lines significantly. However, the cell viability of A549 and MCF-7 cell can be effectively inhibited by ursolic acid.

Keywords: Sular-na-phar (*Oldenlandia corymbosa* L.), antimicrobial activity, antitumor activity, radical scavenging activity, cytotoxic effect, anticancer activity

[1.] PhD Candidate, Department of Chemistry, University of Yangon
[2.] Dr,Associate Professor, Department of Chemistry, Taungoo University
[3.] Dr, Professor, Department of Chemistry, University of Yangon
[4.] Dr,Professor and Head, Department of Chemistry, University of Yangon

Introduction

The plant has been traditionally used as cooling medicine in treatment of fever caused by deranged bile and also used in viral infections, cancer, acne, skin ailments, hepatitis, eye diseases and bleeding. It also shows bitter, acrid, cooling, febrifugal, pectoral, anthelmintic diuretic, depurative, diaphoretic, expectorant, digestive and has stomachic properties (Agrawal, 2013).

Oldenlandia corymbosa L. contains oleanolic acid, ursolic acid and gamma sitosterol, alkaloids, tannins, flavonoids, biflorine, biflorone, r-sitosterol, oleanolic acid, asperulosidic acid, geniposide acid, asperulosidic, deacetylasperuloside and scandoside methyl ester, a polysaccharide composed of glucose, galactose and glucuronic acid. The air dried plantcontains 0.12 %, alkaloids bifloron and biflorin. It contains13.55% inorganic ash that is responsible for it's coolingeffect (Chakraborty *et al.,* 2011; The Wealth of India 1950).

Some bioactivities of Sular-na-phar plant has been investigated by (ThandarAung, 2006). This research work intended to further study for different activities of Sular-na-phar plant, particularly anticancer activity.

Current research has supported the potential of plant-derived natural compounds for the treatment and prevention of cancer and ursolic acid is one such compound. Triterpenoid is one of the important compounds used as an anti-inflammatory, anticancer and anti-microbial agents (Navin and Kim, 2016). One such important and highly investigated pentacyclic triterpenoid, ursolic acid has attracted great attention of late for its potential as a chemopreventive and chemotherapeutic agent in various types of cancer.

Materials and Methods

Sample Collection

Sular-na-phar (the whole plant) (*O. corymbosa* L.) was collected from Shwepyithar Township, Yangon Region. After collection, the air-dried samples were cut into small pieces and ground by using grinding machine. Then the sample was separately stored in the airtight container to prevent moisture and other contamination.

Extraction of Chemical Constituents from Sular-na-phar

Dried powdered samples (400g) were percolated in Pet ether (PE) (60-80°C) (1000mL) for one week and filtered. This procedure was repeated for three times. Then the filtrate was concentrated by a vacuum rotatory evaporator to get respective pet-ether extract.

Similarly, EtOAc, 70% EtOH and H_2O extracts of each dried powdered samples were prepared according to the above procedure.

Screening of Pharmacological Activities of the Whole Plant of Sular-na-phar

This section involves screening of some pharmacological activities such as antitumor activity, antimicrobial activity, antioxidant activity, cytotoxic activity of some crude extracts and anticancer activity of isolated compound of Sular-na-phar.

Screening of Anti-tumor Activity by Potato Crown Gall (PCG) (or) Potato Disc Assay (PDA) method

Anti-tumor activity of EtOH and H_2O extracts of Sular-na-phar was examined by Potato Crown Gall (PCG) (or) Potato Disc Assay (PDA) method (Ferrigni *et al.,* 1982) at Pharmaceutical Research Department (PRD), Ministry of Industry, Yangon, Myanmar.

Fresh, disease-free potatoes were purchased from a local market. Tubers of moderate size were surface sterilized by immersion in 0.1 % sodium hypochlorite for 20 min. Ends were removed and the potatoes were then soaked in sodium hypochlorite solution for an additional 10 min. A core of the tissue was extracted from each end and discarded. The remainder of the cylinder was cut into 1.0 cm thick discs with a surface sterilized scalpel. The discs were then transferred to agar plates (1.5 g of agar dissolved in 100 mL deionized distilled water, autoclaved for 20 minat 121˚C, 20 mL poured into each Petridish). Each plate contained four potato discs and 4 plates, used for each sample dilution.

Samples (0.05, 0.1, 0.2 g) were separately dissolved in DMSO (1 mL) and filtered through Millipore filters (0.22 μm) into sterile tube. This solution

(0.5 mL) was added to sterile distilled water (1.5 mL), and broth culture of *A. tumefaciens* in PBS (2 mL) was added. Controls were made in this way; DMSO (0.5 mL) and sterile DW (1.5 mL) were added to the tube containing 2 mL of broth culture of *A. tumefaciens*. Using a sterile disposable pipette, 1 drop (0.05 mL) each from these tubes was used to inoculate each potato disc, spreading it over the disc surface. After inoculation, Petri dishes were sealed by film and incubated at 27-30 ˚C for 3 days. Tumors were observed on potato discs after 3 days under stereo-microscope followed by staining with Lugol's iodine (10 % KI and 5 % I_2) after 30 min and compared with control. The antitumor activity was examined by observation of tumor produced or not

Screening of Antimicrobial Activity by Agar Well Diffusion Method

The screening of antimicrobial activity of various crude extracts such as PE, EtOAc, 70 % EtOH, H_2O extracts of Sular-na-phar were carried out by agar disc diffusion method at Pharmaceutical Research Department (PRD), Ministry of Industry, Yangon, Myanmar. Six microorganisms namely *Bacillus subtilis*, *Staphylococcus aureus*, *Pseudomonas aeruginosa* , *Bacillus pumilus*, *Candida albicans* and *Escherichia coli* were used for this test.

Screening of Antioxidant Activity by DPPH Free Radical Scavenging Assay

The free radical scavenging activity of EtOH and H_2O extracts from Sular-na-phar was screened by using DPPH Free Radical Scavenging Assay (Marinova and Batchvarov, 2011).

The control solution was prepared by mixing 1.5 mL of 0.002% DPPH solution and 1.5 mL of ethanol in the brown bottle. The blank solution sample solution was also prepared by mixing 1.5 mL of 0.002% DPPH solution and 1.5 mL of test sample solution. These bottles were incubated at room temperature and were shaken on shaker for 30 min. After 30 min, the absorbance values of these solutions were measured at 517 nm and the percentage of radical scavenging activity (% RSA) was calculated by the following equation.

$$\% \text{ RSA} = [(A_{DPPH} - A_{Sample}) - A_{Blank} / A_{DPPH}] \times 100$$

where, % RSA = % radical scavenging activity of test sample

A_{DPPH} = absorbance of DPPH in EtOH solution

A_{Sample} = absorbance of sample + DPPH solution

A_{Blank} = absorbance of sample + EtOH solution

$$\% \text{ Inhibition} = \frac{A_{DPPH\ alone} - A_{Sample}}{A_{DPPH\ alone}} \times 100$$

The antioxidant power (IC_{50}) is expressed as the test substances concentration (μg/mL) that result in a 50 % reduction of initial absorbance of DPPH solution and that allows to determine the concentration. IC_{50} (50% inhibition concentration) values were calculated by linear regressive excel program.

Cytotoxicity Test by Brine Shrimp Lethality Bioassay

Cytotoxic effect of EtOH and H_2O extracts from the whole plant of Sular-na-phar was investigated by brine shrimp lethality bioassay according to the procedure described by Dockery and Tomkins, (2000). Artificial sea water (9 mL) and 1 mL of different concentrations of samples and standard solutions were added to each chamber. Alive brine shrimps (10 nauplii) were then taken with pasteur pipette and placed into each chamber. They were incubated at room temperature for about 24 h. After 24 h, the number of dead or survival brine shrimps was counted and 50% lethality dose (LD_{50}) was calculated (Sahgal *et al.,* 2010).

The control solution was prepared as the above procedure by using distilled water instead of sample solution.

Isolation and Identification of Chemical Constituents from the Sular-na-phar

Methanol extract was then dissolved in methanol and water (9:1) and then washed with hexane. This procedure repeated for three times. The total filtrate were concentrated under rotatory evaporator to obtain defatted

methanol extract. Defatted methanol extracts (7g) was separated by column chromatographic method and eluting with PE : EtOAc (10:1, 9:1, 7:1, 5:1, 3:1, 1:1, 1:3 and 1:5) solvent system. On chromatographic separation, 120 fractions were collected. From the inspection of TLC chromatograms viewed under UV lamp, the fractions having the same appearance on TLC chromatograms were combined to give (VII) fractions. According to the inspection of TLC chromatograms, fraction (FIII) and (FIV) were combined and washed with PE/EtOAc to remove impurities. Then it was recrystallized with MeOH until to get white crystal as compound SL 1.

Structural Identification of Isolated Compound.

The isolated compound was identified by determining their structures using UV-visible, FT IR and NMR spectroscopic data. The Fourier transform infrared spectra of isolated compound (SL 1**)** were recorded by FT IR (8400) spectrophotometer (Shimadzu, Japan) at Department of Chemistry, University of Yangon. The ^{1}H NMR and^{13}C NMR spectra of isolated compound **(**SL 1**)** were recorded in $CDCl_3$ and DMSO by 400 MHz NMR spectrometer at the Department of Organic and Biomolecular Chemistry, Nagoya University and Division of Natural Products Chemistry, Institute of Natural Medicine, University of Toyama, Japan.

Investigation of Anticancer Activity by MTS Assay with Different Cancer Cell Lines

The cytotoxicity of ursolic acid was investigated by using MTS assay against H1299(lung cancer cell line), Clone no.9 (lung cancer cell line), A549 (lung cancer cell line) and MCF-7 (breast cancer cell line) at Laboratory of Biological Chemistry, Department of Chemistry, Faculty of Science, Hokkaido University, Japan. The cell number in the mixture solution was counted by Hemocytometer under microscope. Each cell lines was seeded in 96-well plates and incubated in incubator (37 ºC, 5%CO_2) for one day. And then stimulated with ursolic acid on various cancer cell lines3.0 µL of DMSO was mixed with 697 µL of Opti-MEM. This mixture was assigned as Solution A. 2.8 µL of compound stock solution was mixed with 657 µL Opti-MEM to become 17 µg/mL concentration. From the stock solution concentration of 17

µg/mL of the compound, 440 µL was diluted with 110 µL of Solution A to become 13.6 µg/mLconcentration. This stock solution was continuously diluted with Solution A to get the compound solution with the concentrations of 10.2, 6.8 and 3.4 µg/mL in conical tubes respectively. Each of these solutions 200 µL was mixed with 800 µL of DMEM in conical tube respectively. Finally, 100 µL of each diluted solution was retaken into 96 well plate and incubated (37 ºC, 5% CO_2) in incubator for three days.

Finally, old medium, that containing cancer cell was removed by aspirator and washed with 1000 µL of PBS (phosphate buffered saline) by mutichannels pipette. That PBS (phosphate buffered saline) was removed by aspirator again. 50 µL of DMEM medium and 10 µL of Cell Titter 96 ® Aqueous One Solution Cell Proliferation Assay solution were added into 96 well plate. It was incubated (37ºC, 5% CO_2) in incubator for 30 min. Finally, the absorbance was measured at 490 nm in plate reader.

Results and Discussion

Antitumor Activity of Sular-na-phar

The inhibition of *A.tumefaciens-induced*tumors (or crown gall) in potato disc tissue is an assay based on antimitotic activity that can detect a broad range of known and novel antitumor effects. The validity of this bioassay is predicted on the observation that certain tumorigenic mechanisms are similar in plants and animals. It was demonstrated that inhibition of crown gall tumor initiation on potato disc showed an apparent correlation with compounds and plant extracts. The antitumor activity of the H_2O and EtOH extracts of whole plant of Sular-na-pharwas investigated using PCG test with the bacterium *A. tumefaciens* obtained from Fermentation Department. The tested samples were dissolved in DMSO, diluted and mixed with the bacterial culture for inoculation. After preparing the inoculums, the bacterial suspension was inoculated on the cleaned and incubated for 3 days, at room temperature. After that, the tumors were appeared on potato discs and checked by staining the knob with Lugol's (I_2+KI) solution. In the control, the formation of white knob on the blue background indicated the presence of tumor cells because there is no protein in tumor cells. The active test samples did not form any tumors on the potato discs and its surface remained blue.

From this experiment, it was found that the H_2O extract of whole plant of Sular-na-pharwas good in preventing the tumor formation with the dose 0.05 g/mL, 0.10 g/mL and 0.20 g/mL in *vitro* potato disc assays. The EtOH extract of whole plant of Sular-na-phar did not exhibit the growth of tumor even at the concentration of 0.20 g/mL. The results are shown in Table 1.

Table 1: Tumour Inhibitory Property of Different Concentrations of H_2O and EtOH Extracts of Whole Plant of *O. corymbosa* (Sular-na-phar)

Extracts	Concentration of Samples (g/mL)	Tumor*
Control	0.00	+
H_2O	0.05	-
	0.10	-
	0.20	-
EtOH	0.05	+
	0.10	+
	0.20	+

*(+) Tumor appeared, (-) No tumor appeared

Antimicrobial Activity of Crude Extracts of Sular-na-phar

Four crude extracts of such as PE, EtOAc, EtOH, and H_2O extracts of *O. corymbosa* were screened for antimicrobial activity against six different pathogenic microbes using agar well diffusion method. This method is based on zone diameter including the well diameter, in millimeter (mm).

According to the results presented in Table 2, PE extract of *O. corymbosa* (Sular-na-phar) did not show any antimicrobial activity against all of the microorganisms tested. Moderately significant antibacterial activities were possessed by EtOH extract of selected medicinal plant (13mm-16mm). H_2O extractof the selected medicinal plant inhibited the all strains of microorganisms and significant zone of inhibition ranges between 18mm-22mm. Moreover, EtOAc extract of Sular-na-phar significantly inhibited all strains of microorganisms and significant zone of inhibition ranges between 20mm-32mm. It's zone diameter is wider than the other extracts.

Table 2: Inhibition Zone Diameters of Various Extracts of Sular-na-phar against Six Microorganisms by Agar Well Diffusion Method

No.	Microorganisms	Inhibition Zone Diameters (mm) of Different Extracts			
		PE	EtOAc	EtOH	H_2O
1	*Bacillus subtilis*	-	25 (+++)	13(+)	18(++)
2	*Staphylococcus aureus*	-	32(+++)	15(++)	20(+++)
3	*Pseudomonas aeruginosa*	-	20(+++)	-	20(+++)
4	*Bacillus pumilus*	-	28(+++)	16 (++)	20(+++)
5	*Candida albicans*	-	27(+++)	16 (++)	18(++)
6	*Escherichia coli*	-	30(+++)	14 (+)	22(+++)

Agar well – 10mm
10mm ~ 14mm (+)
15mm ~ 19mm (++)
20mm above (+++)

Antioxidant Activity of Sular-na-phar

The antioxidant activity was measured in terms of hydrogen donating or radical scavenging ability using the stable radical DPPH. The reduction of the radical is followed by a decrease in the absorbance at 517nm. The results are shown in Table 3. From these observations, the radical scavenging activity of EtOH extract was greater than that of H_2O extract. EtOH extract of Sular-na-phar inhibited 50 % of free radical at the concentrations of 112.55 μg/mL (IC_{50}) and also H_2O extract inhibited 50 % of free radical at the concentration of 198.53μg/ mL (IC_{50}). So, antioxidant activity of EtOH extract is more stronger than H_2Othat of extract.

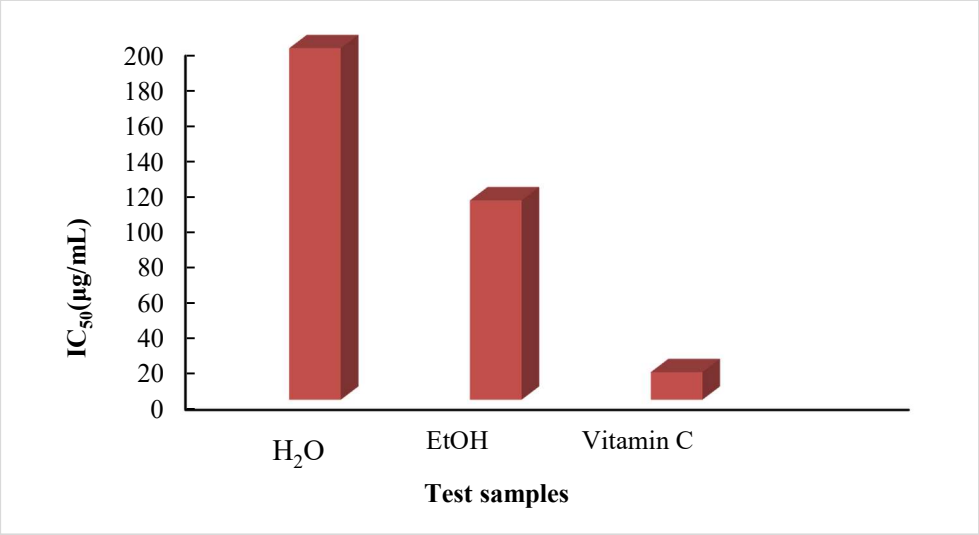

Figure 1: A bar graph of IC_{50}(µg / mL) of H_2O and EtOH crude extracts of (Sular-na-phar)

Table 3: (IC_{50})of H_2OandEtOH Crude Extracts of Sular-na-phar

Samples	IC_{50} (µg/mL)
H_2O extract	198.53
EtOH extract	112.55
Standard Vitamin C	15.55

Cytotoxicity of Sular-na-phar

The cytotoxicity on EtOH and H_2O extracts of whole plant of Sular-na-phar was evaluated by Brine Shrimp cytotoxicity bioassay. This bioassay is general toxicity screening for bioactive plants and their derivatives. A model animal that has been used for this purpose is the Brine Shrimp, *Artemia salina.*

The cytotoxicity of EtOH and H_2Oextracts of the whole plant of Sular-na-phar was expressed in terms of mean SEM (standard error mean) and LD_{50} (50% Lethality Dose) and the results are shown in Table 4. In this experiments, standard potassium dichromate ($K_2Cr_2O_7$) and caffeine were chosen because $K_2Cr_2O_7$ is well-known toxicity in this assay and caffeine is a

natural product. The effect of cytotoxicity was not found on the Brine Shrimp up to maximum dose of 1000 μg/mL.

Table 4: Cytotoxicity of Whole Plant of Sular-na-phar (Sular) against *Artemia salina* (Brine Shrimp)

Tested samples	No. of Death of Brine Shrimp (Mean ± SEM)				LD_{50} (μg/mL)
	1000	100	10	1	
EtOH extract	3.33±0.58	1.33±0.58	0.00±0.58	0.00±0.00	>1000
H_2O extract	1.00±0.58	0.00±0.00	0.00±0.00	0.00±0.00	>1000
$K_2Cr_2O_7$	10.00±0.00	10.00±0.00	2.00±0.00	0.00±0.00	43.74
Caffeine	5.00±1.16	3.00±0.58	2.33±1.20	0.00	1000

Structural Elucidation of Compound SL 1

SL 1 : Ursolic acid: white colour crystal, 0.0285 %, 77.6 mg (R_f= 0.3, PE : EtOAc = 3:1, melting point 286˚C); FT IR of 3400 (OH), 2925, 2687 (CH), 1688 (C=O), 1455 (CH), 1029 (C-O); ^{1}HNMR (400MHz, $CDCl_3$) : δ 0.74 - 2.10 (44H, m), 3.22 (1H, m), 5.22 (1H, m): ^{13}CNMR (400 MHz, $CDCl_3$) δ 15.1, 15.3, 16.6, 16.7, 18, 23.0, 23.2, 23.9, 26, 27.7, 28.0, 29.0, 30.4, 32.8, 36.6, 38.8, 39.2, 39.2 ,41.8, 47.3, 47.5, 53.61, 55.03, 78.57, 125.27, 137.97, 180.41 agreed with the data reported by Guvenalp (2005).

Anticancer Activity of Ursolic acid by MTS Assay with Different Cancer Cell Lines

The compound isolated, ursolic acid was determined the anticancer activities. It indicated the anticancer activities, such as lung cancer cell line and breast cancer cell line. The cytotoxicity of ursolic acid was investigated using MTS assay against H1299, Clone no.9, A549 and MCF-7 cancer cell lines. If percentage of cell viability will be high, the living cell will be

accumulated. If so, anticancer activity will not be effective. According to the result data, cell viability cannot be inhibited by ursolic acid for H1299 and Clone no. 9 cell lines significantly. However, the cell viability of A549 and MCF-7 cell can be inhibited by ursolic acid. That can be evident by comparing with etoposide (positive control). Although inhibition of cell in ursolic acid for A549 cell were 100, 101, 84, 16, 12 and 13 in 0µg/mL, 3.4µg/mL, 6.8µg/mL, 10.2µg/mL, 13.6µg/mL, and 17µg/mL, the etoposide was 67 for concentration of 17µg/mL. For MCF-7, the cell inhibition values of ursolic acid were 96, 46, 22, 20 and 20 in different concentrations, but the cell inhibition of etoposide was 60 for concentration of 17µg/mL. The results are shown in Figure 2 and Table 5. So, the maximum concentration inhibited the cell viability was 13.6µg/mL form A549 and MCF 7 cell lines. On the other hand, H1299 (lung cancer cell line) and Clone no.9 (lung cancer cell line) cannot be inhibited by ursolic acid**,** but A549 (lung cancer cell line) and MCF-7 (breast cancer cell line) can be inhibited by ursolic acid.

Table 5: Average Cell Viability of Various Cell Lines at Different Concentrations of Ursolic Acid of theSular-na-phar

Cell lines	**Average cell viability of various cell lines at different concentrations of ursolic acid(µg/mL)**						**Control**
	0	**3.4**	**6.8**	**10.2**	**13.6**	**17**	**17**
H1299	0.506	0.518	0.530	0.561	0.534	0.401	0.256
	100	102	105	111	105	79	51
Clone no.9	0.453	0.553	0.583	0.562	0.541	0.571	0.251
	100	122	129	124	119	126	55
A549	0.754	0.760	0.631	0.120	0.019	0.096	0.504
	100	101	84	16	12	13	67
MCF –7	0.461	0.443	0.21	0.103	0.009	0.091	0.279
	100	96	46	22	20	20	60

*Absorbance values were measured at 490nm.

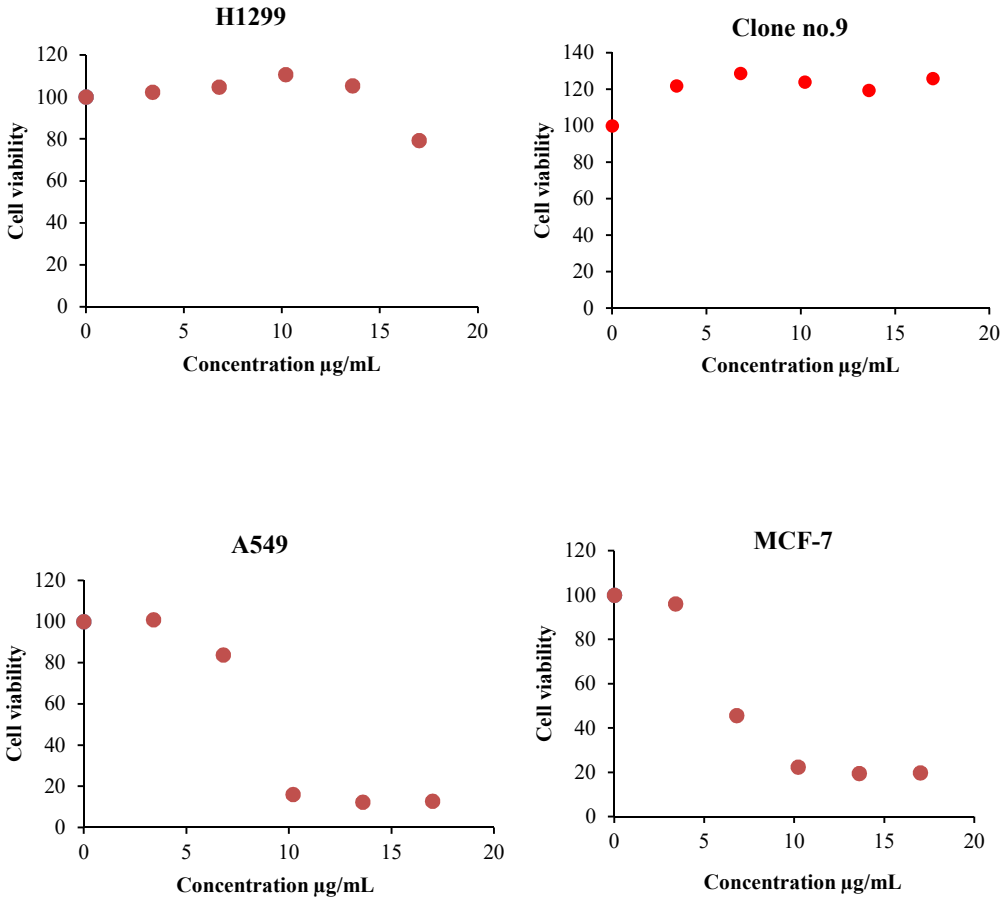

Figure 2: Cell viability of Various Cell Lines at Different Concentrations of Ursolic acid

Conclusion

Antitumor activity investigated by potato crown gall (PCG) assay revealed that H_2O extract of *O. corymbosa* (Sular-na-phar) inhibited tumour formation but EtOH extract could not inhibit.

In antimicrobial activity of four different extracts (PE, EtOH, EtOAc and H_2O) of the whole plant of *O. corymbosa* (Sular-na-phar), PE extract did not show any antimicrobial activity against all of the microorganisms tested. Moderately significant antibacterial activities were possessed by EtOH extract (13mm-16mm) and H_2O extract inhibited the all strains of bacteria with the significant zone of inhibition ranged between 18mm-22mm. Among the four extracts, EtOAc extract significantly inhibited all strains of bacteria with the significant zone of inhibition ranged between 20 mm-32 mm. In screening of free radical scavenging, the IC_{50} values of H_2O and EtOH extracts of Sular-na-pharwere observed to be 198.53 µg/mL and 112.55 µg/mL, respectively. Ethanol extract of sample showed more stronger radical scavenging activity than water extract. The cytotoxicity effect of plant extract was not found on Brine Shrimp up to maximum dose of 1000 µg/mL. The silica gel column chromatographic separation gave : 0.0258%, 77.6mg of ursolic acid (R_f= 0.3, PE : EtOAc = 3:1, melting point 286˚C). The cytotoxicity of ursolic acidas investigated using MTS assay against H1299, Clone no.9, A549 and MCF-7 cancer cell lines. In this experiment, various concentrations such as 3.4, 6.8, 10.2, 13.6, 17 µg/mL were used and etoposide (17 µg/mL) was also used as positive control. Among all these four cell lines, H1299 (lung cancer cell line) and Clone no.9 (lung cancer cell line) could not be inhibited by ursolic acid**,** but A549 (lung cancer cell line) and MCF-7 (breast cancer cell line) can be inhibited by ursolic acid.

Acknowledgements

The authors would like to express their profound gratitude to the Department of Higher Education (Yangon Office), Ministry of Education, Yangon, Myanmar, for provision of opportunity to do this research.

References

Agrawal, S. K. (2013). "Evaluation of Antiulcer Activity of *Oldenlandia corymbosa* (L.)". *International Journal of Research and Development in Pharmacy and Life Sciencies,*vol.2 (2), pp.363-367

Chakraborty, A. K., Rambhade, S. and Patil, U. K. (2011). "*Chromolaena odorata* (L.) : An Overview". *Journal of Pharmacy Research,*vol.4(3), pp.573-576

Dockery, M., and Tomkins, S.(2000). *Brine Shrimp Ecology*. London: 1st Ed., The British Ecology Society, pp. 92-93

Ferrigni N. R., Putnan, J. E., Aderson, B., Jacobsen, L.B., Nicols, D. E., Moore, D. S. and Mclaughlin, J. L. (1982). "Modificationi and Evaluation of the Potato Disc Assay and Antitumor Screening of Euphorviaceae Seeds" *.J. Nat. Prod*, vol. 45(6), pp. 678-686

Guvenalp, Z., Kilic, N., Kazaz, C., Kaya, Y. and Demlrezer, O. (2005). "Chemical Constituents of *Galiumtortumense*". *Turk J Chem,* vol.30, pp.515-523

Marinova, G. and Batchvarov, V. (2011). "Evaluation of the Methods for Determination of the Free Radical Scavenging Activity by DPPH''. *Bulgarian Journal of Agricultural Science*, vol.17, pp.11-24

Navin, R. and Kim, S. M. (2016).Therapeutic Interventions Using Ursolic Acid for Cancer Treatment". *Med chem (Los Angeles)*, vol.6, pp.339-344

Sahgal, G., Ramanathan, S., Sasidharan, S., Mordi, M.N., Ismail, S. and Mansor, S. M. (2010). "Brine Shrimp Lethality and Acute Oral Toxicity Studies on *Swieteniamahagonic* (L.) Jacq. Seed Methanolic Extract''. *Pharmacognosy Res.,* vol. 2(4), pp.215-220

Thandar Aung. (2006). *Isolation, Characterization and Identification of Some Bioactive Constituents and Investigation of Cholesterol Lowering Effect of Euphorbitahirta* L. *(Kywe - Kyaung – Hmin-Say) and Oldenlandia corymbosa* L. *(Sular-Na- Phar*), PhD dissertation, Department of Chemistry, University of Yangon, 9 -51

The Wealth of India. (1950). *A Dictionary of India Raw Materials and Industrial Products*. New Delhi: vol. 2, pp.1-9

INVESTIGATION OF CHEMICAL PROPERTIES AND BIOLOGIICAL ACTIVITIES OF STEM OF *Coccinia cordifolia* COGN. (KIN-PON) AND BARK OF *Dolichandrone serrulata* SEEM. (THA-KHUT)

Kyaw Khaing[1], Aung Phyo Naing[2], Khine Zar Wynn Lae[3], Khin Thida Nyo[4], Daw Hla Ngwe[5]

Abstract

In this research work, stem of *Coccinia cordifolia* Cogn. (Kn-pon) and bark of *Dolichandrone serrulata* Seem. (Tha-khut) were collected from Yekyi Township, Ayarwaddy Region for the investigation of chemical and biological properties such as antimicrobial activity, antioxidant activity, anti-arthritic activity and antitumor activity due to lack of scientific report on these two locally cultivated medicinal plants. Relative abundances of elements analysed by EDXRF showed the presence of calcium, potassium, sulphur, manganese, iron, stronium, zinc and copper in the stems of Kin-pon and calcium, potassium, sulphur, zinc, copper and rubidium in the barks of Tha-khut. Determination of nutritional values has also screen carried out by AOAC method resulting moisture (10.69 %), ash (11.81 %), protein (8.71 %), fiber (36.90 %), fat (0.89 %), carbohydrate (31.00 %) and energy value (169 kcal/100 g) in stems of Kin-pon and moisture (11.25 %), ash (9.55 %), protein (2.29 %), fiber (36.17 %), fat (0.08 %), carbohydrate (40.66 %) and energy value (173 kcal/100 g) in the barks of Tha-khut. In the stems of Kin-pon and the barks of Tha-khut, alkaloids, α-amino acids, carbohydrates, flavonoids, glycosides, organic acids, phenolic compounds, reducing sugars, saponins, starchs, tannins, terpenoids and steroids were found to be present according to preliminary phytochemical tests. However, cyanogenic glycosides were not found in these samples Total phenol contents, total flavonoid contents and reducing ability of the ethanol extracts have been respectively determined by using Folin-Ciocalteu (F-C) method, Kiranmai *et al*. method and Oyaizu method in the ethanol crude extracts from the selcted samples. In addition, antimicrobial activity screening was done on various crude extracts by agar well diffusion method against on *Bacillus subtilis, Staphylococus aureus, Pseudomonas aeruginosa, Bacillus pumilus, Candida albicans and Eschericha coli.* It was observed that EtOAc extract exhibited higher antimicrobial activity than

1. 4 PhD, Candidate, Department of Chemistry, University of Yangon
2. 4 PhD, Candidate, Department of Chemistry, University of Yangon
3. Lecturers, Department of Chemistry, University of Yangon
4. Lecturers, Department of Chemistry, University of Yangon
5. Professor and Head, Department of Chemistry, University of Yangon

other extracts in the stem of Kin-pon whereas EtOH extract showed higher potency in antimicrobial activity than other extracts in the bark of Tha-khut. The antioxidant activity of ethanol and watery crude extracts of the samples was investigated by using DPPH free radical scavenging assay, resulting in the order of Tha-Khut bark (EtOH extract) (IC_{50} = 42.71 µg/mL) > Kin-pon stem (EtOH extract) > Tha-khut bark (watery extract) > Kin-pon stem (watery extract) in antioxidant activity. Antitumor activity screening by Potato Crown Gall (PCG) test revealed that the EtOH and H_2O extracts of stem of Kin-pon and bark of Tha-khut possess the tumor inhibition. Furthermore, antiarthritic activity of the ethanol crude extracts has been studied according to their proteinase inhibitory action and inhibition of protein denaturation action. In antiarthritic activity, ethanol extract of bark of Tha-khut showed proteinase inhibitory action and inhibiion of protein denaturation, however that of stem of Kin-pon did not show activities.

Keywords*:* *Coccinia cordifolia* Cogn., *Dolichandrone serrulata* Seem., chemical properties, antimicrobial activity, antioxidant activity, antitumor activity, antiarthritic activity

Introduction

Coccinia cordifolia Cogn., (Kin-pon), the family Cucurbiace is distributed in Africa country and tropical Asia country. It is a perennial and herbaceous climber with glabrous stems and tuberous roots. Phytochemical screening of stem of Kin-pon reported the presence of saponin, cardenoloids, flavonoids and poly phenols which may be attributed to anti bacterial activity. Major phytoconstituents present in stem of Kin-pon are cardenolides, saponins, flavonoids and polyphenols. *C. cordifolia* have pharmacological activities like analgesic, antipyretic, anti-inflammatory, antimicrobial, antiulcer, antidiabetic, antioxidant, hypoglycemic, hepatoprotective, antimalarial, antidyslipidemic, anticancer, antitussive and mutagenic (Bounmy *et al.,* 2006).

Dolichandrone serrulata Seem., (Tha-khut), the family Bignoniace is distributed in South East Asia. Some chemical constituents of bark of Tha-khut are dolichandroside, decaffeoyl-verbascoside, isoverbascoside, markhamioside, luteocoside B, ixoside, and iridoide glycoside. It is used as anti-fever, anti-inflammatory agent and anti-mutagenicity (Bunbun *et al.,* 2011).

Since Kin-pon and Tha-khut have a lot of useful biological activities, the locally cultivated the stem of Kin-pon and the bark of Tha-khut were chosen to evaluate scientifically some of their bioactivities in this study. In the present work, analyses of some biochemicals such as inorganic elements, nutritional values, total phenol contents, total flavonoid contents and screening of some biological activities such as reducing ability, antimicrobial activities, antitumor activities, antioxidant activities and antiarthritis activities were carried out on the stem of Kin-pon and the bark of Tha-khut.

Materials and Methods

Collection and Preparation of Plant Materials

The stem of Kin-pon and the bark of Tha-khut were collected from Yekyi Township, Ayarwaddy Region, Myanmar in the month of June- July, 2014. The plants were identified and authenticated at the Department of Botany, Yangon University.

After collection, the stem and bark were cleaned thoroughly with distilled water to remove any type of contamination. The washed stem and bark were air dried in shade for about two weeks and ground into the coarse powder with the help of a mechanical grinder. The powders of the samples were separately stored in air tight bottles and kept in a cool, dark and dry place until analyses were commenced.

Qualitative Elemental Analysis by Energy Dispersive X- Ray Fluorescence

Shimadzu EDX-8000 spectrometer can analyze the elements from Na to U under vacuum condition. In this research work relative abundance of elements present in stem of Kin-pon and the bark of Tha-khut was determined by EDXRF spectrometer.

Determination of Nutritional Values

The nutritional values such as moisture, ash, crude protein, crude fiber, crude fat, carbohydrate contents and energy value of the stem of Kin-pon and the bark of Tha-khut were determined according to AOAC method at Food

Industries Development Supporting Laboratory (FIDSL), Myanmar Food Processors and Exporters Association (MFPEA), Yangon, Myanmar.

Preliminary Phytochemical Screening

The stem of Kin-pon and the bark of Tha-khut were subjected to qualitative phytochemical tests for the identification of various bioactive constituents. Phytochemical screenings were carried out by using standard procedures to detect the presence of alkaloids, glycosides, carbohydrates, α-amino acids, phenolic compounds, flavonoids, steroids, terpenoids, saponins, tannins, starch, reducing sugars and organic acids. After the addition of specific reagents to the test solution, the tests were detected by visual observation of colour change or by precipitate formation.

Preparation of the Extracts from the Samples

The crude extracts of stem of Kin-pon and bark of Tha-khut were prepared by extracting the sample with different solvents like petroleum ether, ethyl acetate, ethanol and water by cold percolation method. All of these extracts were kept for the determination of total phenol contents, total flavonoid contents, reducing ability, antimicrobial activity, antioxidant activity and antiarthritic activity.

Determination of Total Phenol Contents

The total phenol content (TPC) in ethanol extract of each sample was estimated by the Folin-Ciocalteu method according to the procedure described by Saxena *et al.* (2013). The sample solution (50 ppm) was prepared by dissolving 0.005 g of extract in methanol making up to 100 mL solution. First, 0.5 mL of the prepared sample was mixed with 0.5 mL methanol. Then, 0.5 mL of Folin-Ciocalteu reagent (FCR: H_2O, 1: 10) was added to the mixture and incubated for 5 min. 4 mL of 1 M sodium carbonate was added to each tube and the tubes were kept at room temperature for 2 h and the UV absorbance of each reaction mixture was read at λ_{max} 765 nm. The blank solution was prepared as the above procedure by using distilled water instead of sample solution. Total phenolic content was estimated as mg gallic acid equivalents per g of EtOH extract.

Determination of Total Flavonoid Contents

Formation of acid stable complexes with the C-4 keto group and either the C-3 or C-5 hydroxyl group of flavones and flavonols in addition with aluminium chloride. Aluminium chloride also forms acid labile complexes with the ortho – dihydroxyl groups in the A- or B- ring of flavonoids. For building the calibration curve, quercetin is used as construction standard materials. Various concentrations of standard solutions were used to make a standard calibration curve (Kalita *et al.,* 2011).

In this method, quercetin was used to make the calibration curve. 0.01 g of quercetin was dissolved in methanol and then diluted to (6.25, 2.5, 25, 50 and 100μg/mL). A calibration curve was made by measuring the absorbance of the dilutions at 415nm (λ_{max} of quercetin) with a Shimadzu UV-1800 spectrophotometer (Kalita *et al.,* 2011).

Each ethanol extract solution in 50 ppm was prepared by dissolving 0.005 g of extract in 100 mL MeOH solution. 0.5 mL of each extract stock solution, 1.5 mL methanol, 0.1 mL of aluminium chloride, 0.1 mL of potassium acetate solution and 2.8 mL of distilled water were added and mixed well. Sample blank was prepared in similar way by replacing aluminium chloride with distilled water. The absorbance was measured at 415 nm (Kalita *et al.,* 2011).

Determination of Reducing Ability

Like the antioxidant activity, the reducing power increased with increasing amount of the extract, when potassium ferricyanide react with ferric chloride in the presence of anti oxidant, potassium ferrocyanide and ferrous chloride are found as a product. Presence of reducers causes the conversion of the Fe^{3+}/ ferricyanide complex used in this method to the ferrous form.

1 mL of different concentrations (6.25, 12.5, 25, 50, 100 μg/mL) of each of the extract was mixed with 2.5 mL of 1 % potassium ferricyanide, 2.5 mL of phosphate buffer (pH 6.6). The mixture was incubated at 50 °C for 20 min. 2.5 mL of 10 % tri chloroacetic acid was added to it and centrifuged at 3000 rpm for 10 min. 2.5 mL of supernatant was taken and 2.5 mL water and

0.5 mL of 0.1 % $FeCl_3$ were added to it. The absorbance was measured at 700 nm. Higher absorbance of the reaction indicated higher reducing power (Kalita *et al.,* 2011).

Determination of Antimicrobial Activity by Agar Well Diffusion Method

Antimicrobial activities of different crude extracts of the stem of Kin-pon and the bark of Tha-khut were screened in *vitro* by agar well diffusion method on nutrient agar medium (Perez *et al*., 1990). In the present study, petroleum ether, ethyl acetate, ethanol, methanol and aqueous extracts were used to study the antimicrobial property of plant sample. Bacterial cultures used in the research were three strains of gram positive (*Bacillus subtilis, Staphyloccous aureus* and *Bacillus pumilus*), two strains of gram negative (*Pseudomonas aeruginosa* and *Escherichia coli*) and one strain of fungi (*Candida albicans*). These experiments were carried out at Pharmaceutical Research Department, Insein, Yangon, Myanmar.

About 0.1 mL of crude extracts of petroleum ether, ethyl acetate, ethanol, methanol and water were added to agar wells. The plates were allowed to stand for 1 h for prediffusion of the extracts to occur. Then, the bacterial (*Bacillus subtilis*, *Staphylococcus aureus*, *Pseudomonas aeruiginosa*, *Bacillus pumilus* and *Escherichia coli*) and fungal (*Candida albicans*) media were incubated at 37 ºC for 24 h. The diameters of inhibition zones including 10 mm well were measured. In the study, the respective pure organic solvents (petroleum ether, ethyl acetate, ethanol, methanol and water) were used as negative control to determine possible inhibitory activity of the solvent. Antimicrobial activity was defined as the diameter (mm) of the clear inhibitory zone formed around the well.

Antioxidant Activity Screening by DPPH Radical Scavenging Assay

The antioxidant activity of 95 % EtOH and H_2O extracts were studied by DPPH Assay Method. DPPH radical scavenging activity was determined by spectrophotometric method. The control solution was prepared by mixing 1.5 mL of 60 µM DPPH solution and 1.5 mL of 95 % ethanol with vortex mixer. The sample solution was also prepared by mixing thoroughly 1.5 mL of 60 µM DPPH solutions and 1.5 mL of test sample solution. The solutions

were allowed to stand at room temperature for 30 min. After 30 min, measurement of absorbance at 517 nm was made by using spectrophotometer UV1800, Shimadzu corporation. Absorbance measurements were done in triplicate for each solution and the mean value was obtained, and then used to calculate % inhibition of oxidation by the following equation,

$$\% \text{ oxidative inhibition} = \frac{A_c - (A - A_b)}{A_c} \times 100\,\%$$

% oxidative inhibition = % oxidative inhibition of test sample

A_c = absorbance of the control (DPPH alone)

A_b = absorbance of the blank (EtOH + Test sample solution)

A = absorbance of test sample solution

Then IC_{50} (50 % inhibitory concentration) values were also calculated by linear regressive excel program (Brand-Williams *et al.,* 1995).

Screening of Antitumor Activity by Potato Discs Assay Method (Potato Crown Gall Test)

95 % EtOH and H_2O extracts of stem of Kin-pon and bark of Tha-khut were studied the tumor activity by Potato Discs Assay Method. Tumor producing bacteria, *Agrobacterium tumerfacien*, isolated from *Sandoricum koetjape* Merr. (Thitto) leaves were used in this study. All of these strains have been maintained as solid slants under refrigeration. For inoculation of the potato discs, 48 h broth cultures containing 5×10^7-5×10^9 cell / mL were used. Fresh, disease free potato tubers were obtained from local markets and were used within 48 h for transfer to the laboratory.

Tubers of moderate sizes were surface- sterilized by immersion in 50% sodium hypochlorite (Clorox) for 20 min. The ends were removed and soaked for 10 min more in Clorox. A core of the tissue was extracted from each tuber by using surface-sterilized (ethanol and flame) 2.5 cm wide cork borer and 2 cm pieces were removed from each end and discarded and the remainder of the cylinder is cut into 1.0 cm thick discs with a surface-sterilized cutter. The discs were then transferred to 1.5 % agar plates (1.5 g of Difco agar was

dissolved in 100 mL of distilled water, autoclaved and 20 mL poured into each petri dish). Each plate contained three discs. This procedure was done in the clean bench in the sterile room. 0.1, 0.2 and 0.3 g of sample was filtered through Millipolefilters (0.22 μm) into a sterile tube. A 0.5 mL of this solution was added to 1.5 mL of sterile distilled water and 2 mL of broth culture of *A. tumefaciens* strain (48 h culture containing 5×10^7-5×10^9cells/mL) were added aseptically.

Controls were made in this way; 0.5 mL of DMSO and 1.5 mL of sterile distilled water were added to the tube containing 2 mL of broth culture of *A. tumefaciens* (from the same 48 h culture). Using a sterile disposable pipette, 1 drop (0.05 mL) from these tubes was used to inoculate each potato disc, spreading it over the disc, surface. The process of cutting the potatoes and incubation must be conducted within 30 min. The plates were sealed with tape to minimize moisture loss and incubated at room temperature counted with microscope and compared with control. The antitumor activity was examined by observation if tumor formation was inhibited or not (Collin, 2001).

Determination of Antiarthritic Activity

The reaction mixture consisted of 0.5 mL of 5 % aqueous solution of bovine serum albumin and 0.05 mL of various concentrations (6.25, 12.5, 25, 50, 100 ug/mL) of the ethanol extract solutions of stems of Kin-pon and that of barks of Tha-khut. The pH of the reaction mixture was adjusted to 6.3 by using 1 M hydrochloric acid and it was then incubated at 37 °C for 20 min and then heated at 57 °C for 3 min. The reaction mixture was allowed to cool and added 2.5 mL of phosphate buffer saline. Turbidity was measured at 340 nm. In control, 0.05 mL distilled water was used instead of test extract while product control lacked bovine serum albumin and diclofenac sodium was used as the standard. The percentage inhibition of protein denaturation was calculated. The control represents 100% protein denaturation. All determinations were done in triplicate.

The reaction mixture consisted of 2.0 mL of 0.06 mg/mL trypsin, 1.0 mL of 0.25 mM tris-HCl buffer pH adjusted to 7.4 and 1.0 mL of ethanol extracts of stems of Kin-pon and barks of Tha-khut. The mixtures were

incubated for 37° C for 5 min. It was then added with 1.0 mL of 0.8 % casein. The mixtures were incubated for additional 20 minutes. Then 2.0 mL of 70 % perchloric acid was added and the cloudy solution was centrifuged at 2500 rpm for 5 min. Diclofenac was used as the standard. Absorbance of the supernatant was measured at 217 nm and buffer was kept as blank. The percentage inhibition of protein denaturation was calculated. All determinations were done in triplicate (Jayaprasam and Ravi, 2012).

Results and Discussion

Relative Abundances of some Elements in the Stem of Kin-pon and the Bark of Tha-khut

As shown in Tables 1 and 2, it can be seen that organic compounds are predominant in the samples, and other elements such as Ca, K and S are also present in reasonable composition but P, Fe and Mn were present in medium amount and Cu, Zn and Rb were present in very little amounts based on the relative abundance of elements.

Table 1: Relative Abundance of Some Elements in Stem of Kin-pon

Element	Relative Abundance (%)
Calcium	3.119
Potassium	1.025
Sulphur	0.172
Manganese	0.015
Iron	0.012
Strontium	0.008
Zinc	0.007
Copper	0.001
Organic Composition	95.641

Table 2: Relative Abundance of Some Elements in Bark of Tha-khut

Element	Relative Abundance (%)
Calcium	3.283
Potassium	0.742
Sulphur	0.128
Iron	0.008
Zinc	0.001
Copper	0.001
Rubidium	0.001
Organic composition	95.836

Nutritional Values of the Stem of Kin-pon and the Bark of Tha-khut

The nutritional values of the stem of Kin-pon and bark of Tha-khut such as moisture, ash, crude protein, crude fiber, crude fat, carbohydrates and energy values were determined by using standard methods for food analysis (AOAC, 2000) and the nutritional composition of the samples are described in Table 3. These analyses revealed some interesting findings. Kin-pon stem was found to contain higher protein content and crude fat content but lower carbohydrate content compared with that in the bark of Tha-khut. The other parameters were observed to be similar in two samples. According to the results, the presence of the important nutrients like fat, fiber, protein, carbohydrate and moisture and ash means that the two samples could be used as a nutritionally valuable and healthy ingredient to improve traditional medicinal formulation and to treat many diseases.

Table 3: Nutritional Compositions of Stem of Kin-pon and Bark of Tha-khut

Parameter	Nutritional Composition (%)	
	Stem of Kin-pon	**Bark of Tha-khut**
Moisture	10.69	11.25
Ash	11.81	9.55
Crude protein	8.71	2.29
Crude fiber	36.90	36.17
Crude fat	0.89	0.08
Carbohydrate	31.00	40.66
Energy value (kcal/100g)	169	173

Preliminary Phytochemical Screening in the **Stem of Kin-pon and the Bark of Tha-khut**

Preliminary Phytochemical screening was performed to investigate the plant materials in terms of its active constituents. In order to detect the various constituents present in the stem of Kin-pon and bark of Tha-khut, the plant extracts were subjected to the qualitative test analysis using standard methods. Test reagents, observations and inferences for the analyses are summarized in Table 4. Various types of organic constituents were found in both samples, except cyanogenic glycosides in both samples.

Table 4: Results of Phytochemical Screening of Stem of Kin-pon and Bark of Tha-khut

Chemical Constituents	Test Reagent	Observation	Inference	
			I	II
Alkaloids	(i) Dragendorff's	Orange ppt.	+	+
	(ii) Wagner's	Brown solution	+	+
	(iii) Mayer's	White ppt.	+	+
	(iv) Hager's	Yellow ppt.	+	+
Glycosides	10% Lead acetate	White ppt.	+	+
Carbohydrates	Molisch's	Red ring	+	+
α-Amino acids	Ninhydrin	Purple colour	+	+
Phenolic	5% Ferric chloride	Brown ppt.	+	+
Compounds	Shinoda's	Green solution	+	+
Flavonoids	LibermanBurchard	Greenish yellow	+	+
Steroids	LibermanBurchard	Pink	+	+
Terpenoids	Foam test	Marked frothing	+	+
Saponins	Ferrous sulphate	Green solution	+	+
Tannins	Sodium picrate	No change	_	_
Cyanogenic	Iodine	Deep violet	+	+
Glycosides	Benedict's	Reddish brown	+	+
Starch		ppt.		
Reducing	Bromocresol green	Deep green	+	+
Sugars		solution		
Organic Acids				

I =Stem of Kin-pon II = Bark of Tha-khut + = present - = absent ppt = precipitate

Total Phenol Contents in the Stem of Kin-pon and the Bark of Tha-khut

Total phenol contents were determined on the ethanol extracts of Kin-pon stem and Tha-khut bark by using Folin-Ciocalteu (F-C) method, where gallic acid was used as the standard. The absorbance values obtained at different concentrations of gallic acid were used for the construction of calibration curve (Figure 3). F-C method is based on the transfer of electrons in alkaline medium from phenolic compounds to phosphomolybedic phosphotun-gallic acid complexes to form blue coloured complexes, $(PMoW_{11}O_{40})^{-4}$ that are determined spectrophotometrically at 760 nm. Total phenol content of the extracts was calculated from the regression equation of calibration curve ($Y = 0.003 x + 0.016$; $R^2 = 0.994$) and expressed as mg

gallic acid equivalents (GAE) per gram of sample in dry weight. The results are presented in Table 5.

It can be seen (Table 6) that the total phenol content (30.49 µg GAE/ mg of the extract) of Tha-khut (75.90 µg GAE/ mg of the extract) is higher than that of Kin-pon indicating that Tha-khut bark might possess more phenolic compounds than Kin-pon stem. Generally, extracts with a high amount of phenolic compounds also exhibit high antioxidant activity.

Table 5: Absorbance of Standard Gallic Acid

Concentration (µg/mL)	Absorbance (Mean value) at 760 nm
6.25	0.024
12.5	0.034
25	0.072
50	0.178
100	0.384

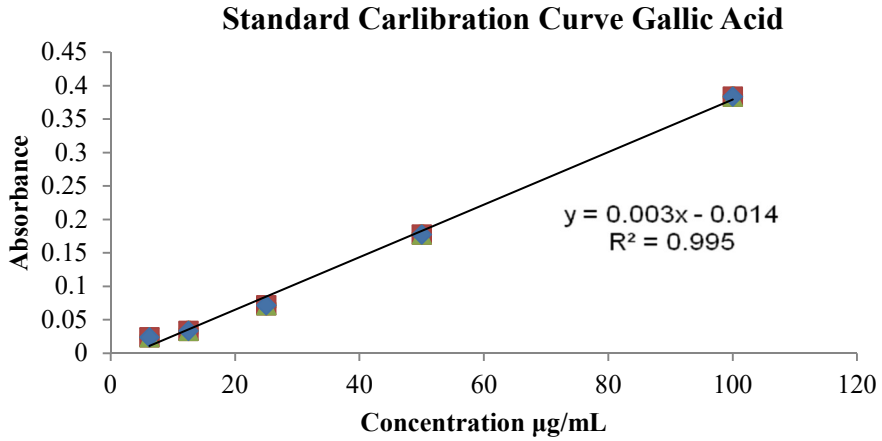

Figure 3: Plot of absorbance vs concentration of standard gallic acid

Table 6. Total Phenol Contents in Ethanol Extracts of Kin-pon Stem and Tha-khut Bark

Ethanol Extract	**Total Phenol Content (mg GAE/g of EtOH extract)**
Kin-pon stem	30.49 ± 2.67
Tha-khut bark	75.90 ± 4.2

Total Flavonoid Contents in the Stem of Kin-pon and the Bark of Tha-khut

To perform the calculation of the total flavonoid content in the samples by using Kiranmai *et al.* (2011) method, a standard curve is needed which is obtained from a series of asorbance of different quercetin concentrations (Table 7 and Figure 4). The total flavonoid content of ethanol extract (51.7 ± 2.9 mg of QE /g of EtOH extract) from the stem of Kin-pon was observed to be similar to that of the bark of Tha-khut (52.4 ± 1.9 ± 2.9 mg of QE /g of EtOH extract) (Table 8). Generally, extracts with a high amount of flavonoid contents also exhibit high antioxidant activity.

Table 7: Absorbance of Standard Quercetin

Concentrations (μg/mL)	Absorbance (Mean value) at 760 nm
6.25	0.005
12.5	0.015
25	0.041
50	0.109
100	0.234

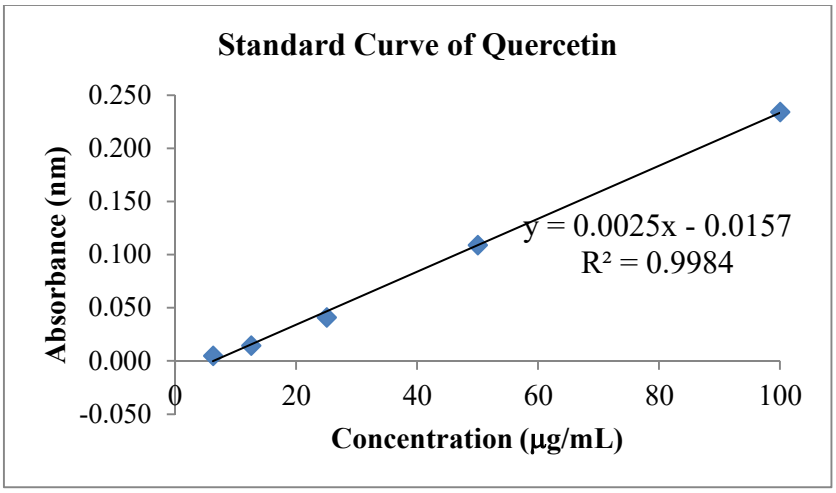

Figure 4: Plot of absorbance vs concentration of standard quercetin

Table 8: Total Flavonoid Contents in Stem of Kin-Pon and Bark of Tha-Khut

Samples	Total Phenolic Content (mg of QE /g of EtOH extract)
Kin-pon EtOH extract	51.7 ± 2.9
Tha-khut EtOH extract	52.4 ± 1.9

Reducing Ability of the Stem of Kin-pon and the Bark of Tha-khut

The reducing capacity of a compound may serve as a significant indicator of its potential antioxidant activity. The estimation of the reductive ability was investigated the Fe^{3+} to Fe^{2+} transformation by using the method of Oyaizu *et al*.,2013, where the change in the absorbance of the final mixture was measured at 700 nm (Table 9). Increase in the absorbance indicates higher reductive ability. The reducing capabilities of the ethanol extracts of bark of Tha-khut and stem of Kin-pon were found to be in dose dependent manner and were found to be slightly lower than standard quercetin (Figure5).

Table 9: Reducing Ability of Ethanol Extracts of Stem of Kin-pon and Bark of Tha-khut

Samples	**Absorbance of different concentrations (µg/mL) at 700 nm**				
	6.25	12.5	25	50	100
Quercetin	0.30	0.41	0.57	0.57	0.61
Tha-khut barks	0.32	0.36	0.39	0.43	0.45
Kin-pon stems	0.27	0.30	0.31	0.35	0.38

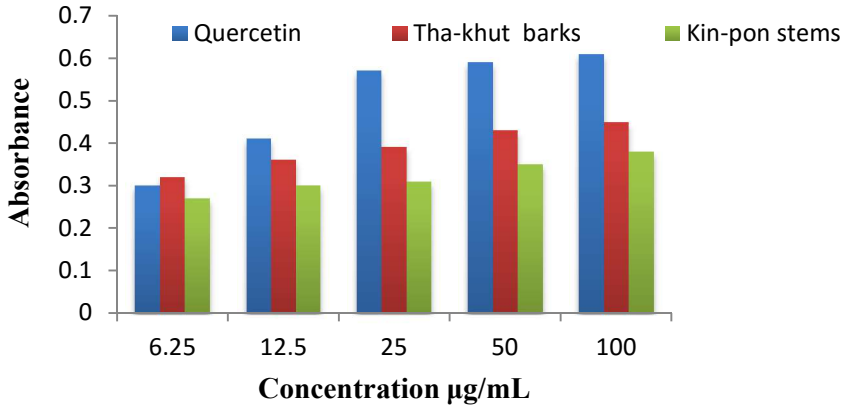

Figure 5: Reducing ability of ethanol extracts from the stem Kin-pon and the bark Tha-khut

Antimicrobial Activity of the Stem of Kin-pon and the Bark of Tha-khut

Antimicrobial activity was studied by agar well diffusion method according to Perez *et al*., 1990. In *vitro* antimicrobial screening of both samples extracts was carried out at Pharmaceuticall Research Department, Insein, Yangon, Myanmar. The antimicrobial activity was assessed by agar well diffusion method which is equally suited to the screening of antibiotics or the products of plant evaluation and is highly effective for rapidly growing microorganisms and the activities of the test extracts are expressed by measuring the zones (mm) of inhibition. Generally the more susceptible the organism, the bigger is the zone of inhibition.

Petroleum ether, ethyl acetate, ethanol, methanol and aqueous extracts of the stem of Kin-pon and the bark of Tha-khut were used to determine th antimicrobial activity against five bacterial strains such as *Bacillus subtilis*, *Staphylococcus aureus*, *Pseudomonas aeruginosa*, *Bacillus pumilus* and *Escherichia coli,* and one fungal strain: *Candida albicans*.

The observed antimicrobial activity of stem of Kin-pon and bark of Tha-khut was expressed as the zone diameters of inhibition shown in Tables 10 and 11. The photographs of agar plates showing the inhibition zones are illustrated in Figures 6 and 7. Among the extracts, EtOAc extract of Kin-pon (14~32 mm) was observed to possess higher antimicrobial activity than EtOAc extract of Tha-khut bark (11 ~ 19 mm). Generally, stem of kin-pon was found to be more potent than bark of Tha-khut in inhibition of microorganisms. Watery extract of Tha-khut bark did not show any activity against all microorganisms.

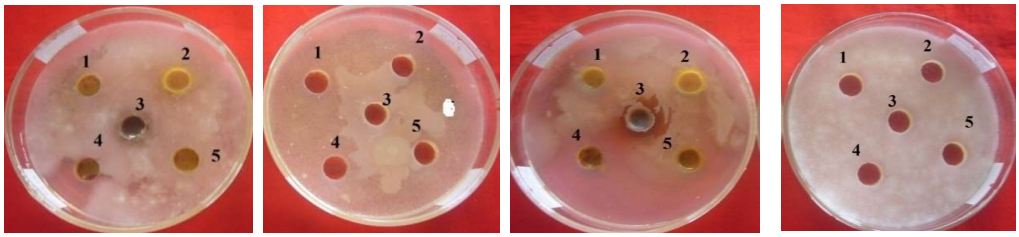

B.subtilis ***S.aureus***

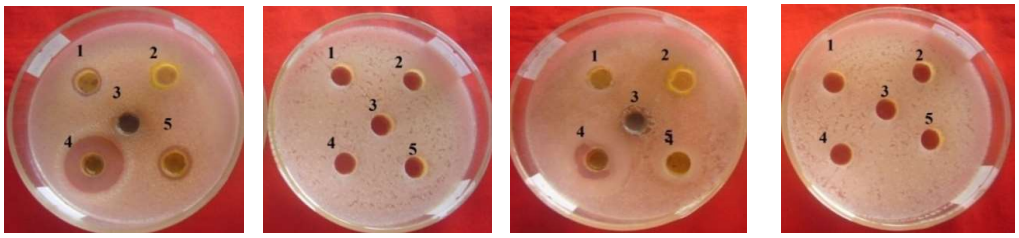

P.aeruginosa ***B.pumilus***

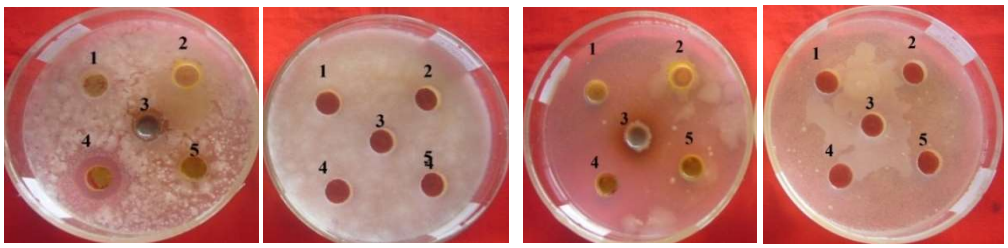

C.albicans ***E.coli***

Figure 6: Agar wells indicating inhibition zones of various extracts from the stem of Kin-pon

1 = EtOH extract 2 = PE extract 3= H_2O extract

4 = EtOAC extract 5 = EtOH extract

Table 10: Inhibition Zone Diameters of Stems of Kin-pon Extracts

Microorganisms	**Inhibition zone diameters (mm) of different extracts**				
	PE extract	**EtOAc extract**	**EtOH extract**	**H_2O extract**	**MeOH extract**
B.subtilis	15 (+)	15 (+)	–	–	–
S.aureus	–	28 (+++)	–	15(++)	–
P.aeruginosa	-	24 (+++)	13 (+)	–	–
B.pumilus	11(+)	14 (+)	–	13(+)	13 (+)
C.albicans	12 (+)	16 (++)	–	12(+)	–
E.coli	-	32 (+++)	–	–	–

Agar well = 10 mm
(+) = 10-14 mm (low activity)
(++) = 15-19 mm (moderate activity)
(+++) = 20 mm & above (high activity)
(-) = no zone of inhibition

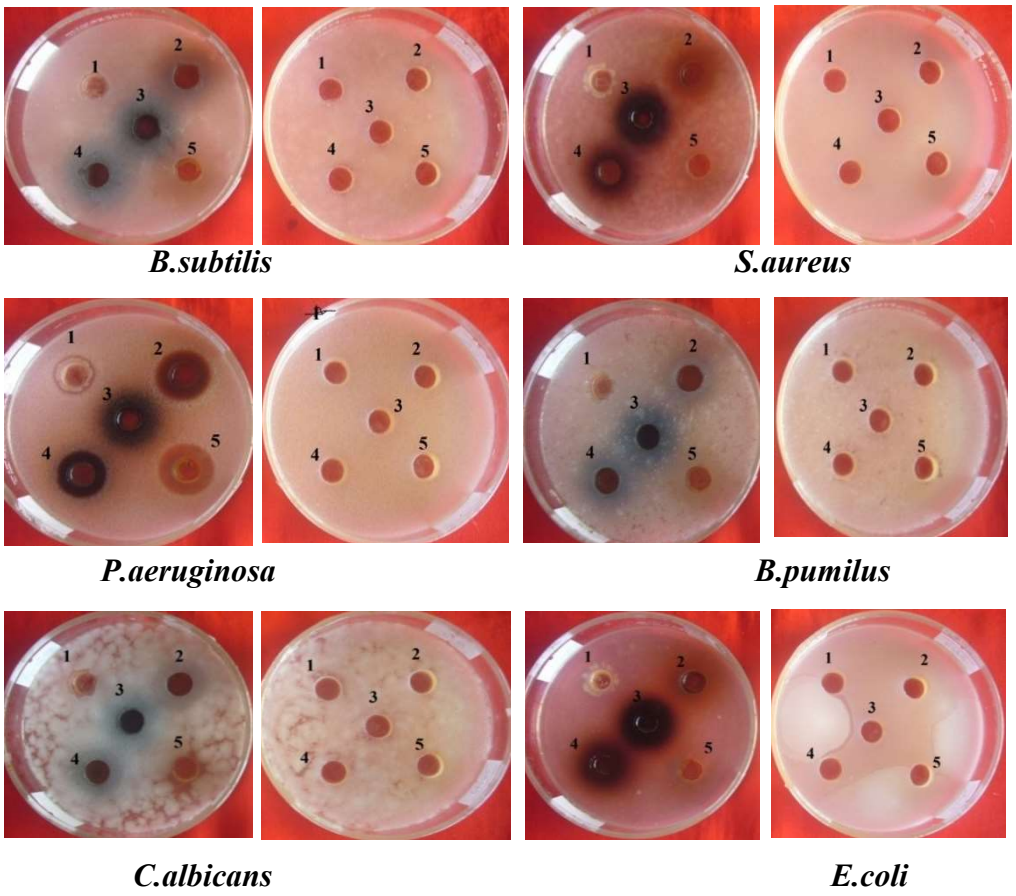

Figure 7: Agar wells indicating inhibition zones of various extracts from the bark of Tha-khut

1 = EtOH extract 2 = PE extract 3= H_2O extract
4 = EtOAC extract 5 = EtOH extract

Table 11: Inhibition Zone Diameters of Barks of Tha-kut Extracts

Microorganisms	Inhibition zone diameters (mm) of different extracts				
	PE extract	**EtOAc extract**	**EtOH extract**	**H_2O extract**	**MeOH extract**
B.subtilis	13 (+)	11(+)	–	–	–
S.aureus	–	13(+)	15 (+)	–	14(+)
P.aeruginosa	14 (+)	19(++)	19 (++)	–	17(+)
B.pumilus	12 (+)	–	–	–	–
C.albicans	13(+)	13(+)	–	–	–
E.coli	–	13(+)	20(+++)	–	14(+)

Agar well = 10 mm
(+) = 10-14 mm (low activity)
(++) = 15-19 mm (moderate activity)
(+++) = 20 mm & above (high activity)
(-) = no zone of inhibition

Antioxidant Activity of the Stem of Kin-pon and the Bark of Tha-khut

The antioxidant activity of ethanol and watery crude extracts of stem of Kin-pon and bark of Tha-khut were investigated with five different concentrations (12.5, 25, 50, 100, 200 µg/mL) by DPPH free radical scavenging assay. According to IC_{50} values, EtOH extract of bark of Tha-khut was more pronounced than other extracts. The antioxidant activity of the tested crude extracts was suggested to be very weak in comparing with the activity of standards ascorbic acid. IC_{50} value of ascorbic acid was found to 21.92µg/mL illustrated in (Table 12).

Table 12: Radical Scavenging Activity (%RSA) and IC_{50} Values of Crude Extracts from the Stem of Kin-pon, the Bark of Tha-khut and Standard Ascorbic Acid on Antioxidant Activity

Test sample	% RSA ± SD at Different Concentration (µg/mL)					IC_{50} (µg/mL)
	12.5	25	50	100	200	
Stem of Kin-pon (EtOH)	21.011±3.358	26.034±1.028	38.371±4.140	64.413±0.211	72.4±1.823	72.33
Stem of Kin-pon (Watery)	26.624±3.241	39.245±3.125	48.136±0.754	83.641±2.336	98.37±0.613	52.62
Bark of Tha-khut (Watery)	20.342±3.607	28.025±1.370	44.436±1.435	68.074±0.754	83.78±0.943	59.14
Bark of Tha-khut (EtOH)	24.012±2.023	41.392±1.963	53.541±0.796	83.193±0.869	92.161±0.827	42.71
Ascorbic acid	42.191±2.443	52.554±0.701	56.382±0.704	83.193±1.001	94.59± 1.365	21.92

Antitumor Activity of the Stem of Kin-pon and the Bark of Tha-khut

The antitumor activity of EtOH and H_2O of stem of Kin-pon and bark of Tha-khut were investigated by using PCG test with the isolated bacterium *A. tumefaciens.* For inoculation of the potato disc, 48 h broth cultures containing $5x10^9$ cells/mL were used. The tested samples were dissolved in DMSO to dilute and the diluted samples were mixed with the bacterial culture for inoculation. After preparing the inoculums, the bacterial suspension was inoculated on the cleaned and sterilized potato discs, and incubated for 3 days, at room temperature. After that, the tumors appeared on potato discs and these were checked by staining the knob with Lugol's (I_2-KI) solution. In the control, the formation of white knob on the blue background indicated the presence of tumor cells because there is no protein in tumor cells. The active test samples did not form any tumors on the potato discs and its surface remained blue.

Antitumor activity screening revealed that two crude extracts of stems of Kin-pon barks of Tha-khut can inhibit tumor growth until the minimum

dose of 0.1 g/mL of EtOH and watery extract of the sample (Tables 12 and 13).

Table 13: Antitumor Activity of Different Crude Extract from the Stem of Kin-pon

No.	Test Sample	Concentration of samples g/mL	Tumor	Remark
1.	Control	0	+	tumor occur
2.	EtOAc extract	0.1	-	No tumor occur
3.	EtOAc extract	0.2	-	No tumor occur
4.	Watery extract	0.1	-	No tumor occur
5.	Watery extract	0.2	-	No tumor occur

(+) Tumor appeared (-) no tumor appeared

Table 14: Antitumor Activity of Different Crude Extract from the Bark of Tha-khut

No.	Test Sample	Concentration of samples (g/mL)	Tumor	Remark
1.	Control	0	+	Tumor occur
2.	Ethanol extract	0.1	-	No tumor occur
3.	Ethanol extract	0.2	-	No tumor occur
4.	Watery extract	0.1	-	No tumor occur
5.	Watery extract	0.2	-	No tumor occur

(+) Tumor appeared (-) No tumor appeared

Anti-arthritic Activity of the Stem of Kin-pon and the Bark of Tha-khut

Inflammatory arthritis is a synovial disease characterized by chronic inflammation of the joints and can result in disability owing to joint destruction. *In vitro* anti-arthritic activity was performed using most popular methods such as inhibition of protein denaturation and proteinase inhibitory (Jayaprakasam and Ravi, 2012). The inhibition of protein denaturation was found in the ethanol extract of bark of Tha-khut but ethanol extract of stem of Kin-pon did not show in the concentrations between 6.25 ~ 100 μg/mL. The

IC_{50} value of the ethanol extract of bark of Tha-khut was 39.42 µg/mL. In this method diclofenac was used as standard for comparing its anti-arthritic potential at much lower concentration with an IC_{50} value of 15.99 µg/mL (Table 14 and Figure 8). In case of arthritis, auto antigens were produced due to protein denaturation. Proteinase inhibitory action was also studied. The ethanol extract of bark of Tha-khut exhibited the proteinase inhibitory action (IC_{50} = 52.33 µg/mL) but ethanol extract of stem of Kin-pon did not show in these concentrations 6.25 ~ 100 µg/mL (Table 15).

Table.15: Inhibition of Protein Denaturation of Stem of Kin-pon and Bark of Tha-khut

Samples	% Inhibition at different concentrations (mg/mL)					
	6.25	12.5	25	50	100	IC_{50} (µg/mL)
Kin-pon (EtOH)	ND	ND	ND	ND	ND	ND
Tha-khut (EtOH)	ND	12.57± 0.86	35.17±0.02	60.88±0.20	71.43±0.38	39.42
DS	10.28±0.11	46.28±0.02	59.58±0.38	72.10±0.11	92.68±0.30	15.99

Data are expressed as mean ± SD for triplicate experiments
ND =Not detected
DS= diclofenac sodium (China)

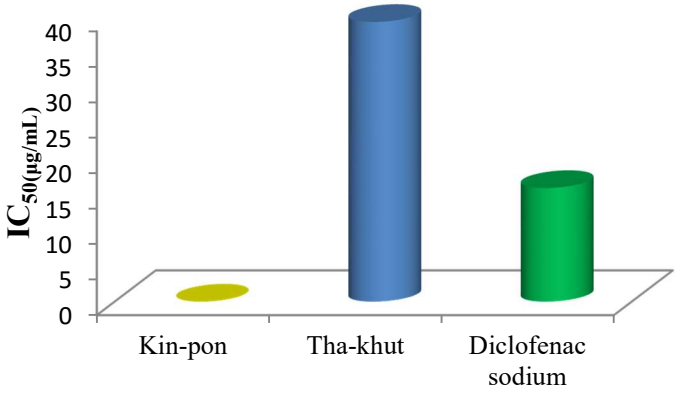

Figure 8: IC_{50} values of protein denaturation of stem of Kin-pon and bark of Tha-khut

Table 16: Proteinase Inhibitory Action Stem of Kin-pon and Bark of Tha-khut

Samples	% inhibition at different concentrations (mg/mL)					
	6.25	12.5	25	50	100	IC_{50} (µg/mL)
Kin-pon (EtOH)	ND	ND	ND	ND	ND	ND
Tha-khut (EtOH)	ND	ND	10.06 ± 0.62	49.66± 0.98	56.37±0.72	52.53
DS	8.96± 0.03	10.48± 0.11	37.71±0.04	68.14±0.96	94.08±0. 52	35.1

Data are expressed as mean ± SD for triplicate experiments
ND =Not detected
DS= diclofenac sodium (China)

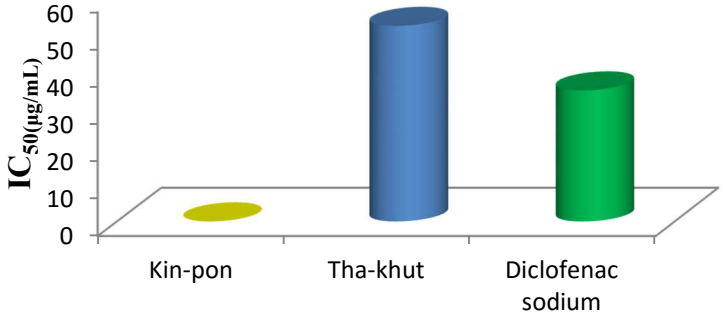

Figure 9: IC_{50} values of proteinase inhibitory action of stem of Kin-pon and bark of Tha-khut

Conclusion

EDXRF analysis showed the presence of calcium, potassium, sulphur, manganese, iron, stronium, zinc, copper in the stem of Kin-pon and calcium, potassium, sulphur, zinc, copper, rubidium in the bark of Tha-khut. According to nutritional composition analyses, the stem of Kin-pon had higher contents in protein and fat than the bark of Tha-khut. Qualitative phytochemical screening of the stem of Kin-pon and the bark of Tha-khut indicated the presence of bioactive constituents like alkaloids, glycosides, carbohydrates, α-amino acids, phenolic compounds, flavonoids, steroids, terpenoids, saponins, tannins, starch, reducing sugars and organic acids which are medicinally valuable. Total phenol contents, total flavonoid

contents and reducing ability of the ethanol extract of bark of Tha-khut was higher than that of stem of Kin-pon. Therefore, the ethanol extract of bark of Tha-khut has highest antioxidant activity than other extracts. From the results of antimicrobial activity screening, it may be concluded that the stem of Kin-pon was more potent than the bark of Tha-khut extracts in antibacterial activity against *Bacillus subtilis*, *Staphylococcus aureus*, *Pseudomonas aeruginosa*, *Bacillus pumilus* and *Escherichia coli*, and antifungal activity against skin pathogen, *Candida albicans*. Antitumor activity screening revealed that EtOH and H_2O extracts of stem of Kin-pon and bark of Tha-khut possessed tumor inhibition up to the minimum dose of 0.1 g/mL extract. In addition, antiarthritic activity of the ethanol crude extracts of stem of Kin-pon and bark of Tha-khut has been evaluated according to their proteinase inhibitory action and inhibition of protein denaturation. In antiarthritic activity, both of the ethanol extracts from bark of Tha-khut showed proteinase inhibitory effect (IC_{50}= 39.42 μg/mL) and inhibition of protein denaturation (IC_{50}= 52.53 μg/mL) however the ethanol extracts from stem of Kin-pon did not exhibit under same conditions. Consequently, it could be deduced that the bark of Tha-khut was more effective than the stem of Kin-pon for the treatment of antiarthritics.

Acknowledgements

The authors would like to thank the Department of Higher Education, Ministry of Education, Myanmar, for the permission of doing this research and Myanmar Academy of Arts and Sciences allowing to present this paper.

References

A.O.A.C. (2000). "*Official Methods of Analysis of the Association of Official Analytical Chemists*". Washington D.C: 17th Ed.

Bounmy, S., Pawadee. N., Somsak. R., Hideaki. O and Tripetch. K (2006). *"*Dolichandroside, A Phenolic Triglycoside from *Dolichandroneserrulata (*DC.) Seem*". The Japanese Society of Pharmacology and Springer-Verlag*, pp. 251-254.

Brand-Williams,W., Cuvelier, M.E. and Berse, C.(1995). "Use of a Free Radical Method to Evaluate Antioxidant Activity". *Lebensm.-Wiss. u.-Technol*., vol. 28, No. 1, pp. 25-30.

Bunbun, I. J., Nahar, N. and Haque, M. (2011). "Antibacterial, Cytotoxic and Antioxidant Activities of Chloroform, n-Hexane and Ethylacetate Extract of Plant *Coccina cordifolia". Agricultural and Biology J. of North America,* vol. 2, No.4, pp. 713 - 714.

Collin, A. (2011). "*Agrobacterium tumefaction*". A class Project for Soilborne Plant Pathogens, Morth Carolina State University, Department of Plant Pathology, pp. 728.

Jayaprakasam, R. and Ravi, T.K. (2012). "Evaluation of Anti Arthritic Activities of Root of *Alalypha indica* Linn. Using *in vitro* Techniques". *International Journal of Phytopharmacy,* Vol. 2, No. 6, pp. 169-173.

Kalita, S., G. Kumar, L. Karthik and K. V. B. Rao (2011), "Phytochemical Composition and In *Vitro* Hemolytic Activity of *Lantana camara* L. (Verbenaceae) Leaves". *Pharmacologyonline*. vol. 1, pp. 59-67.

Kiranmai, M., Mahendra, C. B .K. and Ibrahim, M. (2011). "Comparison of Total Favonoid Content of *Azadirachta indica* Root Bark Extracts Prepared by Different Methods of Extraction. *Res J. Pharm Biol Chem Sci.* vol. 2, No. 3, pp. 254-255.

Patel, S. S. and Zaveri, M. N. (2015). "Trypsin and Protein Denaturation Inhibitory Activity of Leaf and Root of *Justica gendarussa*". *Asian Journal of Pharmaceutical Science & Technology.* vol. 5, No. 4, pp. 217-223

Perez,C., Paul, M. and Bazerque, P. (1990). "Antibiotic Assay by Agar Well Diffusion Method.". *Alta BioMed Group Experiences.* vol. 15, pp. 113-115.

Saxena, M., Saxena, J., Nema, R., Singh, D and Gupta, A. (2013). "Phytochemistry of Medical Plants". *Journal of Pharmacognosy and Phytochemistry,* vol.1, No (6), pp.168-172.

BIOACTIVITY STUDY OF *CLEOME BURMANNI* L.MERR. (TAW-HINGALA) AND *ELEUSINE INDICA* L.GAERTN.(SINNGO-MYET)

Ma Tin Aye[1], Phyu Phyu Win[2], Ni Ni Than[3], Daw Hla Ngwe[4]

Abstract

In the present investigation, two medicinal plants, *Cleome burmanni* L. (Taw-hingala) and *Eleusine indica* L. (Sinngo-inyet) were selected for some bioactivity studies. Antioxidant activity of crude extracts was investigated by using DPPH radical scavenging activity assay. According to the observed data, ethanol extract of Sinngo-myet (IC_{50} = 86.14 µg/mL) showed similar activity with that of Taw-hingala (IC_{50} = 86.18 µg/mL). The cytotoxicity of 70 % ethanol and watery extracts of Taw-hingala and Sinngo-myet was studied by brine shrimp cytotoxicity bioassay. Among the four crude extracts (ethanol and watery extracts from two samples), only ethanol extract of Taw-hingala showed strong cytotoxic effect on brine shrimp at LD_{50}= 1.50 µg/mL but the other crude extracts did not exhibit their cytotoxic effect up to the optimum dose of 1000 µg/mL. Antitumor activity of ethanol and watery extracts of Taw-hingala and Sinngo-myet was also tested on tumor produced bacterium using PCG (Potato Grown Gall) test. From this experiment, the text extracts from all samples were significantly found to inhibit the formation of tumor in the dose of 0.062 g/disc. From the result of screening of antiproliferative activity, it was observed that methanol extracts of the whole plant of Taw-hingala and Sinngo-myet showed mild antiproliferative activity of IC_{50} value at > 100 µg/mL for lung cancer, cervix cancer, breast cancer, normal human fibroblast, liver cancer, pancreatic cancer and pancreas ductal adenocarcinoma respectively.

Keywords*:* *Marne burmanni* L. Merr and *Eleusine indica* L. Gaertn., antioxidant activity, cytotoxicity, antitumor activity, antiproliferative activity

Introduction

Traditional medicinal plants namely *Cleome burmanni* L. Merr. (Taw-hingala) and *Eleusine indica* L. Gaertn. (Sinngo-myet) (Figure 1) were selected in this study. The genus *Cleome* (Capparaceae) is one such genus

1. Demonstrator, Department of Chemistry, Sittway University
2. Associate Professor, Department of Chemistry, Dawei University
3. Professor, Department of Chemistry, Dr, University of Yangon
4. Professor and Head, Department of Chemistry, Dr, University of Yangon

reportedly used in traditional systems of medicine (Bose *et al.,* 2007). *Cleome burmanni* is the most commonly occurring species of *Cleome.* Many species of *Cleome* such as *C.viscosa, C. gynandra, C.chelidonii,* found growing as roadside weeds are reportedly used in traditional systems of medicines. Reports on the phytochemical analysis and medicinal value of this plant are scare or almost absent. However, a preliminary phytochemical screening has shown that many phytochemicals is present in the various extracts of this plant (Sofowora, 1993). *Eleusine indica* (Sinngo-myet) belongs to the family Poaceae. This plant is a common herbage with long, narrow leaves and tubular culm, including cereals, bamboo, sugarcane, fodder grass, goose grass, wire grass etc. Family Poaceae is the largest of the world flora and contain a very wide range of chemical constituent. However, a large proportion of chemical work has been devoted (Sindhia and Bairwa, 2010). There was no scientific information antitumor activity and antiproliferative activity concerning these two plants having in Myanmar. This study intended to illustrate the scientific proof of Myanmar medicinal plants used as good remedies in the treatment of tumor and cancer.

(a) **(b)**

Figure 1: Photographs of (a) Taw-hingala (THG) (b) Sinngo-myet (SNM)

Brine shrimp toxicity test

Artemia found favour as a "standard" organism in toxicological assay, despite the recognition that it is too robust organism to be a sensitive indicator species in pollution research. *Artemia,* the brine shrimp, has extensive use a test organism and in some circumstances is an acceptable alternative to the toxicity testing of mammals in the laboratory. The fact that millions of brine shrimp are also easily reared has been an important help assessing the effects of environment on the brine shrimp under well controlled experimental condition (Lieberman, 1999).

Brine shrimp

Brine shrimp is a small fairly shrimp that lives in vine pool and is used as food for aquarium fish (Figure 2).The scientific classification of brine are as follows:

Scientific	:	*Artemia salina*
Family name	:	Artemiidae
Genus	:	*Artemia*
Marketing name	:	Sea-Monkeys
Species	:	*salina*
Common name	:	Brine shrimp

Figure 2: Image of brine shrimp *(Artemia salina)* (X 200)

Materials and Methods

Screening of Antioxidant Activity by DPPH Assay

DPPH (2, 2- diphenyl-1-picryl hydrazyl) free radical scavenging assay was chosen to assess the antioxidant activity of plant materials. This assay has been widely used to evaluate the free radical scavenging effectiveness of various flavonoids and polyphenols in food system. (Lee *et al,* 2003) In this experiment, the antioxidant activity of ethanol and watery extracts of two selected plant samples was studied by DPPI-1 free radical scavenging assay.

DPPH free radical scavenging activity was determined by UV-visible spectrophotometric method according to the procedure described by Marini-Bettolo *et al*.,(1981).The control solution was prepared by mixing 1.5 mL of 0.002% DPPH solution and 1.5 mL of ethanol in the brown bottle. The sample solution was also prepared by mixing 1.5 mL of 0.002% DPPH solution and 1.5 mL of test sample solution. These bottles were incubated at room temperature and were shaken on shaker for 30 min. After 30 min, the absorbance values of these solutions were measured at 517 nm by using UV-visible spectrophotometer. The percent radical scavenging activity was calculated by the following equation.

$$\% \text{ RSA} = [(A_{DPPH} - A_{Sample}) A_{Blank} / A_{DPPH}] \times 100$$

where,

% RSA = % radical scavenging activity

A_{DPPH} = absorbance of DPPH in EtOH solution

A_{sample} = absorbance of sample + DPPH solution

A_{Blank} = absorbance of sample + EtOH solution

The antioxidant power (IC_{50}) is expressed as the test substances concentration (μg/mL) that result in a 50% reduction of initial absorbance of DPPH solution. IC_{50} (50% inhibitory concentration) values were calculated by linear regressive excel program.

Investigation of Cytotoxicity by Brine Shrimp Lethality Bioassay

Test solution (1 mL) was mixed with 9 mL of artificial sea water and placed in the chamber of ice cup. Alive brine shrimp (10 napulii) was taken with Pasteur pipette and placed into each chamber which was kept at room temperature for about 24 h. After 24 h incubation, the number of survival brine shrimp was counted and 50% lethality dose (LD_{50}) was calculated (Dockery and Tomkins, 2000). The control solution was prepared as the above procedure by using distilled water instead of sample solution.

Screening of Antitumor Activity

In this section, antitumor activity screening of 70 % ethanol, ethyl acetate, methanol extracts of the whole plant of Taw-hingala and Sinngo-myet were carried out by Potato Crown Gall (PCG) test (or) Potato Disc Assay (PDA) method, at Pharmaceutical Research Department, Ministry of Industry, Yangon.

Fresh, disease-free potatoes were purchased from a local market. Tubers of moderate size were surface-sterilized by immersion in 0.1 % sodium hypochlorite for 20 min. Ends were removed and the potatoes were soaked in 0.1% sodium hypochlorite for 10 min. A core of the tissue was extracted from each tuber with a surface-sterilized 1.0 cm cork borer. Pieces of 2 cm were removed from each end and discarded. The remainder of the cylinder was cut into 0.5 cm thick disc with a surface sterilized scalpel. The discs were then transferred to agar plates (1.5 g of agar dissolved in 100 mL distilled water, autoclaved for 20 min at 121 °C, 20 mL poured into each Petri dish. Each plate contained four potato discs and 4 plates were used for each sample dilution.

Sample (0.031, 0.062, 0.125, 0.250, 0.500 and 1 g) of crude extract were respectively dissolved in DMSO (2 mL) and filtered through millipore filters (0.22 mL) into sterilized tube. This solution (0.5 mL) was added to sterilize distilled water (1.5 mL) and broth culture of *A. tumefaciens* in PBS (2mL) was added. Controls were made in this way; DMSO (0.5 mL) and sterilized distilled water(1.5 mL) were added to the tube containing 2 mL of broth culture of *A. tumefaciens.* Using a sterile disposable pipette, 1 drop (0.05 mL) from these tubes was used to inoculate each potato disc, spreading

it over the disc surface. The plates were sealed with tape to minimize moisture loss and incubated at room temperature for three days at 27-30 °C. Tumors were observed on potato discs after 3 days under stereo-microscope followed by staining with Lugol's iodine (10 % K1 and 5 % 1_2) after 30 min and compared with control. The antitumor activity was examined by observation of tumor produced or not.

Investigation of Antiproliferative Activity

Antiproliferative activity of Taw-hingala and Sinngo-myet were studied *in vitro* using cancer cell lines at Division of Natural Product Chemistry, Institute of Natural Medicine, University of Toyama, Japan.

The *in vitro* antiproliferative activity of the methanol crude extract was determined by the procedure described. Briefly, each cell line was seeded in 96-well plates (2×10^3 per well) and incubated in the respective medium at 37 °C under 5 % CO_2 and 95 % air for 24 hr (Dahab and Afifi, 2007).

After the cells were washed with PBS (Nissui Pharmaceuticals), serial dilutions of the tested samples wereadded. After 72 h incubation, the cells were washed with PBS and 100μg/mL of medium containing10 % WST-8 cell counting kit (Dojindo; Kumamoto, Japan) solution was added to the wells. After 2 h incubation, the absorbance at 450 nm was measured. The concentrations of the serial dilutions of the tested samples were 100, 10, 1μg/mL for crude extract and 10, 1, 0.1 mM for positive control. Cell viability was calculated from the mean values of the data from three wells using the equation below and antiproliferative activity was expressed as the IC_{50} (50 % inhibitory concentration) value 5-fluorouracil was used as positive control.

$$(\%)\ \text{Cell viability} = 100 \times \frac{\left\{\text{Abs}_{(\text{test samples})} - \text{Abs}_{(\text{blank})}\right\}}{\left\{\text{Abs}_{(\text{control})} - \text{Abs}_{(\text{blank})}\right\}}$$

Results and Discussion

Cytotoxicity

The cytotoxicity of ethanol and watery crude extracts was expressed in terms of mean ± SEM (standard error mean) and LD_{50} (50 % Lethality Dose). Among the four crude extracts (watery and ethanol crude extract of two samples), only ethanol extract of Taw-hingala showed strong cytotoxic effect on brine shrimp at LD_{50} = 1.50 μg/mL, but the other crude extract did not exhibit cytotoxic effect to brine shrimp up to optimum dose of 1000 μg/mL (Table 1). The LD_{50} values of standard $K_2Cr_2O_7$ and caffeine are 43.741 μg/mL, and 1000 μg/mL, respectively.

These results revealed that the two selected plants were used to prepare one of the traditional medical formulation and were used to folk medicine as anticancer. The reported active (cytotoxic) plant in the study are worth of further pharmacological and medical studies in order to define what kind of antitumor activity they have and to isolate the natural active constituents, which are responsible for the activity.

Table 1: Cytotoxicity of Different Doses of Watery and Ethanol Crude Extracts of Taw-hangala and Sinngo-myet on *Artemia salina* (Brine Shrimp)

Tasted	Sample	No. of Dead Brine Shrimp (Mean± SEM) in various concentration (µg/mL)				
		1	**10**	**100**	**1000**	**LD_{50}µg/mL**
1	Watery Extract	1.50 ± 0.86	2.00 ± 1.15	2.50 ± 1.44	4.00 ± 2.31	> 1000
2	EtOH Extract	2.50 ± 1.44	3.50 ± 2.02	4.50 ± 2.60	5.50 ± 3.17	1.50
3	Watery Extract	1.50 ± 0.86	2.00 ± 1.15	3.00 ± 1.73	4.00 ± 2.31	> 1000
4	EtOH Extract	1.00 ± 0.57	2.00 ± 1.15	2.50 ± 1.44	3.50 ± 2.02	> 1000
5	$K_2Cr_2O_7$	0.67 ± 0.66	2.00 ± 2.00	10.00 ± 0.00	10.00 ± 0.00	43.74
6	Caffeine	0	2.33 ± 1.20	3.00 ± 0.58	5.00 ± 1.16	1000

Antioxidant Activity

From antioxidant screening test, 70 % ethanol and watery extracts of Taw-hingala showed mild antioxidant activity and their IC_{50} values were found to be 86.18 and 34.05 µg/mL respectively (Figure 3). In addition, 70 % ethanol and watery extracts of Sinngo-myet also showed mild antioxidant activity with IC_{50} values of 100.61 and 86.14 µg/mL respectively. The lower the IC_{50} values, the higher the antioxidant activities was found. Therefore, 70 % ethanol extracts are more potent than watery extracts in both samples and all of the extracts showed lower antioxidant activity than standard vitamin C (IC_{50}= 11.4 µg/mL)

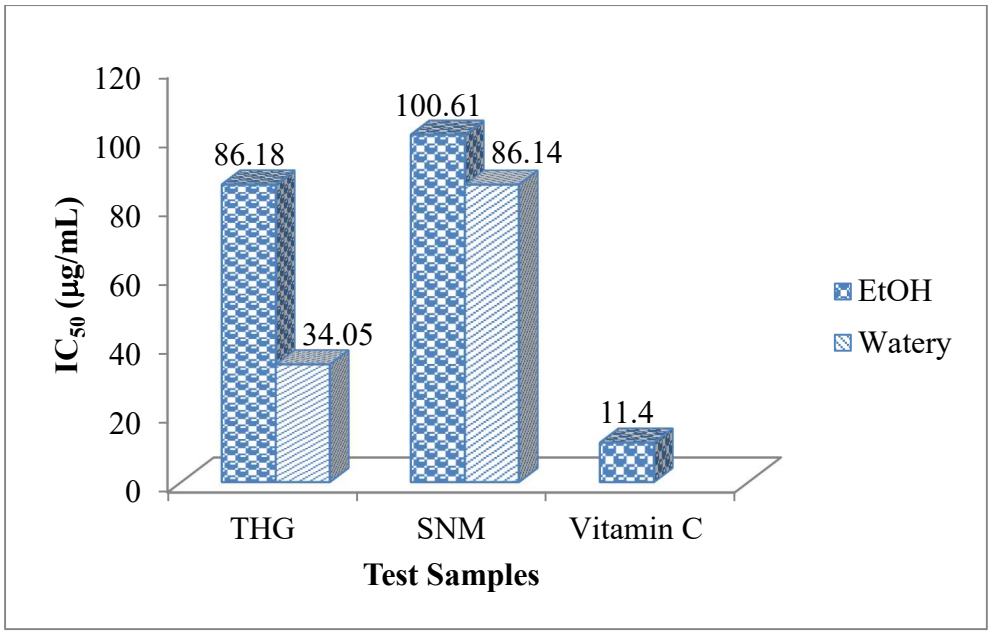

Figure 3: IC_{50} values of crude extract of Taw-hingala and Sinngo-myet

Antitumor Activity

The antitumor activity of watery and ethanol extracts of both plant samples were investigated by using PCG test with the isolated bacterium *A. tuniefaciens.* From this experiment, it was found that watery and 70 % ethanol extracts of both plants sample were effective in preventing the tumor formation with the doses of 1 to 0.062 g/disc in *vitro* potato disc assays (Table 2).

Table 2: Results of Antitumor Activity Screening on 70 % EtOH and Watery Extractsof Taw-hingala and Sinngo-myet

No	Test samples	Concentrations (g/disc)	Tumor Inhibition
1	EtOH (THG)	1	-
		0.500	-
		0.250	-
		0.125	-
		0.062	-
		0.031	+
2	Watery (THG)	1	-
		0.500	-
		0.250	-
		0.125	-
		0.062	-
		0.031	+
3	EtOH (SNM)	1	-
		0.500	-
		0.250	-
		0.125	-
		0.062	-
		0.031	+
4	Watery (SNM)	1	-
		0.500	-
		0.250	-
		0.125	-
		0.062	-
		0.031	+
5	Standard compound (Taxol)	0	+

(-) = tumor appear

(+) = no tumor appear

Screening of Antiproliferative Activity on Cell Lines

Antiproliferative activity is the activity relating to a substance used to prevent or retard the spread of cells, especially malignant cells, into surrounding tissues. Antiproliferative activity were studied *in vitro* using human cancer cell lines. Screening of antiproliferative activity of methanol extracts of Taw-hingala and Sinngo-myet was done by using seven human cancer cell lines. The cell lines used were A 549 (human lung cancer), Hela (human cervix cancer), MCF 7 (human breast cancer), and WI-38 (normal human fibroblast), HePG2 (human liver cancer). PSN 1 (human pancreatic cancer) and PANC1 (pancreas ductal adenocarcinoma).

From the results, it was observed that methanol extracts of the whole plant of Taw-hingala and Sinngo-myet showed mild antiproliferative activity at IC_{50} value = > 100 μg/mL for lung cancer, cervix cancer, breast cancer, normal human fibroblast, liver cancer, pancreatic cancer and pancreas ductal adenocarcinoma (Table 3).

Table 3: Antiproliferative Activity of Methanol Crude Extracts of Taw-hingala and Sinngo-myet against Various Types of Cancer Cell Lines

Samples	IC_{50} (μg/mL) of Various Samples against Tested Cell Lines						
	A549	**Hela**	**MCF7**	**WI-38**	**HePG2**	**PSN1**	**PANC1**
THG (Methanol extract)	> 100	> 100	> 100	> 100	> 100	> 100	> 100
SNM (Methanol extract)	> 100	> 100	> 100	> 100	> 100	> 100	> 100

A 549 = human lung cancer
Hela = human cervix cancer
MCF 7 = human breast cancer
WI-38 = normal human fibroblast
HePG2 = human liver cancer
PSN1 = human pancreatic cancer
PANC1 = pancreas ductal adenocarcinoma

Conclusion

In the present investigation, antioxidant activities of 70% ethanol and watery extracts of Taw-hingala and Sinngo-myet were determined by DPPH assay method using UV spectrophotometer. According tothe observed data, ethanol extract of Sinngo-myet (IC_{50} = 86.14 μg/mL) showed similar activity with watery extract of Taw-hingala(IC_{50} = 86.18μg/mL).

The cytotoxicity of 70 % ethanol and watery extracts of Taw-hingala and Sinngo-myet was studied by brine shrimp cytotoxicity bioassay. Among the four crude extracts(watery and ethanol extract from two samples), only ethanol extract of Taw-hingala showed strong cytotoxic effect on brine shrimp at LD_{50}= 1.50 μg/mLbut the other crude extracts did not exhibit their cytotoxic effect up to the optimum dose of 1000μg/mL.

Antitumor activity of ethanol and watery extracts of Taw-hingala and Sinngo-myet was also tested on tumor produced bacterium using PCG (Potato Grown Gall) test and all of the test extracts from all samples were significantly found to inhibit the formation of tumor in the dose of 0.062 g/disc. From the screening of antiproliferative activity, it was observed that all of methanol extracts of the whole plant of Taw-hingala and Sinngo-myet showed mild antiproliferative activity of IC_{50} value at > 100 μg/mL for lung cancer, cervix cancer, breast cancer, normal human fibroblast, liver cancer, pancreatic cancer and pancreas ductal adenocarcinoma respectively.

Acknowledgement

The authors would like to express their profound gratitude to the Department of Higher Education (Yangon Office), Ministry of Education, Yangon, Myanmar, for provision of opportunity to do this research and Myanmar Academy of Arts and Science for allowing to present this paper.

References

Bose, A., Gupta, J.K., Dash, J.K. and Ghosh ,T.S. (2007). "Diuretic and Antibacterial Activity of Aqueous Extract of *Cleome burmanni* L.Gaertn". *Journal of Pharmaceutical Science,* vol. 69 (2), pp. 292-294

Dahab, R. A. and Afifi, F. (2007). "Antiproliferative Activity of Selected Medicinal Plants of Jordan Against A Breast Adenocarcinoma Cell Line (MCF7)". *Scientia Pharmaceutica (Sci. Pharm.)*, vol. 75, pp. 121-136

Dockery, M. and Tomkins, S. (2000). *Brine Shrimp Ecology*. London: 1st Ed., The British Ecology Society, London, pp. 92-93

Lee, S.E., Hwang, H.J.,Jeong,H.S. and Kim,J.H.(2003). "Screening of Medicinal Plant Extracts for Antioxidant Activity". *Journal* of *Science*, vol. 73, pp. 167-179

Liebermanw, M. (1999), "A Brine Shrimp Bioassay for Measuring Toxicity and Remediation of Chemical " . *Journal of Chemical Education,* vol.76(12), pp. 1689-1691

Marini-Bettolo, G.B., Nicoletti, M., Patamia, M., Geleffi, C. and Messana, I. (1981). "Plant Screening by Chemical and Chromatographic Procedure under Field Conditions". *Journal of Chromato,* vol. 213,pp. 113-127

Sindhia, V.R. and Bairwa, R. (2010). "Compendium of Pharmacological Actions of Medicinal Plants and Their Constituents*". International Journal of Pharmaceutical and Clinical Research*, vol. 2 (2), pp. 90-94

Sofowora, A. (1993). *Medicinal Plants and Traditional Medicine in Africa*. Nigeria: 2nd Ed., Spectrum Books Ltd., pp. 493

INVESTIGATION OF SOME BIOACTIVITIES OF *Peperomia pellucida* L. (THIT-YAY-GYI) AND *Enhydra fluctuans* L. (KANA-PHAW)

Mai Thet Mar Htun[1], Mya Thandar Aung[2], Ni Ni Than[3], Daw Hla Ngwe[4]

Abstract

In the present work, *Peperomia pellucida* L. (Thit–yay–gyi) and *Enhydra fluctuans* L. (Kana-phaw) were chosen to investigate some bioactivities such as antimicrobial, antioxidant, antitumor, anticancer or antiproliferative activities. The antimicrobial activity of different crude extracts from the Thit-yay-gyi and Kana-phaw was determined by agar well diffusion method. Ethyl acetate extracts of both plants samples showed the antimicrobial activity on all tested microorganisms with inhibition zone diameters in the range between 18 mm-35 mm for Thit-yay-gyi and 21 mm-35 mm for Kana-phaw. The antioxidant activity of ethanol and watery crude extracts of Thit-yay-gyi and Kana-phaw were investigated by using DPPH free radical scavenging assay. The antioxidant activity of Kana-phaw ethanol extract (IC_{50} = 22.53 µg/mL) was found to be highest followed by Thit-yay-gyi ethanol extract (IC_{50} = 37.75 µg/mL), then by Kana-phaw watery extract (IC_{50} = 40.63 µg/mL) and Thit-yay-gyi watery extract (IC_{50} = 44.81 µg/mL). In addition, the cytotoxicity of EtOH and H_2O crude extracts from Thit-yay-gyi and Kana-phaw were evaluated by brine shrimp cytotoxicity bioassay. The cytotoxicity of Thit-yay-gyi EtOH extract (LD_{50}=68.2µg/mL) showed more cytotoxic effect than other crude extracts. The antitumor activity of crude extracts was pre-screened by PCG test. It was found that they can inhibit the growth of tumor in the rangs of concentration 1 g/mL, 0.5 g/mL and 0.25 g/mL, 0.12 g/mL. Furthermore, antiproliferative activity of EtOH and H_2O extracts of Kana-phaw and Thit-yay-gyi was investigated by using seven human cancer cell lines. Antiproliferative activity of two extracts were found to be in order of EtOH extract of Thit-yay-gyi>EtOH extract of Kana-phaw> H_2O extract of Thit-yay-gyi> H_2O extract of Kana-phaw. Among the tested crude extracts, EtOH extract of Thit-yay-gyi were found to be more potent than other crude extracts. Therefore, it could be inferred that EtOH extract of Thit-yay-gyi possessed the higher antiproliferative activity than Kana-phaw. By silica gel column chromatographic separation technique, compound A (kaurenoic acid) (white crystal, 0.015 %, m.pt. 172 °C) from PE extract of Kana-phaw was isolated. The isolated compound was identified by physicochemical

1. PhD Candidate, Department of Chemistry, University of Yangon
2. Lecturer, Department of Chemistry, University of Yangon
3. Professor, Department of Chemistry, University of Yangon
4. Professor and Head, Department of Chemistry, University of Yangon

properties and modem spectroscopic technique such as FT IR, NMR, HMBC and ESI MS spectrometry as well as by comparing with their reported data. Isolated compound A (kaurenoic acid) was evaluated by brine shrimp cytotoxicity bioassay. Compound A (kaurenoic acid) showed 50 % death of brike shrimp at concentration of 0.00001 μg/mL.

Keywords: *Peperomida pellucida, Enhydra flucuans*, antimicrobial activity, antioxidant activity, DPPH, brine shrimp cytotoxicity, antitumor activity, antiproliferative activity

Introduction

Peperomida pellucida L. and *Enhydra flucuans* L. belongs to the families Piperaceae and Asteraceae respectively and are called Thit-yay-gyi and Kana-phaw in Myanmar. These plants have been used for treatments of antifungal, antioxidant, anticancer, antiflammatory and antidiarrheal. It is a remarkable medicinal plants that grow wild in India, China and throughout South East Asia (Sarma, 2014).

An antimicrobial activity is an agent that kills microorganisms or inhibits their growth. Medicinal plants represent a rich source of antimicrobial agents. Antioxidants means “against oxidation”. Antioxidants, also known as “free radical scavengers” are compounds that either reduce formation of free radicals or react with an neutralize them. Cytotoxicity is the quality of being toxic to cell. Example of toxic agents are an immure cell or some types of venom.

The extra cells can form a mass called a tumor. Tumors can be benign or malignant. Benign tumors are not cancer while malignant ones are. Cells from malignant tumors can invade nearby tissues. They can also break away and spread to other parts of body. Cancer is not just one disease but many diseases. Most cancers are named for where they start.

Antiproliferative activity is the activity relating to a substance used to prevent or retard the spread of cells, especially malignant cells, into surrounding tissues. Antiproliferative activity were studied *in vitro* using human cancer cell lines.

Materials And Methods

Sample collection

Thit-yay-gyi has been collected from Yangon University Campus and Kana-phaw has been collected from Hlaingtharyar Township, Yangon Region. Its scientific name has been identified at Department of Botany, University of Yangon.

Extraction and Preparation of Crude Extracts from Thit-yay-gyi and Kana-phaw

The dried powdered sample (500 g) was defatted with (2 L) for 95 % EtOH for one week at room temperature by percolation method and followed by filtration. This procedure was repeated for three times. The total combined filtrate was evaporated under reduced pressure by means of a rotary evaporator. Consequently, the defatted EtOH extract was obtained. The defatted sample was then partitioned with PE: H_2O (1 : 2) (300 mL). The combined petroleum ether layers were concentrated under reduced pressure by means of a rotary evaporator. Consequently, pet-ether soluble extract was obtained. The defatted residue was further partitioned between ethyl acetate with water. The combined ethyl acetate layers were concentrated by means of a rotary evaporator. After that ethyl acetate soluble extract was obtained. In this way, 95 % ethanol, pet-ether and ethyl acetate soluble extracts of both plants samples were prepared.

Screening of Antimicrobial Activity by Agar Well Difussion Method

Antimicrobial activities of different crude extracts were tested on six microorganism such as *Bacillus subtilis, Staphylococcus aureus, Pseudomonas aeruginosa, Bacillus pumilus, Escherichia coli* and *Candida albicans* species at the Pharmaceutical Research Department (PRD), Ministry of Industry, Yangon.

To a mixture of 1 g of meat extract, 1 g of peptone, 0.5 g of NaCl and 1.5 g of agar powdered were placed in a sterilized 250 mL conical flask, 100 mL of sterile distilled water were added to obtain nutrient agar medium. The resulting mixture was heated to dissolve the contents. Then the pH of the

resulting solution was adjusted to 7.2 with 0.1 M NaOH solution. It was sterilized in an autoclave at 121 °C for 15 min. About 20-25 mL of agar medium contained test organisms were poured into the sterile petri-dishes under aseptic condition near the flame of the spirit burner and left the agar solid, the cork borer about 10 mm in diameter was sterilized and made a well in the agar plate previously described. Then the extract samples were introduced into the well (about 0.2 mL). They were then incubated at 36 °C for 24 h. The formation of inhibition zone around the well was observed. This observation indicates the presence of antimicrobial active compounds in the extract.

Screening of Antioxidant Activity by DPPH Free Radical Scavenging Assay

In this experiment, the antioxidant activity of ethanol and watery extracts of two selected plant samples was studied by DPPH free radical scavenging assay.

DPPH free radical scavenging activity was determined by UV-visible spectrophotometric method according to the procedure described by Marinova and Batchvarov (2011). The control solution was prepared by mixing 1.5 mL of 0.002 % DPPH solution and 1.5 mL of ethanol in the brown bottle. The sample solution was also prepared by mixing 1.5 mL of 0.002 % DPPH solutions and 1.5 mL of test sample solution. These bottles were incubated at room temperature and were shaken on shaker for 30 min. After 30 min, the absorbance values of these solutions were measured at 517 nm by using UV-visible spectrophotometer. The percent radical scavenging activity was calculated by the following equation.

$$\% \text{ RSA} = [(A_{DPPH} - A_{Sample}) - A_{Blank} / A_{DPPH}] \times 100$$

where,

% RSA = % radical scavenging activity
A_{DPPH} = absorbance of DPPH in EtOH solution
A_{sample} = absorbance of sample + DPPH solution
A_{Blank} = absorbance of sample + EtOH solution

The antioxidant power (IC_{50}) is expressed as the test substances concentration (μg/mL) that result in a 50% reduction of initial absorbance of DPPH solution and that allow to determine the concentration. IC_{50} (50% inhibitory concentration) value were calculated by linear regressive excel program. The standard deviation was also calculated by the following equation.

$$\text{Standard Deviation (SD)} = \sqrt{\frac{(\bar{x} - x_1)^2 + (\bar{x} - x_2)^2 + ...(\bar{x} - x_n)^2}{(n-1)}}$$

Investigation of Cytotoxicity by Brine Shrimp Lethality Bioassay

Cytotoxicity of crude extracts from Kana-phaw and Thit-yay-gyi was investigated by brine shrimp lethality bioassay according to the procedure described by Dockery and Tomkins, 2000.

Artificial sea water (9 mL) and (1 mL) of different concentrations of samples and standard solutions were added to each chamber. Alive brine shrimps (10 nauplii) were then taken with pasteur pipette and placed into each chamber. They were incubated at room temperature for about 24 h. After 24h, the number of dead or survival brine shrimps was counted and 50 % lethality dose (LD_{50}) was calculated (Dockery and Tomkins, 2000). The control solution was prepared as the above procedure by using distilled water instead of sample solution.

Screening of Antitumor activity by Potato Crown Gall (PCG) Test or Potato Disc Assay Method

Fresh potato tubers were obtained from Hledan market, Kamayut Township in Yangon Region and were used within 48 hours before transfer to the laboratory.

Tubers of moderate size were surface-sterilized by immersion in 50% sodium hypochlorite (Clorox) for 20 min. The ends were removed and soaked for 10 min more in Clorox. A core of the tissue was extract from each tuber by using surface-sterlized (ethanol and flame) 1.0 cm wide cork borer and 2 cm pieces were removed from each end and discarded and the remainder of

the cylinder is cut into 0.5 cm thick dics with a surface-sterilized cutter. The discs were then transferred to agar plates (1.5 g of agar was dissolved in 100 mL distilled water, autoclaved for 20 min at 121 °C, 20 mL poured into each petri dish). Each plate contained four potato discs and 4 plates were used for each sample dilution.

Sample (0.125, 0.25 g, 0.5 g and 1 g) of crude extracts were respectively dissolved in dimethyl sulphoxide (DMSO) (2mL) and filtered through Millipore filter (0.22 μm) into sterile tube. This solution (0.5 ml) was added to sterile distilled water (1.5 mL) and broth culture (2 mL) of *Agrobacterium tumefaciens* strains .

Controls were made in this way, DMSO (0.5 mL) and sterile distilled water (1.5 mL) were added to the tube containing broth culture (2 mL) of *Agrobacterium tumesfaciens* strains.

By using a sterile disposable pipette, one drop (0.5 mL) from these tube was used to inoculate each potato discs spreading it over the discs surface. After inoculation, petri dishes were sealed by paraffin and incubated at 27-30 °C for 14. Tumors were observed on potato discs after 14 under stereo-microscope followed by staining with Lugol's solution (5 % I_2 and 10 % KI) after 30 min and compared with control. The anti-Agrobacterium tumefaciens activity was examined by observation of crown gall produced or not.

Screening of Antiproliferative activity on Cell Lines

Antiproliferative activity of Kana-phaw and Thit-yay-gyi was studied *in vitro* using cancer cell lines (lung, cervix, breast, normal human fibroblast, liver, pancreatic, pancreas ductual adenocarcinoma) at Division of Natural Product Chemistry, Institute of Natural Medicine, University of Toyama, Japan.

The *in vitro* antiproliferative activity of the crude extracts was determined by the procedure described (Win *et al.,* 2015). Briefly, each cell line was seeded in 96-well plates (2×10^3 per well) and incubated in the respective medium at 37 °C under 5 % CO_2 and 95 % air for 24 hs. After the cells were washed with PBS (Nissui Pharmaceuticals), serial dilutions of the

tested samples were added. After 72 hrs incubation, the cells were washed with PBS and 100 μL of medium containing 10 % WST-8 cell counting kit (Dojindo; Kumamoto, Japan) solution was added to the wells. After 2 hrs incubation, the absorbance at 450 nm was measured. The concentrations of the serial dilutions of the tested samples were 100, 10, 1 μg/mL for crude extract, 100, 10, 1 μM for isolated compounds and 10, 1, 0.1 mM for positive control. Cell viability was calculated from the mean values of the data from three wells using the equation below and antiproliferative activity was expressed as the IC_{50} (50 % inhibitory concentration) value. 5-fluorouracil was used as positive control.

$$(\%)\ \text{Cell viability} = 100 \times \frac{\left\{\text{Abs}_{(\text{test samples})} - \text{Abs}_{(\text{blank})}\right\}}{\left\{\text{Abs}_{(\text{control})} - \text{Abs}_{(\text{blank})}\right\}}$$

Extraction and Isolation of Chemical Constituents from Kana-phaw

PE extract (5 g) was mixed with silica gel. The mixture was allowed to evaporate with continuous agitation so that freely flowing of dry silica gel on which the sample was uniformly absorbed. The resulting powdered mixture was added to the column using small long necked funnel. The top of the layer was wet with solvent that had previously been allowed to remain above the gel by opening the tap. Some adsorbed gel sticking on the inner wall was washed down with the solvent. The column was then completely filled with adding the solvent system PE:EtOAc (99:1) and fraction was started. The tap was opened and the fractions were collected at the rate of one drop per seconds. Gradient elution was performed successively with PE:EtOA (99:1, 98:2, 95:5, 9:1, 5:1, 2:1, 1:1) v/v and a total of 109 fractions were collected.

The fractions which showed similar TLC behaviours were combined to give successive three main fractions $F_{I\ (1\text{-}20)}$, $F_{II\ (21\text{-}55)}$ and $F_{III\ (56\text{-}109)}$. The collected fractions were monitored by TLC behaviours. After the solvents have been evaporated, fractions F_I and F_{III} were obtained as a mixture. Fraction F_{II} was washed with acetone and purified by crystallization from pet ether to give 30 mg (0.01 %) of compound A (Kaurenoic acid) as white crystal.

Structural Identification

The structures of isolated compound was identified by modern spectroscopic techniques such as FT IR, NMR, HMBC and ESI MS. FT IR spectra of isolated compounds were recorded at Department of Chemistry, University of Yangon. ^{1}H NMR, ^{13}C NMR, HMBC and ESI MS spectra of isolated compound A were measured at Department of Organic and Biomolecular Chemistry, Georg-August University, Goettingen, Germany.

Results and Discussion

Antimicrobial Activity

The antimicrobial activity of Thit-yay-gyi and Kana-phaw was screened by agar well diffusion method on *Escherichia coli*, *Staphylococcus aureus*, *Bacillus subtilis*, *Bacillus pumilus*, *Pseudomonas aeruginosa* and, *Candida albicans* (Figure 1). The resultant inhibition zone diameters are described in Table 1. The larger the inhibition zone diameters, the higher the antimicrobial activity.

According to the results, it was found that EtOAc extract of Thit-yay-gyi and Kana-phaw exhibited more potent antimicrobial activity against all test species with inhibition zone diameter between 18 mm and 35 mm for Thit-yay-gyi and 21mm and 35mm for Kaka-phaw. But Thit-yay-gyi of EtOH extract and Kana-phaw of PE extracts showed less activity.

Therefore, EtOH extract of Thit-yay-gyi and PE extract of Kana-phaw exhibited less antimicrobial activity and EtOAc extract of Thit-yay-gyi and Kana-phaw had the highest antimicrobial activity.

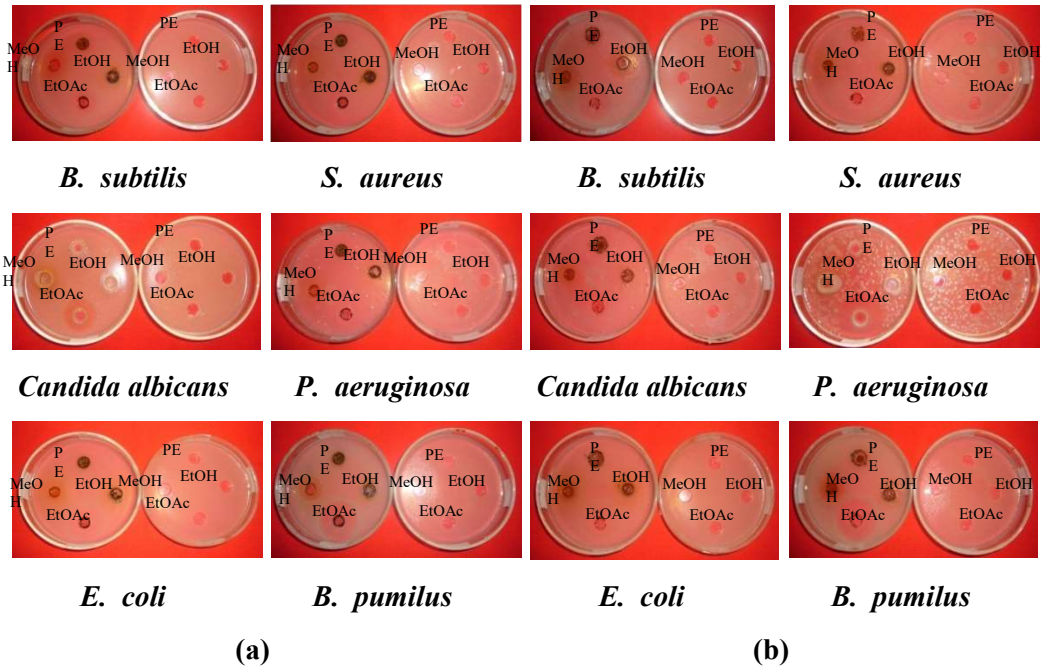

Figure 1: Antimicrobical activity of crude extracts of
(a) Thit-yay-gyi and
(b) Kana-phaw

Table 1. Inhibition Zone Diameters (mm) of Crude Extracts of Thit-yay-gyi and Kana-phaw against 6 Microorganisms

Sample	Solvent	***B. subtilis*** **(mm)**	***S. aureus*** **(mm)**	***P. aeruginosa*** **(mm)**	***B. pumilus*** **(mm)**	***Candida albicans*** **(mm)**	***E. coli*** **(mm)**
Thit-yay-gyi	PE	13 (+)	-	-	-	-	24 (+++)
	MeOH	17 (++)	32 (+++)	-	19 (++)	-	19 (++)
	EtOAc	18 (++)	30 (+++)	19 (++)	**35 (+++)**	25 (+++)	25 (+++)
	EtOH	-	-	-	-	-	-
Kana-phaw	PE	-	20 (+++)	-	-	-	-
	MeOH	20 (+++)	32 (+++)	-	21 (+++)	15 (++)	19 (++)
	EtOAc	21 (+++)	32 (+++)	30 (+++)	**35 (+++)**	14 (+)	25 (+++)
	EtOH	-	17 (++)	15 (++)	-	-	-
Control	PE	-	-	-	-	-	-
	MeOH	-	-	-	-	-	-
	EtOAc	-	-	-	-	-	-
	EtOH	-	-	-	-	-	-

Agar well - 10 mm
10 mm ~ 14 mm (+)
15 mm ~ 19 mm (++)
20 mm above (+++)

Antixoidant Activiy

Antioxidant compounds in plant play an important role as a health-protecting factor. Scientific evidence suggests that antioxidants reduce the risk for chronic diseases including cancer and heart disease.

The antioxidant activity of EtOH and H_2O crude extracts was evaluated by DPPH (2, 2- diphenyl-1-picrylhydrazyl) radical scavenging assay. The radical scavenging activity of crude extracts were expressed in terms of % RSA and IC_{50} (50 % inhibitory concentration). These results are shown in Table 2.

It was found that increasing the concentration of samples, the % RSA was also increased. These results were shown in Figure 2. The antioxidant activity of ethanol and water extracts of Kana-phaw (IC_{50} = 22.53 μg/mL and 40.63 μg/mL) was found to be more potent than of Thit-yay-gyi (IC_{50} = 37.75 μg/mL and 44.81 μg/mL).

Table 2: Radical Scavenging Activity (% RSA) and IC_{50} Values of Crude Extracts from Kana-phaw and Thit-yay-gyi and Standard Ascorbic Acid on Antioxidant Activity

Tested sample	%RSA±SD at Different concentration (μg/mL)					
	12.5	25	50	100	200	IC_{50} (μg/mL)
Kana-phaw (Watery)	42.90±0.80	47.30±0.20	52.41±1.00	57.5±1.41	63.35±1.21	40.63
Thit-yay-gyi (Watery)	46.05±1.03	48.87±0.62	56.87± 0.62	60.67±0.21	74.29±0.60	44.81
Kana-phaw (EtOH)	49.42±0.21	51.16±0.21	57.85±4.73	69.77±0.82	90.41 ±3.29	22.53
Thit-yay-gyi (EtOH)	37.94±0.21	48.11 ±0.41	51.45±0.21	55.67 ±0.21	61.19 ±0.31	37.75
Vitamin C	49.19±2.44	52.55±0.70	55.38±0.70	56.59±0.00	64.25±8.36	15.55

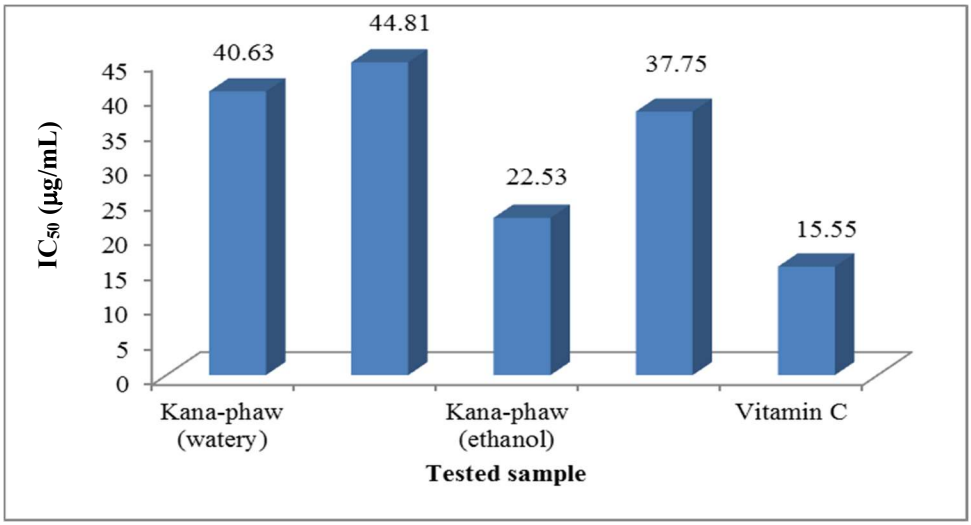

Figure 2: A bar graph of IC_{50} (µg/mL) of EtOH and watery crude extracts of Kana-phaw and Thit-yay-gyi

Cytotoxicity

The cytotoxicity of ethanol and watery of Kana-phaw and Thit-yay-gyi were evaluated by brine shrimp cytotoxicity bioassay. This bioassay is general toxicity screening for bioactive plants and their derivatives. A model animal that has been used for this purpose is the brine shrimp, *Artemia salina* (Tawaha, 2006).

The cytotoxicity of crude extracts were expressed in terms of mean ± SEM (standard error mean) and LD_{50} (50 % Lethality Dose) and the results are shown in Table 3. In this experiment, standard potassium dichromate ($K_2Cr_2O_7$) and caffeine were chosen because $K_2Cr_2O_7$ is well-known toxicity in this assay and caffeine is a natural product.

As shown in Table 3, the cytoxicity of EtOH extracts of Kana-phaw and Thit-yay-gyi were more toxic to brine shrimp than the watery extracts. The LD_{50} values of EtOH extract were 68.2 µg/mL in Thit-yay-gyi and 989 µg/mL in Kana-phaw**.** On the other hand, the LD_{50} values of watery crude extracts were 86.04 µg/mL in Thit-yay-gyi and 224.66 µg/mL in Kana-phaw. The LD_{50} values of standard $K_2Cr_2O_7$ and caffeine are 43.74 µg/mL and 1000 µg/mL respectively.

Table 3: Cytotoxicity of Different Doses of Crude Extracts of Thit-yay-gyi and Kana-phaw against *Artemia salina* (Brine Shrimp)

Sample	No. of Dead of Brine Shrimp (Mean ± SEM) in Various Concentration (µg/mL)					
	0.1	**1**	**10**	**100**	**1000**	**LD_{50} (µg/mL)**
Thit-yay-gyi(EtOH)	0	0	1.33 ± 1.15	7.00 ± 2.00	9.44 ± 2.89	**68.2**
Thit-yay-gyi(Watery)	2.60 ± 4.00	2.98 ± 1.53	3.33 ± 0.58	5.33 ± 0.58	5.67 ± 2.89	86.04
Kana-phaw(EtOH)	0.23 ± 0.58	0.82 ± 0.58	2.00 ± 0.58	2.33 ± 1.53	5±5.46	989
Kana-phaw(Watery)	0.43 ± 1.53	2.35 ± 0.58	3.34 ± 1.15	4.66 ± 1.15	7.66 ± 0.58	224.66
*$K_2Cr_2O_7$	0.52 ± 2.00	0.67 ± 0.66	2.00 ± 2.00	10.00 ± 0.00	10.00 ± 0.00	43.74
*Caffeine	0	0	2.33 ± 1.20	3.00 ± 0.58	5.00 ± 1.16	1000

* Used as Cytotoxic Standard

Antitumor Activity

In this study, tumor producing bacteria, *Agrobacterium tumefaciens* was first isolated from the gall tissues of *Sandoricum koetjape* Merr. (Thitto) leaf and cultured for use in the Patato Crown Gall (PCG) test with plant extracts. Antitumor activity of ethanol and water extracts of Thit-yay-gyi and Kana-phaw were also tested on tumor produced bacteria, *Agrobacterium tumefaciens* isolated from *Sandorium keotjape Merr*. (Thitto) leaves, using PCG (Potato Crown Gall) test. From this experiment, ethanol and water extracts of Thit-yay-gyi significantly inhibited the formation of tumor with the dose of 0.12 and 0.50 g/disc. In addition, it was observed that ethanol and water extracts of Kana-phaw showed to prevent the tumor formation with dose of 0.25 and 1 g/disc. These results are shown in Table 4.

Table 4: Antitumor Activity of Crude Extracts from Thit-yay-gyi and Kana-phaw by PCG Test

Concentrations (g/disc)	Antitumor Activity of Extracts			
	Thit-yay-gyi		Kana-phaw	
	Water extract	EtOH extract	Water extract	EtOH extract
1.00	-	-	-	-
0.50	-	-	+	-
0.25	+	-	+	-
0.12	+	-	+	+
Control	+	+	+	+

(+) Tumor appeared (-) No tumor appeared

Antiproliferative Activity

Antiproliferative Activity

Antiprolifertative activity of EtOH and H_2O extracts of Thit-yay-gyi and Kana-phaw was done by using seven human cancer cell lines. Antiproliferative activity was expressed as the IC_{50} (inhibitory concentration) value. 5-fluorouracil was used as positive control. The antiproliferative activity of crude extracts are summarized in Table 5. The H_2O extract of Kana-phaw did not show antiproliferative activity. The EtOH extract of Thit-yay-gyi and were observed to possess higher antiproliferative activity against breast (MCF 7), cervix (Hela), pancreatic (PSN-1) and pancreas ductal adenocarcinoma (PANC-1) human cancer cell lines than other extracts. In addition, H_2O extract of Thit-yay-gyi found to possess antiproliferative activity against breast human cancer cell line (MCF 7). The EtOH extract of Kana-phaw exihibited potent antiproliferative activity against liver (HePG-2), cervix (Hela) and pancreas ductal adenocarcinoma (PANC-1) human cancer cell lines. It may be concluded that Thit-yay-gyi preserve the high potentially against the breast (MCF 7), cervix (Hela), pancreatic (PSN-1) and pancreas ductal adenocarcinoma (PANC-1) human cancer cell lines than Kana-phaw.

Table 5: Antiproliferative Activity of Crude Extracts against Various Types of Cancer Cell Lines

Sample	IC_{50} (μg/mL) of crude extracts against Tested Cancer Cell Lines						
	A549	**MCF7**	**WI-38**	**Hela**	**HePG 2**	**PSN-1**	**PANC-1**
Thit-yay-gyi (EtOH-extract))	>100	48.70	>100	59.15	>100	62.32	76.45
Thit-yay-gyi (H_2O-extract)	>100	64.12	>100	>100	>100	>100	>100
Kana-phaw (EtOH-extract))	>100	>100	>100	52.06	80.73	>100	74.35
Kana-phaw (H_2O-extract)	>100	>100	>100	>100	>100	>100	>100

A 549 = human lung cancer
Hela = human cervix cancer
MCF 7 = human breast cancer
WI-38 = normal human fibroblast
HePG 2 = human liver cancer
PSN-1 = human pancreatic cancer
PANC-1 = pancreas ductal adenocarcinoma

Conclusion

The antimicrobial activity of different crude extracts from the Thit-yay-gyi and Kana-phaw was determined by agar well diffusion method. Ethyl acetate extracts of both plants samples showed the antimicrobial activity on all tested microorganisms with inhibition zone diameters in the range between 18 mm-35 mm for Thit-yay-gyi and 21 mm-35 mm for Kana-phaw. In antioxidant activity, ethanol extract of Kana-phaw [IC_{50} = 22.53 μg/mL] more potent than the other extracts. In addition, the cytotoxicity of EtOH and H_2O crude extracts from Thit-yay-gyi and Kana-phaw were evaluated by brine shrimp cytotoxicity bioassay. The cytotoxicity of Thit-yay-gyi EtOH extract (LD_{50}=68.2μg/mL) showed more cytotoxic effect than other crude extracts. In

antitumor activity of ethanol and water extracts Thit-yay-gyi and Kana-phaw significantly inhibited the formation of tumor with the dose of 0.12 g/ disc. The EtOH extract of Thit-yay-gyi was possessed the higher antiproliferative activity than other extracts. On silical gel column chromatographic separation, kaurenoic acid (A, 0.015%, m.pt. 172°C) was isolated from PE extract of Kana-phaw. The isolated compound was characterized by some physical and chemical properties and structurally identified by the combination of FT IR, NMR, HMBC and ESI MS spectroscopic methods and also by comparing with the reported data. The cytotoxicity effect of compound A (kaurenoic acid) was found on Brine Shrimp up to minimum dose of 0.00001 μg/mL.

Acknowledgements

The authors would like to express their profound gratitude to the Department of Higher Education (Yangon Office), Ministry of Education, Yangon, Myanmar, for provision of opportunity to do this research.

References

Dockery, M. and Tomkins, S. (2000). *Brine Shrimp Ecology*. London: 1st Ed., The British Ecology Society, pp. 92 – 93

Marinova, G. and V. Batchvarov, (2011). "Evaluation of the Methods for Determination of the Free Radical Scavenging Activity by DPPH". *Bulgarian Journal of Agricultural Science*, vol. 17, pp. 11-24

Tawaha, K. A. (2006). "Cytotoxicity Evaluation of Jordanian Wild Plants using Brine Shrimp Lethality Test". *J. Appl. Sci.*, vol. 8(1), pp. 12 – 17.

Win, N. N., T., Ito, S., Aimaiti, H., Imagawa, H., Ngwe, I. Aboe, and H. J. Morita, (2015). "Kaempulchraols A-H, Diterpenoids from the Rhizomes of *Kaemferia pulchra* Collected in Myanmar". *US National Library of Medicine National Institutes of Health,* vol. 78, pp. 1113

EFFECT OF CHEMICAL RIPENING AGENT (ETHEPHON) ON THE NUTRITIONAL AND METAL COMPOSITIONS OF BANANA (PHEE-GYAN-HNGET-PYAW)

MyaThwet Win[1], Khin Lay Naing[2], Myat Myat Thaw[3]

Abstract

Fruit ripening is a natural process which also can be stimulated using different artificial fruit ripening agents. The effect of chemical ripening agent (ethephon) on the nutritional and metal compositions of banana (Phee-gyan-hnget-pyaw) is investigated work. This includes three types of banana (Phee-gyan-hnget-pyaw): natural ripening (untreated), treatment with different dosages of ethephon (250, 500 and 1000 ppm) and market samples. Nutritional values of banana (Phee-gyan-hnget-pyaw) samples were determined by the method of Association of Official Analytical Chemists (AOAC). The moisture content, total ash and fat contents, the protein, crude fiber, carbohydrate and energy values in all samples were measured. The values of reducing sugar and acidity in treated samples were observed to be higher than natural ripening (untreated) sample. Ascorbic acid (vitamin C) contents have been measured by using two methods, the first AOAC's titrimetric method and the second UV-visible spectrophotometry method. It was observed that the amount of ascorbic acid (vitamin C) content was found to be higher in natural ripening (untreated) sample compared with ethephon-treated and market samples. The pH values of all samples were found within the acid range. Some minerals (K, Na, Ca, Mg, Fe, Mn, Zn, Cu, Cd and Pb) were determined by using atomic absorption spectrometer (AAS). Cadmium and lead contents in all samples were not found. Potassium is the highest value in natural (untreated) samples. Phosphorus contents in all samples were determined by using UV-visible spectrophotometer. Phosphorus content gradually increased in all ethephon-treated samples. It was found that the chemically treated banana samples ripened more faster about three times than untreated ones (natural).

Keywords: banana, ethephon, nutritional values, atomic absorption spectrometer, UV-visible spectrophotometer

1. MRes Student (2016-17), Department of Chemistry, University of Yangon & Senior Scientist, Analysis Department, Department of Research and Innovation
2. Dr, Associate Professor, Department of Chemistry, Moehnyin Degree College
3. Dr , Professor, Department of Chemistry, University of Yangon

Introduction

Banana is one of the major crops which are cultivated all over the world. Banana is grown in more than 120 countries throughout the tropical and subtropical regions (Gunasekara*et al*., 2015). Banana is considered as popular stable food for more than 400 million people (Sanjeev and Eswaran, 2008). It is an alternative perennial fruit crop for farmers due to its high economic gains throughout the year. When considering the production, it is the second important crop in the world. India is the largest producer of banana with 23.205 million metric tonnesof annual productions (Kulkarni*et al*., 2011).Banana is one of the most important and common fruits in Myanmar (SeinHla Bo, 2003). It grows in all states and regions of Myanmar and is available all year round. Banana is a number of species or hybrid in the genus *Musa* of the family *Musaceae*. Thirteen *Musa* species including wilds species are widely grown throughout the country.

Banana fruits are wholesome and fairly well balanced source of nutrients containing various mineral salts, high amount of carbohydrates with a little oil and protein (Ahenkora*et al.*, 1997).The medicinal values of banana are higher than the other common tropical and subtropical fruits. Banana is the cheapest as well as one of the most nutritious fruits.

Bananas have long been recognized for their antacid effects that protect against stomach ulcers and ulcer damage. Fresh banana may protect neuron cell against oxidative stress-induced neurotoxicity and may play an important role in reducing the risk of neurodegenerative disorders such as Alzheimer's disease. The fruit is believed to reduce the worm problems in the kids. Bananas contain minerals and other nutrients that promote hair recovery and rehabilitation (Kumar*et al*., 2012).

The plant hormones are extremely important agents in the integration of developmental activities, and they also are concerned importantly in the response of plants to the external physical environment (Moore, 1994). Ethylene is also an important natural plant hormone, used in agriculture to force the ripening of fruits. Ethylene is produced from essentially all parts of higher plants, including leaves, stems, roots, flowers, fruits, tubers and seeds.In higher vascular plants, a relatively simple biosynthetic pathway produces ethylene (Figure. 1). The amino acid methionine (MET) is the

starting point for synthesis. It is converted to S-adenosyl methionine (SAM) by the addition of adenine, and SAM is then converted to 1-amino-cyclopropane carboxylic acid (ACC) by the enzyme ACC synthase. The production of ACC is often the controlling step for ethylenesynthesis. A number of intrinsic (e.g., developmental stage) and extrinsic (e.g., wounding) factors influence this pathway.

The pool of ACC available for ethylene production can be increased by factors which increase ACC synthase activity, reduced by application of growth regulators(e.g., daminozide), or reduced by a side reaction which forms the relatively biologically inert MACC. In the final step, ACC is oxidized by the enzyme ACC oxidase to form ethylene. This oxidation reaction requires the presence of oxygen, and low levels of carbon dioxide activate ACC oxidase. While the level of ACC oxidase activity is usually in excess of what is needed in most tissues, it can show a dramatic increase in activity in ripening fruit and in response to ethylene exposure (Saltveit, 1999).

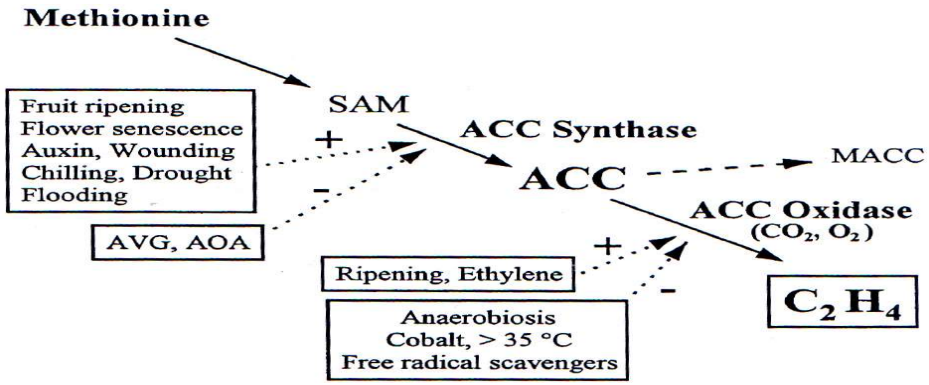

Figure 1: Biosynthesis of ethylene in higher vascular plants. Some of the intrinsic and extrinsic factors that promote (+) or inhibit (-) ethylene (C_2H_4) synthesis in higher vascular plants.

Fruit ripening is a developmentally regulated process resulting from the coordination of numerous biochemical and physiological changes within the fruit tissue that culminates in changes in fruit firmness, color, taste, aroma and texture of fruit flesh (Singh *et al*., 2010). Ripening agents speed up the ripening process. They allow many fruits to be picked prior to full ripening, which is useful. For example, bananas are picked when green and artificially

ripened with specific ripener (Dhembare, 2013). Ethephon, artificial ethylene, ethylene glycol, calcium carbide, carbon monoxide and potassium dihydrogensulfate are major commercially popular artificial ripening agents (Suman *et al*., 2011). Ethephon, 2-chloroethylphosphonic acid, organophosphorus compound is a synthetic plant growth regulator. This class of physiological and biological substance produces similar effects as its endogenous counterparts. Ethephon is used to improve fruit abscission for mechanical harvest, to accelerate post-harvest ripening in fruit, to increase resistance to lodging, to promote or inhibit flowering, to promote maturation and colouring and to enhance sugar content (Hanot *et al*., 2015). Ethephon has been registered with EPA (US Environmental Protection Agency) since 1973 as a plant growth regulator used to promote fruit ripening and flower induction (Bui, 2007). This systemic pesticide translocates into the plant tissues and progressively decomposes to ethylene. Ethylene is the active agent and is associated with various natural physiological processes throughout plant growth and development. Ethephon was found to be the most effective nongaseous ethylene-releasing chemical. Ethephon is a diprotic acid with a phosphonic acid group which provides to this plant growth regulator a high polarity, water solubility and a low volatility. Ethephon is stable in aqueous solution below pH 3.5 and decomposed in ethylene and dihydrogen phosphate under alkali and high temperature conditions (Hanot *et al*., 2015).

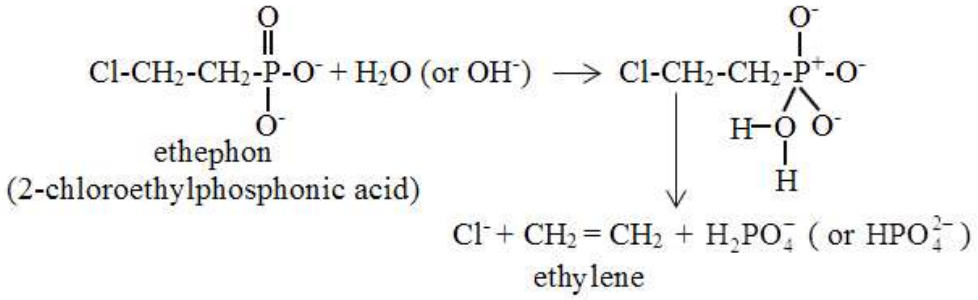

Banana is often harvested in a mature but unripe condition, and is subsequently allowed to ripen further. In natural conditions, they ripen slowly, leading to high weight loss, desiccation, ripening is also uneven and fails to develop good colour and aroma. Hence the marketable quality deteriorates. Therefore, normally banana is artificially ripened (Subbaiah *et al*., 2013).The

use of artificial agents may give more acceptable colour than naturally ripened fruits (Hakim *et al*., 2012) but it may increase the risk of contamination of food materials. With the absence of legislation to control the indiscriminate use of harmful ripening agents, research effort is needed to constantly monitor their presence in foods grown locally. This present study is therefore carried out to investigate the effect of chemical ripening agent (Ethephon) on the nutritional and metal compositions of banana (Phee-gyan-hnget-pyaw) by natural (untreated), treatment with different dosages of ethephon (250, 500, 1000 ppm) and market (treated) samples.

Materials and Methods

Collection of Banana Samples and Chemical Ripening Agent

Freshly harvested bunch of green (mature unripe) banana and banana samples treated with chemical ripening agent (ethephon) from market were collected from Minhla Township (Bago Region). The ripening agent (Ethephon 40 %) (Shanghai Huayi Group Co., Ltd., China) used for the study was also bought from the Kyimyindaing market, Kyimyindaing Township (Yangon Region)(Figure 2).

(a) (b) (c)

Figure 2: (a) Banana (Phee-gyan-hnget-pyaw) plant, (b) Banana (Phee-gyan-hnget-pyaw) fruits and (c) Bottle of ethephon (40%)

Preparation of Banana Samples by Treating with Chemical Ripening Agent (Ethephon)

Banana hands were separated from bunches and washed thoroughly with deionized water to remove the contaminations. Two banana hands were used as untreated control fruits (Natural). For each dosage sample, two banana hands were used. These hands were dipped in different concentrations of ripening agent (Ethephon 40 %) solutions(250 ppm, 500 ppm and 1000 ppm) for 15 min. All samples were packed in each ventilated bamboo basket and covered with polyethylene sheet and kept for ripening at room temperature.

Preparation of Banana Samples for Quantitative Analysis

When all the fruits were completely ripened in yellow peel with black spots, fingers were separated from the hands. For each of the all samples, pulp was homogenized with blender. The suspension mixture solution was obtained. Each of the all samples was carried out in triplicate.

Determination of Changes of Ripening Time and Shelf Life

Natural (untreated) and ethephon-treated banana samples were daily monitored for colour changes of the peel indicative of ripening. The stage of ripeness is judged primarily by colour using a 1-7 scale common in the industry. At colour 1, the finger is hard and completely green; No. 2 is green but with some traces of yellow; No. 3 is more green than yellow; No. 4 is more yellow than green; No. 5 is yellow but with traces of green; No. 6 is fully yellow and No. 7 is yellow with black spots (Sogo-Temi*et al*., 2014). The shelf life was calculated by counting the days required to attain the last stage of ripening but up to the stage when fruit remained still acceptable for marketing (Moniruzzaman*et al*., 2015).

Procedure for the Nutritional and Metal Compositions

Nutritional values of all banana samples were determined according to standard methods of Association of Official Analytical Chemists (AOAC, 1990). Water content by oven drying method, ash content by ashing method in a muffle furnace, protein content by micro Kjeldahl's method, crude fiber content by acid-base digestion method, fat content by Soxhlet extraction method, reducing sugar content by Lane-Eynon's method, titratable acidity

content by titrimetric method, pH value by pH meter and ascorbic acid (vitamin C) content by iodometric titration and UV-visible spectrophotometric methods were used.Some mineral and heavy metal contents of the samples were determined by using atomic absorption spectrometer (AAS, Perkin Elmer Analyst 400) and phosphorus contents were determined by using UV-visible spectrophotometer (UV mini-1240, Japan).

Results and Discussion

Changes of Ripening Time and Shelf Life in Natural and Ethephon-Treated Banana (Phee-gyan-hnget-pyaw) Samples

In this research, the fastest colour change indicated by the peel colour to fully yellow with black spots was observed in 1000 ppm ethephon-treated sample in 35 h while the natural (untreated) banana with no ripening agent ripened in 92 h. It was found that the sample with ripening agent accelerated the rate of ripening faster than natural sample. With high treatment (1000 ppm) on fruits required less shelf life (2 days) while lower dosage (250 ppm) required longer shelf life (3 days) indicating high dosage treatment sample reacted rapidly with fruit samples and quick ripening led to spoilage (Figure 3 and Table 1).

A. Finger is hard and completely green

B. Green but with some trace of yellow

C. More green than yellow

D. More yellow than green

E. Yellow but with traces of green

F. Fully yellow

H. Yellow with black spots

Figure 3: Changes of ripening stage of banana by the treatment of ethephon

Table 1. Observation of Ripening Time and Shelf Life in Natural and Ethephon-Treated Samples

No.	Sample	Ripening time (h)							Shelf life (days)
		A	B	C	D	E	F	G	
1.	Natural	_	54	64	72	79	86	92	6
2.	250ppm (ethephon)	–	36	42	48	53	58	63	3
3.	500ppm (ethephon)	–	29	34	39	44	47	49	2.5
4.	1000ppm (ethephon)	–	24	27	29	31	33	35	2

A = Finger is hard and completely green, B = Green but with some traces of yellow, C = More green than yellow, D = More yellow than green, E = Yellow but with traces of green, F = Fully yellow, G = Yellow with black spots

Calibration Curve for Chromate-diphenylcarbazide Complex with respect to Ascorbic Acid Concentration

In this research, the calibration curve was constructed using a series of solutions of ascorbic acid prepared from 100 ppm stock solution. It was found that absorbance of chromium-diphenylcarbazide complex was related to ascorbic acid concentration. By plotting the absorbance determined versus the corresponding concentration range (0.2-1 ppm) the calibration curve was obtained. The concentrations of ascorbic acid in all samples were determined from this curve (Figure 4).

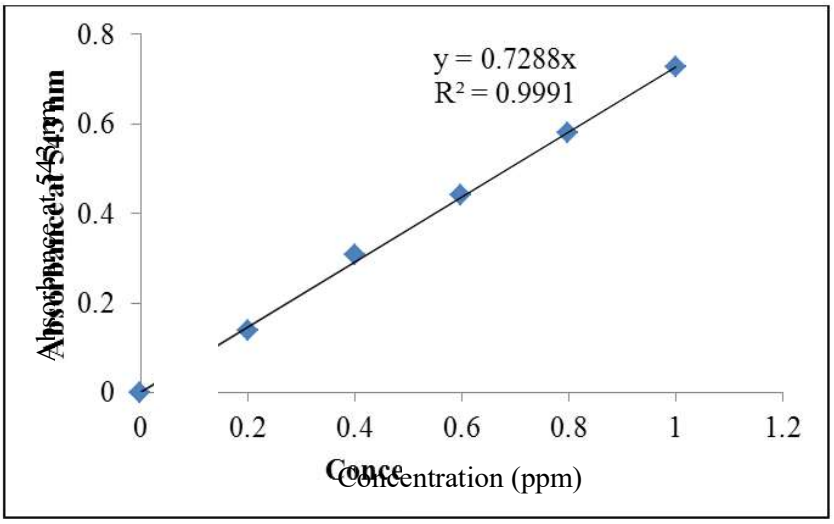

Figure 4: Calibration curve for standard ascorbic acid by UV-visible spectrophotometric method

Standard Calibration Curve for Phosphate

It is necessary to construct a calibration curve from a series of standard solutions(5-100 ppm) for the measurement of phosphorus concentration. In this research, the different absorbance values at 470 nm were obtained for different phosphorus concentrations by using UV-visible spectrophotometer (Vanado-molybdate Colorimetric Method) (Pearson, 1976). It was found that the nature of plot of absorbance vs. concentration of phosphorus was a straight line passing through the original showing that Beer's law was obeyed (Figure 5). Phosphorus contents were determined from this curve.

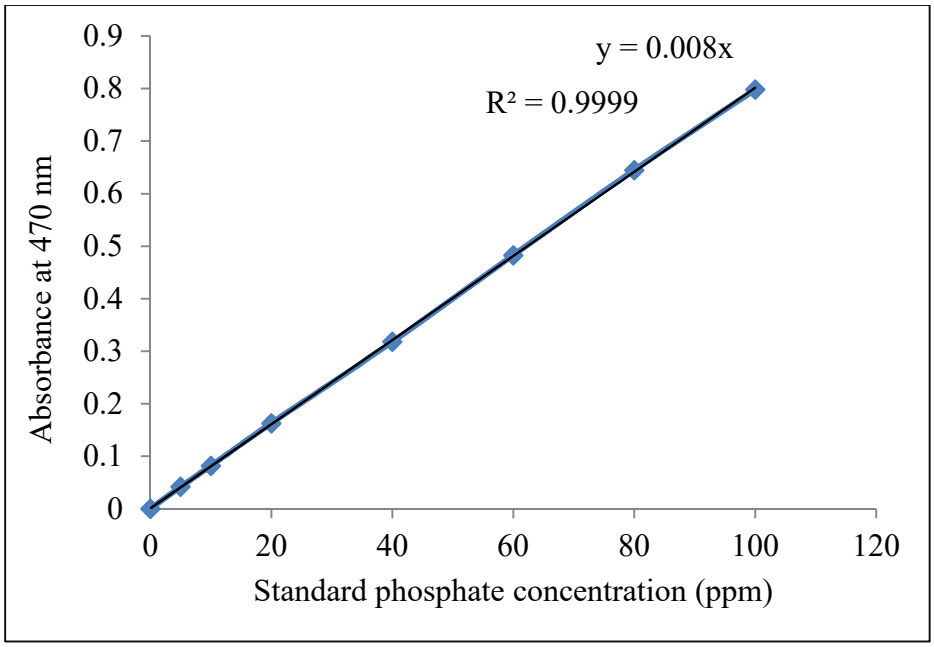

Figure 5: Calibration curve for standard phosphate by spectrophotometric method

Nutritional and Metal Compositions of Natural, Ethephon-Treated and Market Banana (Phee-gyan-hnget-pyaw) Samples

Table 2 shows the nutritional values of natural, ethephon-treated and market banana (Phee-gyan-hnget-pyaw) samples. The water percentage of banana sample was determined by the use of an electric oven at 105 ˚C by drying to obtain constant weight and taking the loss in weight as water.The mean results of water content in natural, (250 ppm, 500 ppm, 1000 ppm) ethephon-treated and market banana samples were found to be 70.69 %, 72.06 %, 72.88 %, 73.90 %, and 73.66 %, respectively(Figure 6). It was found that the water content of all ethephon-treated banana samples were gradually higher than natural (untreated) sample. Water content in banana pulp is observed to increase because of respiratory breakdown of starch to sugar, migration of water from peel to pulp and excess moisture formation (Sen *et al*., 2012; Ayo-omogie*et al*., 2010; Hakim *et al*., 2012). The high percentage of water in chemically treated samples may shortened the shelf life and cause

higher rottenness.The ash percents of all banana samples were found to be in the range of 0.86 – 1.21 %. The amount and composition of ash remained after combustion of fruit material varies considerably according to the part of the fruit, age, treatment etc.

All banana samples contain small amount of protein. It was found that natural (untreated) sample has the maximum content of protein (1.18 %) and market sample has the minimum protein content (0.91 %), whereas the protein content of all ethephon-treated banana samples were less than natural (untreated) sample. This is also in agreement with Adewole and Duruji (2010) who observed a reduction in the protein content during ripening which may be due to reduction of nitrogen during ripening. Crude fiber contents of all banana samples were determined by acid-base digestion method. It was observed that natural (untreated) has slightly higher amount of crude fiber (0.33 %) than the other samples. The higher fiber content in natural sample may be possible due to increase in soluble and insoluble dietary fractions (Khawas*et al*., 2014). It was found that natural sample has slightly high amount of fat (0.05 %) whereas the same fat content (0.03 %) of all ethephon-treated samples were observed. The carbohydrate percentages of all banana samples were calculated by difference. It was observed that carbohydrate content of natural (untreated) sample(26.54 %) was greater than the 1000 ppm ethephon-treated and market samples (23.89 % and 24.25 %)(Figure 7). One of the biochemical changes occurring during ripening is a decrease in carbohydrate content. The starch is degraded by starch degrading enzymes α and β amylases which convert starch to simple sugars (Sogo-Temi*et al*., 2014). It was found that natural (untreated) sample has the highest calorie content (111.33 kcal/ 100 g). Ethephon-treated (1000 ppm) sample has the lowest calorie content (99.71 kcal/ 100 g).

Sugars which possess in their structure free aldehydic or ketonic groups react as weak reducing agents and are termed reducing sugars. These include all the monosaccharides, and the disaccharides maltose, lactose and cellobiose. The highest reducing sugar content (14.44 %) was recorded for market sample. Lower value was observed for natural (untreated) sample. The observed values of reducing sugar (13.02 %, 13.69 %, 14.07 %) for all ethephon-treated samples were gradually higher than natural (untreated)

sample(Figure 8). In another study chemically treated fruits produced higher sugar content due to the increase in soluble pectin, organic acids and hydrolysis of starch to soluble sugars (Hakim *et al.,* 2012).

The titratable acidity of fruit is due to the presence of a mixture of organic acids, whose composition is variable depending on the fruit nature and its maturity. The acids present in the fruits were tartaric, citric, ascorbic, malic and lactic acids. The titratable acidity contents of all banana samples were determined by acid-base titration method. The titratable acidity level was found to be highest in 1000 ppm ethephon-treated sample (0.48 %), while the level was lowest in the natural (untreated) sample (0.35 %). It was reported that high titratable acidity can cause dental erosion, especially among kids (Featherstone *et al*., 2006). Therefore, regular consumption of artificially ripened banana can be hazardous for dental health. Acids play an important role in the post-harvest quality of vegetables, as taste is mainly a balance between sugar and acid contents which is important in evaluation of fruit taste. The changes in titratable acidity and pH of banana indicate a general increase in titratable acidity during ripening (Khawas*et al*., 2014).The pH values of all banana (Phee-gyan-hnget-pyaw) samples were found to be in the acidic range of 4.37-4.69 and pH values of all treated samples were gradually lower than natural (untreated) sample. The decrease in pH of ethephon-treated fruit pulp could be due to increase in titratable acidity during ripening (Kulkarni *et al.,* 2011; Hakim *et al.,* 2012).

The ascorbic acid (vitamin C) contents of natural, ethephon-treated and market samples were determined by iodometric titration and UV-visible spectrophotometric method. In iodometric titration, natural (untreated) sample contained the highest amount of ascorbic acid (12.67 mg/100 g) and the lowest amount was found in the 1000 ppm ethephon-treated sample (6.51 mg/ 100 g) whereas market sample had low level of ascorbic acid amount (6.78 mg/100 g)(Figure 9). In UV-visible spectrophotometric method, ascorbic acid (vitamin C) contents in natural, ethephon-treated and market samples were determined at 543 nm. It was observed that natural (untreated) ripening sample was found to be the highest amount of (13.12 mg/ 100 g). 250, 500 and 1000 ppm ethephon-treated samples and market samples were found to be 9.66 mg/ 100 g, 8.86 mg/ 100 g, 7.17 mg/ 100 g and 6.22 mg/

100g, respectively(Figure 10). According to ripening chemistry, ascorbic acid (vitamin C) decreases with the increase of temperature (Adeyemi and Oladiji, 2009). Ascorbic acid (vitamin C) is also sensitive to oxygen present in the system. Ascorbic acid content of fruits and vegetables decreases even in proper storage treatment due to the prolonged duration (Hakim *et al*., 2012).

Table 2: Comparison of Nutritional Values in Natural, Ethephon-Treated and Market Samples

Sample	Water (%)	Ash (%)	Protein (%)	Fiber (%)	Fat (%)	Carbohyd -rate (%)	Energy value (kcal/100g)	Reducing Sugar (%)	Titratable acidity (%)	pH value	Ascorbic acid[1] (mg/100g)	Ascorbic acid[2] (mg/100g)
S-1	70.69 ± 0.03	1.21 ± 0.02	1.18 ± 0.02	0.33 ± 0.01	0.05 ± 0.02	26.54 ± 0.07	111.33 ± 0.18	13.59 ± 0.02	0.35 ± 0.02	4.62 ± 0.01	12.67 ± 0.02	13.12 ± 0.01
S-2	72.06 ± 0.02	0.96 ± 0.01	1.09 ± 0.03	0.31 ± 0.02	0.03 ± 0.01	25.55 ± 0.04	106.83 ± 0.06	13.02 ± 0.03	0.40 ± 0.01	4.59 ±0.01	9.45 ± 0.01	9.66 ± 0.01
S-3	72.88 ± 0.01	0.91 ± 0.02	0.98 ± 0.02	0.31 ± 0.02	0.03 ± 0.01	24.89 ± 0.01	103.75 ± 0.02	13.69 ± 0.02	0.43 ± 0.02	4.52 ±0.02	8.44 ± 0.01	8.86 ± 0.01
S-4	73.90 ± 0.02	0.91 ± 0.02	0.97 ± 0.02	0.30 ± 0.02	0.03 ± 0.01	23.89 ± 0.03	99.71 ± 0.21	14.07 ± 0.03	0.48 ± 0.02	4.46 ±0.01	6.51 ± 0.01	7.17 ± 0.01
S-5	73.66 ± 0.02	0.86 ± 0.01	0.91 ± 0.01	0.30 ± 0.02	0.02 ± 0.01	24.25 ± 0.02	100.82 ± 0.05	14.44 ±0.02	0.46 ± 0.01	4.37 ±0.02	6.78 ± 0.02	6.22 ± 0.02

S-1= Natural, S-2=250 ppm(ethephon), S-3=500ppm(ethephon), S-4=1000ppm(ethephon), S-5=Market
[1] =Iodometric titration method, [2]=UV–visible spectrophotometric method, Results are expressed as Mean ± S.D, n = 3.

S-1= Natural, S-2=250 ppm(ethephon), S-3=500ppm(ethephon), S-4=1000ppm(ethephon), S-5=Market [1] =Iodometric titration method, [2]=UV–visible spectrophotometric method, Results are expressed as Mean ± S.D, n = 3.

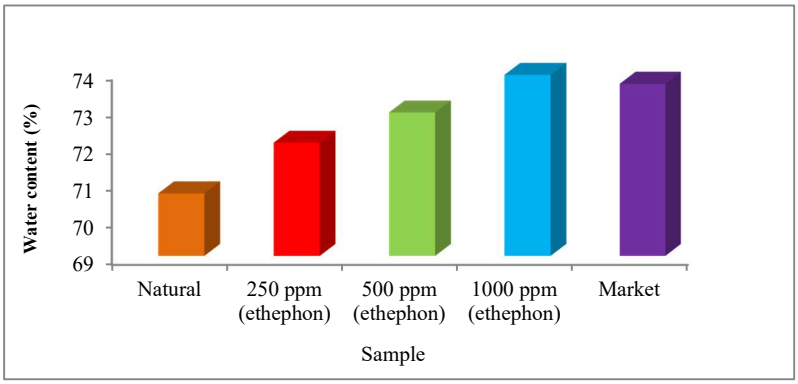

Figure 6: Histogram of water contents in natural, ethephon-treated and market samples

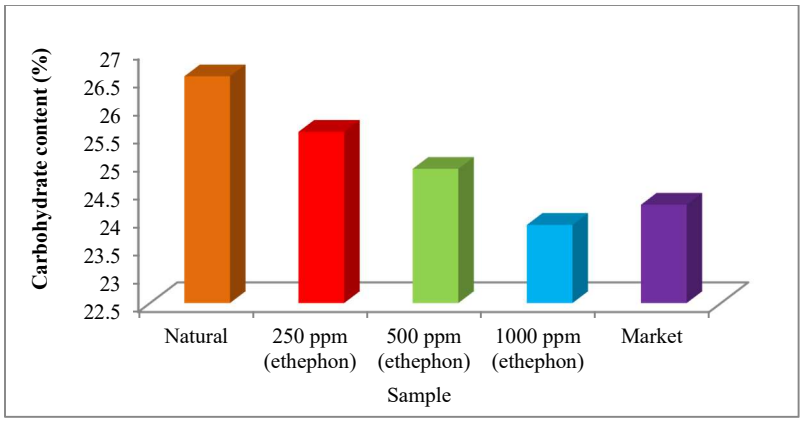

Figure 7: Histogram of carbohydrate contents in natural, ethephon-treated and market samples

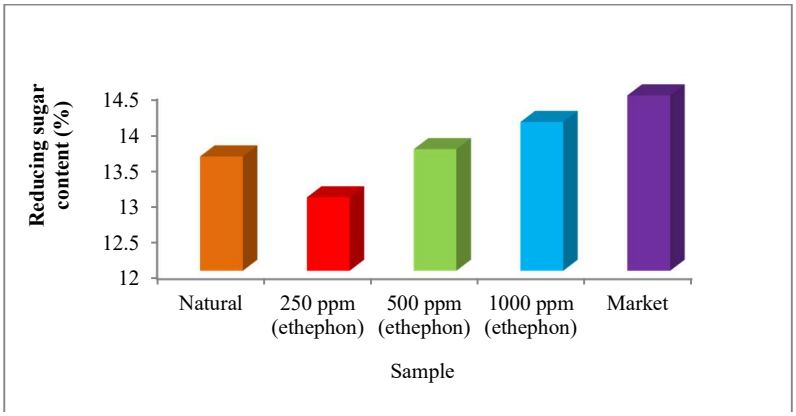

Figur 8: Histogram of reducing sugar contents in natural, ethephon-treated and market samples

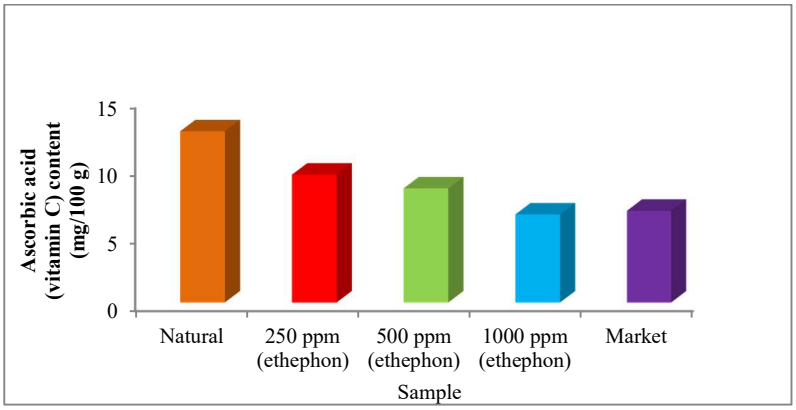

Figure 9: Histogram of ascorbic acid (vitamin C) contents in natural, ethephon-treated andmarket samples by iodometric titration

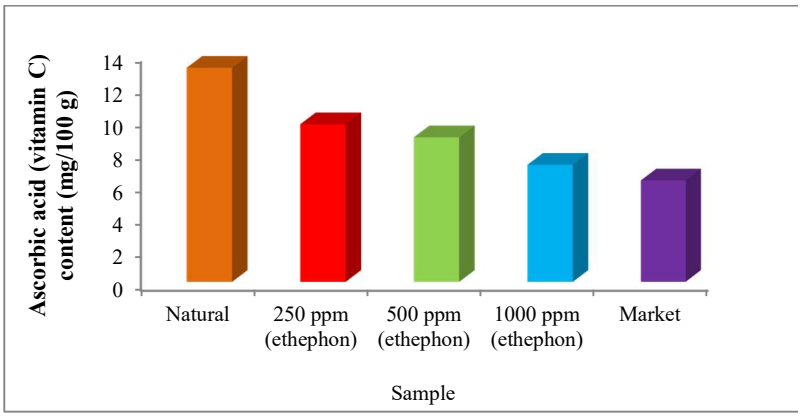

Figure 10: Histogram of ascorbic acid (vitamin C) contents in natural, ethephon-treated and market samples by UV-visible spectrophotometric method

Minerals are important for the various metabolic activities of the living tissue and even more so far the fruit, which exhibits tremendous activity during ripening process. The results of the analysis of some minerals (K, Na, Ca, Mg, P, Fe, Mn, Zn, Cu, Cd and Pb) of all banana (Phee-gyan-hnget-pyaw) samplesare shown in Table 3. In this work, natural (untreated) sample contained the highest content of K followed by Mg, P, Ca, Na, Fe, Zn, Mn and Cu. The mineral contents found in the (250, 500 and 1000 ppm) ethephon-treated and market samples were lower than natural (untreated) sample. Cadmium and lead contents were not found in all samples. In this research work, natural (untreated) sample has the minimum content of phosphorus (38.07 mg/100 g) and market sample has the maximum content of phosphorus (47.01 mg/100 g). Phosphorus contents of 250, 500 and 1000 ppm of ethephon-treated samples were observed to be 39.85, 41.90 and 44.85 mg/ 100 g, respectively. The high amounts of phosphorus in ethephon-treated samples indicate that ethephon is degraded by water resulting in the increase of phosphorus (Hakim *et al*., 2012).

Table 3: Comparison of Mineral Contents in Natural, Ethephon-Treated and Market Samples

Sample	Mineral Contents (mg/100 g)										
	K	Na	Ca	Mg	Fe	Mn	Zn	Cu	P	Cd	Pb
Natural	420.31 ± 0.02	7.38 ± 0.01	29.31 ± 0.01	76.21 ± 0.01	0.84 ± 0.01	0.32 ± 0.02	0.41 ± 0.01	0.17 ± 0.01	38.07 ± 0.02	ND	ND
250 ppm (ethephon)	418.23 ± 0.01	6.54 ± 0.02	27.55 ± 0.03	75.91 ± 0.01	0.79 ± 0.02	0.29 ± 0.02	0.38 ± 0.03	0.15 ± 0.01	39.85 ± 0.02	ND	ND
500 ppm (ethephon)	410.91 ± 0.01	5.73 ± 0.01	26.10 ± 0.02	75.04 ± 0.02	0.79 ± 0.02	0.27 ± 0.02	0.33 ± 0.03	0.12 ± 0.02	41.90 ± 0.02	ND	ND
1000 ppm (ethephon)	409.75 ± 0.01	5.54 ± 0.01	26.06 ± 0.02	74.91 ± 0.02	0.74 ± 0.01	0.26 ± 0.02	0.28 ± 0.02	0.12 ± 0.01	44.85 ± 0.02	ND	ND
Market	394.81 ± 0.01	3.95 ± 0.03	20.29 ± 0.02	74.63 ± 0.03	0.72 ± 0.01	0.24 ± 0.02	0.20 ± 0.02	0.08 ± 0.02	47.01 ± 0.02	ND	ND

ND = not detected, Results are expressed as Mean ± S.D, n = 3.

Conclusion

The current study was an initiation to observe the changes in the basic nutritional parameters upon hindering the natural process of ripening by applying artificial agents. Ripening agent (ethephon) could speed up ripening process than the natural ripening process. This work suggested that the government agencies, scientific communities and any relevant organizations should get involved to follow up the international legislation in monitoring the indiscriminate use of such artificial ripening agents. This research work is of its own merit at least to provide the general guideline. If artificial ripening agent is used the least dosage of about 250 ppm is the highest limit of treatment.

Acknowledgements

The authors would like to thank the Myanmar Academy of Arts and Science for allowing to present this paper and Professor and Head Dr Daw Hla Ngwe, Department of Chemistry, University of Yangon, for her kind encouragement.

References

Adewole, M. B. and Duruji, R. W. (2010). "Quality Assessment of Plantain (*Musa paradisiaca* L.) as Affected by Different Ripening Methods". *African Journal of Biotechnology*, vol. 9(38), pp. 6290-6293

Adeyemi, O. S. and Oladiji, A. T.(2009). "Compositional Changes in Banana (*Musa ssp*.) Fruits during Ripening".*African Journal of Biotechnology*, vol. 8(5), pp. 858-859

Ahenkora, K. M., Key, A., Marfo, K. and Banful, B. (1997)."Nutritional Composition of False Horn *Apantu pa* Plantain during Ripening and Processing".*Afr. Crop Sci. J.,*vol. 5(2), pp. 243-248

AOAC.(1990). *Official Methods of Analysis of the Association of Official Analytical Chemists*. Arlington VA: 15th Ed., Association of Official Analytical Chemists, pp. 1058-10

Ayo-omogie, H. N., Adeyemi, I. A.and Otunola, E. T. (2010). "Effect of Ripening 59 on Some Physiochemical Properties of Cooking Banana (Musa ABB Cardaba) Pulp and Flour".*International Journal of Food Science and Technology,*vol.45, pp. 2605-2611

Bui, Q. Q. (2007). *Ethephon and Jackfruit*. California: Palo Alto, p. 231

Dhembare, A. J. (2013). "Bitter Truth about Fruit with Reference to Artificial Ripener". *Archives of Applied Science Research,* vol. 5(5), pp. 45-54

Featherstone, J. D. B. and Lussi, A.(2006). "Understanding the Chemistry of Dental Erosion, Dental Erosion from Diagnosis to Theory". *Monographs in Oral Science*, vol. 20, pp. 66-67

Gunasekara, S. R. W., Hemamali, K. K. G. U., Dayananada, T. G. and Jayamanne, V. S. (2015)."Post Harvest Quality Analysis of 'EMBUL' Banana Following Artificial Ripening Techniques". *International Journal of Science, Environment and Technology*, vol. 4(6), pp. 1625-1632

Hakim, M. A., Obidul Huq, A. K., Alam, M. A., Saha, B. K.,Formuzul Haque, K. M. and Zaidul, I. S. M. (2012). "Role of Health Hazardous Ethephon in Nutritive Values of Selected Pineapple, Banana and Tomato".*Journal of Food, Agriculture & Environment*, vol. 10(2), pp. 247-251

Hanot, V., Joly,L., Bonnechere, A. and Loco, J. V.(2015). "Rapid Determination of Ethephon in Grapes by Hydrophilic Interaction Chromatography Tandem Mass Spectrometry".*Food Anal. Methods*, vol. 8,pp. 524-530

Khawas, P., Das, A. J., Sit, N.,Badwaik, L. S. and Deka, S. C. (2014). "Nutritional Composition of Culinary *Musa* ABB at Different Stages of Development".*American Journal of Food Science and Technology*, vol. 2(3), pp. 80-87

Kulkarni, S. G., Kudachiker, V. B. and Prakash, M. N. (2011). "Studies on Physico-Chemical Changes during Artificial Ripening of Banana (*Musa sp*) Variety 'ROBUSTA' ". *J. Food SciTechnol*, vol. 48(6), pp. 730-734

Kumar, K. P. S., Bhowmik,D., Duraivel, S. and Umadevi, M. (2012)."Traditional and Medicinal Uses of Banana".*Journal of Pharmacognosy and Phytochemistry*, vol. 1(3), pp. 51-63

Moniruzzaman, M., Khatoon, R., Hossain,M. F. B., Rahman, M. T. and Alam, S. N. (2015). "Influence of Ethephon on Ripening and Quality of Winter Tomato Fruit Harvested at Different Maturity Stages". *Bangladesh J. Agril. Res*., vol. 40(4), pp. 567-580

Moore, T. C. (1994). *Biochemistry and Physiology of Plant Hormones*. New York: 2nd Ed., Narosa Publishing House, pp. 23-25

Pearson, D. (1976). *The Chemical Analysis of Foods*. New York: 7th Ed., Chemical Publishing Co., Inc., pp. 23-24

Saltveit, M. E. (1999). "Effect of Ethylene on Quality of Fresh Fruits and Vegetables". *Postharvest Biology and Technology*, **15**, 279-292

Sanjeev, K. K. and Eswaran, A. (2008)."Efficacy of Micronutrients on Banana *Fusarium* with (*Fusariumoxysporum f. sp. cubense*) and its Synergistic Action with *Trichodermaviride*". *Not. Bot. Hort. Agrobot. Cluj,* vol. 36(1), pp. 52-54

Sein Hla Bo. (2003). *Banana R & D in Myanmar*. Yangon: Ministry of Agriculture and Irrigation, Union of Myanmar, pp. 143-149

Sen, C., Mishra, H. N. and Srivastav, P. P. (2012)."Modified Atmosphere Packaging and Active Packaging of Banana (*Musa spp*): A Review of Control of Ripening and Extension of Shelf Life". *Journal of Stored Products and Post-harvest Research*, vol. 3(9), pp. 122-132

Singh, R., Rastogi, S. and Dwivedi, U. N. (2010)."Phenylpropanoid Metabolism in Ripening Fruits".*Comprehensive Reviews in Food Science and Food Safety*, vol. 9, pp. 398-416

Sogo-Temi, C. M., Idowu, O. A. and Idowu, E. (2014)."Effect of Biological and Chemical Ripening Agents on the Nutritional and Metal Composition of Banana (*Musa*spp)". *J. Appl. Sci. Environ. Manage.*,vol. 18(2), pp. 243-246

Subbaiah, K. V., Jagadeesh,S. L., Thammaiah, N. and Chavan, M. L. (2013). "Changes in Physico-Chemical and Sensory Characteristics of Banana Fruit cv. Grand Naine During Ripening". *Karnataka J. Agric. Sci.,*vol. 26(1), pp. 111-114

Suman, S., Kumud, M. and Thakral, S. (2011)."Application of Apple as Ripening Agent for Banana". *Indian Journal of Natural Products and Resources*, vol. 3(1), pp. 61-64

EFFECT OF ALKALI CONCENTRATION ON THE PREPARATION OF RICE HUSK ASH AND KAOLINITE BASED GEOPOLYMER

Naw Sahblut Moo[1], Khin Khin Latt[2], Thi Thi Aye[3]

Abstract

Geopolymer is a new family of synthetic aluminosilicate materials formed by alkali activation of solidaluminosilicate raw materials. Rice husk ash (RHA) and kaolinite based geopolymer had been prepared from rice husk ash collected from Taungoo Township, Bago region and kaolinite sample from Kyaut Taga, Kyauk Padaung Township, Mandalay Region. The physicochemical properties (moisture content, weight loss on ignition, pH, specific gravity and pozzolanic reactivity) of rice husk ash and kaolinite were determined and these samples were characterized by conventional and modern spectroscopic method (XRD, EDXRF, SEM). Moisture content, weight loss-on-ignition, pH, specific gravity of rice husk ash and kaolinite were found to be 1.9% and 4.6%, 2.6% and 12.3%, 8.8 and 8.3 and 1.87 and 2.82 respectively. The chemical analysis (SiO_2, Al_2O_3, CaO, MgO) was also carried out. It was found that the samples were silica – alumina rich compound. The pozzolanic reactivity of rice husk ash and kaolinite were ranged from 64 % to 94 %. The optimum condition of sodium hydroxide concentration and the ratio of sodium hydroxide and sodium silicate which were used in the preparation of geopolymer have been determined. The physical properties such as apparent porosity, water absorption, apparent density and the mechanical properties such as compressive strength of RHA and kaolinite based geopolymer (GP) were also determined. The apparent porosity and water absorption were ranged from 10.48% to 25.92 % and 5.3% to 16.93 %, respectively. The apparent density values of geopolymer were ranged from 0.52 to 1.89 g/cm^3.The blended cements were prepared by various mixing ratios of GP : commercial cement,(1:1, 2:1,1:2). Compressive strengths of the prepared GP and blended cements at different time intervals have been determined. For all types of cements the maximum compressive strengths were achieved at 28 days after mixing. The optimum ratio of alkali solution was found to be 2:3 volume ratio of 8 M NaOH and Na_2SiO_3.

Keywords: rice husk ash, kaolinite, pozzolanic reactivity, apparent porosity, water absorption, apparent density, compressive strength,

1. 2 PhD, Candidate, Department of Chemistry, University of Yangon
2. Lecturer, Department of Chemistry, University o f Yangon
3. Associate Professor, Department of Chemistry, University of Yangon

Introduction

Nowadays, the whole of the construction of concrete structure like industrial building, high way, dams and bridges are developed and standard ingredients are required in making of concrete. Only of the early part of the eighteen century, Portland Cement came to be known.

Myanmar has been producing cement from available raw materials since 1990, but during the all round the development of the 1990 s, the used of cement has increased (Ajay, 2012). Today, the construction work is more expanded and the demand is supplying construction materials increased. So, cost effective local raw materials are needed for cement replacement.(Kyi Kyi San, 2013)

Geopolymer is an amorphous alumino-silicate material. Its structure is silicon and aluminium atoms bonding together by sharing oxygen atoms (Mehta, 1975). Once alumino-silicate powder was mixed with alkaline solution, a paste forms and transforms to hard material and gained strength. Geopolymer belong to the family of inorganic polymers, which are macromolecules linked by covalent bonds principally aluminium and secondarily other metals such as iron (Davidovits, 1999). Geopolymer was applied in many field such as a replacement of Portland cement because its production lower energy and not release the green house gases and use in building and motar application because of their short time strength developments. Geopolymer was prepared by dissolution of raw materials which have silica and alumina such as rice husk ash and kaolinite in alkaline solution.

Rice husk is a by- product of the rice milling industry. It is a unique crop residue with uniform size and high content of ash (14 %-25%)(James, 1986). The silica content of the rice husk ash (RHA) can be as high as 90% - 98%. This husk can be used as a fertilizer in agriculture or as an additive for cement and concrete fabrication(Hunt, 1984). Due to its high silica content, rice husk has become a source for preparation of elementary silica silicon carbide and silicon nitride.

Kaolinite is the principal mineral of the kaolinite group clay minerals (Bogue, 1995). Soil dominated by oxide and kaolinite clays are characterized

by very stable soil aggregate and they exhibit a low degree of plasticity. Large amount of oxide and kaolinite clays in a soil contribute to the formation of extremely stable soil aggregrates because the clays tend to neutralize each other. Kaolinite has a net negative charge. Kaolinite directly formed from primary minerals in soils of the humid tropics. Although kaolinite is very stable, it can weather to form gibbsite,$Al(OH)_3$ (Jepson, 2007).

Most commom alkali activator used in geo-polymerization is a combination of NaOH or KOH and Na_2SiO_3 or K_2SiO_3 and play important role in polycondensation process. Addition of Na_2SiO_3 solution as the alkaline activator enhances the reaction between the source materials and the solution. OH^- acts as a catalyst for reactivity, and metal cation serves to form a structural element and balance the negative framework carried by tetrahedral aluminum (Hough, 1956).The addition of activators and increase in concentration results in an increase in volume of small pores and lower total porosity.

The main aim of my research work is to study the effect of alkali concentration on the rice husk ash and kaolinite based geopolymer.

Materials and Methods

Sample Collection

Local rice husk samples collected from Taungoo Township, Bago Region and Kaolinite from Kyauk Pa Daung Township, Mandalay Region (Figures 1 and 2) were used in the present work.

Figure 1: Rice husk ash

Figure 2: Kaolinite

Sample Preparation

Rice husk samples (100 g) were placed in a clean dry porcelain basin and their weight were determined. The sample was placed inside the Electric Muffle Furnace and the temperature was raised gradually from 200°C to 700°C until it was burnt completely. After three hours, the samples were cooled and kept in a dessicator and then weighed again. The percent ash of the sample was calculated.

Kaolinite sample was piled up into a cone and dividing it into quarters. Opposite quarters were rejected and the remaining half–portion again treated as before, rolling the sample back and forth on a paper. After quartering, the sample was ground in a motar and pestle and then sieving with 200 mesh sieves.

Methods

Moisture content was determined by oven drying method. Measurement of pH was determined byusing pH meter. The specific gravity of samples was determined by the Pycnometer method ASTM (American Society for Testing Materials).Chemical composition of Rice Husk Ash and Kaolinite was determined by using acid digestion of gravimetric analysis method. Pozzolanic reactivity was determined by titrimeric method. Raw materials were characterized by EDXRF, XRD and SEM techniques. Relative abundance of elemental oxide in rice husk ash and kaolinite samples was determined by ED XRF technique using EDX-8000, Shimadzy Co. Ltd, Japan. X-Ray diffraction pattern of the sample was recorded by X-ray diffractometer (Cat – No. 9240 J101, Japan). SEM micrograph of the samples was recorded by Scanning Electron microscope (Model Jeol – JSM – 5610LV, JEOL Ltd).

Preparation of rice husk ash and kaolinite (1:1 wt. ratio) geopolymer and blended cement

Rice husk ash and kaolinite in1:1, 2:1 and 1:2 wt. ratio was mixed with 3mL of alkali solution (1:1, 1:2, 2:1, 3:1, 2:3)v/v of NaOH : Na_2SiO_3 and 28 mL of water were mixed on a non-absorbent base. Alkali solution, NaOH (4,8,12) M and Na_2SiO_3(0.1) M were used. Immediately the mixture was

placed in the plastic mould. After 28 days, the specimens were removed from the plastic mould. The blended cements were prepared by various mixing ratios of the prepared GP : commercial cement (1:1, 2:1, 1:2) weight ratio.

Table 1: Prepartion of Rice Husk Ash and Kaolinite (1:1 wt. Ratio) Geopolymer Samples Using Various Ratios of NaOH and Na_2SiO_3 Solution

Sample No.	Alkali Solution NaOH: Na_2SiO_3 (v/v)	Concentration of NaOH (M)
A-1	1:1	4
A-2	1:2	
A-3	2:1	
A-4	3:1	
A-5	2:3	
B-1	1:1	8
B-2	1:2	
B-3	2:1	
B-4	3:1	
B-5	2:3	
C-1	1:1	12
C-2	1:2	
C-3	2:1	
C-4	3:1	
C-5	2:3	

Methods Used for Mechanical Test of Rice Husk Ash and Kaolinite Based Geopolymer

Mechanical properties (compressive strength and tensile strength) of rice husk ash and kaolinite based geopolymer were determined at Civil Engineering Department, YTU. Test specimens (5 cm x 5 cm x 5 cm) cubes were used for testing compressive strength.

Figure 3: Compressive strength test machine

Results and Discussion

The result is divided into two parts. The first part is concerned with the physicochemical properties and the characterization of local raw materials (rice husk ash and kaolinite). The second part is concerned with the optimum conditions of sodium hydroxide concentration and sodium silicate for the preparation of rice husk ash – kaolinite based geopolymer. Before preparation of rice husk ash and kaolinite based geopolymer, some physicochemical properties of these raw material were determined. From this investigation, rice husk ash and kaolinite were more or less soluble in all mineral acid and not soluble at all in organic acid, water, hydroxide solvents (Table 2).

Table 2: Solubility of the Rice Husk Ash and Kaolinite

Solvent	Rice Husk Ash	Kaolinite
Nitric Acid	±	±
Sulphuric Acid	±	±
Hydrochloric Acid	±	±
Acetic Acid	-	-
Ethanol	-	-
Sodium Hydroxide	-	-
Water	-	-

(+) = soluble (±) = slightly soluble (-) = insoluble

Physicochemical properties of rice husk ash and kaolinite

The physicochemical properties such as moisture content, loss-on-ignition, pH and specific gravity in rice husk ash and kaolinite were 1.9% and 4.6%, 2.6% and 12.3 %, 8.8 and 8.3, 1.87 and 2.82, respectively, as shown in (Table 3).The moisture content of the rice husk ash and kaolinite contain 1.9 % and 4.6 %. It is possibly due to basic oxides and those of silicon, iron and aluminium. These are potentially are able to absorb moisture and have the property to become wetted which is one unique property of a cement ingredient. So, the content of moisture in kaolinite was slightly high. Loss on ignition (LOI) was eventually a measure of the un-burnt carbon in rice husk ash and kaolinite. LOI value of kaolinite was relatively high (12.3 %) residual carbon content of the ash. pH value of rice husk ash was 8.8 and kaolinite was 8.3 which is highly alkaline, not surprising of the nature of basic oxide. The inorganic composition of SiO_2, Al_2O_3, CaO, MgO and Fe_2O_3 are present in these samples (Table 4).

Table 3: Physicochemical Properties of Rice Husk Ash and Kaolinite

Samples	Moisture (%)	Loss – on – ignition (%)	pH	Specific Gravity
Rice Husk Ash	1.9	2.6	8.8	1.87
Kaolinite	4.6	12.3	8.3	2.82

Table 4: Relative Abundance of Elemental Oxide by ED XRF Analysis of Rice Husk Ash and Kaolinite Samples

Samples	Relative abundance (%)									
	SiO_2	Al_2O_3	Fe_2O_3	CaO	K_2O	TiO_2	MnO_2	SO_3	SnO_2	ZnO
Rice husk ash	96.70	-	0.30	0.59	1.73	0.30	0.20	0.37	0.03	0.01
Kaolinite	57.48	23.31	7.13	9.62	1.37	0.76	0.14	-	-	0.01

Characterization of rice husk ash and kaolinite samples

Figures 4 and 5 show the relative composition of the rice husk ash and kaolinite samples. According to ED-XRF pattern, silicon were found to be major in rice husk ash and Kaolinite samples. According to XRD result, kaolinite samples of the 2Θ value from 28 to 32 which is an indication of crystalline form. For rice husk ask samples, the pyrolysis was carried out in the range 450-700 ˚C, the silica was predominantly amorphous. (Figure 6 and 7). According to SEM micrograph, small pore and particles with diameter < 10 μm were seen on the surface of both rice husk ash and kaolinite samples (Figure 8).

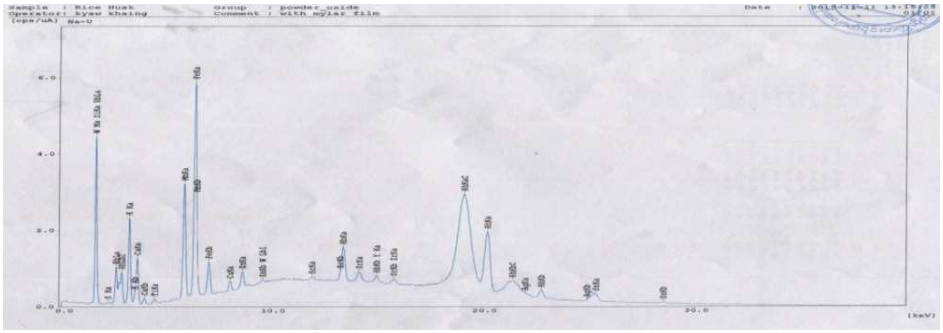

Figure 4: ED XRF spectrum of rice husk ash sample

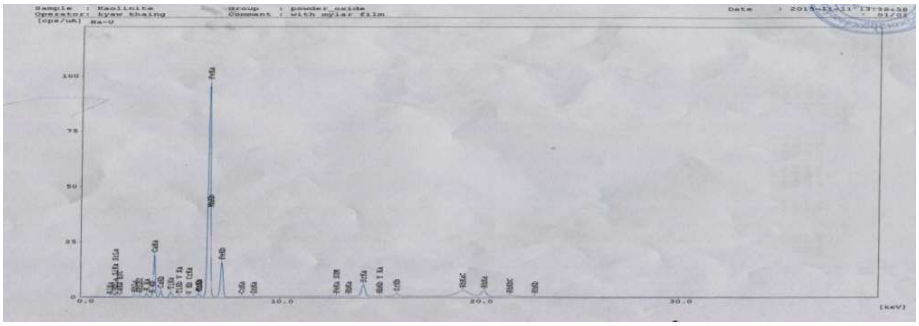

Figure 5: ED XRF spectrum of kaolinite sample

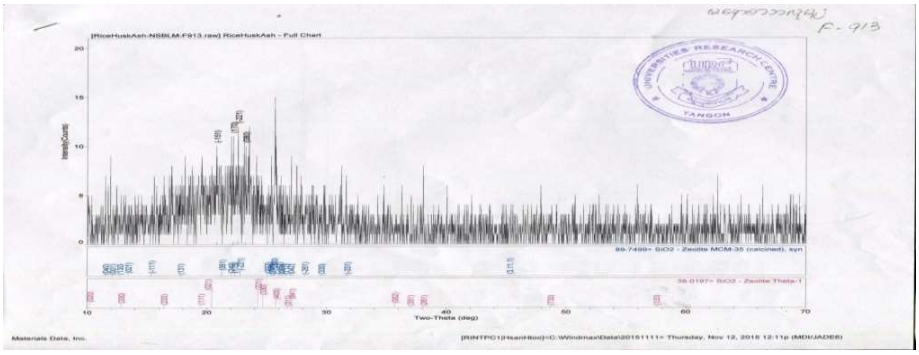

Figure 6: XRD spectrum of Rice Husk Ash sample

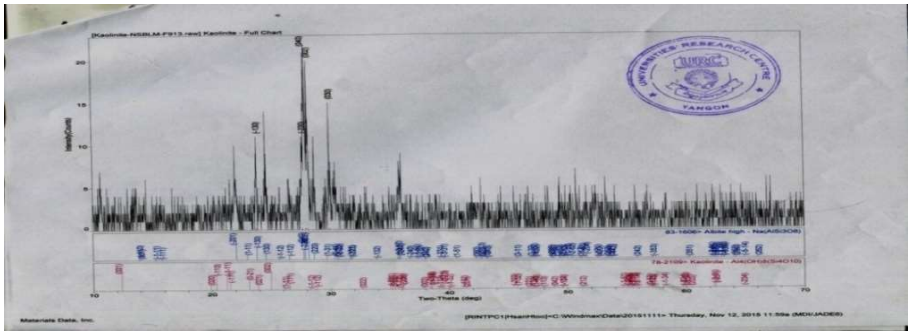

Figure 7: XRD spectrum of kaolinite sample

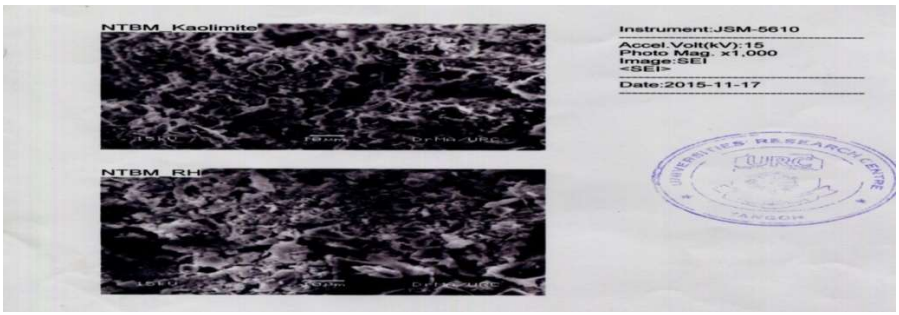

Figure 8: SEM images of rice husk ash and kaolinite samples

Pozzolanic Reactivity of Rice Husk Ash and Kaolinite Samples

In this research work, the pozzolanic reactivity of rice husk ash and kaolinite was found between 64 % to 94 %.These two samples allowed to react with calcium hydroxide nearly to 90 percent and the amount of $Ca(OH)_2$ reacted was increased as the time of reaction increased (Table 5 and 6).

Table 5: Pozzolanic Reactivity of Rice Husk Ash Sample

Experiment	Time (min)	Reacted Value of Ca $(OH)_2$ with Rice Husk Ash
1	30	79.17
2	60	82.96
3	90	86.75
4	120	90.60
5	150	94.40

Table 6: Pozzolanic Reactivity of Kaolinite Sample

Experiment	Time (min)	Reacted Value of Ca $(OH)_2$ with Kaolinite
1	30	64.10
2	60	71.60
3	90	77.28
4	120	82.96
5	150	90.60

The optimum condition of effect of alkali concentration on the prepared rice husk ash and kaolinite based geopolymer

Smaller the pole in prepared geopolymer, it become less permeable to water and lead to more denser. It was found that the less apparent porosity and water absorption percent, the more apparent density values. Sample no. B-5 has the highest value of apparent density, 1.89 g/cm^3 (Table 7).For the apparent density and compressive strength (28 days) were found to be maximum (sample no. B-5). Compressive strength is directly proportional to density value (Table 8).According from these data, the optimum condition for alkaline activator is 2:3. The more the hydroxide content in the ratio the more

micro-cracking would be observed. In addition, the more silica content the time become slower. The higher concentration results in higher strength capabilities. However the higher concentration increases the setting and delays polymer formation.

Table 7: Apparent Porosity, Water Absorption and Apparent Density of Prepared Geopolymer Samples (prepared by 1:1 wt. ratio of RHA: kaolinite)

Concentration of NaOH (M)	Sample No.	Apparent Porosity(%)	Water Absorption (%)	Apparent Density (g/cm^3)
4	A-1	12.14	8.72	0.81
	A-2	13.33	9.26	0.73
	A-3	14.12	10.95	0.71
	A-4	26.19	10.42	0.52
	A-5	10.48	5.33	1.21
8	B-1	19.33	10.82	1.72
	B-2	24.16	14.88	1.69
	B-3	24.81	15.48	1.70
	B-4	25.92	16.93	0.81
	B-5	18.52	11.58	1.89
12	C-1	19.93	9.17	1.21
	C-2	17.30	8.55	1.02
	C-3	20.21	10.22	0.93
	C-4	20.01	11.23	0.84
	C-5	18.12	5.11	1.38

Table 8: Compressive Strength of Rice Husk Ash – Kaolinite (1:1 wt. Ratio) Based Prepared Geopolymer Samples (28 days)

concentration of NaOH (M)	Sample No.	Compressive Strength (N/mm^2)		
		7 days	14 days	28 day
	A-1	6.01	6.24	12.48
	A-2	4.22	5.12	7.22
4	A-3	5.91	7.23	10.23
	A-4	3.24	3.59	5.61
	A-5	6.58	9.29	15.76
	B-1	8.23	12.11	15.12
	B-2	5.19	7.24	8.58
8	B-3	9.88	13.81	11.21
	B-4	5.25	7.03	6.42
	B-5	10.62	15.17	19.03
	C-1	5.24	5.98	14.12
	C-2	4.05	4.84	11.74
12	C-3	6.25	7.25	10.92
	C-4	3.15	4.06	5.02
	C-5	6.47	12.70	17.14

Table 9: Apparent Porosity, Water Absorption and Apparent Density of Geopolymer Samples Prepared by Different Weight ratio of RHA and Kaolinite

Conc: of NaOH (M)	Mix Ratio of RHA:Kaolinite	Apparent Porosity	Water Absorption	Apparent Density
4	1: 1	16.01	10.91	1.21
	2:1	17.30	12.04	0.34
	1:2	15.91	9.22	1.51
8	1: 1	25.92	16.11	1.89
	2: 1	27.59	18.04	1.53
	1: 2	22.43	15.82	2.33
12	1: 1	20.10	11.21	1.38
	2: 1	23.99	16.39	1.35
	1: 2	19.04	14.60	1.71

Mechanical strength of rice husk ash and kaolinite based geopolymer

The apparent density and compressive strength values is high in (1: 2wt. ratio) of RHA : kaolinite (Table 9).And also, the compressive strength value was found to be high in (1:2 wt. ratio) at 28 days (Table 10). Compressive strength value increased as the densities increased**.** In this research work, the compressive strength was found to be increased as the curing time increased. The maximum compressive strength of blended cement: commercial cement (1: 2) is 29.81 N/mm^2 at 28 days (Table 11).

Table 10: Relationship Between Time and Compressive Strength of Prepared Geopolymer (GP) in Various Ratios of Rice Husk Ash and Kaolinite

Concentration of NaOH (M)	**Prepared GP Rice Husk Ash: Kaolinite (Weight Ratio)**	**Compressive Strength (N/mm^2) in Different Time Intervals**		
		7 days	**14 days**	**28 days**
	1:1	16.01	10.91	1.21
4	2:1	17.30	12.04	0.34
	1:2	15.91	9.22	1.51
8	1:1	25.92	16.11	1.89
	2:1	27.59	18.04	1.53
	1:2	22.43	15.82	2.33
12	1:1	20.10	11.21	1.38
	2:1	23.99	16.39	1.35
	1:2	6.72	12.60	18.81

Table 11: Relationship between Time and Compressive Strength of Blended Cement and Commercial Cement (Elephant Brand)

Blended Cement : Commercial Cement (weight Ratio)	**Compressive Strength (N/mm^2) in Different Time Intervals**		
	7 days	**14 days**	**28 days**
1:1	17.64	21.50	23.94
2:1	9.21	15.72	19.32
1:2	22.24	25.65	29.81
Cement (Elephant Brand)	31.41	36.14	40.77

Conclusion

The physicochemical properties of rice husk ash and kaolinite were determined by conventional and modern instrumental techniques. The physical properties such as moisture content and loss-on-ignition in rice husk ash and kaolinite were respectively to be found that 1.9 % and 4.6 %,2.6 % and 12.3 %. pH and specific gravity in rice husk ash and kaolinite are 8.8 and 8.3. and 1.87 and 2.82, respectively. Rice husk ash and kaolinite have good pozzolanic properties which react with calcium hydroxide forming calcium silica hydrate. Pozzolanic reactivity of these sample increase with increase of reaction time. The optimum ratio of alkaline activator is 2:3 v/v sodium hydroxide and sodium siicate. The optimum concentration of sodium hydroxide concentration is 8M.Investigation about rice husk ash and kaolinite based geopolymer have found a potential material for replacing the use of Portland cement in infrastructure development thus decrease the carbon dioxide emission. However the different samples may give different reactivities due to their varying chemical compositions. The influence of NaOH molarity and alkaline activator ratioare essential for achieving the optimum strength of geopolymer. The use of rice husk ash and kaolinite as geopolymer are more environmentally friendly and cost compared to ordinay Portland cement.

Acknowledgements

The authors would like to express their profound gratitude to the Department of Higher Education (Yangon Office), Ministry of Education, Yangon, Myanmar, for provision of opportunity to do this research and Myanmar Academy of Arts and Science for allowing to present this paper.

References

Ajay,K. and Kalyani M. (2012). " Properties and Industrial Applications of Rice Husk ": A review. *International Journal of Emerging Technology and Advanced Engineering*, vol**10**(2), pp.86-88

Bogue, R. H. (1995). *The Chemistry of Portland Cement*, New York, Rheinhold Publishing Corp : 83-95

Davidovits, J.(1999). "Chemistry of Geopolymeric System, Terminology", Proceedings of Geopolymervol99, Geopolymer Institute, France ,pp. 9-14

Hough, J.H. and Barr. H.T. (1956). ''Possible Use for Waste Rice Husks in Building Materials and Other Products'', Agricultural Experimental Station , *Louisiana State Bulletin*, vol 150(1),pp.106-115

Hunt, LP, Dismukes JP and Amrick J. A. (1984). ''Rice hulls as a Raw Material for Producing Silicon'', *Journal of the Electrochemical Society* vol.131(7), pp. 1683-1684

James, J. (1986). *Chemistry of Silica from Rice Husk and Rice Husk Ash cement* ,Ph.D Thesis, Bangalore, Indian Institute of Science

Jepson, W.B., (2007). ''Kaolins: Their Properties and Uses'', *Philosophical Transaction of the Royal society*, London, 31, 411-432

Khin Moe Aye, (2013*). Study on Fly-ash Bentonite Based Geopolymer in Concrete Production*. Ph.D Disseration, Department of Chemistry, Yangon University.

Kyi Kyi San, Myat Hla Wai and Thazin Lwin.(2013). "Preparation, Characterization and properties of Kaolinite and Fly Ash-Based Geopolymer". *Jour. Myan. Acda. Arts & Sci*, vol11**(**1), pp.21-22

Mehta, P. K. (1975). ''Rice usk Ash Cement-High Quality, Acid Resisting''*, J.Amer. Concrete Instit*., 72 (5), 235-236

STUDY ON THE EFFECT OF PRESSING TEMPERATURE AND FIBER LENGTH ON PHYSICOMECHANICAL PROPERTIES OF PREPARED PARTICLEBOARDS DERIVED FROM BETEL NUT FIBER TREATED WITH CASHEW NUT SHELL LIQUID

Saw Win[1], Yee Yee Than[2], Thet Thet Hla Aung[3]

Abstract

The objective of the paper is to evaluate the physicomechanical properties of the fabricated single-layer experimental particleboards. Particleboards were made from treated betel nut fiber bonded with 40% modified cashew nut shell liquid. The particleboards were prepared by varying pressing temperature (130 °C, 140 °C, 150 °C, 160 °C, 170 °C and 180 °C). Different lengths of betel nut fiber (0.5cm, 1.0cm, 2.0cm, 3.0cm and 4.0cm) were also used for the preparation of particleboards. The experimental particleboards were tested for their physicomechanical properties such as modulus of rupture (MOR) and density by British Standard Method (BS) and then water absorption (WA) and swelling thickness (ST) according to the procedures defined by Indian Standard Method (IS). The tensile strength (T.S) and hardness of prepared particleboards were also studied by using Tensile Tester and Hardness Tester. The surface morphology of prepared particleboards was analyzed by scanning electron microscope (SEM) to measure the fiber pull out and fracture behavior. Thermal gravimetric analysis was also carried out to study the thermal degradation of prepared particleboards using TG-DTA. The study revealed that the sample of betel nut fiber length 2.0cm and pressing temperature 170°C showed highest MOR, TS and least WA, ST and highest density and hardness when compared with other prepared particleboards due to the physicomechanical properties of 3273 psi (MOR), 3.6 lb (TS) and 9% (WA), 22.28% (ST)and 1.20 gcm^{-3} (density) and 88.75 Shore D (hardness). It was found that the fiber length and pressing temperature have a significant effect on the board properties.

Keywords: Betel nut fiber, modified cashew nut shell liquid, particleboards, physicomechanical properties.

1. 4 PhD Candidate, Department of Chemistry, University of Yangon
2. Dr, Associate Professor, Department of Chemistry, Kyaington University
3. Dr, Associate Professor, Department of Chemistry, Sagaing University

Introduction

Particleboard (PB) is a wood-based or non-wood-based panel product manufactured under pressure and temperature from particles of wood or other lignocelluloses fibrous materials and a binder. It is used widely in the manufacture of furniture (box, cupboard, tabletop and speech shelf, etc.) and building materials (wall and ceiling paneling etc.) (Palakpuja, 2015). These particleboards are intended for use in the production of furniture and building materials that can be exposed to the action of higher humidity (e.g. kitchens. bathrooms, and laundries) (Wazny 1994).

Betel nut fiber is composed of cellulose with lignocelluloses, pectin, protopectin, wax and ash. Betel nut fiber can be easily and cheaply obtained and found in large amount at regional level. By using these fibers, it can reduce environmental pollution and has no harm to health and can also decrease the final cost of the product (Negsa, 2011). The average betel nut fiber length is 4cm long.The density of particleboard decreases with increase in fiber length (Mirski, 2014).

Cashew nut shell liquid is applied as lignins, paints and laminating resins. By using cashew nut shell liquid in manufacture of particleboards, it can provide particleboard to expose with higher humidity and can also damage the fungal species occurring on the surface of particleboards (Maulida, 2013). Ureaformaldehyde is a good resin for bonding particle and not poisonous in nature. It can be easily obtained with low cost. By using ureaformaldehyde, particleboard has very high tensile strength, the capacity of low water absorption and high surface hardness (Clausen *et al.,* 2003).

The particleboard without using cashew nut shell liquid or laminating favours to fungi growth. Fungi species break down cellulose and cause decreasing mechanical properties. The growth of fungi not only deteriorates aesthetic value and causes weakness of the building structure (Clausen *et al*., 2003) but also affects health of people who lived in that environment (Maulida, 2013).

Particleboards may be processed from 100°C to 230°C temperature range for duration of up to 30 min. The pressing parameters (temperature, pressure and time) normally lead to the degradation of the fiber's mechanical

properties. Control of hot press temperature and duration enhance in service ability cause less degradation of chemical components. Control of exposure of particleboards to high temperature can enhance resistance to moisture absorption, swelling thickness and ultimately durability (Palakpuja, 2015).

The parameters affecting the physicomechanical properties of particleboards are wood type (fiber type), fiber content, fiber length (particle size), resin type, resin content, pressing temperature, pressing pressure and pressing time (Mirski, 2014).

In the form of particleboard composite, many Myanmar researchers have reported as well. However, some known reports are those of Myat Myat Nwe (2008) on preparation and characterization of composite (plaster) board derived from renewable resource Bagasse and Aung Khine Tun (2012) on feasibility study on the production of quality wood adhesive using renewable cashew nut shell liquid.

This paper is concerned with the fabrication of durable particleboards using readily available and affordable cashew nut shell liquid as a composite resin compounded with modified adhesive UF resin at different pressing temperature and using different fiber lengths of betel nut fiber.

Materials and Methods

Materials

The raw materials utilized for the process are betel nut fiber (BNF), cashew nut shell liquid (CNSL) and ureaformaldehyde (UF) resin. The betel nut fiber collected from Min Bya Township, Rakhine State was prepared by Retting process (Ramachandra and Ashok, 2011).

Betel nut fiber was treated with 2% NaOH followed by cleaning with dilute acetic acid to neutralize excess NaOH. The treated betel nut fibers were dried for 7 days under ambient conditions to 10.7% moisture content, before use. The fibers were manually cut into fiber lengths 0.5cm, 1.0cm, 2.0cm, 3.0cm and 4.0cm long (Figure1).

0.5 cm 1.0 cm 2.0 cm 3.0 cm 4.0 cm

Figure 1: Betel nut fiber with different lengths

Cashew nut shell liquid was collected from Myeik, Thaninthayi Region. It was extracted from cashew nut shell by hot oil bath process.

Moisture content of reddish brown cashew nut shell liquid was 4.84%. Ureaformaldehyde(UF) was collected from Wartara glue factory, Yangon, Myanmar.Cashew nut shell liquid was modified with ureaformaldehyde with solid content of 58%, in the ratio of (1:1) by weight to improve the strength and the bonding between matrix resin and fibers. Betel nut fiber (120g) was blended with (40%) modified cashew nut shell liquid (40g CNSL and 40g UF).

Methods

Six types of particleboards to study the effect of pressing temperature labelled as (PBT1-PBT6) and five types of boards for effect of fiber length labelled as (PBL1-PBL5) were fabricated by using BNF and modified CNSL. Pre-weighed raw material (120 g of BNF with fiber length 2.0cm) for pressing temperature and 120g of BNF with fiber length 0.5cm; 1.0cm, 2.0cm, 3.0cm and 4.0cm for effect of fiber length was placed separately into HenschelMixer (2.2 HP, 2800 rpm). The glue mixture (40% modified CNSL-UF) was then poured on to the fiber and blended for 5 min at ambient temperature in the Henschel Mixer to obtain a homogenized mixture. The mat configuration was single layer boards measuring (6" x 6") were manually formed and pressed in a hydraulic hot press at 2200psi at 130ºC to 180ºC for pressing temperature effects and pressed only at 170ºC for fiber length effects for 15 min. The experimental design was shown in Table 1.

Table 1: Production Parameters of Single Layer Particleboards

Parameter	**Value**
Pressing temperature (°C)	130, 140, 150, 160, 170, 180
Pressing time (min)	15
Pressing pressure (psi)	2200
Dimension (inches)	6 x 6 (15.24 cm x 15.24 cm)
Thickness (inches)	0.19-0.28 (0.45 cm-0.67cm)
Number of boards of each type	2

Two replicate panels were made for each board type. After pressing under hydraulic hot press for 15 min, each board was pressed under cool press for 5 min. The particleboards were then conditioned at ambient temperature for one week in a vertical position (Figure2). The particleboards were trimmed to avoid edge effects to a final size of 6" x 6", and then cut into various sizes for property evaluationaccording to IS: 3087-1965 and BS: 1811-1961 (Figure 3)

Figure 2: Finished particleboards during conditioning at ambient temperature

Figure 3: Particleboards samples stored after the assessment

Some physical properties were determined in accordance with appropriate standards density (BS:1811-1961), water absorption (WA) and swelling thickness (ST) after a 24 himmersion in distilled water (IS:3087,1965). The mechanical properties determined were modulus of rupture (MOR) (BS:1811:1961), tensile strength (TS) (Electro-hydraulic Tensile Tester, Philadelphia, USA). For a particleboard, the mechanical properties (MOR) and water absorption (WA) tests are more important since it decides the strength of the material and porosity for a particleboard. Hardness measurement is done using Wallace Micro Hardness Tester: DIN-Normen, 1987.

Each panel was cut to get two WA/ST samples (2.54 cm x 2.54cm), two density samples (2.54 cm x 2.54 cm) and two TS/MOR samples (14 cm x 2.54 cm).

The scanning electron microscope(SEM: JSM 560 LV, JEOL, Ltd Japan) was used to identify the tensile fractured morphology of particleboard samples. The thermogravimetric differential thermal analysis (TG-DTA, Pyris Diamod TG-DTA High Temp 115 V) was used to measure the thermal stability of particleboard samples.

Results and Discussion

Some physicochemical properties of betel nut fiber are determined according to moisture content by TAPPI-T 210 om.86, 1992-93, Ash content by ASTM test method (D- 1102, 1986), fat and waxes content by Soxhlet extraction Method, cellulose content by AOAC method, pH by pH meter, lignin content by TAPPI method (TAPPI, 1992) hemicelluloses content by TAPPI method (TAPPI, 1992) and bulk density by Tapped method 1.

Table 2: Physicochemical Properties of Betel Nut Fiber

No	Characteristics	Observed value	Reported value *
1	Moisture content % (w/w)	10.7	10.92
2	Ash content % (w/w)	2.14	1.05
3	pH	6.1	-
4	Bulk density (g cm^{-3})	0.04	-
5	Fats and Waxes (%)	0.05(fats)	0.64
6	Lignin % (w/w)	12.31	7.20
7	Hemicellulose % (w/w)	17.52	32.98
8	Cellulose %(w/w)	70.17	53.20 (α-cellulose)

* Ramachandra and Ashok, (2011)

Effect of Pressing Temperature on the Physicomechanical Properties

The thickness of the prepared particleboards (PBT 1 – PBT 6) ranged from 0.46cm to 0.65cm. The density ranged from 0.92 $gcm^{-3}$to 1.24gcm^{-3}. The average water absorption and swelling thickness of the specimens following a 24h immersion ranged from 18.20% to 4.54% and 37.50% to 19.92% respectively. Particle board (PBT6) had the highest board density due to highest pressing temperature. The WA and ST values increased with decreasing the board density. The MOR ranged from 2516 psi to 3273 psi for PBT 1– PBT 6respectively. Particleboards having the greatest values of densities had the greatest values of MOR except (PBT6). The TS ranged from 2.1lb to 3.6 lb respectively. It was found that PBT 6 (180ºC) had the less MOR and TS than PBT 5 (170ºC) due to the more brittleness of fiber and resin, as expected. It can be suggested that the particleboard density plays a very important role on the bending strength. The pressing temperature increased which tend to increase the density of boards, as expected. The physicomechanical properties of prepared particleboards are shown in Table 3 and variation of properties at different pressing temperatures are shown in their respective figures 4.

Table 3. Physicomechanical Properties of Prepared Particleboard at Various Pressing Temperatures

Physicomechanical Property	**PBT1**	**PBT2**	**PBT3**	**PBT4**	**PBT5**	**PBT6**
Thickness (cm)	0.65	0.57	0.53	0.50	**0.50**	0.46
Density (gcm^{-3})	0.92	0.98	1.07	1.12	**1.20**	1.24
Water Absorption (%)*	18.20	15.80	14.43	13.04	**9.0**	4.54
Swelling Thickness (%)*	37.50	30.29	29.77	28.50	**22.28**	19.92
Hardness (Shore D)	81.25	85.00	86.75	88.00	**88.75**	90.7
Tensile Strength (lb)	2.1	2.5	2.6	3.5	**3.6**	3.1
Modulus of Rupture (psi)	2516	2537	2544	2731	**3273**	3237

Pressing Temperature = 130º C, 140º C, 150º C, 160º C, 170º C, 180º C

Pressing Time = 15 min

Fixed loaded Pressure = 2200 psi

Fixed Fiber Length = 2- cm, Adhesive = CNSL – UF

* = after 24 h

PBT1 = PB (130º C) PBT2 = PB (140º C) PBT3 = PB (150º C)

PBT4 = PB (160º C) PBT5 = PB (170º C) PBT6 = PB (180º C)

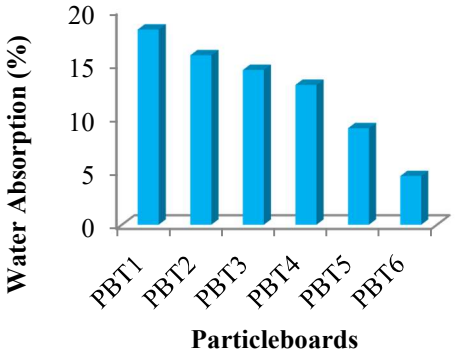

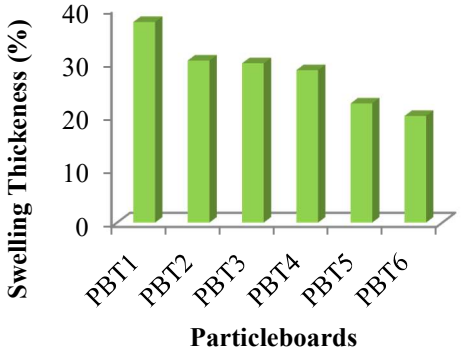

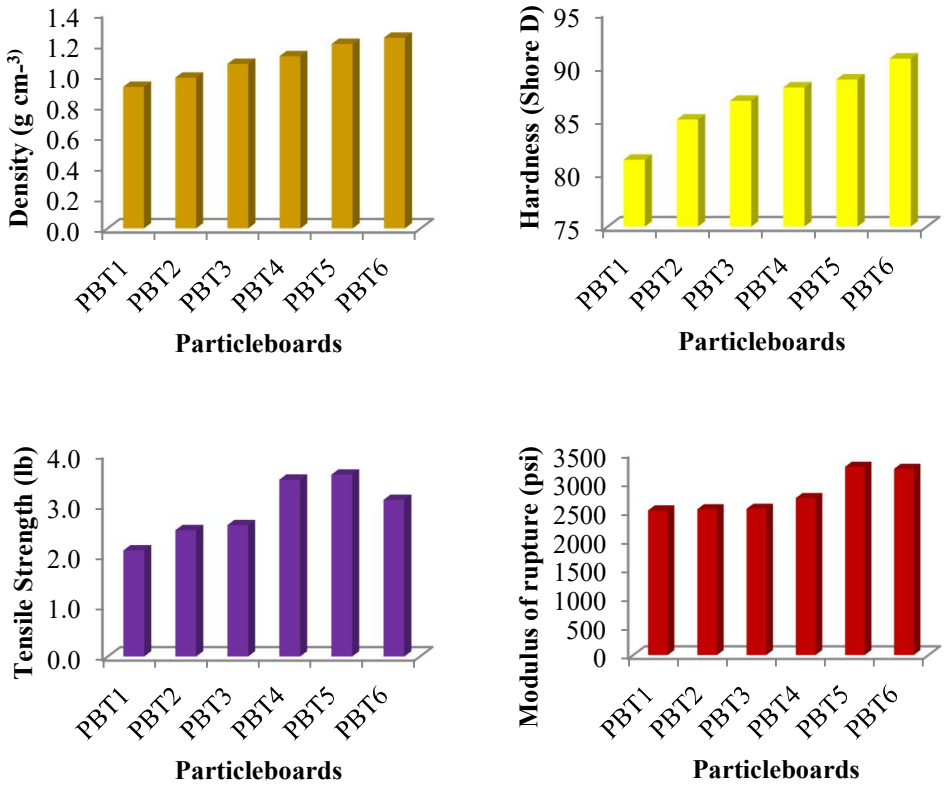

PBT1 = PB (130º C) PBT2 = PB (140º C) PBT3 = PB (150º C)

PBT4 = PB (160º C) PBT5 = PB (170º C) PBT6 = PB (180º C)

Figure 4: Variation of physicomechanical properties of particleboards at different pressing temperatures

Effect of Fiber Length on the Physicomechanical Properties

The thickness of prepared particleboards (PBL 1-PBL 5) ranged from 0.45cm to 0.67cm. The density ranged from 0.88gcm^{-3} to 1.29gcm^{-3}. The average water absorption and swelling thickness of the specimens following a 24 h immersion ranged from 9% to 38.1% and 22.28% to 56.69% respectively. The PBL 5 had the highest board density due to the shortest fiber length. The WA and ST of PBL3 (2.0cm) was less than that of the others.

There are more voids between the longer fiber, so WA and ST of PBL1 (4.0cm) and PBL2 (3.0cm) increased. But there are greater surface area contacting with water for the shorter fiber, so WA and ST of PBL 4 (1.0cm) and PBL 5 (0.5cm) increased, as expected. The MOR and TS ranged from2095 psi to 3273 psi and 1.90 lb to 3.60lb respectively PBL3 (2.0cm) had the greater values of MOR than others (PBL 1 (4.0cm), PBL 2 (3.0cm))which had more voids and PBL4 (1.0cm), PBL 5 (0.5cm) had greater surface area. The hardness ranged from 79.38 Shore D to 91.70 Shore D for PBL1-PBL5. It was found that the hardness of particleboard increases with decrease in fiber length when compared to other fiber lengths. The fiber length was important factor to determine the quality of product particleboard. The physicomechanical properties of prepared particleboards are shown in Table 4 and variation of properties at different fiber lengths are also shown in respective figures 5.

Table 4: Physicochemical Properties of Prepared Particleboards at Various Fiber Lengths

Physicomechanical Property	**PBL1**	**PBL2**	**PBL3**	**PBL4**	**PBL5**
Thickness (cm)	0.67	0.55	**0.5**	0.5	0.45
Density (gcm^{-3})	0.88	0.96	**1.20**	1.25	1.29
Water Absorption (%)*	32.5	30.5	**9.0**	37.5	38.1
Swelling Thickness (%)*	34.17	30.43	**22.28**	48.24	56.69
Hardness (Shore D)	79.38	80.38	**88.75**	90.50	91.70
Tensile Strength (lb)	3.05	3.30	**3.60**	2.30	1.90
Modulus of Rupture (psi)	2095	2776	**3273**	2387	2148

Fixed Pressing Temperature = 170º C

Pressing Time = 15 min

Fixed loaded Pressure = 2200 psi Adhesive = CNSL – UF

Fiber lengths = 0.5 cm, 1.0 cm, 2.0 cm, 3.0 cm, 4.0 cm

* = after 24 h

PBL1 = PB (L = 4.0 cm) PBL2 = PB (L = 3.0 cm) PBL3 = PB (L = 2.0 cm)

PBL4 = PB (L = 1.0 cm) PBL5 = PB (L = 0.5 cm)

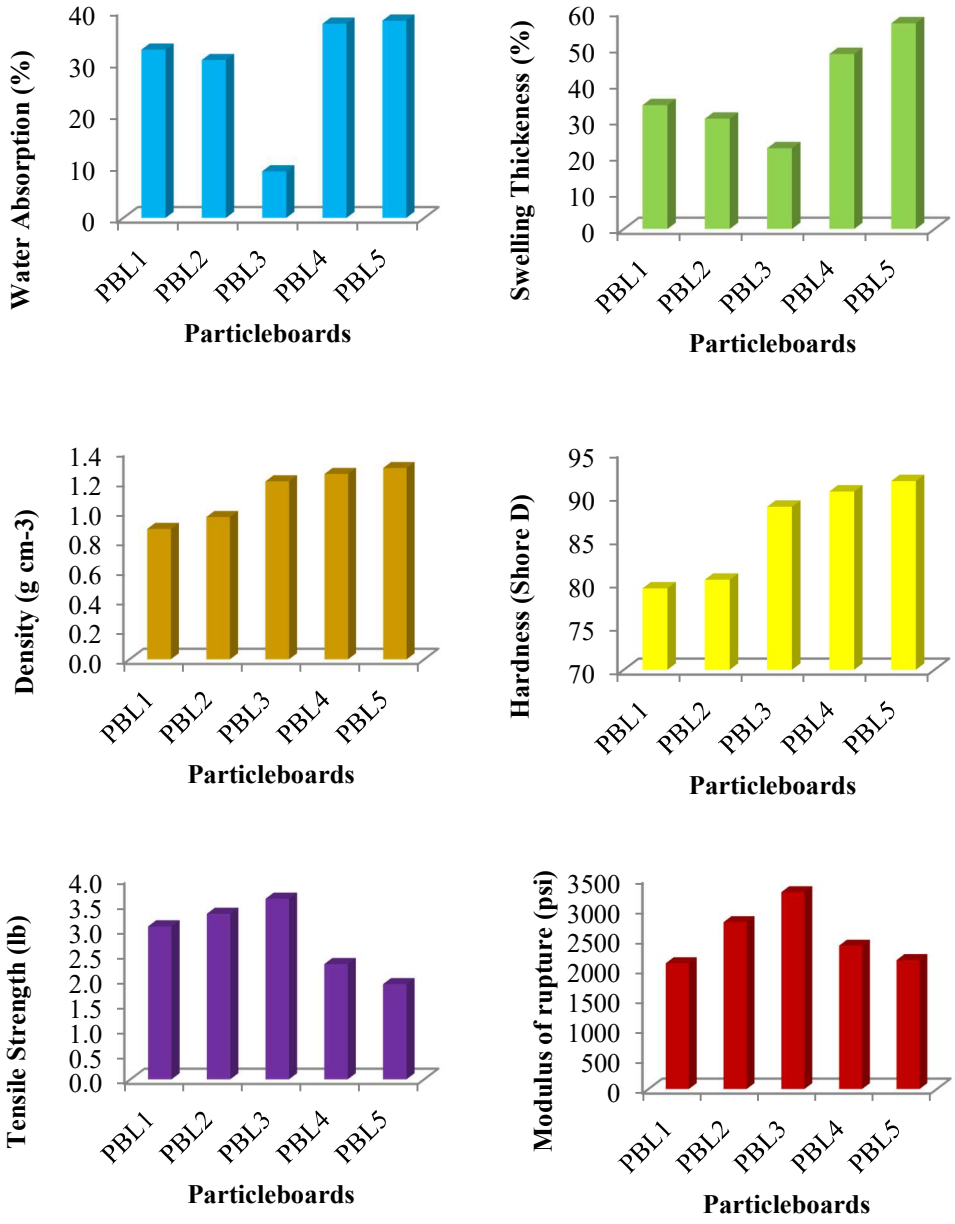

PBL1 = PB (L = 4.0 cm) PBL2 = PB (L = 3.0 cm) PBL3 = PB (L = 2.0 cm)
PBL4 = PB (L = 1.0 cm) PBL5 = PB (L = 0.5 cm)

Figure 5: Variation of physicomechanical properties of particleboards at different fiber lengths

Screw holding (SH) and connection of boards

The screws and nails were strongly held by particleboards without breaking, racking and brusting (Figure 6).

Figure 6: Photographs of screw holding for PBT6 (or) PBL3

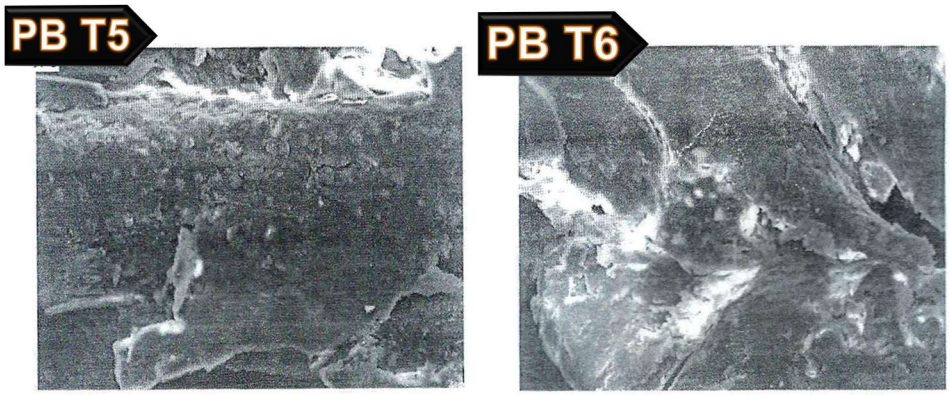

Figure 7: SEM micrographs of PBT5 and PBT6 particleboards

The surface of PBT 5 (170ºC) was more uniform than that of others. It also had less micropores and microcracks than PBT6. It was found that the more uniform and less micropores, microcracks as more compactability and tend to enhance more MOR and less WA and ST.

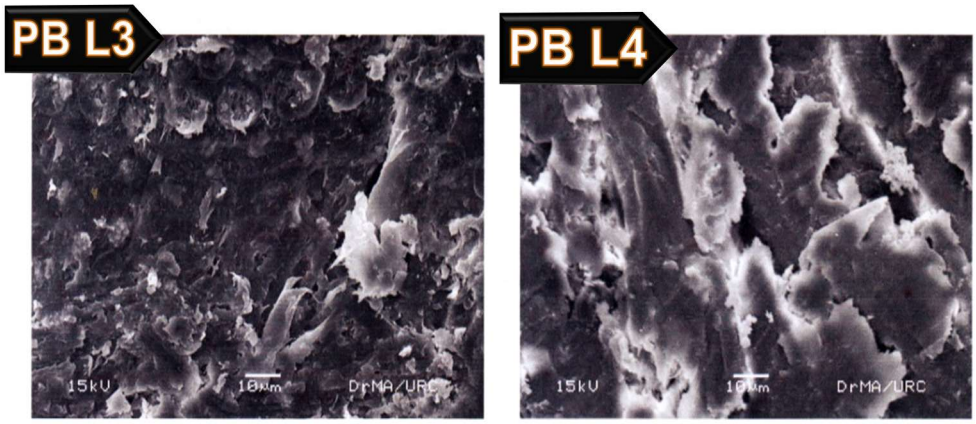

Figure 8: SEM micrographs of PBL3 and PBL4 particleboards

From the SEM analysis it was found that the long fibers PBL 3 (2.0cm) can withstand maximum stress, and showed better strength compared to short fiber (PBL 4 (1.0cm)). The short fibers (PBL4) were not uniformly distributed in the specimen resulted in lesser strength. PBL3 had agglomerate structure tend to compact and enhance MOR. The PBL4 had cluster form with less compact and decrease MOR. The SEM photo images of fractured surface of the particleboards were shown in Figures7 and 8.

TG-DTA Thermograms of PBT 5 and PBT 6

TG-DTA Thermograms of PBT 5 and PBT 6 are shown in Figure 9.

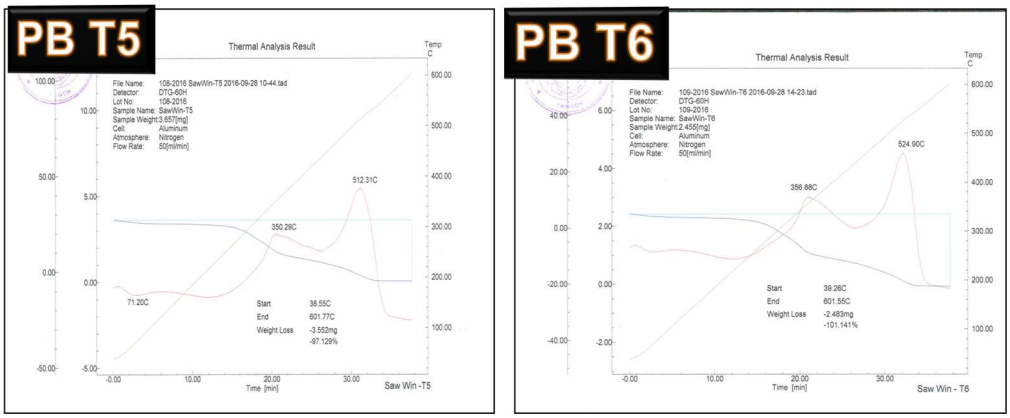

Figure 9: TG-DTA thermograms of PBT5 and PBT6 particleboards

PBT 5 (170°C) was more thermally stable due to the less weight loss than PBT 6 (180°C) until 440°C.

TGD-TA Thermograms of PBL 3 and PBL 4

PBL 3 (2.0cm) was more thermally stable (or) more thermally resistant due to the less weight loss than PBL 4 (1.0cm) Figure 10.

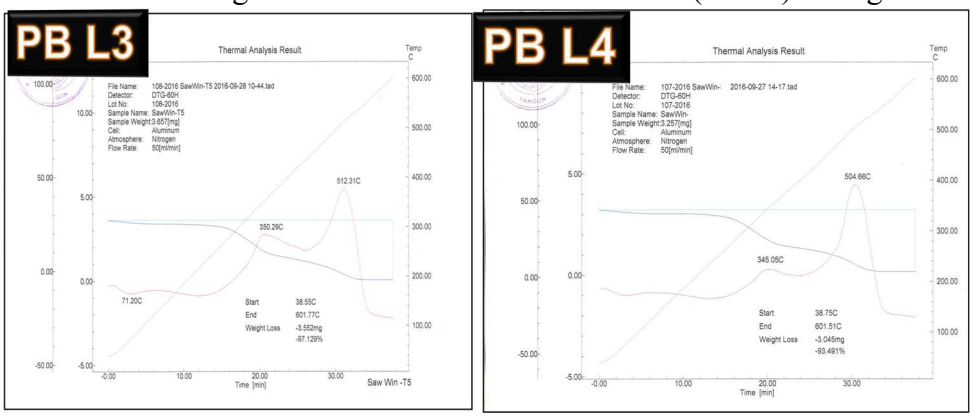

Figure 10: TG-DTA thermograms of PB L3 and PB L4 particleboards

Table 5: Thermal Analysis Data of Prepared Particleboards

Item	TG Break in Temp: (°C)	TG Weight Loss (%)	DTA Peak Temp: (°C)	DTA Nature of Peak	Remark
PBT5	38.55-170	7.030	71.20	Endo	Loss in weight due to dehydration
	170-440	58.820	350.29	Exo	Due to combustion
	440-601.77	31.219	512.31	Exo	Due to combustion Residual weight is 2.87%
PBT6	38.57-180	7.093	-	-	Loss in weight due to dehydration
	180-466.70	58.947	344.44	Exo	Due to combustion
	466.70-601.51	33.318	536.98	Exo	Due to combustion. Residual weight is 0.634%
PBL3	38.55-170	7.030	71.20	Endo	Loss in weight due to dehydration
	170-440	58.820	350.29	Exo	Due to combustion
	440-601.77	31.219	512.31	Exo	Due to combustion Residual weight is 2.87%
PBL4	38.75-140	7.890	-	-	Loss in weight due to dehydration
	140-430	58.333	345.05	Exo	Due to combustion
	430-601.51	27.268	504.66	Exo	Due to combustion Residual weight is 6.509%

Surface finish

After formation of particleboard, the surface can be made attractive by using sun mica laminates since the particleboard are laminated with different lamination films, different finished touches, can be given like teak wood finish, padauk wood finish, mahogany wood finish etc. Some of surface finishes are shown in Figure 11.

Figure 11: Photographs of surface finishes for PBT5 (or) PBL3

Application

Some of the application of the particleboards (PBT5 or PBL3) made from betel nut fiber and modified cashew nut shell liquid are shelves, furniture, boxes and cupboards ceilings etc., are shown in Figure 12.

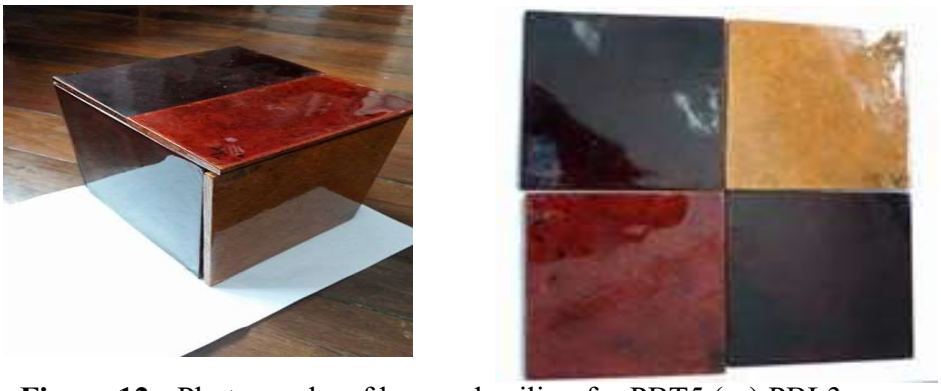

Figure 12: Photographs of box and ceiling for PBT5 (or) PBL3

Conclusion

The results presented here suggest that it is completely feasible to manufacture acceptable or high quality particleboard using betel nut fiber as an alternative lignocellulosic raw material. Since particleboards produced with pressing temperature at 170ºC had the most desirable quality, the production of such pressing temperature is recommended for the milling of the culms. Fiber length (2.0cm) was also found to have a great effect on the properties of modified CNSL-UF bonded betel nut fiber particleboards. The use of renewable materials such as betel nut fiber for manufacturing particleboards, could help to alleviate the scarcity of raw material for the particleboard industry.

Acknowledgements

The authors would like to express their profound gratitude to the Department of Higher Education (lower Myanmar), Ministry of education, Yangon, Myanmar, for provision of opportunity to do this research.

References

Aung Khine Tun. (2012).*Feasibility Study on the Production of Quality Wood Adhesive Using Renewable Cashew Nut Shell Liquid.* PhD Dissertation, Chemistry Department, University of Yangon.

Clausen, C. A., Haughton, L. and Murphy, C. (2003). *Evaluating Wood-based Composites for Incipient Fungal Decay with the Immunodiagnostic Wood Decay Test.* Madison, WI : Gen. Tech. Rep.,FPL-GTR 142 U.S. Department of Agriculture, Forest Service, Forest Products Laboratory, 7

Maulida, S. T., Jayanto, E. R. and Hendry, S. (2013). *Characteristic Mechanic of Polyester Composite Particleboard with Filler Particle of Area Nut Fiber.*

http://www.Mining.eng.cmu.ac.th (Accessed 4 September 2015)

Mirski, R., Dziurka, D. Dukarska, D. Czarnecki, R. and Cofta, G. (2014). *"*Microfungi and Particleboards*". Bio Resources.,* vol.9(4), pp. 6329 – 6339

Myat Myat New. (2008).*Preparation and Characterization of Composite (Plaster) Board Derived from Renewable Resource, Non-Wood Plant Fiber (Bagasse).* PhD Dissertation, Chemistry Department, University of Yangon.

Negsa, E. (2011). "Effect of Temperature and Durations of Heating on Coir Fibers*". Journal of Industrial Crops and Products,* vol, 33 (3), pp. 638-643

Palakpuja, P. (2015). *Properties and Uses of Ureaformaldehyde Resin.*

http://blog.oureducation.in/properties-and-uses-of-urea-formaldehyde-resin/ (Accessed 8 August 2015)

Ramachandra, R. G. and Ashok, K. M. (2011). "Fabrication and Performance of Hybrid Betel Nut Short Fiber Sansevieria Cylindrical Epoxy Composites".*International Journal of Materials and Biomaterials Applications,* vol.1(1), pp. 6-13

Wazny, J. (1994). *The Present Classification of Wood Degradation Factors.* Revised Version, International Research Group on Wood Preservation, Document No. IRG/WP/94-10071

X-RAY DIFFRACTION CHARACTERIZATION FOR OPTIMAL CRYSTALLITE AGGREGATES OF PHYTO-SYNTHESIZED SILVER NANOPARTICLES (AgNPs) BY *OCIMUM SANCTUM* L. LEAF EXTRACT

Su Thiri Kyaw[1], Myo Maung Maung[2], Mya Kay Thi Aung[3]

Abstract

ABSTRACT

In this research work, the holy basil leaves were collected from Hpa-an Township, Kayin State and verified its botanical name at Department of Botany, Hpa-an University. Preparation of silver nanoparticles and characterization of prepared silver nanoparticles by X-ray diffraction are described in the present work. A cost effective and environmental friendly method has been carried out for phytosynthesis of silver nanoparticles (AgNPs) from different volumes (2, 4, 6, 8 and 10 mL) of silver nitrate solution (1.0 mM) as metal precursor by using different amounts (5, 10, 15, 20 and 25 µL) of *Ocimum sanctum* L. leaf extract as reducing agent without using other chemicals of reducing agents. Based on the volume of metal precursor solution, the phyto-synthesized silver nanoparticles were designated as AgNP-2, AgNP-4, AgNP-6, AgNP-8 and AgNP-10 for further characterization. From the X-ray diffraction characterization, it was observed that the XRD patterns of AgNP-8 and AgNP-10 from synthesized AgNPs only showed the optimal crystallite aggregates for cubic crystal system. Comparing with (JCPDS, DB card No. 00-006-0480) reference, the peaks at 2θ values of both AgNP-8 and AgNP-10 corresponded to the Miller indices ($h\ k\ l$) of cubic system of Ag nanoparticles. From indexing XRD patterns of cubic system, it could be confirmed that the optimal phyto-synthesized AgNP-8 and AgNP-10 were face-centered cubic (FCC) crystal system because of having Miller indices with all odd or all even. It was observed that the average crystallite sizes of AgNP-8 and AgNP-10 were found to be 57.65 nm and 49.82 nm by using Scherrer formula.

Keywords : Silver nanoparticles, phyto-synthesis, *Ocimum sanctum* L., XRD, aggregates, single crystallite size

1. 2PhD, Candidate, Department of Chemistry, University of Yangon
2. Lecturer, Department of Chemistry, Dagon University
3. Lecturer, Department of Chemistry, University of Yangon

Introduction

Nanotechnology is a rapid growing science of producing and utilizing nano-sized particles. The uses of nano-sized particles are even more remarkable. They are mostly prepared from noble metals like silver, gold, platinum and palladium (Anuradha *et al.,* 2014). A number of approaches are available for the synthesis of silver nanoparticles, such as thermal decomposition, electrochemical, microwave assisted process and green chemistry. Many of the nanoparticle synthesis or production methods of nanoparticles involve the use of hazardous chemicals, low material conversions and high energy requirements (Logeswari *et al.,* 2015).

Biological methods have emerged as an alternative to the conventional methods for synthesis of nanoparticles. Synthesis of inorganic nanoparticles by biological systems make nanoparticles more biocompatible. Silver was recognized as a disinfecting agent; in its nanoparticles forms induce their ability in functions from medicine to culinary items. Human beings are frequently infected by micro-organisms such as bacteria, yeast, mold, virus, etc. Silver and silver ion based materials are usually used for their bactericidal and fungicidal activity.

The antimicrobial activity of silver is much superior to other metals, such as mercury, copper, lead, chromium and tin. Hence, silver and silver ion containing materials are used as prostheses, catheters, vascular grafts and as wound dressings in several biomedical applications.

Various methods, including physical and chemical methods were developed to synthesize metal nanoparticles, such as chemical reduction, electrochemical reduction, photochemical reduction etc. Biological method of nanoparticles synthesis using microorganisms, enzyme and plant or plant extract offers numerous benefits to offer a valuable contribution as eco-friendly technologies into nano-material science. In other hand, biological methods are free from the use of toxic solvents for synthesis of nanoparticles which are hazardous to the environment.

Nanoparticles are generally characterized by their size, shape, surface area and dispersity (jiang *et al*., 2009). The common techniques of characterizing nanoparticles are UV-visible spectrophotometry, Fourier transform infrared spectroscopy (FTIR), powder X-ray diffraction (XRD) (Shahverdi *et al*., 2011) .

The UV-visible spectroscopy is a commonly used techniques (Pal *et al*., 2007). Light wavelengths in the 300-800 nm are generally used for characterizing various metal nanoparticles in size range of 2 to 100 nm. FTIR spectroscopy is useful for characterizing the surface chemistry (Chithrani *et al*., 2006). XRD is used for the phase identification of the crystal structure of the nanoparticles (Sun *et al*., 2000).

Among the various known biosynthesis methods, plant mediated nanoparticle synthesis is preferred as it is cost-effective, eco-friendly and safe for human therapeutic applications (Paramasivam *et al*., 2015). Nowadays, the use of different types of medicinal plants has been increased by traditional medical practitioners for the treatments of various types of diseases.

The plant extract may act both as reducing and stabilizing agent. The most common and important medicinal plant i.e., *Ocimum sanctum* L. which have different medicinal properties such as anticancer, antimicrobial, cardio-protective, antidiabetic, analgesic, antispasmodic, antiemetic, hepatoprotective, antifertility, adaptogenic and diaphoretic actions (Birendra and Panigrahi, 2015).

The health benefits of *O.sanctum* include skin care, dental care, relif from respiratory disorders, asthma, fever, lung disorders, heart diseases and stress. *O.sanctum* protects all sorts of infections from viruses, bacteria, fungi and protozoa.

The use of plant extract reduce the cost as well as we do not require any special culture preparation and isolation techniques. The advantages of using plants and their extracts for the synthesis of metal nanoparticle is that they are easily available, safe to handle and possess a broad variability of metabolites that may aid in reduction (Gavade *et al*., 2015).

Materials and Methods

Collection of Holy Basil Leaves

Freshly green leaves of Holy basil (Kala-pin-sein) were collected from Hpa-an in Kayin State and identified by authorized botanists at Botany Department, Hpa-an University.

Preparation of Leaf Extract

Small finely pieces of 5 g of dried holy basil leaf sample was accurately weighed and placed into Erlenmeyer flask or beaker. Double distilled water (100 mL) was poured into the flask. The flask was then boiled for 5 min. The watery extract was cooled, filtered and kept in the refrigerator at 4 °C for further experiments and used within a week.

Preparation of 1 mM $AgNO_3$ Solution

Silver nitrate solution was prepared by adding 0.0169 g of $AgNO_3$ to 100 mL of deionized water in the Erlenmeyer flask and stored for further experiments.

Synthesis of Colloidal Solution of Silver Nanoparticles

Colloidal solution of silver nanoparticles were synthesized in accordance with the following procedure.

Different volumes (5, 10, 15, 20 and 25 μL) of Holy basil leaf extract were typically added to 2, 4, 6, 8 and 10 mL of silver nitrate solution (0.001M) respectively to be reduced Ag^+ ion to Ag^0 (nanoparticles). The colloidal solution of silver nanoparticles colouring colloidal brown was obtained within an hour (for about 50 min). The solution was allowed to incubate at room temperature overnight. The colloidal solution obtained were stored in refrigerator until further use to analyse.

Confirmation for The Existence of Silver Nanoparticles in Solution by Tyndall Effect

A laser pointer was taken and wrapped a rubber band around the on-switch so it was on continuously. The laser pointer was placed to the edge of the bottles containing GNP colloidal solution and the light was passed through the solution. The observation was recorded. The laser pointer was then rotated at 90° intervals and recorded any new observations.

The photograph of observation about the existence of silver nanoparticles in solution are represented in Figure 1.

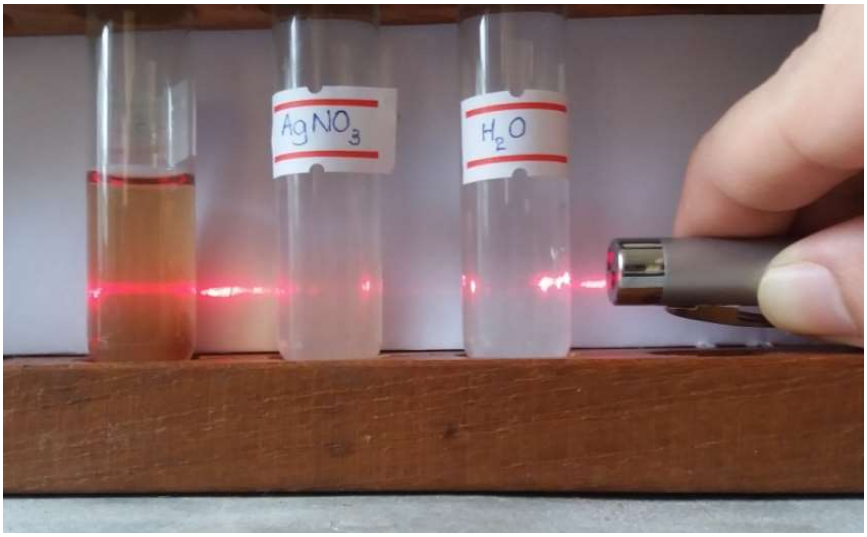

Figure 1: Dispersion of light (by laser beam) through AgNPs in aqueous medium

Confirmation the Formation and the Presence of Silver Nanoparticles (a Colloidal Solution) by the Spectra of the UV-Visible Spectrophotometry

The sample solutions were first diluted with distilled water. The UV-visible spectroscopic measurements of holy basil leaf extract, AgNP-8 and AgNP-10 were carried out by a computer controlled on a UV-visible Spectrophotometer (Shimadzu) at the West Yangon University.

Confirmation of the Functional Groups of Silver Nanoparticles by FTIR Spectrophotometry

The characterization of functional groups on the surface of AgNPs by plant extract were investigated by FTIR analysis (Shimadzu) and the spectra was scanned in the range of 4000-400 cm^{-1} range. The sample were prepared by dispersing the AgNPs uniformly in a matrix of dry KBr, compressed to form an almost transparent disc. KBr was used as a standard analyse the samples.

Determination of Crystallite Size Using Scheerer's Formula and Identification for Structure of Prepared Silver Nanoparticles from XRD Diffractograms

The synthesized colloidal AgNP solution was incubated at room temperature for least 2 days. The next day, the solution was observed to have distinctly deposited precipitate at the bottom of flask, leaving the colloidal supernatant at the top. The upper aliquot (colloidal AgNP) was decanted stored in refrigerator for further use. The precipitated silver nanoparticle powder was obtained from 5 mL of silver nitrate solution (0.001 M) and it was designated as AgNP-2 and the others as AgNP-4, AgNP-6, AgNP-8 and AgNP-10 respectively according to their concentrations.

The samples of silver nanoparticle powder (AgNP-2, AgNP-4, AgNP-6, AgNP-8 and AgNP-10) were analysed by X-ray diffraction technique to identify the crystallite size and structure. The recommended procedure used was in accordance with the catalogue.

The XRD spectra of the sample are presented in Figures 2 to 6. The average crystallite size of AgNP samples was calculated by using Scherrer's formula.

$$L = \frac{K\lambda}{\beta \cos\theta}$$

where, L = average crystallite size

K = constant crystallite shape

λ = wavelength of X-ray radiation $CuK\alpha_1$

β = FWHM of 2θ

θ = diffraction Bragg angle

Tables 1 and 2 show the average cryatsllite size of prepared silver nanoparticles.

Results and Discussion

Existence of Silver Nanoparticles in Solution by Tyndall Effect

The Tyndall effect is the scattering of light as a light beam passes through the colloid. Figure 1 shows the existence of silver nanoparticles in aqueous solution (as colloids). This Tyndall effect could be evident that the colloids have dispersed particles, making them nanoparticles. Hence, the particles will not settle out of the mixture.

According to this evidence, it was found that laser beam does not pass through water and silver nitrate solution. The dispersion of light passes through AgNPs in aqueous medium.

Confirmation to Colloidal AgNP-8 and AgNP-10 in Aqueous Solution by UV-Visible Spectrophotometry

UV-visible spectroscopy is a valuable tool for structural characterization of silver nanoparticles.

Figures 2 to 4 show the UV absorption spectra of colloidal AgNP-8, AgNP-10 and watery extract of holy basil leaf, respectively. It indicated that the silver nanoparticles were highly formed in aqueous phase, being stable with no precipitation. The maximum UV-visible absorption peak of colloidal AgNP-8 and AgNP-10 were appeared at 415 nm and 424 nm whereas watery extract of holy basil leaf absorbed the UV light at 268 nm.

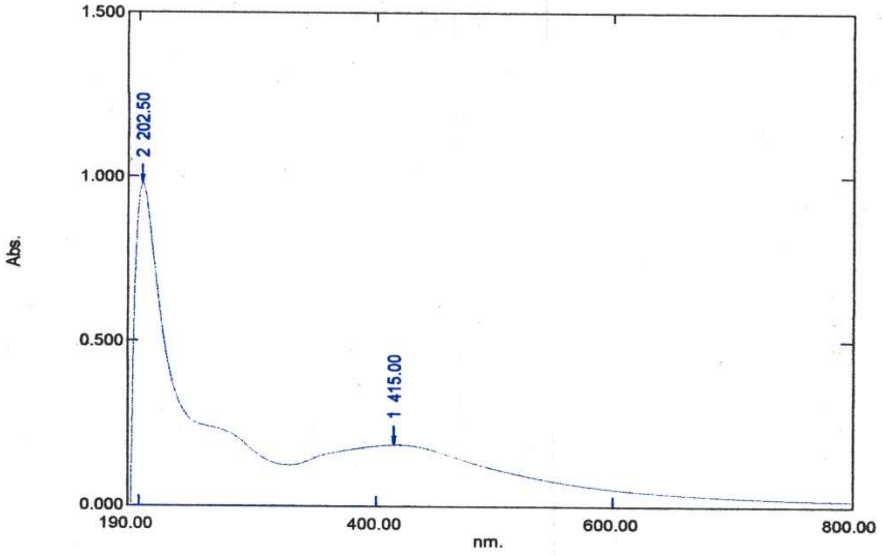

Figure 2: UV spectrum of colloidal AgNP-8

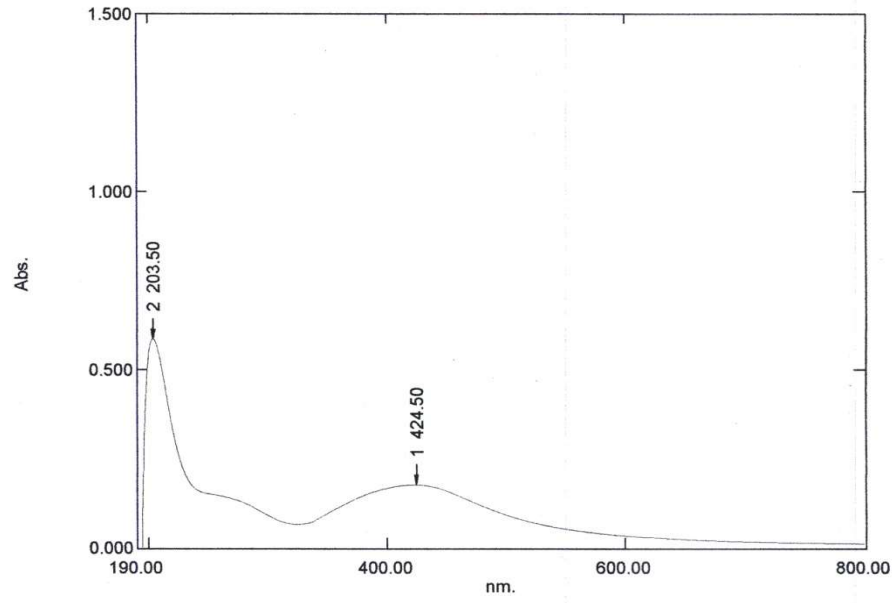

Figure 3: UV spectrum of colloidal AgNP-10

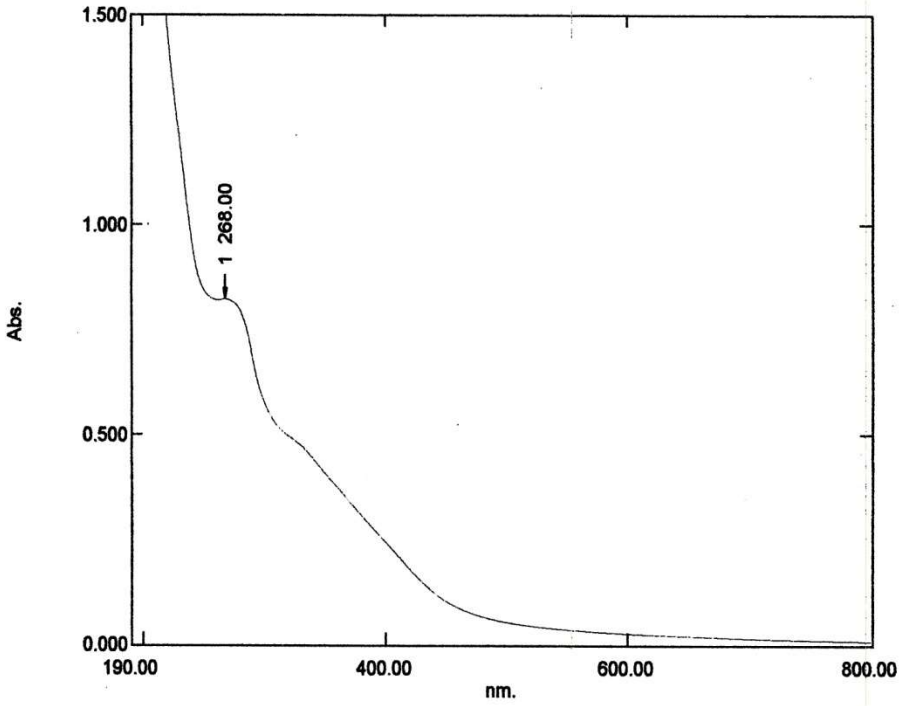

Figure 4: UV spectrum of watery extract of holy basil leaf

Confirmation of the Functional Groups of Silver Nanoparticles by FTIR Spectrophotometry

FTIR measurements were carried out to identify the biomolecules for capping and efficient stabilization of the metal nanoparticles synthesized. The FTIR spectra of silver nanoparticles show figures 5 and 6 and the bands at 3348 cm^{-1} and 3361 cm^{-1} corresponds to O-H stretching of alcohols and phenols. The peak found that 1636 cm^{-1} and 1647 cm^{-1} showed C=O stretching of conjugated system.

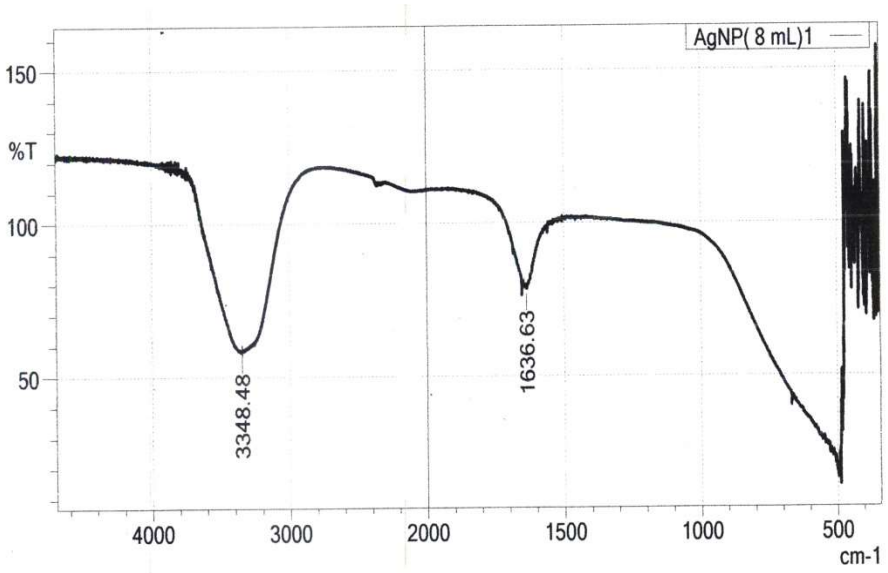

Figure 5: FTIR spectrum of colloidal AgNP-8

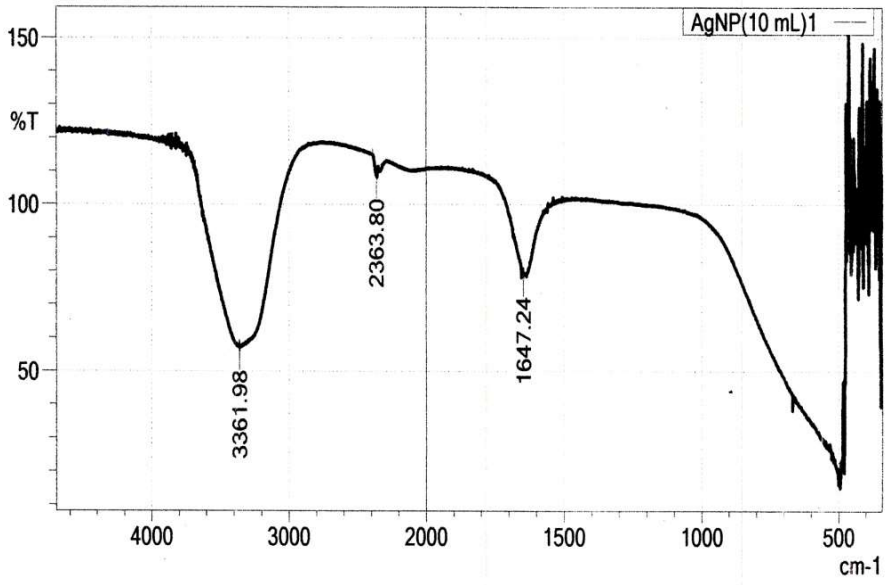

Figure 6: FTIR spectrum of colloidal AgNP-10

Structure of Prepared Silver Nanoparticles and the Crystallite Size by Using Scheerer's Formula from X-Ray Diffractograms

Figures 7 to 11 represent the X-ray diffractograms of the AgNP and Tables 1 and 2 describe the average crystallite size with respect to their relating parameters of 2θ, d and FWHM (the full-width at half maximum). The Bragg reflections corresponding to the (1 1 1), (2 0 0) and (2 2 0) sets of lattice planes were observed from the patterns.

These Miller indices corresponding to the (1 1 1), (2 0 0) and (2 2 0) all-odd or all-even sets of lattice planes designate the face-centred cubic (FCC) structure of silver nanoparticle.

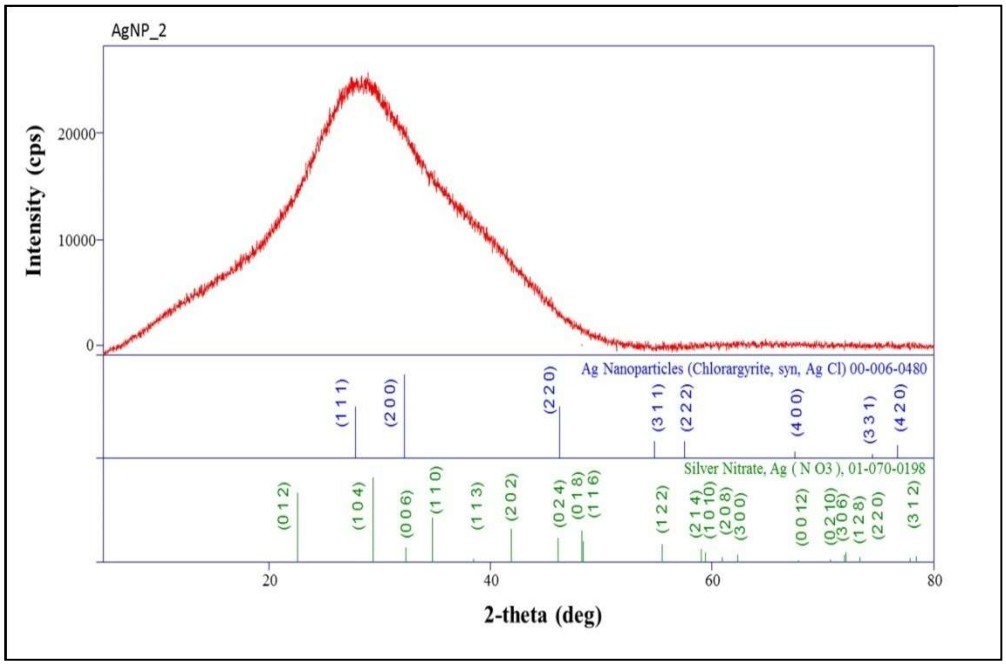

Figure 7: X-ray diffractogram of AgNP-2

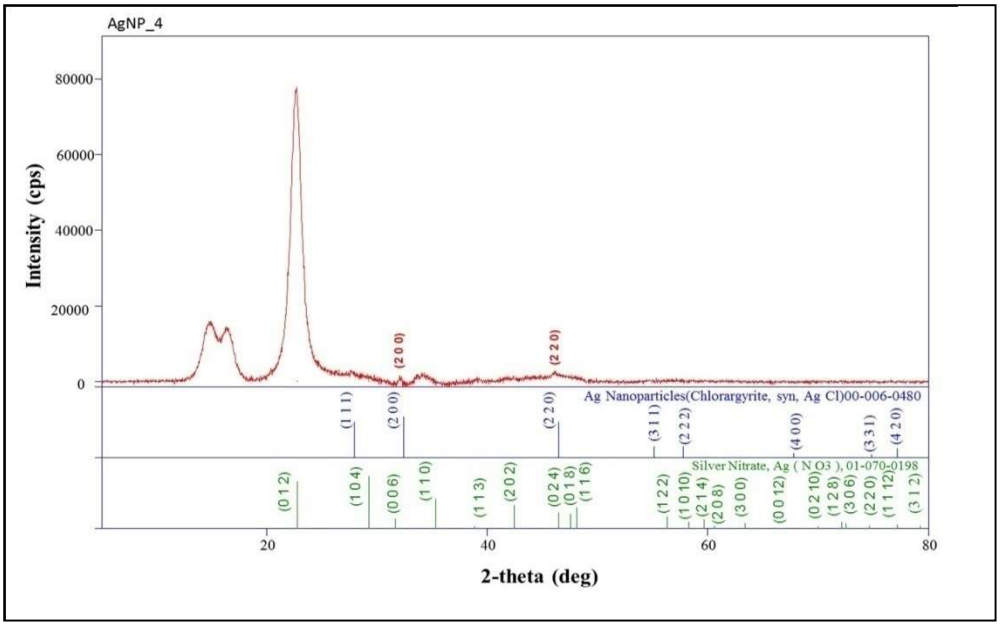

Figure 8: X-ray diffractogram of AgNP-4

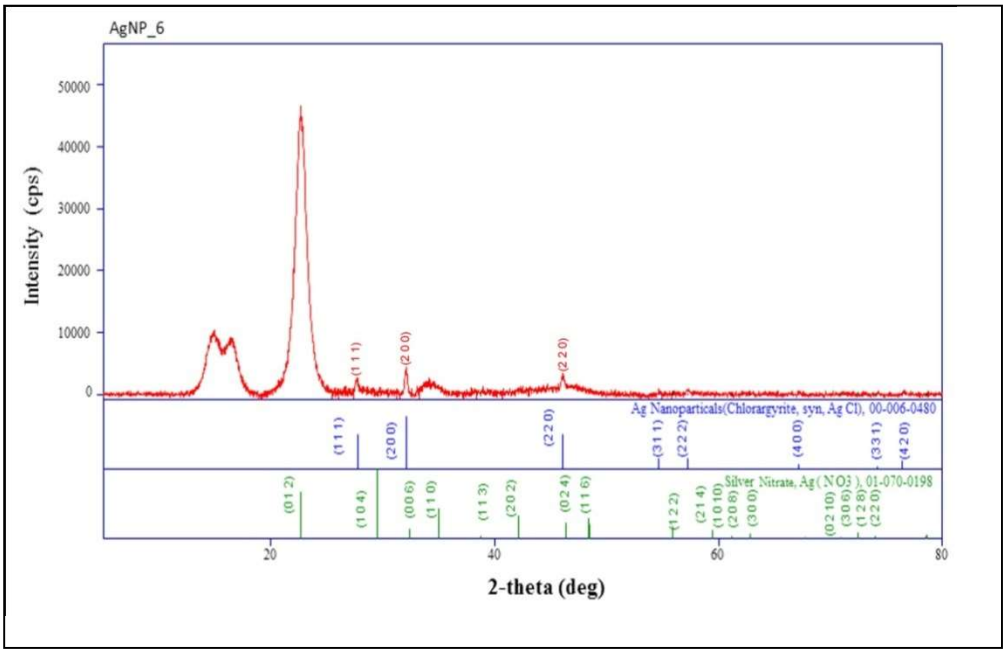

Figure 9: X-ray diffractogram of AgNP-6

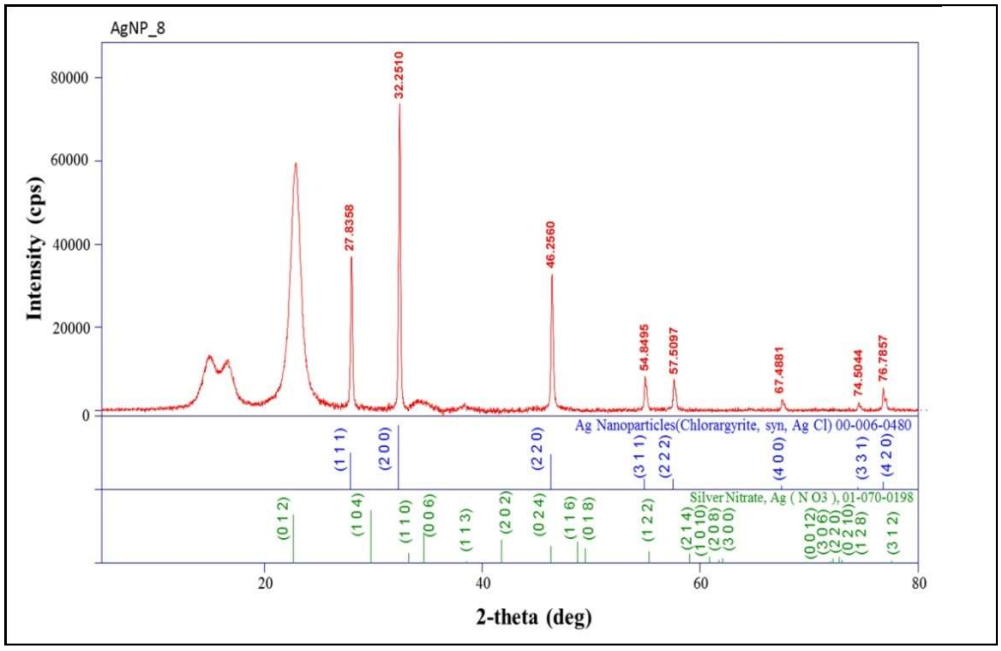

Figure 10: X-ray diffractogram of AgNP-8

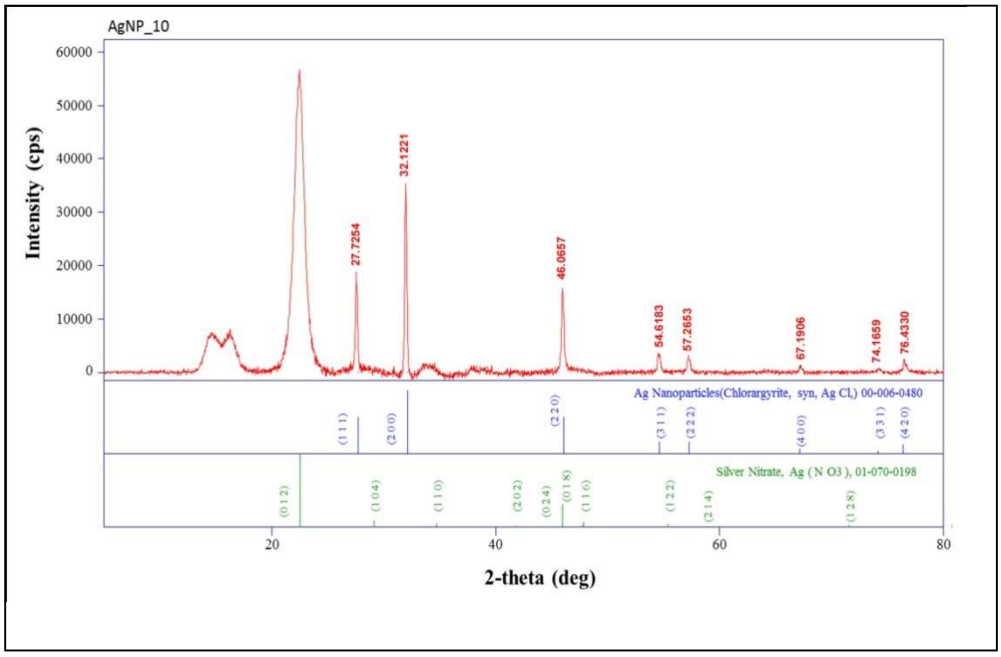

Figure 11: X-ray diffractogram of AgNP-10

Table 1: Data for Calculation of Average Crystallite Size of AgNP-8

Peak	2θ (deg)	θ (deg)	cosθ (rad)	β of FWHM (deg)	β (rad)	L (nm)
1	27.8358	13.9179	0.9706	0.1634	0.002852	50.09
2	32.2510	16.1255	0.9607	0.1618	0.002824	51.11
3	46.2560	23.1280	0.9196	0.1577	0.002752	54.78
4	54.8495	27.4248	0.8876	0.1561	0.002724	57.34
5	57.5097	28.7549	0.8767	0.1558	0.002719	58.16
6	67.4881	33.7441	0.8315	0.1556	0.002716	61.40
7	74.5044	37.2522	0.7960	0.1565	0.002731	63.77
8	76.7854	38.3927	0.7838	0.1571	0.002742	64.52
				Average crystallite size, L =		57.65

Table 2: Data for Calculation of Average Crystallite Size of AgNP-10

Peak	2θ (deg)	θ (deg)	cosθ (rad)	Bof FWHM (deg)	β (rad)	L (nm)
1	27.7254	13.8627	0.9709	0.1860	0.003246	43.99
2	32.1221	16.0611	0.9610	0.1855	0.003238	44.57
3	46.0657	23.0329	0.9203	0.1838	0.003208	46.97
4	54.6183	27.3092	0.8885	0.1827	0.003189	48.94
5	57.2653	28.6327	0.8777	0.1824	0.003183	49.62
6	67.1906	33.5953	0.8330	0.1809	0.003157	52.72
7	74.1659	37.0830	0.7978	0.1798	0.003138	55.38
8	76.4330	38.2165	0.7857	0.1794	0.003131	56.36
				Average crystallite size, L =		49.82

Conclusion

Ocimum sanctum L. (holy basil) leaves having positive and sound benefits have to be used in synthesis of silver nanoparticles. The UV absorption peaks of AgNP-8 and AgNP-10 were found to be 414 nm and 425 nm indicate the synthesis of AgNPs. FTIR confirmed the biofabrication of the AgNPs by the action of different phytochemicals with its different groups present in the extract solution. From the X-ray diffraction characterization, it

was observed that the XRD patterns of AgNP-8 and AgNP-10 from synthesized AgNPs only showed the optimal crystallite aggregates for cubic crystal system. Comparing with (JCPDS, DB card No. 00-006-0480) reference, the peaks at 2θ values of both AgNP-8 and AgNP-10 corresponded to the Miller indices ($h\ k\ l$) of cubic system of Ag nanoparticles. From indexing XRD patterns of cubic system, it could be confirmed that the optimal phyto-synthesized AgNP-8 and AgNP-10 occupied by face-centered cubic (FCC) crystal system because of having Miller indices with all odd or all even. It was observed that the average crystallite sizes of AgNP-8 and AgNP-10 were found to be 57.65 nm and 49.82 nm by using Scherrer formula.

Acknowledgements

The authors would like to express their profound gratitude to the Department of Higher Education (Yangon Office), Ministry of Education, Myanmar for provision of opportunity to do this research.

References

Anuradha, G., Sunda, B.S., Ramana, M.V., Kumar, J.S and Sujatha, T. (2014). "Single Step Synthesis and Characterization of Silver Nanoparticles from *Ocimum tenuiflorum* L. Green and Purple". *Journal of Applied Chemistry*, vol. **7**(5), pp 123-127

Birendra, K.B. and Panigrahi, A.K. (2015). "Biosynthesis and Characterization of Silver Nanoparticles (SNPs) by Using Leaf Extracts of Ocimum sanctum L (Tulsi) and Study of its Antibacterial Activities". *Journal of Nanomedicine and Nanotechnology*, pp 1-5

Chithrani B.D., Ghazani, A.A. and Chan, W.C.W. (2006). "Determining the Size and Shape Dependence of Gold Nanoparticle Uptake into Mammalian Cells". *Nano Lett*, pp 662-668

Gavade, S.J.M., Nikam, G.H., Sabale, S.R., Mulik, G.N. and Tamhankar, B.V. (2015). "Green Synthesis of Silver Nanoparticles by Using *Acacia concinna* Fruit Extract and Their Antibacterial Activity". *Journal of Nano Science and Nano Technology*, vol. **9**(3), pp 89-94

Jiang, J., Obersorster, G. and Biswas, P. (2009). "Characterization of Size, Surface Change, and Aggolmeration State of Nanoparticle Dispersions for Toxicological Studies". *J Nanopart Res*, pp 77-89

Longeswari, P., Silambarasan, S. and Abraham, J. (2015). "Ecofriendly Synthesis of Silver Nanoparticles from Commercially Available Plant Powders and Their Antibacterial Properties". *J.scient,* vol. **20** (3), pp 1049-1054

Pal, S., Tak, Y.K. and Song J.M. (2007). "Does The Antimicrobial Activity of Silver Nanoparticles Depend On The Shape of The Nanoparticle? A Study of the Gram-Negative Bacterium *Escherichia coli*". *Appl Envoron Microbiol*, pp 1712-1720

Paramasivam, P., Venkataramana, M., Abirami, M., Vanathi, P., Krishria, K. and Rajendran, R. (2015). "Biological Synthesis and Characterization of Silver Nanoparticles Using *Eclipta alba* Leaf Extract and Evaluation of its Cytotoxic and Antimicrobial Potential". *J.Scient*, pp 1-14

Shahverdi A.R., Shakibaie, M. and Nazari, P. (2011). "Basic and Practical Procedures for Microbial Synthesis of Nanoparticles". *Metal Nanoparticles in Microbiology*, pp 177-197

Sun, S., Murray, C., Weller, D., Folks, L. and Moser A. (2000). "Monodisperse FePt Nanoparticles and Ferromagnetic FePt Nanocrystal Superlattices". *Nano Science*, pp 1989-1992

EVALUATION OF WATER QUALITIES FOR WATER SAMPLES COLLECTED FROM FLOODED AND NON-FLOODED AREAS IN BAGO CITY DURING 2014-2016

Thein Hla Kyaw[1], Moe Ohmmar[2], Win Aung[3]

Abstract

Bago City is situated on the Bago River. Some parts of this cityis frequently being flooded in rainy season. The comparative studies on the quality of water body sites in the flooded and non-flooded areas of Bago City, during the time frame (2014-2016) have been studied. Flooding causes changes of water quality. The physicochemical properties (pH, temperature, DO, COD, BOD, total alkalinity, total hardness, total dissolved solid, nitrate nitrogen, phosphate, chlorinity, salinity and turbidity were determined on a quarterly basis throughout each year. Microbiological properties (total coliform and *E. coli*) of the water samples were also determined. Atomic absorption spectrophotometric method was used to determine the toxic elements (As, Pb, Hg, and Cd). The qualities of water resources from flooded and non-flooded areas in Bago City and its vicinity have been assessed.

Keywords: Bago City, flooded site, flooded and non-flooded areas, water quality, toxic elements

Introduction

Bago city is the administrative site of the Bago region. It is only about 80 km north west of Yangon, Myanmar. It is situated as stride the Bago river which flows down from the Bago mountain ranges. Normally, during the monsoon period some sites of the Bago city were prone to be flooded while other sites were not.

Usually, during the flooding time period the downtown area of Bago city because of its high embankment remain non-flooded while the lowline municipal areas were often impacted by flooding.

In Bago city, domestic water was either supplied from a reservoir Kandawgyi lake or some communities have to depend on tube well water.

[1]. PhD Candidate, Department of Chemistry, Nationalities Youth Resource Development of Degree College, Yangon
[2]. Associate Professor, Department of Chemistry, University of Hinthada
[3]. Associate Professor, Department of Chemistry, University of Myitkyina

As mentioned above, due to continual flooding within the city limit of Bago city, the underground water as well as the reservoir can be affected by the accumulation of toxic elements, such as arsenic, mercury, lead and cadmium. The water quality assessment of dams situated in the Bago region has been assessed by Myanmar researchers (Win Aung, 1996); (Khin Maw MawSoe, 2009); (Yin Thu, 2009) and (Nwe Ni Win, 2014).

This paper is comparative assessment of the water quality of the flooded and non-flooded sites in Bago region within the time-frame of period 2014 to 2016.

Materials and Methods

Sample Collection

Water samples were collected separately from the flooded and non-flooded areas of BagoCity. These samples have been quarterly collected since 2014.

The sites in non-flooded areas are:-**Site 1** (Laik Pyar Kan) [N17º 20.078' ; E 96º 29.164']; **Site 2** (Basic Education High School (BEHS) 1-tube well:390ft depth) [N17º 20.078'; E 96º 29.164']; and **Site 3** (Kandawgyi-the main fresh water source for the city)[N17º 22 36.03' ; E 96º 25 50.71']; **Site 8** (Mingalar Zayyon Monastery)[N17º 19.542' ; E 96º 28.414']; and **Site 9** (Dakkhina Monastery) [N17º 19.284' ; E 96º 28.245']. Similarly, the sites in the flooded areas are:-**Site 4** (Kyauk Kyisu) [N17º 20.581' ; E 96º 28.854']; **Site 5** (Basic Education High School (BEHS) 4/sub lake) [N17º 20.106' ; E 96º 28.575']; **Site 6** (Basic Education High School (BEHS) 4/sub TW) [N17º 20.137' ; E 96º 28.532'];and **Site 7** (Basic Education High School (BEHS) 5) [N17º 19.995' ; E 96º 28.415'].

Determination of Physicochemical and Microbiological Properties of Water Samples

The pH values of water samples were measured directly by using portable pH meter in the field.

The contents of dissolved oxygen in water samples and their temperatures were measured by using HANNA oxygen meter incorporated

with temperature probe in the field. These changes in values of dissolved oxygen and temperatures for the year 2015 were not significant (American Public Health Association, 1992).

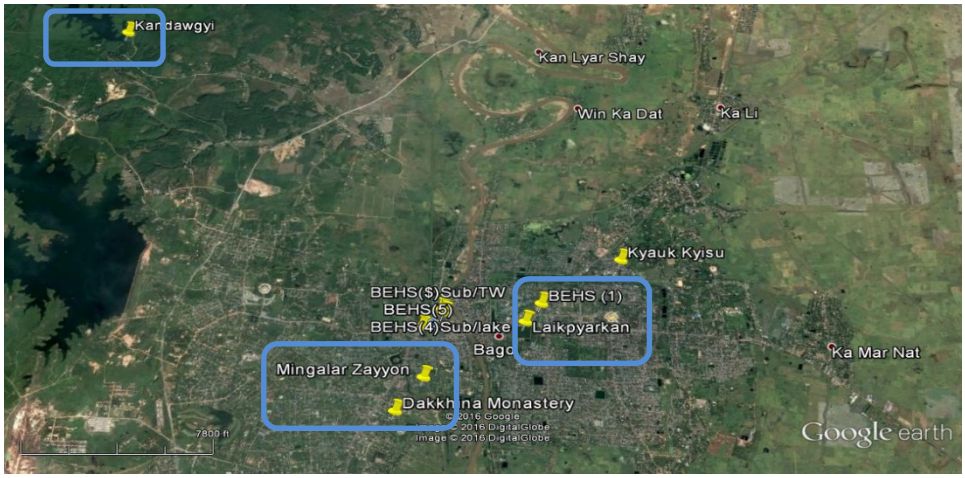

Figure 1: Google map of sample collecting sites (site 1 – site 9) in Bago city and its vicinity(The places in rectangle are non-flood areas)

The BOD_5 was carried out promptly after collecting the samples according to the water examination standard procedures. COD values of the collected water samples were measured by permanganate titrimetric method.

The dissolved solid contents in the samples were determined by using adissolved oxygen meter. Chlorinity of the water samples were determined by Mohr titrimetric method. By using Knudsen equation, the salinity of water was calculated. Total hardness was determined by EDTA titrimetric method. Total alkalinity of water samples was measured by titrimetric method. These laboratory works were carried out in the Analytical Research Laboratory (ACRL), Department of Chemistry, University of Yangon (Holden and Churchill, 1970).

The concentrations of nitrate and total phosphate were determined by spectroscopic methods at the Quality Control Laboratory, Fisheries' Enterprise, Ministry of Fisheries and Livestock (Crocodile Breeding Pond), Tharkayta Township. Moreover, the toxic metals (As, Hg, and Pb) were determined by Atomic Absorption Spectrophotometer at ISO 17025

Certificate Quality Control Laboratory, Fisheries' Enterprise, Tharkayta Township, Yangon.

The enumeration of *E.coli* and coliform counts were carried out at Analytical Research Laboratory (ACRL), Department of Chemistry, University of Yangon (Kumar and Kakrani, 2000).

Results and Discussion

In this research, the physicochemical and microbiological properties of water samples collected from the selected flooded and non-flooded areas of Bago city and its vicinity were measured by conventional standard methods at Analytical Research Laboratory, Department of Chemistry, University of Yangon.

The pH, temperature and dissolved oxygen (DO) were taken in the field by using portable pH meter, DO meter incorporated with thermometer probe. The data were compared with UNEP (United Nations Environmental Protection-2012) standards, this recent data are in the acceptable range of domestic water. The pH values of the water samples collected from the respective sampling sites quarterly during 2014-2016 did not significantly change.

The dissolved solid contained in the samples were determined by dissolved oxygen meter. It is noted that TDS values were not changed by flooding suddenly due to the slow perforation rate into the underground aquifers (Tables 11,13,15, and 17).

Although the impact areas were flooded for a few days in 2015, the parameter such asBOD and COD were also found to be low (Stone, 2012).

The conductivity of Laik Pyar Kan and Kandawgyi were abruptly changed by the flow of rain water into these lakes. Similarly, the salinity and chlorinity values of these two lakes were also significantly changed,(Tables 1 and 5).

The total hardness values of Laik Pyar Kan and Kandawgyi were suddenly dropped by the dilution effect of rain water. The tube well are

sources of water, so the changes in these parameters were not significant (Tables 1 and 5).

The total alkalinity values of water collected in August were abruptly increased. Explanation is given by comparing the data obtained for successive years, i.e., there have been remaining works in 2017 (Tables 1,3,11, and 15).

The values concerned with microorganisms were contributed to the people resided these respective areas. There were some impacts on water samples collected from BEHS (1) and BEHS (4) (Table 19).

The nitrate contents in most of the sampling sites were not noticeably changed. But the phosphate contents changed due to the effect of runoff from agricultural farms.

Table 1: Comparison of Water Quality Parameters for Laik Pyar Kan (Non-Flooded Area) (2014-2016)

	pH	**DO (ppm)**	**BOD (ppm)**	**COD (ppm)**	**Alkalinity (ppm)**	**Hardness (ppm)**	**Turbidity (NTU)**	**TDS (ppm)**	**Conductivity (μS/cm)**
	7.3	6.2	2.1	4.90	45.0	20	15.0	28.0	56
2015 Feb	6.8	4.5	0.6	0.37	4.0	104	9.0	56.2	83
2015 May	6.8	5.0	0.5	1.84	5.6	260	18.7	45.7	118
2015 Aug	6.7	5.0	4.5	4.78	20.0	16	11.8	43.8	48
2015 Nov	6.9	5.5	3.7	3.44	15.2	88	10.3	50.9	78
2016 Feb	6.7	5.0	1.5	0.84	28.0	34	82.0	20.0	75
2016 May	6.5	5.0	2.0	1.11	40.0	40	120.0	20.5	114
2016 Aug	6.5	5.5	2.0	1.62	24.0	48	58.0	160.0	47
2016 Nov	6.8	4.0	2.0	1.75	100.0	60	85.0	20.5	50
UNEP (2012)	6.0-8.0	-	10.0	5.0	-	-	-	-	-

Table 2: Comparison of Water Quality Parameters and Toxic Metal Contents for Laik Pyar Kan (Non-Flooded Area) (2014-2016)

	Chlorinity (‰)	**Salinity (‰)**	**Phosphate (ppm)**	**Nitrate (ppm)**	**Lead (ppm)**	**Cadmium (ppm)**	**Mercury (ppm)**	**Arsenic (ppm)**
2014 Nov	0.27	0.52	ND	ND	ND	ND	ND	ND
2015 Feb	0.02	0.06	0.30	ND	0.101	ND	ND	ND
2015 May	0.07	0.16	1.20	ND	0.192	ND	ND	ND
2015 Aug	0.06	0.13	0.40	0.01	0.189	0.0009	0.0009	0.002
2015 Nov	0.04	0.11	0.80	ND	0.174	ND	ND	0.001
2016 Feb	Nil	Nil	0.02	0.02	ND	0.0123	0.0004	0.006
2016 May	Nil	Nil	0.03	0.02	1.018	0.0510	0.0005	0.009
2016 Aug	Nil	Nil	0.10	0.01	1.205	0.0600	0.0005	0.015
2016 Nov	Nil	Nil	0.02	0.30	ND	0.0220	0.0004	0.002
UNEP (2012)	-	-	-	-	0.05	-	0.01	0.01

ND = not detectable

2015, there was an impact of flood on ground water with respect to the perforation of toxic elements such as arsenic, mercury, lead, and cadmium. These toxic elements entered the water body due to the increase in level of aquifer or underground water table.

The rainfall in August was the highest and also the river water level was also high but the river water level did not exceed the critical level of Bago (910 cm) (Figure 2). It may be summarized that the impact of flooding was not significant according to the viewpoints of physicochemical properties. However, a little effect of short term flooding, the population of microorganism (Table 19) (Edberg, *et al.,* 2000) (Dubey, *et al.,* 2002) and contents of toxic elements were noticeable(Tables 12, 14, 16, and 18).

Table 3: Comparison of Water Quality Parameters for BEHS (1) (Non-Flooded Area) (2014-2016)

	pH	DO (ppm)	BOD (ppm)	COD (ppm)	Alkalinity (ppm)	Hardness (ppm)	Turbidity (NTU)	TDS (ppm)	Conductivity (μS/cm)
2014 Nov	6.9	6.7	1.9	4.00	61.0	36	11.0	156.0	312
2015 Feb	7.2	4.5	0.5	0.37	15.4	104	2.4	207.0	314
2015 May	6.8	5.5	3.5	1.47	19.8	325	1.2	198.6	337
2015 Aug	6.7	5.9	4.0	1.10	100.0	32	1.9	188.1	298
2015 Nov	7.0	5.9	3.0	0.99	28.1	94	1.6	200.6	301
2016 Feb	6.8	5.0	1.5	1.82	130.0	30	7.0	15.0	294
2016 May	6.9	5.0	1.5	2.21	100.0	60	7.0	10.0	326
2016 Aug	7.2	2.0	1.0	0.42	132.0	64	12.0	189.0	296
2016 Nov	7.2	3.5	2.0	0.32	140.0	70	25.0	210.0	302
UNEP (2012)	6.0-8.0	-	10.0	5.0	-	-	-	-	-

Table 4: Comparison of Water Quality Parameters and Toxic Metal Contents for BEHS(1) (Non-Flooded Area) (2014-2016)

	Chlorinity (‰)	Salinity (‰)	Phosphate (ppm)	Nitrate (ppm)	Lead (ppm)	Cadmium (ppm)	Mercury (ppm)	Arsenic (ppm)
2014 Nov	0.56	1.04	ND	ND	ND	ND	ND	ND
2015 Feb	0.02	0.06	0.80	ND	0.236	ND	ND	ND
2015 May	0.05	0.13	1.50	ND	0.541	ND	ND	ND
2015 Aug	0.48	0.90	1.20	ND	0.363	0.002	0.0007	0.025
2015 Nov	0.35	0.67	1.10	ND	0.404	ND	ND	0.011
2016 Feb	Nil	Nil	0.02	0.002	ND	0.013	0.0001	0.031
2016 May	Nil	Nil	0.01	0.020	1.029	0.058	0.0004	0.023
2016 Aug	Nil	Nil	0.05	0.020	1.221	0.067	0.0012	0.013
2016 Nov	Nil	Nil	0.07	0.050	ND	0.032	0.0003	0.009
UNEP (2012)	-	-	-	-	0.05	-	0.01	0.01

Table 5: Comparison of Water Quality Parameters for Kandawgyi(Non-Flooded Area) (2014-2016)

	pH	DO (ppm)	BOD (ppm)	COD (ppm)	Alkalinity (ppm)	Hardness (ppm)	Turbidity (NTU)	TDS (ppm)	Conductivity (μS/cm)
2014 Nov	7.1	5.8	1.80	0.70	12.0	7	6.00	11.0	23
2015 Feb	6.7	4.5	1.85	0.37	14.0	13	0.00	16.7	24
2015 May	6.9	4.3	1.50	1.84	14.0	31	0.42	10.5	27
2015 Aug	6.8	3.4	2.00	1.10	16.0	24	0.99	11.7	18
2015 Nov	7.0	5.8	2.20	0.59	14.5	19	0.09	14.8	21
2016 Feb	6.6	4.5	2.50	1.86	16.0	10	10.00	15.0	21
2016 May	6.5	4.5	2.50	2.87	12.0	20	8.00	10.5	27
2016 Aug	6.5	5.0	2.50	1.36	20.0	40	17.00	15.1	18
2016 Nov	6.7	4.0	2.50	1.32	20.0	25	6.00	20.5	18
UNEP (2012)	6.0-8.0	-	10.0	5.0	-	-	-	-	-

Table 6: Comparison of Water Quality Parameters and Toxic Metal Contents for Kandawgyi (Non-Flooded Area) (2014-2016)

	Chlorinity (‰)	Salinity (‰)	Phosphate (ppm)	Nitrate (ppm)	Lead (ppm)	Cadmium (ppm)	Mercury (ppm)	Arsenic (ppm)
2014 Nov	0.04	0.11	ND	ND	ND	ND	ND	ND
2015 Feb	0.01	0.06	0.10	ND	0.011	ND	ND	ND
2015 May	0.04	0.11	1.50	ND	0.016	ND	ND	ND
2015 Aug	0.03	0.10	0.03	0.01	0.159	0.001	0.0006	0.003
2015 Nov	0.03	0.08	0.00	ND	0.034	ND	ND	ND
2016 Feb	Nil	Nil	0.01	0.03	ND	0.012	0.0005	0.001
2016 May	Nil	Nil	0.02	0.12	1.015	0.047	0.0003	0.003
2016 Aug	Nil	Nil	0.06	0.08	1.069	0.052	0.0006	0.011
2016 Nov	Nil	Nil	0.08	0.20	ND	0.029	0.0005	0.001
UNEP (2012)	-	-	-	-	0.05	-	0.01	0.01

ND = not detectable

Table 7: Comparison of Water Quality Parameters for MingalarZayyon Monastery (Non-Flooded Area) (2014-2016)

	pH	DO (ppm)	BOD (ppm)	COD (ppm)	Alkalinity (ppm)	Hardness (ppm)	Turbidity (NTU)	TDS (ppm)	Conductivity (µS/cm)
2016 Feb	6.6	4.5	2.0	1.32	50	24	2	30	107
2016 May	6.8	5.5	1.5	2.78	36	36	3	25	109
2016 Aug	6.6	5.3	2.5	2.28	24	56	3	160	59
2016 Nov	6.9	5.0	2.0	2.87	65	32	5	102	73
UNEP (2012)	6.0-8.0	-	10.0	5.0	-	-	-	-	-

Table 8: Comparison of Water Quality Parameters and Toxic Metal Contents for MingalarZayyon Monastery (Non-Flooded Area) (2014-2016)

	Chlorinity (‰)	Salinity (‰)	Phosphate (ppm)	Nitrate (ppm)	Lead (ppm)	Cadmium (ppm)	Mercury (ppm)	Arsenic (ppm)
2016 Feb	ND	ND	0.02	0.02	ND	0.012	0.0001	0.071
2016 May	ND	ND	0.01	0.28	1.017	0.059	0.0003	0.004
2016 Aug	ND	ND	0.04	0.04	1.175	0.060	0.0007	0.025
2016 Nov	ND	ND	0.02	0.01	ND	0.019	0.0002	0.005
UNEP(2012)	-	-	-	-	0.05	-	0.01	0.01

ND = not detectable

Table 9: Comparison of Water Quality Parameters for Dakkhina Monastery (Non-Flooded Area) (2014-2016)

	pH	DO (ppm)	BOD (ppm)	COD (ppm)	Alkalinity (ppm)	Hardness (ppm)	Turbidity (NTU)	TDS (ppm)	Conductivity (µS/cm)
2016 Feb	6.2	5.0	2.0	1.87	20	14	1	10.5	47
2016 May	6.0	4.0	2.0	5.57	20	20	2	20.0	42
2016 Aug	6.5	4.0	2.0	1.88	28	44	3	147.0	46
2016 Nov	6.8	4.0	2.0	2.36	80	42	2	85.0	49
UNEP (2012)	6.0-8.0	-	10.0	5.0	-	-	-	-	-

Table 10: Comparison of Water Quality Parameters and Toxic Metal Contents for Dakkhina Monastery (Non-Flooded Area) (2014-2016)

	Chlorinity (‰)	**Salinity (‰)**	**Phosphate (ppm)**	**Nitrate (ppm)**	**Lead (ppm)**	**Cadmium (ppm)**	**Mercury (ppm)**	**Arsenic (ppm)**
2016 Feb	ND	ND	0.01	0.001	ND	0.012	0.0005	0.007
2016 May	ND	ND	0.01	0.110	1.019	0.059	0.0002	0.008
2016 Aug	ND	ND	0.07	0.050	1.178	0.061	0.0004	0.018
2016 Nov	ND	ND	0.03	0.010	ND	0.027	0.0004	0.006
UNEP (2012)	-	-	-	-	0.05	-	0.01	0.01

ND = not detectable

Table 11: Comparison of Water Quality Parameters for Kyauk Kyisu (Flooded Area) (2014-2016)

	pH	**DO (ppm)**	**BOD (ppm)**	**COD (ppm)**	**Alkalinity (ppm)**	**Hardness (ppm)**	**Turbidity (NTU)**	**TDS (ppm)**	**Conductivity (μS/cm)**
2014 Nov	6.8	6.6	1.3	2.90	80.0	38	8.00	143.0	287
2015 Feb	6.8	4.0	0.5	0.37	13.8	52	0.17	188.0	287
2015 May	6.7	5.5	3.5	0.74	15.4	130	0.53	176.8	263
2015 Aug	7.2	5.3	1.5	1.10	92.0	28	2.02	166.9	250
2015 Nov	6.9	5.4	3.1	0.55	26.0	56	1.27	179.2	272
2016 Feb	6.5	4.0	2.5	1.87	118.0	30	16.00	125.0	273
2016 May	6.8	4.0	2.5	4.65	84.0	40	12.00	115.5	276
2016 Aug	6.5	5.3	2.5	3.82	28.0	56	13.00	179.0	264
2016 Nov	6.9	5.0	2.0	3.62	125.0	45	28.00	100.0	270
UNEP(2012)	6.0-8.0	-	10.0	5.0	-	-	-	-	-

Table 12: Comparison of Water Quality Parameters and Toxic Metal Contents for Kyauk Kyisu (Flooded Area) (2014-2016)

	Chlorinity (‰)	Salinity (‰)	Phosphate (ppm)	Nitrate (ppm)	Lead (ppm)	Cadmium (ppm)	Mercury (ppm)	Arsenic (ppm)
2014 Nov	0.65	1.21	ND	ND	ND	ND	ND	ND
2015 Feb	0.03	0.09	0.20	ND	0.024	ND	ND	ND
2015 May	0.09	0.19	1.00	ND	0.158	ND	ND	ND
2015 Aug	0.08	0.17	0.50	ND	0.215	0.004	0.0001	0.008
2015 Nov	0.06	0.14	0.30	ND	0.116	ND	ND	0.004
2016 Feb	ND	ND	0.01	0.04	ND	0.013	0.0004	0.020
2016 May	ND	ND	0.01	0.22	1.026	0.053	0.0002	0.010
2016 Aug	ND	ND	0.20	0.06	1.220	0.065	0.0011	0.015
2016 Nov	ND	ND	0.03	0.06	ND	0.031	0.0005	0.002
UNEP (2012)	-	-	-	-	0.05	-	0.01	0.01

ND = not detectable

Table 13: Comparison of Water Quality Parameters for BEHS(4) Sub/Lake (Flooded Area) (2014-2016)

	pH	DO (ppm)	BOD (ppm)	COD (ppm)	Alkalinity (ppm)	Hardness (ppm)	Turbidity (NTU)	TDS (ppm)	Conductivity (µS/cm)
2014 Nov	7.0	5.1	1.6	3.70	23.0	10	19	92.0	183
2015 Feb	6.8	4.0	0.5	0.37	20.0	13	ND	20.3	31
2015 May	6.7	3.3	0.5	1.47	23.4	35	ND	25.8	47
2015 Aug	6.8	5.0	1.5	1.10	16.0	28	ND	22.5	34
2015 Nov	6.8	5.3	2.3	0.66	15.2	22	2	21.1	30
2016 Feb	6.8	5.0	1.5	1.84	20.0	20	3	15.0	30
2016 May	6.8	5.5	2.0	1.47	20.0	36	8	20.0	52
2016 Aug	6.7	3.5	1.5	0.23	40.0	48	16	164.0	34
2016 Nov	6.8	3.5	2.5	0.57	45.0	48	4	180.0	31
UNEP (2012)	6.0-8.0	-	10.0	5.0	-	-	-	-	-

ND = not detectable

Table 14: Comparison of Water Quality Parameters and Toxic Metal Contents for BEHS(4) Sub/Lake (Flooded Area)(2014-2016)

	Chlorinity (‰)	**Salinity (‰)**	**Phosphate (ppm)**	**Nitrate (ppm)**	**Lead (ppm)**	**Cadmium (ppm)**	**Mercury (ppm)**	**Arsenic (ppm)**
2014 Nov	0.12	0.24	ND	ND	ND	ND	ND	ND
2015 Feb	0.01	0.06	0.10	ND	0.042	ND	ND	ND
2015 May	0.04	0.12	1.20	ND	0.039	ND	ND	ND
2015 Aug	0.04	0.11	1.40	ND	0.336	0.001	0.0002	0.004
2015 Nov	0.03	0.09	0.10	ND	0.076	ND	ND	ND
2016 Feb	ND	ND	0.02	0.003	ND	0.012	0.0006	0.005
2016 May	ND	ND	0.02	0.020	1.102	0.050	0.0007	0.001
2016 Aug	ND	ND	0.03	0.050	1.169	0.058	0.0007	0.012
2016 Nov	ND	ND	0.06	0.040	ND	0.029	0.0006	0.004
UNEP (2012)	-	-	-	-	0.05	-	0.01	0.01

ND = not detectable

Table 15: Comparison of Water Quality Parameters for BEHS(4) Sub/TW (Flooded Area)(2014-2016)

	pH	**DO (ppm)**	**BOD (ppm)**	**COD (ppm)**	**Alkalinity (ppm)**	**Hardness (ppm)**	**Turbidity (NTU)**	**TDS (ppm)**	**Conductivity (μS/cm)**
2014 Nov	6.8	5.2	1.1	2.50	44.0	36	4.00	127.0	255
2015 Feb	7.2	5.0	1.0	1.47	110.0	65	0.32	193.0	291
2015 May	7.5	4.0	1.0	0.37	13.8	273	11.14	179.4	273
2015 Aug	8.3	5.2	3.5	2.21	104.0	52	ND	181.5	292
2015 Nov	7.3	5.0	2.5	1.99	94.0	70	ND	188.2	286
2016 Feb	7.2	5.0	2.0	0.32	106.0	52	12.00	120.0	291
2016 May	7.3	4.8	2.0	0.74	100.0	76	5.00	130.0	370
2016 Aug	7.5	5.5	2.5	0.58	108.0	72	9.00	192.0	317
2016 Nov	7.6	5.0	3.0	0.53	118.0	78	30.00	198.0	319
UNEP (2012)	6.0-8.0	-	10.0	5.0	-	-	-	-	-

ND = not detectable

Table 16: Comparison of Water Quality Parameters and Toxic Metal Contents for BEHS(4) Sub/TW (Flooded Area)(2014-2016)

	Chlorinity (‰)	**Salinity (‰)**	**Phosphate (ppm)**	**Nitrate (ppm)**	**Lead (ppm)**	**Cadmium (ppm)**	**Mercury (ppm)**	**Arsenic (ppm)**
2014 Nov	0.79	1.46	ND	ND	ND	ND	ND	ND
2015 Feb	0.02	0.06	0.20	ND	0.128	ND	ND	ND
2015 May	0.09	0.19	1.50	ND	0.157	ND	ND	ND
2015 Aug	0.07	0.16	0.20	ND	0.286	0.008	0.0004	0.082
2015 Nov	0.04	0.11	0.10	ND	0.223	ND	ND	0.002
2016 Feb	ND	ND	0.03	0.02	ND	0.122	0.0005	0.003
2016 May	ND	ND	0.01	0.01	1.021	0.052	0.0009	0.002
2016 Aug	ND	ND	0.10	0.01	1.135	0.061	0.0006	0.012
2016 Nov	ND	ND	0.05	0.12	ND	0.024	0.0006	0.007
UNEP (2012)	-	-	-	-	0.05	-	0.01	0.01

ND = not detectable

Table 17: Comparison of Water Quality Parameters for BEHS(5) Sub/TW (Flooded Area) (2014-2016)

	pH	**DO (ppm)**	**BOD (ppm)**	**COD (ppm)**	**Alkalinity (ppm)**	**Hardness (ppm)**	**Turbidity (NTU)**	**TDS (ppm)**	**Conductivity (µS/cm)**
2014 Nov	7.1	6.4	0.8	2.10	67	26	5.00	76.0	152
2015 Feb	6.7	4.0	0.5	0.37	90	52	0.25	118.3	177
2015 May	6.8	5.5	3.0	1.47	48	247	0.34	124.6	219
2015 Aug	6.6	5.4	4.5	2.94	60	56	ND	129.8	137
2015 Nov	6.8	5.1	3.2	1.76	73	87	3.14	119.1	150
2016 Feb	6.5	4.5	2.0	1.82	94	40	18.00	25.0	172
2016 May	6.8	5.2	1.5	2.77	56	60	14.00	15.0	199
2016 Aug	6.8	5.0	2.0	1.12	68	72	7.00	191.0	147
2016 Nov	7.2	4.0	2.0	0.18	110	65	4.00	160.0	167
UNEP (2012)	6.0-8.0	-	10.0	5.0	-	-	-	-	-

Table 18: Comparison of Water Quality Parameters and Toxic Metal Contents for BEHS(5) Sub/TW (Flooded Area)(2014-2016)

	Chlorinity (‰)	**Salinity (‰)**	**Phosphate (ppm)**	**Nitrate (ppm)**	**Lead (ppm)**	**Cadmium (ppm)**	**Mercury (ppm)**	**Arsenic (ppm)**
2014 Nov	0.52	0.96	ND	ND	ND	ND	ND	ND
2015 Feb	0.01	0.05	0.10	ND	0.104	ND	ND	ND
2015 May	0.04	0.10	1.00	ND	0.223	ND	ND	ND
2015 Aug	0.04	0.70	0.80	ND	0.259	0.005	0.0008	0.008
2015 Nov	0.29	0.55	0.10	ND	0.179	ND	ND	0.001
2016 Feb	ND	ND	0.02	0.01	ND	0.012	0.0004	0.009
2016 May	ND	ND	0.03	0.01	1.022	0.055	0.0002	0.007
2016 Aug	ND	ND	0.03	0.06	1.130	0.062	0.0016	0.014
2016 Nov	ND	ND	0.02	0.01	ND	0.015	0.0007	0.008
UNEP(2012)	-	-	-	-	0.05	-	0.01	0.01

ND = not detectable

Table 19: Total Coliform and *E. coli* of Water Samples Collected from Flooded and Non-flooded Areas in Bago City

Site No.	Location	Total coliform and *E. coli* (cfu/mL)															
		2015 Feb		2015 May		2015 Aug		2015 Nov		2016 Feb		2016 May		2016 Aug		2016 Nov	
		Coli form	*E.coli*	Coli form	*E.coli*	Coli form	*E.coli*	Coli form	*E.coli*	Coli form	*E.coli*	Coli form	*E.coli*	Coli form	*E.coli*	Coli form	*E.coli*
1	LaikPyarKan	2	0	11	0	11	2	5	1	25	1	23	1	13	3	24	0
2	BEHS(1)TW	2	0	12	4	8	11	4	0	3	0	20	11	12	4	28	14
3	Kandawgyi	0	0	0	0	20	1	4	0	11	0	10	0	11	0	5	0
4	KyaukKyisu	0	0	0	0	5	0	3	0	4	2	8	2	30	0	16	2
5	BEHS (4/sublake)	3	0	16	0	3	1	5	0	0	0	7	0	12	0	10	2
6	BEHS (4/sub TW)	0	0	2	1	20	6	10	2	8	1	15	1	13	0	6	0
7	BEHS (5)	2	0	4	1	15	1	4	0	10	0	6	0	26	0	30	16
8	MingalarZayon	-	-	-	-	-	-	-	-	0	0	0	0	28	16	40	25
9	Dakkhina Monastery	-	-	-	-	-	-	-	-	5	0	3	0	8	5	11	2
UNEP standard (2012)		< 3 (*E. coli*)															

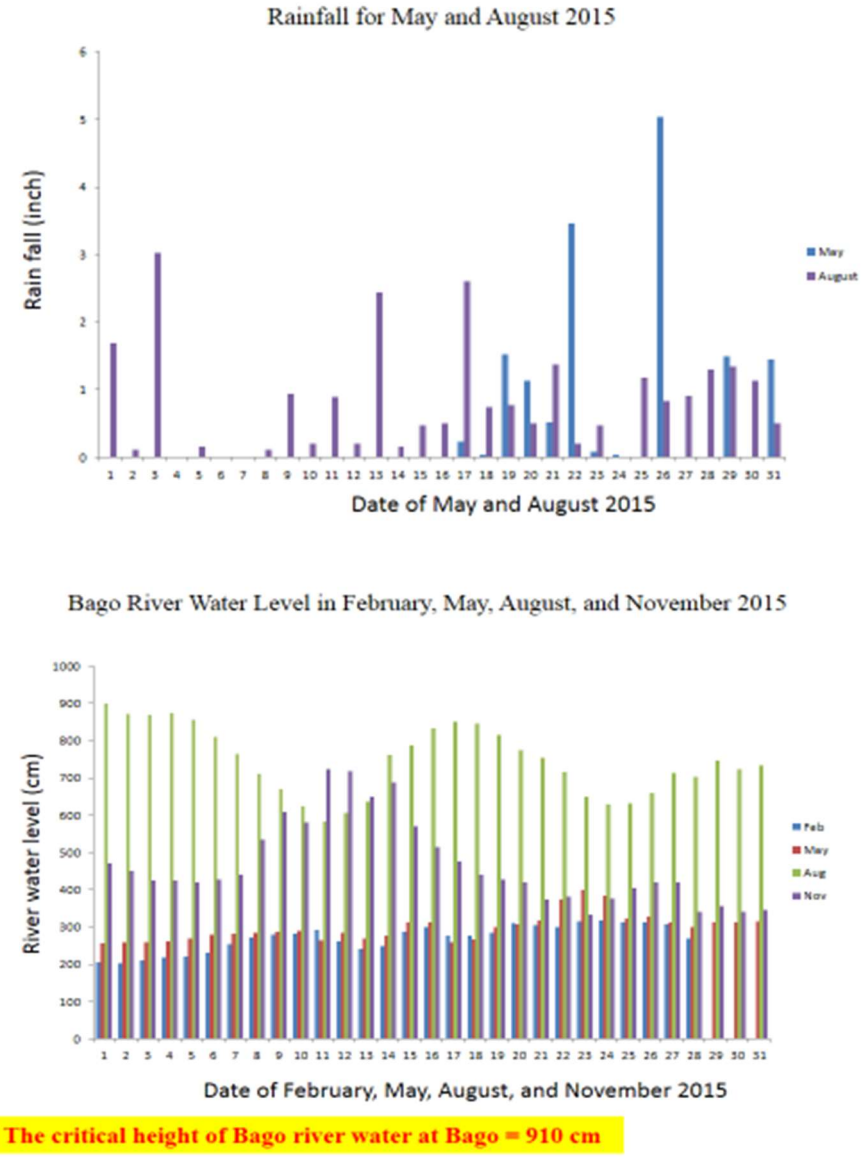

Figures 2: Histograms for rainfall in Bago and Bago river water level at Bago in 2015

Conclusion

In the three year study period (2014-2016), the assessment of water quality of those targeted sites which became flooded was found to show higher quantity of the toxic elements such as Ag, Hg, Pb and Cd. By comparingwith those targeted sites, the remaining non-flooded sites were found to show lower or resilient quantity of toxic element.

There are two probable aspects; firstly, it may be due to perforation or permeation of the toxic elements through the ground strata or ground water flow. Secondly, it may be due to the dissolved chemicals corresponding to excel respective trace toxic elements. It may be polluted by use of fertilizer, insecticides, pesticides and battery plants etc., carried during the water flood flow.

The intensity of the presence of toxic metals (As, Pb, Hg and Cd) was high at the target flooded sites, whereas the non-flooded sites remain resilient as it was. Higher intensity of toxic metals was perhaps due to the over accumulation of the dissolved metal complexes which occurred during the flooding time period. This occurred during the heavy monsoonrainy period. The high level dissolved toxic metals compounds was attributed to thesurface water body flow to & fro.

Acknowledgements

The authors would like to express their profound gratitude to the Department of Higher Education (Yangon Office), Ministry of Education, Yangon, Myanmar, for provision of opportunity to do this research and Myanmar Academy of Arts and Science for allowing to present this paper.

References

American Public Health Association.(1971). *Standard Methods for the Examination of Water and Waste Water*. Washington: Academic Press, pp. 500-515

Dubey, R.C. and Maheshwari, D. K. (2002).*Practical Microbiology*. New Delhi: Schand and Company Ltd. Ram Nagar

Edberg, S.C., E.W. Rice, R.J. Karlin and M.J. Allen. (2000). "*Escherichia coli*: The Best Biological Drinking Water Indicator for Public Health Protection". *J. Appl. Microbiol.,* 88, 106S–116S

Holden, W.S. and Chrcchill, J. (1970).*Water Treatment and Examination.* London: Gloucester Place,
pp. 259-260

Khin Maw MawSoe.(2009). *Effective and Efficient Water Management System Based on the Water Quality Assessment of Mazin Dam (Bago Division)*. PhD Dissertation, Department of Chemistry, University of Yangon, Myanmar

Kumar, U. and Kakrani, B. (2000).*Water Environmental and Pollution*. New Delhi, pp. 43-47

Nwe Ni Win. (2014). *Effective and Efficient Water Management System Based on the Water Quality Assessment of Kawliya Dam (Bago Region)*. Department of Chemistry, University of Yangon, pp. 13-18

Stone, J. (2012). *The Chemistry of Chemical Oxygen Demand.* http://www.envexp.com (Accessed October 6, 2014)

United Nations Environmental Program. (2012). *Analytical Method for Environmental Water Quality*. Vienna: IAEA Office. pp. 1-161

Win Aung. (1996). *Environmental Studies on Bago River Water at Bago*. M.Sc Thesis, Department of Chemistry, University of Yangon, pp. 10-16

Yin Thu.(2009). *Effective and Efficient Water Management System Based on the Water Quality Assessment of Zalettaw Dam (Bago Division)*. PhD Dissertation, Department of Chemistry, University of Yangon, Myanmar

EFFECT OF BIOFERTILIZER WITH *TRICHODERMA HARZIANUM* ON GROWTH AND YIELD OF TOMATO (*LYCOPERSIUM ESCULENTUM* M.)

Thet Su Min[1], Khaing Sanda Wint[2], Zaw Naing[3]

Abstract

In the present work, biofertilizer was prepared from farm waste materials such as cow dung, rice straw and rice bran with bioinoculant *Trichoderma harzianum* (Yezin Isolate). All materials such as cow dung, rice straw, rice bran, bioinoculant *Trichoderma harzianum* and water were used in composting process for preparation of biofertilizer by open heap layering method. Using the compost products mixed with pure soil at different rates, pot experiment was conducted to test the effect of *Trichoderma harzianum* as inoculated compost on the growth of tomato plant. The experiment was laid out in Randomized Complete Block Design (RCBD) with four treatments and five replications. Physical parameters and chemical compositions of soil samples before sowing and after harvesting were analysed by conventional methods and modern techniques. Statistical analysis was carried out using International Rice Research Institute (IRRISTAT Version 5.0) in this study. The results from this study indicated that the prepared biofertilizer is a suitable and effective replacement for chemical fertilizers for the growth and production of tomato.

Keywords*:* biofertilizer, *Trichoderma harzianum* (Yezin Isolate), composting process, tomato

Introduction

Tomato (*Lycopersicum esculentum* M.) is one of the most important vegetables in Asia and Africa and these continents account for more than 65% of global tomato production. Tomato is a warm season crop that originated in South America. Tomato is rich in nutrients such as vitamins, minerals and antioxidants which are important to well-balanced human diets. Tomato is also an important dietary component because it contains high levels of lycopene, an antioxidant that reduces the risks associated with several cancers and neurodegenerative diseases (Srinivasan, 2010).

1. 4PhD, Candidate, Department of Chemistry, University of Yangon
2. Associate Professor, Department of Chemistry, Taung Goke Degree College
3. Associate Professor, Department of Chemistry, Maubin University

Tomato is one of the promising main vegetables in Myanmar. Nowadays, the commercial production of vegetables is increasing as a result of rapid population growth. Moreover, improper use of chemical fertilizers have adverse effect on the environment and costly (Oguzar, 2007). These day's people are trying to reduce the use of inorganic fertilizers to sustain the natural resources. Organic manures improve the physical and chemical condition of the soil. Uptake of macro and micro nutrients improved with application of organic manures (Maskina *et al*., 1988).

The term biofertilizer, represent everything from manures to plant extracts. Biofertilizers are microbial preparations containing living cells of different microorganisms which have the ability to mobilize plant nutrients in soil from unusable to usable form through biological process. Biofertilizers are used in live formulation of beneficial microorganism which on application to seed, root or soil, mobilize the availability of nutrients particularly by their biological activity and help to build up the lost microflora and in turn improve the soil health in general. The microorganisms used for the biofertilizer are bacteria of *Bacillus*, *Pseudomonas*, *Lactobacillus*, photosynthetic bacteria, nitrogen fixing bacteria, fungi of *Trichoderma* and yeast. Biofertilizers have shown great potential as a renewable and environmental friendly source of plant nutrient (Ismail *et al*., 2014).

Trichoderma species present in nearly all agricultural soils and in other environment (Harman, 2000). The fungus *Trichoderma harzianum* (Figure 1) is a biological control organism against a wide range of soil-borne pathogens and has plant growth-promote capacity. It has been shown that *T.harzianum* stimulated the growth of tomato (Datnoff and Pernezny, 1998). In the present study, growth and yield of tomato under pot experiment was studied by using biofertilizer with *Trichoderma harzianum.*

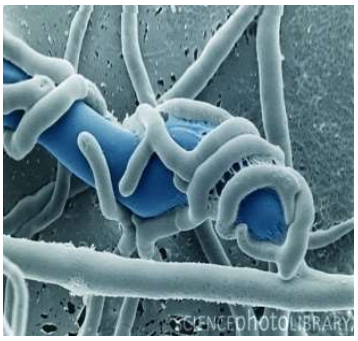
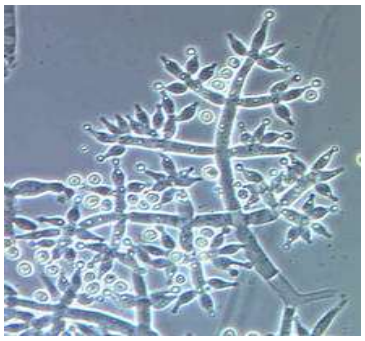

Figure 1 : Trichoderma harzianum

Materials and methods

Sample Collection and Preparation

Cow dung, rice straw and rice bran were collected from Sein Sar Pin Village, Maeutaw village group, Zaeyarthiri Township, Naypyitaw. All materials such as cow dung, rice straw, rice bran, bioinoculant *T. harzianum* (200: 40: 4: 1) and water (18L) were to be used in composting process for preparation of biofertilizer by open heap layering method. Size of box used in composting (pile size) was 8' × 4' × 2.5'. After about 75 days, the compost was ready to be used. The fertilizers were packed in bags, stored in a cool place. By using inoculated biofertilizer, the pot experiment was conducted at the Department of Agricultural Research, Yezin. The experiment was laid out in Randomized Complete Block Design (RCBD) with four treatments and five replications. The treatments used in this study were :

Treatment 1 (T1) = Soil treated with 10 % inoculated biofertilizer

Treatment 2 (T2) = Soil treated with 20 % inoculated biofertilizer

Treatment 3 (T3) = Soil treated with 30 % inoculated biofertilizer

Treatment 4 (T4) = control

Weekly plant height measurements were taken from two weeks after transplanting and shoot fresh weight, root fresh weight, shoot dry weight, root dry weight and fruit yield per plant were recorded after the harvest. Land preparation was done by cutting the vegetation of scraping the soil surface.

Methods

Four treatments were analysed by conventional and modern techniques before sowing and after harvesting. Qualitative elemental composition of biofertilizer was determined by EDXRF technique. Soil texture was determined by international pipette method. Moisture content was determined by oven drying method and soil pH was measured with a glass electrode using a 1:2.5 soil to water ratio. Organic carbon was determined by Tyurin's method, electrical conductivity was determined by conductivity meter, available nitrogen content was determined by alkaline permanganate method and available phosphorous content by Olsen's method. Available potassium, exchangeable calcium, magnesium and potassium were determined by AAS. In the analytical procedures of the experiments, recommended methods and techniques were applied (FAO, 2008; AOAC, 1980). Statistical analysis was carried out using International Rice Research Institute (IRRISTAT version 5.0) in this study.

Results and Discussion

Elemental Analysis of Prepared Fertilizer by EDXRF

Qualitative elemental compositions in soil fertilized with biofertilizers were detected by EDXRF. These spectra are shown in Figure 2 and the data are presented in Table 1. According to EDXRF spectra, essential elements for plants and no toxic elements were found in the four treatments. All the treatments, silicon peaks were the most prominent and so it showed the highest content of silicon.

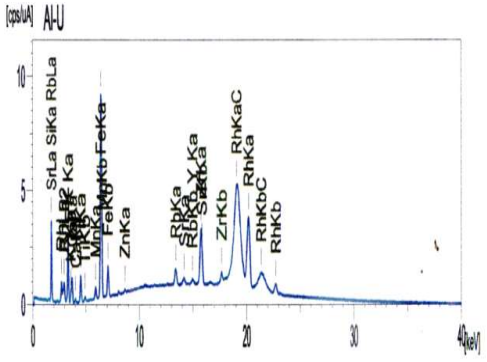

(T1)

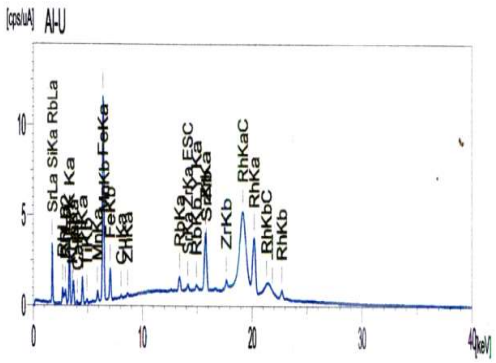

(T2)

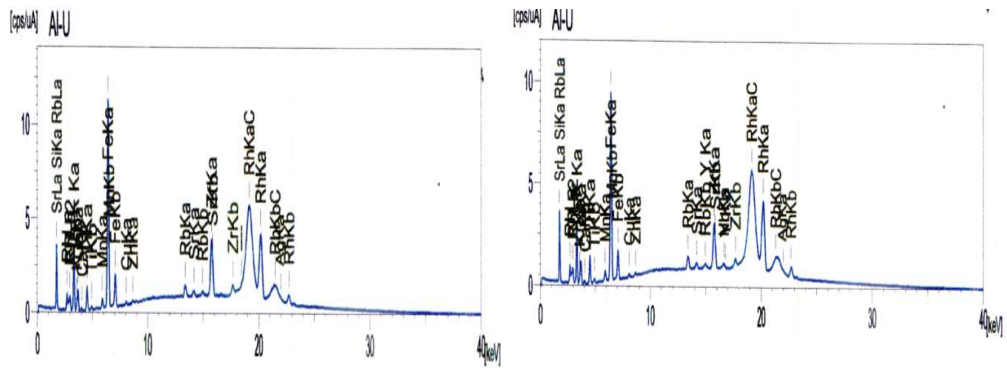

(T3) **(T4)**

Figure 2 : EDXRF spectra of soil treated with biofertilizer

Table 1: Elemental Composition of Soil Treated with Biofertilizer by EDXRF

Element	Elemental Composition (%)			
	T1	**T2**	**T3**	**T4**
Si	74.448	71.612	70.115	74.699
K	12.159	13.517	13.774	11.266
Al	3.914	4.677	4.483	4.474
Ca	3.469	3.816	3.278	3.460
Fe	3.476	4.212	4.018	3.349
Ti	1.576	1.873	1.574	1.480
S	0.380	0.382	0.485	0.377
Mn	0.285	0.294	0.248	0.264
Zr	0.128	0.119	0.107	0.130
Ag	-	-	0.134	0.128
P	0.175	0.245	0.321	0.108
Rb	0.085	0.087	0.071	0.071
Zn	0.024	0.040	0.032	0.033
Cu	-	0.028	0.033	0.032
Sr	0.035	0.033	0.030	0.029
Nb	-	-	-	0.023
Y	0.012	0.015	-	0.011

T1 = Soil treated with 10 % biofertilizer T2 = Soil treated with 20 % biofertilizer

T3 = Soil treated with 30 % biofertilizer T4 = Control

Analysis of Soil for Four Treatments before Sowing

Soil is one of the most important natural resources for agricultural production, which heavily depends on soil fertility. It is therefore an essential mandate survey and to classify soil, and to apply fertilizers in order to increase yield. Table 2 shows the physical parameters and chemical compositions of four treatments before sowing. Soil texture depends on the relative proportions of sand, silt and clay in the soil. It indicates high percentage amount of sand in four treatments. This type of soil falls in the domain of loamy sand soil. This type of soil's texture has less capacity to retain water but afford to penetration of roots and being exposed to good aeration and retention of plant nutrients. The pH values of the fertilizer treated soils were found to be slightly increased than that of the original control soil. The pH values of treated soils were found to be in the range of 6.61-6.84. The observed pH values were suitable for plant growth. The values of electrical conductivity of the treated soils were higher than that of the original free soil. Electrical conductivity of soils informs the ionic nature of the soluble compound to supply the needs of plants. Soil humus is also important in increasing the water holding capacity of the soil and it plays a part in the retention of plant nutrients. The humus content increased from 1.79 % to 2.05 % and organic carbon increased from 1.04% to 1.19 %.

As for the total N content in the case of four treatments, T3 has the highest N content. It is a common fact that for plant growth nitrogen (N) is required to promote development of stem and leaf, phosphorous (P) acts to stimulate growth, accelerate fruits and seed formation and the function of potash (or) K is essential to development of starches, sugar and fibers. The highest content of available nitrogen, phosphorous and potassium in T3 were 38.00 ppm, 48.03 ppm and 796.69 ppm and the amounts of exchangeable Ca, Mg and K were about 8.50 me/100g, 0.55 me/100g and 2.68 me/100g respectively. On the context of what has been described above, T4 (control) has the lowest N, P and K contents. Regarding the observed values, it was considered that the four treatments can be used in crop production to enhance the soil fertility.

Table 2: Analysis Data of the Soil Before Sowing

Analytical Item	**T1**	**T2**	**T3**	**T4**
Texture - Sand (%)	83.92	83.80	83.76	83.96
Silt (%)	7.96	7.40	7.84	7.44
Clay **(%)**	8.12	8.80	8.40	8.60
Moisture (%)	1.14	1.44	1.64	0.74
pH	6.66	6.76	6.84	6.61
Electrical Conductivity (dS/m)	0.58	0.86	1.19	0.23
Organic Carbon (%)	1.05	1.15	1.19	1.04
Humus (%)	1.81	1.98	2.05	1.79
Total N (%)	0.11	0.23	0.32	0.06
C/N ratio	9.54	5.00	3.71	17.33
Available N (ppm)	22.00	25.00	38.00	20.00
Available P (ppm)	21.83	39.30	48.03	18.73
Available K (ppm)	350.41	605.79	796.69	272.48
Exchangeable Ca (me/100g)	7.28	7.63	8.50	7.13
Exchangeable Mg (me/100g)	0.45	0.48	0.55	0.34
Exchangeable K (me/100g)	1.76	1.89	2.68	0.47

T1 = Soil treated with 10 % biofertilizer T2 = Soil treated with 20 % biofertilizer

T3 = Soil treated with 30 % biofertilizer T4 = Control

Figure 3 : View of pot experiment for tomato

Analysis of the Soil used for Tomato at Harvesting

The texture, moisture percent, electrical conductivity, organic carbon content, humus percent, total nitrogen content, C/N ratio, available nitrogen, phosphorous and potassium, exchangeable calcium, magnesium, potassium and pH values of soil after harvesting tomato are shown in Table 3. The soils were subjected to different treatments by using inoculated compost (biofertilizer). Comparison for all cases is made with respect to the physicochemical composition of the soil samples. After harvesting, all type of soils are loamy sand type.

The soil organic carbon contents under the biofertilizer application were higher than these under the control. The C/N ratio of T3 is lower than that of other treatments for all crops because large amount of organic fertilizer utilization can cause nitrogen depletion and decrease the C/N ratio. A variety of treated soils was compared with the control soil after harvesting stage. Moreover, it was observed that the pH of the soil before sowing and after harvesting stages lie between 6.61 and 7.61.These can be considered as the slightly acidic and neutral type of soil.

The fertility status of the soil is expected to benefit from poultry manure application since the manure is known to improve soil organic matter, macro-nutrient status and micro nutrient qualities of the soil (Akande and Adediran, 2004). On reviewing the results of the data presented in Table 3 even after the harvesting stage nitrogen, phosphorous, potassium and as well as the organic carbon and humus contents in the case of soil T1, T2 and T3 were significantly changed under cultivation because most of them were frequently removed from the soil permanently by the crop produced.

Figure 4: The growth of four treated tomato plants

Table 3: Analysis Data of the Soil Using for Tomato After Harvesting

Analytical Item	**T1**	**T2**	**T3**	**T4**
Texture - Sand (%)	84.52	81.40	79.44	86.84
Silt (%)	10.48	12.56	16.04	8.08
Clay **(%)**	5.00	6.04	4.52	5.08
Moisture (%)	0.51	0.55	0.62	0.45
pH	7.59	7.61	7.27	7.01
Electrical Conductivity (dS/m)	0.30	0.32	0.34	0.20
Organic Carbon (%)	0.87	1.08	1.10	1.01
Humus (%)	1.49	1.86	1.89	1.74
Total N (%)	0.10	0.14	0.15	0.05
C/N ratio	8.70	7.71	7.33	20.20
Available N (ppm)	15.30	15.60	22.20	12.70
Available P (ppm)	84.76	105.68	116.59	60.26
Available K (ppm)	174.38	176.86	189.26	155.37
Exchangeable Ca (me/100g)	5.89	6.07	7.19	5.46
Exchangeable Mg (me/100g)	0.36	0.39	0.45	0.32
Exchangeable K (me/100g)	0.21	0.28	0.30	0.14

T1 = Soil treated with 10 % biofertilizer T2 = Soil treated with 20 % biofertilizer
T3 = Soil treated with 30 % biofertilizer T4 = Control

Effect of *T. harzianum* on Growth and Yield of Tomato

From the pot experiment investigation, it was observed that *T.harzianum* inoculated biofertilizer promoted plant growth and also enhanced the growth of tomato. Time frame of sowing to the harvested time was of 120 days. The growth factors of the crops were evaluated in terms of the plant height (cm), shoot fresh weight (g), root fresh weight (g), shoot dry weight (g), root dry weight (g), number of total fruit per plant and total yield (g plant^{-1}).

There was no significant difference in plant height for all treatments (Table 4). There was significant difference in shoot fresh weight, root fresh weight, shoot dry weight, root dry weight between either treated soil and the original free soil. A major feature of that *T.harzianum* is its capability to grow along roots during their elongation, thus colonizing the whole root system and benefiting the crop for its entire life (rhizosphere competence). *T.harzianum* has beneficial effects on plant growth and vigour and on the development efficiency of the root systems of several crops (Bjorkman *et al*, 1998).

Number of total fruits of T3 was significantly higher than those of T1, T2 and T4. The total yield (g plant^{-1}) in pot experiment are presented in Table 4. There were highly significantly different in total yield of T3. This study revealed that application of *T. harzianum* showed positive results in growth and yield of tomato.

Fruits (T1)

Fruits (T2)

Fruits (T3) **Fruits (T4)**

Figure 5: Yield of tomato fruits by treated biofertilizers and control

T1 = Soil treated with 10 % biofertilizer T2 = Soil treated with 20 % biofertilizer
T3 = Soil treated with 30 % biofertilizer T4 = Control

Table 4: Effect of Biofertilizer on Growth and Yield of Tomato

Treatment	Life time (day)	Plant height (cm)	Shoot fresh weight (g)	Root fresh weight (g)	Shoot dry weight (g)	Root dry weight (g)	Number of total fruit plant^{-1}	Total yield (g plant^{-1})
T1	120	35.48	70.42	10.31	20.95	3.07	44.20	867.68
T2	120	36.58	106.45	9.40	23.83	3.49	50.20	1055.52
T3	120	37.02	162.97	11.88	34.44	5.07	59.00	1242.46
T4	120	30.62	62.74	7.75	19.35	3.30	39.20	750.80
F-test		ns	**	**	**	**	**	**
LSD (5%)		9.78	6.91	0.94	1.98	0.38	5.37	160.90
CV (%)		20.30	5.00	6.90	5.80	7.40	8.10	11.90

T 1= 10 % Biofertilizer, T 2= 20 % Biofertilizer, T 3= 30 % Biofertilizer, T 4= Control
** ($P < 0.01$), ns= non significant

Conclusion

In this research work, it was conducted to know the effect of biofertilizer with *T.harzianum* on plant growth and yield of tomato. Based on the specific properties such as total carbon and nitrogen content, the value of macro and micronutrients, pH value and soil texture, EDXRF spectra of prepared biofertilizers and the growth and yield of tomato are reliable to enhance the soil fertility and soil productivity. It was observed that T3 (30% biofertilizer) was found to be enhanced better growth and yield than other treatments. Therefore, this study creates a platform to encourage the agricultural industry to use biofertilizer with *T.harzianum* as a substitute to the commercial chemical fertilizer which is more economical and environmental friendly.

Acknowledgements

The authors would like to express their profound gratitude to the Department of Higher Education (Lower Myanmar), Ministry of Education, Yangon, Myanmar, for provision of opportunity to do this research and Myanmar Academy of Arts and Science for allowing to present this paper.

References

Akande, M.O. and Adediran, J.A. (2004). "Effects of Terralyt Plus Fertilizer on Growth Nutrients Uptake and Dry Matter Yield of Two Vegetable Crops". *Moor J. of Agric.Res.,* vol. 5, pp. 12-17

AOAC. (1980). "*Official Methods of Analysis*". Washington DC: 13th Ed, Association of Official Analytical Chemists, pp. 3-27

Bjorkman, T., Blanchard L. M. and Harman, G.E. (1998). "Growth Enhancement of Shrunken-2(sh2) Sweet Corn by *Trichoderma harzianum* 1295-22 : Effect of Environmental Stress". *J. Am. Soc. Hortic. Sci.,* vol. 125, pp 35-40

Datnoff, L. E. and Pernezny, K. L. (1998). "Effect of Bacterial and Fungal Microorganisms to Colonize Tomato Roots, Improve Transplant Growth and Control of Fusarium Crown and Root Rot". *Florida Tomato Institute Proceedings* PRO, vol. 111, pp. 26-33

FAO. (2008). *Guide to Laboratory Establishment for Plant Nutrient Analysis.* Rome: FAO, pp. 30-44

Harman, G. E. (2000). "Myths and Dogmas of Biocontrol, Changes in Perceptions Derived from Research on *Trichoderma harzianum* T-22". *Plant Dis*., vol. 84**,** pp. 377-393

Ismail, E.G., Salah, W.M, Salah, K. and Fadia,E.S. (2014). "Effect of Manure and Biofertilizers on Growth, Yield, Silymarin Content and Protein Expression Profile of *Silybum marianum*". *Adv Agric. Biol*., vol. 1 (1), pp. 36-44

Maskina, M.S., Singh, B., Singh, Y. and Meelu, O. P. (1988). " Fertilizer Requirement of Rice-Wheat and Maize-Wheat Rotations on Coarse Textured Soils Amended with Farmyard Manure". *Fert. Res*., vol. 17, pp. 153-164

Oguzar, N.S. (2007). "Effect of Palm Bunch Ash on Growth of Groundnut". *J. Agronomy*., vol. 1 (2), pp. 59-61

Srinivasan, R. (2010). *Safer Tomato Production Techniques*, *A Field Guide for Soil Fertility and Pest Management*, Taiwan: The World Vegetable Centre, Shanhua, AVRDC Publication, vol. 97, pp. 10-74

PREPARATION AND CHARACTERIZATION OF COMPOSTED ORGANIC FERTILIZERS PREPARED FROM ORGANIC WASTES (COW DUNG, CORN STALK AND KOKKO LEAVES)

Thin Thin Nwe[1], Tin Moe Khaing[2], Thi Thi Aye[3]

Abstract

Organic wastes from animals, plants and agricultural sources, posing serious environmental and health problems can be managed, through production of compost. In the present research work, raw organic materials (cow dung, corn stalk and kokko leaves) that are well suited for application to the soil as a fertilizer or soil conditioner were used as materials for composting. Five kinds of composted organic fertilizers were prepared by using various ratios of these organic waste materials and EM solution and then some physicochemical properties (pH, moisture, EC, Organic matter, C:N ratio, total N, total P_2O_5, total K_2O, Ca, Mg, S) and trace elements (Fe, Zn, Mn and Cu) necessary for plants of composted organic fertilizers were qualitatively and quantitatively characterized by EDXRF, AAS, and others modern and conventional methods. According to these data, the nitrogen and phosphorus contents of sample 3 (cow dung+ EM) are higher than the others (sample 1,2,4 & 5). However, secondary nutrients, micronutrients and trace elements were higher in samples 1, 2, 4, & 5. Therefore, macronutrients, micronutrients and trace elements needed for plant growth were found in these fertilizers. Thus, making combination of different organic wastes as compost is beneficial for plants by fulfilling of plant nutrients through organic resources and their application in a balanced way for maintaining soil productivity. Furthermore, the use of composted organic fertilizer will not only supplement the chemical fertilizers, but also reduce environmental pollution.

Keywords: Composted organic fertilizer, EM, Macronutrient, Micronutrient

Introduction

Composting is the natural process of decomposing and recycling organic materials into a humus-rich soil amendment by the successive action of bacteria, fungi, actinomycetes, or earthworms. Many common materials can be composted on-site, including food wastes, leaves, grass clippings, plant

1. 3 PhD, Candidate, Department of Chemistry, University of Yangon
2. Lecturers, Department of Chemistry, University of Yangon
3. Associate Professor, Department of Chemistry, University of Yangon

trimmings, straw, shredded paper, animal manure, and municipal solid wastes. Many of these materials were composted to destroy weed seeds and potential human and plant pathogens; to enhance their nutrient availability; and to facilitate their storage, transport, and application to land. The final product is a stable dark-brown or black humus material with an earthy smell. Like other recycling efforts, composting has many benefits to agriculture, the environment, the economy, and the society.

In this study, raw materials (cow dung, corn stalk and kokko leaves) were used in composting. These materials can be available in Myanmar. Cow dung has been used for centuries as a fertilizer for farming (Bokhtia and Sakurai, 2005). It can improve the soil structure (aggregation) so that the soil holds more nutrients and water, and therefore becomes more fertile. Cow dung also encourages soil microbial activity which promotes the soil's trace minerals supply, improving plant nutrition. Corn stalk is a waste product from the harvest of other economically important plant parts and high in cellulose, hemi-cellulose, lignin and other components (minerals and moisture) and a source of nutrients and organic matter which helps keep soil fertile. Composting of maize residues is useful method of producing a stabilized product and substantial organic matter because a high C/N ratio also produces humus that can be used as a source of organic materials and slow the release of nutrients. Kokko leaves are a source of organic fertilizer on the soil chemical properties and the highest value for organic carbon, total nitrogen and potassium (Haque, 2000).

EM is a fermented mixed culture of naturally occurring species of co-existing microorganisms in acidic medium (pH below 3.5). Among the main microorganisms in EM culture are the species of photosynthetic bacteria (Rhodopseudomonas plastris and Rhodobacter sphacrodes), lactobacilli (L.plantarum, L.casei, and streptococcus lactis), yeast (saccharomyces spp) and actinomycetes (stretomycetes (Streptomyces spp). Microorganisms in EM improve crop health and yield by increasing photosynthesis, producing bioactive substance such as hormones and enzymes, accelerating decomposition of organic materials and controlling soil borne disease.

Compost has been considered as a valuable soil amendment for centuries. Most people are aware that using composts is an effective way to

increase healthy plant production, help save money, reduce the use of chemical fertilizers, and conserve natural resources. Compost provides a stable organic matter that improves the physical, chemical and biological properties of soils, thereby enhancing soil quality and crop production. Nowadays, Organic fertilizers are needed in organic farming. Organic farming preserves the ecosystem. Organic farming neither demands the use of synthetic nor the harmful chemicals (pesticides and fungicides) for controlling weeds, insects and pests. Organic farming relies on large-scale application of animal or farmyard manure (FYM), compost, crop rotation, residues, green manure, vermicompost, bio-fertilizers and bio-pesticides (Naeem & Iqbal,2006).

Materials and Methods

Sample Collection and Preparation

Cow dung, corn stalk and kokko leaves were collected from Einkyitaw village, Mahlaing Township, Mandalay Region. Each sample was dried in air, ground and sieved into mesh size 150 μm and stored in air-tight plastic bags. Then, some physicochemical properties of raw materials were qualitatively and quantitatively characterized by EDXRF, AAS and other moderns and conventional methods. Five piles (approximately 3m length, 3m width and 3m height) were made for the preparation of compost. Then all materials viz., raw materials (cow dung, corn stalk and kokko leaves) were used in the composting process. Firstly, a layer of raw materials was spread on the bottom of the pile. Then EM solution (EM: molasses: water = 1:1:98 v/v) was sprinkled to attain adequate moisture content (Apnan, 1995). The procedure was repeated three times. Then, they were covered with plastic sheet. Temperature of the compost pile was measured two times (9 am and 5 pm) daily and the average of two was recorded. Generally, the temperature gradually up and reached its optimum (62˚C). The mixture was maintained its optimum temperature for several days and then dropped (32 ˚C) gradually.

After one month later, when the temperature of the pile was dropped to ambient temperature, the pile was turned over. The pile was covered with plastic sheet and measured temperature daily. After another one month later, the pile was turned over and the temperature of the pile was again dropped to

ambient temperature (Mi Mi Hliang, 2011). Finally, after 75 days, the compost was ready to be used. The fertilizers were kept in air-tight container and used for chemical analyses. The following different types of composted organic fertilizers were prepared.

- Sample 1 ➡ Cow dung + Corn stalk + kokko leaves +EM (30kg+ 20kg+ 10kg +5L)
- Sample 2 ➡ Cow dung + Corn Stalk + EM (30 kg+ 30 kg + 5L)
- Sample 3 ➡ Cow dung + EM (60 kg + 5L)
- Sample 4 ➡ Cow dung + Corn stalk + kokko leaves +EM (30kg+ 10kg + 20kg +5L)
- Sample 5 ➡ Cow dung + Corn stalk + kokko leaves +EM (20kg+ 20kg+ 20kg +5L)

Methods

Measurement of pH was carried out by a pH meter (Digital pH Meter), moisture content was determined by oven drying method. Nitrogen content was determined by Kjeldahl's method. Phosphorous content was determined by UV-Visible Spectrophotometric technique and potassium content was determined by Flame photometric technique. Qualitative elemental contents of raw materials were determined by EDXRF technique and quantitative elemental contents were determined by AAS technique. Organic matter was determined by Walkley and Black's method and Electrical conductivity contents of composted organic fertilizers were determined by Conductivity meter. Total sulphur of composted organic fertilizers was determined by turbidity method. In the analytical procedures of the experiments, recommended methods and techniques were applied (Vogel, 1968 ; AOAC, 1984).

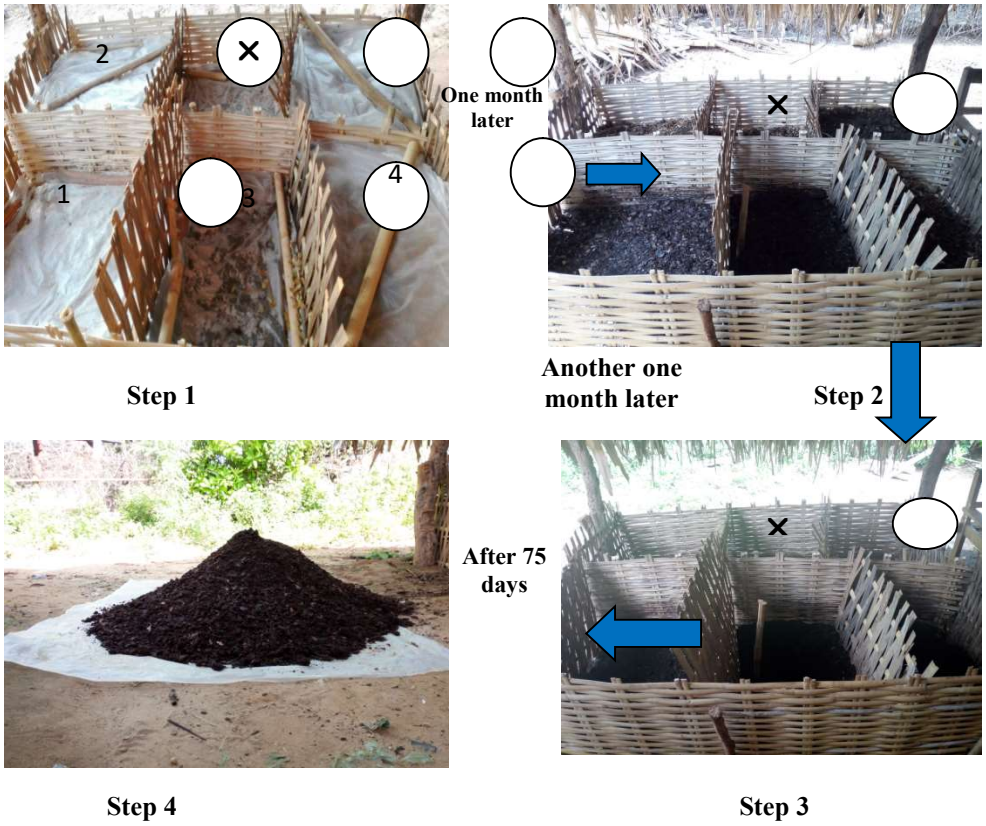

Figure 1: Procedure for the Preparation of composted organic fertilizers

Methods

Measurement of pH was carried out by a pH meter (Digital pH Meter), moisture content was determined by oven drying method. Nitrogen content was determined by Kjeldahl's method. Phosphorous content was determined by UV-Visible Spectrophotometric technique and potassium content was determined by Flame photometric technique. Qualitative elemental contents of raw materials were determined by EDXRF technique and quantitative elemental contents were determined by AAS technique. Organic matter was determined by Walkley and Black's method and Electrical conductivity contents of composted organic fertilizers were determined by Conductivity

meter. Total sulphur of composted organic fertilizers was determined by turbidity method. In the analytical procedures of the experiments, recommended methods and techniques were applied (Vogel, 1968 and AOAC, 1984).

Results and Discussion

This research is mainly concerned with the preparation of composted organic fertilizers by using organic wastes (cow dung, corn stalk and kokko leaves). These raw materials are plentiful in rural areas. Before preparing composted organic fertilizers, some physicochemical properties of these organic wastes were determined. Some physicochemical properties are pH, moisture, total N, total P_2O_5, total K_2O and then qualitative and quantitative elemental contents of raw materials were determined. The resulting data are shown in Table 1, 2 and 3. According to these experimental data indicated that macronutrients (NPK) and the other micronutrients necessary for the growth of plants and soil fertility were found in cow dung, corn stalk and kokko leaves. Therefore, these raw materials were used in composting as organic fertilizers. Then, five kinds of composted organic fertilizers were prepared by using these raw materials. After lasting 75 days, composted organic fertilizers were ready to be used in the field. During the composting process, temperature of compost pile was measured. Temperature is also a good indicator of the various stages of the composting process. Composting is a method of speeding natural decomposition under controlled conditions. Raw organic materials are converted to compost by a succession of organisms. During the first stages of composting, bacteria increase rapidly. Later actinomycetes (filamentous bacterial), fungi and protozoans go to work. After much of the carbon in the compost has been utilized and the temperature has fallen, centipedes, millipedes, sowbugs, earthworms and other organisms continue the decomposition. As microorganisms decompose the organic materials, their body heat causes the temperature in the pile to rise dramatically.

Table 1: Some Physicochemical Properties of Raw Materials (Cow dung, Corn stalk and Kokko leaves)

No	Raw Materials	Parameters				
		pH	Moisture (%)	Total N (%)	Total P_2O_5(%)	Total K_2O(%)
1	Cow dung	8.82	8.142	0.942	0.585	0.554
2	Corn stalk	6.20	9.244	2.302	0.730	0.501
3	Kokko leaves	5.57	8.287	3.249	0.312	0.290

Table 2: Elemental Analysis of Raw Materials (Cow dung, Corn stalk and Kokko leaves) by EDXRF

Elements	Relative Abundance (%)		
	Cow dung	Corn stalk	Kokko leaves
Si	44.300	19.540	4.086
K	19.208	29.342	22.696
Ca	14.576	41.089	59.363
Fe	10.965	3.645	6.249
Al	3.794	-	-
Ti	1.742	1.277	0.522
S	1.700	1.939	3.455
Mn	1.666	1.277	3.189
P	1.458	1.680	0.050
Zn	0.153	0.193	0.247
Sr	0.127	0.112	0.144
Cr	0.075	-	-
Rb	0.070	0.079	-
Zr	0.068	-	-
Cu	0.054	0.094	-
V	0.043	-	-

Table 3: Elemental Contents in Raw Materials (Cow dung, Corn stalk and Kokko leaves) by AAS

No	Raw Materials	Elements (ppm)				
		Ca	**Mg**	**Mn**	**Cu**	**Zn**
1	Cow dung	17.26	8.595	1.057	0.045	0.063
2	Corn stalk	9.989	8.597	0.579	0.052	0.114
3	Kokko leaves	15.71	8.451	2.603	0.051	ND

ND= Not Detected

Table 4: Temperature Changes of Compost Pile (1, 2 and 3) during Composting Process (75 days)

Day	Temperature (˚C)			Day	Temperature (˚C)			Day	Temperature (˚C)		
	Sample 1	Sample 2	Sample 3		Sample 1	Sample 2	Sample 3		Sample 1	Sample 2	Sample 3
1	33	33	33	26	52	44	46	51	47	48	50
2	33	33	33	27	50	43	46	52	50	49	50
3	37	33	33	28	49	42	46	53	54	49	53
4	39	35	36	29	46	42	45	54	57	50	54
5	42	35	36	30	46	39	40	55	61	52	55
6	43	36	38	31	44	37	40	56	61	52	55
7	46	38	39	32	40	37	40	57	59	52	55
8	47	38	40	33	39	35	39	58	59	51	57
9	52	40	40	34	38	32	38	59	55	51	57
10	53	42	43	35	37	32	36	60	55	49	56
11	54	45	45	36	37	32	36	61	54	49	54
12	55	45	46	37	35	33	34	62	53	49	53
13	57	47	46	38	35	33	34	63	52	48	52
14	58	47	50	39	36	35	34	64	50	46	52
15	59	48	52	40	36	37	32	65	46	46	52
16	60	49	52	41	37	38	32	66	44	42	52
17	60	50	55	42	39	40	32	67	44	42	50
18	60	50	55	43	39	42	33	68	40	40	47
19	59	48	55	44	40	42	35	69	38	39	45
20	58	48	54	45	40	42	35	70	38	38	43
21	57	47	53	46	42	43	35	71	36	36	40
22	56	46	50	47	42	43	37	72	34	33	40
23	55	46	50	48	46	45	39	73	34	33	35
24	55	46	49	49	46	46	44	74	34	33	35
25	53	45	47	50	47	46	44	75	34	33	35

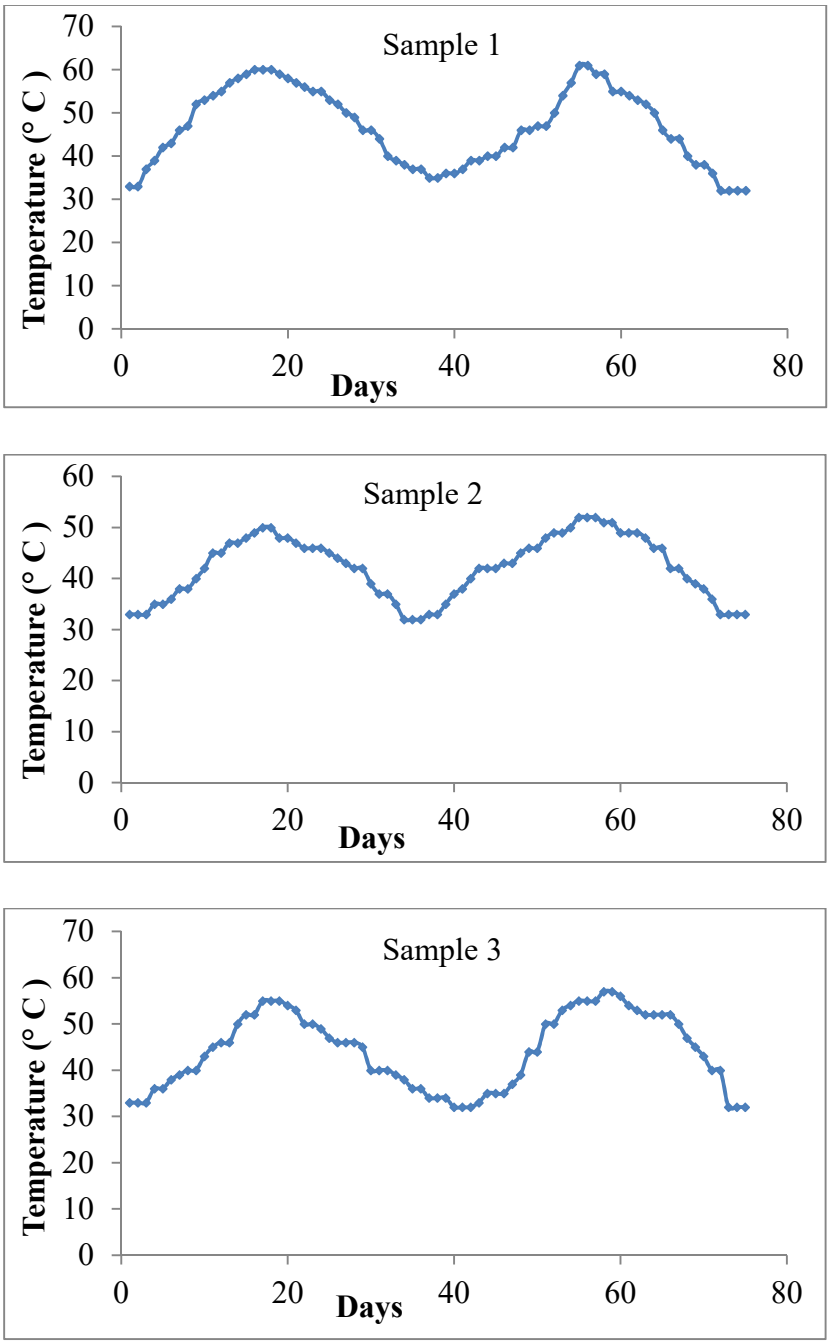

Figure 2: Temperature changes of compost samples (1, 2 and 3) during composting process

Table 5: Temperature Changes of Compost Pile (4 and 5) during Composting Process (75 days)

Day	Temperature (˚C)		Day	Temperature (˚C)		Day	Temperature (˚C)	
	Sample 4	Sample 5		Sample 4	Sample 5		Sample 4	Sample 5
1	33	33	26	47	44	51	50	43
2	33	33	27	47	44	52	54	45
3	35	33	28	46	43	53	55	45
4	36	34	29	43	42	54	57	48
5	38	35	30	43	42	55	59	49
6	39	37	31	42	40	56	60	50
7	40	37	32	40	40	57	62	52
8	41	37	33	40	40	58	62	53
9	42	40	34	38	38	59	62	54
10	45	42	35	37	37	60	61	54
11	45	43	36	36	35	61	61	54
12	48	45	37	35	32	62	58	53
13	50	46	38	34	32	63	58	52
14	53	47	39	33	31	64	54	51
15	57	49	40	33	30	65	53	49
16	59	49	41	35	30	66	50	48
17	60	50	42	37	33	67	46	48
18	60	50	43	37	33	68	44	45
19	58	50	44	38	34	69	43	41
20	57	48	45	38	34	70	43	38
21	55	47	46	38	34	71	40	37
22	54	46	47	40	36	72	32	35
23	52	45	48	44	36	73	32	33
24	50	45	49	44	40	74	32	33
25	49	44	50	48	40	75	32	33

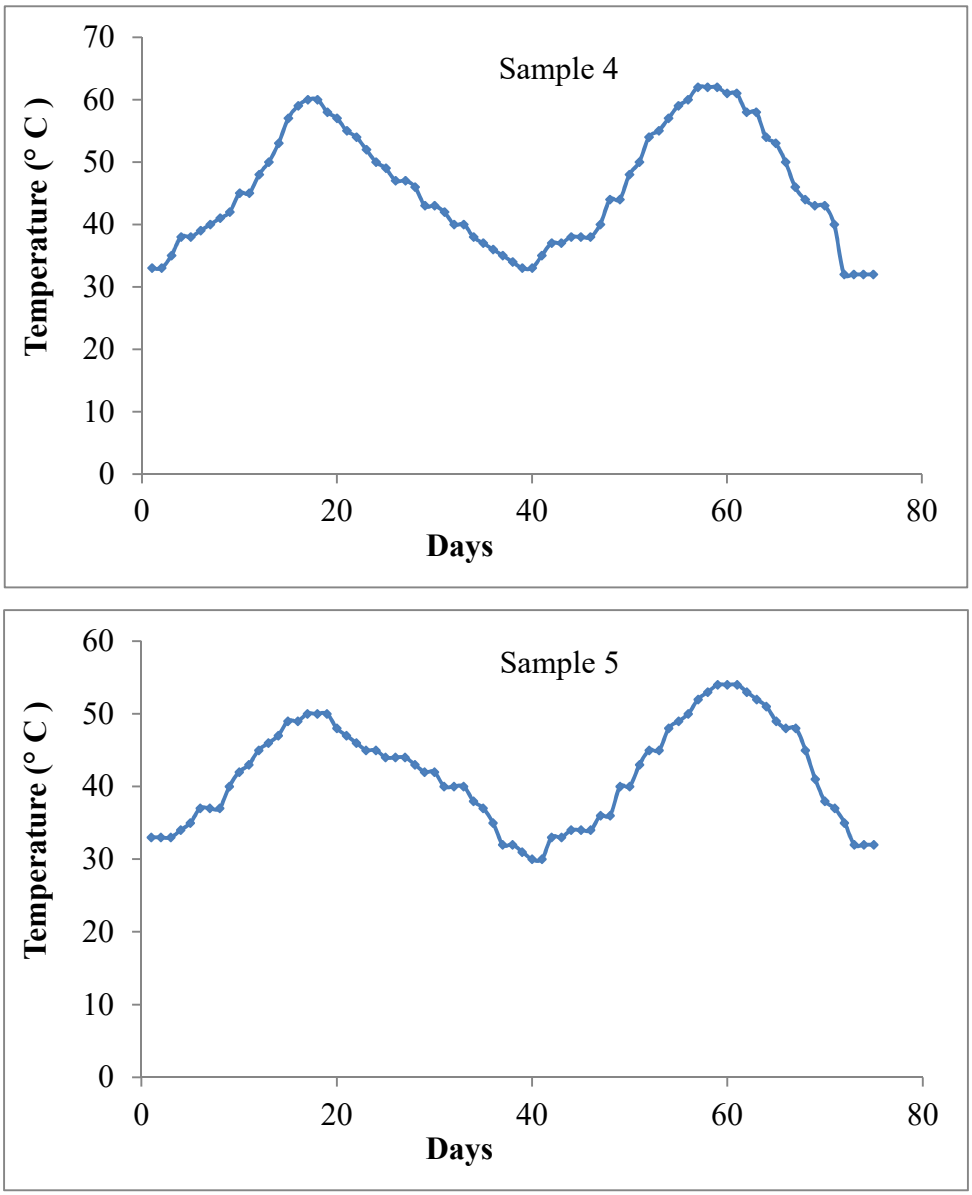

Figure 3: Temperature changes of compost Sample (4 and 5) during composting process

Some Physicochemical Properties of Composted Organic Fertilizers

Some physicochemical properties of composted organic fertilizers are pH, moisture, electrical conductivity, total organic carbon, total organic matter, C:N ratio, total nitrogen, total phosphorus, total potassium, calcium, magnesium, sulphur and trace elements were determined. Composted organic fertilizers have pH above 7. The pH values of composts are slightly alkaline. The moisture contents ranged from 7.478 to 15.838% for different compost types. The lowest value of moisture content (7.478%) was found in sample no 5 and the highest value of moisture content (15.838%) was obtained for sample no 3. The EC values ranged from 2.42 to 3.62 dSm^{-1}. This EC range is in the optimum range (2.0 to 4.0 dSm^{-1}) for growing media. Regarding total organic carbon was found to be 13.589 -19.951% for different compost types which are higher than the reported value 10% (Batjes., 1996). The total organic matter values ranged from 23.428 to 34.396%. Regarding the C/N ratio, it ranged from 14.406:1 to 16.647:1 for different compost types. These results are in agreement with the results ranged from 15:1 to 20:1 is ideal for ready to use compost (Rosen et al., 1993). These resulting data are shown in Table 6.

Table 6 Physicochemical Properties of Composted Organic Fertilizers

Samples	Parameters					
	pH	Moisture (%)	EC	Organic Matter (%)	Organic C (%)	C:N
Sample 1	7.61	9.628	2.95	27.818	16.136	14.406
Sample 2	7.70	9.582	2.60	23.428	13.589	15.529
Sample 3	7.60	15.838	3.62	34.396	19.951	15.833
Sample 4	7.75	7.564	2.69	24.109	13.984	16.647
Sample 5	7.73	7.478	2.42	25.529	14.808	16.271

EC = Electrical conductivity

Nitrogen is an essential element required for successful plant growth. The total nitrogen values ranged from 0.84 to 1.26% for different compost types. The lowest value of total nitrogen 0.84% for sample no. 4 and the highest value of total nitrogen (1.26%) were found in sample no. 3. These

results are in agreement with those obtained by Bento et al. (2006) whose found that the total nitrogen rate ranged from 0.99 % to 2.01%. Like nitrogen, phosphorus and potassium are also essential elements for plant growth. Phosphorus stimulates root growth, helps the plant set buds and flowers, improves vitality and increases seed size. Potassium improves overall vigor of the plant. It helps the plants make carbohydrates and provides disease resistance. The total phosphorus and total potassium values ranged from 0.420% to 0.594% and 0.906% to 1.488%, respectively, for different compost types. According to these phosphorus and potassium, the contents of phosphorus and potassium in these composted organic fertilizers are suitable for plant growth. The secondary nutrients-calcium, magnesium and sulphur and trace elements (iron, zinc, manganese and copper) necessary for plants were found in these composted organic fertilizers. The resulting data are shown in Table 7 and 8.

Table 7: Macronutrient Contents of Composted Organic Fertilizers

Samples	Macronutrients					
	Total N(%)	**Total P_2O_5(%)**	**Total K_2O(%)**	**Ca(ppm)**	**Mg (ppm)**	**S (%)**
Sample 1	1.120	0.480	1.488	154.4	9.264	0.077
Sample 2	0.875	0.442	1.296	151.8	9.251	0.071
Sample 3	1.260	0.594	1.152	151.2	9.125	0.069
Sample 4	0.840	0.420	0.906	152.3	9.158	0.076
Sample 5	0.910	0.467	1.008	146.8	8.994	0.061

Table 8: Micronutrient Contents of Composted Organic Fertilizers

Samples	Micronutrients			
	Fe (%)	**Zn (ppm)**	**Mn (ppm)**	**Cu (ppm)**
Sample 1	1.90	1.391	8.415	0.157
Sample 2	2.09	1.240	10.300	0.179
Sample 3	1.78	0.761	4.475	0.112
Sample 4	1.94	2.069	7.020	0.137
Sample 5	2.15	1.278	6.213	0.125

Elemental Contents in Composted Organic Fertilizers by EDXRF Technique

The relative abundance of some elemental contents in composted organic fertilizers was determined by EDXRF technique. According to these data in Table 9, all composted organic fertilizers contained high amounts of Si, Ca, Fe, K, Al, Ti and S and many trace elements necessary for plants were found.

Table 9: Relative Abundance of Composted Organic Fertilizers by EDXRF

Elements	Relative Abundance (%)				
	Sample 1	**Sample 2**	**Sample 3**	**Sample 4**	**Sample 5**
Si	29.057	34.261	24.675	24.239	30.704
Ca	27.376	20.117	35.528	36.03	26.689
Fe	16.972	20.188	17.045	15.854	18.835
P	-	0.138	0.194	-	0.047
K	16.379	13.251	12.87	13.459	13.086
Al	5.929	7.345	5.051	5.925	6.085
Ti	1.532	1.86	1.547	1.47	1.641
S	1.109	0.912	1.33	1.195	1.103
Mn	0.699	0.772	0.72	0.769	0.735
Sr	0.335	0.321	0.453	0.412	0.348
Zr	0.118	0.171	-	0.13	0.128
Zn	0.117	0.083	0.165	0.157	0.11
Rb	0.11	0.117	0.109	0.107	0.108
Cr	0.092	0.144	0.118	0.081	0.141
V	0.063	0.066	0.063	0.065	0.077
Br	0.058	-	0.082	0.062	0.049
Ni	-	0.052	-	-	0.058
Cu	0.053	0.045	0.052	0.043	0.056
Y	-	0.016	-	-	-

Conclusion

In this research work, some physicochemical properties of five kinds of composted organic fertilizers prepared by using organic wastes (cow dung, corn stalk and kokko leaves) have been studied. Before making composted organic fertilizers, some physicochemical properties of raw materials were characterized by conventional methods and modern instrumental techniques. According to the results, these raw materials contain macronutrients, micronutrients and trace elements necessary for plants and therefore were used in composting. Five kinds of composted organic fertilizers were prepared and some physicochemical properties of these different compost types were determined. The obtained results indicate that the pH value ranged from 7.61 to 7.75, moisture contents ranged from 7.478% to 15.838% and EC values ranged from 2.42 to 3.62 dSm^{-1}. The total organic carbon values ranged from 13.589 to 19.951%, the total organic matter contents ranged from 23.428 to 34.396% and the C/N ratio values ranged from 14.406:1 to 16.647:1. Macronutrients (primary and secondary nutrients), primary nutrients-total nitrogen values (0.840 to 1.260%), total phosphrous values (0.420 to 0.594%), total potassium values (0.960 to 1.488%) and secondary nutrients- calcium contents (146.8 to 154.4 ppm), magnesium contents (8.994 to 9.264 ppm) and sulphur contents (0.061 to 0.077%). The trace elements contents were iron (1.78 to 2.15%), manganese (4.475 to 10.300 ppm), copper (0.112 to 0.179 ppm) and zinc (0.761 to 2.069 ppm), respectively for different compost types. According to the experimental results, macronutrients, micronutrients, trace elements for plants and organic matter for good soil fertility were found in all composted organic fertilizers. Organic matter enhances root growth and nutrient uptake resulting in higher yields. Organic fertilizers add humus to the soil and this has the ability to hold positively charged ions (cations) and negatively charged ions (anions) make them available to the plants through the process of exchange capacity. Composted organic fertilizers provide plant nutrients, and improve soil biophysical properties, soil organic matter and crop yields (Naeem and Iqbal, 2006). Therefore, these composted organic fertilizers can be used to grow various kinds of crops in agriculture.

\

Acknowledgements

The authors would like to express their profound gratitude to the Department of Higher Education (Yangon Office), Ministry of Education, Yangon, Myanmar, for provision of opportunity to do this research

References

AOAC. (1984). *Official Methods of Analysis*. Washington, DC: 14th Ed., Association of Official Analytical Chemists

APNAN . (1995). *EM Application Manual for APNAN Countries*. Asia-Pacific Natural Agriculture Network, pp. 3-6

Batjes,N.H. (1996). Total Carbon and Nitrogen in the Soils of the World. *Eur.J. Soil Sci*., vol.47, pp.151-163

Benito, M.,A. Masaguer, A. Moliner, and R.De Antonio. (2006). "Use of Pruning Waste Compost as a Component in Soilless Growing Media". Bioresour. Technol. 97:2071-2076

Bokhtia, S. M. and Sakurai K. (2005). "Effects of Organic Manure and Chemical Fertilizer on Soil Fertility and Productivity of Plant and Ratoon Crops of Sugarcane". *Archieves of Agronomy and Soil Science*, vol. 51, pp. 325-334

Haque, M.O. (2000). *Effect of Different Fertilizers Management Practices on the Growth and Yield of Main and Ratoon Crop of Cabbage*. MSc Thesis, Dept. of Hort., BAU, Mymensingh, 96

Mi Mi Hlaing .(2011). *Recycling Wastes into Organic Fertilizers by Vermicomposting using Earthworms*. PhD Dissertation, Chemistry Department, Yangon University

Naeem, M., and Iqbal J. (2006). "Comparative Study of Inorganic Fertilizers and Organic Manures on Yield and Yield Components of Mungbean (Vigna radiat L.)", *Journal of Agriculture & Social Sciences*, 1813-2235/2006

Rosen, C.J., Halbach T.R., and Swanson B.T., (1993). Horticultural uses of municipal solid waste components. Hortic. Technol. vol.3, pp. 167-1773

Vogel, A.L. (1968). *A Text Book of Quantitative Inorganic Analysis*, 3rd Ed., New York, Longmans, Green, and Co., Ltd., pp. 800-884

GREEN SYNTHESIS OF SILVER NANOPARTICLES USING CHITOSAN AS REDUCING AGENT

Tin Moe Swe[1], Khin Aye May[2], KhinThan Yee[3]

Abstract

The development of eco-friendly process for the synthesis of nanoparticle is one of the main steps in the area of nanotechnology research. In this study, the synthesis of silver nanoparticles was conducted from silver nitrate ($AgNO_3$) by using chitosan solution as reducing agent. Silver nanoparticles (Ag nanoparticles) were prepared by adding different volumes of silver nanoparticles (1mL,2mL,3mL,4mL) of 0.01M $AgNO_3$ solution to various concentrations of chitosan solution (1% and 0.5% w/v). To avoid the chemical toxicity, biosynthesis (green synthesis) of metal nanoparticles is proposed as a cost-effective and environmental friendly alternative. The existence of nanoparticles in colloidal solution was confirmed by Tyndall effect. The synthesized silver nanoparticles were characterized by UV-visible spectroscopy, FT IR, SEM, XRD, EDXRF and determined their antimicrobial activities. The maximum absorption of prepared silver nanoparticles using chitosan solution as reducing agent were observed at the wavelengths of near 390 nm indicating the presence of Ag nanoparticles in colloidal solution. According to antimicrobial activity tests, Ag nanoparticles prepared using 1% (w/v) chitosan solution as reducing agent were found to be more active than 0.5%(w/v) chitosan solution. Among them, the Ag-nanoparticle prepared from 4mLof 0.01 M $AgNO_3$ in 1% w/v of chitosan solution exhibit the highest activity on *P.aeruginosa*. From the SEM micrograph of this sample, the prepared Ag nanoparticles had spherical shape of various size. XRD analysis of Ag nanoparticles showed the amorphous form. The functional groups of Ag nanoparticles in this sample was identified by FT IR analysis which indicates the presence of Ag-O stretching and deformation. The relative abundance of silver in the prepared sample was investigated by EDXRF.

Keywords: chitosan, silver nanoparticles, antimicrobial activity, Tyndall effect

[1.] 3PhD, Candidate, Department of Chemistry, University of Yangon
[2.] Associate Professor, Department of Chemistry, Dagon University
[3.] Lecturer, Department of Chemistry, University of Yangon

Introduction

In recent years, noble metal nanoparticles have been the subject of focused research due to their unique electronic, optical, mechanical, magnetic and chemical properties that are significantly different from those of bulk counterpart. Nowadays, silver nanoparticles has gain tremendous popularity in the world in the field of sensors because of outstanding significant optical, electronic and chemical properties (Kumar and Rani, 2013). Silver nanoparticles exhibit new optical properties, which are observed neither in molecules nor in bulk metals. One example is presence of absorption band in visible light region. This band appears due to the surfaceplasmon-oscillation modes of conduction electrons which are coupled through the surface to external electromagnetic fields(Hussain*et al*., 2011). The green synthesis is a concept that is introduced to define the method used in synthesis, which is favored over solvent medium. This is because it is environmentally friendly and contains a reducing agent that is benign to the environment. Besides, it also utilizes a non-toxic stabilizer in forming Ag nanoparticles. Chitosan, a polysaccharide biopolymer, is a product of deacetylation of chitin, which is the second most abundant natural polymer in the world after cellulose. The biocompatibility and antibacterial properties of chitosan and its being an environmentally friendly polyelectrolyte makes it attractive in academic research (Mansor *et al.,* 2011).

Silver exhibits the highest electrical and thermal conductivities among all the metals for centuries. People have used silver for its antibacterial qualities. Nanoparticles usually have better or different qualities than the bulk material of the same element. In the case of silver nanoparticles the antibacterial effect is greatly enhanced and because of their tiny size (Link*et al*., 1999). Nanoparticles have immense surface area relative to volume. Therefore minuscule amounts of silver nanoparticles can lend antimicrobial effects to hundreds of square meters of its hostmaterial. Nanomaterials are the leading requirement of the rapidly developing field of nanomedicine and bionanotechnology (Mandal and Sastry, 2014).

Nanoparticles are being utilized as therapeutic tools in infections, against microbes thus understanding the properties of nanoparticles and their effect on microbes is essential to clinical application (Khan *et al*., 2014).

Among noble metal nanoparticles, silver nanoparticles have received considerable attention owing to their attractive physicochemical properties. Silver nanoparticles exhibit distinct optical activities that have found wide use in electronics, catalysis and in sensing based applications (Matti *et al*., 2012). Moreover, it displays antimicrobial activity against a broad spectrum of bacteria and fungi and thus finds use as a biocide and also in the preparation of bactericidal nanomaterials for wound dressings and surgical purposes. Silver nanoparticles are nontoxic to human in low concentrations. The silver-nanoparticles can inactivate proteins, blocking respiration and electron transfer (Ramos *et al*., 2010).

Silver nanocrystals, mostly hydrosols are one of the most attractive inorganic material not only because of its tremendous applications in photography, catalysis**,** biosensor, biomolecular detection, diagnostics, and particularly antimicrobial activities but also because of its environmentally benign nature**.** Synthesis of different morphologies of advanced silver nanomaterials (nanotubes, nanowires, nano cubes, nanorods, and nanosheets) has been the subject of a large number of researchers in many laboratories (Shah *et al*.,2012). Silver, a naturally occurring element, is non-toxic, hypoallergenic, does not accumulate in the body to cause harm and is considered safe for the environment. Many manufactured goods like washing machines, air conditioners and refrigerators are using linings of silver nanoparticles for their antimicrobial qualities. Sportswear, toys and baby articles, food storage containers, HEPA filters, laundry detergent etc. are made with silver nanoparticles. The medical field also is using products with silver nanoparticles, such as heart valves & other implants, medical face masks, wound dressings and bandages (Nagaonkar and Rai, 2015). Nanomaterials are the leading in the field of nanomedicine, bionanotechnology and in that respect nanotoxicology research is gaining great importance. Silver exhibits the strong toxicity in various chemical forms to a wide range of microorganism is very well known and silver nanoparticles have recently been shown to be a promising antimicrobial material. Analysis of bacterial growth showed that the toxicity of silver nanospheres is higher than that of gold nanospheres. In addition, noresearch has discovered any bacteria able to develop immunity to silver as they often do with antibiotics (Zhang*et al*., 2007). Therefore, eco-friendly or green chemistry and non-toxic biological

methods have also been widely considered for synthesis of silver nanoparticles.

Aim

To synthesize silver nanoparticles by green synthesis and apply on burn wound healing.

Materials and Methods

Materials

Commercial chitosan sample from shrimp shell was purchased from Asian Technology Groups Co., Ltd., Local Industry,Yangon, Myanmar. All other chemicals used were of analytical reagent grade. In all investigations, the recommended standard methods and techniques involving both conventional and modern methods were provided.

Preparation of Chitosan Solutions (1% and 0.5%)

Chitosan (1g) was dissolved in 1%(v/v) acetic acid solution. It was stirred until the chitosan was completely dissolved. Then the solution (1 % w/v) was filtered and stored for further use and analyses. The above solution was diluted with acetic acid solution to form 0.5 % (w/v) chitosan solution.

Synthesis of Silver Nanoparticles (Ag nanoparticles)

Silver nanoparticles (Ag nanoparticles) were prepared using chitosan solutions (1% and 0.5% w/v) as reducing agents as well as stabilizing agents. 100 mL of 1% and 0.5% (w/v) chitosan solution was heated to 80 ± 3 ºC. The collagen when heated at 80±3 ºC denatures chitosan which acts as reducing/stabilizing reagent. 1,2,3,4 mL each of the $AgNO_3$ solution (0.01M) was added rapidly at a stirring rate of 3000 rpm. A colour changesto pale yellow was observed due to the complex formation between chitosan and Ag ion. The reaction was carried out under dark conditions and the contents were subjected to vigorous stirring at 80±3 ºC to ensure the complete formation of chitosan capped silver nanoparticles. The prepared (Ag nanoparticles were denoted as samples

1,2,3,4 when using 1,2,3,4 mL of 0.01 M $AgNO_3$ solution respectively in 1% (w/v) chitosan solution. Samples 5,6,7 and 8 were prepared by addition of 1,2,3,4 mL each of 0.01M $AgNO_3$ solution to 0.5% w/v of chitosan solution.

Characterization of Prepared Ag nanoparticles

The prepared Ag nanoparticles(Samples1-8) were characterized by UV-vis sprectroscopy, XRD analysis and determined their antimicrobial properties.

Results and Discussion

Tyndall Effect

Tyndall effects on Ag nanoparticles are shown in Figures 1 and 2. It was found that the laser light passes through the solutions due to the presence of nanoparticles.

Sample 1 Sample 2 Sample 3 Sample 4

Figure 1: Tyndall effect on Ag nanoparticles (Samples 1, 2, 3, 4)

Sample 5 Sample 6 Sample 7 Sample 8

Figure 2: Tyndall effect on Ag nanoparticles (Samples 5, 6, 7, 8)

Analysis of Silver Nanoparticles by UV-vis Spectroscopy

The synthesized nanoparticles were confirmed using UV-vis spectroscopy as depicted in Figures3 to 10.The maximum absorption wavelengths of Ag nanoparticleswere found to be near 390nm (Table 1) which confirmed that the presence of nanoparticles in colloidal solutions were Ag nanoparticles with the size of 1-5nm.

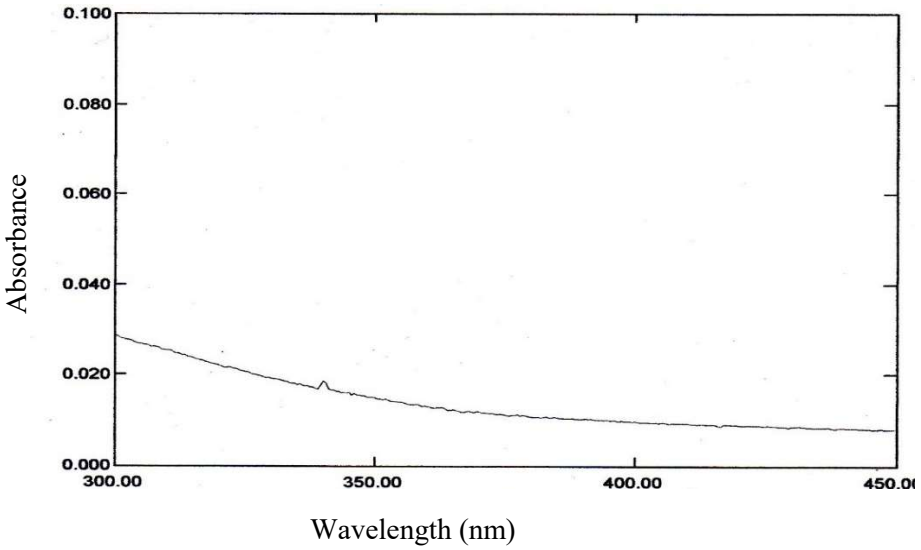

Figure 3: UV-vis spectrum of silver nanoparticles in colloidal solution (Sample 1)

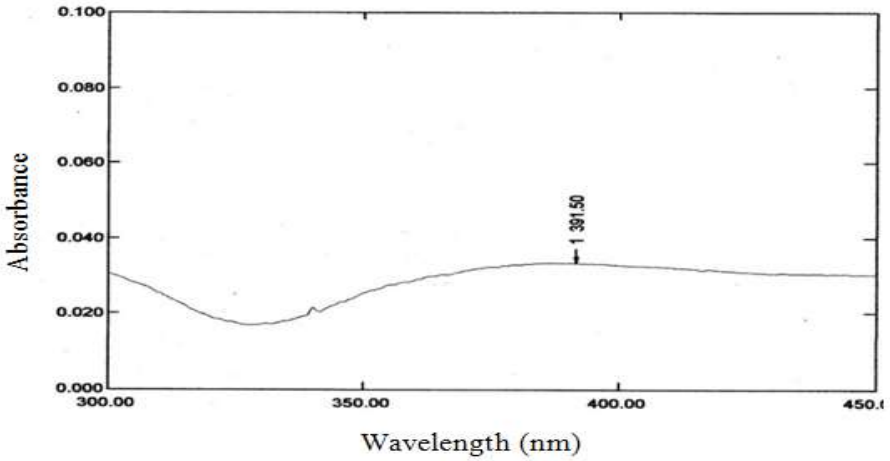

Figure 4: UV-vis spectrum of silver nanoparticles in colloidal solution (Sample 2)

Wavelength (nm)

Figure 5: UV-vis spectrum of silver nanoparticles in colloidal solution (Sample 3)

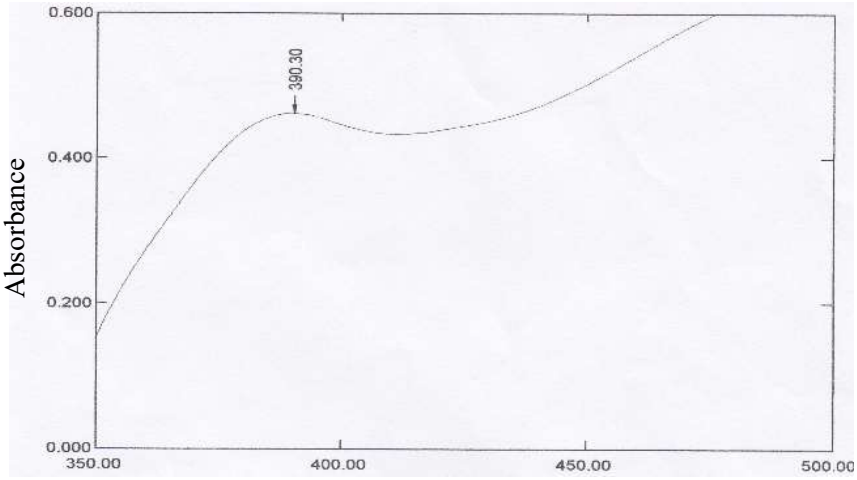

Wavelength (nm)

Figure 6: UV-vis spectrum of silver nanoparticles in colloidal solution (Sample 4)

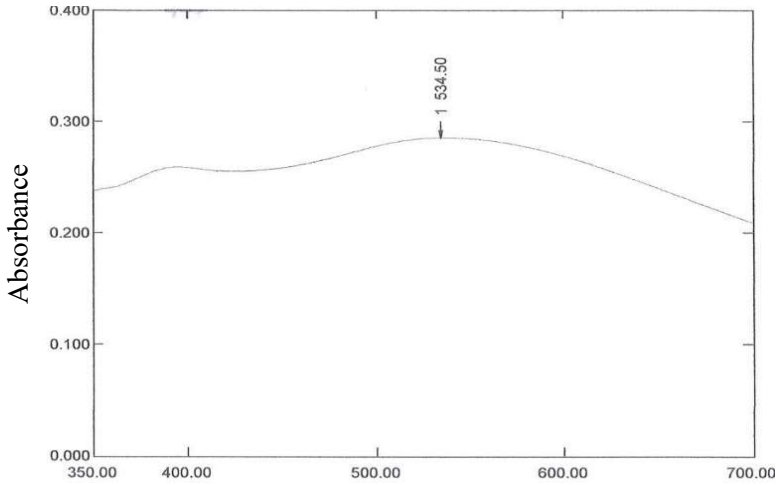

Figure 7 : UV-vis spectrum of silver nanoparticles in colloidal solution (Sample 5)

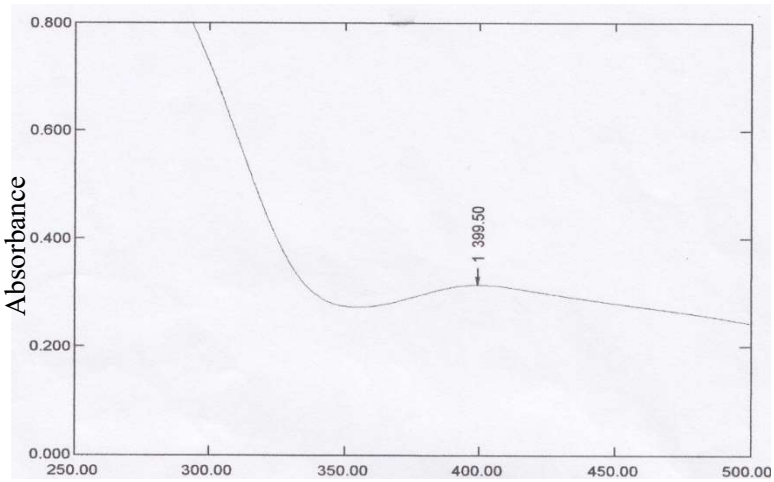

Figure 8: UV-vis spectrum of silver nanoparticles in colloidal solution (Sample 6)

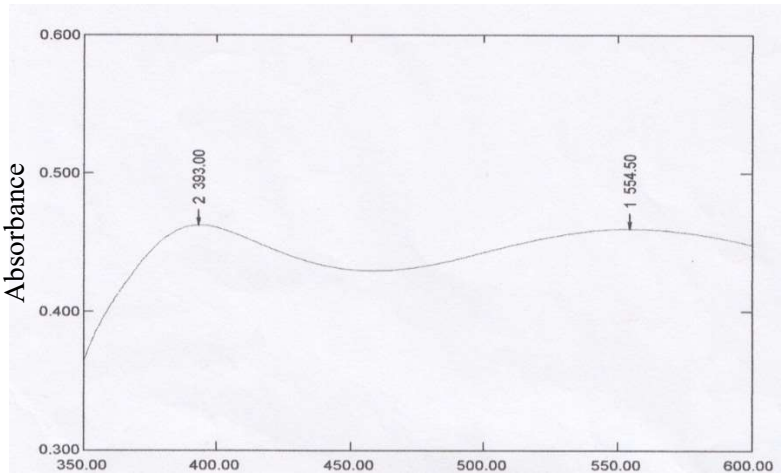

Figure 9: UV-vis spectrum of silver nanoparticles in colloidal solution (Sample 7)

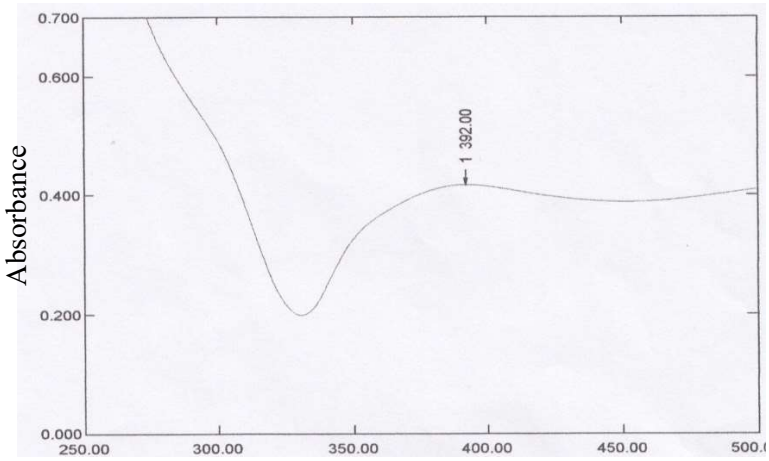

Figure 10 : UV-vis spectrum of silver nanoparticles in colloidal solution (Sample 8)

Table 1: Wavelength of Maximum Absorption of Ag Nanoparticles

Ag nanoparticles Sample	Observed wavelengths of maximum absorption (nm)
1	-
2	391
3	392
4	**390**
5	390,534
6	399
7	399,554
8	392

X-ray Diffraction Analysis

X-ray diffractograms of synthesized Ag nanoparticlesare shown in Figures11 to 18. All of the XRD sprectra show the amorphous nature of prepared silvernanoparticles.

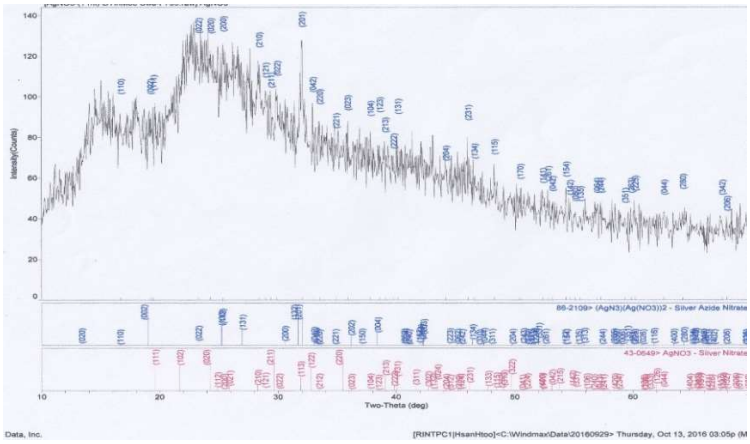

Figure 11 : X-ray diffractogram of silver nanoparticles (Sample 1)

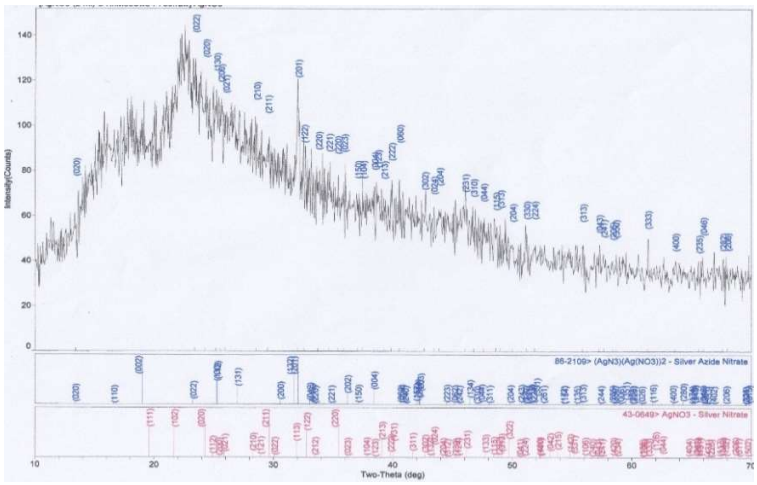

Figure 12: X-ray diffractogram of silver nanoparticles (Sample 2)

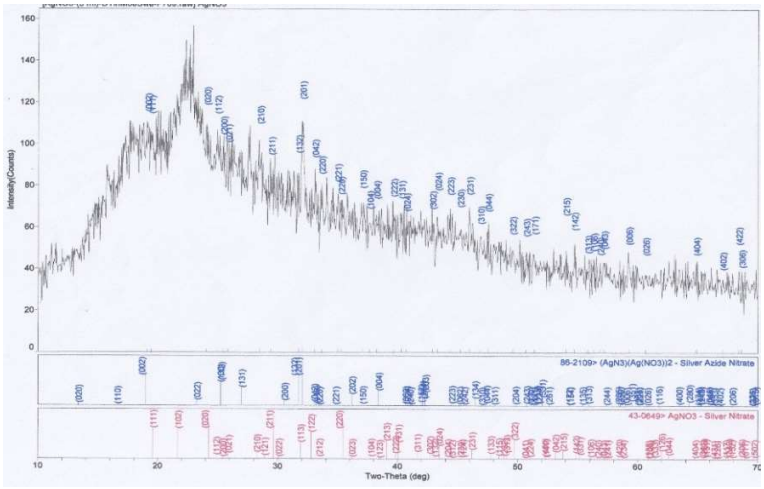

Figure 13 : X-ray diffractogram of silver nanoparticles (Sample 3)

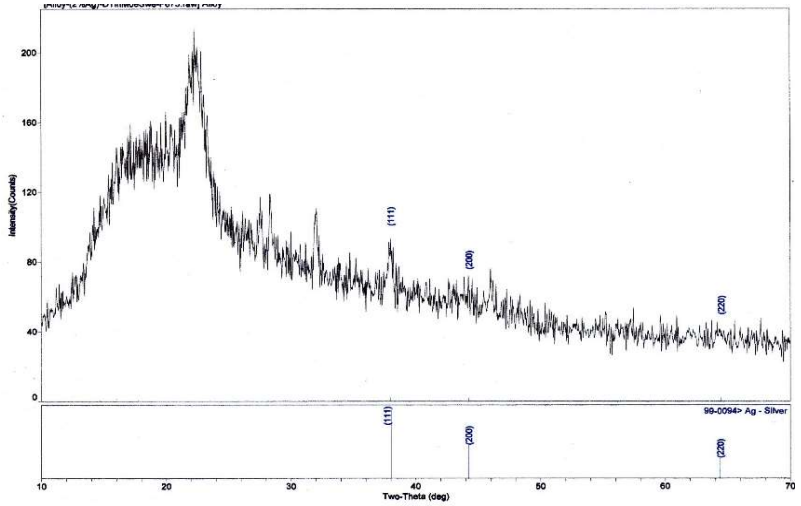

Figure 14: X-ray diffractogram of silver nanoparticles (Sample 4)

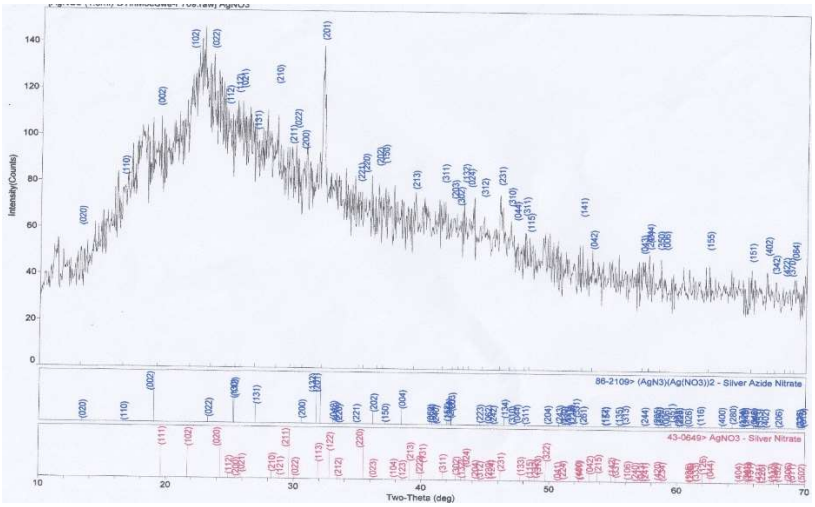

Figure 15: X-ray diffractogram of silver nanoparticles (Sample 5)

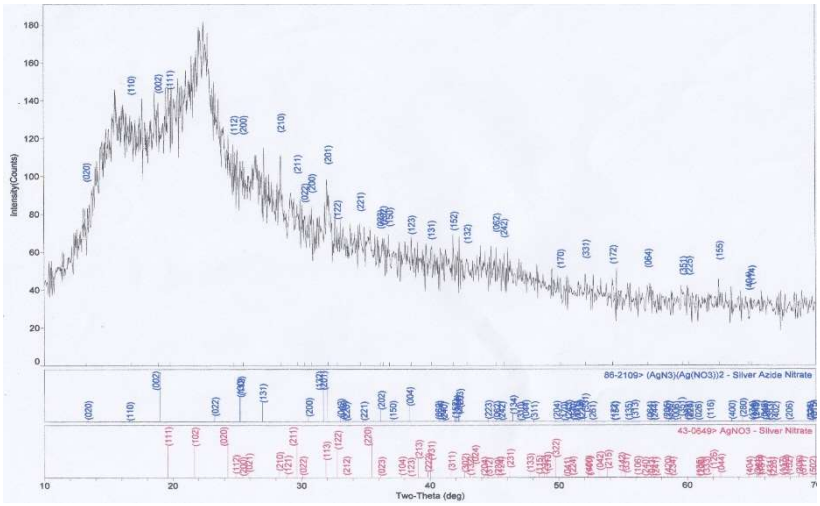

Figure 16: X-ray diffractogram of silver nanoparticles (Sample 6)

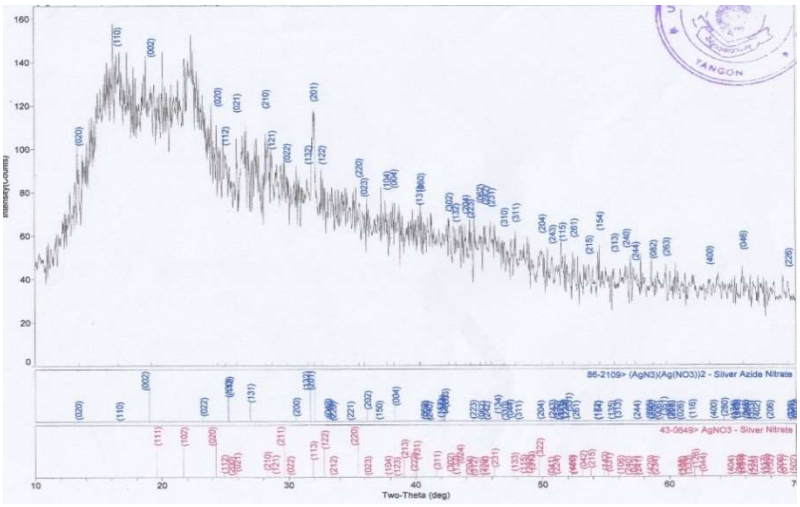

Figure 17: X-ray diffractogram of silver nanoparticles (Sample7)

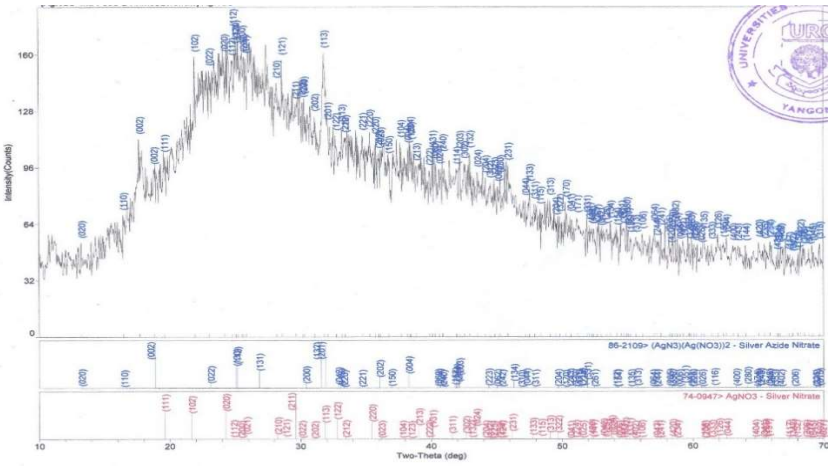

Figure 18: X-ray diffractogram of silver nanoparticles (Sample 8)

Antimicrobial Activities of Silver Nanoparticles

The antimicrobial activities of Ag nanoparticlestested against 6 microorganisms are shown in Figures19 and 20 and Tables 2 and 3.. According to the results, although chitosan itself show the avtivity on microorganisms, the presence of silver nanoparticles enhance the activitysignificantly.Samples5,6,7,8 were less active than samples 1,2,3,4 except *S. aureus.* So 1% (w/v) chitosan was chosen for the preparation of Ag nanoparticles. Among samples 1 to 4, the most active sample 4 was chosen for the preparation of Au-Ag bimetallic nanoparticles based on UV-vis spectroscopic analyses and antimicrobial activities.

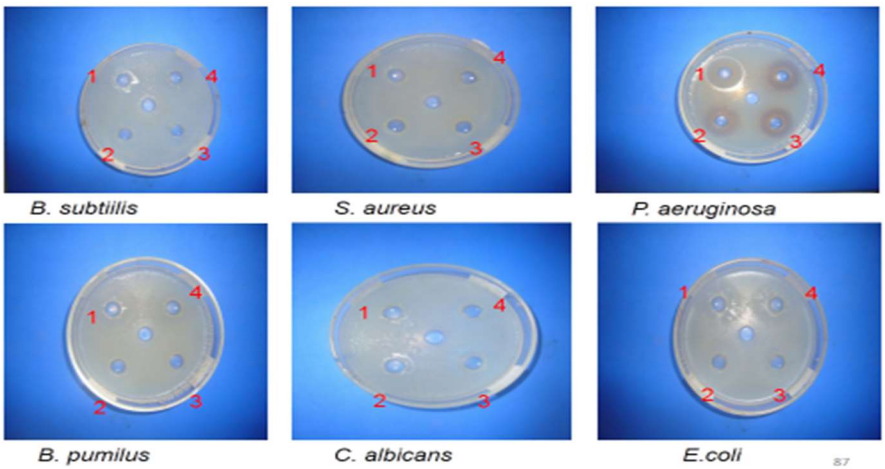

Figure 19: Antimicrobial activities of Ag nanoparticles (Samples 1,2,3 and 4)

Table 2: Antimicrobial Activities of the Prepared Silver Nanoparticles (Samples 1-4) against Six Microorganisms

Sample No	Inhibition Zone Diameter (mm)					
	B. subtilis	*S. aureus*	*P. aeruginosa*	*B. pumilus*	*C. albicans*	*E. coli*
1	13 (+)	-	30 (+++)	26 (+++)	12 (+)	30 (+++)
2	13 (+)	-	25 (+++)	25 (+++)	13 (+)	30 (+++)
3	13 (+)	-	24 (+++)	25 (+++)	12 (+)	30 (+++)
4	11 (+)	-	26 (+++)	29 (+++)	11 (++)	30 (+++)
1%Chitosan	-	-	-	-	-	-

Agar well – 10 mm

10 mm ~ 14 mm (+)

15 mm ~ 19 mm (++)

20 mm above (+++)

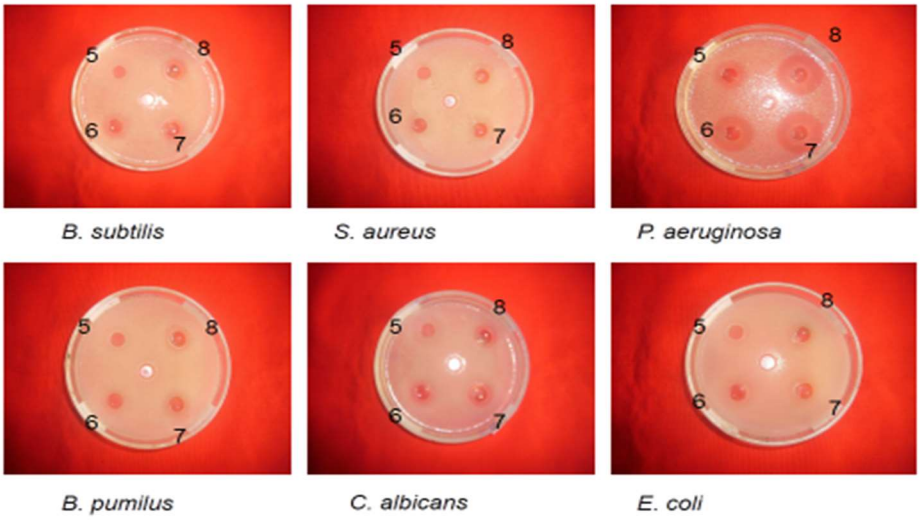

Figure 20: Antimicrobial activities of Ag nanoparticles (Samples 5,6,7,8)

Table 3: Antimicrobial Activities of the Prepared Silver Nanoparticles (Samples 5-8) against Six Microorganisms

Sample No	Inhibition Zone Diameter (mm)					
	B. subtilis	*S. aureus*	*P. aeruginosa*	*B. pumilus*	*C. albicans*	*E. coli*
5	13 (+)	12 (+)	15 (++)	12 (+)	13 (+)	13 (+)
6	15 (++)	11 (+)	21 (++)	13 (+)	15 (+)	15 (++)
7	17 (++)	12 (+)	24 (+++)	13 (+)	12 (+)	15 (++)
8	17 (++)	12 (+)	25 (+++)	13 (+)	11 (++)	13 (+)
0.5% Chitosan	-	-	-	-	-	-

Agar well - 10mm

10mm ~ 14mm (+)

15mm ~ 19mm (++)

20mm above (+++)

Scanning Electron Microscopic (SEM) Analysis

Structural and surface morphology of silver nanoparticles (Sample 4)was analyzed by SEM analysis. The micrograph is presented in Figure 21. The various spherical shape of silver nanoparticles were observed.

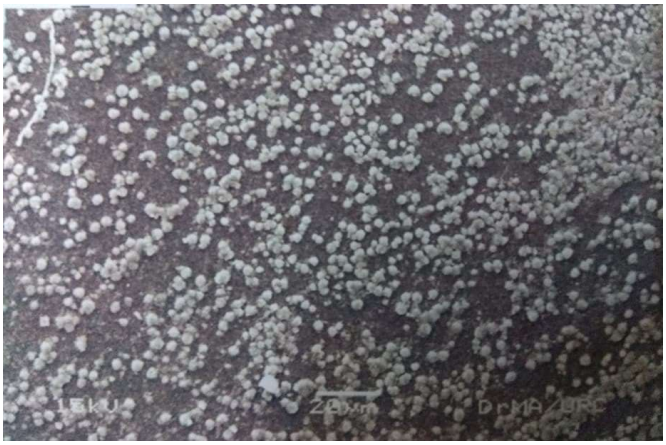

Figure 21: SEM micrograph of silver nanoparticles (Sample 4)

Fourier Transform Infrared Spectrpscopy (FT IR)

The synthesized silver nanoparticles (Sample 4) was characterized by FT IR spectroscopy. The FT IR sprectra of Ag nanoparticleswas shown in Figure 22.Infraed studies was carried out in order to ascertain the purity and nature of the metal nanoparticles. Metals generally give absorption band in finger print region i.e. below 1000cm^{-1} arising from inter-atomic vibrations. The peak observed at 3448cm^{-1} are may be due to O-H stretching. The peaks at 1397 and 650 cm^{-1} are corresponding to Ag-O stretching and deformation, respectively. The observed wave numbers of prepared Ag nanoparticles (Sample 4) were accordance with the literature values (Mansor *et al.,* 2011).

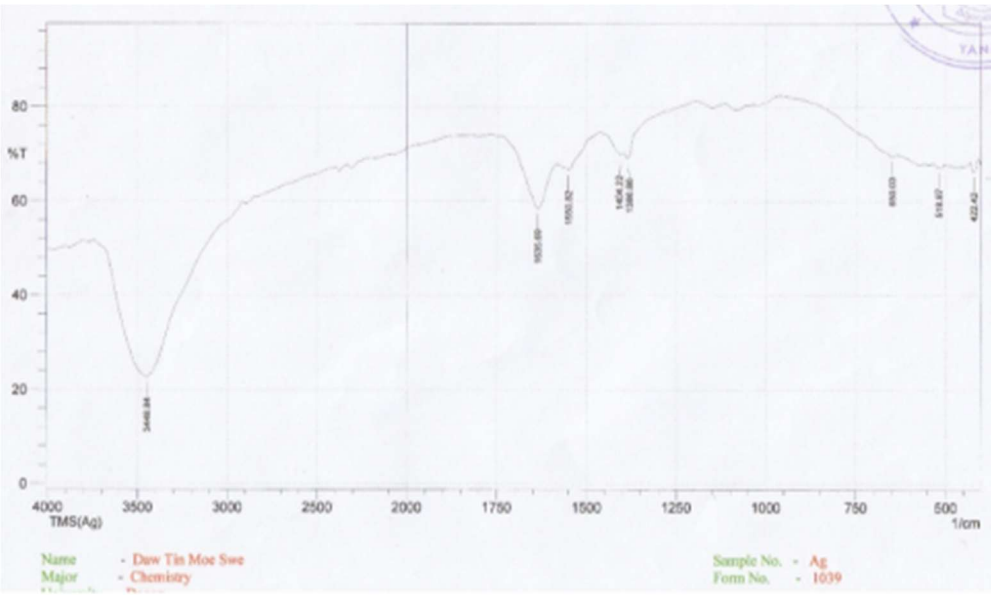

Figure 22: FT IR spectrum of silver nanoparticles (Sample 4)

Table 4: FT IR Spectral Assignment for Silver Nanoparticles (Sample 4)

Observed wavenumber (cm^{-1})	**Literature wavenumber (cm^{-1})**	**Band assignment**
3448	3200-3600	-OH stretching
1397*	~ 1400	Ag-O stretching
650	~ 650	Ag-O deformation

* Mansor *et al,* 2011

Energy Disperse X-ray Florescence (EDXRF)

EDX RF spectrum confirms the presence of silver (%) in sample 4. (Figure 23)

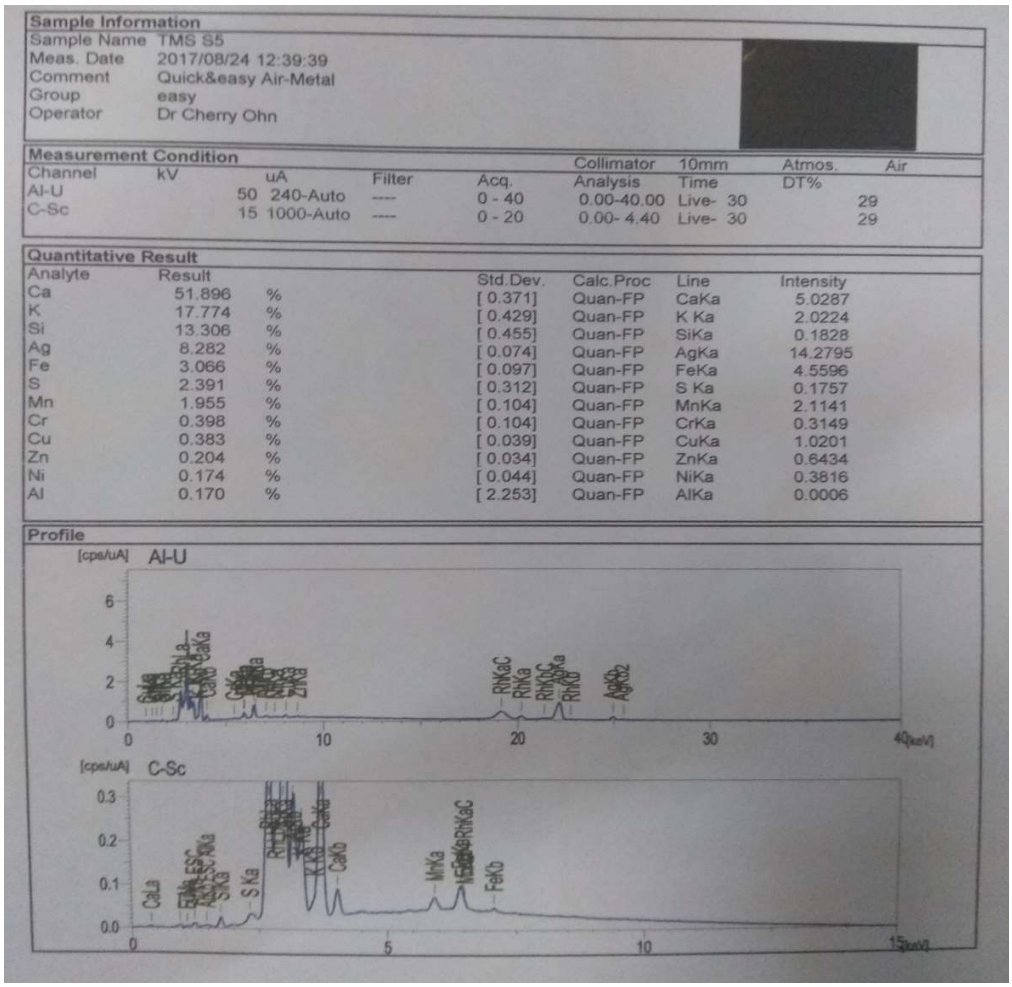

Figure 23: EDXRF spectrum of silver nanoparticles (Sample 4)

Conclusion

From the overall assessment of the present work, the following inferences can be deduced. Pale yellow colour of Ag nanoparticles was successfully synthesized. The prepared particles which were in the nano range was confirmed by Tyndall scattering. The laser light passes through the solution due to the presence of nanoparticle. The prepared particles which were in the wavelength of nano range was confirmed by UV-visible spectroscopy. The maximum absorption wavelengths of Ag nanoparticles were found near 390nm. All of the X-ray diffractogram shows the amorphorus nature. According to the results of antimicrobial activities of silver nanoparticles using 1% w/v chitosan solution as reducing agent it showed high activities for five tested microorganisms except *S. aureus*. Based on UV-vis and antimicrobial activities of samples 1 to 4, the maximum mixing ratio of 4 mL and 0.01M $AgNO_3$ in 1% w/v chitosan was chosen for further studies. The EDXRF results of sample 4 was found to be 8.282% of Ag. From the SEM micrograph of sample 4, the prepared Ag nanoparticles had spherical shape with various sizes. According to the FT IR spectrum of sample 4, three obvious infrared bands were observed at 3448cm^{-1}, 1397 cm^{-1} and 650cm^{-1}due to the presence of O-H stretching, Ag-O stretching and Ag-O deformation, respectively.

Acknowledgement

The authors would like to thank Professor and Head, Dr Daw Hla Ngwe, Department of Chemistry, University of Yangon, for the permission of doing this research and allowing the writing of this paper. Special thanks are extended to Universities' Research Centre, University of Yangon.

References

Hussain, J.I., Hashmi,A.A. and Khan, Z. (2011).“Silver Nanoparticles: Preparation, Characterization, and Kinetics”. *Advanced Materials Letters*, vol.2(3), pp.188-194

Khan, A.K., Rashid, R., Mutaza, G. and Zahra, A. (2014). “Gold Nanoparticles: Synthesis and Applications in Drug Delivery”. *Tropical Journal of Pharmaceutical Research*,vol.13(7), pp. 1168-1177

Kumar, H. and Rani, R. (2013). “Structural Characterization of Silver Nanoparticles Synthesized by Micro Emulsion Route”. *International Journal of Engineering and Innovative (IJEIT),* vol. 3(3), pp. 2277-3754

Link, S., Wang, Z.L. and El-Sayed, M.A. (1999). “Alloy Formation of Gold-silver Nanoparticles and the Dependence of the Plasmon Absorption on Their Composition”. *J.Phys. Chem. B*, vol.103,pp.3529-3533

Mandal, A. and Sastry, T.P. (2014). “Fabrication of Gelatin Based Composites Containing BimetallicAg-Au Nanoparticles for Biomedical Applications”.*IJRSET*, vol. 3(5), pp.12463-12472

Mansor, B. A., Jenn, J. L., Kamyar, S., Nor, A. I. and Mei, Y. T. (2011). “Synthesis of Silver Nanoparticles in Chitosan, Gelatin and Citosan/Gelatin Bionanocomposites by a Chemical Reducing Agent and Their Characterization”. *Journal of Faculty of Science,* vol. 16, pp. 7237-7248

Matti, M., Schooneveld, V., Carlos, C.C., Pet, J., Meeldijk, J.D., Rijissel, J.V., Meijerink, A., Erne, B.H. and Groot, F.M.F. (2012). “Composition Tunable Cobalt-Nickel and Cobalt-Iron Alloy Nanoparticles Below 10 nm Synthesized Using Acetonated Cobalt Carbonyl”. *J Nanopart Res,* vol. 14(991), pp. 1-13

Nagaonkar, D. and Rai, M.(2015). “Sequentially Reduced Biogenic Silver-gold Nanoparticles with Enhanced Antimicrobial Potential over Silver and Gold Monometallic Nanoparticles”. *Advanced Materials Letters*, vol.(4),pp.334-341

Ramos, M., Ferrer, D.A., Chianelli,R.R., Correa, V., Matos, J.S. and Flores, S. (2010). “Synthesis of Ag-Au Nanoparticles by Galvanic Replacement and Their Morphological Studies by HRTEM and Computational Modeling”. *Journal of Nanomaterials*, vol.20(11), pp.1-5

Shah, A., Rahman, L., Qureshi, R.and Rehman, Z. (2012). “Synthesis, Characterization and Applications of Bimetallic (Au-Ag, Au-Pt, Au-Ru) Alloy Nanoparticles”. *Rev. Adv. Mater.Sci*., vol.30, pp.133-149

Zhang, Q., Lee, J.Y., Yang, J., Boothroyd, C. and Zhang, J. (2007). “Size and Composition Tunable Ag-Au Alloy Nanoparticles by Replacement Reaction”. *Nanotechnology*, vol.18,pp.1-8

DISSOLUTION OF RICE STRAW IN 1-BUTYL-3-METHYLIMIDAZOLIUM ACETATE [BMIM][OAc]

Tun Tun Win[1], Win Aung[2], Ni Ni Sein[3]

Abstract

Dissolution of rice straw (RS) in an ionic liquid (IL), 1-butyl-3-methylimidazolium acetate [BMIM][OAc] was studied with regard to effects of size, amount of rice straw powder, dissolution time and dissolution temperature. Highest yield percent (76.65 %) of regenerated cellulose was achieved using 0.149 mm size and 0.2 g of rice straw powder. Effect of dissolution time (10, 30, 90 min) on the yield percent of regenerated cellulose showed that higher yield percentages of 78.08 % and 76.65 % were achieved for dissolution times of 90 min and 30 min respectively. Three dissolution temperatures were set for dissolution study and it was found that the shortest dissolution time (10 min) was observed at 160 ºC. Surface morphology of the regenerated cellulose samples showed amorphous and porous structure compared to highly organized fibril structure of raw rice straw powder. Amorphous structure of regenerated cellulose samples were also confirmed by FT IR spectral data. The appearance of amorphous band around 900cm^{-1} of cellulose was observed in regenerated cellulose indicating the reduction of crystallinity. Crystalline peak of cellulose at (101) plane at 2θ value of 22º was clearly observed in raw rice straw powder whereas the peak intensity decreased or absent in regenerated sample. By the optimization of the dissolution condition, 0.2 g of rice straw powder with 0.149 mm size was chosen for dissolution of rice strow at 120 ºC for 30 min.

Keywords : 1-butyl-3-methylimidazolium acetate,[BMIM][OAc], rice straw, ionic liquid, regenerated cellulose

Introduction

The search for renewable feed stocks to produce useful chemicals, materials and fuels has become an important goal, with the ever-growing energy demands and environmental concerns, together with the diminishing fossil fuel reserves (Tuck *et al*., 2012; Chatterjee *et al*., 2015). Lignocellulosic biomass is a promising alternative to fossil resources because of its

1. 4 PhD,Candidate Department of Chemistry, University of Yangon
2. Associate Professor, Department of Chemistry, Myitkyina University
3. Professor (Retired), Department of Chemistry, University of Yangon

abundance, renewability and versatility. Recently, lignocellulosic biomasses attract great attention of scientists as a potential feedstock for bioethanol production (Poornejad *et al*., 2014). Lignocellulosic biomass is generated in large quantities, especially in countries that are predominantly agricultural. One of the examples of biomass is rice straw.

Lignocellulose is a composite material synthesized by plant cells, consisting mainly of polymeric carbohydrates (cellulose and hemicelluloses) and the aromatic polymer lignin (Figure 1).

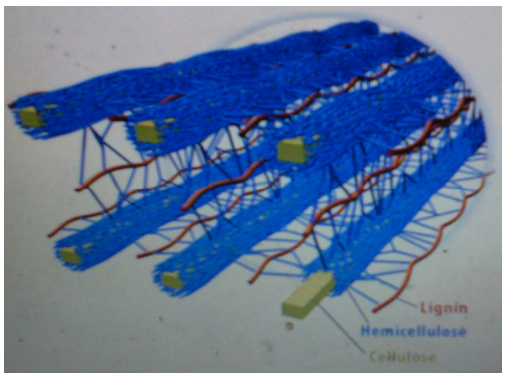

Figure 1: Spatial arrangement of cellulose, hemicellulose and lignin in the cell walls of lignocellulosic biomass.

Cellulose may exist in crystalline or amorphous forms. Amorphous structures are less ordered than crystalline regions. The crystalline structures are highly ordered and poorly depolymerized by cellulose (Yong, 2005). The cellulose fibers are usually embedded in an amorphous matrix of hemicellulose and lignin. Lignocellulosic biomass is suitable source for conversion to bioethanol because of the abundance and cheapness. However, conversion of lignocelluloses to bioethanol is faced with physical and chemical barriers. More specifically, crystalline structure of cellulose, presence of lignin, and covalent cross-linkages between lignin and hemicelluloses in cell wall obstruct the decomposition process of lignocellulosic materials (Mood *et al.*, 2013). Therefore, the goal of pretreatment is defined to overcome these obstacles including breaking down lignin structure, disrupting the crystalline structure of cellulose and cross-linked matrix of lignin and hemicelluloses, and increasing the porosity and

surface area of cellulose (Alvira *et al.*, 2010; Li *et al.*, 2010). The most commonly applied methods involved, for example include steam or carbon dioxide explosions and hot water treatment. Chemical processes involve acid or alkali treatments and organosolv process for example, however, all these pretreatment methods have several disadvantages. Some of the solvents cause the degradation of lignocelluloses upon dissolving. These unwanted by-products can inhibit a subsequent hydrolysis or fermentation step (Larsson *et al*., 1999). Some pretreatment methods are too slow (even weeks), and these methods cannot be considered as "green" since hazardous or toxic compounds are released. Therefore, more efficient pretreatment procedures are required. One potential alternative is the use of ionic liquids (ILs).

Ionic liquids (ILs) are a group of new organic salts that are liquids at relative low temperatures (below 100 ˚C). As the name suggest they are completely ionic with most ionic liquids consisting of an organic cation and an inorganic or organic anion. Many ionic liquids are also liquids at room temperature making it an ideal solvent to work with. Compared with traditional molecular solvents, ionic liquids express very interesting properties like broad liquid regions, high thermal stabilities and negligible vapour pressures (Brennecke and Maginn, 2001). Ionic liquids are also called green solvents because no toxic or explosive gases are formed when used (Anderson *et al*., 2002). The ability of ionic liquids to dissolve cellulose depends on the nature of the native cellulose (its degree of polymerization and crystallinity) on the operating conditions (temperature, reaction time, initial concentration of cellulose in the IL) and the presence of impurities (water). Dissolved cellulose can be precipitated and separated from lignin and hemicelluloses by the addition of anti-solvents, such as water (Fort *et al*., 2006).

This research is aimed to study the dissolution of rice straw powder in 1-butyl-3-methylimidazolium acetate [BMIM][OAc].

Materials and Methods

Sample

1-Butyl-3-methylimidazolium acetate [BMIM][OAc] was procured from Sigma-Aldrich and used without further purification. Rice straw sample was collected from Pyinmagyi village in Kyaukpadaung Township, Mandalay Region.

Sample Preparation

The collected sample was cut into small pieces and pulverized into powder with machine. The powdered samples were sieved with 30, 60 and 100 mesh size to obtain 0.595 mm, 0.250 mm and 0.149 mm sizes of rice straw respectively. The powdered samples were stored at room temperature.

Dissolution Experiments

Dissolution of rice straw powder in [BMIM][OAc] was carried out according to the procedure of Poornejad *et al.* (2014) with some modifications.

Investigation of the Effect of Size of Rice Straw on Dissolution in Ionic Liquid

A suspension of rice straw (0.595 mm) in [BMIM][OAc] with 2% solid loading was prepared in a 100 mL beaker. It was then put in an oil bath at 120 ºC. The suspension was stirred every 15 min by a glass rod to ensure complete distribution of solid in the solvent. At the end of the pretreatment, the dissolved solid was regenerated by sudden addition of 30 mL boiling water. The precipitated solid was recovered by vacuum filtration and washed by ethanol and boiling water till clear filtrate was achieved. The regenerated cellulose was dried at 105 ºC in oven for 3 h, and then stored in sealed bags for further use and analysis. The above procedure was also carried out with 0.250 mm and 0.149 mm rice straw samples in place of 0.595 mm rice straw while other parameters were kept constant.

Investigation of the Effect of Mass of Rice Straw on Dissolution in IL

A suspension of rice straw (0.1 g, 0.2 g and 0.3 g each) of 0.149 mm size in [BMIM][OAc] was prepared in three separate 100 mL beakers. Then the beakers were put in an oil bath at 120 ºC and heated for 30 min. The remaining procedure was the same as that described above.

Investigation of the Effect of Time on Dissolution of RS in IL

A suspension of rice straw (0.149 mm) in [BMIM][OAc] with 2 % solid loading was prepared in a 100 mL beaker. It was then put in an oil bath at 120 ºC and heated for 10 min. The suspension was occasionally stirred by a glass rod to ensure complete distribution of solid in the solvent. The remaining procedure was the same as that described above. Heating times of 30 min and 90 min were also studied using 0.2 g of rice straw (0.149 mm).

Investigation of the Effect of Temperatures on Dissolution of Rice Straw

A suspension of rice straw (0.149 mm) in the ionic liquid with 2 % solid loading was prepared in a beaker. It was heated in an oil bath at 120 ºC and the suspension was stirred every 15 min by a glass rod to ensure complete distribution of solid in the solvent. The remaining procedure was the same as that described above. The same procedure was carried out using two different temperatures of 140ºC and 160ºC while other parameters were kept constant.

Characterization Techniques

Surface morphologies of raw rice straw and regenerated cellulose were investigated by scanning electron microscope (model Jeol-JSM-5610 LV, Japan) operating at an accelerating voltage of 15 kV and 550 X magnification at Universities' Research Center, Yangon.

Fourier Transform Infrared (FT IR) spectra of raw rice straw and regenerated cellulose were recorded in a range of wavenumber from 4000 to 550 cm^{-1} on a FT IR spectrometer (FT IR-8400 SHIMADZU, Japan) at Universities' Research Center, Yangon.

X-ray diffraction patterns of raw rice straw and regenerated cellulose were recorded on X-ray diffractometer (Rigaku, Tokyo, Japan), using CuK_{α}

radiation (λ= 1.54 ˚A) at 40 kV and 40 mA at Universities' Research Center, Yangon. The intensity data were collected over a 2θ range of 10˚ to 70˚.

Results and Discussion

Effect of Size of Rice Straw on Dissolution in Ionic Liquid

The dissolution process was studied by three different sizes of rice straw (RS) *viz*., 0.595 mm, 0.250 mm and 0.149 mm. From the investigation, RS with 0.149 mm size completely dissolved in [BMIM][OAc] within 30 min at 120 ºC (Table 1). The dissolution time of RS with 0.250 mm mesh size was 90 min and that for 0.595 mm size was 110 min. The larger the size of rice straw powder the longer the dissolution time. Thus, for shorter time for dissolution, 0.149 mm size of rice straw was chosen for further experiments.

Table 1. Relationship between Size and Dissolution Time of Rice Straw in Ionic Liquid

No	Size (mm)	Dissolution time (min)
1	0.595	110
2	0.250	90
3	0.149	30

Mass of RS =0.2 g, Temperature = 120 ºC

After dissolution in [BMIM][OAc], the regenerated cellulose yield percentages were found to be 69.4±0.15%, 70.00±0.13% and 76.65±0.15% for rice straw with 0.595 mm, 0.250 mm and 0.149 mm respectively (Table 2). As the size decreased, the rice straw particles dissolved more easily and higher yield of cellulose was achieved.

Table 2: Yield Percent of Regenerated Cellulose of Rice Straw Particles

No.	Size (mm)	Mass of regenerated cellulose (g)	Yield (%)
1	0.595	0.1388	69.40±0.15
2	0.250	0.1401	70.00±0.13
3	0.149	0.1533	76.65±0.15

Mass of RS= 0.2 g, Time = 30 min, Temperature = 120 ºC

SEM analysis of regenerated cellulose obtained using different sizes of rice straw

SEM micrograph of rice straw sample in Figure 2 shows rigid and highly ordered fibrils. This compact and unavailable form could not assist and accelerate the penetration of the enzyme to the carbohydrates. Also there are spots on the rice straw. These spots are silica which is one of the problematic component of rice straw in conversion to ethanol (Poornejad *et al.*, 2014). SEM images showed that the surface morphologies of regenerated cellulose were quite different from that of raw RS. On the other hand amorphous form of cellulose were seen in the SEM images of regenerated cellulose.

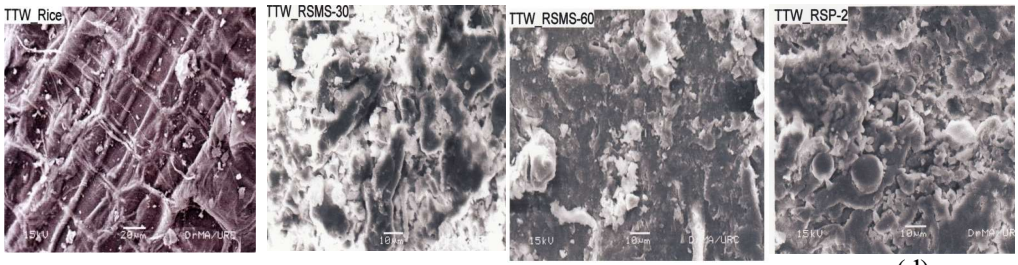

(a) (b) (c) (d)

Figure 2: SEM images of (a) raw RS and regenerated cellulose from different sizes of RS (b) 0.595 mm (c) 0.250 mm and (d) 0.149 mm

FTIR analysis of raw RS and regenerated cellulose obtained using different sizes of RS

Figure 3 shows the FT IR spectra of raw particles and regenerated cellulose from RS particle of different sizes dissolved in [BMIM][OAc]. The corresponding spectral data are shown in Table 3. A broad band around 3400 cm^{-1} was assigned to –OH stretching vibration and the bands at about 2900 and 2800 cm^{-1} attributed to asymmetric and symmetric vibration of C-H in CH_2 group. The appearance of absorption band around 1640cm^{-1} corresponds to the C-O stretching vibration of C-OH. The peak became stronger after cellulose was regenerated. The peak around 1090 cm^{-1} attributes to the C-O bond stretching vibration of C-O-C group in the anhydroglucose ring. The peaks around 900cm^{-1} corresponds to the glycosidic C-H deformation with ring vibration and O-H bending which is the characteristic of glycosidic linkages between glucose in cellulose. This peak is designed as an amorphous band which is observed only in the regenerated cellulose (Ciolacu *et al.*, 2011). This may be indicated that the crystal structure of RS transformed from crystalline to amorphous.

In addition, the FT IR absorption band around 1430 cm^{-1}, assigned to symmetric CH_2 bending vibration decreased in regenerated cellulose. This band is also known as "crystallinity band", indicating that a decrease in its intensity reflects reduction in the crystallinity of sample.

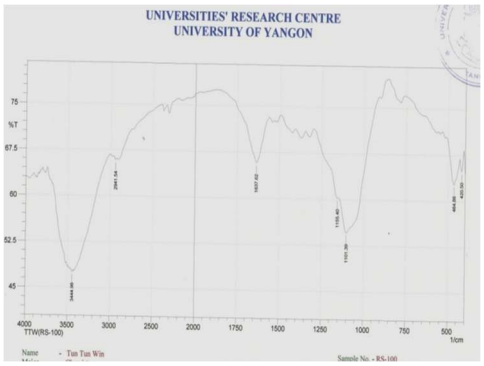

(a)

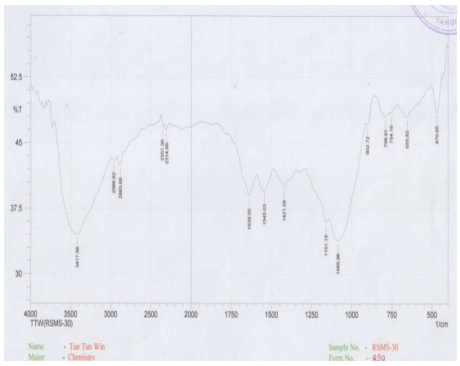

(b)

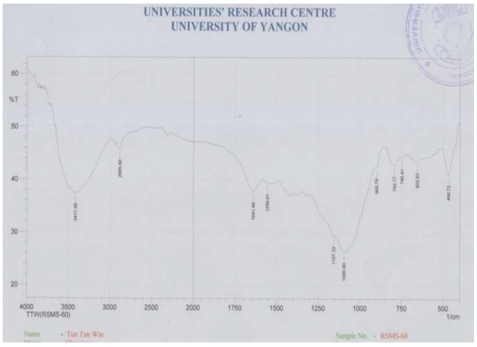

(c)

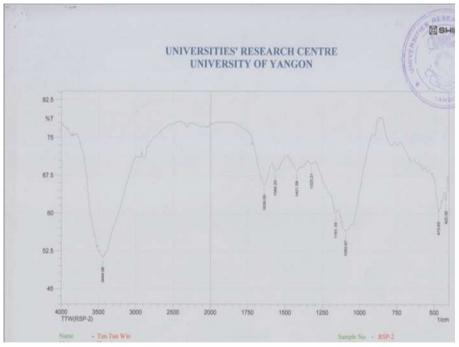

(d)

Figure 3:FT IR spectra of (a) raw RS and regenerated cellulose from different sizes of RS (b) 0.595 mm (c) 0.250 mm and (d) 0.149 mm

Table 3: FT IR Spectral Data of Raw RS Particles and Regenerated Cellulose Obtained from Different Sizes of RS

No	Observed wave number (cm^{-1})				Reported value* (cm^{-1})	Remark
	Raw RS	Regenerated cellulose				
		0.595 mm	0.250 mm	0.149 mm		
1	3444	3417	3417	3444	3362	-OH stretching vibration
2	2941	2966	2960	2966	2918	Asymmetric stretching band of C-H
3	2830	2833	2885	2880	2860	symmetric stretching band of C-H
4	1637	1639	1641	1634	1637	C-O stretching vibration of C-O-H of lignin
5	1540	1545	1556	1566	1598	C=C stretching vibration of aromatic ring (lignin)
6	1430	1421	1421	1421	1456	-CH_2symmetric bending
7	1155	1161	1157	1161	1152	C-O asymmetric vibration of C-O-C in ring
8	1101	1085	1095	1093	1079	C-O bond stretching vibration of C-O-C group in anhydroglucose ring
9	-	902	900	900	896	Glycosidic C-H deformation with ring vibration.

*Ciolacu *et al.,* (2011) ; Zheng *et al.,* (2013)

XRD analysis of raw RS and regenerated cellulose obtained using different sizes of RS

X-ray diffractograms of raw RS and regenerated cellulose obtained from different sizes of RS are shown in Figure 4. In the X-ray diffractograms of raw rice straw and regenerated cellulose samples, a peak of (101) plane at 2θ value of 22º shows the crystalline peak of cellulose structure. After the dissolution and regeneration process, the diffractograms of regenerated cellulose showed the decrease in the peak intensity. This finding indicates that IL [BMIM][OAc] breaks intermolecular and intramolecular hydrogen bonds of cellulose during dissolution process. The crystallinity percents for regenerated cellulose are shown in Table 4.The dissolution of the rice straw in [BMIM][OAc] was confirmed by decrease in crystallinity of the regenerated cellulose. The crystallinity percent was determined from the XRD analysis by the equation,

Percent crystallinity = (crystalline area / total area) x 100

Crystallinity percent of raw rice straw was 37.27%.This result in accordance with reported value of 37.72(Sakdaronnarong and Jongiertjunya, 2012). Crystallinity percents of regenerated cellulose were found to be 12.63%, 12.25 % and 12.77 % for different sizes of RS dissolved in [BMIM][OAc] for 30 min. Crystallinity percents were not much different but noticeably decreased from that of raw RS particle. From this study, 0.149 mm size rice straw was chosen for further experiments because of higher yield of regenerated cellulose.

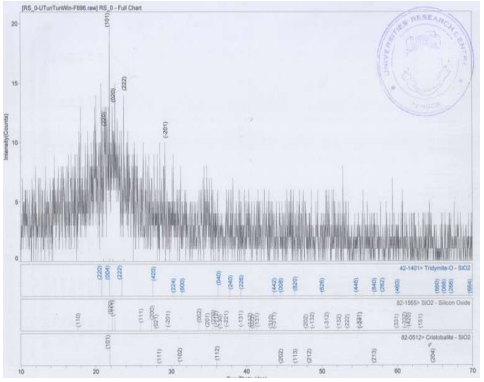

(a)

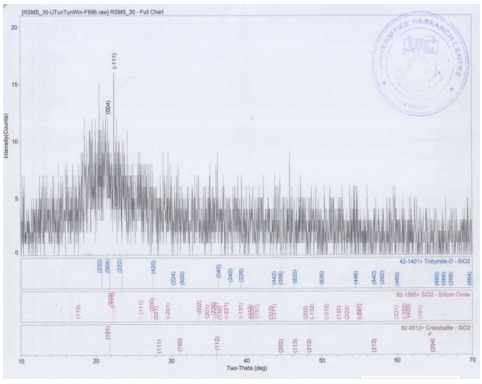

(b)

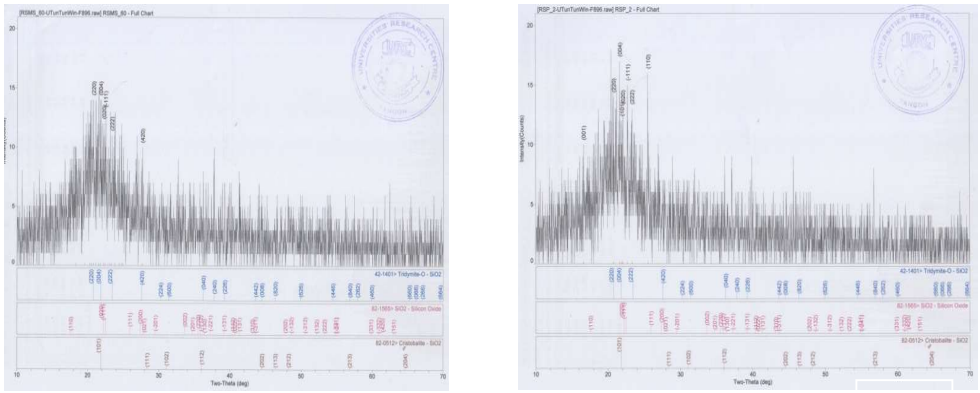

(c) (d)

Figure 4: X-ray diffractograms of (a) raw RS and regenerated cellulose from different sizes of RS (b) 0.595 mm (c) 0.250 mm and (d) 0.149 mm

Table 4: Crystallinity Percent of Regenerated Cellulose Obtained by Dissolution of Different Sizes of RS

No	Size of rice straw (mm)	Crystalline peaks area (nm^2)	Total area of all peaks (nm^2)	Crystallinity (%)
1	Raw	53.6	143.6	37.27
2	0.595	22.8	180.5	12.63
3	0.250	22.3	182.1	12.25
4	0.149	23.2	181.7	12.77

Mass of RS= 0.2 g, Temperature = 120ºC , Time = 30 min

Effects of Mass of Rice Straw on Dissolution in IL

In this study different amounts of RS powder were used to investigate the dissolution process. Yield percentages were in the range of 74.85% to 76.65% (Table 5). Highest yield percentage was obtained from 0.2 g of RS. Thus, 2 % solid loading of suspension of RS was appropriate amount for dissolution in [BMIM][OAc].

Table 5: Yield Percent of Regenerated Cellulose Obtained by Dissolution of Different Amounts of Rice Straw

No.	Amount of RS (g)	Mass of regenerated cellulose (g)	Yield (%)
1	0.1	0.0758	75.80±0.20
2	0.2	0.1533	76.65±0.15
3	0.3	0.2275	75.83±0.23
4	0.4	0.2994	74.85±0.20

Temperature = 120ºC, Time = 30 min, Size = 0.149 mm

SEM analysis of regenerated cellulose obtained using different amount of RS

SEM images of regenerated cellulose are shown in Figure 5. Regenerated cellulose showed amorphous form indicating breakage of intermolecular hydrogen bond and intramolecular hydrogen bond by the ionic liquid. Therefore, the structure of the straw was changed from a compact and unavailable form to an open up and widely accessible form. This could assist and accelerate the penetration of the enzymes to the carbohydrates.

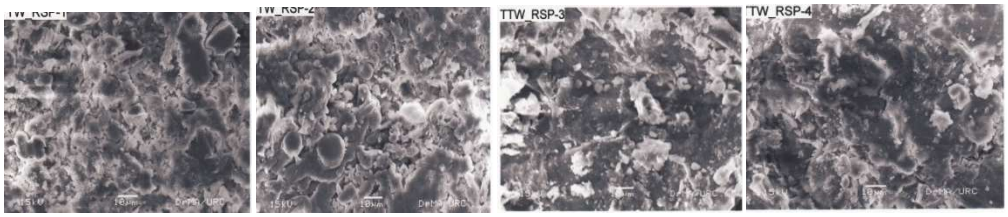

(a) (b) (c) (d)

Figure 5: SEM images of regenerated cellulose obtained from different amounts of RS (a) 0.1 g (b) 0.2 g (c) 0.3 g and (d) 0.4 g

FT IR analysis of regenerated cellulose obtained using different amount of RS

Figure 6 shows the FT IR spectra of regenerated cellulose from different amounts of RS particles dissolved in [BMIM][OAc]. The peaks around 900 cm^{-1} corresponds to the glycosidic C-H deformation with ring vibration was observed in the regenerated cellulose. This may be indicated that the crystal structure of RS transformed from crystalline to amorphous.

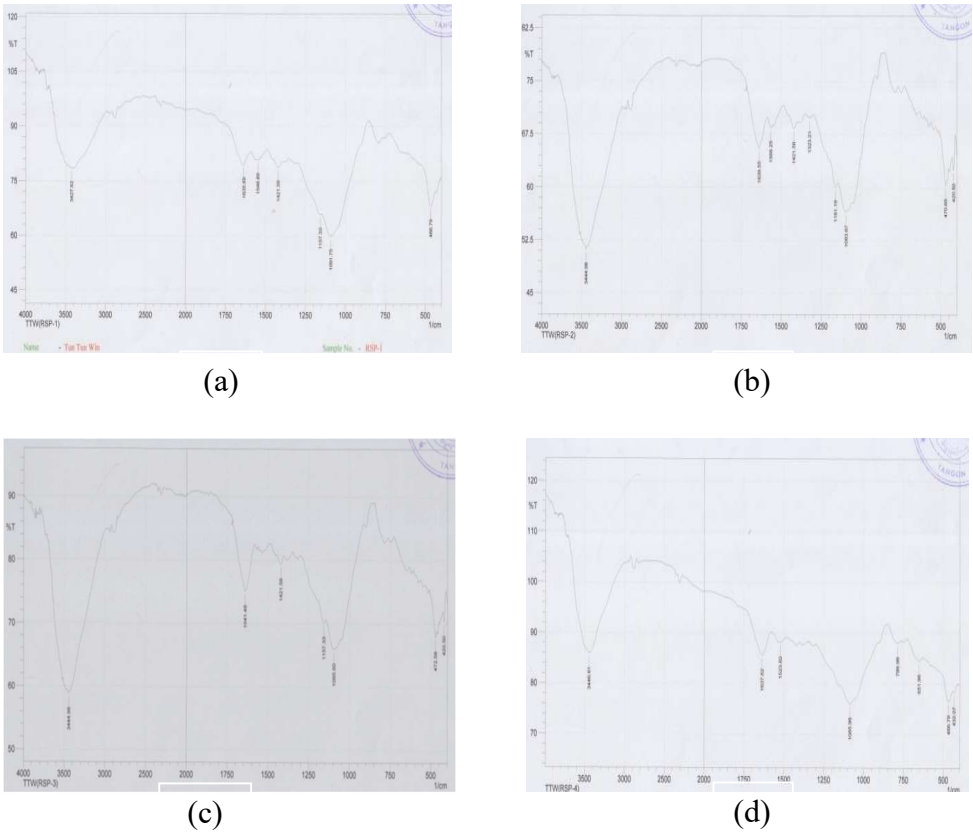

(a) (b)

(c) (d)

Figure 6: FT IR spectra of regenerated cellulose obtained from different amounts of RS (a) 0.1 g (b) 0.2 g (c) 0.3 g and (d) 0.4 g

XRD analysis of regenerated cellulose obtained using different amount of RS

X-ray diffractograms of regenerated cellulose obtained from different amounts of RS are shown in Figure 7. After the dissolution and regeneration process, the diffractograms of regenerated cellulose showed the decrease in the peak intensity of the crystalline peak at 2θ value of 22°. Breakage of intermolecular and intramolecular hydrogen bonds of cellulose by [BMIM] [OAc] was observed during dissolution process. The crystallinity percents for regenerated cellulose are shown in Table 6. Crystallinity percent of regenerated cellulose were found to be 12.37 %, 12.76 % , 9.12 % and 9.61 % for different amount of RS dissolved in [BMIM] [OAc] for 30 min. All the regenerated cellulose showed lower crystallinity percents than raw rice straw of 37.27 % indicating the transformation of crystalline to amorphous forms. It was noticed that crystallinity percents were decreased by using 0.3 g and 0.4 g of RS particles compared to 0.1 g and 0.2 g. In this study, mass of 0.2 g was chosen for further experiments because of higher yield of regenerated cellulose.

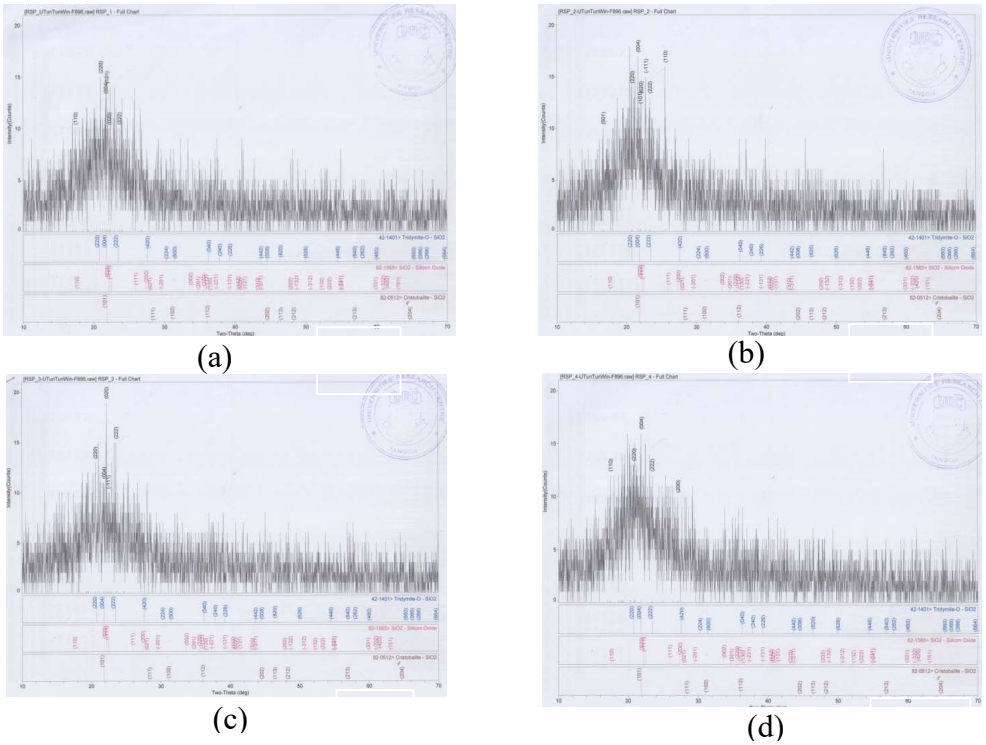

Figure 7: X-ray diffractograms of regenerated cellulose obtained from different amounts of RS (a) 0.1 g (b) 0.2 g (c) 0.3 g and (d) 0.4 g

Table 6: Crystallinity Percent of Regenerated Cellulose Obtained by Dissolution of Different Sizes of RS

No	Mass of rice straw (g)	Crystal area (nm^2)	Total area (nm^2)	% Crystallinity
1	0.1	22.2	179.4	12.37
2	0.2	23.2	181.7	12.76
3	0.3	16.1	176.4	9.12
4	0.4	18.8	195.5	9.61

Temperature = 120 ºC, Time = 30 min, Size= 0.149 mm

Effect of Time on Dissolution of RS in IL

In this study, effect of time on the dissolution of RS powder in IL was investigated at 120 ºC for 10 min, 30 min and 90 min. Yield percentage of regenerated cellulose was shown in Table 7. Yield percentage increased as the dissolution time increased. Higher yield percents were obtained for 30 min and 90 min dissolution times. It was noted that 10 min dissolution time was not sufficient for complete dissolution. Since yield percent of regenerated cellulose was not much different for 30 min and 90 min shorter dissolution time of 30 min was chosen for pretreatment of the rice straw.

Table 7: Yield Percentage of Regenerated Cellulose of RS Powder during Different Dissolution Time

No.	Time (min)	Regenerated Cellulose (g)	Yield (%)
1	10	0.0490	24.50±0.22
2	30	0.1533	76.65±0.15
3	90	0.1561	78.05±0.22

Mass of RS=0.2 g, Temperature=120ºC, Size = 0.149 mm

SEM analysis

Figure 8 shows SEM images of regenerated cellulose. It was observed that the organized structure of RS is not completely destroyed in regenerated cellulose observed from 10 min dissolution time. The Change in the structure of RS was observed in widely accessibly amorphous form in regenerated cellulose by using dissolution times of 30 min and 90 min. This could assist and accelerate the penetration of the enzyme to carbohydrate.

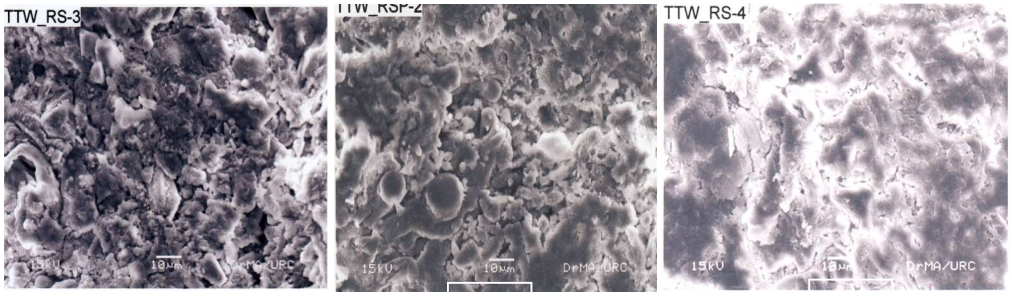

(a) (b) (c)

Figure 8: SEM images of regenerated cellulose obtained using different dissolution times (a) 10 min, (b) 30 min and (c) 90 min of RS at 120 ºC

FT IR analysis of regenerated cellulose obtained using different dissolution times

FT IR spectra of regenerated cellulose obtained by different dissolution times are shown Figure 9. As noted as earlier, C=C stretching of aromatic ring of lignin peak around 1630 cm^{-1}became shorter as compared to that of raw RS. Crystallinity peak around 1430 cm^{-1} due to bending of C-H in - CH_2 decreased and amorphous peak around 900 cm^{-1}appeared in regenerated cellulose. This indicates the breakage of inter- and intra-hydrogen bonds of cellulose. It was also noted that the peak around 1630 cm^{-1} in regenerated cellulose obtained for 30 min and 90 min dissolution times are shorter than that obtained for 10 min. The crystal peak around 1430 cm^{-1} obtained for 10 min dissolution time is more intense than those for 30 min and 90 min. It indicates that dissolution time for 10 min is not sufficient for complete dissolution.

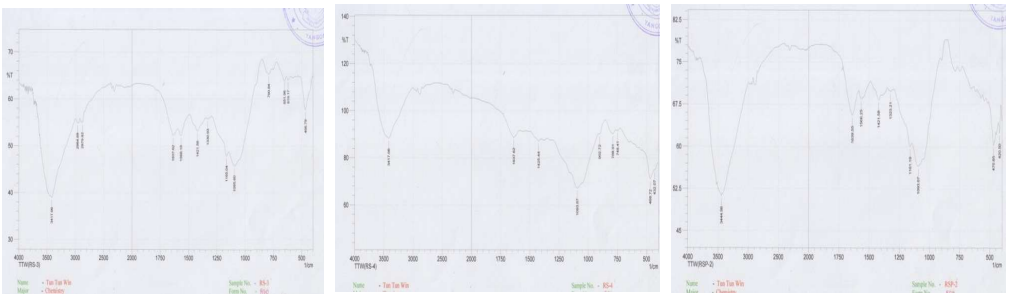

Figure 9: FT IR spectra of regenerated cellulose obtained from (a) 10 (b) 30 and (c) 90 min dissolution times

XRD analysis of regenerated cellulose obtained using different dissolution times

XRD patterns of regenerated cellulose obtained by different dissolution times are shown in Figure 10. Amorphous form of cellulose were seen by the diffuse lines in the XRD patterns. As shown as before crystalline peak of (101) plane at 2θ of 22º became less intense indicating the change of crystalline to amorphous form. X-ray diffractogram of regenerated cellulose obtained for 10 min show crystalline peak at 2θ =22º indicating dissolution time for 10 min is not sufficient for complete dissolution.

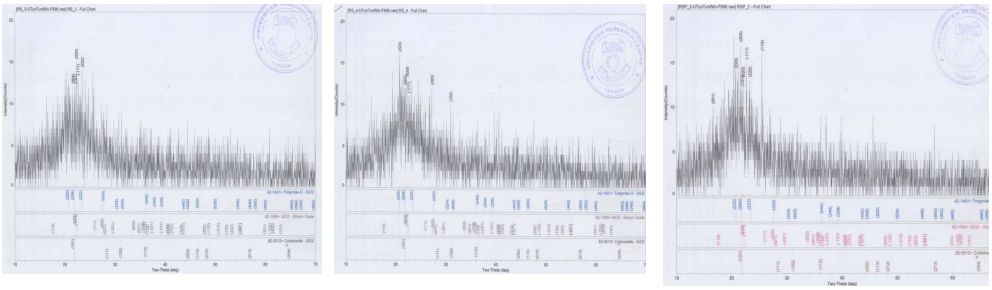

(a) (b) (c)

Figure 10: X-ray diffractograms of regenerated cellulose obtained from (a) 30 (b) 60 and (c) 90 min dissolution times

The crystallinity percent of regenerated cellulose obtained by dissolution time of 10 min was found to be higher than those obtained by 30 min and 90 min (Table 8). This is because within 10 min RS did not completely dissolve in IL. RS powder were found to completely dissolved within 30 min. The crystallinity percent of regenerated cellulose obtained by dissolution time of 30 min was slightly higher than that of 90 min.

Table 8: Crystallinity Percent of Regenerated Cellulose Obtained by Dissolution of Different Times

No	Time (min)	Crystalline peak area (nm^2)	Total peak area (nm^2)	Crystallinity (%)
1	10	36.2	176.4	20.52
2	30	23.2	179.8	12.96
3	90	23.2	181.7	12.78

Mass of RS=0.2 g, Temperature = 120 ºC, Size= 0.149 mm

Effect of Temperature on Dissolution of RS in IL

Three different temperatures *viz.,* 120 ºC, 140 ºC and 160 ºC were chosen to study the effect of temperature on dissolution of RS powder. It was observed that at 120 ºC RS powder completely dissolved within 30 min (Table 9). When the temperature was increased to 140 ºC the dissolution time decreased to 25 min whereas at 160 ºC the dissolution time was found to be 10 min. It was reported that 1-ethyl-3-methylimidazolium acetate, [Emim][OAc], is very effective at 160 °C for dissolution of rice straw within 10 min (Myint *et al*., 2015; Myint *et al*., 2016).

Table 9: Dissolution Time of RS powder in [BMIM][OAc] with Different Temperatures

No	Temperature (ºC)	Dissolution time (min)
1	120	30
2	140	25
3	160	10

Mass of RS =0.2 g, Size =0.149 mm

Yield % of regenerated cellulose at 120 ºC, 140 ºC and 160 ºC are shown in Table10. It was found that yield percentage of regenerated cellulose at 120 ºC was 76.65%. As the temperature increased the yield percentage of regenerated cellulose were found to decrease, *i.e.,* at 140 ºC was 63.58 % and at 160 ºC was 60.85 % .

Table 10: Yield Percentages of Regenerated Cellulose Obtained from Dissolution Different Temperatures and Times

No	Temperature (ºC)	Dissolution time (min)	Mass of regenerated cellulose(g)	Yield (%)
1	120	30	0.1533	76.65±0.15
2	140	25	0.1271	63.58±1.5
3	160	10	0.1217	60.85±0.30

Mass of RS =0.2 g, Size= 0.149 mm

Conclusion

Dissolution of rice straw powder in ionic liquid (IL) of [BMIM][OAc] was investigated in this study. Among three different sizes of rice straw (0.595 mm, 0.250 mm and 0.149 mm), the highest yield percent (76.65 %) was obtained using smallest size of 0.149 mm. Effect of mass of RS on dissolution in [BMIM][OAc] revealed that higher yield percent was achieved using 0.2 g of RS. Effect of dissolution time on regeneration of cellulose was studied for 10 min, 30 min and 90 min and the lowest yield percent (24.50 %) was obtained for the shortest dissolution time. The yield percentages of regenerated cellulose were comparable, i.e., 76.65 % and 78.08 % for dissolution time of 30 min and 90 min respectively. Shorter dissolution time of 30 min was chosen for treatment of RS. For ease of carrying out the experiment, 120 ºC was chosen for dissolution of RS. SEM images of regenerated cellulose samples showed the destruction of the highly ordered fibrils of raw rice straw. FT IR spectral data showed that the peak intensities of 1630 cm^{-1} and 1430 cm^{-1} (crystalline peak) decreased in all regenerated cellulose sample compared to those of raw RS. Amorphous peak of cellulose (900 cm^{-1}) appeared after dissolution and regeneration of cellulose. After dissolution in [BMIM][OAc] and regeneration, the intensity of the crystalline

peak of (101) plane at 2θ value of 22º in raw RS sample decreased in all regenerated cellulose samples. Crystallinity percents of regenerated cellulose were lower than that of raw RS indicating the breakage of inter- and intra-hydrogen bonding in cellulose. Based on the results, the suitable conditions for dissolution of RS powder in [BMIM][OAc] were chosen as 0.2 g of 0.149 mm size RS with dissolution temperature for 30 min at 120 ºC for pretreatment of rice straw powder for bioethanol preparation.

Acknowledgements

The authors would like to express their profound gratitude to the Department of Higher Education (Yangon office), Ministry of Education, Yangon, Myanmar, for provision of opportunity to do this research.

References

Alvira, P., Tomás-Pejó, E., Ballesteros , M. and Negro, M.J. (2010). "Pretreatment Technologies for An Efficient Bioethanol Production Process Based on Enzymatic Hydrolysis: A Review". *Bioresour Technol*, vol.101, pp.4851–4861.

Anderson, J.L., Ding, J., Welton, T. and Armstrong, D.W. (2002)."Characterizing Ionic Liquids on the Basis of Multiple Solvation Interactions". *Journal of the American Chemical Society,* vol.124, pp.14253-14254.

Brennecke, J. F. and Maginn, E. J. (2001). "Ionic liquids: Innovative Fluids for Chemical Processing". *AIChE Journal,* vol.47(11), pp.2384-2389.

Chatterjee, C., Pong, F. and Sen, A. (2015). "Chemical Conversion Pathways for Carbohydrates". *Green Chem.* vol.17, pp.40–71.

Ciolacu, D., Ciolacu, F. and Popa, V. I. (2011) . "Amorphous Cellulose –Structure and Characterization. *Cellulose Chem. Technol.,*vol.45 (1-2), pp.13-21

Fort, D. A., Remsing, R.C., Swatloski, R.P., Moyna, P. and Rogers, R.D. (2006)."Can Ionic Liquids Dissolve Wood? Processing and Analysis of Lignocellulosic Materials with 1-n-Butyl-3-Methylimidazolium Chloride". *Green Chemistry*, vol.9, pp. 63-69.

Larsson, S., Palmqvist, E., Hahn-Hägerdal, B., Tengborg, C., Stenberg, K., Zacchi, G. and Nilvebrant, N.O. (1999). "The Generation of Fermentation Inhibitors during Dilute Acid Hydrolysis of Softwood". *Enzyme and Microbial Technology*, vol.24, pp.151-159.

Li ,C., Knierim, B., Manisseri, C., Arora, R., Scheller, H. V., Auer, M., Vogel, K.P., Simmons, B.A. and Singh, S. (2010). "Comparison of Dilute Acid and Ionic Liquid Pretreatment of Switchgrass: Biomass Recalcitrance, Delignification and Enzymatic Saccharification". *Bioresour Technol.* vol.101, pp.4900–4906.

Mood, S. H., Golfeshan, A.H., Tabatabaei, M., Jouzani, Gh. S., Najafi, Gh., Gholami, M. and Ardjmand, M. (2013). "Lignocellulosic Biomass to Bioethanol; A Comprehensive Review on Pretreatment". *Renew Sust Energ Rev*, vol. 27, pp.77-93

Myint, H. H., Kurniawan, W., Hinode, H., Sein, N.N., Salim, C. and Cross, J. S. (2015). "Dissolution Model of Ball Milled Rice Straw Particles in 1-Ethyl-3-Methyl Imidazolium Acetate at Elevated Temperature". *J Bioprocess Biotech*., vol., 5(11), p. 260

Myint, H. H., Kurniawan, W., Hinode, H., Sein, N. N. and Cross, J. S. (2016). "Optical and Confocal Microscopic Studies on Dissolution of Rice Straw Particles in 1-Ethyl-3- Methylimidazolium Acetate ." *ASEAN Engineering Journal Part B,* vol. 5(2), pp. 4-18

Poornejad, N., Karimi1, K. and Behzad, T. (2014) . "Ionic Liquid Pretreatment of Rice Straw to Enhance Saccharification and Bioethanol Production" . *Journal of Biomass to Biofuel*, vol.1, pp.8-13

Sakdaronnarong, C. and Jonglertjunya, W. (2012). "Rice Straw and Sugarcane Bagasse Degradation Mimicking Lignocellulose Decay in Nature: An Alternative Approach to Biorefinery". *Science Asia*, vol. 38, pp. 364-372

Tuck, C.O., Pérez, E., Horváth, I. T., Sheldon, R. A. and Poliakoff, M. (2012). "Valorization of Biomass: Deriving More Value from Waste". *Science* , vol. 337, pp.695–699.

Yong, J. L. (2005). *Oxidation of Sugarcane Bagasse Using a Combination of Hypochlorite and Peroxide*. MSc Thesis, The Department of Food Science, Chonnam National University.

Zheng, C. Y., Tao, H. X. and Xie, X. A. (2013). "Distribution and Characterization of Liquefaction of Cellulose in Sub-and Super-Critical Ethanol: Liquefaction of Biomass". *Bio Resources*, vol.8(1), pp.655-656.

PREPARATION OF CELLULOSE HYDROGEL FILMS FROM SUGAR CANE BAGASSE

Thinzar Aye[1], Thinzar Nu[2], Cho Cho[3]

Abstract

Several million dry tons of sugar cane bagasses are annually produced throughout the world. Bagasse is a waste product mainly deriving from sugar cane production. Thus, sugar cane bagasse is a big problem of their production. As a result, convertion of bagasse to valuable products like cellulose hydrogel films is important issues to be concerned. In the present work, sugar cane bagasse was used as a cellulose resource which was chemically treated using sulphuric acid (H_2SO_4) and sodium hydroxide (NaOH).When this pretreated sample was bleached by sodium hypochlorite (NaOCl), treated bagasse cellulose fiber was obtained. FTIR, SEM and XRD measurements were used to characterize the properties of raw and treated fiber samples. Following this, solvent exchange processes were performed by use of water, ethanol and Dimethylacetamide (DMAc) respectively. Using (DMAc/LiCl) system was possible to obtain cellulose hydrogel solution and cellulose hydrogel film was prepared by phase inverse method without cross linker. The resultant hydrogel film was found to be transparent and flexible.

Keywords: cellulose hydrogel film, sugar cane bagasse, cellulose, phase inverse method

Introduction

In recent years, there has been an increase in the level of research on the development of new biodegradable materials for use in packaging, agriculture, medicine and other areas. Generally, biodegradable polymer materials are increasingly important as environmental contamination and waste disposal problems associated with plastics and related products from synthetic polymers become more severe. Natural polymers have various advantages over synthetic polymers due to their low-cost, great availability and biodegradability (Zhou, *et al.,* 2008).

Cellulose hydrogel has become especially attractive to "tissuse engineering" as matrices for repairing and regenerating a wide variety of tissue and organs. Hydrogels consisted of hydrophilic polymer networks

1. 2 PhD, Candidate, Department of Chemistry, University of Yangon
2. Associate Professor, Department of Chemistry, University of Yangon
3. Professor, Department of Chemistry, Yenangyaung Degree College

which can absorb from 10-20 % up to thousands of times of their dry weight in water. Various hydrogels from natural polymers were fabricated by using hyaluronate, chitosan and its derivatives, and cellulose in which there is a potential application in the biomaterials field. Among them, cellulose is the most abundant renewable resource on earth and may become a main chemical resource in the future. Therefore, this sustainable material in plants has numerous functional possibilities and can be expected with the demand for environmentally and biocompatible products (Svensson *et al.,* 2005). A wide range of lingocellulosic agricultural by-products has successfully been converted into cellulose hydrogel film including agave tequilana Weber bagasse (Karla Lizette Tovar Carrillo *et al*., 2013), sugar cane bagasse (Kazuki Nakasone *et al*., 2016).

Sugarcane bagasse (SB), as the fibrous by-product remaining after sugar extraction from sugarcane, is one of the most important byproducts. About 54 million dry tons of SB are produced annually throughout the world (Ren *et al.,* 2006). Bagasses offer the advantages of being a cheap, plentiful and low polluting fuel (Mothe and Miranda, 2009). Commonly, all plant biomass consists of cellulose, hemicellulose, lignin, pectin and protein. Most of the plant biomass consists of about 33 % of cellulose as the major component of the rigid cell walls. Table 1. shows the percentage composition of sugarcane bagasse.

Table 1: Percentage Composition of Sugarcane Bagasse

Component	**%Composition***
Cellulose	43.6
Hemicellulose	33.5
Lignin	18.1
Ash	2.3
Wax	0.8
Other	0.7

Sun *et al.,* 2004

Cellulose is a linear and high molecular weight polymer as well as natural, renewable and biodegradable material (Rachtanapun, 2009). Cellulose is aligned parallel to each other in fibrils, which are surrounded by a matrix of lignin and hemicellulose (Figure 1). In addition, cellulose has properties such as low density, good mechanical properties as well as biodegradability. Cellulose, the major chemical component of fiber wall and contributing 40-45% of the dry weight. It is composed of linear chain of D-glucose linked by β-1,4-glycosidic bond with the degree of polymerization (DP) from 10,000 in native wood to 1,000 in bleached kraft pulps. Each D-anhydroglucopyranose unit possesses hydroxyl groups at C2, C3, and C6 positions, capable of undergoing the typical reactions known for primary and secondary alcohols. The molecular structure imparts cellulose with its characteristic properties: hydrophylicity, chirality, degradability, and broad chemical variability initiated by the high donor reactivity of hydroxyl groups.

Cellulose has a strong tendency to form intra - and inter-molecular hydrogen bonds by the hydroxyl groups on these linear cellulose chains, which stiffen the straight chain and promote aggregation into a crystalline structure and give cellulose a multitude of partially crystalline fiber structures and morphologies. Crystalline cellulose has very limited accessibility to water and chemicals (Edgar *et al.,* 2001).

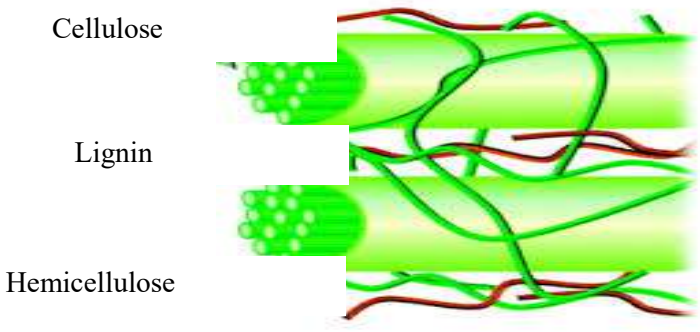

Figure 1: Components of primary cell wall

It is well known that native cellulose is very difficult to dissolve in common solvents. This is due to formation of strong hydrogen bond between abundant hydroxyl groups in the polymer chains. In addition, crystalline and

aggregated fibers of the cellulose also make it difficult in the solubilization. For this reason, studies on native cellulose hydrogel are fewer than cellulose derivatives. Therefore, solvents such as alkali-based aqueous system, N-methylmorpholine-N-oxide (NMMO), lithium chloride (LiCl)/ N, N-dimethylacetamide (DMAc) and ionic liquids (ILS) were developed for cellulose dissolutions. These solvent system provides great opportunities to prepare native cellulose hydrogel through physical cross-linking (Striegel, 1997).

For cellulose hydrogel films preparation has been reported by which a DMAc/LiCl system enables flexible cellulose hydrogel films using phase inversion processes. Hydrogels are networks of hydrophilic polymer chains in natural or synthetic polymers. They are highly water absorbent without being soluble in water. Here, the phase inversion process involves transformation from a liquid phase polymer solution to a solid state of the polymer (Kazuki and Kobayashi, 2016). In the present study, sugar cane bagasse was used to obtain cellulose hydrogel solution and the hydrogel film.

Materials and Methods

Collection of Sugar Cane Bagasse

Sugar cane bagasse was collected from Nawaday Sugar Mill, Pyay Township, Bago Region.

Bagasse Treatment

The bagasse was firstly washed with distilled water to remove remaining sugar components and then heated in oven at 50˚C. For acid treatment, 10 g of bagasse was added into 300 mL of 4 vol% H_2SO_4 aqueous solution and stirred for 2 h at 90 ˚C. Then, sample was washed with abundant distilled water five times to eliminate residues of the H_2SO_4 solution. And then 300 mL of 10 wt% NaOH solution was added and kept under stirring for 12 h at 90 ˚C until a black liquor solution was obtained. The residues of fiber were washed with excess distilled water until neutral pH. After that the fiber was added into 300 mL of 10 vol% NaOCl solution and stirred for 3 h at 40˚C. NaOCl was used as bleaching agent to obtain light colored fiber for

preparation of cellulose solution. Figure 2 shows sugar cane bagasse raw sample, acid treated sample, base treated sample and cellulose fiber. The obtained cellulose fiber was used for preparation of cellulose solution in DMAc/LiCl system.

(a) (b) (c) (d)

Figure 2: (a) Sugar cane bagasse raw sample (b) acid treated sample (c) base treated sample and (d) cellulose fiber

Preparation of Cellulose Solution

The treated bagasse cellulose fiber (1 g) was stirred in 300 mL of distilled water at room temperature for 24 h to swell the fiber. After the swelling fiber was filtered by an adapter glass filter under vacuum, ethanol (300 mL) was added to the swelled fiber and the mixture was stirred for 24 h at room temperature. Ethanol was removed and the swelled fiber was added to 300 mL of DMAc. The mixture was then left overnight under stirred condition. Both dried LiCl and DMAc were added to the swelled bagasse fiber to dissolve the cellulose fiber and stirred at room temperature for 3 days. About 1 wt% cellulose in DMAc/LiCl containing 8 wt% LiCl was obtained.

Preparation of Cellulose Hydrogel Films

For preparation of cellulose hydrogel films, 10 g of cellulose solution was poured into glass dish (9.1 cm diameter), and kept for 24 h in a plastic container filled with ethanol. In this step, cellulose was gradually progressed in the vapor at room temperature. Finally, the cellulose hydrogel film was obtained by the phase inversion process from liquid to solid gel. The resultant transparent film as shown in Figure 3 was washed with excess distilled water and then placed in distilled water for 24 h to remove DMAc. The obtained

hydrogel films were kept in plastic container filled with distilled water until further experiments.

Figure 3: Transparent cellulose hydrogel film from sugar cane cellulose fiber

Characterization

The formation of prepared samples was monitored by FTIR, SEM and XRD. The structural changes of samples were analyzed by FTIR spectrometer (FTIR – 8400 SHIMADZU, Japan). FTIR analysis was in a range of wave number from 4000 to 400 cm^{-1}. Surface morphology of the samples was investigated by SEM (JSM-5610 LV Scanning Microscope, JEOL, Japan). X-ray diffraction pattern of the sample was recorded on X-ray diffractometer (Rigaku, Tokyo, Japan), using CuK_{α} radiation (λ= 1.54 Å) at 40 kV and 40 mA. The diffraction angle ranged from 10˚ to 70˚ of 2θ.

Results and Discussion

Figure 4 shows FTIR spectra of the sugarcane bagasse, treated fibers and cellulose fibers at different treatment conditions. The FTIR spectra of all sample show the strong broad band around 3400 cm^{-1}which is due to the O-H stretching vibration. The strong band at around 2900 cm^{-1} which is due to C-H stretching vibration referred to CH_2 group. The absorption band at around 1730 cm^{-1} indicates the C=O stretching in carbonyl group of pyrone. Appearance of the band around 1600 cm^{-1} is a relative pure ring stretching mode strongly associated with the aromatic ring C=C in benzene as well as in pyrone ring. From the comparison of the FTIR spectra, the appeared peaks around 1510 cm^{-1} showed the presence of lignin and lignocellulose in the initial raw sample. Moreover, the band around 1200 cm^{-1} disappeared in

treated fiber which is assigned the removal of hemicelluloses. This clearly indicated that the amount of lignin from the sugar cane bagasse raw sample was successfully reduced by the chemical and temperature treatments.

SEM microphotographs of treated samples indicated the clearly appearance surface morphologies of the samples. Figure 5(a) is SEM micrograph of sugar cane bagasse sample which shows the major constituents of natural fibers such as cellulose, hemicelluloses and lignin. The SEM images of treated samples in Figures 5(b) and (c) have been changed in their morphologies due to the removal of lignin and hemicelluloses. Finally Figure 5(d) can be seen that the main structural unit of cellulose in the plant wall consists of cellulose microfibrils bonded together in a polymeric matrix.

XRD measurement was carried out to evaluate the effect of treatment condition on the crystalline structure of bagasse, treated fibers and cellulose fibers. Figure 6 shows the XRD patterns of the bagasse and the purified fibers. The patterns of (a) – (d) exhibited typical crystalline lattice of cellulose with peaks at 22.3˚ and 16.4˚. The crystalinity indexes of sugar cane bagasse raw sample, acid treated sample, base treated sample and cellulose fiber were 44.1%, 58.8%, 59.1% and 60.2% respectively. The increment of crystalinity in cellulose fiber was due to the removal of hemicelluloses and lignin by NaOH and NaOCl treatment.

The crystalinity index (CI) was calculated by using following equation:

$$CI\ (\%) = (I_{002} - I_{am}) / I_{002} \times 100$$

I_{002} = the maximum intensity of the peak (002) lattice diffraction

I_{am} = the intensity of diffraction attributed to amorphous cellulose

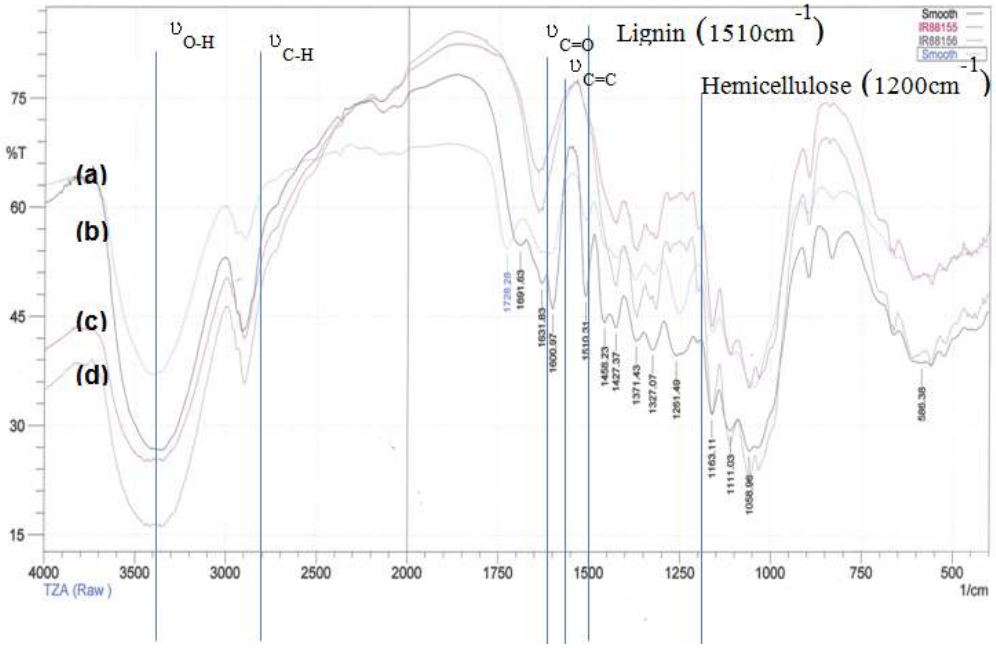

Figure 4: FTIR spectra of (a) sugar cane bagasse raw sample (b) acid treated sample (c) base treated sample and (d) cellulose fiber

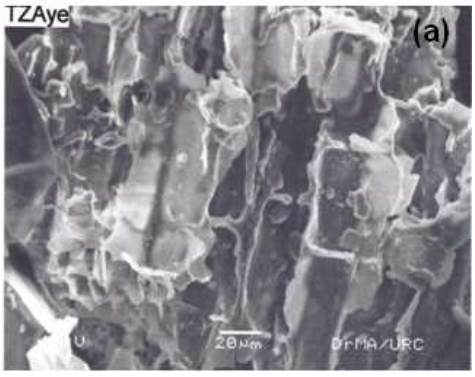

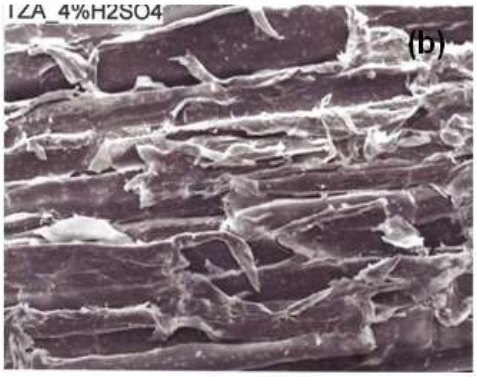

Figure 5: SEM photographs of (a) sugar cane bagasse raw sample (b) acid treated sample (c) base treated sample and (d) cellulose fiber

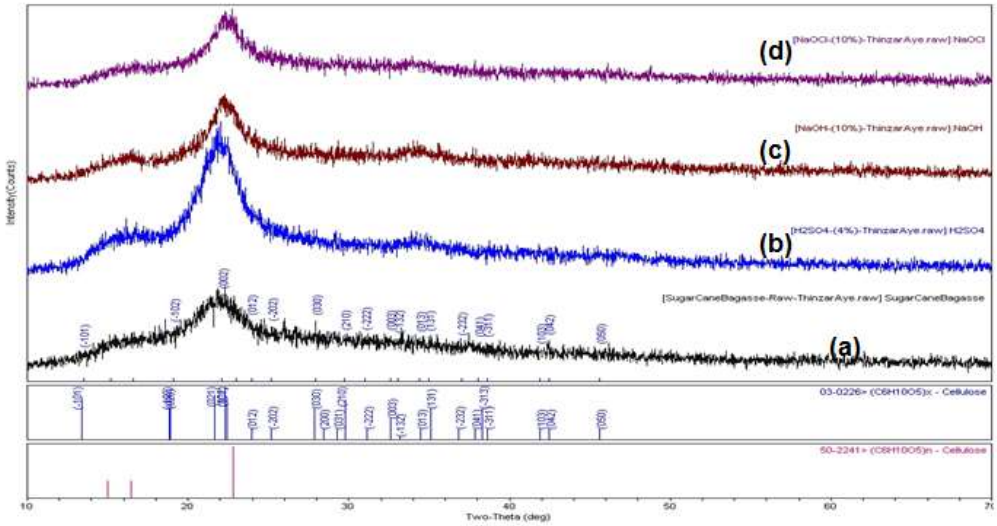

Figure 6: XRD patterns of (a) sugar cane bagasse raw sample (b) acid treated sample (c) base treated sample and (d) cellulose fiber

Conclusion

The sugar cane bagasse was used as starting material which was treated using sulphuric acid, sodium hydroxide and then bleached with sodium hypochlorite. The treated samples were characterized by FTIR, SEM and XRD. From the XRD data, crystalinity indexes of sugar cane bagasse raw sample, acid treated sample, base treated sample and cellulose fiber were 44.1%, 58.8%, 59.1% and 60.2% respectively. SEM and FTIR analyses clearly showed that the amount of liginin and hemicellulose from sugar cane bagasse sample was successfully reduced by chemical treatment and also proved that the final product was cellulose fiber. From the observation, obtained bagasse fiber was pure cellulose fiber which was used for preparation of cellulose hydrogel films. Sugar cane bagasse hydrogel films were successfully prepared by phase inversion of the DMAc solution with LiCl. Later, sugar cane bagasse cellulose hydrogel films will be utilized for biomedical applications.

Acknowledgements

The authors wish to thank to Professor Dr Daw Hla Ngwe, Head of the Department of Chemistry, University of Yangon for her encouragement. Warmest thanks are also extended to Professor Dr Ye Chan, Head of Department, Universities' Research Centre, University of Yangon for providing necessary research facilities

References

Edgar, K.J., Buchanan C.M., Debenham J.S., Rundquist P.A., Seiler B.D., Shelton M.C. and Tindall D. (2001). " Advanced in Celluloic Ester Performance and Application*", Prog. Polym. Sci,* vol. 26**,** pp.1605

Karla, L.T., Satoshi S.S., Tagaya M. and Kobayashi T. (2013). " Fibroblast Compatibility on Scaffold Hydrogels Prepared from Agave Tequilana Weber Bagasse for Tissue Regeneration "*.J.Ind.Eng.Chem.Res*.,vol.52,pp.11607-11613

Kazuki, N. and Kobayashi T. (2016). " Effect of Pre-treatment of Sugar Cane Bagasse on the Cellulose Solution and Application for the Cellulose Hydrogel Films". *J. Polym. Adv. Technol*.,vol. 27, pp. 973-980

Mothe, C.G. and Miranda I.C. (2009). "Characterization of Sugarcane and Coconut Fibers by Thermal Analysis and FTIR". *Journal of Thermal Analysis and Calorimetry*, vol. 97 (2), pp. 661- 665

Rachtanapun, P. (2009). "Blended Films of Carboxymethyl Cellulose (CMCp) from Papaya Peel and Corn Starch". *Kasetsart Journal (Natural Sciences)*, vol. 43(5), pp. 259-266

Ren,J., Kong W. and Sun R. (2006). "Bagasse-acrylic Absorbent". *Journal of bioresources*, vol. 9 (2), pp. 3290-3303

Svensson, A., E. Nicklasson, Harrah T., Panilaitis B., KaplanD. L., Brittberg M. and Gatenholom P. (2005). "Bacterial Cellulose as a Potential Scaffold for Tissue Engineering of Cartilage". *Biomaterials* , vol. 26, pp. 419

Striegel, A., (1997). "Theory and Applications of DMAc/LiCl in the Analysis of Polysaccharides, Carbohydr. Polym.". vol. 34, pp. 267-274

Sun, J.X., Sun X.F., Zhao H. and Sun R.C. (2004). "Isolation and Characterization of Cellulose from Sugarcane Bagasse". *Polymer Degradation and Stability*, vol. 84, pp. 331-339

Zhou, R., Mo Y., Li Y., Zhao Y., Zhang G. and Hu Y. (2008). "Quality and Internal Characteristics of Huanghua Pears (Pyrus pyrifolia Nakai, cv. Huanghua) Treated with Different Kinds of Coating during Storage". *Postharvest Biology and Technology*, vol 49, pp. 171-179

AN INVESTIGATION ON THE EFFECTIVENESS OF PREPOLYMERIZATION, DRYING AGENTS AND PROTECTIVE COATING ON THE CHARACTERISTICS OF LACQUERWARE*

Phyo Phyo Thwe[1], Thwe Linn Ko[2], Pansy Kyaw Hla[3]

Abstract

Thitsi (Myanmar Lac) sample was collected from Kawlin Township, Sagaing Region during October and November, 2012. The physico-chemical characteristics of raw and prepolymerized (purified) Thitsi such as colour, odour, ash, viscosity, boiling range, pH and specific gravity were determined. Moreover, chemical constituents such as moisture and volatile matter, thitsiol, nitrogenous matter, gummy matter and fatty or oily matter were investigated. Bamboo lacquerwares were prepared by applying raw and purified Thitsi several time and hardened in the underground cellar. Effect of number of coating and drying agents on the hardening time of Thitsi-coat on lacquerwares were investigated at the relative humidity (70 – 87)% and the temperature (27.1 – 31.8)ºC of the underground cellar. Evaluation of the quality of the prepared lacquerwares was studied by investigating the pencil hardness, cross hatch, adhesion, coating thickness, specular gloss, immersion resistances, resistance to steam at 100ºC, and weathering resistance were determined. The best quality of lacquerware was achieved by restricted increased number of coatings and lacquerwares coated six or seven times occupied the perfectness. Although drying agents can accelerate the polymerization time, it can impair the properties of lacquerware. Thitsi coated lacquerwares are safe and adaptable for use in house-hold purposes and can also be kept in special environments for several years without diminution of their aesthetic attraction. Additionally, the quality of lacquerware was upgraded by applying a protective coating to give a high gloss lacquerware with a lesser number of consecutive lacquer coatings (two coats) and the upgraded ware could be employed for exterior uses.

Keywords: Thitsi, kurome lacquer, prepolymerize, underground cellar, specular gloss

1. Dr, Assistant Lecturer, Department of Industrial Chemistry, Yadanabon University
2. Dr, Professor, Department of Industrial Chemistry, University of Mandalay
3. Dr, Professor (Retired), Department of Industrial Chemistry, University of Yangon

*. **Best Paper Award winning Paper in Industrial Chemistry, (2017)**

Introduction

Lacquer used in Myanmar is called "Thitsi", literally meaning wood varnish. It is the sap of *Melanhorrea usitata*, a tree native to Southeast Asia. Lacquer tree grows wild up to elevations of three thousand feet in the drier forests of Myanmar. There seems to have been no attempt to cultivate it using plantation management techniques (Fraser-Lu, 1996).

Thitsi consists of phenolic matter, water, gum, nitrogen containing matter and laccase, all of which are known to be necessary for hardening of Thitsi. No organic solvent evaporates during the drying process, only water. Because of the self-drying system, natural lacquer is an eco-friendly product that is expected to be useful in the future as a coating material (http://www. intechopen.com). Thitsi was first used as an adhesive for fixing gold foil, chipped porcelain, or attaching arrowheads to the wooden shaft. Then, with the accumulation of experience and awareness, Thitsi was applied to bamboo, wood and other furniture. It is still used in daily life in crafts and industrial equipment (http://www.jsaweb.recent-advances-in-research-on-lacquer-allergy. html).

Indeed, lacquerware has many of the characteristics of modern plastic. It is light, waterproof, easily moulds and dries to a hard state. It can be applied to virtually any surface: plain or carved wood, bamboo, paper, fabric, even metal and stone. It stiffens, strengthens and preserves the surface to which it is applied. It is decorative, inexpensive, hygenic and can be painted, moulded, and carved. When polished, it takes on a flawless sheen (Fraser-Lu, 1996).

The objectives of this study were to get the scientific data concerning with Myanma Thitsi and lacquerwares, eco-friendly products and to investigate the upgraded lacquerware for exterior uses.

Materials and Method

Materials

Thitsi sample was collected from Kawlin Township, Sagaing Region during October and November. Matured stalks of bamboo (Wa-ya) (*Gigantochloa rostrata Wong*) from Yangon Region were used as the substrates to prepare the lacquerwares. Turpentine oil and linseed oil were

also obtained from Kemiko Cosmetics and Chemical Dealers, Yangon Region. UPG protective coating was provided from United Paint Group Co., Ltd, Yangon Region.

Methods

Purification or Prepolymerization of Thitsi

Raw Thitsi was homogenized by a make-shift homogenizer. About 500 g. of Thitsi was taken and homogenized in a make-shift homogenizer for 0.5 hr., 1 hr., 1.5 hr. and 2 hr. respectively. After that, it was filtered by using a filter cloth. During filtration and homogenization, heating was made by halogen lamp (1000 W.) from 1 ft. above the homogenizer and filtering medium to facilitate the flow of Thitsi and evaporation of water.

Determination of Physico-chemical Characteristics of Raw and Purified Thitsi

Physico-chemical characteristics like ash content, viscosity, boiling range, pH and specific gravity were determined by ASTM D29, D562, D850, pH meter and D1963 respectively.

Determination of Constituents of Raw and Purified Thitsi

Constituents of Thitsi samples such as moisture and volatile matter, thitsiol content, nitrogenous matter, gummy matter and fatty or oily matter were determined by ASTM D29, and Pearson, 1908.

Characterization of Functional Groups of Thitsiol

The various functional groups of thitsiol of purified Thitsi were examined by Fourier Transform Infrared Spectroscopy (FT-IR, Perkin Elmer, 8400, Shimadzu).

Preparation of Bamboo Lacquerwares

Preparing the Bamboo Substrates

Air-dried matured stalks of bamboo (Wa-ya) (*Gigantochloa rostrata Wong*) substrates were cut into 2 inches in length and 1 inch in width and polished with abrasive paper to smooth the surface and cleaned to free from dust and dirt.

Lacquering and Hardening in Local Underground Cellar

The prepared bamboo substrates were lacquered with raw Thitsi and purified Thitsi. Lacquering was made carefully with a flat brush in all the prepared lacquerware to form a thin layer of uniform coating. Then, the coated materials were hardened in the underground cellar. After each coating, the freshly dried coat was rubbed with an abrasive paper (paper No. 400 and 600) to get a smooth surface. The specimen was said to be dried if no tackiness was felt by a finger press on the lacquered surface. As a preliminary study, standard deviation for hardening time of raw Thitsi-coat on bamboo substrates was firstly determined.

Determination of Physico-chemical Properties of Processed Lacquerwares and Export Quality Myanma Commercial Lacquerwares

Physico-chemical properties of lacquerwares such as pencil hardness, cross hatch, adhesion, coating thickness, specular gloss, water immersion resistance, salt immersion resistance, resistance to steam at 100ºC, acid immersion resistance, alkali immersion resistance and weathering resistance were determined.

Characterization of Morphological Features of Lacquer Film

The morphological feature of seven times coated lacquer film was studied on the original film and also after weathering test by Scanning Electron Microscope (SEM) (JSM – 5610).

Study on the Effect of Drying Agents on the Hardening Time

Purified Thitsi was blended with varying amounts of turpentine to enhance the hardening time. 10 g. each of purified Thitsi was blended with varying amounts of turpentine oil such as 0.025 g., 0.05 g., 0.075 g. and 0.1 g. and stirred for 30 min. under sunlight. Then the respective mixtures were painted on bamboo substrates. The above procedure was again conducted with linseed oil, another drying agent.

Determination of Physico-chemical Properties of Lacquerwares Coated by Thitsi Mixed with Drying Agents

Physical and chemical properties of coated lacquerwares by purified Thitsi mixed with respective drying agents were determined.

Study on the Effect of Protective Coating on Myanma Lacquerwares for Exterior Uses

High performance heavy duty, protective coating was prepared by mixing 4:1 ratio of 2K polyurethane top coat clear (HPU 90200) and hardener coat (HPH 65200), and 10 – 20% (%w/w) of thinner (UT 91). The protective coating was coated on the hardened lacquerwares and dried for 3 hr. at room temperature. Then, weathering effect on the protective film coated lacquerwares was inspected.

Results and Discussion

As shown in Table (1), it was observed that the colour of Thitsi changed from deep brown to black due to the purification process. The colour of Thitsi represented their quality. Thitsi samples possessed a peculiar sweetish odour. It was also found that ash content of purified Thitsi sample was slightly increased by the purification process and also it was clearly observed that the viscosity of Thitsi increased markedly, whereas specific gravity was decreased. Thus, purified Thitsi became lighter than that of raw Thitsi. But the boiling range of purified Thitsi did not change apparently. pH of Thitsi samples were 5.6. By the purification process, their physico-chemical characteristics did not entirely deviate. These physico-chemical characteristics of Thitsi were within the range of literature values of Thitsi.

Table1: Physico-chemical Characteristics of Raw and Purified Thitsi

Sr. No.	Characteristic	Thitsi Sample		Literature Value*
		Raw	Purified	
1	Colour	deep brown	black	grayish – black
2	Odour	peculiar sweetish	peculiar sweetish	peculiar sweetish
3	Ash (%w/w)	0.074	0.089	0.041 – 0.130
4	Viscosity (cP.)	3482	8000	200 – 14100
5	Boiling Range (ºC)	50 – 83	53 – 82	18.8 – 387.7
6	pH	5.6	5.6	4 – 6
7	Specific Gravity	1.012	0.996	0.985 – 1.013

* Data – http://www.material-safety-data-sheet-lacquer.html

Constituents of raw and purified Thitsi are displayed in Table (2). Due to the purification process, the contents of thitsiol and nitrogenous matter were increased whereas the remaining constituents, moisture and volatile matter, gummy matter and fatty or oily matter of raw Thitsi were decreased. Moisture and volatile matter content decreased from 10.0 %w/w to 5.0 %w/w and Thitsiol content increased from 80.0 %w/w to 87 %w/w. Decrease in moisture and volatile matter content and fatty or oily matter and increase in nitrogenous matter of Thitsi facilitate the hardening, meanwhile increase in thitsiol content impair the hardening, but it could provide the best gloss and high resistance to physical and chemical attacks. The quality of Thitsi depends on its content of Thitsic acid, now termed thitsiol. The best quality lacquer contains the highest percentage of thitsiol.

Table 2: Constituents of Raw and Purified Thitsi

Sr. No.	Constituent	Thitsi Sample		Literature Value* (Japanese Urushi)
		Raw	Purified	
1	Moisture and Volatile Matter (%w/w)	10.0	5.0	20 – 30
2	Thitsiol (%w/w)	80.0	87.0	60 – 70
3	Nitrogenous Matter (%w/w)	1.0	2.0	1.5 – 5
4	Gummy Matter (%w/w)	4.5	3.0	4 – 10
5	Fatty or Oily Matter (% w/w)	0.5	0.3	0 – 1

*Data - http://www.jsaweb.recent-advances-in-research-in-lacquer-allergy.html

To improve the quality of lacquerware products and to speed up the polymerization time, raw Thitsi were prepolymerized or purified. Table (3) shows the effect of prepolymerization time on the moisture and volatile matter content and thitsiol content of Thitsi. It was found that moisture and volatile matter content decreased meanwhile thitsiol content increased with increased prepolymerization time. The most suitable prepolymerization time was observed at 1 hr. because of the needs for the reliable Thitsi to be of minimum moisture and volatile matter content, 3 – 5% w/w. At this prepolymerization time, the highest thitsiol content was found to be 87%w/w.

Table 3: Effect of Prepolymerization Time on the Moisture, Volatile Matter and Thitsiol Contents of Raw Thitsi

Sr. No.	Constituent	Prepolymerization Time (hr.)					Remarks
		0.0	0.5	1.0*	1.5	2	
1	Moisture and Volatile Matter (%w/w)	10.0	8.0	5.0	1.0	0.0	1. Thitsi should have minimum moisture and volatile matter content (3 – 5)%w/w.
2	Thitsiol (%w/w)	80.0	84.0	87.0	88.0	88.0	2. All constituents are essential for hardening of Thitsi.

*Most suitable condition,
Remark (1) - http://www.development.of.a.fast.drying.lacquer.based.on.raw.lacquer.sap. Pdf
Remark (2) - http://www.intechopen.com

Various functional groups of thitsiol from Thitsi were examined by FTIR and it proved that the sample was Thitsi. As shown in Table (4), the frequency at 3441cm^{-1} represented the presence of phenolic groups which has O – H stretching vibration assignment. The frequency at 3009 cm^{-1} corresponded to the presence of = CH – group of the aromatic system. The band at 2924 cm^{-1} frequency indicated the saturated alkyl group which has – CH_2 – asymmetric stretching vibration and the frequency at 2852 cm^{-1} of sample showed the saturated alkyl group which has –CH_2 – symmetric stretching vibration. The band at 1280 cm^{-1} frequency represented the characteristics of O – H in-plane bending vibration of phenolic group whereas at the frequency of 731 cm^{-1} corresponded to the O – H out-of-plane bending

vibration of phenolic group. The infrared spectrum of thitsiol obtained was found to be the same with urushiol from Japanese urushi virtually.

Table 4: FTIR Absorption Frequencies of Functional Groups of Thitsiol from Purified Thitsi

Sr. No.	Observed Frequency (cm^{-1})	Literature Frequency* (cm^{-1}) (Urushiol)	Band Assignment	Remarks
1	3441	3431	O – H stretching vibration	Phenol
2	3009	3012	= CH – stretching vibration	Aromatic ring
3	2924	2926	– CH_2 – asymmetric stretching vibration	Saturated alkyl group
4	2852	2853	– CH_2 – symmetric stretching vibration	Saturated alkyl group
5	1280	1310-1200	O – H in-plane bending vibration	Phenol
6	731	750-650	O – H out-of-plane bending vibration	Phenol

* http://www.atsem09-owjung.pdf

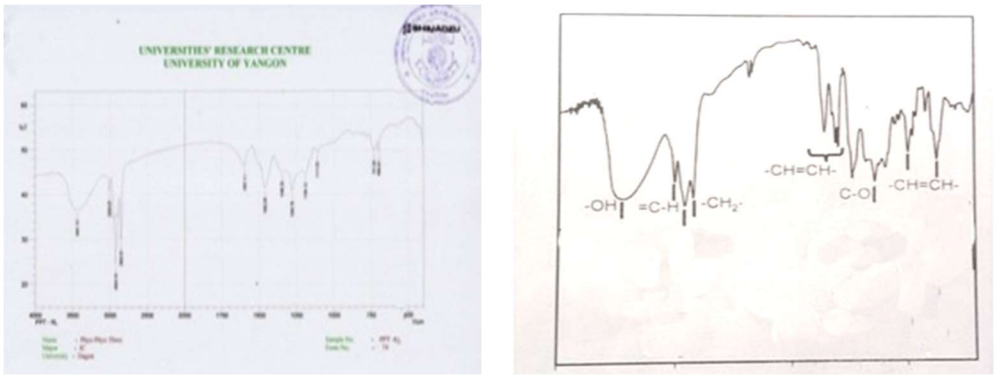

(a) **(b)**

Figure 1: FTIR Spectra of (a) Thitsiol and (b) Urushiol

It was studied that standard deviation for hardening time of raw Thitsi-coat on bamboo substrates hold 0.58 hr.. For further studies, this deviation time covered on the hardening time of raw and purified Thitsi-coat on bamboo lacquerwares.

Total hardening time of coat of raw and purified Thitsi on bamboo lacquerwares are shown in Table (5). It was found that, high moisture and volatile matter content and high nitrogenous matter content of Thitsi facilitate the hardening whereas high thitsiol content curtails the hardening. The presence of nitrogenous constituent was essential for the drying of Thitsi. It was also found that the hardening time of Thitsi coats were slightly decreased with consecutive increased number of coatings. Moreover, high relative humidity of underground cellar diminished the hardening time.

Since, purification or prepolymerization accelerated the polymerization of thitsiol monomer to the lacquer dimer, trimer, ……, oligomer and polymer, it can be clearly observed that the hardening time of coated lacquerwares with purified Thitsi in all the coating was greatly shorter than the wares coated with raw Thitsi.

For the same of number of coatings (i.e. eight coats), hardening time was very much shorer, 216.3 hr. for purified Thitsi compared to 315 hr. for raw Thitsi.

Table 5: Total Hardening Time of Coat of Raw and Purified Thitsi on Bamboo Lacquerwares

Thitsi Sample	**Hardening Time (hr.) of Coats of Thitsi**							
	1st coat	**2nd coat**	**3rd coat**	**4th coat**	**5th coat**	**6th coat**	**7th coat**	**8th coat**
Raw	60.3	106.6	151.3	195.1	227.5	257.8	287.0	315.0
Purified	36.3	66.3	94.6	120.8	146.6	171.0	194.3	216.3

Physical properties of bamboo lacquerwares coated with raw and purified Thitsi from Kawlin Township are described in Table (6). It can be observed that the increase in number of consecutive coatings, resulted in harder the scale of hardness. From these data, the hardness values of lacquerwares initially from four to eight times were the highest (i.e. 6H) and the commercial product, export quality Myanma lacquerware had also 6H. Cross hatch and adhesion qualities of Thitsi (raw/purified) coated on bamboo substrates were completely perfected, 100%.

It was observed that the wet film thickness of each coating in all lacquerwares occupied 120 μm. The dry film thicknesses of coated

lacquerwares with purified Thitsi were much thicker than that coated with raw Thitsi in all consecutive lacquer coatings because of purified Thitsi had high viscosity.

Determination of the specular gloss of processed lacquerwares is an essential test for assessment of their quality. Because of purified Thitsi had higher thitsiol content than raw Thitsi, it was observed that the gloss values of coated lacquerware with purified Thitsi were much higher than the wares coated with raw Thitsi. Rather high gloss values, >80G.U. were obtained starting from five times coated lacquerwares with purified Thitsi. The highest gloss value, 100 G.U. was obtained in eight times coating for purified Thitsi.

Moreover, the gloss value of processed lacquerwares painted with purified natural Thitsi were higher than the gloss value of commercial product, export quality Myanma lacquerware. It was also found that the gloss values increased with increase in number of consecutive coatings. This test confirmed that the thitsiol content of Thitsi could greatly influence the specular gloss of lacquerwares. Therefore, Thitsi products can last hundreds of years while retaining their glossiness, smoothness and elegance.

Table 6: Physical Properties of Coated Lacquerwares with Raw and Purified Thitsi

Sr. No	Coat on Lacquerware	Physical Property									
		Pencil Hardness		Cross Hatch (%)		Adhesion (%)		Dry Film Thickness (μm)		Specular Gloss (GU)	
		Raw	Purified	Raw	Purified	Raw	Purified	Raw	Purified	Raw	Purified
1	1st coat	4H	4H	100	100	100	100	26	43	28.5	45.5
2	2nd coat	5H	5H	100	100	100	100	52	86	33.2	54.6
3	3rd coat	5H	5H	100	100	100	100	78	129	45.8	63.8
4	4th coat	6H	6H	100	100	100	100	104	172	59.0	70.6
5	5th coat	6H	6H	100	100	100	100	130	215	71.8	85.6
6	6th coat	6H	6H	100	100	100	100	156	258	80.1	94.8
7	7th coat	6H	6H	100	100	100	100	182	301	87.7	98.2
8	8th coat	6H	6H	100	100	100	100	208	344	93.0	100.0
9	Myanma Export Product	6H		100		100		-		98.1	

Wet film thickness of Thitsi = 120 □m, H = Hard pencil

Chemical properties of bamboo lacquerwares coated with raw and purified Thitsi from Kawlin Township are described in Table (7). It was observed that after the treatment of water, salt and steam, the resultant gloss values of lacquerwares were higher than the wares before treatment in respective mediums in all coatings and also the gloss value of the export quality commercial product. In these tests, the increased in consecutive coatings, resulted in higher the gloss value and increased to withstand the chemical and heat resistances.

It was found that the gloss values of lacquerwares were slightly decreased by acid and alkali treatments (1-3 G.U.) than the original gloss values but they were still higher than the gloss values of commercial product. Although the gloss value of wares slightly decreased after determination of acid immersion resistance they could be said that they were rather resistant to acid solution because no cracking, blistering, rusting and water spotting were observed.

Table 7: Gloss Values of Coated Lacquerwares with Raw and Purified Thitsi in Different Mediums

Sr. No	Coat on Lacquerware	Specular Gloss of Thitsi-Coat on Lacquerware (G.U) after Chemical Treatment									
		Water Immersion (2 months)		5% NaCl Immersion (2 months)		Steam Treatment (6 hr)		5% HCl Immersion (1 month)		5% NaOH Immersion (1 month)	
		Raw	Purified	Raw	Purified	Raw	Purified	Raw	Purified	Raw	Purified
1	1st coat	35.5	57.2	37.5	58.8	39.4	56.2	26.2	45.1	20.8	37.5
2	2nd coat	43.4	63.0	40.4	65.1	45.2	65.4	31.5	51.8	25.9	45.0
3	3rd coat	57.2	72.2	56.3	73.5	59.3	74.5	44.1	61.7	38.1	55.2
4	4th coat	68.8	79.1	70.2	80.8	71.5	82.3	57.2	68.8	50.9	61.8
5	5th coat	78.7	87.9	81.4	91.3	82.6	90.5	70.0	83.7	63.2	76.3
6	6th coat	89.6	96.8	89.9	99.8	92.4	98.3	77.8	91.4	71.8	85.4
7	7th coat	96.2	99.9	97.9	100.0	98.1	100.0	85.1	97.0	80.5	91.2
8	8th coat	100.0	100.0	100.0	100.0	100.0	100.0	91.4	100.0	87.2	95.9
9	Myanma Export Product	98.9		99.2		99.8		89.6		45.9	

Gloss values of coated lacquerwares with different raw and purified Thitsi after weathering effect are shown in Table (8). From this test it was found that the gloss value of lacquerwares gradually decreased with prolonged exposure time to UV radiation. Because of decreased in gloss value, the appearance of the wares was unsatisfactory but their qualities were acceptable, and they could not be scratched with a finger nail. There was no chalking, cracking, blistering, rusting, water spotting and dirt retention too.

Thus, hardened Thitsi film is an excellent coating material due to its lustre and stiffness, but its drawback is that it is sensitive to light, especially UV radiation. Part of the polymerized thitsiol was decomposed and may be volatile, leaving the film in a heterogeneous condition when the film was exposed to UV radiation. After assessing the weathering resistance which is equivalent to nine years and five months, the gloss value of processed wares were higher almost double the value than the gloss of commercial products. Thus, the processed wares could sustain the exterior weather condition.

Table 8: Gloss Values of Coated Lacquerwares with Raw and Purified Thitsi after Weathering Test

Sr. No.	Exterior Weather		Specular Gloss of Thitsi-Coat on Lacquerware (G.U.)		
	hr. Used	Affected yr.	Raw Thitsi	Purified Thitsi	Myanma Export Product
1	-	-	86.5	96.8	98.1
2	164	0.68	76.2	83.5	85.3
3	352	1.47	65.8	77.1	69.5
4	776	3.23	43.7	70.3	52.1
5	1088	4.53	38.8	62.7	46.2
6	1492	6.22	35.6	58.3	39.7
7	1812	7.55	32.9	50.0	28.9
8	2192	9.13	30.8	43.4	19.6
9	2264	9.43	27.1	37.9	12.1

SEM photomicrograph of original lacquer film and SEM microphotograph of the film after weathering test which include the exposure to UV radiation are shown in Fig (2). SEM image of seven times coated original lacquer film was packed densely and a well-defined surface texture

with an equally smooth surface with only very few minute grains which was responsible for its excellent durability. When the film was exposed to UV radiation, the lacquer film might absorb UV and suffer from photo-oxidative degradation and part of the polymerized thitsiol was decomposed and volatilized. So, SEM photographs of lacquer films after weathering effect showed well-defined microstructure with irregular scratches, large nodules and turning marks.

(i) **(ii)**

Figure 2: SEM Photographs of Kawlin Thitsi Coated Lacquer Film
(i) Seven Times Coated Original Lacquer Film
(ii)Seven Times Coated Lacquer Film after Exposing to Weathering Test Equivalent to Nine Years and Five Months

In order to speed up the polymerization time of Thitsi-coat on lacquerwares, turpentine and linseed oil were used as drying agents and their hardening effect was studied. Effect of turpentine and linseed oil on the hardening time of Thitsi-coat on lacquerwares is described in Tables (9) and (10) respectively. It was observed that the most suitable ratio of Thitsi and turpentine was found to be 1:0.005, which gave the shortest hardening time, and the most suitable ratio of Thitsi and linseed oil was 1:0.0075. It was found that drying oils truly enhanced the polymerization time of Thitsi-coat on lacquerwares. The hardening time of Thitsi-coat on lacquerwares decreased by mixing Thitsi with appropriate amount of drying agents because solvent drying agent, turpentine accelerated the polymerization ability of Thitsi by evaporation of water, and drying oil, linseed oil speeded up to harden Thitsi by a chemical reaction in which the components crosslinked by the action of oxygen.

Table 9: Effect of Turpentine on the Hardening Time of Thitsi-Coat on Lacquerwares

Sr. No.	Ratio of Thitsi and Turpentine	Hardening Time of Thitsi-Coat on Lacquerware (hr.)							
		1st coat	2nd coat	3rd coat	4th coat	5th coat	6th coat	7th coat	8th coat
1	1:0.0000	36.25	30.00	28.33	26.25	25.75	24.42	23.25	22.00
2	1:0.0025	32.00	27.67	26.00	24.50	23.00	22.25	21.33	19.83
3	1:0.0050*	26.67	22.17	21.50	20.33	18.50	17.17	16.25	15.50
4	1:0.0075	30.33	26.50	24.17	23.83	21.25	20.67	19.58	18.67
5	1:0.0100	49.00	46.67	38.33	34.83	30.50	29.17	27.25	26.67

* Most suitable ratio of Thitsi and turpentine

Table 10: Effect of Linseed Oil on the Hardening Time of Thitsi-Coat on Lacquerwares

Sr. No.	Ratio of Thitsi and Linseed Oil	Hardening Time of Thitsi-Coat on Lacquerware (hr.)							
		1st coat	2nd coat	3rd coat	4th coat	5th coat	6th coat	7th coat	8th coat
1	1:0.0000	36.25	30.00	28.33	26.25	25.75	24.42	23.25	22.00
2	1:0.0025	26.50	24.15	23.33	21.67	20.75	18.00	17.25	16.17
3	1:0.0050	23.00	22.75	21.67	19.17	17.25	16.17	15.83	14.33
4	1:0.0075*	21.50	19.17	18.50	16.83	14.67	13.50	12.83	12.00
5	1:0.0100	27.50	25.17	24.83	22.17	21.50	19.83	18.17	16.83

* Most suitable ratio of Thitsi and linseed oil

Pencil hardness of lacquerwares coated by purified Thitsi mixed with drying agents are shown in Table (11). It was observed that the pencil hardness of lacquerwares coated by purified Thitsi mixed with linseed oil was harder than that mixed with turpentine. It was also found that the hardness degree increased with increase in number of consecutive coatings. These hardness values were lower than the wares painted by purified Thitsi alone. Thus, drying agents improved the polymerization time but; these agents impaired the hardness of lacquerwares.

Table 11: Pencil Hardness of Different Types of Thitsi Coated Lacquerwares

Sr. No.	Coat on Lacquerware	Pencil Hardness of Thitsi-Coat on Lacquerware		
		PTK + T (1 : 0.0050) Thitsi-Coat	PTK + LO (1 : 0.0075) Thitsi-Coat	Purified Thitsi-Coat
1	1st coat	F	H	4H
2	2nd coat	F	H	5H
3	3rd coat	F	2H	5H
4	4th coat	F	2H	6H
5	5th coat	H	3H	6H
6	6th coat	2H	3H	6H
7	7th coat	3H	4H	6H
8	8th coat	4H	4H	6H

PTK = Purified Thitsi from Kawlin Township, T = Turpentine oil, LO = Linseed oil, F = Fine pencil, H = Hard pencil

Cross hatch and adhesion of lacquerwares coated by purified Thitsi mixed with drying agents are described in Table (12). It revealed that the cross hatch and adhesion of painted lacquerwares by purified Thitsi mixed with turpentine and linseed oil were 100%. Thus the application of drying agents in lacquering process did not influence the cross hatch and adhesion strength of processed lacquerwares.

Table 12: Cross Hatch and Adhesion of Different Types of Thitsi Coated Lacquerwares

Sr. No.	Coat on Lacquerware	Cross Hatch and Adhesion of Thitsi-Coat on Lacquerware (%)		
		PTK + T (1 : 0.0050) Thitsi-Coat	PTK + LO (1 : 0.0075) Thitsi-Coat	Purified Thitsi-Coat
1	1st coat	100	100	100
2	2nd coat	100	100	100
3	3rd coat	100	100	100
4	4th coat	100	100	100
5	5th coat	100	100	100
6	6th coat	100	100	100
7	7th coat	100	100	100
8	8th coat	100	100	100

Table (13) shows the specular gloss values of lacquerwares coated by purified Thitsi mixed with drying agents. It was observed that the gloss values of coated lacquerwares by purified Thitsi mixed with linseed oil were higher than the wares that mixed with turpentine. However, these gloss values of lacquerware were slightly lower than the ware coated with original purified Thitsi. Although the drying agents promoted the polymerization time of Thitsi, it slightly lower the gloss of lacquer film.

Table 12: Specular Gloss of Different Types of Thitsi Coated Lacquerwares

Sr. No.	Coat on Lacquerware	Specular Gloss of Thitsi-Coat on Lacquerware (G.U.)		
		PTK + T (1 : 0.0050) Thitsi-Coat	PTK + LO (1 : 0.0075) Thitsi-Coat	Purified Thitsi-Coat
1	1st coat	37.8	39.2	45.5
2	2nd coat	45.3	45.9	54.6
3	3rd coat	54.8	58.6	63.8
4	4th coat	62.0	69.8	70.6
5	5th coat	74.2	78.5	85.6
6	6th coat	83.5	87.0	94.8
7	7th coat	91.7	94.8	98.2
8	8th coat	94.6	95.2	100.0

Specular gloss values of coated lacquerwares by purified Thitsi mixed with respective drying agents after chemical treatments and weathering effect are shown in Tables (14), (15) and (16) respectively. From these Tables, it was found that the gloss values of painted lacquerware by purified Thitsi mixed with linseed oil were higher than that mixed with turpentine. But, these gloss values of lacquerware were slightly lower than gloss values of lacquerware coated by purified Thitsi alone.

Table 14: Specular Gloss of Coated Lacquerwares by Purified Thitsi mixed with Turpentine (1: 0.005) after Chemical Treatments

Sr. No.	Coat on Lacquerware	Specular Gloss of Thitsi-Coat on Lacquerware (G.U)				
		Water Immersion (2 months)	5% NaCl Immersion (2 months)	Steam Treatment (6 hr)	5% HCl Immersion (1 month)	5% NaOH Immersion (1 month)
1	1st coat	37.2	37.4	37.5	33.8	31.7
2	2nd coat	43.0	43.1	43.3	40.3	39.1
3	3rd coat	52.8	52.1	53.4	49.8	46.3
4	4th coat	59.6	59.8	59.3	57.1	54.9
5	5th coat	69.5	69.8	69.2	65.4	61.2
6	6th coat	80.1	81.2	81.0	76.5	69.1
7	7th coat	87.5	87.8	88.0	86.2	79.8
8	8th coat	91.6	92.0	91.6	92.1	87.5

Table 15: Specular Gloss of Coated Lacquerwares by Purified Thitsi mixed with Linseed Oil (1 : 0.0075) after Chemical Treatments

Sr. No.	Coat on Lacquerware	Specular Gloss of Thitsi-Coat on Lacquerware (G.U)				
		Water Immersion (2 months)	5% NaCl Immersion (2 months)	Steam Treatment (6 hr)	5% HCl Immersion (1 month)	5% NaOH Immersion (1 month)
1	1st coat	39.5	40.8	39.1	36.6	33.7
2	2nd coat	52.8	53.2	49.5	45.8	42.8
3	3rd coat	57.3	58.1	56.7	53.7	49.2
4	4th coat	63.4	63.0	64.0	63.0	60.4
5	5th coat	74.8	74.1	75.1	70.3	66.3
6	6th coat	84.4	86.6	85.4	82.5	74.1
7	7th coat	89.2	90.5	89.9	89.1	82.6
8	8th coat	92.6	93.8	92.4	93.4	89.1

Table 16: Specular Gloss of Coated Lacquerwares by Purified Thitsi mixed with Drying Agents after Weathering Effect

Sr. No.	Exterior Weather		Specular Gloss of Thitsi-Coat on Lacquerware (G.U.)		
	hr. Used	Affected yr.	PTK + T (1 : 0.0050) Thitsi-Coat	PTK + LO (1 : 0.0075) Thitsi-Coat	Purified Thitsi-Coat
1	-	-	91.7	94.8	96.8
2	164	0.68	81.3	82.1	83.5
3	352	1.47	70.8	73.4	77.1
4	776	3.23	62.4	65.3	70.3
5	1088	4.53	52.6	56.4	62.7
6	1492	6.22	47.2	50.6	58.3
7	1812	7.55	40.8	44.1	50.0
8	2192	9.13	30.1	35.2	43.4
9	2264	9.43	24.7	30.8	37.9

Fast drying resulted in an opaque and non-uniformly hardened film when the rate of water evaporation from the Thitsi coated surface did not harmonize well with the hardening rate, i.e., the oxygen-absorbing rate to form a uniform and transparent hardened film. Thus, application of drying agents diminished both physical and chemical properties of lacquerware because these drying agents quickly dried the Thitsi. (Monreal, 1985)

With the aid of protective coating, lightly coated lacquerwares, (i.e. only two or three coats) could be upgraded in lustre. Besides, they withstood attacks from weathering as heavily coated lacquerwares. Gloss values of coated lacquerware with thin film protective layer after weathering effect are shown in Table (17).

It was observed that the gloss values of all consecutive lacquer coating did not decrease by weathering effect. The protective coating prevented the exposure of the lacquer film to UV radiation and the decomposition of polymerized thitsiol, and thus the gloss values, 100 G.U. remain constant after exposure to UV radiation which is equivalent to nine years and five months. Therefore, lacquerwares can be used for exterior uses like outdoor decorations for hotel, restaurants and parks, etc., by providing with high performance protective coating.

By this experiment, application of protective coating over the lacquered surface not only enhanced the using of lacquerwares for outdoor purposes but it also saved the required time and amount of Thitsi needed as lacquerwares are coated by natural purified Thitsi only.

Table 17: Gloss Values of Coated Lacquerwares with Protective Coating after Weathering Effect

Sr. No.	Exterior Weather		Specular Gloss of Thitsi-Coat on Lacquerware (G.U.)					
	hr. Used	Affected yr.	1st coat	2nd coat	3rd coat	4th coat	5th coat	6th coat
1	-	-	90.6	100	100	100	100	100
2	164	0.68	90.6	100	100	100	100	100
3	352	1.47	90.6	100	100	100	100	100
4	776	3.23	90.6	100	100	100	100	100
5	1088	4.53	90.6	100	100	100	100	100
6	1492	6.22	90.6	100	100	100	100	100
7	1812	7.55	90.6	100	100	100	100	100
8	2192	9.13	90.6	100	100	100	100	100
9	2264	9.43	90.6	100	100	100	100	100

(a) **(b)**

Figure 3: Smooth and Glossy (a) Bamboo Lacquerwares (b) Lacquerware Cups

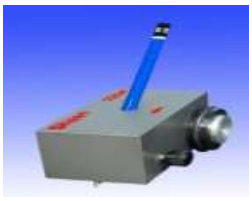

Figure 4: Wolff-Wilborn Pencil Tester

Figure 5: Cross Hatch Cutter

Figure 6: Wet Film Thickness Comb

Figure 7: Dry Film Thickness Tester

Figure 8: Tri-micro Gloss Meter

Figure 9: QUV Accelerated Weathering Tester

Conclusion

The constituents and properties of Thitsi vary with the age of tree, grown region and collected season. Quality of Thitsi depends on its thisiol content. Moreover, the best quality Thitsi can give the lustrous lacquerwares, possessing outstanding qualities with marvelous gloss, good chemical resistance and high durability. Purification of Thitsi produces fine lacquer. Thus purified Thitsi can provide further appropriate seasoning, viscosity and glossiness when laid upon any surfaces.

Lacquer could not set by the aid of heat, sun light and dry air and hence, polymerization of Thitsi should be allowed to take place in the dark underground cellar to dry the lacquerwares. Purification process saved the time required for polymerization of raw Thitsi and also gave high quality lacquerwares. In addition, the prepolymerization was to hopefully be used to prepare a fast drying Thitsi on a large scale and promote the application of Thitsi as an industrial paint. Using appropriate amount of solvent and drying oil reduced the hardening time of Thitsi but slightly affect the some properties of lacquerwares (with the exception of cross hatch and adhesion). Using large amount of these drying agents retarded the polymerization time and impaired the quality of lacquerwares.

Processed lacquerwares had hardness and good adhesive power so they can keep their aesthetic appearance. From the point of chemical strength, lacquerwares had ability to resist not only water, salt and steam but also withstand acid and alkali. But, their drawback was found on the exposure to UV radiation. The properties of lacquerwares especially glossiness could increase by using them in various environments and different conditions. The good quality lacquerware obtained by restricted increased number of coating

and it was noted that six or seven times coated lacquerwares with pure Myanma Thitsi occupied the perfectness. Since thin film protective coating on harden lacquerwares (only second times coated wares) prevents photo-oxidative degradation and decomposition of polymerized thitsiol, they could be used for exterior application under UV radiation. Therefore, Myanma lacquerwares could be upgradeable for various outdoor decorations like synthetic materials. Thitsi, a renewable resource and an eco-friendly biopolymer material, can be used in special environments and can also be kept for several years without declining their true attractiveness.

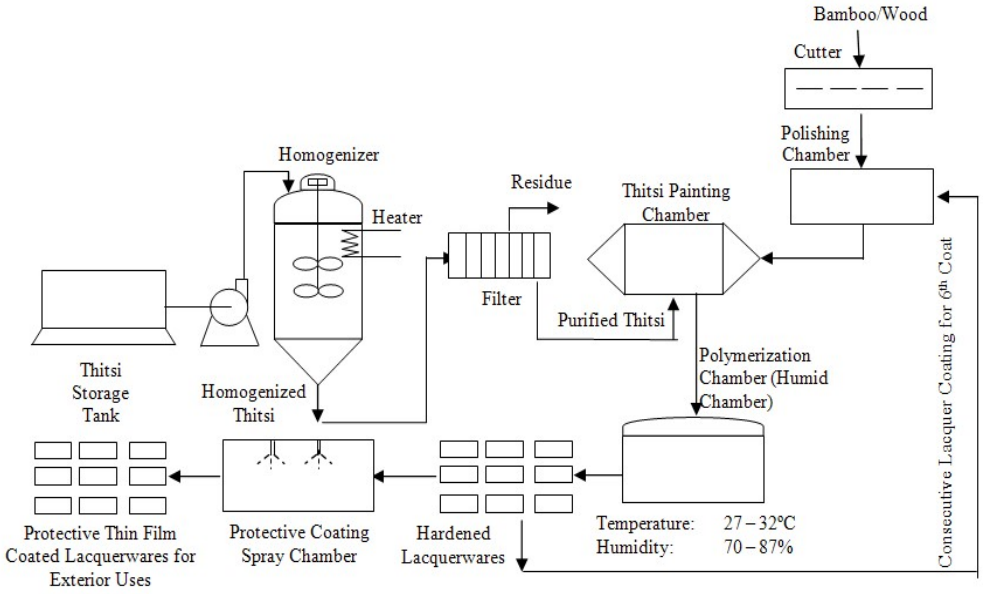

Figure 10: Process Flow Diagram for the Production of Protective Thin Film Coated Lacquerwares

Acknowledgements

The author is grateful to my supervisor, Dr Pansy Kyaw Hla, Professor (Retired) of the Department of Industrial Chemistry, University of Yangon for her invaluable suggestions and advices during the tenure of this research work. I would like to express my profound respect and deepest gratitude to my co-supervisor Dr Thwe Linn Ko, Professor of the Department of Industrial Chemistry, University of Mandalay for her invaluable suggestions, kind encouragement, advice and constant guideline throughout this research work.

I feel heartily a deep sense of gratitude to Dr Nwe Ni Wai, Executive Director (PDD, R&D, QAD), United Paints Group Co., Ltd, for giving permission to conduct the research and kind support and also Daw Myint Myint Thein, Lab Technician, Research and Development Department, United Paints Group Co., Ltd, Hlaing Thayar Industrial Zone (1), Hlaing Thayar Township, Yangon Region, for her kindly help in the determination of physico-chemical properties of lacquerwares, invaluable encouragement and also comments on the data.

References

Annual Book of ASTM Standards, 1986, *Paints, Related Coatings and Aromatics,* Volume 06.01 and 06.02 Section 6, United States of America.

APHA-AWWA-WPCF of A-*merica, 1981, *Standard Methods for the Examination of Water and Wastewater*, 15th edition, United State of America.

Fraser-Lu, S., 1996, *Burmese Lacquerware*, 1st Edition, Sirivatana Printing, Bangkok, Thailand.

Hundley, H.G., and U. Chit Ko Ko, 1961, *List of Trees, Shrubs, Herbs and Principal Climber, etc.*, Yangon, Myanmar.

Pearson, R. S., 1908, "A Chemical Investigation of the Constituents of Burmese Varnish", Volume I, Part IV, Calcutta, India.

Rong, L. *et al*., 2004, *Development of a Fast Drying Lacquer Based on Raw Lacquer Sap*, Japan.

Websites

1. http://www.intechopen.com
2. http://www.jsaweb.recent-advances-in-research-on-lacquer-allergy.html

EXTRACTION AND CHARACTERIZATION OF OIL FROM MEZE SEEDS (*MADHUCALONGIFOLIA*)

Kyi Kyi Sein[1], Yi Yi Myint[2], Pansy Kyaw Hla[3]

Abstract

In this research work, meze seed oil was extracted from meze seeds (*Madhuca longifolia*). Meze seeds were collected from Simehtun village near the vicinity of Yadanabon University, Amarapura Township, Mandalay Region. Firstly, the characteristics of meze seed kernelssuch as moisture content, ash content, protein content, crude fiber content and crude fat content were investigated. The phytochemicals and elemental composition present in meze seeds kernels were also investigated. Meze seed oil was extracted by two different methods; with expeller and by using different solvents such as 95% ethanol, Special Boiling Point (SBP 62/82) and petroleum ether, followed by either simple or vacuum distillation. Among these solvents, petroleum ether is the most suitable to get the highest oil yield. The effect of volume of solvent and extraction time on yield of extracted oil was also studied .The most suitable extraction time is 4 hours for each solvent respectively. Extracted meze seed oil was identified by FT-IR spectroscopy. The physico-chemical properties such as specific gravity, refractive index, colour, relative density, moisture, acid value, saponification value, unsaponifiable matter, iodine value and peroxide value of extracted meze seedoils were also determined. The fatty acids composition of meze seedoil such as 25.913% palmitic acid, 19.330% stearic acid, 43.716% oleic acid, 9.824% linoleic acid and traces of other fatty acids was revealed by Gas Chromatography Analysis.

Keywords: meze seed oil,expeller, SBP 62/82, petroleum ether

Introduction

Mahua (*Madhuca longifolia)* is an important economic plant, growing throughout the tropical and subtropical region. It is a native plant of India, Sri Lanka and also Myanmar (tropical region). Myanmar name is Meze or Myintzuthaka. It is a fast growing tree that grows up to approximately 20 meters in height, possesses evergreen or semi-evergreen foliage with wider and round canopy. It belongs to the family Sapotaceae. *Madhuca longifolia*

[1]. Lecturer, Department of Industrial Chemistry, University of Yangon
[2]. Dr, Professor and Head (Retd.), Department of Industrial Chemistry, Yadanabon University
[3]. Dr, Professor (Retd.), Department of Industrial Chemistry, University of Yangon

have tremendous therapeutic and potential use but due to unawareness of people it is not fully utilized.(http:// www. grow-tree.com, Why Tree).

Its flowers appear with new leaves between February and April and fruits ripening begin from May to August. Fruits (berries) are ovoid or sub-globose, generally 2.5 to 5 cm long, greenish in colour but they turn reddish-yellow or orange when ripe and fleshy with few seeds (Mishraet al. 2013).

The seeds have been used to produce oil usually by using mechanical expression method, solvent extraction method, or both methods. Mechanical pressing is the most common method for oil extraction which includes of different types of press such as hydraulic press, screw press and rolling press. Solvent extraction is a method which is able to extract over 98% oil. However, this method has its own disadvantages such as the necessary equipment is high in cost, the process is quite dangerous in correlation with fire and explosion and the solvent used, requires specific process before conducting the next process (International Food Research Journal 18 (4) 2011).

Mahua seed oil (semisolid at ambient temperature) is used for the care of the skin, used for the manufacture of soaps, detergent and as a vegetable butter. It can also be used as fuel oil. The seed fat has emulsion property so it is mostly used as an emulsifying agent in few pharmaceutical industries. It is generally applied as massage oil in many parts of India as it is good to moisturize skin (http:// www. grow-tree.com, Why Tree).

Thus, the objectives of this study is to compare the different extraction methods of meze (Mahua) seed oil and, to give information of different characteristics of meze seed oil depending on the extraction methods.

Materials and Methods

Materials

Mature meze seeds were collected from Simehtun village near the vicinity of Yadanabon University Campus, Amarapura Township, Mandalay Region from August to October for a particular year. Best Oil Press machine was used to express the meze seed oil. For solvent extraction, three types of solvents such as 95% ethanol(BDH, Analar grade, boiling point of 78-80ºC),

SBP (62/82) (boiling point of 60-80ºC) and petroleum ether (boiling point of 35-60ºC)were used to extract meze seed oil.

Methods

Pretreatment of Meze Seeds

The collected meze seeds were dehulled by hand in order to obtain the inner kernels. The seed kernels were then sun-dried to reduce the moisture content (in the range of 4-6%)for 2-3 days. Then they were kept tightly in tin or plastic bags at room temperature (27-30 °C) and ready to extract the oil.

Extraction of Meze Seed Oil by using Expeller

The dried meze seed kernels were crushed using expeller (Best Oil Press Machine with Heater ,Model No.02, Taiwan made)between 45-50ºCto obtain meze oil and oil cake residues separately. The pressed oil was settled and filtered to remove the residual solids.

Extraction of Meze Seed Oil by Using Different Solvents

Solvent Extraction

For solvent extraction, dried meze seed kernels were subjected to grinding in the grinder for reduction of size from lump form to coarse particles. Further grinding was done by recycling coarse particles to produce the pulverized seed kernels (size of -10 mesh). About 5 g of pulverized dried meze seed kernels and 200 mL of 95% ethanol were used to extract the meze seed oil at the boiling point of solvent. Extraction time for about 4 hr was used to obtain the maximum yield of oil.

Distillation

The miscella obtained from the solvent extraction was distilled (either simple or vacuum)to remove the solvent. Simple distillation was carried out at the boiling point of each solvent. The conditions used for vacuum distillation were 60°C and 530 mmHg for 95% ethanol, 50°C and 420 mmHg for SBP (62/82), 30ºC and 480-500 mmHg for petroleum ether. The traces of solvent in the oil were driven off by keeping in the oven for about 1 hr at 110 °C. The oil extracted was accurately weighed.

The same procedure was done with250, 300,350,400mL of 95% ethanol respectively. Similarly, extraction of meze seed oil was also conducted with SBP (62/82) and petroleum ether at their boiling points as described above.

Effect of the volume of solvent and that of extraction time on the yield of extracted meze oil was also studied.

Methods of Identification and Analysis

Physico-chemical properties, phytochemical characteristics and elemental composition of meze seed kernel were firstly investigated. The functional groups present in the extracted meze oil was identified by Fourier Transform Infrared (FT-IR) spectrum. To evaluate the quality of meze seed oil such as specific gravity, refractive index, colour, relative density, moisture, acid value, saponification value, unsaponifiable matter, iodine value and peroxide value were determined and compared with the commercial oil. Gas Chromatography analysis was also conducted to find out the fatty acid composition of meze seed oil.

Results and Discussion

The physico-chemical properties such as moisture, ash, protein, crude fibre, crude fat and carbohydrate content of Myanmar meze seed kernels are shown in Table(1). It is seen that the percentage of crude fat is the highest in Myanmar meze seed kernel and it is also higher than literature values. Its Protein content is significantly different from the literature values. From the results of phytochemical investigations shown in Table(2), it can be seen that meze seed kernel contains alkaloids, flavonoids, glycosides, phenolics, reducing sugar, tannin, saponin, carbohydrate and α - animo acid except starch. Elemental composition of meze seed kernels analyzed by EDXRF spectroscopy was illustrated in Figure (1). According to Table (3), it was found that meze seed kernel contains K, Ca, Fe and C.

Table (4) and Figure (2) show that different yield percentages of oil were extracted with respect to the different volumes of 95% ethanol, SBP and petroleum ether used. From these results, it is seen that increasing the amount

of solvent did not increase the oil yield significantly. Although the increase amount of each of the solvent was used, each percentage of oil yield was not significantly increased. So, to recover the cost of solvent, 250 ml of 95%ethanol, 300 ml of SBP and 250 ml of petroleum ether were chosen as the suitable amount for each extraction. From these results, it can be considered that petroleum ether is the most suitable solvent to achieve the maximum oil yield. Effect of extraction time on yield of oil extracted with 95% ethanol, SBP and petroleum ether is shown in Table (5). Due to these results, it is seen that the most suitable extraction time is (4) hr for the respective solvent depending on the highest yield (Figure 3). This observation shows that the longer the extraction time beyond the most suitable time results in lower the oil yield. This result agrees to the finding reported by Mani et al.(2007) that any further increase in extraction time beyond suitable time did not increase the oil yield.

Interpretation data of FT-IR spectrum, shown in Figures (4) and (5), Tables (6) and (7) to identify that both the extracted meze seed oil and commercial oil contain the functional groups such as carboxylic acid and alkenes group significantly. Fatty acid composition of extracted oil investigated by Gas Chromatography is indicated in Figure (6) and Table (8). The results shown in Table (8) represent that extracted oil mainly contains palmitic acid (25.9%), oleic acid acid (43.7%)as predominant compounds while stearic acid (19.3%) and linoleic acid (9.8%)were low. The results are in agreement with Mishraet al. (2013).The results shown in Table (9) represent the comparative study on physico-chemical properties of extracted meze seed oil and commercial oil with literature value. Peroxide value, acid value and iodine value of extracted meze seed oil are much less than that of commercial oil and these lower values indicate the freshness and lower rancidity of extracted oil. This observation is in agreement with the findings of Chakrabarty (2003)that these detections give the initial evidence of rancidity in unsaturated fats and oils.

The results shown in Table (10) represents the comparative study of physico-chemical properties of meze seed oils extracted by different solvents. Because of higher boiling range of ethanol, oil extracted with 95% ethanol has greater peroxide value and acid value than that extracted with SBP and

petroleum ether. In addition to simple distillation, vacuum distillation was also conducted to obtain meze seed oil. According to Table (11), it can be seen that the characteristics such as colour, acid value, peroxide value and saponification value of vacuum-distilled oil are less than that of simple-distilled oil indicating a better quality of meze seed oil. Besides these, the time taken for vacuum distillation is less than half of that taken for simple distillation.

Meze Tree and Fruits

Meze Seeds

Meze Seed kernels

Meze Seed Oilby expeller

Meze Seed Oilby petroleum ether

Table 1: Physico-Chemical Properties of Meze Seed Kernels(Myanmar)

Sr. No	Characteristics	Meze seed	Literaturevalues *
1.	Moisture content (w/w%)	4.18	7.8
2.	Ash content (w/w%)	1.64	3.4
3.	Protein (w/w%)	5.90	16.9
4.	Crude fiber (%)	8.86	3.2
5.	Crude fat (%)	53.71	46.7
6.	Carbohydrate (%)	25.71	22

Table 2: Phytochemical Characteristics of Meze Seed Kernel (Myanmar)

Sr. No.	Tests	Extract	Reagents	Observation	Inference
1	Alkaloids	1%HCl	Mayer's reagent Dragendorff's reagent	White ppt Orange ppt	+
2	Flavonoids	EtOH	H_2SO_4(conc:) +Mg turning	Pink colour	+
3	Glycosides	H_2O	10%$FeCl_3$	Purple colour	+
4	Phenolics	H_2O	10%$FeCl_3$	Blue-black colour	+
5	Reducing Sugar	H_2O	Fehling's solution	Brick red ppt	+
6	Tannins	H_2O	2% NaCl+ 1%$FeCl_3$	Deep blue ppt	+
7	Saponin	H_2O	-	Persistent foam	+
8	Carbohydrate	H_2O	10%α naphthol &H_2SO_4(conc:)	Red ring	+
9	α-amino acid	H_2O	Ninhydrin reagent	Purple colour	+
10.	Starch	H_2O	Iodine solution	-	-

Table 3: Elemental Composition of Meze Seed Kernel Analyzed by Energy Dispersive X-ray Fluorescence (EDXRF) Spectroscopy Method

Element	Composition (w/w%)
K	0.079
Ca	0.018
Fe	0.002
C	99.901

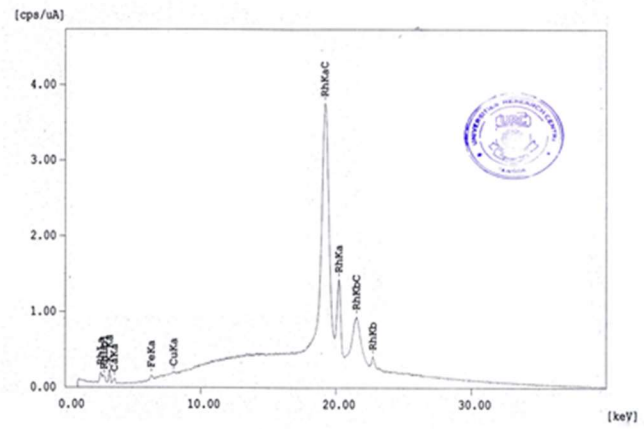

Figure 1: EDXRF Spectrum for Elemental Composition of Meze Seed Kernel

Table 4: Effect of the Volume of Solvent on Yield of Meze Seed Oil Extracted Using

Different Solvents

Weight of meze seed kernel = 5 g
Time of extraction = 4hr
Particle size of kernel powder = 10 mesh

Sr. No	Volume of Solvent (mL)	Ratio of meal to solvent (w/v)	95% Ethanol		SBP (62/82)		Petroleum Ether	
			Weight of oil (g)	Oil yield (%)	Weight of oil (g)	Oil yield (%)	Weight of oil (g)	Oil yield (%)
1.	200	1:40	2.52	50.4	2.61	52.2	2.830	56.6
2.	250 *	1:50	2.58	51.6	2.62	52.4	2.890	57.8
3.	300**	1:60	2.62	52.4	2.48	53.1	2.905	58.1
4.	350	1:70	2.64	52.8	2.65	54.4	2.915	58.3
5.	400	1:80	2.67	53.4	2.74	54.8	2.925	58.5

* Most suitable volumes of 95% ethanol and petroleum ether
** Most suitable volume of SBP

Table 5: Effect of Extraction Time on Yield of Meze Seed Oil, Extracted Using **Different Solvents (based on most suitable volume of each solvent)**

Weight of Meze seed kernel = 5 g
Volume of 95% ethanol / Petroleum ether = 250 mL
Volume of SBP(62/82) = 300 mL
Particle size of kernel = 10 mesh

Sr. No	Extraction Time (hr)	95% Ethanol		SBP (62/82)		Petroleum Ether	
		Weight of oil (g)	Oil yield (%)	Weight of oil (g)	Oil yield (%)	Weight of oil (g)	Oil yield (%)
1.	1	1.4	28	2.1	42	2.32	46.4
2.	2	1.52	30.4	2.53	50.6	2.61	52.2
3.	3	1.4	37.6	2.6	52	2.62	52.4
4.	4*	2.58	51.6	2.48	53.1	2.89	57.8
5.	5	1.76	45.2	2.42	48.4	2.87	57.4

* Most suitable extraction time using 95% ethanol, SBP(62/82) and petroleum ether

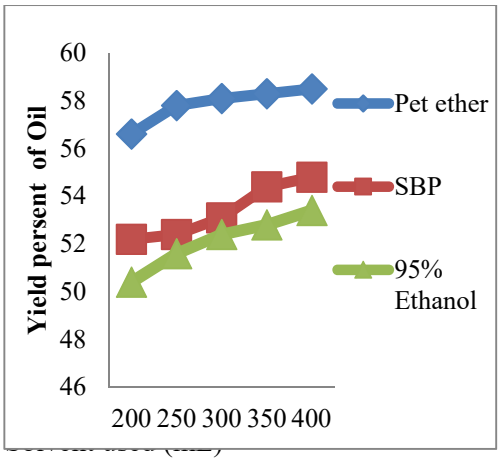

Figure 2: Effect of Extraction Timeon Yield of Meze Seed Oil ,Extracted Using Different Solvents

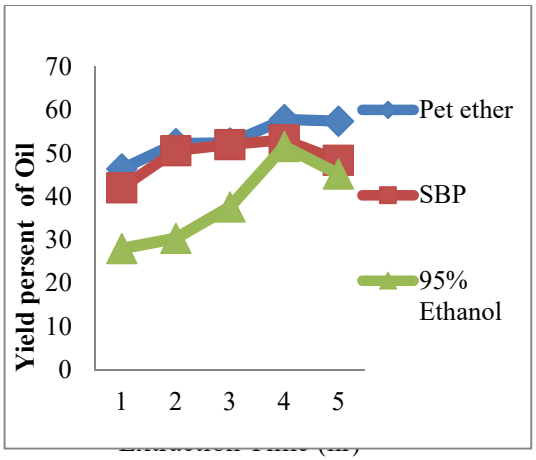

Figure 3: Effect of Extraction Timeon Yield of Meze Seed Oil, Extracted Using Different Solvents

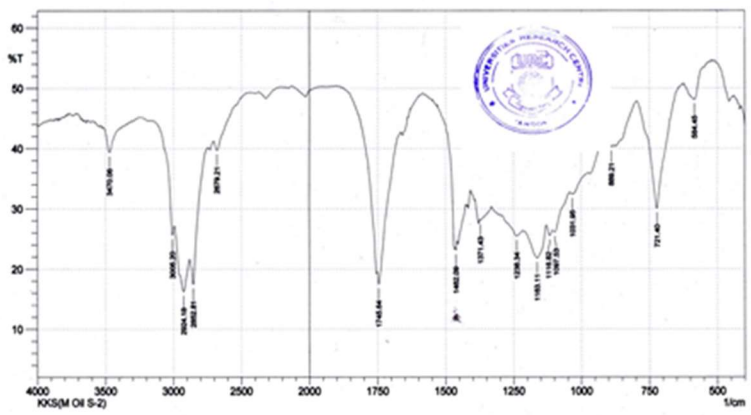

Figure 4: FT-IR Spectrum of Extracted Meze Seed Oil

Table 6: FT-IR Spectrum Data of Extracted Meze Seed Oil

Wave number, cm^{-1}			
Observed	**Literature ***	**Functional group**	
3470	3500-3300	υ– NH	Stretching vibration of amines groups
3005	3560-3500	υ– OH	Stretching vibration of carboxylic acid
2924 2852	3000-2840	υ– CH	Stretching vibration of alkane group
2679	2700-2500	υ– OH	OH-in plane bending and C-O stretching
1745	1740-1720	υ – C=O	Stretching vibration of carboxylic acid
1462	1550-1220	υ – CO-H	Stretching vibration of alcohol and phenol group
1371	< 1400	υ– CH	CH symmetric bending vibration
1238 1163 1116	1260-1000	υ – C-O	Stretching vibration of alcohol and phenol group
889	~ 890	υ– CH	Stretching vibration of alkenes group (1,1-disubstituted)
721	~ 700-750	υ– CH	Stretching vibration of alkenes group (cis 1,2- disubstituted alkenes)

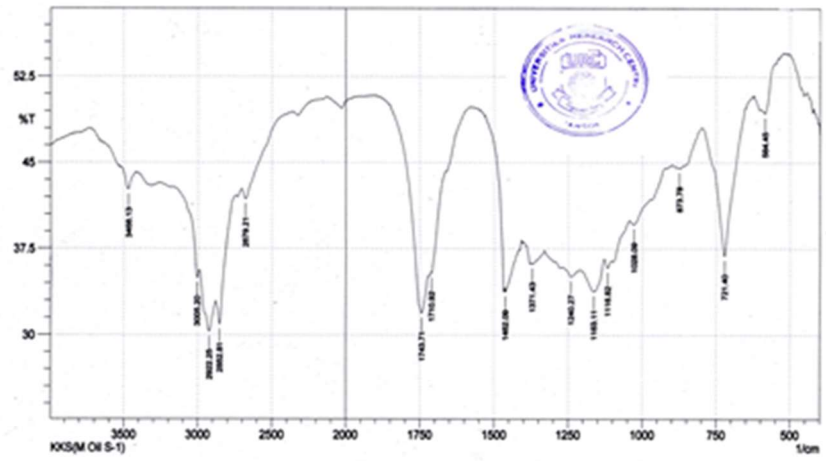

Figure 5: FT-IR Spectrum of Commercial Oil

Table 7: FT-IR Spectrum Data of Commercial Meze Seed Oil

Wave number, cm^{-1}		Functional group	
Observed	**Literature ***		
3468	*3500-3300*	***υ**– NH*	*Stretching vibration of amines groups*
3005	3560-3500	*υ*– OH	Stretching vibration of carboxylic acid
2922 *2852*	*3000-2840*	***υ**– CH*	*Stretching vibration of alkane group*
2679	~2700-2500	*υ*– OH	OH-in plane bending and C-O stretching
1743 *1710*	*1740-1720*	***υ** – C=O*	*Stretching vibration of carboxylic acid*
1462	1550-1220	*υ*– OH	Stretching vibration of alcohol and phenol group
1371	< 1400	*δs*- CH	CH symmetric bending vibration
1240 1163 1117	1260-1000	*υ* – C-O	Stretching vibration of alcohol and phenol group
874	~ 890	*υ*– CH	Stretching vibration of alkenes group (1,1-disubstituted)
721	~ 700-750	*υ*– CH	Stretching vibration of alkenes group (cis 1,2- disubstituted alkenes)

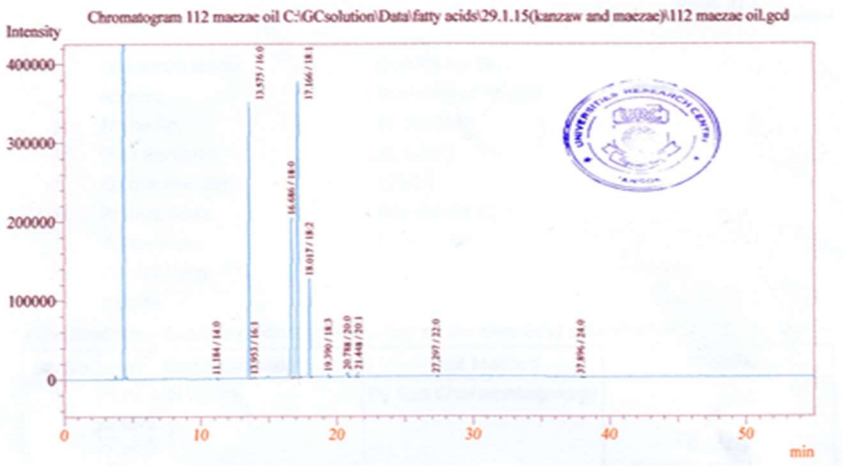

Figure 6 : Fatty Acid Gas chromatogramme of Extracted Meze Seed Oil

Table 8: Fatty Acid Composition of Extracted Meze Seed Oil by GC Analysis

Fatty acids composition by GC	**Values (%w/w)**	**Literature values (%w/w) ***
C 12:0 (Lauric)	Not detected	-
C 14:0 (Myristic)	0.073	-
C 14:1	Not detected	-
C 16:0 (Palmitic)	25.913	24.5
C 16:1 (Oleo-Palmitic)	0.059	-
C 18:0 (Stearic)	19.330	22.7
C 18:1 (Oleic)	43.716	37
C 18:2 (Linoleic)	9.824	14.3
C 18:3 (Linolenic)	0.283	-
C 20:0 (Arachidic)	0.526	-
C 20:1	0.125	-
C 22:0 (Behenic)	0.052	-
C 22:1	Not detected	-
C 24:0 (Lignoceric)	0.1	-

*International Journal of Humanities and Social Science Invention

Table 9: Comparison of Physico-Chemical Properties of Extracted Meze Seed Oil with Commercial Oil

Sr. No	Properties	Extracted meze seed oil	Commercial oil *	Literature values **
1.	Refractive index	1.465± 0.02	1.466± 0.01	1.452-1.462
2.	Specific gravity	0.908± 0.01	0.193± 0.53	0.862-0.875
3.	Colour	2.3R, 1.5B, 20Y	2.5 R, 0.2 B, 40.5Y	Pale Yellow
4.	Saponification value (mg KOH per g)	195.49± 0.56	197.223± 0.53	187-196
5.	Unsaponifiable matter (%)	0.984± 0.09	2.95± 0.06	1-3
6.	Iodine value (mgI_2/g)	53.50± 0.32	55.352± 0.372	58-70
7.	Peroxide value (milliequi peroxide oxygen per kg)	9.369± 0.62	26.422± 0.67	-
8.	Acid value (mg KOH per g)	1.752± 0.22	5.044± 0.045	0.5-20
9.	Moisture (loss on drying) %	0.046± 0.01	1.27 ± 0.11	-
10.	Relative density (at 20°C)	0.913± 0.01	0.182± 0.006	-

*Purchased from Daw San Oil Milll, Amarapura Township, Mandalay Region.
** :en.m.wikipedia. org/-----/ *Madhucalongifolia*

Table 10: Comparison of Physico-Chemical Properties of Meze Seed Oils Extracted by Different Solvents

Sr. No.	Properties	Extracted meze seed oil			Literature values *
		95% Ethanol	SBP(62/82)	Petroleum Ether	
1.	Refractive index	1.466±0.01	1.469±0.02	1.465±0.1	1.452-1.462
2.	Specific gravity	0.918±0.002	0.945±0.29	0.907±0.02	0.862-0.875
3.	Colour	2.5R, 0.9B, 25.5Y	2.3R, 1.3B, 20Y	2.1R, 1.2B, 25.2Y	Pale Yellow
4.	Saponification value (mg KOH per g)	197.892±0.06	196.167±0.81	192.659±0.75	187-196
5.	Unsaponifiable matter (%)	2.372±0.14	1.617±0.01	1.612±0.005	1-3
6.	Iodine value (mg I_2/g)	54.126±0.66	54.486±0.23	54.124±0.88	58-70
7.	Peroxide value (milliequi peroxide oxygen per kg)	28.753±0.52	7.226±0.5	15.66±0.27	-
8.	Acid value (mg KOH per g)	22.598±0.22	6.689±0.19	8.569±0.37	0.5-20
9.	Moisture (loss on drying) %	0.045±0.008	0.039±0.03	0.099±0.01	-
10.	Relative density (at 20°C)	0.921±0.03	0.928±0.01	0.918±0.008	-

* :en.m.wikipedia. org/-----/ *Madhucalongifolia*

Table 11: Comparison of Physico-Chemical Properties of Extracted Meze Seed Oil using Simple and Vacuum Distillation

Sr. No	Properties	Extracted with 95% Ethanol		Extracted with SBP(62/82)		Extracted with Petroleum Ether		Literature values*
		Simple-distillation	Vacuum-distillatio	Simple-distillati	Vacuum-distillatio	Simple-distillati	Vacuum-distillatio	
1.	Colour	2.5 R, 0.9 B, 17.5 Y	4.8 R, 0 B, 17 Y	2.3R, 1.3B, 17 Y	6.2 R, 0 B, 17 Y	2.1R, 1.2B, 17 Y	5.8 R, 0 B, 17 Y	Pale Yellow
2.	Saponification value (mg KOH per g)	197.892 ±0.06	189.912 ±0.29	196.167 ±0.81	189.636 ±0.21	192.659± 0.75	198.665 ±0.23	187-196
3.	Peroxide value (milliequivalent peroxide oxygen per kg)	28.753 ±0.52	14.510 ±0.19	7.226 ±0.5	2.491 ±0.21	15.66 ±0.27	12.560 ±0.2	-
4.	Acid value (mg KOH per g)	22.598 ±0.22	7.32 ±0.32	6.689 ±0.19	5.921 ±0.1	8.569 ±0.37	6.176 ±0.05	0.5-20

Conclusion

The seed kernels having average moisture content between 4 and 6 % gave the maximum oil yield. Extraction of oil from meze seeds were conducted by using expeller and also by using the organic solvents like 95% ethanol, SBP and petroleum ether. 4 hours of extraction time gave a maximum oil yield percentage of 51.6% by 95% ethanol, 53.1% by SBP and 57.8% by petroleum ether. Petroleum ether is the most suitable solvent to achieve the maximum oil yield. But the defect of using petroleum ether and SBP is that the odour of these solvents remained in the extracted oil although the oil colour is better than using ethanol. The properties like acid value, peroxide value, saponification value and colour of meze seed oil extracted by solvents are also better than that extracted by expeller. But to extract the oil by solvent extraction is more expensive than using the expeller. Using vacuum distillation in oil extraction can give meze oil of better quality. Meze seed oil can be used to make soaps, candles and biodiesel production.

Acknowledgements

The author would like to acknowledge Professor Dr Cho Cho Oo, Head of the Department of Industrial Chemistry, University of Yangon, for giving permission to perform this research and advice on this research work.

I would like to express my gratitude to Dr Pansy Kyaw Hla, Professor (Retd.) of the Department of Industrial Chemistry, University of Yangon and Dr Yi Yi Myint, Professor and Head (Retd.) of the Department of Industrial Chemistry, Yadanabon University for their valuable suggestions and advice throughout this research work.

References

AbuAl-Futuh, I.M., (1983), United Nations Industrial Development Organization Report.

Harborne, JB, (1973), Phytochemical Methods, Chapman and Hall Ltd., New York.

International Food Research Journal 18 (4) 2011.

Mishra Sunita & Padhan Sarojini ,International Journal Of Humanities and Social Science Invention ISSN, Vol:2,May 2013.

Mohan,.J.,(2000). Organic Spectroscopy Application, Principle and Narosa Publishing House, New delhi.

Mani. S, Jaya.S and Vadivambal. R (2007), Food Bioprod. Process. 85 328

M.M, Chakrabarty, (2003), Chemistry and Technology of Oils and Fats.

Perry, J.H., Chemical Engineer's Hand Book. Mc. Graw Hill Book Company, Inc. Toyo. Kogakusha Company, Ltd.

Ratnabhargavi. A.R, (2013), Project Report on Setting Up Of a Mahua Oil Extraction Unit, India.

Websites

http :// en.m. wikipedia org/ Maducalongifolia

http :// www. mother herbs. com / madhuca-india

http :// shivorganics.com/ madhuca- india

http :// www . Jhssi-org/papers/----3/F253036,pdf

http :// www . Ijpsr.com/--/ 8% 20 vol % 203 % 20 IS

http :// www. grow- tree. com, Why Tree.

http://en.wikipedia.org/wiki/Ethanol)

http://en.m.wikipedia.org>wiki) Petrol….

TREATMENT OF DISTILLERY WASTEWATER BY USING THERMALLY AND CHEMICALLY ACTIVATED KAOLIN

Lei Lei Aung[1], Thin Yu Mon[2], Aye Mar Htun[3], Kay Khine Hnin[4]

Abstract

Large volumes of dark brown molasses spent wash is generated from the distillation step in Distilleries and consequently, detrimental to the sustainability of the environment. In this study, kaolin from Wallan village, Mon State was activated to prepare low cost adsorbent for removal of colour and specific organic pollutants from the wastewaters. The removal efficiencies of kaolin were firstly investigated by treating the effluentwith natural kaolin using various dosages of kaolin (3 to 9% wt/v) and different contact time (30 min to 150 min). Then the effects of combined mechanical and thermal activation (from 100 to 600ºC),and chemical activation (2.5 to 5.5 M sulphuric acid) on the contaminant removal efficiencies of kaolin were examined. The physico-chemical characteristics of wastewater such as colour, turbidity, chemical oxygen demand (COD) and UV/Vis absorbance at 436 nm before and after treatment were systematically analysed. The collected wastewater is characterized by extremely high chemical oxygen demand, turbidity and solid contents, apart from low pH, unpleasant odor and dark brown color. The experiments showed that natural kaolin (NK) largely removed colour imparting contaminants than turbidity and COD from wastewater. Activating the NK by methods such as grinding, grinding and heating, acid activation decreased its colour removal efficiencies while its turbidity and COD removal efficiencies dramatically increased upon activation.Among the natural and activated kaolin samples, acid activation of kaolin enhanced its turbidity and colour removal efficiencies. The maximum turbidity and COD removalefficiencies of ~80% and ~60%, respectively were achieved with acid activated kaolin (4.5 M sulphuric acid) for 30 min contact time whereas those of ~17% and ~36%, respectively with natural kaolin for 150 min.

Keywords: distillery wastewater, kaolin, mechanical and thermal activation, chemical activation, contaminant removal efficiencies

[1.] Dr, Lecturer, Department of Industrial Chemistry, University of Yangon
[2.] MSc. Student, Department of Industrial Chemistry, Yadanabon University
[3.] Assistant Lecturer, Department of Industrial Chemistry, Yadanabon University
[3.] Assistant Lecturer, Department of Industrial Chemistry, Yadanabon University

Introduction

The molasses spent wash (MSW)released from distilleries contains colouring compound called melanoidin, high chemical oxygen demand, biochemical oxygen demand, suspended solids, inorganic solids and low pH (Saha *et al.,* 2005). It is conventionally treated by anaerobic digestion for generation of methane and then aerobically using trickling filter or by activated sludge system prior to disposal. Although biological treatment can significantly remove COD, the effluent still has the dark color due to the presence of melanoidin. Furthermore, multistage biological treatment not only reduces the organic contaminants but also intensifies the color due to re-polymerization of colored compounds (Pena *et al.,* 2003).Adsorption is the most popular physicochemical treatment for the removal of dissolved organics from water (Meroufel *et al.,* 2013).Activated carbon is widely used due to its large surface area, microporus structure, high adsorption capacity and high degree of surface reactivity. Since large volume of water is used in distillery industries, activated carbon is not cost effective for treating the large volumes of distillery spent wash. Thus, there exist a potential to reach for low cost adsorbents.

Kaolin, one of the low-cost adsorbents that is commonly used in wastewater treatments (Nandi, *et al.,* 2009; Shirsath, *et al.,* 2013),is abundantly found in Myanmar. Kaolin consists of clay minerals such as kaolinite, illite, halloysite, and montmorillonite, and of non-clay minerals as quartz and feldspar, anastase, and gibbsite (Panda *et al.,* 2010). Kaolinite, 1:1 type aluminosilicate clay mineral, $(Si_4)_{IV}(Al_4)_{VI}O_{10}(OH)_8$, has variable charge that depends on the pH, on alumina face and on the edges arising from the protonation and deprotonation of exposed hydroxyl groups (James, 1995). Since the terminal OH groups have either a partial positive or partial negative charge groups, they also possibly chemisorb certain types of ions, regardless of the pH value. The industrial applications depend on the surface modifications of kaolin. Many researchers have reported that the mineralogical and textural properties of kaolin can be altered by activating it mechanically or chemically, in particular using sulfuric acid (Nguetnkam *et al.,* 2008; Didi *et al.,* 2009). However, there are limitations in the existing

methods and it is necessary to evaluate the treatment processes that provide a better solution for distillery spent wash.

The objectives of this study are (i) to prepare kaolin which is abundantly found in Myanmar as an adsorbent for wastewater treatment and (ii) to evaluate the effect of mechanical, thermal and chemical activation on their contaminant removal efficiencies.

Materials and Methodology

Materials

Kaolin from Wallan village, Chaunghsone Township, Mon State was supplied by Mupon Ceramic Factory.The distillery wastewater was collected from the effluent storage tank at the Shwe Myanmar Factory, Industrial Zone 2, Mandalay.

Figure 1: Raw Materials. (a) Kaolin; (b) Distillery Wastewater

Methodology

Preparation of Kaolin

The pale yellow-colored kaolinwas washed with distilled water until the pH of kaolin suspension reached about 7to remove the soluble mineralogical impurities. The sample was dried in an oven (Pelion 0°C-300°C) at 100°C for 24 hr and then sieved to 200 mesh kaolin powder, referred to as NK (Natural Kaolin). Less than 2 μm fraction is also better size for studying coarser-grained clay minerals such as kaolinite and chlorite (Srodon, 2006).

Combined Mechanical and Thermal Activation of Kaolin

Natural kaolin was ground using the iron pot pulverizer (Labtechnics). NK was ground with the three centrifugal rings rotatingat 300 rpm for 15 min to test the effect of small particles on the kaolin's contaminant removal efficiency. The ground kaolin (GK) was heated for 1 hr in a muffle furnace (O Lab) at 600°C and then, screened with 200 mesh sieve. The resulting sample is regarded as GHK (Ground and Heated Kaolin).The same procedure was repeated at different temperatures such as 100°C, 200°C and 400°C.

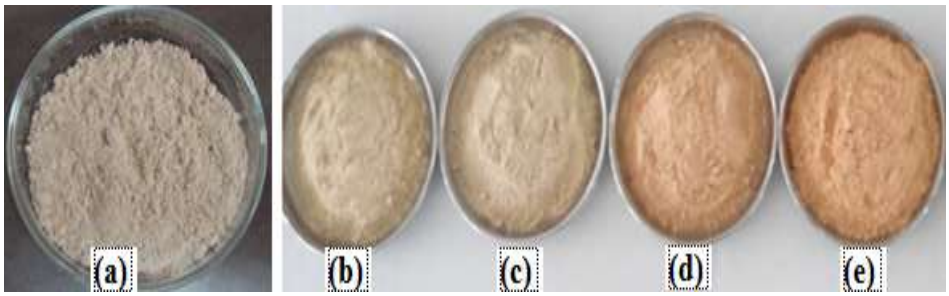

Figure 2: Ground Kaolin (a); Ground and Heated Kaolin Prepared at Different Temperatures (b) 100°C (c) 200°C (d) 400°C and (e) 600°C

Chemical Activation of Kaolin

The kaolin powder was refluxed with 2.5M sulphuric acid solution in the solid-liquid ratio of 1:50 (10 g of kaolin to 500 mL of H_2SO_4) at 80°C for 4 hr under mechanical stirring. The acid-refluxed kaolin samples were washed with distilled water until reaching pH of 3. It was dried at 100°C for 24 hr and then, screened with 200 mesh sieve. The sample produced is referred to as AAK (Acid Activated Kaolin).The same procedure was repeated using various sulphuric acid concentrations of 3.5M, 4.5 M and 5.5 M.

Figure 3: Natural Kaolin (a); Acid Activated Kaolin Prepared using Various Sulphuric Acid Concentrations(b) 2.5 M (c) 3.5 M (d) 4.5 M and (e) 5.5 M

Preparation of Distillery Wastewater

Collected distillery wastewater was filtered using filter cloth to remove sand and other undissolved impurities.

Adsorption Studies

Treatment of Distillery Wastewater

Natural kaolin (3% (w/v)) was mixed with the distillery wastewater under agitation at 150 rpm for 30 min. The mixture was then centrifuged at 2,000 rpm for 15 min and filtered through a filter paper.

To study the effect of kaolin dosage on the removal of contaminants from wastewater, the same procedure was repeated using different NK dosages such as 5%, 7% and 9% (w/v). Wastewater was treated with NK 7% (w/v) (the most suitable dosage in this study) for different contact time (30-150 min) to evaluate the optimum treatment time. The effects of physical and chemical activation on kaolin were also studied. The same experiments were done using activated kaolins such as ground and heated kaolin (GHK) and acid activated kaolin (AAK) samples in the kaolin dose of 7% (w/v) for 30 min. All the adsorption experiments were done at room temperature. Values reported in tables and figures are the means of duplications.

Analysis of Raw and Treated Distillery Wastewater

The true colour (TCU- True Colour Units) of filtrate was determined at 565 nm and 635 nm absorbance for green and red colour, respectively after scanning the wavelength at 430 nm, 470 nm, 565 nm and 635 nm using colourimeter (labquest). Turbidity (NTU-Nephelometric Turbidity Units) was determined with Vernier turbidity sensor using Absorptometric method. The pH of the distillery wastewaters before and after treatments with optimized kaolin samples was tested with VernierpH meter. Chemical Oxygen Demand (COD) was determined by titration method. The filtrate was tested to measure the yellow colour representing organic compounds in wastewater using the UV/Vis spectrophotometer (LABOMED UV-2550). In the Photometric method, the filtered distilled water was calibrated at zero and the spectrophotometer was set at visible range 436 nm.

Results and Discussion

In this research, the contaminant removal efficiencies of natural and activated kaolin on distillery wastewater were studied. The physical and chemical characteristics of distillery wastewater were compared with literature values as shown in Table (1). It had extremely high COD (256000 mg/L), Turbidity (~52 mg/L), but pH was low, unpleasant odor and dark brown color. The characteristics of the spent wash depend on the raw material used (Mall and Kumar, 1997). The contaminants removal efficiencies of kaolin were firstly investigated by treating the wastewaters with natural kaolin using various dosages of kaolin (3 to 9% wt/v) and the results are shown in Table (2). Some contaminants imparting green and red colour, turbidity and COD were increasingly decreased with increasing kaolin doses. The removal efficiencies on green color is from ~31% to ~72%, red color is from ~44% to ~46% and turbidity is from ~16% to ~80% (Figure 4). This is due to the increase in surface area and active sites on kaolin and consequently, causing the kaolin to be adsorbed with organic matter from the effluent. However, COD removal was slightly increased from ~5% to ~16% when kaolin dosage was increased from 3% to 7% (wt/v). Further increased to 9% (wt/v) of kaolin, the COD removal efficiency was decreased to ~11% (Figure 4-b). This

means increasing natural kaolin (NK) doses had slightly affected COD and also yellow-colored organic materials removal efficiencies of NK.

The characteristics of distillery wastewater before and after treatment with NK for 30 min, 90 min and 150 min are shown in Tables (3).True colour measured at 565 nm and 635 nm and visible absorbance at 436 nm of treated wastewater were also decreased except the contact time 90 min was applied for wastewater treatment. This means the materials imparting green, red and yellow colour representing organic compounds in wastewater were removed by adsorption. The color removal efficiencies were high whereas turbidity and COD removal efficiencies of NK were low when wastewater was treated with 7% (wt/v) of kaolin for 30 min. Further increasing of treatment time to 150min, the green colour, yellow colour and turbidity removal efficiencies decreased from ~70% to ~28%, ~13% to ~5% and ~13% to ~5% (Figure 5). However, COD reduced from 196300 mg/L to 164800 mg/L when wastewater treatment time was increased from 30 min to 150 min. The slight increase in COD removal efficiency (from ~24% to ~36%) with increasing time also indicates that treatment time did not significantly affect on the NK. Therefore, the suitable conditions are selected as kaolin dosages (7% wt/v) and treatment time (30 min) for distillery wastewater treatment.

Ground Kaolin was activated with different temperatures ranging from 100°C to 600°C and the results are shown in Table (4) and Figure (6). All the pollution parameters of treated wastewater decreased upon treating with GK. When ground kaolin was heated to 100°C, the yellow colour removal efficiencies were decreased from ~22% to ~2% while removal for COD and turbidity were increased from ~23% to ~46% and ~33% to ~58% (Figure 6). However, heating GK above 100°Cduring activation slightly decreased the colours (@ 565 nm and 635 nm) of distillery wastewater at 600°C from 1.087 to1.017 and from 0.484 to 0.365 (Table 4).Among of the ground and heated kaolin (GHK samples), the ground kaolin heated at 100°C gave the most suitable conditions for distillery wastewater treatment. At this temperature, COD and turbidity of treated wastewater were at the least value (137600 mg/L and 22 NTU units)as shown in Table (4). The analyzed parameters (COD and turbidity) were increased with increasing heating temperatures from 100°C to 600°C: COD and turbidity values increased to 174400 mg/L and to 35.1 NTU

units, respectively and removal efficiencies for COD was decreased to ~32% and turbidity to ~32%. Mechanical activation breaks down kaolinite structure and OH bonds which lead to changes in fineness of solid particles, surface area and number of active sites of the materials (Pacheco-Torgal et al., 2011). In the course of a thermal activation, kaolinite loses the most part of its structural water and passes into a metastable state (Dudkin et al., 2005) resulting in collapsed and disarranged clay structure (Sabir et al., 2001) and hence a decrease in the specific surface area which leads to decrease in color removal (James et al., 2008).

Effect of different sulphuric acid concentrations (2.5 M to 5.5 M) on the contaminant removal efficiencies of kaolin were shown in Table (5) and Figure (7). When the natural kaolin was activated using 2.5 M sulphuric acid, the turbidity values was dramatically decreased from ~43 to ~15 NTU units whereas other parameters such as colour and COD values were increased. The turbidity removal efficiency of AAK (2.5 M sulphuric acid) was increased from ~16% to ~71% upon acid activation (Figure 7-b). However, further increasing the acid concentration to 4.5 M increased the contaminant removal efficiencies of AAK samples. The colour at 565 nm, colour at 635 m, turbidity and COD values were decreased to~0.99, 0.47, 10.4 NTU units and 104000 mg/L, respectively. Acid activated kaolin (4.5 M sulphuric acid) gave the maximum COD and turbidity removal of ~60% and ~80%, respectively. The colour and COD removal efficiencies of AAK decreased when the acid concentration was increased to 5.5 M. Acid activation leaves a large number of highly active silanol and aluminol groups on the adsorbent sites (Dudkin et al., 2005). Upon acid activation, specific surface area, porosity and number of acid centers are also changed in the activated clay due to the leaching of alumina and other mineral impurities (Rhodes and Brown, 1992). However, sorption properties decreased at high acid concentrations along with the extensive leaching of alumina from the clay corresponding to the collapse of clay structure.

The contaminants removal efficiencies of natural kaolin, ground kaolin, ground and heated kaolin (at 100°C), and acid activated kaolin (4.5 M) was shown in Table (6) and illustrated in Figure (8). NK gave the lowest colour value and the highest turbidity and COD values. This indicates that NK

largely removed colour imparting contaminants than turbidity and COD from wastewater. Activating the kaolin (NK) such as grinding, grinding and heating, acid activation decreased its colour removal efficiencies while its turbidity and COD removal efficiencies largely increased. Among these activated kaolin samples, acid activated kaolin (AAK) gave the maximum turbidity and COD removal efficiencies of ~80% and ~60%, respectively (Figure 8). The pH value of treated wastewater was increased from 4.76 to 8.08 after treatment with natural kaolin and to 7.42 with ground kaolin. However, pH value was changed to ~4.4 when the wastewater was treated with activated kaolin (such as GHK and AAK).Though kaolinite is the least reactive clay, its high pH dependency enhances or inhibits the adsorption of metals according to the pH of the environment (Bhattacharyya and Gupta, 2008). Based on the COD and turbidity removal efficiencies, the acid activated kaolin (4.5 M sulphuric acid) gave the most suitable conditions for distillery wastewater treatment.

Table 1: Physical and Chemical Characteristics of Distillery Wastewater

Sr. No	Parameters	Distillery Wastewater	Literature[a] Values
	Physical Characteristics		
1	Colour TCU (at 565 nm) TCU (at 635 nm)	 1.417 0.785	 - -
2	Turbidity (NTU unit)	51.5	-
	Chemical Characteristics		
3	pH	4.76	3-5.4
4	COD (mg/L)	256000	104000-134400
	Absorbance @ 436nm		
5	Vis_{436}	2.826	-

[a] Pathate (1999)

Table 2: Characteristics of Distillery Wastewater Before and After Treatment with Various Dosages of Natural Kaolin (NK)

Sr. No	Parameters	Before Treatment	After Treatment (Treated with Various NK Doses (wt/v))			
			3%	5%	*7%	9%
1	Colour TCU (at 565 nm) TCU (at 635 nm)	 1.417 0.785	 0.982 0.44	 0.964 0.44	 0.429 0.435	 0.401 0.422
2	Turbidity (NTU unit)	51.5	46.2	45.1	43.3	42.1
3	COD(mg/L)	256000	243558	234675	215111	227558
4	Vis_{436}	2.826	2.66	2.446	2.46	2.47

* Most Suitable Condition

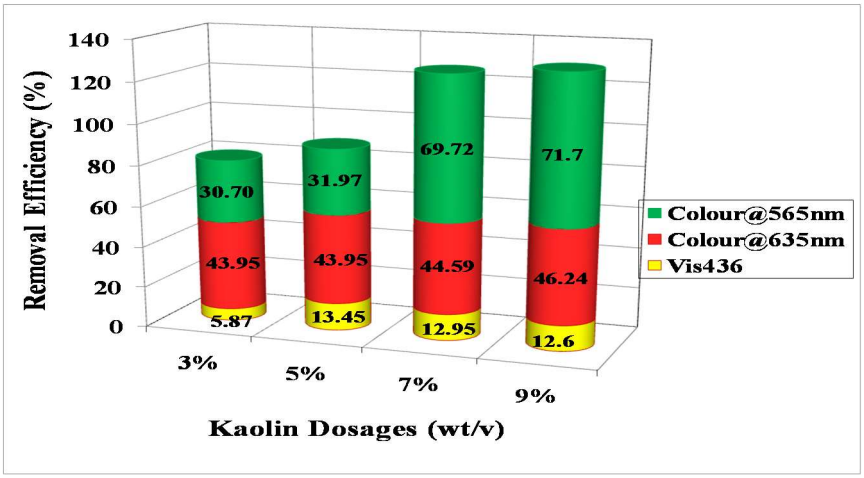

(a)

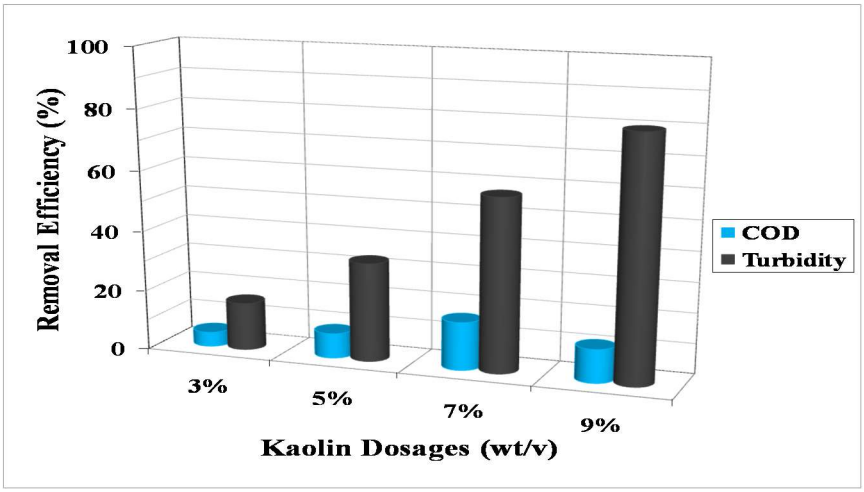

(b)

Figure 4: Effect of Different Dosages on NK for Removal of Contaminants from Wastewater. (a) Color Removal; (b) COD and Turbidity Removal

Table 3: Characteristics of Distillery Wastewater Before and After Treatment with Natural Kaolin (NK) for Different Treatment Time

Sr. No	Parameters	Before Treatment	After Treatment with NK (Treated for Different Time)		
			*30min	90 min	150 min
1	Colour TCU (at 565 nm) TCU (at 635 nm)	 1.417 0.785	 0.429 0.435	 1.223 0.924	 1.017 0.365
2	Turbidity(NTU unit)	51.5	43.3	38.5	42.6
3	COD (mg/L)	256000	193600	172800	164800
4	Vis_{436}	2.826	2.46	2.634	2.673

* Most Suitable Condition

(a)

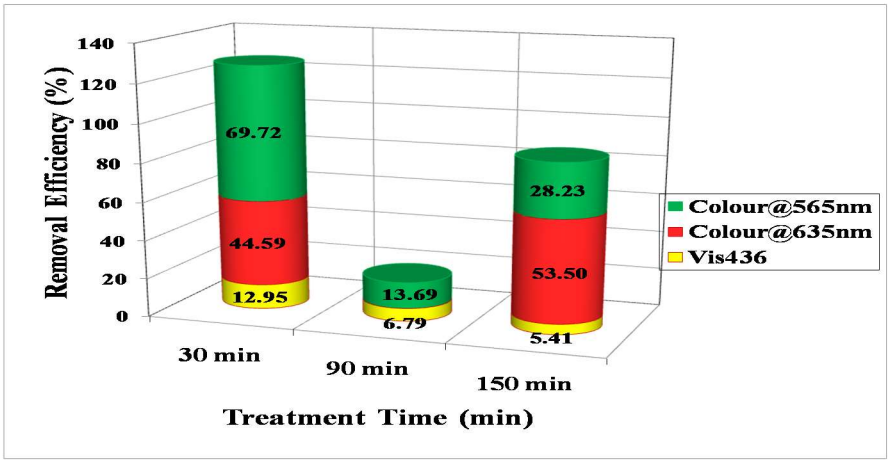

(b)

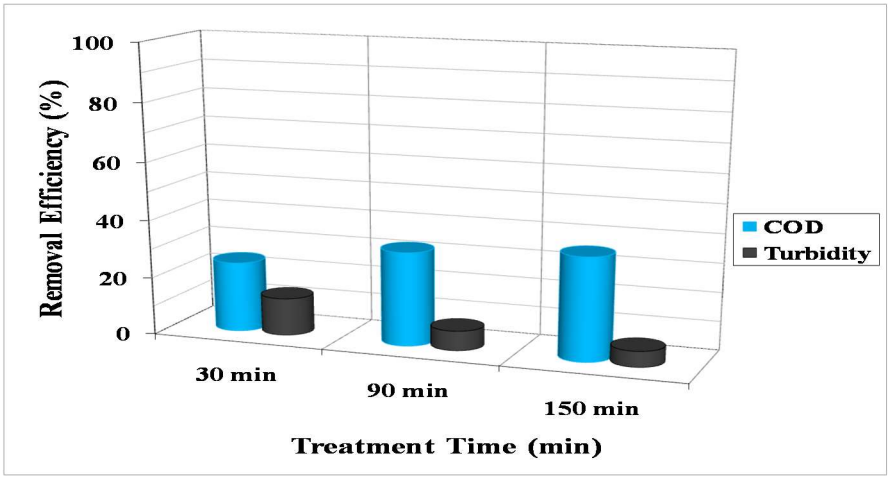

Figure 5: Effect of Wastewater Treatment Time on NK for Removal of Contaminants from Wastewater. (a) Color Removal; (b) COD and Turbidity Removal

Table 4: Characteristics of Distillery Wastewater Before and After Treatment with Ground Kaolin (GK) and Ground and Heated Kaolin (GHK)

Sr. No	Parameters	Before Treatment	After Treatment with GK and GHK				
			GK	GHK: Activated at Different Temperatures			
				*100°C	200°C	400°C	600°C
1	Colour TCU (at 565 nm) TCU (at 635 nm)	 1.417 0.785	 1.124 0.484	 1.087 0.484	 1.079 0.408	 1.072 0.407	 1.017 0.365
2	Turbidity (NTU unit)	51.5	34.6	22	30.1	34.1	35.1
3	COD (mg/L)	256000	196800	137600	148800	176000	174400
4	Vis_{436}	2.826	2.21	2.775	2.768	2.748	2.738

* Most Suitable Condition
Treatment Conditions: Time = 30 mins, Kaolin Dosage = 7 % (wt/v)

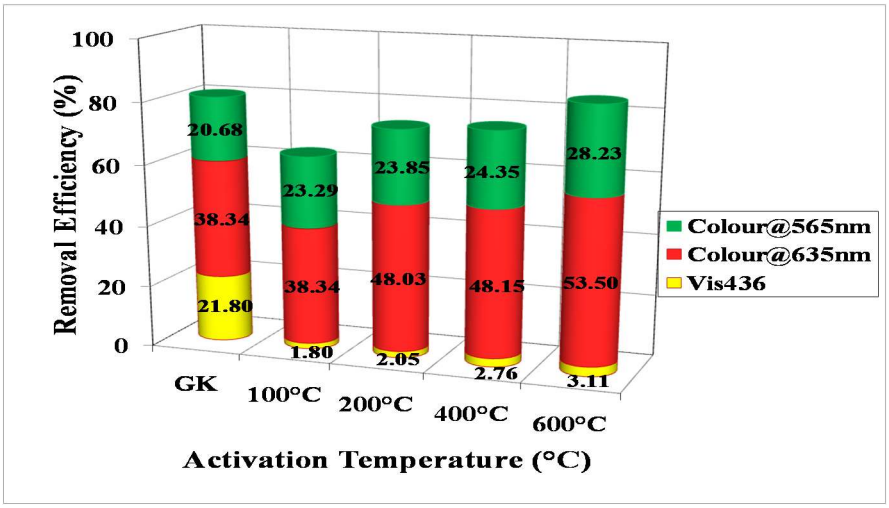

(a)

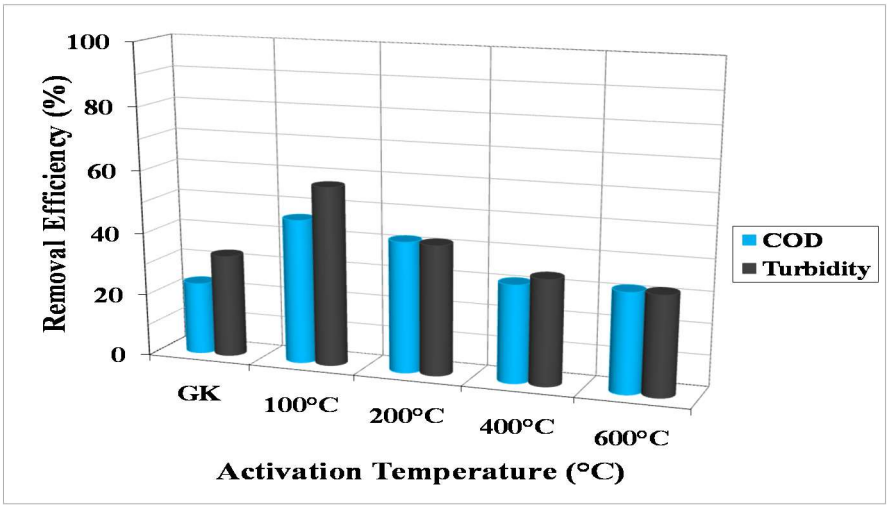

(b)

Figure 6: Effect of Activation Temperature on GK for Removal of Contaminants from Wastewater. (a) Color Removal; (b) COD and Turbidity Removal

Table 5: Characteristics of Distillery Wastewater Before and After Treatment with Acid Activated Kaolin (AAK)

Sr. No	Parameters	Before Treatment	After Treatment with NK and AAK				
			NK	AAK: Activated using Various Sulphuric Acid Concentrations			
				2.5 M	3.5 M	*4.5 M	5.5 M
1	Colour TCU (at 565 nm) TCU (at 635 nm)	 1.417 0.785	 0.429 0.435	 1.132 0.564	 1.126 0.549	 0.991 0.475	 1.172 0.647
2	Turbidity (NTU unit)	51.5	43.3	14.8	12.6	10.4	9.9
3	COD (mg/L)	256000	215111	217600	187200	104000	213600
4	Vis_{436}	2.826	2.46	2.728	2.716	2.699	2.763

* Most Suitable Condition

Treatment Conditions: Time = 30 mins, Kaolin Dosage = 7 % (wt/v)

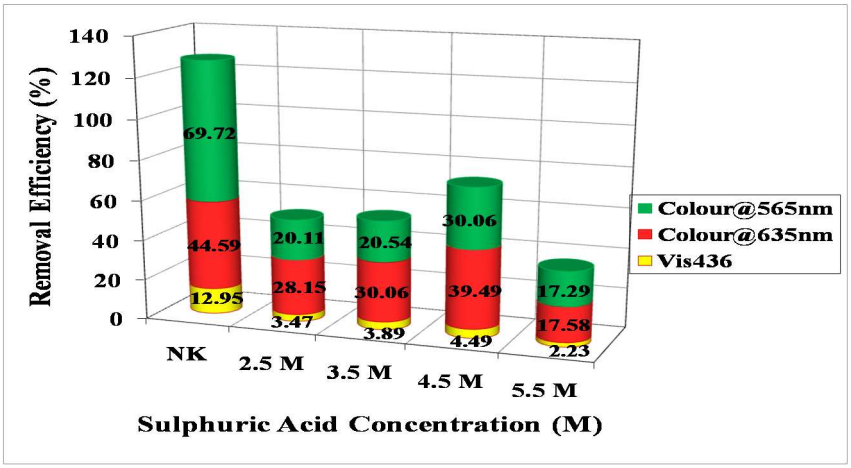

(a)

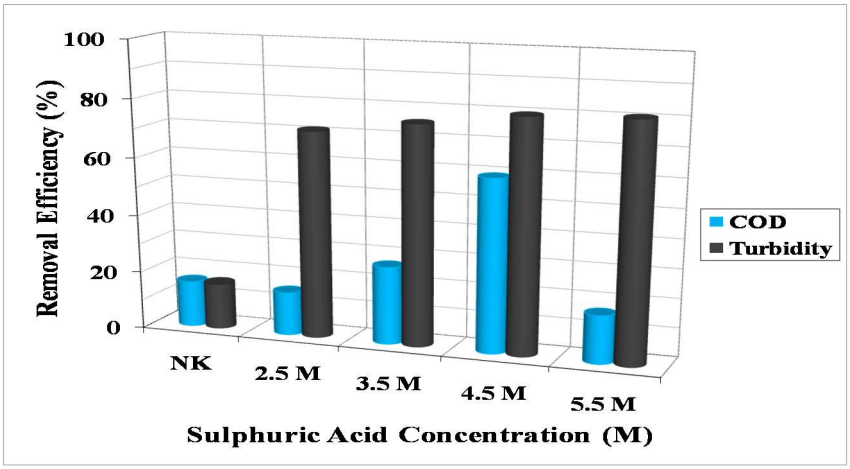

(b)

Figure 7: Effect of Sulphuric Acid Concentration on NK for Removal of Contaminants from Wastewater. (a) Colour Removal; (b) COD and Turbidity Removal

Table 6: Comparison of Distillery Wastewater's Characteristics Before and After Treatment with Optimized Natural and Activated Kaolin

Sr. No	Parameters	Before Treatment	After Treatment (Treated with Different Kaolin Samples)			
			NK	GK	GHK	*AAK
1	Colour TCU (at 565 nm) TCU (at 635 nm)	 1.417 0.785	 0.429 0.435	 1.124 0.484	 1.087 0.484	 0.991 0.475
2	Turbidity (NTU unit)	51.5	43.3	34.6	22	10.4
3	pH	4.76	8.08	7.42	4.46	4.41
4	COD (mg/L)	256000	215111	196800	137600	104000
5	Vis_{436}	2.826	2.46	2.21	2.775	2.699

* Most Suitable Condition;

NK=Natural Kaolin, GK=Ground Kaolin, GHK= Ground Kaolin heated at 100°C, AAK= Kaolin Activated using 4.5 M Sulphuric Acid;

Treatment Conditions; Time = 30 mins, Kaolin Dosage= 7 % (wt/v)

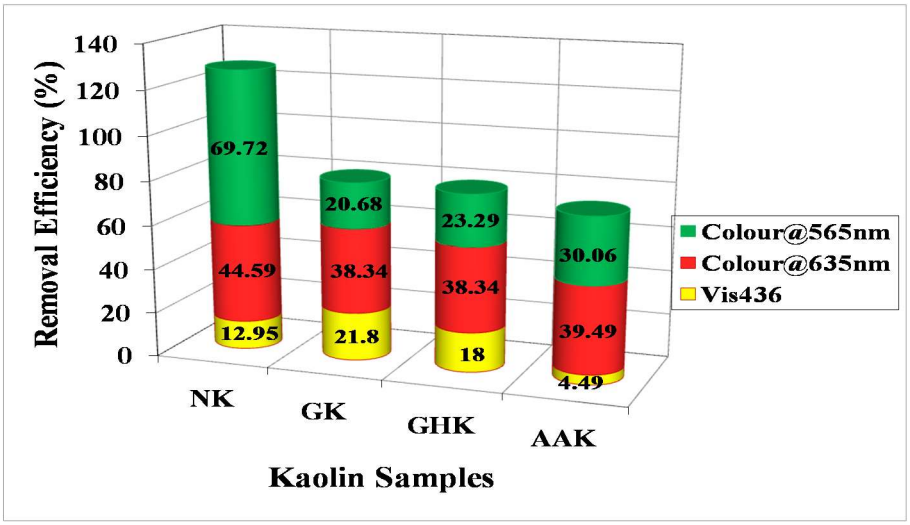

(a)

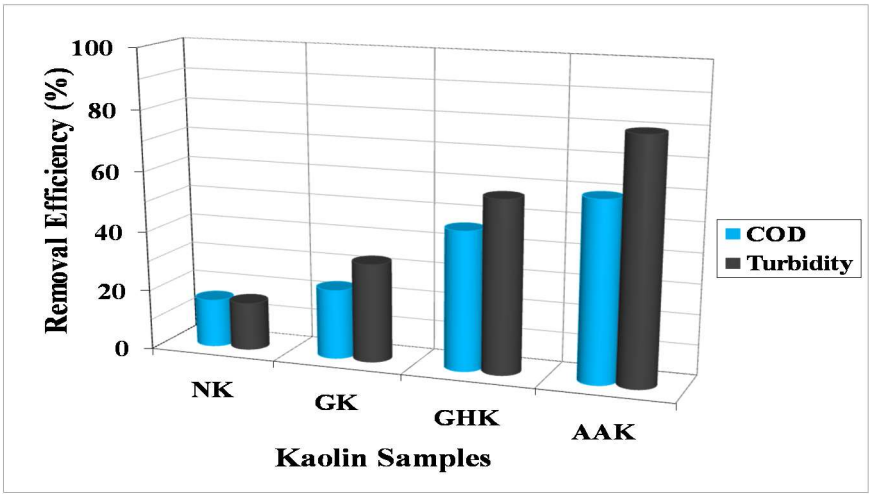

(b)

Figure 8: Comparison of the Contaminant Removal Efficiencies of Natural and Activated Kaolin. (a) Color Removal; (b) COD and Turbidity Removal

(NK=Natural Kaolin, GK=Ground Kaolin, GHK= Ground and Heated Kaolin at 100°C, AAK= Activated Kaolin using 4.5 M Sulphuric Acid; Treatment Conditions: Time = 30 mins, Kaolin Dosage= 7 % (wt/v))

Conclusion

It was noted that the wastewater should be pretreated by an appropriate method before discharging into the receiving watercourses. Upon treatment, COD, turbidity, colour and the absorbance measured at 436 nm were reduced as compared with those of raw wastewater. Among GHK samples. preheating the ground kaolin at 100°C gave better results for removal of turbidity and COD. These removal capacities decreased with increasing heating temperatures. The colour removal capacities of acid activated kaolins were decreased while those of COD and turbidity increased with increasing sulphuric acid concentrations from 2.5M to4.5M during activation. Beyond this optimum acid concentration (5.5 M H_2SO_4), the contaminants removal efficiency was decreased.This study finds that the acid activation of kaolin (using 4.5 M H_2SO_4)is a suitable method for preparing kaolin as an adsorbent for distillery wastewater treatments.

Acknowledgements

The authors are extremely grateful to Professor Dr Cho Cho Oo, Head of the Department of Industrial Chemistry, University of Yangon, for her encouragement and valuable suggestions for writing this research paper. We wish to express our sincere gratitude to Dr Yi Yi Myint, Professor and Head (Retd.) of the Department of Industrial Chemistry, Yadanabon University, for giving us permission to do research and support research facilities throughout this research work. We also would like to deeply appreciate Dr Khin Hnin Aye, Professor and Head of the Department of Industrial Chemistry, and Professor Dr Nwe Nwe Aung, Yadanabon University for giving permission us to use the necessary facilities of the laboratory at the Industrial Chemistry Department, Yadanabon University.

References

Bhattacharyya, K.G. & Gupta, S.S.(2008). Influence of Acid Activation on Adsorption of Ni(II) and Cu(II) on Kaolinite and Montmorillonite: Kinetic and Thermodynamic Study. *Chemical Engineering Journal*136, 1-13.

Didi, M.A., Makhoukhi, B., Azzouz, A.& Villemin, D.(2009).Colza Oil Bleaching through Optimized Acid Activation of Bentonite: A Comparative Study.*Applied Clay Science*42, 336–344.

Dudkin, B.N., Loukhina, I.V., Isupov, V.P.& Avvakumov, E.G. (2005).Mechanical Activation of Kaolinite in Presence of Concentrated Sulfuric Acid. *Russian Journal of Applied Chemistry*78, 33-37.

James, O.O., Mesubi, M.A., Adekola, F.A., Odebunmi, E.O., Adekeye, J.I.D. & Bale, R.B. (2008). Bleaching Performance of a Nigerian (Yola) Bentonite. *Latin American Applied Research* 38, 45-49.

James, S.R. (1995). Principles of Ceramics Processing.*John Wiley & Sons*, New York, p. 492.

Mall, I.D.& Kumar, V.(1997). Removal of Organic Matter from Distillery Effluents using Low Cost Adsorbent. *Chemical Engineering World XXXII* 7,89–96.

Meroufel, B., Benali, O., Benyahia, M., Benmoussa, Y., & Zenasni, M.A. (2013). Adsorptive Removal of Anionic Dye from Aqueous Solutions by Algerian Kaolin: Characteristics, Isotherm, Kinetic and Thermodynamic Studies. *Journal of Materials and Environmental Sciences* 4 (3), 482-491.

Nandi, B.K., Goswami, A. & Purkait, M.K.(2009). Adsorption characteristics of brilliant green dye on kaolin. *Journal of Hazardous Materials*161,387-395.

Nguetnkam, J.P., Kamga, R., Villiéras, F., Ekodeck, G.E. & Yvon, J.(2008).Assessing the Bleaching Capacity of Some Cameroonian Clays on Vegetable Oils.*Applied Clay Science* 39, 113–121.

Panda, A. K., Mishra, B.G., Mishra, D.K. & Singh, R.K.(2010).Effect of Sulphuric Acid Treatment on the Physico-chemical Characteristics of Kaolin Clay. *Colloids and Surfaces A: Physicochemical and Engineering Aspects*363, 98-104.

Pena, M., Coca, M., Gonzalez, R., Riojia, R.,& Garcia, M. T. (2003). Chemical Oxidation of Wastewater from Molasses from Molasses Fermentation with Ozone. *Chemosphere* 51 (9), 893-900.

Rhodes, C. N. & Brown, D.R.(1992).Structural Characterization and Optimization of Acid-treated Montmorillonite and High-porosity Silica Supports for $ZnC1_2$Alkylation Catalysts. *Journal of the Chemical Society, Faraday Transactions* 88, 2269-2274.

Sabir, B.B., Wild, S. & Bai, J.(2001). Metakaolin and Calcined Clays as Pozzolans for Concrete: a Review. *Cement and Concrete Composites* 23, 441-454.

Saha, Balakrishnan, M.,& Batra., V. (2005).Improving Industrial Water Use: Case Study for an Indian Distillery.*Journal of Resource Conservation Recycling*43, 163–174.

Shirsath, S.R., Patil, A.P., Patil, R., Naik, J.B., Gogate, P.R. & Sonawane, S.H. (2013). Removal of Brilliant Green from wastewater using conventional and ultrasonically prepared poly (acrylic acid) hydrogel loaded with kaolin clay: A comparative study. *Ultrasonics Sonochemistry* 20, 914-923.

Srodon J. (2006). Identification and quantitative analysis of clay minerals, In: Handbook of Clay Science, Developments in Clay Science1,*Elsevier*, Amsterdam, 765–786.

STUDY ON THE PREPARATION OF MIXED FRUIT JAM (PINEAPPLE AND WATERMELON)

Khin Swe Oo[1], Khine Myat Myint[2], Dr Yee Yee Win[3]

Abstract

The main objective of this research is to reduce fruit losses, to supply wholesome and safe preserved fruits to utilize during the off-season and develop new value-added products. The present research placed it emphasis on preparing mixed fruits jam products (pineapple and watermelon) retaining its natural flavor, aroma and a longer shelf-life. Their characteristics such as pH, acidity, viscosity, fiber content, ash content, colour, soluble solid (°Brix) and organoleptic properties were determined. Effect of chemical preservatives, effect of concentration of sugar, effect of heating temperature on the quality of mixed fruits jam product were investigated to produce good quality products. The results so obtained would in some way be helpful or supplement the local cottage industries.

***Keywords*:** mixed fruit jam, pineapple, watermelon

Introduction

Pineapple and watermelon are the popular fruits of the Myanmar. Pineapples are grown during in Shan State, Kachin State and Bago Division. Watermelons are especially grown in Yangon Division and Bago Division. In Myanmar, these fruits are abundantly available.

Among preserved fruits, jams, and jellies form an important class of products. Sweet spreads are a class of foods with many textures, flavours, and colours. Jam is a prepared fruit cooked to a precise formula so that the natural pectin and acid are extracted and, together with added sugar, forms a colourful and tasteful mixture which sets well and keeps for a long time. A good jam possesses the qualities, firm in consistency, brilliant in colour, even in fruit distribution, soft in texture of skin and flesh, true flavour of the fruit, filled to the jar top, and capable of storage without the formation of syrup, crystals, mould or ferment. Jam also will hold its shape, but it is less firm than jelly. Jam is made from crushed fruits and sugar. Generally citric, tartaric or malic

[1.] Lecturer, Department of Industrial Chemistry, University of Yangon
[2.] MRes, Department of Industrial Chemistry, East Yangon University
[3.] Professor and Head(Retired), Department of Industrial Chemistry, East Yangon University

acids are used to supplement the acidity of fruits for jam making. Addition of the acid to fruits is necessary because appropriate combination of pectin, sugar, and acid is essential to give a 'set' to the jam. The amount of added pectin needed to give a good gel also depends on the type of fruit used in the jam. Sugar serves as a preserving agent, contribute flavor, and acids gelling (Manay and Shadaksharaswamy, 2005).

The finished product of jam should contain 30-50% invert sugar to avoid the crystallization of cane sugar in the jam during storage. When packed in cans are pasteurized for about 30 minutes (N. Shakuntala Manay.etal, 2003).

About 30% of the vitamin C present in fresh fruit is destroyed during the jam making process, but that which remains in the finished product is stable during storage (Dauthy, M.E., 1995).

The aim of this research work is to supply wholesome, safe, nutritious and acceptable mixed fruits jam products containing natural flavour and aroma characteristics to consumers throughout the year.

Materials and Methods

Materials

In this research work, good, sound and matured ripe pineapple (yellow colour) and watermelon (red colour) obtained from Thanlyin Township, Southern Yangon Area. Food additives such as sugar, salt, citric acid, sodium carboxy methyl cellulose, pectin and commercial grade preservatives (potassium sorbate, potassium metabisulfite and sodium benzoate) were purchased from local markets.

Preparation of Pineapple-watermelon Jam

A good, sound and ripe pineapple of yellow colour was thoroughly washed with water. The washed pineapple was then cored and sliced into1cm cube.

A good, sound and ripe watermelon of deep red colour was thoroughly washed with water. The washed watermelon was then cored, sliced and placed

in a juice extractor to obtain juice. (1000g) of extracted juice was heated and stirred thoroughly at 85°C for 75 minutes until soluble solid content of juice was obtained 20°Brix.

(200g) of 20°Brix watermelon juice and (100g) pineapple (1cm cubic) were placed in the stainless steel pan. 35% of sugar, 0.17% citric acid, 0.5% salt and 0.4% sodium carboxmethyl cellucose were added into it. The mixture was heated under controlled temperature at 90˚C and stirred thoroughly. Heating was continued to obtain the desired soluble solid content range 60-75 °Brix of pineapple-watermelon jam. And then, 0.1 % of potassium sorbate were added and thoroughly agitated. Finally the firm pineapple-watermelon jam was carefully poured into the sterilized glass bottle and sealed with sterilized cap and then storage at room temperature.

Results and Discussion

Jam is product of sugar and pectin contained fruits. It has characteristics of texture, colour and taste. It should be capable of storage for a reasonable period after opening of bottle without risk of spoilage.

The physical and chemical characteristics of raw pineapple and watermelon are indicated in Table (4.1).

Table (4.2) shows that the effect of sugar concentration on pineapple-watermelon jam. From this table, the most favourable sugar concentration of pineapple-watermelon jam was 35% because this sugar amount gave good sweet taste and attractive colour.

Table (4.3) displays the effect of chemical preservative on the properties of pineapple-watermelon jam. From the table, it was observed that the optimum potassium sorbate concentration was 0.1% due to the pH, acidity, ºBrix, colour, shelf-life and odour of mixed fruits jam.

Table (4.4) indicates that the effect of heating temperature on the properties of pineapple-watermelon jam. From the results, heating time 1:15 hours and heating temperature 90ºC were the most favorable condition because the more attractive colour of mixed fruits jam were obtained.

Acidity is the measure of shelf-life of the product. Acidity studied to ensure physico-chemical changes during preparation and storage (Kalra and Tandon, 1985). Table (4.5) shows the effect of storage time on acidity, pH and soluble solids content (ºBrix) of pineapple-watermelon jam.

In pineapple-watermelon jam, acidity content was increased to 0.21% at 2 weeks, 0.28% at 4 weeks, 0.35% at 6 weeks, 0.36% at 8 weeks of storage respectively. There was no change in the acidity after 8 weeks at room temperature. Increase in acidity of fruit jam is due to ascorbic acid degradation or hydrolysis of pectin (Cruess, W.V., 1958, Sogi, D.S and S.Singh, 2001).

Fruit products are being effectively preserved at low pH (Sindhu et.al., 1984). Significant pH changes were noticed during 8 weeks storage of pineapple-watermelon jam. No appreciable changes in pH occured in both prepared jams after 8 weeks storage at room temperature.

The results from Table (4.5) also show that soluble solid content increase during 8 weeks storage at room temperature.

Table (4.6) indicates the physico-chemical characteristics of prepared pineapple-watermelon jam. These characteristics were found to be acceptable limit.

Table (4.7) displays the effect of storage period on vitamin C (ascorbic acid) of pineapple-watermelon jam product. From this table, it was observed that vitamin C (ascorbic acid) content of all mixed fruits jam decreased during storage. Ascorbic acid deceases because it is easily oxidized in presence of oxygen by both enzymatic and enzymatic catalyst. Assuming that glass containers are impermeable to oxygen, the principal causes of L-ascorbic acid destruction are oxidation by residual oxygen in the headspace followed by anaerobic decomposition and destructive influence of light (Maeda E.E and D.M.D.N Mussa, 1986).

In the presence of free oxygen (e.g., oxygen present in the headspace and dissolved in the jam) ascorbic acid would be oxidized to dehydro ascorbic acid and this might be followed by ring cleavage and the formation of di-ketogulonic acid. Once the free oxygen has been consumed by the chemical reactions, degradation of ascorbic acid might proceed an aerobically. Under

anaerobic conditions, ascorbic acid degrades by several steps to form furfural (Nagy, S. and J. M. Smoot, 1980).

Table(4.1): Physical and Chemical Characteristics of Raw Pineapple and Watermelon

Sr. No	Characteristics	Pineapple	Watermelon
1	Soluble Solids Content (°Brix)	8	9
2	Moisture Content (%)	83.4	89.4
3	Ash Content (%)	3.4	0.2
4	Fibre Conrent (%)	5.5	2
5	Acidity (v/w%)	1.7	0.03
6	pH	4.62	6.91
7	Vitamin C	10.6	35.2

These data were determined at the Department of Industrial Chemistry, East Yangon University.

Table (4.2): Effect of Sugar Concentration on Characteristics of Pineapple - watermelon Jam

Watermelon	-200g	Sodium Carboxymethyl Cellulose	-1.2g
Pineapple	-100g	Potassium Sorbate	-0.1g
Citric acid	-0.5g	Salt	-1.5g

Sample No.	Sugar (w/w%)	Acidity	H	°Brix	Flavour	Colour
1	25	0.25	4.53	70	Slightly sweet	Red
2	30	0.29	4.20	65	Sweet	Red
*3	35	0.28	4.45	70	Good Sweet taste	Red
4	40	0.27	4.12	65	More sweeter taste	Red
5	45	0.21	4.48	70	More sweeter taste	Red

* Suitable sugar concentration

These data were determined at the Department of Industrial Chemistry, East Yangon University.

Table (4.3): Effect of Chemical Preservative on the Properties of Pineapple-watermelon Jam

Watermelon	-200g	Sodium Carboxymethyl Cellulose	-1.2g
Pineapple	-100g	Salt	-1.5g

Characteristics	Pineapple-watermelon jam		
	*PS (w/w%)	SB (w/w%)	PMBS (w/w%)
pH	4.43	4.15	4.21
Acidity	0.17	0.15	0.13
Soluble Solid Content	70	70	70
Colour	Red	Red	Red
Shelf-life	6months	6months	3months
Odour	Good smell	Good smell	Sour smell

* PS = Potassium Sorbate (Suitable Preservative)
SB = Sodium Benzoate, PMBS = Potassium Metabisulphite
These data were determined at the Department of Industrial Chemistry, East Yangon University.

Table (4.4): Effect of Heating Temperature on the Properties of Pineapple-watermelon Jam

Watermelon	- 200g	Sodium Carboxymethyl Cellulose	- 1.2g
Pineapple	- 100g	Potassium Sorbate	- 0.1g
Citric acid	- 0.5g	Salt	- 1.5g
Sugar	- 35g		

Temperature (°C)	Pineapple-watermelon jam			Colour	Time (hours)
	°Brix	pH	Acidity		
80	70	4.45	0.28	Red	1: 25
*90	70	4.43	0.17	Red	1:15
100	70	4.39	0.15	Deep red	1: 00

* Suitable temperature
These data were determined at the Department of Industrial Chemistry, East Yangon University.

Table (4.5): Effect of Storage Time on Acidity, pH and Soluble Solid Content of Pineapple-watermelon Jam

Watermelon -200g Pineapple - 100g

Stroage Time (weeks)	Sugar (w/w%)	PS (w/w%)	SCMC (w/w%)	Salt (w/w%)	CA (w/w%)	Acidity	pH	Soluble Solid Content (°Brix)
Initial	35	0.1	0.4	0.5	0.17	0.21	4.42	70
2	35	0.1	0.4	0.5	0.17	0.21	4.42	70
4	35	0.1	0.4	0.5	0.17	0.28	4.44	70.5
6	35	0.1	0.4	0.5	0.17	0.35	4.45	71
8	35	0.1	0.4	0.5	0.17	0.36	4.46	72
10	35	0.1	0.4	0.5	0.17	0.36	4.46	72
12	35	0.1	0.4	0.5	0.17	0.36	4.46	72

PS = Potassium Sorbate
SCMC = Sodium carboxymethyl cellulose
CA = Citric acid
These data were determined at the Department of Industrial Chemistry, East Yangon University.

Table (4.6): Effect of Storage Period on Vitamin C (ascorbic acid) of Prepared Pineapple-watermelon Jam

Sr.No.	Storage Period	Pineapple-watermelon jam
1.	Initial	4.8
2.	1 months	3.9
3.	2months	3
4.	3months	2.5
5.	4months	1.9
6.	5months	1.76
7.	6months	1.74

These data were determined at the Department of Industrial Chemistry, East Yangon University.

Table (4.6): Physical and Chemical Characteristics of Prepared Pineapple-watermelon Jam

Sr. No.	Characteristics	Pineapple-watermelon jam
1	Soluble Solid Content (°Brix)	60
2	Moisture Content (w/w%)	36.4
3	*Sugar Content (%)	53
4	Ash Content (w/w%)	2.8
5	Fibre Content (w/w%)	0.9
6	Acidity (v/w%)	0.11
7	pH	4.9
8	Vitamin C	4.8
9	*Colour	4 Red, 50 Yellow

*Sugar content and colour were determined at Laboratory of Small Scale Industry Department, Ministry of Co-operative . The others were determined at the Department of Industrial Chemistry, East Yangon University.

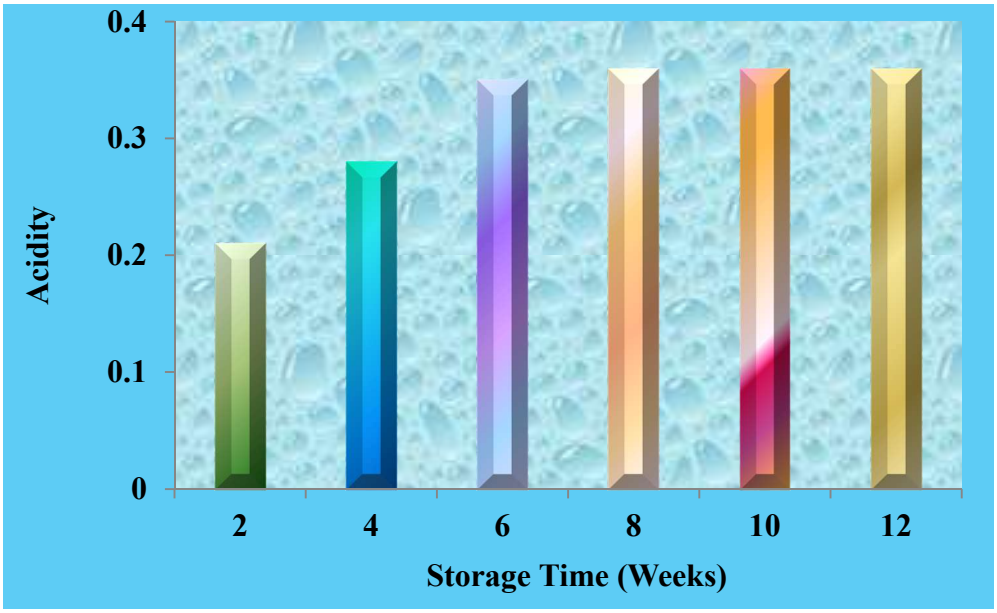

Figure (4.2): Effect of Storage Time on Change in Acidity of Pineapple-watermelon Jam

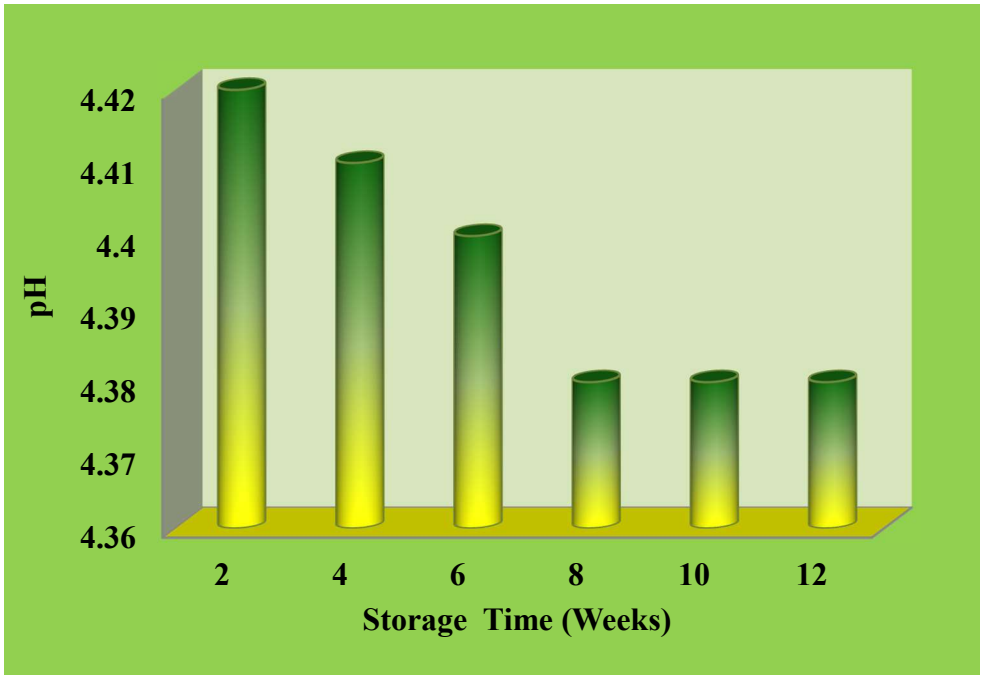

Figure(4.3): Effect of Storage Time on Change in pH of Pineapple-watermelon Jam

Figure (4.3): Pineapple - Watermelon Jam

Acknowledgements

I would like to express my gratitude to Dr Cho Cho Oo, Professor and Head, Department of Industrial Chemistry, University of Yangon, for allowing us to submit this article. The authors would like to acknowledge Dr Yee Yee Win, Professor (Retired), Head of the Department of Industrial Chemistry, East Yangon University, for providing research facilities, for her valuable suggestions and advice throughout this research work.

References

Cruess, W.V., **(**1958). "Principles of fruit preservation in commercial Fruit and Vegetable Products", 4th Ed, pp: 426-462, 465- 488, M Graw Hill, New York.

Dauthy, M.E., (1995), "Fruit and Vegetable Processing", FAO Agricultural Services Bulletin 119, Rome.

Kalar SK, Tandon DK (1985). "Physico-chemical changes in mango pulp during ambient storage in glass containers", J. Food Sci. Technol." 22: 343- 345

Maeda E.E. and D.M.D.N. Mussa, (1986). " The stability of vitamin C (L- ascorbic acid) in bottle and canned orange juice". J. Food Chem., 22: 51-58.

Manay SN, Shadak sharaswamy N (2005). "Foods, Facts and Principles", New Age International (P) Limited, New Delhi pp: 197.

N. Shakuntala Manay and M. Shadaksharawamy, (2003), "Food Fasts and Principles", New Age International (P) Ltd, Publishers, New Delhi. Seven wonders of watermelon [dead link]

Nagy, S. And J.M. Smooth, 1980. "Effects of storage temperature and duration on total vitamin C content of canned single-strength grapefruit juice". J. Agric Food Chem., 28: 417-421.

Sindhu S, Bhumbla K, Joshi (1984). "Preservation of Tomato juice under acid condition", Food Sci. Agric. 35: 345- 352

CHARACTERIZATION AND UTILIZATION OF GUM FROM*ACACIA CATECHU(SHA)*

San San Htwe[1], Yi Yi Myint[2], Pansy KyawHla[3]

Abstract

Gum arabic or gum acacia is the oldest and best known of natural gums obtained from different acacia species. This research was focused on characterization and utilization of purified gum from *Acacia catechu* (Sha), found in Sagaing Region of Upper Myanmar. Raw gum was manually collected in Summer, and purified by dissolving, filtration, and decolourization using hydrogen peroxide and drying the gum solution in vacuum dryer at 70ºC and 650 mm Hg. Solubility test, chemical tests and hydrolysis products test by thin layer chromatography were conducted to identify the purified gum. For the assessment of the quality of purified gum, purity tests (loss on drying, ash content, starch and dextrin, tannin bearing gum, heavy metals, microorganisms, etc.), physicochemical properties and emulsion stability of purified gum were investigated. Purified gum was used in clarification of three different wines comparatively regarding the characteristics of wines. As a result, the effective clarifying efficiency varied from one wine to another. Purified gum was utilized in making tamarind toffee and it is found that small amount (5%) of gum was efficient for the emulsification of the fat present in toffees. Moreover, purified gum powder was used as drying carrier in the preparation of dehydrated tamarind powder and the results indicate that the purified gum greatly affected the drying time (reduced from 23 hr to 3.5 hr) and solubility of this product.

Key words: Gum arabic, Clarification, Emulsification, Drying carrier

Introduction

Gum arabic or gum acacia is a tree gum exudate with high quality obtained from acacia species such as *Acacia Senegal* and *Acacia seyal* grown in Sudan which is the main gum arabic producing country. In Myanmar, gum Arabic can be obtained from *Acacia nilotica* (Subyu), *Acacia leucophloea* (Tanaung) and *Acacia catechu* (Sha) distributed in Mandalay, Sagaing and Magwe Regions of Upper Myanmar. The gum oozes from the stems and branches of trees (usually five years of age or more) when subjected to stress conditions such as drought, poor soil or wounding. Gum is soft and tacky as it

[1.] Dr, Lecturer, Department of Industrial Chemistry, University of Yangon
[2.] Dr, Professor and Head (Retd.), Department of Industrial Chemistry, Yadanabon University
[3.] Dr, Professor (Retd.), Department of Industrial Chemistry, University of Yangon

exudes from trees and so the outer layer become contaminated with foreign substances such as sand, dirt, insects, pieces of bark and leaves etc. To remove the insoluble impurities, gum nodules are dissolved in a solvent, screening, filtering and recovering the gum from solution. Gum arabic readily dissolved in cold and hot water in concentration up to 50%. Because of the compact, branched structure, gum arabic solutions are characterized by low viscosity, allowing the use of high gum concentration in various application (Verbenken, 2003). Gums arabic is mainly used in the confectionery industry, where it is incorporated in a wide range of products. It has a long tradition of use in wine gums, where it produces a clarity that is higher than can beobtained with other hydrocolloids. Thus, it can be used for clarification of wine (Phillips and Williams et al., 2000).

Gum arabic is used in toffees and caramels as an emulsifier, to maintain a uniform distribution of the fat across the products. Emulsification, acid stability, low viscosity at high concentration, adhesive and binding properties and good mouth feel characteristics have been applied in five main food areas; confections, beverages and emulsions, flower encapsulation, baked goods and brewing (Chapman and Hall, 1997).

Thus, the objectives of this study is to produce a variety of value added products from natural sources, to give the knowledge for the application of plant materials to rural people in tropical regions and to upgrade the quality of local natural exudates to substitute the imported food additives.

Materials and Methods

Materials

Gum arabic from Sha (*Acacia catechu*) grown in Salingyi Township, Sagaing Region, was collected from February to May yearly and hydrogen peroxide (commercial grade) was purchased from Academy Chemical Store, Pabedan Township, Yangon Region.

Methods

Processing of Gum

In order to facilitate the purification, raw gum nodules collected from Sha trees were crushed and ground by using grinding machine. The resulting gum particles were sieved in a sieve shaker (up to -60mesh size). And then, the gum particles were dissolved individually in distilled water to obtain the gum solution of 10%, 20% and 30% (w/v) concentrations. The insoluble impurities were removed by filtering the gum solution with nylon filter (200nm and 400nm).After that, the filtrate was decolourized by using different concentration (10% w/v, 20% w/v, 30% w/v) of hydrogen peroxide solution. Finally, the decolourized gum solution was dried at about 70ºC for about 6 hr in vacuum drying oven.

Identification and Analysis of Purified Gum from Sha

The identification of the purified gum powder were carried out by solubility test by using water and 95% ethanol, chemical tests (*Fehling's* test**,** *Benedict's* test**,** *Barfoed's* test) and thin layer chromatography. The physico-chemical characteristics of purified gum powder such as moisture content, ash content, heavy metals, protein content, crude fiber, density, relative viscosity, emulsion stability etc., were also determined.

Applications

Purified gum was applied in the clarification of wines (Strawberry, Damson and Grape obtained from Pyin Oo Lwin District, Mandalay Region); as an emulsifier, the purified gum was also used in making tamarind toffees and as a drying carrier, in the preparation of dehydrated tamarind powder.

Results and Discussion

Raw gum arabic containing insoluble impurities can be removed by conventional filtration methods. Soluble colour impurities could be removed by using different amount and different concentrations (10%, 20%, 30% w/v) of hydrogen peroxide (H_2O_2). The extent of decolourization was assessed by Spectrometric measurement using UV-Vis Spectrophotometer. The results of Table (1) indicate that decolourization time was affected by concentration and amount of H_2O_2. For decolourization, the higher the concentration and the larger the amount of H_2O_2, the shorter the decolourization time. The lower absorbance values of the decolourized gum solutions indicate the extent of decolorization.

The purified gum was identified by solubility test using different solvents (cold and hot water, 95% ethanol), test on hydrolysis products by chemical tests and TLC analysis. From the results in Table (2), it is clearthat, gum arabic is soluble in both cold and hot water but insoluble in ethanol. The results of Tables (3) and (4) point out that the purified gum composed of reducing sugars containing four monosaccharides such as galactose, rhamnose, arabinose and glucuronic acid, etc., which is in agreement with literature (Phillips and Williams, et al., 2000).

The results in Table (5) show that the percent of loss on drying (moisture content) of purified gum is lower than that of France gum and that of standard value (15%max). Total ash content of purified gum was slightly higher than that of standard value reported by IS-3988 (1967). The total ash content is used to determine the critical levels of foreign matter, insoluble matter in acid (Mocak et al., 1998). Sha gum does not contain acid insoluble ash and heavy metals (lead and arsenic). According to the results of Table (6), purified gum has no crude fibre.

From the results, showing the effect of concentration of purified gum solution on relative densities and relative viscosity, in Tables (7) and (8), it is obvious that increase in the relative densities and viscosity of gum solution were proportional to their increasing concentrations. This is because the highly branched structure of the gum arabic molecules leads to compact relatively small hydrodynamic volume and consequently gum arabic will only become a viscous solution at high concentrations cited by Williams et al.,

1990. The results of the influence of pH of gum solution on its relative viscosity show that the relative viscosities increase with increase in pH up to pH 5 and decrease again beyond the pH values of 5(Table 9). This results agree with Anderson et al., 1990 cited that in very acidic solutions, acid groups neutralize so inducing a more compact conformation of the polymer which leads to a decreased viscosity; while a higher pH (less compact molecule) results in maximum viscosity whereas in very basic solution, the ionic strength increment reduces the electrostatic repulsion between gumarabic molecules producing a more compact conformation of the biopolymer and thus reducing the viscosity of the solution.

From the results as presented in Table (10), it is clear that the swelling capacities of purified Sha gum, 1.5 indicates the hydrophilic nature of the gum, the results of bulk and tapped densities show the volume reduction under applied tapped pressure and the value(1.004) of Hausner's ratio of the Sha gum points out the good flow property of gum. The results of the emulsion stabilities of Sha gum with regard to different types of edible oil (sunflower, groundnut, sesame, corn and soya oils) in Table (11) points out that soya oil gave the highest emulsion stability. Table (12) illustrates that the emulsion stability increases significantly with increase in stirring time from 1 to 5 minutes. The results in Table (13)revealed that emulsion stability increases with increasing the concentration of the gum solution. Emulsion stability at a temperature regime of 50, 100, 150, 200 and 250ºC slightly increases with increase in heating temperature as shown in Table (14).

Purified gum from Sha prepared under most suitable conditions was used in the clarification of three types of wine such as Damson, Grape and Strawberry Wine. It is clear that the optimum amounts of gum are 2g, 0.5g and 1g for Grape, Damson and Strawberry wine respectively as shown in Tables (15), (16) and (17). This finding is in agreement with Ribereuet al., (2006) that the effective amount of gum arabic varied from one wine to another. The results representing the use of purified Sha gum as an emulsifier in making tamarind toffee, in Table (18)point out that the amounts of gum from Shaaffect the texture, flavour and mouth feel of tamarind toffees and the most suitable amount of gum was 2 g or 5% (w/w) of tamarind based on the organoleptic properties. As shown in Table (19), moisture content of toffee

made with Sha gum is less than that of toffee made with France gum but greater than the toffee from the Market which in turn, total dry matter of toffee made of Sha gum is greater than that of toffee made with France gum and less than that of toffee from Market. The results in Table (20) indicate that the microorganism load fell within the specifications. The effect of amount of drying aid (purified Sha gum) and drying temperatures on drying times and yield percent are shown in Table (21). It is obvious that drying times greatly decreased in the presence of gum arabic and solubility time also significantly decreased and the solubility time of samples was 60 seconds for 40(%w/w) purified Sha gum. It means that the tamarind powder could be dissolved in water at room temperature without difficulty. The drying carriers, gum arabic, is easily dissolved in water (Cano-Chauca*et al.*, 2005) thus, it enhances the dissolution ability of the tamarind powders. Also, the drying temperature had a positive effect on the solubility because the higher drying temperature resulted in more porosity of the powders. The higher porosity led to the more specific surface area of powder, resulting in larger contact surface area between powder and water. If the lower proportion of drying carrier is applied, the layer of drying carrier on the tamarind powder surface will be subsequently thinner.

The effect of drying temperature on physical properties of dehydrated tamarind powder was determined and the results are shown in Table (22). Bulk densities of tamarind powder decreased with increasing drying temperature. The bulk density is an important characteristic for the packaging design and the calculation of transportation volume. The drying temperature and the formula of feed are deemed as the causes of this occurrence. The higher drying temperature resulted in the lower bulk density (Chegini and Ghobadian, 2005).The higher drying temperature led to a higher rate of moisture evaporation from the feed resulting in a higher porosity and lower bulk density of the dried powder. Furthermore, at the same drying temperature, the higher proportion of drying aids would lower the bulk density. Drying temperature and drying aids also similarly affected on tapped density as shown in Table (22).

Table 1: Effect of Concentration of Hydrogen Peroxideon Decolourization of Gum Arabic from Sha

Amount of gum arabic = 50 mL (10%, w/v) = 5 g
Drying temperature and time = 70°C, 6 hr

Sr. No.	Concentration of H_2O_2 (%w/v)	Volume of H_2O_2 (mL)	Decolourization Time (hr), 70°C	**Absorbance		Weight of product (g)	Purified Gum Yield (%w/w)
				Before decolourization	After decolourization		
1	10	3	3.5	0.635	0.379	2.96	59.2
		5	3.0	0.635	0.363	3.23	64.6
		7	2.73	0.635	0.327	3.38	67.6
		*9	2.2	0.635	0.220	4.0	80.0
		11	2.2	0.635	0.205	3.93	78.6
2	20	3	2.00	0.635	0.190	4.03	80.6
		5	1.73	0.635	0.180	4.06	81.2
		7	1.65	0.635	0.159	4.02	80.4
		*9	1.12	0.635	0.155	4.17	83.4
		11	1.10	0.635	0.151	4.13	82.6
3	30	3	1.28	0.635	0.139	3.9	78.0
		5	0.92	0.635	0.122	4.0	80.0
		7	0.78	0.635	0.114	3.64	74.8
		*9	0.68	0.635	0.098	4.04	80.8
		11	0.66	0.635	0.084	4.0	80.0

*Most suitable condition
** Absorbanceindicatingtheextent of decolourization of gum

(a) (b) (c)

Figure 1: Sha(a)Gum Modules(b) Gum Particles(c) Purified Gum Powder

Table 2: Solubility Test for Purified Gum Arabic from Sha

Drying temperature = 70ºC
Drying time = 6 hr

Sr. No.	Solvent	Ratio of Gum to Solvent (w/v)	Observation	
			Sha Gum	France Gum
1	Ethanol (95%)	1:2	Insoluble	Insoluble
2	Cold water (20°C)	1:2	Soluble	Soluble
3	Hot water (65 °C)	1:2	Soluble	Soluble

Table 3: Chemical Tests for Monosaccharide (Reducing Sugar) in Purified Gum Arabic from Sha

Drying temperature = 70ºC
Drying time = 6 hr

Sr. No.	Experiments	Observation		Remark
		Sha Gum	France Gum	
1	Benedict's Test	Reddish precipitate	Reddish precipitate	Reducing sugar present
2	Fehling's Solution Test	Reddish precipitate	Reddish precipitate	Reducing sugar present
3	Barfoed's Test	Red precipitate	Red precipitate	Reducing sugar present

Table 4: R_f Value of Four Monosaccharides by Three Solvent System in TLC Analysis of Purified Gum Arabic from Sha

Drying temperature=70ºC
Drying time = 6 hr

Sr.No.	Solvent System	Galactose		Rhamnose		Arabinose		Glucuronic/a	
		Literature Value*	Gum from Sha	Literature Value*	Gum from Sha	Literature Value*	Gum from Sha	Literature Value*	Gum from Sha
1	BEW	0.16	0.16	0.22	0.22	0.38	0.4	0.21 0.33	0.34
2	BAW	0.16	0.16	0.22	0.22	0.33	0.33	0.37	0.43
3	PhOH	0.38	0.36	0.52	0.49	0.6	0.62	0.13	0.11

BEW ⇨ n. Butanol : Ethanol : Water (4: 1 : 2.2 v/v)
Ph OH ⇨ Phenol Saturated with water
BAW ⇨ n-Butanol: Acetic :Water (9:6:1 v/v)*(Aparna, 2000)

Table 5: Physicochemical Properties of Purified Gum Arabic from Sha

Drying temperature = 70ºC
Drying time = 6 hr

Sr.No	Characteristics	*Literature	Sha Gum	France Gum
1	Loss on drying (%)	15% max	8.47	13.09
2	Total ash (%)	4% max	4.23	2.91
3	Acid insoluble ash (%)	0.5%max	0.0	0.0
4	Lead (mg/kg)	10	Nil	Nil
5	Arsenic (mg/kg)	3	Nil	Nil

Table 6: Nutritional Values of Purified Gum Arabic from Sha

S r. No.	**Composition**	**Sha Gum**	**France Gum**	**Methods**
1	Protein (%w/v)	5	5.81	AOAC-2000-920
2	Sugar (%w/v)	9.8	9.0	Refractometer (Master-
3	Crude fibre (%w/v)	0	0	AOAC-2000-978
4	Soluble fibre (%w/v)	83.34	78.19	Sabah El-Kheir et al.,

Table 7: Effect of Concentration of Sha Gum Solution on Relative Density

Sr. No.	**Concentration of Gum Solution(%w/v)**	**Relative Density**	
		Purified Sha Gum	**France Gum**
1	1	1.074	0.9980
2	10	1.086	1.0280
3	20	1.136	1.0588
4	30	1.150	1.0832
5	40	1.272	1.1056

Table 8: Effect of Concentration of Sha Gum Solution on Relative Viscosity

Sr. No.	**Concentration of Gum Solution(%,w/v)**	**Relative Viscosity**	
		Purified Sha Gum	**France Gum**
1	5	1.45	1.272
2	10	1.6	7.348
3	20	1.7	19.65
4	30	5.57	56.76
5	40	74.6	105.7

Table 9: Effect of pH of Sha Gum Solution on Relative Viscosity Concentration of gum solution = 10% (w/v)

Sr. No.	**pH of Gum Solution**	**Relative Viscosity**	
		Sha Gum Solution	**France Gum Solution**
1	3	1.44	1.84
2	5	1.45	2.07
3	7	1.14	4.74
4	9	1.11	4.71
5	11	1.10	3.66
6	13	1.10	2.96

Table 10: Physical Properties of Purified Gum Arabic Powder(Sha)

Sr. No.	Properties	Purified Sha Gum	Gum powder (France)
1	Bulk density (g/L)	0.556	0.558
2	Tapped density (g/L)	0.558	0.645
3	Swelling capacity	1.5	1.600
4	Hausner ratio	1.004	1.156
5	Hydration capacity	1.51	1.430

Table 11: Effect of Types of Edible Oil on Emulsion Stability of Gum Solution (Sha)

Stirring time =1 min

Ratio of oil to gum solution (20%w/v) =1:2

Stirring temperature = Room temperature (28-30º C)

Sr. No.	Types of Edible Oils	Emulsion Stability
1	Sunflower oil	0.864
2	Peanut oil	0.912
3	Sesame oil	0.886
4	Corn oil	0.867
5	Soya oil*	1.015

*Most suitable type of oil

Table 12: Effect of Stirring Time on Emulsion Stability of Gum Solution (Sha)

Ratio of soya oil to gum solution (20%w/v) =1:2

Stirring temperature = Room temperature (28-30ºC)

Sr. No.	Stirring Time(min)	Emulsion Stability
1	1	1.015
2	2	1.118
3	3	1.274
4	4	1.391
5	5	1.440

Table 13: Effect of Concentration of Gum Solution (Sha)on Emulsion Stability

Stirring time =1 min

Ratio of soya oil to gum solution (20%w/v) =1:2

Stirring temperature = Room temperature (28-30º C)

Sr. No.	Concentration of Gum Solution(v/v)	Emulsion Stability
1	1/1000	1.015
2	2/1000	1.016
3	3/1000	1.020
4	4/1000	1.024
5	5/1000	1.027

Table 14: Effect of Different Heating Temperatures on Emulsion Stability of Gum Solution (Sha)

Stirring time =1 min

Ratio of soya oil to gum solution (20%w/v) =1:2

Stirring temperature = Room temperature (28-30ºC)

Sr. No.	Temperature (ºC)	Emulsion Stability
1	50	0.930
2	100	0.934
3	150	0.942
4	200	0.944
5	250	0.947

Table 15: Effect of Amount of Gum(Sha)on Clarification of Grape Wine

Amount of Wine = 50mL
Turbidity of Untreated Wine (after 1month) = 221.2 NTU
Turbidity ofUntreated Wine (after 3months) = 318.8NTU
Turbidity of Untreated Wine (after 5months) = 448.8NTU

Sr. No.	Amount of Gum (g)	Turbidity of Wine after Treatment (NTU)			Transmittance	Absorbance
		After 1 month	After 3 months	After 5 months	After 5 months	After 5 months
1	0.1	149.8	174.4	256.6	68.6	0.167
2	0.5	157.2	198.8	240.1	70.2	0.192
3	1.0	197.6	190.2	219.0	72.8	0.157
4	1.5	170.6	164.2	183.6	75.2	0.146
5	2.0*	*140.1	236.4	144.4	84.2	0.104

*Most suitable condition

Table 16: Effect of Amount of Gum (Sha)on Clarification of Damson Wine

Amount of Wine = 50mL
Turbidity of Untreated Wine (after 1month) = 145.1 NTU
Turbidity of Untreated Wine (after 3months) = 445.1NTU
Turbidity of Untreated Wine (after 5months) = 681.0NTU

Sr. No.	Amount of Gum (g)	Turbidity of Wine after Treatment (NTU)			Transmittance	Absorbance
		After 1 month	After 3 months	After 5 months	After 5 months	After 5 months
1	0.1	70.0	97.4	113.5	75.4	0.126
2	0.5*	***52.3**	84.4	66.3	101.8	0.005
3	1.0	70.6	102.1	133.3	83.4	0.078
4	1.5	53.2	102.2	104.0	62.7	0.199
5	2.0	186.3	457.3	407.0	28.5	0.546

*Most suitable condition

Table 17: Effect of Amount of Gum(Sha)on Clarification of Strawberry Wine

Amount of Wine = 50mL

Turbidity ofUntreated Wine (after 1month) = 40.40 NTU

Turbidity of Untreated Wine (after 3months) = 260.0NTU

Turbidity of Untreated Wine (after 5months) = 470.0NTU

Sr. No.	Amount of Gum (g)	Turbidity of Wine after Treatment (NTU)			Transmittance	Absorbance
		After 1 month	After 3 months	After 5 months	After 5 months	After 5 months
1	0.1	29.0	11.6	27	93.7	0.028
2	0.5	28.4	21.5	21.1	98.5	0.069
3	1.0*	35.3	*2.1	16.4	115.0	0.063
4	1.5	40.2	12.7	17.6	111.8	0.067
5	2.0	77.9	41.7	46.3	86.6	0.115

*Most suitable condition

Grape Wine (before and after clarification)

Strawberry Wine (before and after clarification)

Damson Wine (before and after clarification)

Tamarind Toffees

Table 18: Effect of Amount of Gum from Sha on Characteristics of Tamarind Toffee

Tamarind = 40g, Sugar = 105g, Glucose = 12g, Milk Powder = 8g, Margarine = 3g, Essence = 0.5ml, Salt = 3.5g,
Cooking Time = 50min, Cooking Temperature = 80°C

Sr. No.	Amount of Gum (g)	Acidity (%)	pH	Moisture (%)	Total Dry Matter (%)	Yield (%)	Shelf-life (Months)	Organoleptic Properties
1	1.0	4.9	2.7	8.6	91.4	81	5	Soft texture, pleasant taste, slightly creamy mouthfeel
2	1.5	4.5	2.8	7.9	92.1	84	5	Soft texture, pleasant taste, creamy mouthfeel
3	2.0*	4.5	2.8	7.8	92.2	81	5	Soft texture, pleasant taste, creamy mouthfeel
4	2.5	4.7	2.8	7.3	92.7	81	5	Soft texture, pleasant taste, creamy mouthfeel
5	3.0	4.6	2.8	8.6	91.4	85	5	Soft texture, pleasant taste, creamy mouthfeel

*Most suitable condition

Table 19: Physicochemical Properties of Tamarind Toffees

Sr. No.	Characteristics	Toffee made with Sha Gum	Toffee made with France Gum	Toffee from Market (Duwon)
1	Moisture (%)	7.9	8.2	5.7
2	Total dry matter	92.1	91.8	94.3
3	Acidity (%)	4.5	6.3	6.0
4	pH	2.8	2.7	2.7
5	Shelf-life (months)	5	5	5

Table 20: Microbial Loads of Tamarind Toffees

Sr. No.	Characteristics	Toffee made with Sha Gum	Toffee made with France Gum	Toffee from Market (Duwon)	International Specification
1	TPC (cfu/gm)	2.2×10^3	6.1×10^3	7×10^3	10^6
2	Yeast and mold	1×10^2	3×10^2	5×10^3	10^6

Table 21: Effect of Amount of Drying Aid (Sha, Gum Arabic) on Drying Time and Yield % of Dehydrated Tamarind Powder at Different Drying Temperatures

Amount of tamarind flesh =100 g

Sr. No.	Gum arabic Concentration (% w/w)	Drying Temperature (°C)	Drying Time (hr)	Moisture % (w/w)	Yield % (w/w)	Soluble Time (s)at (70° C) in
1	0	50	22.5	18.33	5.47	1200
		60	22.5	17.85	5.36	1200
		70	23	17.24	5.42	1200
		80	23	16.73	5.40	1200
		90	23	15.88	5.31	1200
2	10	50	10	14.63	9.31	205
		60	10	14.31	9.25	200
		70	9	14.25	10.34	180
		80	8	10.24	10.54	160
		90	8	10.11	10.23	150
3	20	50	9.5	13.61	30.22	120
		60	9	13.46	30.13	120
		70	8.5	13.22	33.30	110
		80	6.5	9.46	36.08	95
		90	5	8.47	32.54	90
4	30*	50	8.5	12.32	40.34	100
		60	8	12.15	40.35	100
		70	7	11.04	42.67	95
		80	5	6.65	42.80	80
		90*	3.5	7.08	49.93	70
5	40	50	7	9.73	41.25	90
		60	6.5	9.12	41.44	90
		70	6	8.76	41.25	75
		80	5	6.41	42.80	60
		90	3.5	6.22	42.93	60

*most suitable condition

Table 22: Effect of Drying Temperature and Time and Drying Aid (Sha Gum Arabic) on the Physical Properties of Dehydrated Tamarind Powder

Amount of tamarind flesh=100 g

Sr. No.	Gum arabic Concentration (% w/w)	Drying Temperature (°C)	Drying Time (hr)	Bulk density (g/mL)	Tapped density (g/mL)	Water solubility Index (WSI)	Water absorption Index (WAI)
1	0	50	22.5	1.32	1.50	10.35	2.85
		60	22.5	1.30	1.47	10.56	2.81
		70	23	1.26	1.42	10.74	2.50
		80	23	1.14	1.33	10.81	2.47
		90	23	1.17	1.24	10.88	2.45
2	10	50	10	0.95	1.22	21.12	2.27
		60	10	0.94	1.13	21.36	2.21
		70	9	0.93	1.10	22.62	2.18
		80	8	0.86	0.91	22.90	2.15
		90	8	0.85	0.90	23.54	2.10
3	20	50	9.5	0.93	1.10	42.15	2.03
		60	9	0.91	1.01	42.47	2.01
		70	8.5	0.84	0.95	42.11	1.96
		80	6.5	0.78	0.82	43.05	1.85
		90	5	0.76	0.80	10.35	2.85
4	30*	50	8.5	0.82	0.90	64.13	1.68
		60	8	0.77	0.81	66.24	1.58
		70	7	0.65	0.72	71.16	1.36
		80	5	0.62	0.70	71.44	1.31
			3.5	0.55	0.64	72.96	1.28
5	40	50	7	0.78	0.85	63.24	1.69
		60	6.5	0.70	0.72	63.20	1.67
		70	6	0.67	0.71	63.18	1.64
		80	5	0.61	0.69	64.02	1.50
		90	3.5	0.53	0.65	65.89	1.46

*most suitable condition

Conclusion

Raw gum arabic from Sha can be purified by filtration and decolourization using hydrogen peroxide solution. It can be concluded that 20% w/v of hydrogen peroxide solution is the most suitable for decolourization with respect to decolouring time (40 min) and safety. Because, high concentration of hydrogen peroxide is irritating to skin, eyes and mucous membranes. Moreover, the explosion hazard is usually present with high strength. For these reason, 20% H_2O_2 was considered to be appropriate decolourizing agent.

The purity of gum from Sha can be assessed by moisture content, ash content, and heavy metals, (lead and arsenic). Bulk density and tapped density of purified gum determined can provides further use of gum other than as an emulsifier. The viscosity of gum arabic solution depends on its pH. It can be observed that gum solution has highest viscosity within acid pH and thus, it may conclude that the gums are more suitable for many acidic foods. The function of gum in tamarind toffees is to emulsify the fats and prevent the releasing of fats into outer layer of toffees. Moreover, gums contribute the flavour and mouth feel of tamarind toffee. Gum from Sha is the most suitable drying carrier for the preparation of dehydrated tamarind powder which cannot be dehydrated tamarind alone.

The comparative production cost of purified gum arabic from Sha (local source) and that of gum from France were 5077.9 K/kg and 29000 K/ kg, respectively. Thus, this research would be implemented in some way for substituting the imported additives used in food, pharmaceutical and cosmetic industries to produce cheaper value-added products.

Acknowledgements

The author would like to acknowledge Professor Dr Cho Cho Oo, Head of the Department of Industrial Chemistry, University of Yangon, for giving me permission to present this research paper at Research Paper Reading Session sponsored by Myanmar Academy of Arts and Science.

I would like to express my gratitude to my supervisor, Dr Pansy Kyaw Hla, Professor (Retd.) of the Department of Industrial Chemistry, University of Yangon, Dr Yi Yi Myint, Co-supervisor, Professor and Head (Retd.) of the Department of Industrial Chemistry, Yadanabon University, and Dr Khin Thet Ni, Professor and Head (Retd.) of the Department of Industrial Chemistry, University of Yangon for their valuable suggestions and advice throughout this research work.

References

Anderson DMW, Weiping W (1990) Composition of the gum from Combretumpaniculatum and four other gums which are not permitted food additives. Phytochemistry 29:1193–1195.

Cano-Chauca, M., Stringheta, P.C., Ramos, A.M. and Cal-Vidal, J. (2005) Effect of the carriers on the microstructure of mango powder obtained by spray drying and its functional characterization, Innovative Food Science and Emerging Technologies. 6, 420-428.

Chapman and Hall, (1997) Hydrocolloid Application, T.J Press, Padstow, Cornwall, in Great Britain, First Edition.

Chegini, G.R. and Ghobadian, B. (2005) Effect of spray-drying conditions on physical properties of orange juice powder, Drying Technology, 23, 657-668.

Mocak, J, Jueasek. P, Phillips G.O, Virgas. S (1998) The classification of natural gums.X, Chemometric characterization of exudates gums that conform to the revised specification of the gum Arabic for food use and the identification of adulterants. Food Hydrocolloids, Vol.12, No.2, (April 2002) pp.353-361,ISSN: 0031-8655.

Phillips G.O and Williams P. A. (2000) Handbook of hydrocolloids. Woodhead publishing limited, Cambridge England.

Pua, C.K., Hamid, N.S.A., Tan, C.P. Mirhosseini, H.Rahman, R.B.A. and Rusul, G. (2010) Optimization of drum drying processing parameters for production of jackfruit (*Artocarpusheterophyllus*) powder using response surface methodology. LWT-Food Science and Technology. 43, 343-349.

Rib´ereau-Gayon P., Glories Y. and Maujean A., (2006) Handbook of Enology; The Chemistry of Wine Stabilization and Treatments; Volume 2, 2nd Edition, John Wiley & Sons Ltd, Chichester, West Sussex PO19 8SQ, England.

Shri V.S. Mathur (1973) *Indian Standard Specification for Acacia (Arabic) Gum, Food Grade, Indian Standard Institution.*

Verbeken, D., Dierckx, S. and Dewettinck .K. (2003) Exudate gums: occurrence, production, and application,

Williams PA, Phillips GO, Stephen AM (1990) Spectroscopic and molecular comparison of three fractions from Acacia senagal gum. Food Hydrocolloids 4:305–311.

EVALUATION OF NONI (*MORINDA CITRIFOLIA* L.) EXTRACT AND ITS APPLICATIONS IN COSMETIC AND MEDICINAL PRODUCTS

Ohnmar Kyi[1], Cho Cho Oo[2], Khin Thet Ni[3]

Abstract

The first portion of this research work was to prepare fermented Noni fruit extract and leaf extract from indigenous Noni which was cultivated as organic farming in Taungoo Township, Bago Region. The Noni fruit extract was prepared by Drip extraction method and was also determined the optimum fermentation period. The optimum fermentation period was found to be three months. The moisture, ash, protein, crude fiber, crude fat, carbohydrate contents and energy value of Noni fruit extract were examined. The vitamin content of Noni fruit extract was determined and the elemental analysis by EDXRF were also conducted. The Noni leaf extract was prepared as leaf juice and water extract. The amino acid content of leaf juice was determined and elemental analysis of water extract by EDXRF was conducted. The second portion was making the Noni cream as a cosmetic product prepared with resultant fruit extract and the Noni pain relieving cream as medicinal product prepared by using both the Noni leaf juice and Noni leaf water extract. It was found that the most suitable conditions were obtained by using Noni cream (a) and pain relieving cream PR I and PR II (a) according to the characteristics of the creams.

***Keywords*:** Noni, Noni fruit extract, Noni leaf extract, Noni cream, Noni pain relieving cream

Introduction

The genus Morinda (Rubiaceae) consists of about 80 species. The most well-known species of this genus is *Morinda citrifolia* L., commonly known as Noni. Ye'yo is the Myanmar name of plant *Morinda citrifolia* L. and grows very well in Myanmar. In traditional Myanmar medicine Ye'yo has been used for many health conditions. People in Myanmar cooked unripe fruits in curries, and ate the ripened fruits with salt or jaggery. Noni leaves were used to wrap fresh fish for cooking. Noni juice is a rich source of carbohydrates and proteins. It is also rich in vitamins like vitamin A and

1. Dr. Associate Professor, Industrial Chemistry Department, Dagon University
2. Dr. Professor and Head, Industrial Chemistry Department, University of Yangon
3. Dr. Professor and Head (Retired), Industrial Chemistry Department, University of Yangon

vitamin C, along with adequate amounts of iron and niacin. The fruit juice is in high demand as an alternative medicine for various illnesses such as arthritis, diabetes, high blood pressure, muscle pains, menstrual difficulties, headaches, heart disease and drug addiction. It was reported that the fruits of Noni suppress the growth of tumors by stimulating the immune system. Because of containing the nutrient anthraquinone in Noni juice, it was shown to be potentially useful as an anti-wrinkle agent when use externally or internally. It is valued for its many unique health promoting components that are well known treatment for skin conditions of all kinds. Noni increases the production of collagen and is good to use for the skin. Noni acts an anti-inflammatory agent. It is effective with muscular and joints conditions such as arthritis. Juice from the leaves is used for arthritis in Philippines.

Materials and Methods

Raw Materials

Noni fruits and Noni leaves, stearic acid, cetyl alcohol, lanolin, olive oil, petroleum jelly, beeswax, glyceryl monostearate, KOH, triethanolamine, methyl paraben, propyl paraben, essence, ethylene glycol distearate, light liquid paraffin, cajeput oil, menthol, eucalyptus oil, camphor and propylene glycol and polymer (Visc Optima SE).

Methods

Preparation of Fermented Noni Juice

Firstly, Noni fruits, mainly whitish in colour with tinges of green were washed, air-dried and then the ripe, soft and translucent fruits were obtained. The soft fruits were placed into 3 separate stainless steel fermentation vessels and stood for 1 month, 3 months and 6 months respectively. The contact between the juice and fresh air was minimized throughout the process. During aging, the Noni juice was fermented gradually. The golden colour fermented juice was gradually darkened on aging. At the end of each fermentation period, the juice was drained from spigots at the base of containers. Then the fermented Noni fruit extract was decanted, filtered and kept in sterilized bottles.

Preparation of Noni Leaf Water Extract

The ground Noni leaves were extracted with cold water (solvent to ground leaves ratio of 1:10) at room temperature for 1 hr. Then the mixture was filtered with cheesecloth bag and Noni leaf water extract was obtained.

Preparation of Noni Leaf Juice

Ground Noni leaves were put into the cheesecloth bag and squeezed. Then the resultant leaf juice was centrifuged to obtain a clear Noni leaf juice.

Preparation of Noni Cream

Formula of Noni Cream (a)

As an oil phase, 15 g of stearic acid, 8 g of cetyl alcohol, 2 g of lanolin, 3 g olive oil, 0.5 g petroleum jelly, 0.2 g beeswax and 5 g glyceryl monostearate were heated to 70 °C for 10 min with constant stirring until all the contents dissolved into a clear solution. As a water phase, 54.6 g of fermented Noni fruit extract, 0.9 g KOH, 7.0 g distilled water and 0.35 g triethanolamine were stirred at 70 °C. 0.1 g of methyl paraben, 0.05 g of propyl paraben and 3.0 g water were heated to 70 °C until a clear preservative solution was obtained. The water phase and preservative solution were gradually added to the oil phase. The oil phase and water phase were thoroughly stirred 1000 rpm for 10 minutes at 70 °C. After cooling to 40 °C, 0.3 g of lavender essence was added and stirred. The cream obtained was cooled to room temperature and poured into sterilized glass bottles.

Formula of Noni Cream (b)

Noni cream was prepared by the procedure as described in formula of Noni cream (a). The amount of fermented Noni fruit extract 44.6 g and amount of water 20 g were used. The amounts of other ingredients were the same.

Formula of Noni Cream (c)

The procedure was the same as described in formula of Noni cream (a) with same ingredients but fermented Noni fruit extract was 34.6 g and water was 30 g.

Preparation of Pain Relieving Cream

Formula of Pain Relieving Cream PR I

As a primary oil phase, 1 g of stearic acid, 1 g of ethylene glycol distearate, 3 g of light liquid paraffin, 0.3 g methyl hydroxyl benzoate and 0.2 g of propyl hydroxyl benzoate were heated to 70 °C with constant stirring. 1.2 g of cajeput oil, 12 g of menthol, 1g of eucalyptus oil, 8 g of camphor and 0.5 g of propylene glycol were warmed gently to 40 °C and stirred slowly. It was noted as secondary oil phase. Primary oil phase and secondary oil phase were mixed thoroughly and it was noted as Part A. After that, 2 g of polymer was added to the mixture of 54.2 g of water and 15 g Noni leaf extract and then stirred until a thick paste was obtained. Then 0.3 g of triethanolamine was added to this mixture with continued stirring and it was noted as part B. Part A and part B were mixed with constant stirring at 1000 rpm for 4 minutes. Then the prepared cream was poured into sterilized bottles.

Formula of Pain Relieving Cream PR II (a), II (b) and II (c)

Pain relieving cream was prepared by the same procedure as described in formula PR I. In PR II (a) 12 g of Noni leaf water extract and 47.2 g of water, in PR II (b) 22 g of Noni leaf water extract and 37.2 g of water, and in PR II (c) 32 g of Noni leaf water extract and 27.2 g of water were used. But the amounts of other ingredients were the same for these three formulae.

Results and Discussion

The fermented juices were obtained by drip extraction method with different fermentation periods (1 month, 3 months and 6 months). The three months fermentation product was satisfactory because its colour, odour and taste were better than that of the other fermented Noni juices. There was no significant difference in the percent (w/w) yields of fermented juices with

periods as shown in Table (1). The shelf life of all fermented juices without preservative was one year. The compositions and nutritional facts of the 3 months fermented juice and 6 months fermented juice are shown in Table (2). The results were consistent with the literature values. Because of the lower yield of Noni leaf juice, water extract was prepared by using water and ground leaves ratio of 1: 10.The results are shown in Table (3). The vitamin C content of fruit extract and amino acid content of leaf extract are shown in Tables (4) and (5) respectively. Noni fruit extract contains 567.18(μg/mL) vitamin C and that value had led to the preparation of skin cream because vitamin C creates a brighter complexion and evens out skin tones, and also diminishes the appearance of fine lines and wrinkles.

Table 1: Percent Yield and Physical Characteristics of Fermented Noni Fruit Extract

Property	**Fermentation Period of Fermented Juice**		
	1 month	**3*months**	**6 months**
Yield, % (w/w)	60.83	66.25	66.44
pH	3.17	3.17	3.16
Specific gravity	1.01	1.03	1.03
Colour	brown	brown	dark brown
Odour	strong smell	pungent	less pungent
Taste	slightly sour	sour	more sour with a bitter taste

* refer to the most favorable fermentation period

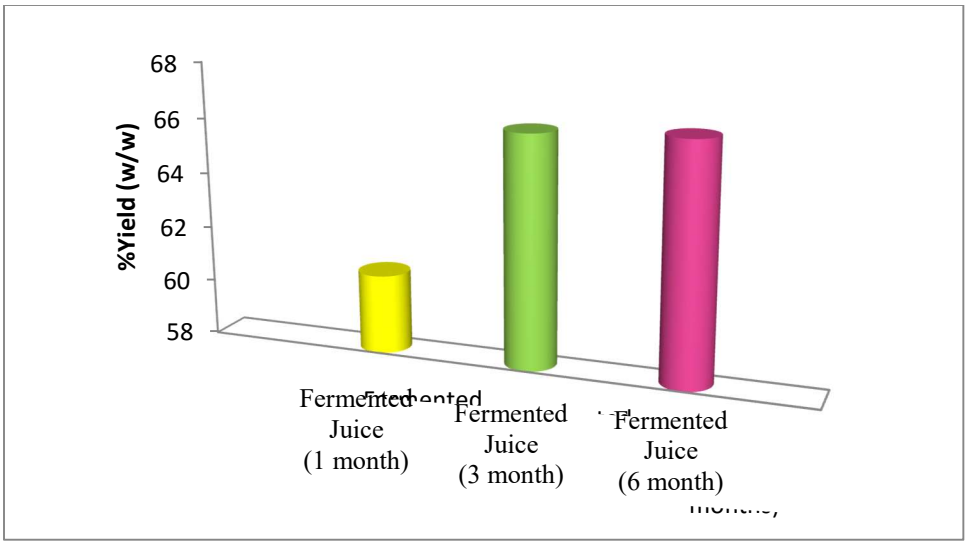

Figure 1: Percent Yields of Noni Juice with Different Fermentation Periods

Table 2: Composition of Noni Fruit Extracts (Juices)

Sr. No.	Constituent/ Nutritional Fact	Fermented Juice %(w/w)		
		(3 months)	(6 months)	*Literature Value
1	Moisture	94.71	95.5	91.6
2	Ash	0.56	0.52	0.46
3	Protein	0.65	0.55	0.39
4	Crude fiber	0	0	0.72
5	Crude fat (ether extract)	0	0	0.14
6	Carbohydrate	4.08	4.08	3.84
7	Energy value (kcal/100g)	20	19	15.4

* refer to (https:www.University of Hawaii/ctahr/noni/nut…)

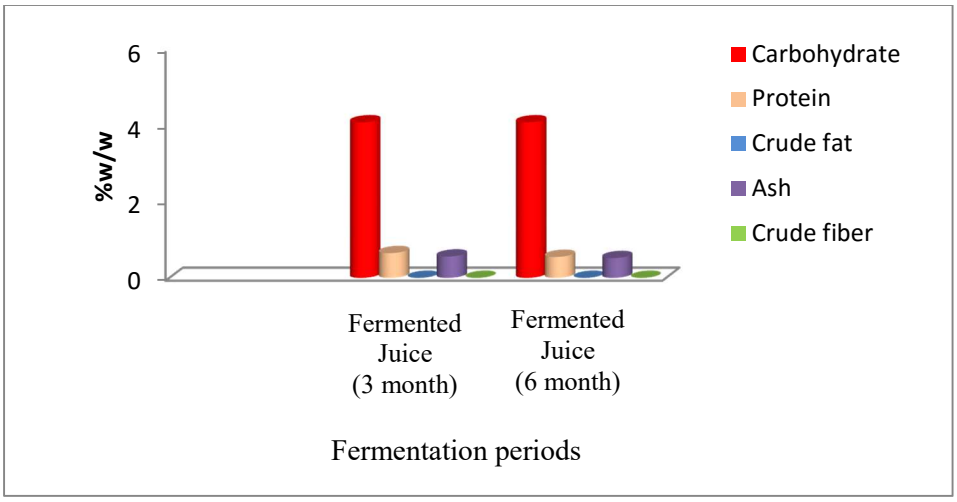

Figure 2: Percent Composition of Noni Juices

Table 3: Percent Yields of Noni Leaf Juice and Water Extract

Sr. No.	Type of Noni Leaf Extract	Yield % (w/w)
1	Leaf juice	18.99
2	Water extract	40.12

Table 4: Vitamin Contents of Noni Fruit Extract

Test Item	Result (µg/mL)	Limit of Detection, (µg/mL)	Test Method
Vitamin A (Retinyl)	ND	1.03	Asian Manual of Food Analysis(2011)
Vitamine E (α-Tocopherol)	ND	1	
Vitamin B_1	ND	0.05	EN 14122:2003
Vitamin B_2	ND	0.05	EN 14152:2003
Vitamin C (L-ascorbic acid)	567.18	-	Method for Food Analysis (2003)

The parameters were determined at Food Research and Testing Laboratory, Faculty of Science, Chulalongkorn University, Bangkok, Thailand.

Table 5: Amino Acid Contents of Noni Leaf Juice

Sr.No.	Amino Acid	Result (g/100 g)	Limits of Detection (g/100g)	Test Method
1	Alanine	ND	0.05	Amino Acid Analysis of Protein Hydrolysates by LC-MS/MS
2	Arginine	ND	0.1	
3	Aspartic acid	0.86	-	
4	Cystine	ND	0.14	
5	Glutamic acid	0.25	-	
6	Glycine	ND	0.05	
7	Histidine	ND	0.09	
8	Hydroxylysine	ND	0.1	
9	Hydroxyproline	ND	0.08	
10	Isoleucine	ND	0.08	
11	Leucine	0.12	-	
12	Lysine	0.13	-	
13	Methionine	0.16	-	
14	Phenylalanine	0.13	-	
15	Proline	0.34	-	
16	Serine	0.08	-	
17	Threonine	0.15	-	
18	Tryptophan	ND	0.08	
19	Tyrosine	ND	0.11	
20	Valine	ND	0.07	

The parameters were determined at Food Research and Testing Laboratory, Faculty of Science, Chulalongkorn University, Bangkok, Thailand.

Table 6: Compositions of Noni Creams with Fermented Noni Fruit Extract

Reaction condition	= 70 °C (30min)	Stearic acid	= 15 g
Glyceryl mono stearate	= 5 g	Cetyl alcohol	= 8 g
Petroleum jelly	= 0.5 g	Total	= 100 g
Lanolin	= 2 g	TEA	= 0.35g
Fragrance	= 0.3 ml		

Sample	Olive Oil (g)	Bees Wax (g)	Paraben Mixture (g)		KOH (g)	TiO_2 (g)	Fermented Noni Fruit Extract (g)	H_2O (g)
			Methyl Paraben	Propyl Paraben				
Noni Cream (a)*	3	0.2	0.1	0.05	0.9	0.4	54.6	10
Noni Cream (b)	3	0.2	0.1	0.05	0.9	0.4	44.6	20
Noni Cream (c)	3	0.2	0.1	0.05	0.9	0.4	34.6	30

*the most suitable formula

The larger amount of fermented Noni fruit extract was used in formula of Noni cream (a) and a cream with good texture and white colour was obtained as shown in Table (6). TiO_2 was used to increase the opaqueness and also reduce the transparency of product. Moreover, TiO_2 absorbs and reflects light which can cause products to deteriorate. Moreover in formulating of Noni cream (a) olive oil was used because olive oil contains three major antioxidants: vitamin E, polyphenols and phytosterols. Among the samples of Noni cream with fermented fruit extract, Noni cream (a) was taken as the most suitable formula because it was smooth, spreadable and contained relatively larger amount of fermented Noni fruit extract as shown in Table (9). Table (7) indicates percent composition of Noni pain relieving cream PR I in which Noni leaf extract was found to be 15 %. Table (8) shows the formulation of pain relieving cream samples.

Table 7: Compositions of Noni Pain Relieving Cream, Formula PR I

Sr. No.	Ingredients	% (w/w)	Remarks
1	Noni leaf extract	15.00	A stable emulsion was observed up to 12 months
2	Methyl hydroxy benzoate	0.30	
3	Propyl hydroxy benzoate	0.20	
4	Light liquid paraffin	3.00	
5	Stearic acid	1.00	
6	Ethylene glycol distearate	1.00	
7	Propylene glycol	0.50	
8	Menthol	12.0	
9	Eucalyptus oil	1.00	
10	Cajeput oil	1.20	
11	Camphor	8.00	
12	fragrance	0.30	
13	Triethanolamine	0.30	
14	Water	54.2	
15	Visc Optima SE	2.00	
	Total	**100.0**	

The compositions of Noni leaf water extract in PR II (a), PR II (b) and PR II (c) were 12 % (w/w), 22 % (w/w) and 32 % (w/w) and respectively. Table (9) shows the characteristics such as pH, colour, viscosity and stability of Noni pain relieving cream samples PR I, PR II(a), PR II(b) and PR II(c). Among these 4 samples, PR I and PR II (a) gave the best results due to their viscosity, smoothness and absence of irritation and redness to skin.

Figure 3: Noni Cream

Figure 4: Noni Pain Relieving Cream

Table 8: Composition of Noni Pain Relieving Cream, Formula PR II (a), II (b) and II (c)

Sr. No.	Ingredients	PR II (a)	PR II (b)	PR II (c)
		% (w/w)	% (w/w)	% (w/w)
1	Noni leaf water extract	12.00	22.00	32.00
2	Methyl hydroxy benzoate	0.30	0.30	0.30
3	Propyl hydroxy benzoate	0.20	0.20	0.20
4	Light liquid paraffin	3.00	3.00	3.00
5	Stearic acid	1.00	1.00	1.00
6	Ethylene glycol distearate	1.00	1.00	1.00
7	Propylene glycol	0.50	0.50	0.50
8	Menthol	12.0	12.0	12.0
9	Eucalyptus oil	1.00	1.00	1.00
10	Cajeput oil	1.20	1.20	1.20
11	Camphor	8.00	8.00	8.00
12	fragrance	0.30	0.30	0.30
13	Triethanolamine	0.30	0.30	0.30
14	**Water**	**57.2**	**47.2**	**37.2**
15	ViscOptima SE	2.00	2.00	2.00
Total		**100.0**	**100.0**	**100.0**

Note: A stable emulsion was observed up to 12 months

Figures (3) and (4) show prepared Noni cream and pain relieving cream. Figures (5) and (6) present elemental analyses of Noni fruit extract and leaf extract. Figures (7) and (8) depict the elemental analysis of Noni pain relieving cream samples PR I and PR II (a) by EDXRF. It can be concluded that elements potassium and calcium were present in Noni leaf extract were also present in the samples of Noni pain relieving cream.

Table 9: Characteristics of Noni Cream and Pain Relieving Cream using Noni Extract

Sample	**pH**	**Colour**	**Viscosity (cP)**	**Emulsion Stability (1 year)**	**Remarks**		
					Smooth-ness	**Spreadability**	**Absence of irritation, redness**
Noni cream (a)*	5.2	white	9310	stable	4	4	5
Noni cream (b)	5.3	white	9440	stable	3	3	5
Noni cream (c)	5.3	white	9460	stable	3	3	5
PR I*	5.5	dark brown	1728	stable	4	4	5
PR II(a)*	6.1	light brown	1484	stable	4	4	5
PR II(b)	5.4	light brown	1384	stable	3	3	5
PR II(c)	5.4	brown	1267	stable	3	3	5

* The most suitable formula Note: 1 = very poor, 2 = poor, 3 = fair, 4 = good and 5 = excellent

Table 10: Elemental Analysis of Fermented Noni Fruit Extract, Noni Leaf Water Extract and Pain Relieving Creams by EDXRF

Sr. No.	Element/ Compound	Noni Fruit Extract (mg/L)	Noni Leaf Water Extract, (mg/L)	Noni Pain Relieving Cream	
				PR I (ppm)	PR II(a) (ppm)
1	K	1443.023	5760.107	684.572	308.493
2	Cl	-	1592.749	-	-
3	Ca	-	1307.268	357.660	168.434
4	S	89.982	188.375	-	-
5	Rb	-	32.923	-	-
6	Zn	-	18.287	-	-
7	Fe	17.638	27.403	-	-
8	Cu	8.270	17.280	-	-
9	Mn	-	16.737	-	-
10	Sr	-	15.102	-	-
11	$C_6H_{10}O_5$	12.500 mg/L	12.500 mg/cm^2	-	-
12	H_2O		-	99.896	99.952

The elements were determined at Universities' Research Centre, Yangon Region.

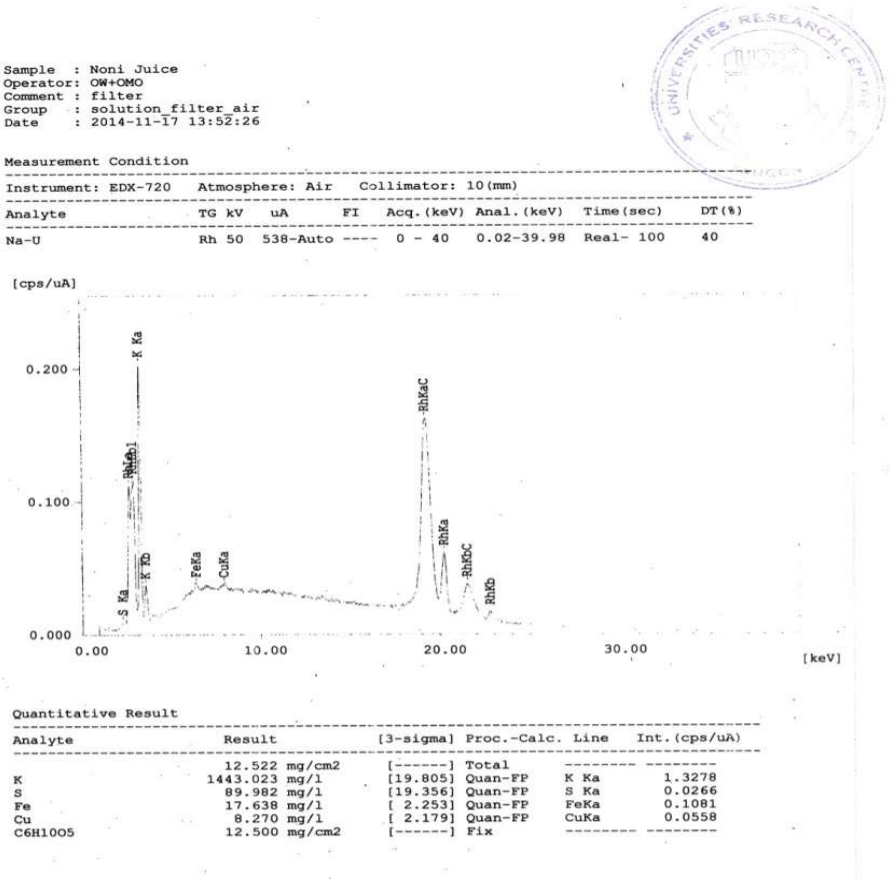

Figure 5: EDXRF Spectrum of Noni Fruit Extract Sample

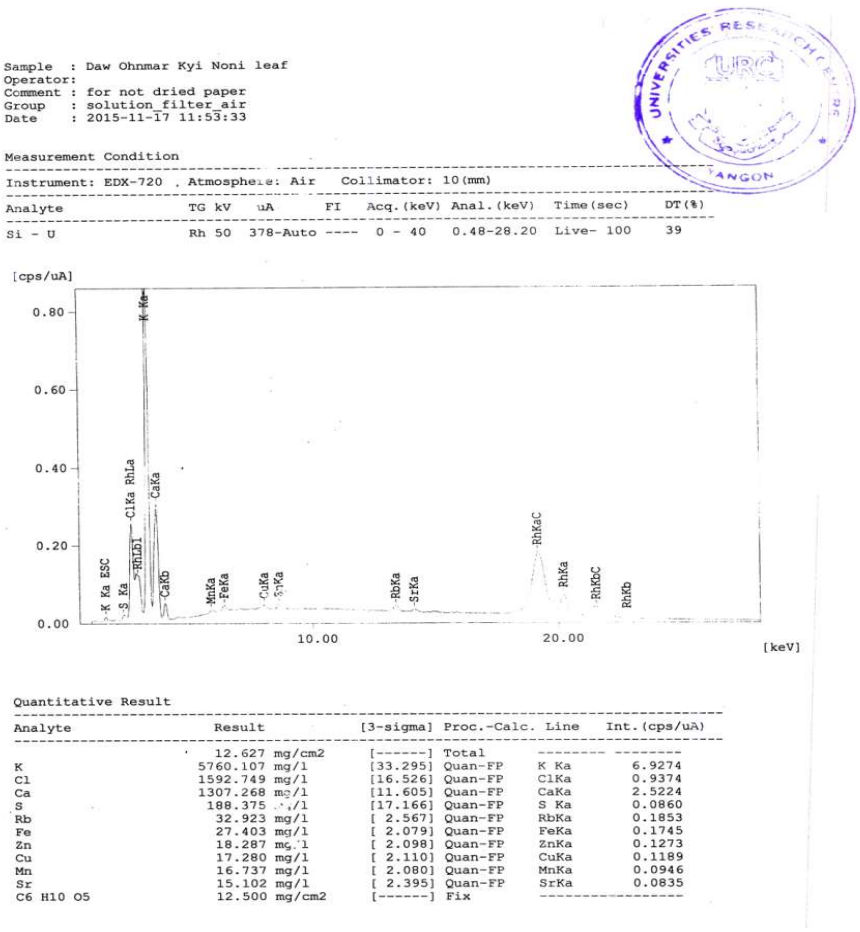

Sample : Daw Ohnmar Kyi Noni leaf
Operator:
Comment : for not dried paper
Group : solution_filter_air
Date : 2015-11-17 11:53:33

Measurement Condition

Instrument: EDX-720 , Atmosphere: Air Collimator: 10(mm)

Analyte	TG	kV	uA	FI	Acq.(keV)	Anal.(keV)	Time(sec)	DT(%)
Si - U	Rh	50	378-Auto	----	0 - 40	0.48-28.20	Live- 100	39

Quantitative Result

Analyte	Result	[3-sigma]	Proc.-Calc.	Line	Int.(cps/uA)
	12.627 mg/cm2	[------]	Total		
K	5760.107 mg/l	[33.295]	Quan-FP	K Ka	6.9274
Cl	1592.749 mg/l	[16.526]	Quan-FP	ClKa	0.9374
Ca	1307.268 mg/l	[11.605]	Quan-FP	CaKa	2.5224
S	188.375 mg/l	[17.166]	Quan-FP	S Ka	0.0860
Rb	32.923 mg/l	[2.567]	Quan-FP	RbKa	0.1853
Fe	27.403 mg/l	[2.079]	Quan-FP	FeKa	0.1745
Zn	18.287 mg/l	[2.098]	Quan-FP	ZnKa	0.1273
Cu	17.280 mg/l	[2.110]	Quan-FP	CuKa	0.1189
Mn	16.737 mg/l	[2.080]	Quan-FP	MnKa	0.0946
Sr	15.102 mg/l	[2.395]	Quan-FP	SrKa	0.0835
C6 H10 O5	12.500 mg/cm2	[------]	Fix		

Figure 6: EDXRF Spectrum of Noni Leaf Extract Sample

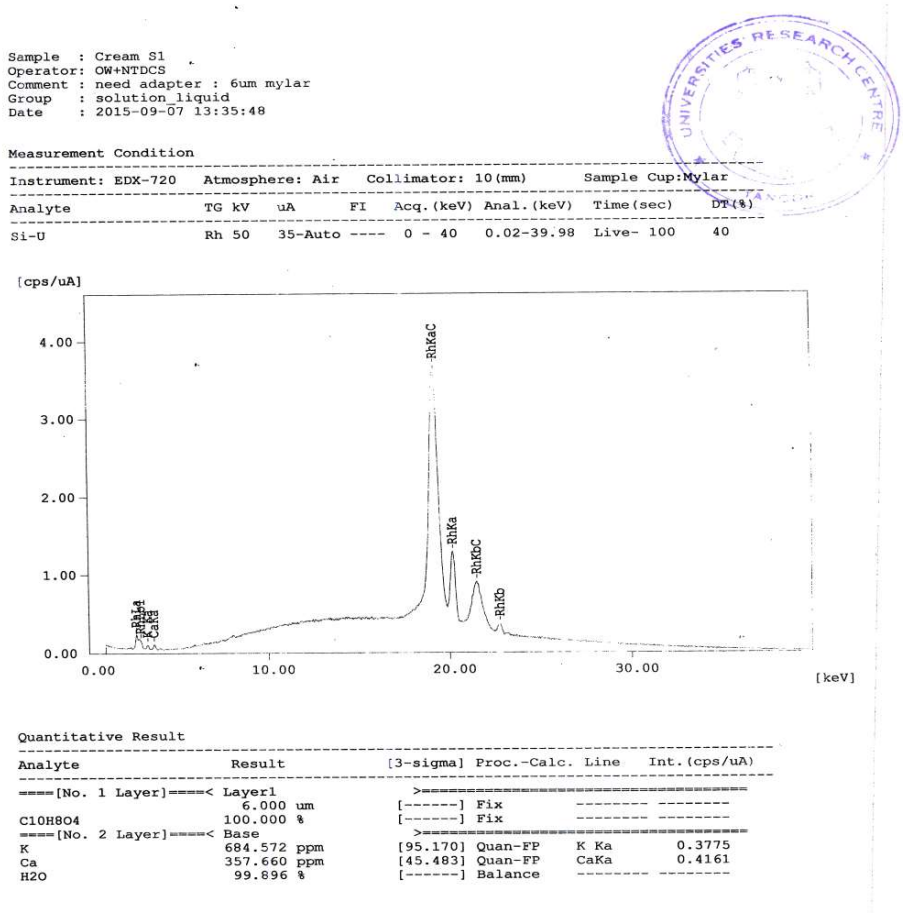

Figure 7: EDXRF Spectrum of Noni Pain Relieving Cream Sample PR I

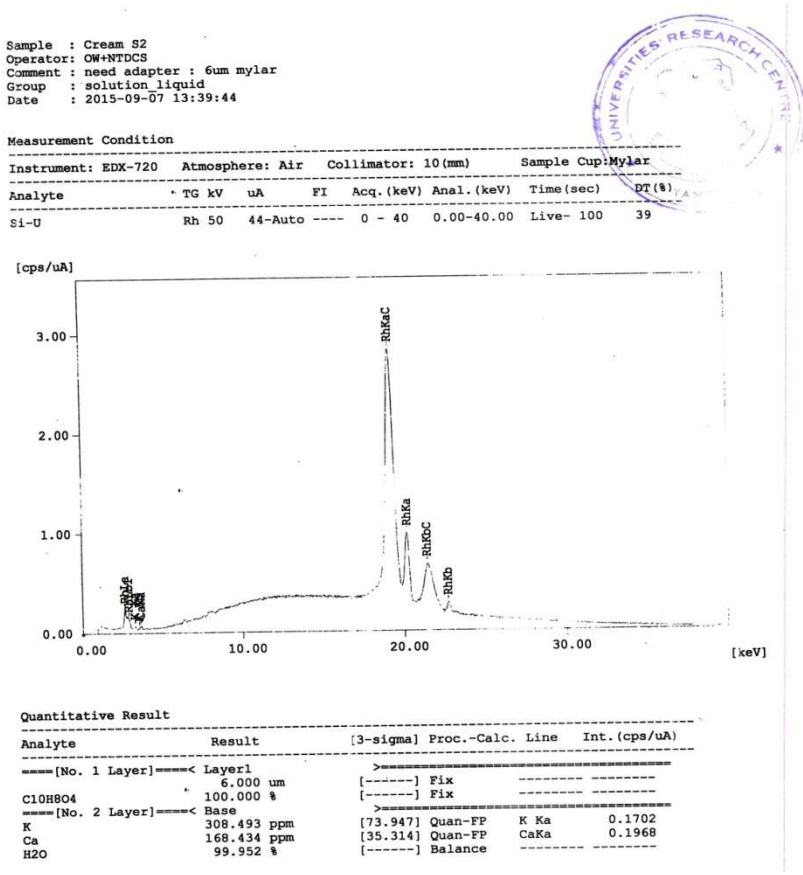

Figure 8: EDXRF Spectrum of Noni Pain Relieving Cream Sample PR II(a)

Conclusion

In this research, cosmetic and medicinal products of Noni were prepared with leaf extract and fermented fruit extract. Good quality fermented Noni fruit extract was obtained within 3 months yielding 66.44 %. The composition of Noni juice is consistent with literature value. Noni cream was prepared with fermented Noni fruit extract due to its vitamin C content of 567.18 μg/mL. In the preparation of Noni cream, amount of ratios of fruit extract and water were varied as 54.6:10, 44.6:20 and 34.6:30. The most

suitable formula is Noni cream (a) which was prepared with 54.6 g of fermented Noni fruit extract and 10 g of water. The creams obtained were smooth, spread easily, no redness and no irritation when applied onto the skin. The emulsion of cream samples was stable up to one year. Noni leaf extracts were prepared as leaf juice and water extract. The pain relieving cream PR I was prepared with 15 g of leaf juice and 54.2 g of water. Moreover, pain relieving cream Pr II (a), II (b) and II (c) were prepared by different ratios of Noni leaf water extract and water i.e 12.0:57.2, 22.0:47.2 and 32.0:37.2. The most suitable formula is PR II (a).

Acknowledgements

I would like to express my greatest appreciation to Dr Khin Hla Mon, Professor and Head, Department of Industrial Chemistry, Dagon University for her permission to submit this research paper. I wish to express my profound respect and deepest gratitude to my supervisor Dr Khin Thet Ni, Professor and Head (Retired), Department of Industrial Chemistry, University of Yangon, and co-supervisor Dr Cho Cho Oo, Professor and Head, Department of Industrial Chemistry, University of Yangon, for their constructive advice and valuable suggestions.

References

Balsam, M.S and E. Sagarin, 1972. Cosmetic Science and Technology, Vol. I. 2nd Edition, John Wiley and Sons, Inc.

Harry's Cosmeticology, 2011. 7th edition, Longman Scientific and Technical Inc.

Hirazumi, A. and E. Fususawa. 1999. An immuno modulatory polysaccharide-rich substance from the fruit juice of *Morinda citrifolia* (noni) with anti-tumor activity. Phytotherapy Research, Vol 13: pp 380–7.

Hirazumi, A., E. Furusawa, S. C., Chou, and Y. Hokama, 1996. Immunomodulation contributes to anti-cancer activity of Morinda citrifolia (noni) fruit juice. Proceedings of the Western Pharmaceutical Society Vol 39: pp 7–9.

Nelson, S. C., & Elevitch, C. R., 2006. Noni: The Complete Guide for Consumers and Growers, Gardening – 104.

https://www.healingnoni.com>skin-care
https:www.University of Hawaii/ctahr/noni/nut…)

OPTIMIZATION OF FERMENTATION CONDITION FOR THE PREPARATION OF FRUIT YOGHURT

Bo Bo Thet[1], Pansy Kyaw Hla[2]

Abstract

In this research, yoghurt was prepared from goat and cow milks. Available cow milks in the market such as Ngwe Sin Palei and Sein Lei KanThar Brands were purchased from Hledan Market, Kamayut Township and native cow milk was collected from YwarThit Village, Htantabin Township, Yangon Region. Native goat milks were also collected from Ywar Thit Village, Htantabin Township and Insein Township. In the preparation of fruit yoghurt, 5%, 10% and 15% of fruits were used. Three kinds of fruits such as strawberry, avocado and banana were used in yoghurt. The physico-chemical characteristics, yield percent and shelf-life of prepared fruit yoghurt were also investigated. Starter culture, pH, fermentation temperature, time and fruit percent were important to control the parameters for preparation of fruit yoghurt. It was observed that at 43°C of fermentation temperature, 15g of starter culture, 5hr of fermentation time and 10% fruit were the most suitable conditions for the preparation of fruit yoghurt based on its pH, taste and texture.

Keywords: fruit yoghurt, starter culture, pH, fermentation temperature and time, fruit percent

Introduction

Milk is a unique substance in that it is both consumed as fluid milk with minimal processing and it is the raw material used to manufacture a wide variety of products. Milk also has a unique nutritional property that makes it an especially important food, particularly for the young. Milk and milk products have formed an important part of the diet of man (Potter, 1986).

The milk from cows and goats will vary in composition and many other factors. These include the breed, individuality of the animal, age, stage of lactation, season of the year, the feed, time of milking, period of time between milking, the physiological condition of the cow whether it is calm or excited, whether it is receiving drugs and so on (Eckles, 1982).

[1.] Dr, Lecturer. Department of Industrial Chemistry, University of Yangon
[2.] Dr, Professor (Retired). Department of Industrial Chemistry, University of Yangon

Processing milk into a dairy product makes it more stable for storage over extended period of time. In the tropics where ambient temperature are high and refrigeration is not readily available, milk may be concentrated by boiling or made into butter or ghee or other products which keep better at room temperatures. When there is an abundant local supply, storage and marketing may have a low priority, leading to wastage (Edgar, 1995).

Yoghurt is a dairy production that has more profits than milk. Digestive system in some people has an allergy to lactose (sugar of milk), but lactose is transformed to lactic acid in yoghurt and does not create allergy. Fermented milk products are traditional, particularly in countries with warm climates, primarily because raw milk rapidly sour as a result of the production of lactic acid by microorganisms, which inevitably gain access to the milk. This souring, or fermentation, constitutes an important means of preventing spoilage by *proteolytic* and other bacteria which cannot tolerate acid conditions and inhibits the growth of certain common pathogens (Meyer, 1960).

Lactic acid bacteria are used also to produce fermented milks other than yoghurt, most with a national original significance. One of the oldest fermented milk is known as yoghurt. Yoghurt consists of pasteurized, homogenized whole milk that is inoculated with *Streptococcus thermophilus* and *Lactobacillus bulgaricus* and incubated for a short time (2-3 hours) at 43-45°C (Hall,1976).

The objectives of this research work were to convert milk, which is perishable, into yoghurt with a longer shelf-life whilst preserving most of its nutrients and to explore the possibility for the commercial production of yoghurt from cow and goat milks.

Materials and Methods

Sampling and Analysis of Raw Milks

Available cow milks in the market such as Ngwe Sin Palei and Sein Lei KanThar Brands were purchased from Hledan Market, Kamayut Township and native cow milk was collected from YwarThit Village, Htantabin Township, Yangon Region. Native goat milks were also collected

from YwarThit Village, Htantabin Township and Insein Township, Yangon Region.

Milk Analyzer (MILKOTESTER) was used in the determination of physico-chemical characteristics of milk samples. Milk Analyzer (MILKOTESTER) is designed for percentage analysis of Fat, Solids-Not-Fat (SNF), Protein, Lactose, Water Content, Temperature(°C), Freezing point, Total Solids, Density and pH. These components can all be measured at the same time.

Pasteurization and Homogenization of Milk

1liter of Cow Milk (Sein Lei KanThar Brand) was poured into a stainless steel pot. The milk was heated up to 85°C and it was held there for at least 15 min. The heated milk was homogenized by using magnetic stirrer for about 10 min.

Similarly, cow milk (Ngwe Sin Palei Brand and YwarThit Village) and goat milk (Insein and YwarThit Village), were prepared in the same manner.

Preparation of Fruit Yoghurt

1 liter of pasteurized milk was added to a sterilized stainless steel pot, stirred and heated at 95°C using a magnetic stirrer, and held for 2 minutes. It was then cooled until it reached the required incubation temperature of 43 - 46°C that is the critical temperature for yoghurt culture growth. 15g of starter culture was added to the milk and held at 45°C, for 4 - 5 hr to reach a pH range of 4.3 to 4.6. Then, 70 g of sugar, 1.5 g of sodium carboxymethyl - cellulose, 50 mg of sodium sorbate and 5% strawberries by weight of yoghurt were added respectively and blended by using a blender. The mixture is again pasteurized at 75°C for 3 minutes and poured carefully into a previously sterilized bottle and capped tightly, labeled and stored in a cool dry place.

Similarly, the same procedure was also carried out with strawberries 10% and 15%.

The same procedure was repeated by using bananas and avocados. The effect of fruit percent on the pH and taste of fruit yoghurt were determined and its result shown in Table (4).

Results and Discussion

Physico-chemical characteristics of milk samples such as Cow milk Ngwe Sin Palei brand, Sein Lei KanThar brand and native cow milk from YwarThit Village, Htantabin Township were determined by Milk Analyzer (MILKOTESTER). Similarly, goat milk from YwarThit Village, Htantabin Township and Insein Township were also analyzed. The comparison between cow milk and goat milk samples is shown in Table (1). The protein and fat content of cow milk (Sein Lei KanThar Brand) were the highest and so it was the best for making yoghurt.

Table (2) shows the effect of starter culture on the fermentation time in the preparation of yoghurt. It was observed that starter culture (15g), fermentation time (5hours) and fermentation temperature (43°C) were the most suitable condition. At 43°C, pH of prepared yoghurt reached the range of 4.3 to 4.6 during fermentation time of 5hr and the data are shown in Table (3).

In the preparation of fruit yoghurt, 5%, 10% and 15% of fruits by weight of yoghurt were used and the experimental data are shown in Table (4). It was evident that 10% fruit by weight of yoghurt was the most suitable condition in the preparation of fruit yoghurt according to pH, taste and type of prepared fruit yoghurt. Physico-chemical characteristics of fruit yoghurt are shown in Table (5) and it was found that fat content and protein content of avocado yoghurt were greater than other fruit yoghurt samples. Table (6) shows the comparison of physico-chemical characteristics of prepared yoghurt and commercial yoghurt. It was found that fat content and protein of prepared yoghurt were greater than the commercial yoghurt.

During storage, the acidity of prepared fruit yoghurt decreased. The determination of the acidity of prepared yoghurt was conducted seven times at three days interval and the data are shown in Table (7).

Table 1: Comparison of Physico-chemical Characteristics of Cow and Goat Milk Samples

Sr. No.	Characteristics	Cow Milk Samples			Goat Milk Samples		*Literature value
		Ngwe Sin Palei	Sein Lei KanThar	Ywar Thit Village	Ywar Thit Village	Insein	
1	Milk yields (viss/head/day)	5-6	6-7	2-2.5	0.5-1	0.7-1	-
	Chemical characteristics						
2	Fat content (%)(w/w)	3.6	4.3	3.8	3.8	4.1	3.80
3	Protein content (%)(w/w)	3.2	3.6	3.3	3.2	3.4	3.35
4	Solid not fat (%)(w/w)	8.8	12.2	8.5	8.6	8.9	8.80
5	Water content (%)(w/w)	87.6	83.5	87.7	87.6	87	87.25
6	Total solids content (%)(w/w)	12.4	16.5	12.3	12.4	13.0	12.60
7	Ash content (%)(w/w)	0.63	0.65	0.60	0.68	0.65	0.70
	Physical characteristics						
8	Specific gravity	1.018	1.04	1.009	1.02	1.007	1.03
9	Refractive index	1.35	1.33	1.32	1.34	1.31	-
10	pH	6.60	6.62	6.64	6.62	6.61	6.65

The experiments were conducted at the Laboratory of Department of Industrial Chemistry, West Yangon University.

*Winton, L.A., 2000.

Table 2: Effect of Starter Culture on the Fermentation Time

Volume of milk = 1 liter

Sr. No.	Temperature(°C)	Starter Culture(g)	Fermentation Time(hours)	
			Experiment	**Literature value
1	40	10	8	4-5
		15	7	
		20	6	
2	*43	10	7	4-5
		*15	*5	
		20	4	
3	45	10	6	4-5
		15	4	
		20	3	

* The most suitable condition

**Winton, L.A., 2000

The experiments were conducted at the Laboratory of Department of Industrial Chemistry, West Yangon University.

Table 3: Changes in pH of Yoghurt During Fermentation

Volume of milk = 1 liter , Starter culture = 15g,
Fermentation temperature = 43˚C

Sr. No.	Source		pH at Different Fermentation Times (hour)						
			0	1	2	3	4	*5	6
1	Cow milk	Ngwe Sin Palei	6.6	6.1	5.7	5.2	4.8	4.3	3.8
		Sein Lei KanThar	6.7	6.3	5.6	5.4	4.9	4.4	4.0
		YwarThit Village	6.5	6.1	5.6	5.3	4.7	4.2	3.6
2	Goat milk	YwarThit Village	6.6	6.2	5.8	5.5	4.9	4.5	4.0
		Insein	6.5	6.0	5.6	5.3	4.9	4.6	3.9

*Optimum fermentation time = 5hr

The experiments were conducted at the Laboratory of Department of Industrial Chemistry, West Yangon University.

Table 4: Effect of Fruit Percent on the pH and Taste of Yoghurt

Milk Sample = Sein Lei KanThar

Sr. No.	Source	Characteristics	Fruits (%)(w/w)			*Literature value
			5	**10	15	
1	Strawberry	pH	4.9	4.2	3.7	4.1-4.3
		Yoghurt type	liquid	liquid	semi-solid	liquid
		Taste	slightly sweet	slightly sour	sour	sour
2	Avocado	pH	5.1	4.3	4.0	4.1-4.3
		Yoghurt type	liquid	liquid	semi-solid	liquid
		Taste	slightly sweet	slightly sour	sour	sour
3	Banana	pH	4.8	4.4	3.9	4.1-4.3
		Yoghurt type	liquid	liquid	semi-solid	liquid
		Taste	slightly sweet	slightly sour	sour	sour

*Winton, L.A., 2000

**The most suitable condition

The experiments were conducted at the Laboratory of Department of Industrial Chemistry, West Yangon University.

Table 5: Physico-chemical Characteristics of Prepared Fruit Yoghurt
Milk Sample = Sein Lei KanThar

Sr. No.	Characteristics	Fruit Yoghurt			*Literature value
		Strawberry	Avocado	Banana	
	Chemical characteristics				
1	**Fat content (%)(w/w)	6.2	7.3	6.5	≥3
2	**Protein content (%)(w/w)	3.24	4.15	3.48	3-8
3	Total solids content (%)(w/w)	15.36	16.34	16.20	11.20
4	Solid not fat (%)(w/w)	9.16	9.04	9.70	≥8.2
5	Ash content (%)(w/w)	0.82	0.98	0.90	0.92
6	Lactic acid content(%)(w/w)	1.2	1.7	1.8	1.1-1.8
	Physical characteristics				
7	Water content(%)(w/w)	80.52	75.38	77.23	88.80
8	pH	4.2	4.3	4.4	4.1-4.3
9	Yoghurt type	liquid	liquid	liquid	liquid
10	Taste	sour	slightly sour	slightly sour	sour

*Winton, L.A., 2000

**Fat and protein content were determined at SGS (Myanmar) Company limited.
The experiments were conducted at the Laboratory of Department of Industrial Chemistry, West Yangon University.

Table 6: Comparison of Physico-chemical Characteristics of Prepared Yoghurt and Commercial Yoghurt

Sr. No.	Characteristics	Prepared Fruit Yoghurt (Sein Lei KanThar)	Commercial Yoghurt (Hlegalay Yoghurt)
	Chemical characteristics		
1	*Fat content (%)(w/w)	4.2	3.2
2	*Protein content (%)(w/w)	6.8	6.3
3	Total solids content (%)(w/w)	18.2	16.4
4	Solid not fat (%)(w/w)	13.95	13.2
5	Ash content (%)(w/w)	0.90	0.87
6	Lactic acid content(%)(w/w)	1.5	1.4
	Physical characteristics		
7	Water content (%)(w/w)	81.8	83.6
8	pH	4.3	4.2
9	Yoghurt type	liquid	liquid
10	Taste	slightly sour	slightly sour
11	Shelf-life (week)	2	2

*Fat and protein content were determined at SGS (Myanmar) Company limited.
The experiments were conducted at the Laboratory of Department of Industrial Chemistry, West Yangon University.

Table 7: Effect of Storage Time on the Acidity of Prepared Yoghurt
Milk Sample = Sein Lei KanThar
Storage temperature = Refrigeration Temperature (0-4°C)

Sr. No.	Yoghurt	Storage Time (days)	Acidity (%) (v/w)	*Literature value
1	Strawberry Yoghurt	0	4.30	3.9
		3	4.24	
		6	4.21	
		9	4.18	
		12	4.12	
		15	3.70	
2	Avocado Yoghurt	0	4.60	3.9
		3	4.53	
		6	4.48	
		9	4.40	
		12	4.25	
		15	3.95	
3	Banana Yoghurt	0	4.50	3.9
		3	4.45	
		6	4.40	
		9	4.32	
		12	4.15	
		15	3.85	

*Winton, L.A., 2000

The experiments were conducted at the Laboratory of Department of Industrial Chemistry, West Yangon University.

Conclusion

Standard fermented milk products are made from raw milk (Cow or Goat) that has good quality such as yield, fat, protein, total solids and pH. This means fresh, pure and clean milk from healthy animals and the milk should be free from odors and taints that could affect the quality of products. In this research work, milk products – yoghurt was prepared from cow milk as well as from goat milk. In the preparation of fruit yoghurt, the effect of starter culture on fermentation time, the effect of fermentation time on pH and the

effect of fruit percent on the pH and taste of the products were investigated. In the preparation of fruit yoghurt, different ratios of fruit (5%, 10%, 15%) were used. It was observed that at 43°C of fermentation temperature, 15g of starter culture, 5hr of fermentation time and 10% fruit were the optimum conditions for the preparation of fruit yoghurt based on its pH, taste and texture. Prepared fruit yoghurt was compared with commercial fruit yoghurt (Hlegalay Yoghurt). It was found that the quality of prepared fruit yoghurt were higher than that of commercial yoghurt samples.

Acknowledgements

I would like to express deeply thank to Dr. Pansy Kyaw Hla, Professor (Retd), Industrial Chemistry Department, University of Yangon for providing research facilities and also for her invaluable suggestions and guidance during the research work. We are greatly indebted to Dr. Cho Cho Oo, Professor and Head, Industrial Chemistry Department, University of Yangon for allowing us to submit this article.

References

Eckles, C.H., W.B. Combs and H. Macy (1982) *Milk and Milk Products*, 4th Edition, McGraw Hill, New York.

Edgar, S. M. (1995) *Milk and Dairy Product Technology*, Marcel Dekker, Inc. New York.

Hall, H.S. (1976) *Standardized Pilot Milk Plants*, Food and Agriculture Organization of United Nations, Rome.

Meyer, L.H. (1960) *Food Chemistry*, Reinhold Publishing Corporation, New York.

Potter, N. (1986) *Food Science*, 4th Edition, AVI Publishing Co. Ltd., New York.

Winton, L.A. and K.B. Winton.(2000) *Milk and Milk Products*, Agrobio, India.

PREPARATION OF MODIFIED STARCH FROM SWEET POTATO AND ITS APPLICATION IN SOME FOOD PRODUCTS

Khin Hla Mon[1], Sandi Bo Bo[2]

Abstract

Starch is a carbohydrate consisting of a large number of glucose units joined by glycosidic bonds. It can be modified chemically to increase their positive attribute. The present research work was focused on the preparation of modified starch from sweet potato using both acid treatment method and cross-link method. The prepared modified starch was used in the preparation of some food products such as biscuit and mayonnaise. Fresh and mature sweet potatoes were collected from Pyin Oo Lwin Township, Mandalay Region. The most suitable conditions for the preparation of starch were 1:6 (w/v) ratio of sweet potato to water at 4 hr settling time. The most favourable conditions for the preparation of modified starch from sweet potato by acid treatment were 0.5 mL of 10 % hydrochloric acid at room temperature for 15 min. In cross-link method, the most suitable conditions were 5mL of 0.1 % sodium tripolyphosphate at room temperature for 30 min. The characteristics of starch and modified starches such as ash, moisture, pH, gelatinization temperature, solubility, swelling power and amylose content were investigated. Both sweet potato starch and prepared modified starches by two different methods were identified by FT-IR and SEM method. It was used in the preparation of mayonnaise and biscuit.

***Key words*:** glycosidic bonds, cross-link method, gelatinization

Introduction

Sweet potato (*Ipomoea batatas* L.) is a tuberous rooted perennial plant belonging to the convolvulaceae or morning glory family and the main commercial producers of sweet potatoes are China, Indonesia, Vietnam, Japan, India, Myanmar and Uganda. The main utilization of sweet potato is in the starch manufacture and has many applications due to its starch composition. The quality of sweet potato tubers flour and starches appear not only to be affected by the content of the starch in the tuber, but also the amylose- amylopectin ratio of the starch and the chemical composition of the

[1] Professor and Head, Department of Industrial Chemistry, Dagon University.
[2] MSc Student, Department of Industrial Chemistry, Dagon University.

tuber (Hoover, 1985; Moorthy, 2002). In Myanmar, sweet potatoes are farmed in Sagaing Region, Mandalay Region, Ayeyarwaddy Region, Yangon Region, Bago Region and other tropical places. Starches have limitations which reduce their use at industrial level due to the inability tolerate a wide range of processing techniques, distribution and storage conditions. Modified starches are superior to starches due to their improved functional properties and are widely employed in processed food in several years. It is used in pharmaceuticals, biodegradable polymers and as food additives. Starch is a carbohydrate consisting of a large number of glucose units joined by glycosidic bonds. Pure starch is a white, tasteless and odorless powder that is insoluble in cold water or alcohol. It consists of two types of molecules: the linear and helical amylose and the branched amylopectin. Depending on the plant, starch generally contains 20 to 25% amylose and 75 and 80% amylopectin by weight. Amylose is also an important thickener, water binder, emulsion stabilizer and gelling agent in both industrial and food based contexts. Amylopectin is a soluble polysaccharide and highly branched polymer of glucose found in plants. (http://www.wikipedia.org.com)

The present research investigated the preparation of modified starch from sweet potato using two different methods: acid treatment method and cross-linked method. This modified starch was identified by FT-IR method, followed by the determination of amylose and amylopectin content.

Materials and Methodology

Materials

Fresh and mature sweet potatoes were collected from Pyin Oo Lwin Township, Mandalay Region. All the chemicals used were India made, Analar grade hydrochloric acid, sodium hydroxide, sodium tripolyphosphate.

Methodology

Preparation of Sweet Potato Starch

Fresh sweet potatoes were thoroughly washed with tap water to remove the impurities such as dirt, grit and dust. Then, raw sweet potatoes were peeled and washed with tap water. 100g of sweet potatoes were crushed

in a blender. The resultant paste was soaked in water in the ratio of 1:6 (w/v%) for 60 min at 30ºC by stirring with a constant rate of 150 rpm. The sweet potato starch slurry was filtered through a nylon cloth to obtain the starch granules. The starch granules in the filtrate were settled for 4 hr, and then water was decanted to separate out the starch. The starch granules were washed with tap water two times. The starch was sun-dried and pulverized using mortar and pestle to obtain a fine powder. The prepared sweet potato starch is shown in Figure (2). Effect of sweet potato to water ratio (1:3,1:4,1:5,1:6,1:7 and 1:8) and effect of settling time (1,2,3,4,5) hr on the yield of sweet potato starch were investigated using the same procedure mentioned above.

Figure 1: Sweet Potato

Figure 2: Sweet Potato Starch

Preparation of Modified Starch from Sweet Potato by Acid Treatment Method

Dried sweet potato starch 5g was thoroughly mixed with 0.5 mL of 20% hydrochloric acid in a 250 mL beaker and stirred for 15 min at 40ºC. The slurry was completely neutralized with 1 mL of 0.01 % sodium hydroxide. The slurry was washed with water and settled for one day. After that, it was separated by decantation of water. The starch was sun-dried for 90 min and pulverized using mortar and pestle to obtain fine powder. The prepared modified sweet potato starch by acid treatment is shown in Figure 3(a). Effect of volume of 20% hydrochloric acid (0.25,0.5,1.0,1.5,2.0,2.5) ml, effect of concentration of 0.5ml of HCL (5,10,20,30,40,50) % and effect of reaction temperature (30,40,50,60)°C on the yield of sweet potato modified starch were determined using the same procedure as mentioned above.

Preparation of Modified Starch from Sweet Potato by Cross-link Method

Dried sweet potato starch 5g was mixed with 10 mL of water for 10 min. 5 mL of 0.1% sodium tripolyphosphate and 5 mL of 0.1% sodium hydroxide were added into the starch slurry and stirred in a small scale batch type mixer for 30 min at 30ºC. The pH of the slurry obtained was adjusted to 6-7 using 0.3% hydrochloric acid. The slurry was washed two times with tap water and settled for one day. Then, water was decanted to separate out the starch. The starch was sun-dried for 90 min and pulverized using mortar and pestle to obtain a fine powder. The prepared sweet potato modified starch by cross-linked method is shown in Figure 3(b). Effect of volume of 0.1% sodium tripolyphosphate (1,3,5,7,9) ml, effect of concentration of 5 ml sodium tripolyphosphate (0.05,0.10,0.15,0.20 and 0.25) and effect of reaction temperature (30,40,50, 60,70) ºC on the yield of sweet potato modified starch were investigated the same procedure as mentioned above.

(a) Acid Treatment Method **(b)** Cross-linked Method

Figure 3: Modified Starch

Determination of the Characteristics of Starch and Modified Starch

The characteristic of starch and modified starch such as ash, gelatinization temperature, moisture, pH, solubility, swelling power, amylose and amylopectin content were determined.

Results and Discussion

Figure (4) shows the results of the effect of ratio of sweet potato to water on the yield percent of sweet potato starch. Although the ratio of sweet potato to water was increased to 1:7 (w/v) and 1:8 (w/v), the yield percent of

sweet potato starch does not apparently increased. So, 1:6 (w/v) ratio of sweet potato to water was chosen as the most suitable condition because of the least amount of used water. The effect of settling time on the yield percent of sweet potato starch was investigated in the range of 1, 2, 3, 4 and 5 hr, respectively. It is obvious that, no appreciable increased amount of starch was obtained beyond 4hr settling time. So, 4hr settling time was selected as the most favourable condition. The results are shown in Figure (5).

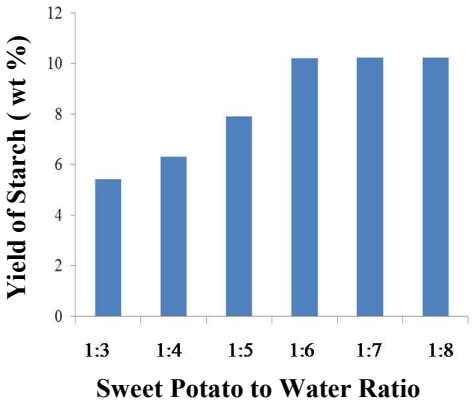

Figure 4: Effect of Sweet Potato to Water Ratio on the Yield of Sweet Potato Starch

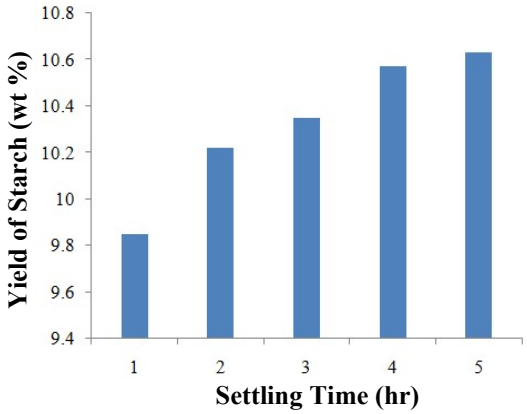

Figure 5: Effect of Settling Time on the Yield of Sweet Potato Starch

The results of Table (1) show the effect of volume of 20% hydrochloric acid on the yield of sweet potato modified starch by acid treatment. Higher volume of 20% hydrochloric acid beyond 0.5 ml gave a starch of rough texture and also the yield percent of sweet potato modified starch was decreased. When higher concentration of hydrochloric acid was used in the treatment of starch, most of the non-starchy materials were removed from the slurry. Therefore, 0.5 ml of 20% hydrochloric acid was chosen as the most suitable condition. The effect of concentration of 0.5 mL of hydrochloric acid on the yield percent of modified starch is shown in Table (2). The lower the acid concentration, the higher the yield percent of modified starch was obtained. Moreover, lower concentration of hydrochloric acid gave a smooth texture of modified starch and it was more economic. And also, it can reduce the side effect of the application of high concentration of hydrochloric acid. Therefore, 10% of 0.5 ml hydrochloric acid was selected as

the most suitable condition. Table (3) tabulates the results of the effect of reaction temperature on the yield of modified starch. 30°C reaction temperature gave the highest yield percent of modified starch (90.6%) than the others. Beyond this temperature, modified starch formed a gel due to the absorption of water.

Table 1: Effect of Volume of 20% HCl on the Yield of Modified Starch (Acid Treatment)

Weight of Starch - 5 g
Volume of 0.01(w/v)% NaOH - 1 mL
Reaction Temperature - 40°C
Reaction Time - 15 min

Sr. No.	Volume of 20% HCl (mL)	Yield (wt%)	Colour	Texture
1	0.25	84.2	odd white	smooth
2*	0.50	86.4	odd white	smooth
3	1.00	82.2	odd white	smooth
4	1.50	78.0	odd white	slightly rough
5	2.00	74.2	odd white	slightly rough
6	2.50	72.6	odd white	rough

* the most favourable condition

Table 2: Effect of Concentration of HCl on the Yield of Modified Starch (Acid Treatment)

Weight of Starch - 5g
Volume of HCl - 0.5 mL
Volume of 0.01(w/v)% NaOH - 1 mL
Reaction Temperature - 40°C
Reaction Time - 15 min

Sr. No.	Concentration of HCl (%)	Yield (wt%)	Colour	Texture
1	5	83.2	odd white	smooth
2*	10	87.6	odd white	smooth
3	20	86.4	odd white	slightly rough
4	30	84.0	odd white	slightly rough
5	40	80.2	odd white	rough
6	50	77.6	odd white	rough

* the most favourable condition

Table 3: Effect of Reaction Temperature on the Yield of Modified Starch (Acid Treatment)

Weight of Starch - 5 g
Volume of 10(v/v)% HCl - 0.5 ml
Volume of 0.01(w/v) % NaOH - 1 ml
Reaction Time - 15 min

Sr. No.	Reaction Temperature (°C)	Yield (wt%)	Colour	Texture
1*	30 (R.T)	90.6	white	smooth
2	40	87.6	white	smooth
3	50	78.8	white	smooth
4	60	77.9	white	smooth

* the most favourable condition

By varying the volume of 0.1 (w/v)% sodium tripolyphosphate such as 1, 3, 5, 7 and 9 mL, the effect of volume of 0.1 (w/v)% of sodium tripolyphosphate on the yield of sweet potato modified starch was studied. It was found that 5 mL of 0.1 (w/v)% sodium tripolyphosphate gave 92.4 (wt)% of sweet potato modified starch, which is the highest yield amongst them. The results are shown in Table (4).

Lowest concentration of sodium tripolyphosphate gave a white and smooth texture of modified starch. 0.05 (w/v) % and 0.1(w/v) % of sodium tripolyphosphate gave the 90.6% and 92.4% of sweet potato modified starch respectively. Between them, 0.1(w/v)% of sodium tripolyphosphate was selected as the most suitable condition due to its higher yield percent. The results are shown in Table (5).

The effect of reaction temperature on the yield percent of modified sweet potato starch was investigated in the range of (30, 40, 50, 60 and 70)°C, respectively. Among of them, 30°C of reaction temperature gave the highest yield percent of modified starch 93.8 wt% than the others. Beyond this temperature, modified starch absorbed water resulting in gel formation. The results are shown in Table (6).

Table 4: Effect of Volume of Sodium Tripolyphosphate on the Yield of Modified Starch (Cross-Link Method)

Weight of Starch - 5g
Volume of Water - 10 mL
Volume of 0.1(w/v %) NaOH - 5 mL
Volume of 0.3(v/v%) HCl - 3 mL
Reaction Temperature - 40ºC
Reaction Time - 60 min
Concentration of Sodium Tripolyphosphate - 0.1 % (w/v)

Sr. No.	Volume of Sodium Tripolyphosphate (mL)	Yield (wt%)	Colour	Texture
1	1	85.0	white	smooth
2	3	91.0	white	smooth
3*	5	92.4	white	smooth
4	7	92.8	odd white	slightly rough
5	9	92.2	odd white	slightly rough

* the most favourable condition

Table 5: Effect of Concentration of Sodium Tripolyphosphate on the Yield of Modified Starch (Cross-Link Method)

Weight of Starch - 5g
Volume of Water - 10 mL
Volume of 0.1(w/v%) NaOH - 5 mL
Volume of 0.3(v/v%) HCl - 3 mL
Volume of Sodium Tripolyphosphate - 5 mL
Reaction Temperature - 40ºC
Reaction Time - 60 min

Sr. No.	**Concentration of Sodium Tripolyphosphate (w/v%)**	**Yield (wt%)**	**Colour**	**Texture**
1	0.05	90.6	white	smooth
2*	0.10	92.4	white	smooth
3	0.15	90.8	odd white	slightly rough
4	0.20	90.2	odd white	slightly rough
5	0.25	89.4	odd white	slightly rough

* the most favourable condition

Table 6: Effect of Reaction Temperature on the Yield of Modified Starch (Cross-Link Method)

Weight of Starch - 5g
Volume of Water - 10 ml
Volume of 0.1(w/v%) $Na_5P_3O_{10}$ - 5 ml
Volume of 0.1(w/v%) NaOH - 5 ml
Volume of 0.3 (v/v)% HCl - 3 ml
Reaction Time - 60 min

Sr. No.	Reaction Temperature (°C)	Yield (wt%)	Colour	Texture
1*	30°C (R.T)	93.8	white	smooth
2	40°C	92.4	white	smooth
3	50°C	86.2	odd white	gel type
4	60°C	82.4	odd white	gel type
5	70°C	80.4	odd white	gel type

* the most favourable condition

Table (7) tabulates the result of characteristics of starch and modified starch such as ash, gelatinization temperature, moisture, pH, solubility, swelling power, amylose and amylopectin contents. The ash contents of starch and modified starches are similar to that of literature value. Gelatinization temperatures for starch and modified starches were found to be well comparable with the literature value. The moisture (wt%) for starch, acid treated starch and cross-linked starches were 7.08%, 6.28% and 7.16 % respectively. pH for starch, acid treated starch and cross-linked starch were found to be 6.88, 6.82 and 6.91 respectively.

Solubility and swelling power of starch, acid treated modified starch and cross- link modified starch were 24.37%, 28.12%, 32.71% and 25.45%, 33.51%, 35.87% respectively. Amylose and amylopectin contents of starch, acid treated modified starch and cross- link modified starch were 18.93%, 25.12%, 28.78% and 81.07%, 74.88%, 71.22% and respectively.

Table 7: Characteristics of Starch and Modified Starch

Characteristics	Starch		AMS		CMS	
	Experimental Value	*Literature Value	Experimental Value	*Literature Value	Experimental Value	*Literature Value
Ash (wt %)	0.13	1.64 ± 0.01	0.15	1.98 ±0.02	0.15	1.20 ± 0.05
Gel.Temp (°C)	60	62	71	70-80	75	70-80
Moisture (wt %)	7.08	8.72 ± 0.03	6.27	9.02 ± 0.07	7.16	9.08 ± 0.09
pH	6.88	6.50	6.82	6.65	6.91	6.71
Solubility(w/w%)	24.37	-	28.12	-	32.71	-
Swelling Power(w/w%)	25.45	-	33.51	-	35.87	-
Amylose Content (wt%)	18.93	-	25.12	-	28.78	-
Amylopectin Content (wt%)	81.07	-	74.88	-	71.22	-

AMS - Acid Treated Modified Starch

CMS - Cross-Link Modified Starch

* Pakistan Journal of Nutrition, 2009

The results of FT-IR spectrum of sweet potato modified starches prepared by (acid treated and cross-link methods) and commercial modified starch are demonstrated in Figures (6).The mid-infrared spectrum (4000 – 400 cm^{-1}) is approximately divided into four regions. The nature of a group frequency was determined by the region in which it is located. The regions are generalized as follows: the X – H stretching region (4000 – 2500 cm^{-1}), the triple bond region (2500 – 2000 cm^{-1}) and the fingerprint region (1500 – 600 cm^{-1}). The spectral characteristics of the prepared modified starch and commercial modified starch were found to be similar. The infrared spectra of sweet potato starch samples that originate mainly from the vibrational modes of amylose and amylopectin reflected the changes in molecular structure.

The O-H stretching region (3000-3600 cm^{-1}),C-H stretching region (2800-3000 cm^{-1}), the skeletal mode vibration of the glycosidic linkage (900-950 cm^{-1}) in infrared spectra are clearly seen for all the sweet potato modified starch. In the finger print region, there were several discernible absorbencies at 1157.73, 1080.17, 1014.59, 1157.33, 1080.17, 1018.45 and 1016.52, which were attributed to C – O bond stretching. Another characteristics peak occurred at 1641.48 cm^{-1}, which presumably originated from tightly bound

water present in the starch granules. The extremely broad band appearing most intense at 3000-3700 cm^{-1} could be attributed to the vibration of hydroxyl (O-H) groups. The band at 2931.90 and 2936.90 cm^{-1} were characteristic of C-H stretching associated with ring methane hydrogen atoms.

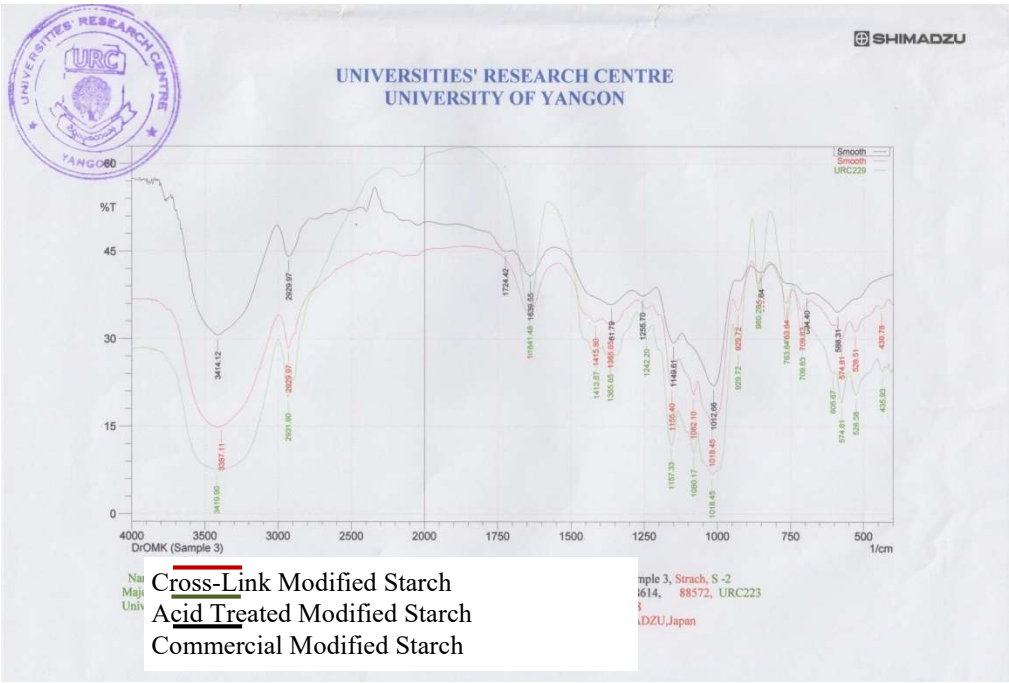

Figure 6: Comparison of FT-IR Spectrum for Acid Treated Modified Starch, Cross-Link Modified Starch and Commercial Modified Starch

Table 8: Effect of the Weight of Modified Starch on the Organoleptic Properties of Mayonnaise

Weight of Egg - 53.0 g
Weight of Sugar - 10 g
Weight of Vinegar - 20 g
Weight of Soybean Oil - 55 g
Weight of Guar Gum - 0.4 g
Room Temperature - 25-30 ºC
Weight of Common Salt - 2.0 g

Sr. No.	Weight of Modified Starch(g)	pH	Organoleptic Properties		
			Taste	Color	Texture
1	-	5.4	bad taste	pale yellow	very soft and stable emulsion
2	1.0	5.4	bad taste	pale yellow	very soft and stable emulsion
3	2.0	5.3	slightly sour taste	pale yellow	very soft and stable emulsion
4	3.0	5.3	slightly sour taste	pale yellow	very soft and stable emulsion
5	4.0	5.3	slightly sour taste	pale yellow	slightly soft and stable emulsion
6	*5.0	5.3	good taste	pale yellow	soft and stable emulsion
7	6.0	5.3	good taste	pale yellow	thick and slightly sticky
8	7.0	5.3	good taste	pale yellow	very thick and sticky

*the most favourable condition

Table 9: Formulae for the Preparation of Butter Biscuit

Formulae	Ingredient (wt %)			Organoleptic Properties			
	Starch	M.S	F	Colour	Texture	Taste	Odour
I	-	-	30	pale yellow	very rough	good taste	pleasant smell
II	30	-	-	pale yellow	bland	good taste	pleasant smell
III	-	30	-	pale yellow	very soft	good taste	pleasant smell
IV	10	-	20	pale yellow	very rough	good taste	pleasant smell
*V	-	20	10	pale yellow	smooth	good taste	pleasant smell
VI	-	15	15	pale yellow	slightly rough	good taste	pleasant smell
VII	-	10	20	pale yellow	very rough	good taste	pleasant smell

M.S - Modified Starch
F - Wheat Flour
*the most favorable condition

Mayonnaise

Biscuit

Conclusion

Starch was firstly produced from sweet potato and then it was modified using both acid treatment method and cross-link methods. According to the results of the characteristics and yield % of modified starch using two different modified starch. When equal amount of modified and flour were used in formulation of biscuit, it gave a slightly rough texture biscuit. The ratio of modified starch to flour 2:1 gave a smooth texture biscuit. In conclusion, if 20% of modified starch was used in the preparation of biscuit, the texture of biscuit was smooth and good. The prepared mayonnaise using

only the modified starch instead of the mixture of guar gum and modified starch gave a good texture, smooth and stable emulsion. It can be controlled by the syneresis and increase the viscosity, mouthfeel and stability of mayonnaise.

Acknowledgement

We would like to express our sincere gratitude to Dr Aye Aye Tun, Pro-rector, Dagon University for her permission and the financial support in this research work. We are grateful to Dr Yin Shwe, Professor and Head (Retd), Department of Industrial Chemistry, Dagon University for her kind encouragement and numerous invaluable suggestions.

References

Abbas K.A., et al., (2010). Modified Starches and Their Usages in Selected Food Products: A Review Study, Journal of Agricultural Science, Vol. 2, No. 2.

Bo Bo., Sandi.(2016,).Preparation of Modified Starch from Sweet Potato and its Application in Food Processing

Hoover, R. and Sosulski, F.W. (1985).Studies on the Functional Characteristics and Digestibility of Starches from Phaselous Vulgaris Biotypes.

Kavlani N, et al., (2012).Various Techniques for the Modification of Starch and the Applications of its Derivatives, International Research Journal of Pharmacy.

Ko., Phyu Hnin. (2017)Utilization of Sweet Potato Modified Starch for Some Food Products

Moorthy, S. N. (2002). Physico-chemical and Functional Properties of Tropical Tuber Starches.

Mohan, J., (2000), Organic Spectroscopy Principle and Applications, Narosa Publishing New Delhi.

STUDY ON THE YIELD OF ALCOHOL IN THE PRODUCTION OF WINE FROM DIFFERENT INDIGENOUS FRUITS

Ko Win[1], Aye Aye Aung[2] , Swe Swe Aung[3]

Abstract

The vast majority of all wine found almost anywhere is fermented grape juice, but wine can technically be made from other fruits. In this research work, grape, pineapple, strawberry, and plum were selected for winemaking. They were purchased from Thirimingalar market. Fermentation was carried out at room temperature by using yeast (*Saccharomyces Cerevisiae*). Yield of alcohol was studied by varying the process condition such as sugar content, dosage of yeast and amount of water. Alcohol content, pH, acidity, sugar content, specific gravity and color of prepared wines were determined. The data obtained from the study suggested that the addition of 250g of sugar, 1.5g of yeast, and 900mL of water to 500g of grape is most suitable to obtain the highest yield of alcohol in the production of wine.

Keywords : Wine, fermentation, indigenous fruits, alcohol content

Introduction

Wine is any fermented fruit juice. People typically associate wine solely with grapes and it's true that the vast majority of all wine found almost anywhere is fermented grape juice, but wine can technically be made from other fruits.

Grape wine is the alcoholic product of the fermentation of grape juice, and the essential feature of this fermentation is the conversion of the grape sugars, glucose and fructose, to ethyl alcohol (ethanol), carbon dioxide (released as a gas), and flavor components. This complex process is accomplished by living yeast cells and is illustrated in the following chemical equation :

$$C_6H_{12}O_6 \xrightarrow{\text{yeast}} 2CH_3CH_2OH + 2CO_2$$

[1.] Dr., Professor, Department of Industrial Chemistry, Dagon University
[2.] Dr., Assistant Lecturer, Department of Industrial Chemistry, Dagon University
[3.] Assistant Lecturer, Department of Industrial Chemistry, Dagon University

The alcohol produced through fermentation is a wine's major flavor component. It also affects the solubility of many wine constituents. Some is used in forming other flavor compounds. It also enhances wine's resistance to spoilage. Moreover, wines traditionally are classified according to their alcoholic content. Indeed the amount of alcohol formed from a given amount of grape sugar is of considerable practical importance to the wine (http://scopius.spaceports.com/goodwine/pineapple.htm).

People's interest in wine is largely focused on its taste, but it probably wouldn't taste very good if it were simply a matter of leaving jugs of grape juice in the basement for a couple of months. There are a lot different factors which go into creating each wine's unique taste. Wine tasting is the sensory examination and evaluation of wine. Wines contain many chemical compounds similar or identical to those in fruits, vegetables, and spices.

The sweetness of wine is determined by the amount of residual sugar in the wine after fermentation, relative to the acidity present in the wine. Dry wine, for example, has only a small amount of residual sugar (Anderson, 1973).

Materials and Methods

The fruits were washed with water. The flesh was cut away from the core and 500g of the flesh was chopped into small pieces. All the juice liberated during chopping was collected. Chopped fleshes were put into a nylon straining bag and tied closed. It was then transferred into the primary fermenter and crushed by hand. Sugar was added to the boiling water and it was stirred until sugar was completely dissolved. The sugar solution was poured into the primary fermenter just to cover the fruits and allowed to cool to room temperature. When it reached room temperature, all the ingredients except yeast were added, stirred into bag and tied again. After 24 hr, yeast was added and stirred again. Fermenter was covered and allowed to ferment the must for 7 days, stirring twice daily. Then the nylon bag was taken from the primary fermenter and it was allowed to drip without squeezing. Pulps were discarded and the fermentation was continued for three weeks. Then the clear liquid was withdrawn and investigated for its quality. Alcohol content, pH, acidity, specific gravity, color and sugar content of wines were determined.

Results and Discussion

In this research work, the yield of alcohol in the preparation of pineapple wine, strawberry wine, plum wine and grape wine were studied by varying the amount of sugar, dosage of yeast and amount of water while the amount of fruit, the dosage of sodium bisulfite, ammonium sulfate, pectic enzyme, tartaric acid and fermentation period were kept constant.

The effects of sugar content, dosage of yeast, and water content on the yield of alcohol in the preparation of pineapple wine are shown in Tables (1), (2) and (3), respectively. According to the results it was clearly seen that highest yield percent of alcohol was obtained by using 300g of sugar, 1.5g of yeast, 900mL of water, 0.4g of sodium bisulfite, 0.2g of pectic enzyme, 0.2g of tartaric acid and 1.5g of ammonium sulfate for 500g of pineapple. In the preparation of pineapple wine, it was found that when the amount of sugar was increased over 300g, the yield of alcohol decreased because excess sugar inhibits the growth of yeast and may affect the yield of alcohol (Potter, 1973). If the amount of sugar is less than 300g, the yield of alcohol decreases because the amount of sugar is insufficient for fermentation with respective dosage of yeast. According to Table (2), when the dosage of yeast was higher than 1.5g, the yield of alcohol decreased. This was probably due to the inactivity of yeast inoculated in winemaking. Excess amount of yeast might affect the flavor of wine (Frazer,1981). When the dosage of yeast was lower than 1.5g, no alcohol was observed because of the insufficient dosage of yeast. From the result of the Table 3, if more than 900ml of water were used, the yield of alcohol decreased. But it less than 900mL of water were used, the yield of alcohol also decreased. From this study, it is clearly seen that the yield of alcohol also depends upon the amount of water used.

The effects of sugar content, dosage of yeast, and water content on the yield of alcohol in the preparation of strawberry wine are shown in Tables (4), (5) and (6), respectively. The results shown in these Tables demonstrated that the highest yield percent of alcohol could be obtained by using 350g of sugar, 1g of yeast, 900mL of water, 0.4g of sodium bisulfite, 0.2g of pectic enzyme, 0.2g of tartaric acid and 1.5g of ammonium sulfate for 500g of strawberry. Moreover, the effect of sugar content, the effect of dosage of yeast and the

effect of water content on the yield of alcohol in the preparation of strawberry wine were quite similar to that of pineapple wine.

The effects of sugar content, dosage of yeast, and water content on the yield of alcohol in the preparation of plum wine are illustrated in Tables (7), (8) and (9), respectively. These data suggested that the highest yield percent of alcohol could be obtained by using 300g of sugar, 4g of yeast, 500mL of water, 0.4g of sodium bisulfite, 0.2g of pectic enzyme and 1.5g of ammonium sulfate for 500g of strawberry. The effect of sugar content, the effect of dosage of yeast and the effect of water content on the yield of alcohol were quite close to that of pineapple wine.

The effects of sugar content, dosage of yeast, and water content on the yield of alcohol in the preparation of grape wine are shown in Tables (10), (11) and (12), respectively. The results indicated that the highest yield percent of alcohol was obtained by using 250g of sugar, 1.5g of yeast, 900mL of water, 0.4g of sodium bisulfite, 0.2g of pectic enzyme, 0.2g of tartaric acid and 1.5g of ammonium sulfate for 500g of grape. The effect of sugar content, the effect of dosage of yeast and the effect of water content on the yield of alcohol were also similar to that of pineapple wine.

Optimum conditions for the highest yield of alcohol in the production of wine from different indigenous fruits are summarized in Table (13).

The quality of wines was assessed by some parameters like pH, alcohol content, acidity, and specific gravity. In conclusion , although the quality of prepared pineapple wine, strawberry wine, grape wine, and plum wine are quite different, it was observed that the experimental results are compatible with the literature values and the products can be used as beverage.

Grapes were planted in Myanmar on an experimental scale in 1959 at Kyaukpadaung Township, and Myingyan District, in the dry zone of Central Myanmar. As it was shown that cultivation of this crop was feasible in this climatic zone, planting of grape was extended to Kyaukpadaung, Meikhtila, Nyaung Oo, Yamethin, Pyawbwe and Pakokku Townships. These townships are very dry areas of Central Myanmar. The climatic conditions of grape growing areas of Myanmar are probably different from that of other grape

growing countries. Therefore, cultivation practices for grapes in Myanmar may not be the same as in other countries.

Myanmar is a tropical country, which can be a disadvantage for wine grapes: Monsoons can damage vines, summer days in the region are shorter than in Europe (eight hours compared to 10 to 12), and there is plenty of heat and humidity. In Myanmar, grapes are grown mainly for the fresh fruit market. Grapes are grown not only in state farms but also in private farms. There is not enough wine production for local consumption and export in Myanmar. Fruit wines have traditionally been popular with home winemakers. Fruit wine making is no more difficult than making wines from fresh grapes. The basic process is the same, and consideration is given to the same aspects as when preparing grape juice for home winemaking (http:// www.eckraus.com/fruit-wine-making).

Grape, pineapple, strawberry, and plum are commonly grown fruits in Myanmar. Grape from Meiktila, pineapple from Bago, strawberry from Pyin Oo Lwin, and plum from Pakokku Townships were selected for winemaking in this study. Influence of pH, acidity, sugar content, water content, dosage of yeast, duration of fermentation on yield of alcohol were investigated and this study is intended as a guide to optimize these factors by wine composition and quality. These factors must be studied in more detail in order to develop vinification technologies which would ensure production of wine with the best sensory characteristics from locally grown fruits.

Table 1: Effect of Sugar Content on the Yield of Alcohol in the Preparation of Pineapple Wine

Weight of Pineapple = 500g Volume of Water = 900 mL
Weight of Yeast = 1.5g Fermentation Period = 28 days

Sr. No.	Wt. of Sugar (g)	pH	Acidity (w/v%)	Specific Gravity	Yield of Alcohol (v/v %)
1.	200	3.3	0.78	1.00	4
2.	250	3.0	0.70	1.00	7
3.	300*	3.0	0.70	1.00	8
4.	350	3.4	0.86	1.02	0
5.	400	3.2	0.76	1.06	0

* Optimum condition

Table 2: Effect of Dosage of Yeast on the Yield of Alcohol in the Preparation of Pineapple Wine

Weight of Pineapple = 500g Volume of Water = 900 mL
Weight of Sugar = 300g Fermentation Period = 28 days

Sr. No.	Wt. of Yeast (g)	pH	Acidity (w/v %)	Specific Gravity	Yield of Alcohol (v/v %)
1.	1	3.3	1.37	1.00	0
2.	1.5*	3.0	0.70	1.00	7
3.	3	3.0	0.63	1.00	5
4.	4	3.4	0.87	1.00	4
5.	5	3.2	0.91	1.00	4

* Optimum condition

Table 3: Effect of Water Content on Yield of Alcohol in the Preparation of Pineapple Wine

Weight of Pineapple = 500g Weight of Yeast = 1.5 g
Weight of Sugar = 300g Fermentation Period = 28 days

Sr.No.	Volume of Water (mL)	pH	Acidity (w/v%)	Specific Gravity	Yield of Alcohol (v/v %)
1.	200	3.2	1.30	1.09	0
2.	500	3.1	0.93	1.05	2
3.	700	3.3	0.93	1.01	6
4.	900*	3.0	0.70	1.00	7
5.	1100	3.2	0.71	1.00	5

* Optimum condition

Table 4: Effect of Sugar Content on the Yield of Alcohol in Preparation of Strawberry Wine

Weight of Strawberry = 500g Volume of Water = 900 mL
Weight of Yeast = 1g Fermentation Period = 28 days

Sr. No.	Wt.of Sugar (g)	pH	Acidity (w/v%)	Specific Gravity	Yield of Alcohol (v/v %)
1.	200	3.1	0.57	1.00	0
2.	250	3.6	0.69	1.00	5
3.	300	3.8	0.67	1.00	5
4.	350*	3.3	0.69	1.00	8
5.	400	3.3	0.72	1.00	1

* Optimum condition

Table 5: Effect of Dosage of Yeast on the Yield of Alcohol in the Preparation of Strawberry Wine

Weight of Strawberry = 500g Volume of Water = 900 mL
Weight of Sugar = 350g Fermentation Period = 28 days

Sr. No.	Wt.of Yeast (g)	pH	Acidity (w/v%)	Specific Gravity	Yield of Alcohol (v/v %)
1.	1*	3.4	0.6	1.00	6
2.	1.5	3.6	0.69	1.00	5
3.	3	3.5	0.67	1.00	4
4.	4	3.6	0.65	1.00	4
5.	5	3.6	0.67	1.00	4

*Optimum condition

Table 6: Effect of Water Content on Yield of Alcohol in the Preparation of Strawberry Wine

Weight of Strawberry = 500 g Weight of Yeast = 1 g
Weight of Sugar = 350 g Fermentation Period = 28 days

Sr. No.	Volume of Water (mL)	pH	Acidity (w/v%)	Specific Gravity	Yield of Alcohol (v/v %)
1.	200	4.7	1.05	1.00	0
2.	500	3.4	2.52	1.06	0
3.	700	3.7	1.54	1.00	1
4.	900*	3.6	0.69	1.00	5
5.	1100	3.9	0.71	1.00	3

* Optimum condition

Table 7: Effect of Sugar Content on the Yield of Alcohol in the Preparation of Plum Wine

Weight of Plum = 500g Volume of Water = 500 mL
Weight of Yeast = 4g Fermentation Period = 28 days

Sr. No.	Wt. of Sugar (g)	pH	Acidity (w/v%)	Specific Gravity	Yield of Alcohol (v/v %)
1.	200	3.5	0.95	1.03	0
2.	250	3.3	1.43	1.00	3
3.	300*	3.3	1.70	1.00	4
4.	350	3.6	1.38	1.00	1
5.	400	3.5	1.29	1.02	0

* Optimum condition

Table 8: Effect of Dosage of Yeast on the Yield of Alcohol in the Preparation of Plum Wine

Weight of Plum = 500g Volume of Water = 500 mL
Weight of Sugar = 300g Fermentation Period = 28 days

Sr. No.	Wt. of Yeast (g)	pH	Acidity (w/v%)	Specific Gravity	Yield of Alcohol (v/v %)
1.	1	3.2	1.84	1.03	0
2.	1.5	3.3	1.43	1.00	3
3.	3	3.4	1.20	1.00	4
4.	4*	3.5	0.99	1.00	5
5.	5	3.5	0.92	1.00	4

* Optimum condition

Table 9: Effect of Water Content on the Yield of Alcohol in the Preparation of Plum Wine

Weight of Plum = 500g Weight of Yeast = 4 g
Weight of Sugar = 300g Fermentation Period = 28 days

Sr. No.	Volume of Water (mL)	pH	Acidity (w/v%)	Specific Gravity	Yield of Alcohol (v/v %)
1.	200	3.4	1.54	1.07	0
2.	500*	3.5	1.28	1.00	3
3.	700	3.3	1.43	1.00	3
4.	900	3.5	1.41	1.03	1
5.	1100	3.7	1.38	1.00	0

* Optimum condition

Table 10: Effect of Sugar Content on the Yield of Alcohol in the Preparation of Grape Wine

Weight of Grape = 500g Volume of Water = 900 mL
Weight of Yeast = 1.5g Fermentation Period = 28 days

Sr. No.	Wt. of Sugar (g)	pH	Acidity (w/v %)	Specific Gravity	Yield of Alcohol (v/v %)
1.	200	3.2	0.54	1.00	4
2.	250*	3.0	0.58	1.00	4
3.	300	4.3	0.68	1.01	3
4.	350	3.4	0.64	1.00	1
5.	400	3.2	1.43	1.03	0

* Optimum condition

Table 11: Effect of Dosage of Yeast on the Yield of Alcohol in the Preparation of Grape Wine

Weight of Plum = 500g Volume of Water = 900 mL
Weight of Sugar = 250g Fermentation Period = 28 days

Sr. No.	Wt. of Yeast (g)	pH	Acidity (w/v%)	Specific Gravity	Yield of Alcohol (v/v %)
1.	1	3.2	0.56	1.00	1
2.	1.5*	3.0	0.58	1.00	7
3.	3	3.0	0.68	1.00	3
4.	4	3.4	0.60	1.00	3
5.	5	3.4	0.64	1.00	2

* Optimum condition

Table 12: Effect of Water Content on the Yield of Alcohol in the Preparation of Grape Wine

Weight of Plum = 500g Weight of Yeast = 1.5 g
Weight of Sugar = 250g Fermentation Period = 28 days

Sr. No.	Volume of Water (mL)	pH	Acidity (w/v%)	Specific Gravity	Yield of Alcohol (v/v %)
1.	200	3.3	0.93	1.10	0
2.	500	3.8	1.13	1.02	3
3.	700	3.3	0.71	1.01	4
4.	900*	3.0	0.58	1.00	7
5.	1100	3.3	0.65	1.00	5

* Optimum condition

Table 13: Production and Analysis of Wine from Locally Grown Fruits
Weight of fruit = 500g

Sr. No.	Fruit	Optimum Dosage of Sugar(g)	Optimum Dosage of Yeast (g)	Optimum Volume of Water (mL)	Color of Wine	Sugar Content (% Brix) of Wine
1	Pineapple	300	1.5	900	White 0.3, Yellow 1.2	5
2	Strawberry	350	1	900	Red 0.9, Yellow 1.8	5
3	Plum	300	4	500	Red 2, Blue 3.1, yellow 0.5	6
4	Grape	250	1.5	900	Red 5, Yellow 0.2	6

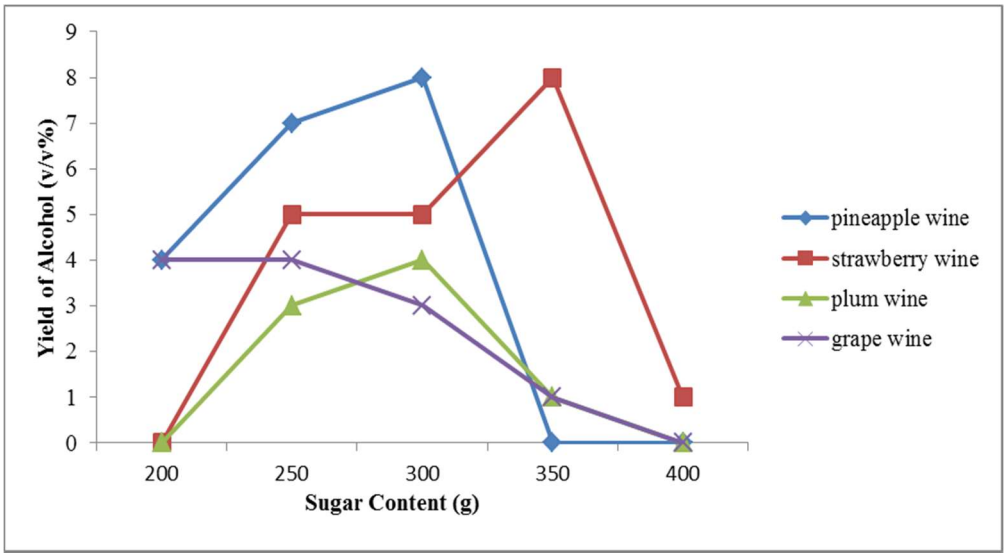

Figure 1: Effect of sugar content on the yield of alcohol in the preparation of pineapple, strawberry, plum and grape wines

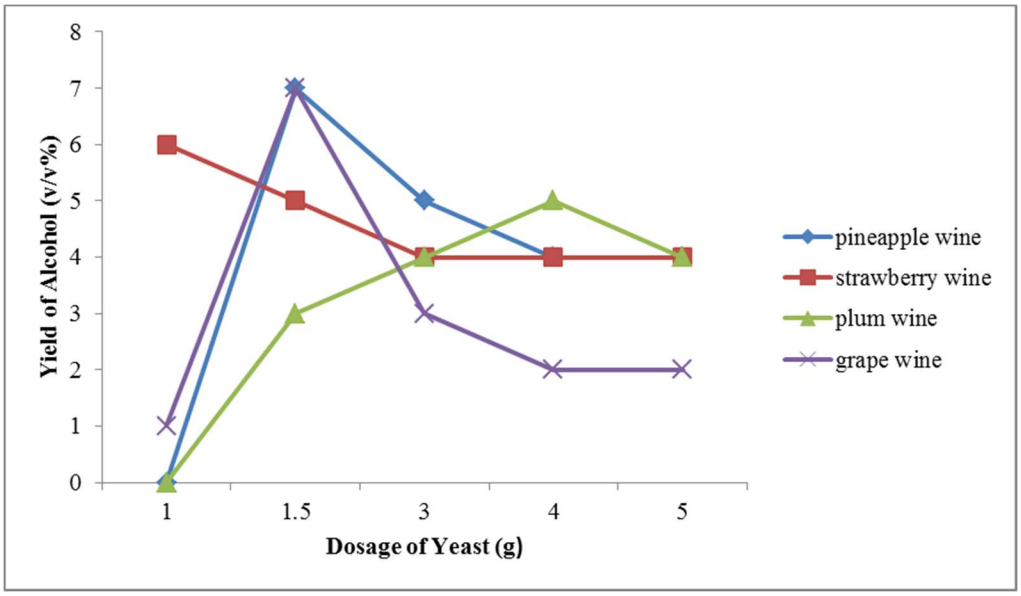

Figure 2: Effect of dosage of yeast on the yield of alcohol in the preparation of pineapple, strawberry, plum and grape wines

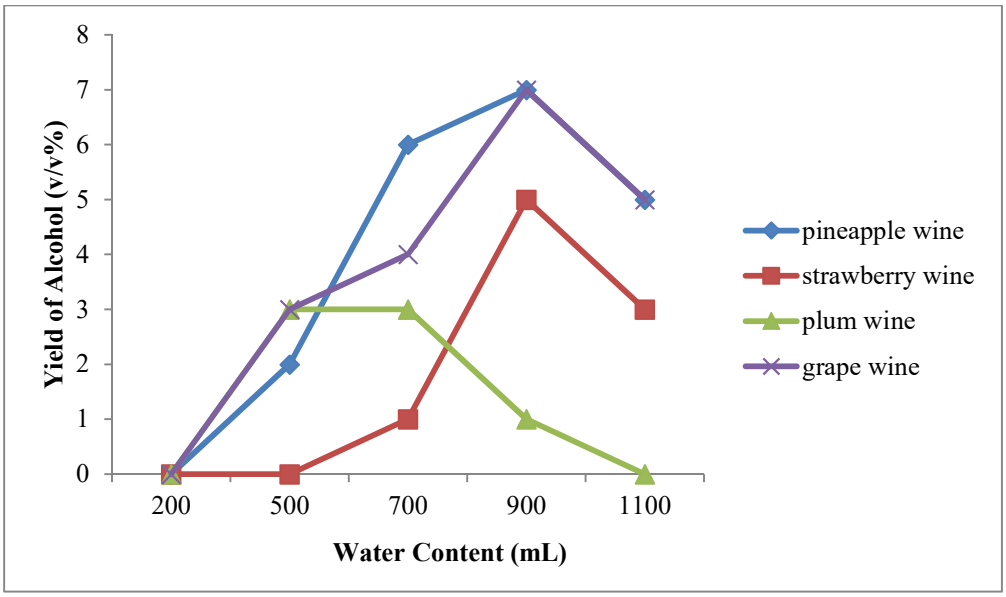

Figure 3: Effect of water content on the yield of alcohol in the preparation of pineapple, strawberry, plum and grape wines

Conclusion

The data obtained from this study suggested that the addition of 250g of sugar, 900mL of water, and 1.5g of yeast to 500g of grape is most suitable to obtain the highest yield percent in production of wine. Pineapple, strawberry, and plum grow extremely well in Myanmar. The quality wines can be produced from these fruits other than grape. The results of this study are significant for improvement of fruit wine production. The factors which determine the quality of fruit wine should also be studied in order to produce the wine with the best sensory characteristics from various indigenous fruits.

Acknowledgements

Appreciation is expressed to the Department of Higher Education, Ministry of Education for giving the opportunity to launch this research programme. Profound thanks are extended to Dr. Yin Shwe (Retired), Professor and Head of Department of Industrial Chemistry, Dagon University, for her encouragement and suggestions to accomplish this study.

References

Anderson, F. and Raymon, H., ‘‘The Art of Making Wine’’, Hawthorn Books Inc., United States of America. (1970)

Frazier, W.C.& Westhoff, D.C. Food Microbiology,3rd edition, McGraw-Hill, Publishing Company Ltd.(1981)

Potter, N.N., ‘‘Food Science’’, 4th edition, Department of Food Science, Cornell University, Ithaca, New York.(1973)

Tayler , W.H.T., ‘‘ The Penguin Book of Home Brewing and Wine Making’’, Penguin Books Ltd, Harmondswirth, Middlesex, England.(1973)

http://4Globalspec.com/thread/41293/How to make pineapple wine

http:// en Wikipedia.org/wiki/Grape

http://scopius.spaceports.com/goodwine/pineapple.htm

http:// www.eckraus.com/fruit-wine-making

SMALL SCALE PRODUCTION OF ZINC SULPHATE AND ITS APPLICATION

Ohnmar Kyi[1],Yin Shwe[2], Khin Thet Ni[3]

Abstract

Zinc sulphate is a water soluble inorganic compound. It can be prepared by treating virtually any zinc containing material (metal, minerals, oxides) with sulfuric acid followed by evaporation and crystallization. Zinc and its alloys have been used as a protective and decorative coatings over a variety of metal substrates. In this research, commercial grade zinc oxide was used as raw material for the preparation of zinc sulphate. Moreover, a make-shift stainless steel reactor was constructed for the production of zinc sulphate. Prepared zinc sulphate was used in zinc electroplating process. The purity of zinc oxide was found to be 98.58(% w/w) by volumetric analysis method and 99.953 (%w/w) by EDXRF method. The maximum yield of zinc sulphate 79.50 (%w/w) was obtained by treating 10 g of zinc oxide with 75 mL of 3 M sulphuric acid. Prepared Zinc sulphate was identified by X-ray Diffraction (XRD) and the purity and composition was determined using Energy Dispersive X-ray Flourescence (EDXRF). 2 kg of zinc sulphate per batch was produced from 488 g of zinc oxide by using a make-shift stainless steel stirred tank reactor. Iron sheet was electroplated in the zinc sulphate solution using different parameters by varying the voltage, current and electroplating time. The acceptable bright colour and suitable thickness was obtained at 6V, 5A, 15 min electroplating time. The corrosion rate of selected zinc coated layer in artificially simulated environments (tap water, 3.5 % NaCl solution and dilute acid solution) and standard salt spray test (ASTM B 117) was also studied. The selected zinc coated layer give 72 hr protection for salt spray test. The surface morphology of the zinc coating before and after corrosion were studied by Scanning Electron Microscopy (SEM).

Keywords**:** zinc sulphate , electroplating

Introduction

Zinc and its alloys have been used as a protective and decorative coatings over a variety of metal substrates for more than 100 years ago. It gives excellent corrosion resistance, particularly in industrial and urban environments. Zinc coating can be obtained by different techniques such as

1. Dr., Assistant Lecturer, Industrial Chemistry Department, Dagon University
2. Dr., Professor (Retired), Department of Industrial Chemistry, Dagon University
3. Dr, Professor (Retired), Department of Industrial Chemistry, University of Yangon

batch hot-dip galvanizing, continuous sheet galvanizing, zinc painting, zinc spray metalizing, mechanical plating, electrogalvanizing and zinc electroplating. Of these, zinc electroplating is the most prevalent for functional and decorative applications. Its relatively low cost makes the zinc plating process the top choice for affordable corrosion protection.(T.J Tuaweri et. al,2013) Typical zinc electroplating applications include coating nuts, bolts, washers and various automotive parts. Other common uses include the production of electrical transmission components and plating fasteners. (H.B. Muralidhara,2011) Three main types of zinc plating are being done today; cyanide zinc solution, chloride zinc solution and zinc sulphate solution. With the never-ending environmental pressures that are being placed on industry, there is a worldwide push to move away from cyanide zinc into chloride and sulphate plating. The toxicity and stringent regulation against water pollution and hence costly effluent disposal of cyanide based baths has led to the increased interest and accelerated growth of acid zinc based baths in the past few years. Many of the acid types bath utilize zinc sulphate and are used to electroplate cast iron and malleable irons.

Zinc electroplating is amenable to both rack plating or barrel plating processes. The former is preferable for providing suitable thickness distribution on larger or more complex parts. Barrel plating is recommended for coating smaller objects such as nuts and bolts.(Bamidele. MDurodala)

In this research, zinc sulphate was prepared from zinc oxide with sulphuric acid. Prepared zinc sulphate solution was used as a source of zinc in zinc electroplating bath to replace cyanide electroplating process which causes environmental impact. Electroplating of iron sheet was carried out by using prepared zinc sulphate solution as electrolyte under different conditions. The assessment of the quality of zinc coated sheets by different solutions were also studied. The main objective of this study was to produce zinc sulphate and to study the effective utilization of zinc sulphate in electroplating process in place of cyanide electroplating process.

Materials and Methods

Raw Materials

Zinc oxide (commercial grade), Iron Sheet (H 490143) were obtained from Khin Maung Nyunt Trading Co.,Ltd. South Dagon Township, Yangon Region. Analar grade chemicals (India) such as aluminium sulphate, boric acid, sulphuric acid, hydrochloric acid, chromic acid and sodium hydroxide were purchased from Golden Lady Chemical Sale Centre, Pabedan Township, Yangon Region. Distilled water and deionized water were obtained from Department of Industrial Chemistry, Dagon University.

Methods

Preparation of Zinc Sulphate from Zinc Oxide

Effect of Volume of 2M H_2SO_4 on Yield Percent of Zinc Sulphate

65 mL of 2 M sulpuric acid was placed in a 250 mL beaker. 10 g of zinc oxide powder was added and stirred with a magnetic stirrer at 100 rpm for 10 min to dissolve all of the zinc oxide powder. When the zinc oxide powder was completely dissolved, the solution was heated at 70ºC in a water bath for 30 min. After the precipitation of zinc sulphate, the solution was filtered. After that saturated zinc sulphate solution was cooled down to room temperature and left for 2 days. Zinc sulphate was filtered and washed with 30 mL of ethanol and dried in a desiccator. Yield percent of zinc sulphate was calculated as follows:

$$\text{Yield of zinc sulphate}, \% = \frac{\text{experimental weight of the product}}{\text{theoretical weight of the product}} \text{x } 100$$

Other experiments were conducted by the above procedure but by varying the volumes of sulphuric acid (70 mL, 75 mL and 80 mL) were used. The results are shown in Table (1).

Effect of Strength of H_2SO_4 on Yield Percent of Zinc Sulphate

The same procedure as described in the above experiment was carried out using 75mL of sulphuric acid at the various concentrations of 3M and 4M. The results are shown in Table (2).

Construction of Reactor Design for Production of Zinc Sulphate

A make-shift stirred tank reactor was constructed based on the amount of zinc sulphate crystals to be prepared. The inner tank (304 grade stainless steel) was surrounded by outer layer (202 grade stainless steel) with the water jacket between them. The impeller was inserted at the centre of the inner tank which was connected to the 15W DC electric motor for agitation. Electric heater (1000 W) was used to heat water and zinc sulphate solution. Digital thermometer was used to measure the temperature of zinc sulphate solution thoroughout the experiment until the completion of reaction.

The volume of the reactor was (346.185 in^3) and size of agitator (1.77 in D, 7.5 in length) was made of 304 grade stainless steel. It was fabricated at Shwe Family Equipment and Metal Moulding, Company. No (198C), Sintae St., Industrial Zone(3),South Dagon Township, Yangon. Maximum yield of zinc sulphate 2 Kg per batch was obtained by using 488 g of zinc oxide.

Electroplating of Iron Sheet

Preparation of Electrolyte Solution

Distilled water 8.5 L was poured into a container and other ingredients such as 2400 g of zinc sulphate, 300 g of aluminium sulphate, 300 g of boric acid were added with agitation to enhance complete dissolution. The solution was finally made up to 10 L by adding distilled water.

Pretreatment of Iron Sheet for Electroplating

The iron sheets were cut into pieces of 80.32 cm^2. They were punched in machine and washed with detergent to remove any grease and oil adhering on the iron sheet and then washed with water. After that, the sheets were pickled in 6M hydrochloric acid for 5 min to remove scales and rust and then brushed with iron brush. After acid pickling, the iron sheets were washed again with water to remove traces of acid and dried in an oven and weighed.

Electroplating of Iron Sheet

In electroplating bath, two pure zinc plates were used as anodes. The pre-weighed iron sheet 80.32 cm^2 already attached to the flexible copper wire

was hanged at the cathode of the zinc electroplating bath. Both anodes and cathode were dipped in the electrolyte solution containing zinc sulphate when a direct current was passed through the electrolyte, zinc ions were plated onto the iron cathode. The whole process was carried out at room temperature. Electroplating process was carried out at different electric voltages such as (3V, 4V, 5V,6Vand 7V), electroplating time (5 min, 10 min, 15 min and 20 min) at electrodes distances of 12.7cm. After electroplating, zinc coated iron sheet was removed and rinsed with water, then it was dipped in sodium chromate solution to fix the zinc layer for 5 sec and then washed with water and caustic soda solution. Finally, it was washed with water again and dried in an oven for 5 min. Zinc coated iron sheet was obtained and weighed again.

Results and Discussion

The purity of zinc sulphate to be used in electroplating process is important. Therefore, the purity of zinc oxide was examined both by volumetric analysis and EDXRF. The purity of zinc oxide was 98.58% by volumetric method (ASTM E 56) and 99.953 % by EDXRF. The XRD result of zinc oxide is shown in Fig. (1). From Tables (1) and ( ), a high yield 79.50(%w/w) of zinc sulphate was obtained by using 10 g of zinc oxide with 75 mL of 3 M sulphuric acid. Although the concentration of sulphuric acid was increased up to 4 M, the yield percent of zinc sulphate did not increase considerably. XRD spectrum shows the high purity of prepared zinc sulphate sample. The composition of the commercial grade, analar grade and prepared zinc sulphate were determined by EDXRF. The content of zinc in prepared zinc sulphate is higher than commercial grade but lower than that of the analar grade. The results are shown in Fig. (8), (9) and (10).

Zinc sulphate is the primary component for zinc ion in electrolyte solution. Aluminium sulphate was used to give a bright deposit on the substrate. Apart from bright deposit, aluminium sulphate gave good adhesion of metal on the surface of the substrate. It was also used to improve the uniformity of deposition of zinc on iron sheet. One of the most important additives in an electroplating bath was boric acid which serves as a weak buffer to control the pH and to give a smooth deposit. The elemental

composition of electrolyte solution was examined by EDXRF. The respective spectra is shown in Fig. (10).

Zinc electroplating process was studied by varying the electroplating parameters such as voltage, current and electroplating time. The effect of voltages (3V,4V,5V,6V and 7V) on thickness of zinc coating on iron sheet at different electroplating times (5 min, 10 min,15 min and 20 min) are shown in Table (3). Electroplating at low current and voltage takes longer electroplating time to obtain a certain thickness. The deposited zinc increased with the increase in voltage (3 V to7 V) but gray colour appears at high voltage and electroplating time longer than 15 min. Bright silvery colour and smooth surface was obtained at 6 V and electroplating time of 15 min. Beyond these process conditions, rough coated zinc layer or burning occurred on the iron sheet.

The quality of the best parameters of zinc electroplated sheet was assessed by the resistance in artificially simulated environments. Tap water (pH=6.7), 3.5 % NaCl solution (pH=6.5) and dilute sulphuric acid solution (pH= 5.3) were used as corrosion medium. The corrosion rate of electroplated sample by different environments are shown in Table (4). From these results, the corrosion rate of zinc electroplated sample increased with increasing treatment time in all the different environments. During 60 days, the corrosion rate of zinc coating in sodium chloride solution was faster than in sulphuric acid solution and tap water.

In NaCl solution, the corrosion rate of zinc coating was the highest in the first 15 days due to the dissolution of zinc followed by passivation of an impermeable film (Redox reaction) on the intended metal surface and no rusting occurs for a test period of 60 days. The corrosion resistance of zinc coating to the neutral salt spray test was also conducted by using (ASTM B117) method. The number of hr for the formation of white rust on zinc layer indicated the corrosion resistance. In the present case, selected zinc coated sheet produced white rust after 72 hr treatment. Zinc coated sample could be used in various environments according to the salt spray test period of 72 hr. The surface morphology of the deposited zinc layer before and after corrosion tests are shown in Fig. (12).

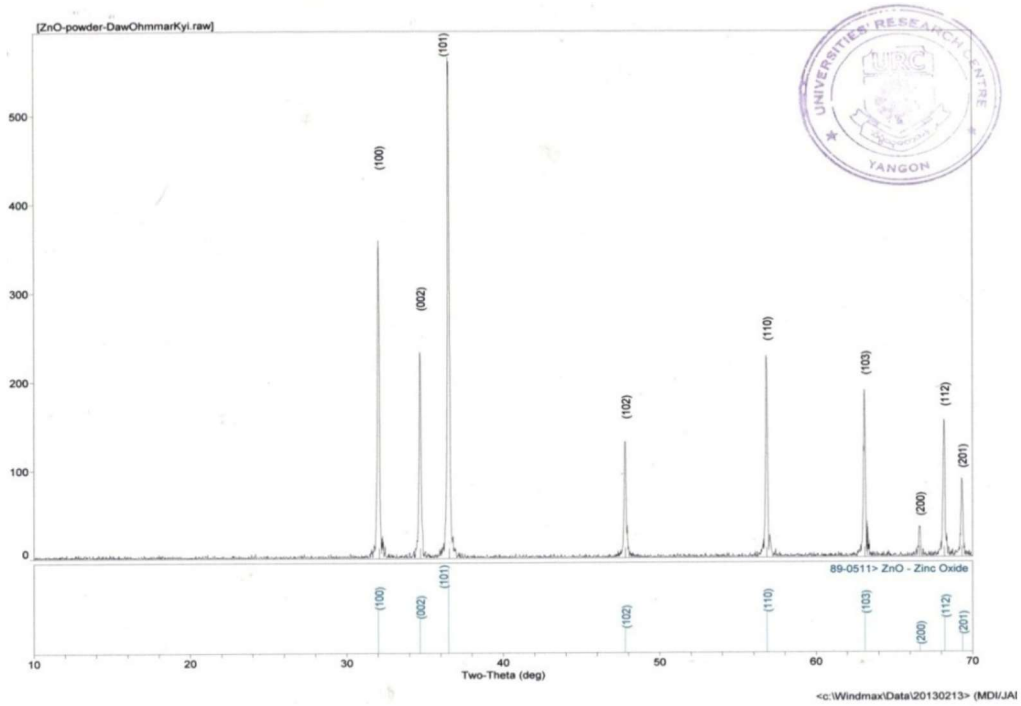

Figure 1. XRD Spectrum for Zinc Oxide

Table 1: Effect of Volume of 2M Sulphuric Acid on Yield of Zinc Sulphate from Zinc Oxide

Evaporation time at 70°C = 30 min
Reaction time = 10 min
Weight of zinc oxide = 10 g

Sr. No.	Reaction Time (min)	Rate of Agitation (rpm)	Concentration of H_2SO_4 (M)	Volume of H_2SO_4 (mL)	Yield Percent of $ZnSO_4$ (% w/w)
1.	10	100	2	65	71.51
2.	10	100	2	70	73.45
3.	10	100	2	75*	78.47
4.	10	100	2	80	78.49

* The most suitable condition.

The experiments were conducted at the Department of Industrial Chemistry, Dagon University.

Table (2) Effect of Strength of Sulphuric Acid on Yield of Zinc Sulphate From Zinc Oxide

Evaporation time at 70°C = 30 min
Reaction time = 10 min

Sr. No.	Reaction Time (min)	Rate of Agitation (rpm)	Concentration of H_2SO_4 (M)	Volume of H_2SO_4 (mL)	Yield Percent of $ZnSO_4$ (% w/w)
1.	10	100	2	75	78.47
2.	10	100	3*	75	79.50
3.	10	100	4	75	79.51

* The most suitable condition.

The experiments were conducted at the Department of Industrial Chemistry, Dagon University.

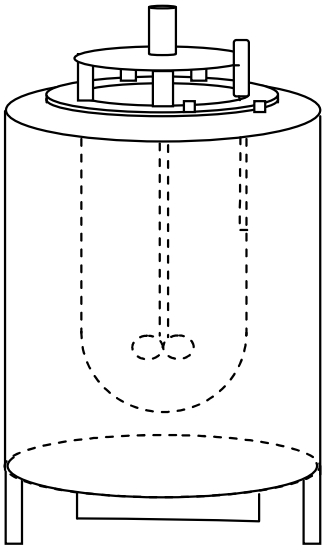

Figure 2: Schematic Diagram of Stirred Tank Reactor for the Production of Zinc Sulphate

Figure 3: Stirred Tank Reactor for the Production of Zinc Sulphate

Figure 4: Zinc Oxide (Commercial grade)

Figure 5: Prepared Zinc Sulphate

Figure 6 : Zinc Coated Iron Sheet

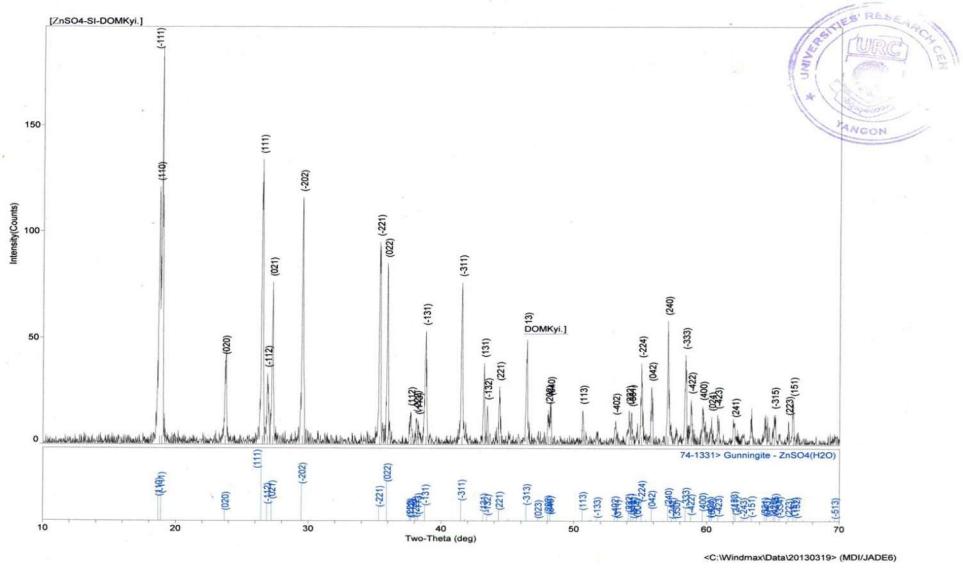

Figure 7: XRD Spectrum of Prepared Zinc Sulphate

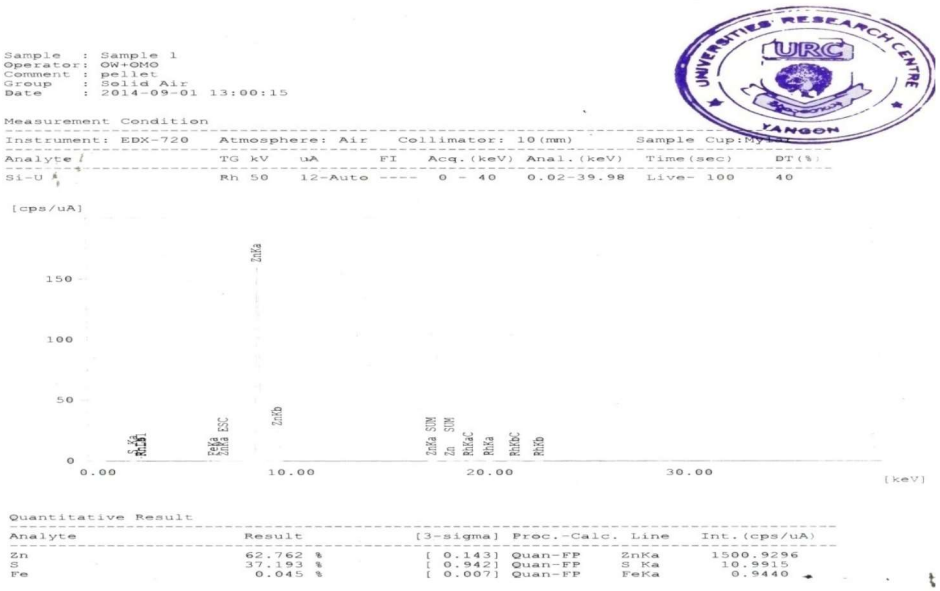

Figure 8: EDXRF Results of Prepared Zinc Sulphate

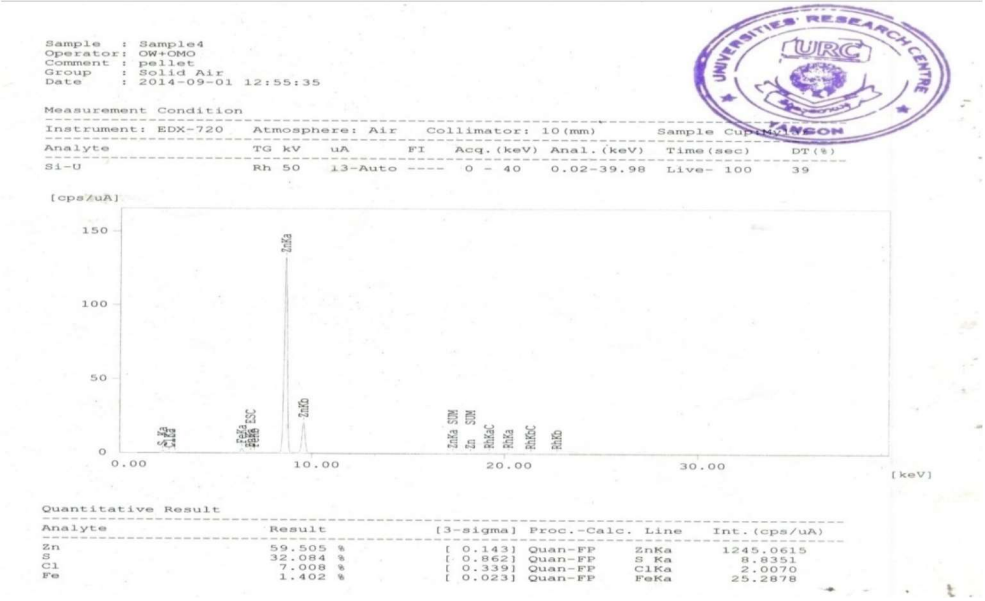

Figure 9: EDXRF Results of Zinc Sulphate (Commercial grade, India)

Figure 10: EDXRF Results of Zinc Sulphate (Analar grade, India)

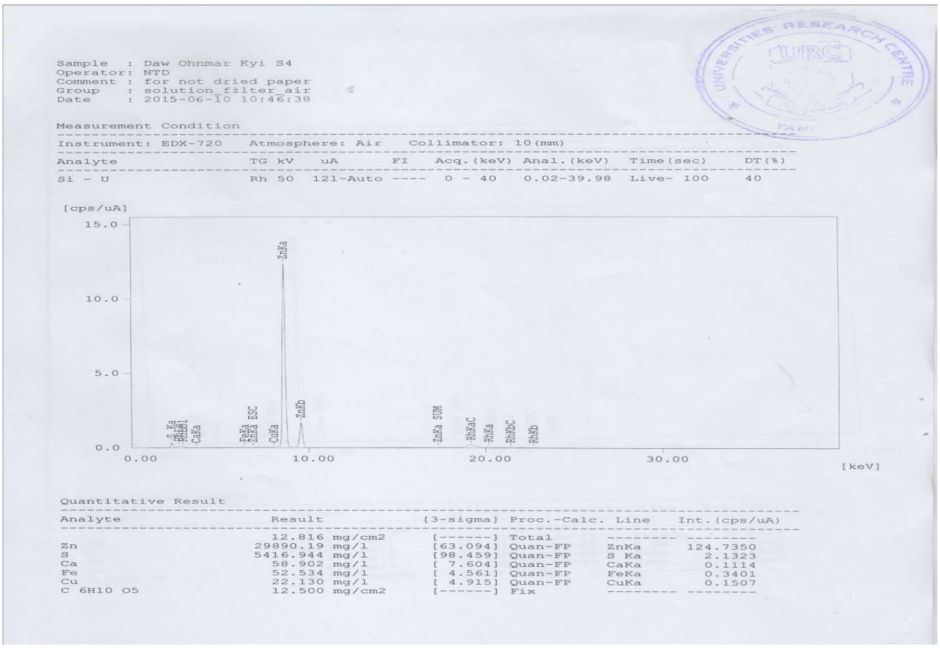

Figure 11: EDXRF spectrum of Electrolyte Solution

J. Myanmar Acad. Arts Sci. 2018 Vol. XVI. No. 1B 539

Table 3: Effect of Voltage on Thickness of Zinc Coating on Iron Sheet at Various Electroplating Time

Thickness of iro … a electrodes = 12.7 cr

Sr. No.	Electric Voltage (V)	Electric Current (A)	Actual …												Zinc Coated Lay … Service Conditi…							
			5 min	10 min	15min	20 min	5 min	10 min	15min	20 min	5 min	10 min	15min	20 min	5 min	10 min	15min	20 min	5 min	10 min	15min	20 min
1.	3	2	3.14	6.62	9.73	14.05	3.54	7.09	10.63	14.18	B	B	B	B	< SC 1	SC 1	>SC 2	>SC 3	S	S	S	S
2.	4	3	4.72	10.39	14.53	19.37	5.32	10.63	15.95	21.27	B	B	B	B	< SC 1	>SC 2	>SC 3	>SC 3	S	S	S	S
3.	5	4	6.29	10.85	20.44	25.44	7.09	14.18	21.27	28.35	B	B	B	B	>SC 1	>SC 2	>SC 3	SC 4	S	S	S	R
4.	6*	5	7.87	16.71	23.57*	34.07	8.86	17.73	26.59	35.43	B	B	B	B	>SC 1	>SC 3	>SC 3	>SC 4	S	S	S	R
5.	7	6	10.31	20.29	29.63	-	10.63	21.27	31.90	-	B	B	B	-	>SC 2	>SC 3	>SC 4	-	S	SR	R	-

The experiments were conducted at KMN Manufacturing Co.,Ltd.South Dagon, Yangon Region *The most suitable condition. **T.J.Tuaweri et.al , A Study of Process Parameters for Zinc Electrode position from a Sulphate Bath, 2013. (Faraday's Law of Electrolysis) B = Bright Silvery Colour, S=smooth , SR=slightly rough, R=rough

Classification of Thickness Class for Electrodeposited Coatings of Zinc on Iron and Steel (ASTM B 633)

Service Condition	Thickness, min (μm)
SC 4 (very severe)	25
SC 3 (severe)	12
SC 2 (moderate)	8
SC 1 (mild)	5

Examples of Appropriate Service Conditions and Description of Service Conditions

SC 4 (Very Severe) - Exposure to harsh conditions, or subject to frequent exposure to moisture, cleaners, and saline solutions, plus likely damage by denting, scratching, or abrasive wear. e.g: plumbing fixtures, pole line hardware.

SC 3(Severe) - Exposure to condensation, perspiration, infrequent wetting by rain, and cleaners. e.g: tubular furniture, insect screens, window fittings, builder's hardware, military hardware, washing machine parts, bicycle parts.

SC 2(Moderate) - Exposure mostly to dry indoor atmospheres but subject to occasional condensation, wear, or abrasion. e.g: tools, zippers, pull shelves, machine parts

SC 1 (Mild) - Exposure to indoor atmospheres with rare condensation and subject to minimum wear or abrasion. e.g: buttons, wire goods, fasteners.

[1] Dr., Assistant Lecturer, Industrial Chemistry Department, Dagon University
[2] Dr., Professor (Retired), Department of Industrial Chemistry, Dagon University
[3] Dr, Professor (Retired), Department of Industrial Chemistry, University of Yangon

Table 4: Change in Appearance, Colour and Weight Loss of Zinc Coating on Iron Sheets After Treatment in Artificially Simulated Environments

Thickness of z

Artificially Simulated Environments	Zinc Coat on Iron Sheet Before Treatment	Zinc Coating on Iron Sheet After Treatment											
		15 days			30 days			45 days			60 days		
	colour and surface appearance	wt. loss of zinc (% w/w)	colour	surface appearance	wt. loss of zinc (% w/w)	colour	surface appearance	wt. loss of zinc (% w/w)	colour	surface appearance	wt. loss of zinc (% w/w)	colour	surface appearance
Tap Water	silvery white, smooth	0.074	silvery white	smooth	0.156	silvery white	smooth	0.216	silvery white	smooth	0.232	silvery white	smooth
3.5 % NaCl Solution (pH=6.5)	silvery white, smooth	2.23	silvery white	white rust on surface	6.15	gray	corroded surface	9.35	gray	corroded surface	12.21	gray	corroded surface
Dilute Sulphuric Acid Solution (pH= 5.3)	silvery white, smooth	0.19	silvery white	white rust on surface	1.24	silvery white	corroded surface	2.63	gray	corroded surface	4.25	gray	corroded surface

The experiments were carried out at the Department of Industrial Chemistry, Dagon University.

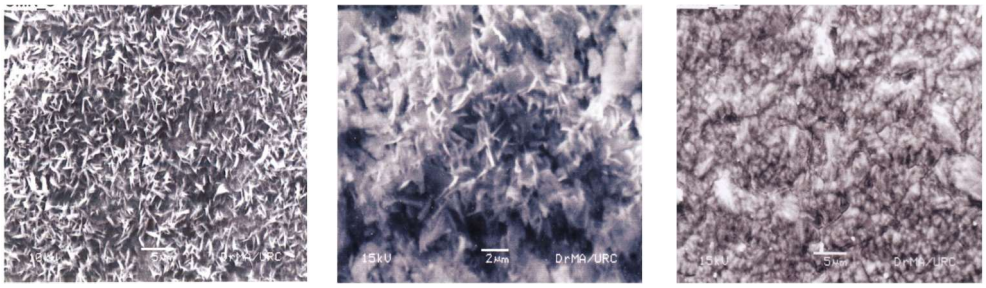

(a) Bright Silvery Colour of Zinc Coat (60 days)

(b) Deterioration of Zinc Coat after Treatment with 3.5 % NaCl Solution (60 days)

(c) Deterioration of Zinc Coat after Treatment with Acid Solution (60 days)

Figure 12: SEM Micrograph for Morphology of Zinc Coated Iron Sheet

Conclusion

In this research, zinc oxide (commercial grade,China) which has a purity of 99.953 % obtained from KMN Manufacturing Co., Ltd. was used to produce zinc sulphate. The maximum yield of zinc sulphate 79.50 (% w/w) was obtained by using 10g of zinc oxide with 75 mL of 3 M sulphuric acid. Analysis by X-ray Diffraction (XRD) method shows the purity of the prepared zinc sulphate which is the same as the technical grade zinc sulphate. Based on the required amount of zinc sulphate, make-shift stirred tank reactor was constructed. Maximum yield of zinc sulphate 2 Kg per batch was obtained by using 488 g of zinc oxide. Prepared zinc sulphate was used in the preparation of electrolytes solutions for zinc electroplating. The best operating conditions were 6V, 5 A, 15 min electroplating time at distance between electrodes of 12.7 cm. From salt spray test, it can be observed that the prepared zinc coated iron sheet resists up to 72 hr using salt spray test method according to ASTM B117.Therefore zinc coated iron sheet with selected parameters can be used in various environments.

Acknowledgement

The author would like to express her gratitude to Dr Yin Shwe, Professor and Head (Retired), Department of Industrial Chemistry, Dagon University, for her kind encouragement and close supervision and guidance throughout the research. I am greatly indebted to my supervisor Dr Khin Thet Ni, Professor and Head(Retired), Department of Industrial Chemistry, University of Yangon and Dr Than Htaik , Director General, Department of Cottage Industry(Retired) , Ministry of Cooperatives, for his advice given to me while the research work is being conducted. I would also like to thank Khin Maung Nyunt Trading,Co.,Ltd, for providing research facilities during the electroplating process of the research work.

References

H.B. Muralidhara,2011." Electrodeposition of Nanocrystalline Zinc on Steel Substrate from Acid Sulphate Bath and its Corrosion Study.".

B.M. Dorodola,2011." Study of Influence of Zinc Plated Mild Steel Deterioration in Seawater Environment".

S.A Moshood, “Study of Influence of Zinc Plated Mild Steel Deterioration in Seawater Environment”. International Journal of Electrochemical Science. http// www.electrochemsci.org.

T.J .Tuaweri, E.M, Adigio and P.P. Jombo, August 2013 .“ A Study of Process Parameters for Zinc Electroplating from a Sulphate Bath”. International Journal of Engineering Science Invention. Volume2 Issue8.